Chemical and biological investigations of cytotoxic metal complexes

Dissertation

(kumulativ)

zur Erlangung des akademischen Grades doctor rerum naturalium
(Dr. rer. nat.)

vorgelegt dem Rat der Chemisch-Geowissenschaftlichen Fakultät
der Friedrich-Schiller-Universität Jena

von
M.Sc. M.Sc. Jana Hildebrandt

Gutachter:

1. Prof. Dr. Wolfgang Weigand, Friedrich-Schiller Universität Jena
2. Prof. Dr. Matthias Dürst, Universitätsklinikum Jena
3. Prof. Dr. Nils Metzler-Nolte, Ruhr-Universität Bochum

Tag der Verteidigung: 29.05.2019

אִם-אֶשְׁכָּחֵךְ יְרוּשָׁלִָם

תִּשְׁכַּח יְמִינִי

Psalm 137:5

Table of contents

Abbreviations

A	
A	Adenine
Asp	Aspirin
Aspy-NMe_2	*p*-dimethylaminophenylazopyridine
ATM	Ataxia telangiectasia mutated
ATP	Adenosinetriphosphate
azpy	2-phenylazopyridine
B	
bpy	2,2'-bipyridine
But	Butyl
t-BuOK	Potassium *tert*-butoxide
C	
C	Carbon
CAM	Cell-to-cell adhesion molecule
CAPE	Caffeic acid phenyl ester
CatB	Cathepsin B
CHEK	Checkpoint kinase
CN	Cyanide
COX	Cyclooxygenase
CS_2	Carbon disulfide
CTR	Copper transporter
Cu	Copper
CYP450	Cytochrom P450
Cys	Cysteine
CytC	Cytochrome C
D	
DACH	(1R, 2R)-1,2-diaminocyclohexane
DCA	Dichloroacetate
DCM/dcm	Dichloromethane
DMF/dmf	Dimethylformamide
dmpa	*N,N*-dimethyl-1-phenethyl-amine

DMSO/dmso	Dimethylsulfoxide
DNA	Desoxyribonucleic acid
dppe	1,2-bis(diphenylphosphino)ethane
E	
E.coli	*Eschericha coli*
EDC	1-Ethyl-3-(3-dimethylaminopropyl)carbodiimide
e.g.	*Exempli gratia*
EGFR	Epidermal growth factor receptor
EI	Electrospray ionization
en	Ethylenediamine
EPR	Enhanced permeability and retention
equiv.	Equivalente
ER(+)/ER(-)	Estrogen-receptor positive/ negative
Et	Ethyl
F	
FACS	Fluorescence-activated cell sorting
FDA	Food and Drug Administration
FGF	Fibroblast growth factor
G	
G	Guanine
GABA	Gamma amino-butyric acid
GFS	Growth factors
Glu	Glutamic acid
GLUT	Glucose-transporter
Gly	Glycin
GS	Growth signal
GSH	Glutathione
GST	Glutathione S-transferase
5'-GMP	5'-guanosinemonophosphate
H	
H	Hydrogen
harmine	7-methoxy-1-methyl-9H-pyrido[3,4-b]indole

HDAC	Histone deacetylase
HIm	Imidazole
HInd	Indazole
HMG	High mobility group
HMGB1	High mobility group protein B1
HRPC	Hormone refractory prostate cancer
HSA	Human serum albumin
HSAB	Hard and soft acids and bases
H2AX	Histone H2AX
I	
I	Iod
i	Inhibitor
Ibu	Ibuprofen
IC50	Half maximal inhibitory concentration
K	
K	Potassium
L	
L	Ligand
M	
m-	*Meta*-
MAPK	Mitogen-activated protein kinase
Me	Methyl
MMR	Mismatch repair
MRP	Multi-drug-resistant protein
MS	Mass spectrometry
MTT	3-(4,5-dimethylthiazol-2-yl)-2,5-diphenyltetrazolium bromide
N	
N	Nitrogen
Na	Sodium
NER	Nucleotide exicision repair

NF-κB	Nuclear factor 'kappa-light-chain-enhancer' of activated B-cells
NHS	N-Hydroxysuccinimide
Ni	Nickel
nm	Nano molar
NMR	Nuclear magnetic resonance
NSCLC	Non-small cell lung cancer
O	
O	Oxygen
o-	*Ortho*-
OCT	Organic cationic transporter
Os	Osmium
P	
P	Phosphor
p-	*Para*-
PARP	Poly((ADP-ribosyl)alted) protein
Pd	Palladium
PDHC	Pyruvate dehydrogenase complex
PDK	Pyruvate dehydrogenase kinase
Ph	Phenyl
PhB	Phenylbutyrate
pRb	Retinoblastoma protein
Pt	Platinum
pta	1,3,5-triaza-7-phosphatricyclo-[3.3.1.1]decane
Pur	Purine
R	
RNA	Ribonucleic acid
RNase	Ribonuclease A
ROS	Reactive oxygen species
r. t.	Room temperature
rt	Retention time
Ru	Ruthenium

S

S	Sulfur
sac	Saccharinate
SAR	Structure-activity-relationship
SCLC	Small cell lung cancer
Se	Selenium

T

terpy	2,2’:6,2’’-terpyridine
Tf	Transferrin
tfa	Trifluoroacetic acid
TGF	Transforming growth factor
THF/thf	Tetrahydrofurane
Ti	Titanium
TrXr	Thioredoxin reductase

V

Val	Valoproate
VEGF	Vascular endothelial growth factor
VRAC	Volume-regulated anion channels

Documentation of Authorship

1. List of Publications

[JH1] Unusual mode of protein binding by a cytotoxic π-arene ruthenium(II) piano-stool compound containing an O,S-chelating ligand

Jana Hildebrandt, Helmar Görls, Norman Häfner, Giarita Ferraro, Matthias Dürst, Ingo B. Runnebaum, Wolfgang Weigand, Antonello Merlino

Dalton Transactions **2016**, *45*, 12283-12287.

[JH2] Highly cytotoxic Osmium(II) compounds and their Ruthenium(II) Analogues targeting Ovarian Carcinoma cell lines and evading Cisplatin resistance mechanisms

Jana Hildebrandt, Norman Häfner, Daniel Kritsch, Helmar Görls, Matthias Dürst, Ingo B. Runnebaum, Wolfgang Weigand

in preparation

[JH3] Platinum(II) O,S complexes as potential metallodrugs against Cisplatin resistance

Jana Hildebrandt, Norman Häfner, Helmar Görls, Daniel Kritsch, Giarita Ferraro, Matthias Dürst, Ingo B. Runnebaum, Antonello Merlino ,Wolfgang Weigand

Dalton Transactions **2016**, *45*, 18876-18891.

[JH4] Novel Nickel(II), Palladium(II), and Platinum(II) complexes with O,S-bidendate cinnamic acid ester derivatives: An *in vitro* cytotoxic comparison to Ruthenium(II) and Osmium(II) Analogues

Jana Hildebrandt, Norman Häfner, Helmar Görls, Matthias Dürst, Ingo B. Runnebaum, Wolfgang Weigand

in preparation

[JH5] Synthesis, characterization and biological investigation of platinum(II) complexes with asparagusic acid derivatives as ligands

Jana Hildebrandt, Ralf Trautwein, Daniel Kritsch, Norman Häfner, Helmar Görls, Matthias Dürst, Ingo B. Runnebaum, Wolfgang Weigand

Dalton Transactions **2019**, *48*, 936-944.

[JH6] Asparagusic Acid Derivatives and their Cytotoxic Platinum(II) Complexes

Jana Hildebrandt, Tobias Niksch, Ralf Trautwein, Norman Häfner, Helmar Görls, Marie-Christin Barth, Matthias Dürst, Ingo B. Runnebaum, Wolfgang Weigand

Phosphorous, Sulfur, and Silicon and the Related Elements **2017**, *192*, 182-186.

Additional Publications:

[1] Platinum(II) Complexes with O,S Bidentate Ligands: Biophysical Characterization, Antiproliferative Activity, and Crystallographic Evidence of Protein Binding

Carolin Mügge, Tiziano Marzo, Lara Massai, Jana Hildebrandt, Giarita Ferraro, Pablo Rivera-Fuentes, Nils Metzler-Nolte, Antonello Merlino, Luigi Messori, Wolfgang Weigand

Inorganic Chemistry **2015**, *54*, 8560-8570.

[2] Diselenolane-mediated cellular uptake

Nicolas Chuard, Amalia I. Poblador-Bahamonde, Lili Zong, Eline Bartolami, Jana Hildebrandt, Wolfgang Weigand, Naomi Sakai, Stefan Matile

Chemical Science **2018**, *9*, 1860-1866.

Additional Presentations:

[1] Synthesis and biological behavior of O,S-chelating platinum(II) and ruthenium(II) complexes

Jana Hildebrandt, Norman Häfner, Helmar Görls, Matthias Dürst, Ingo B. Runnebaum, Wolfgang Weigand

7th Postgraduate Symposium on Cancer Research, **2015**.

[2] Cytotoxic Ruthenium(II) and Platinum(II) Complexes with Cinnamic Acid Derivatives as Ligands

Jana Hildebrandt, Norman Häfner, Helmar Görls, Matthias Dürst, Ingo B. Runnebaum, Wolfgang Weigand

GDCh-Wissenschaftsforum Chemie, **2015**.

[3] Combating Cisplatin Resistance: Biological Activity of Platinum(II) Complexes with Cinnamic Acid Derivatives as Ligands

Jana Hildebrandt, Norman Häfner, Helmar Görls, Daniel Kritsch, Matthias Dürst, Ingo B. Runnebaum, Antonello Merlino, Wolfgang Weigand

Frontiers in Medicinal Chemistry, **2016**.

[4] Combating Cisplatin Resistance: Biological Activity of Platinum(II) Complexes with Cinnamic Acid Derivatives as Ligands

Jana Hildebrandt, Norman Häfner, Helmar Görls, Daniel Kritsch, Matthias Dürst, Ingo B. Runnebaum, Antonello Merlino, Wolfgang Weigand

8th Postgraduate Symposium on Cancer Research, **2016**.

[5] Are Ru(II)/ Pt(IV) complexes useful compounds to overcome drug resistance?

Jana Hildebrandt, Dan Gibson, Wolfgang Weigand

3rd International Symposium on Functional Metal Complexes that Bind to Biomolecules – 4th Whole Action Meeting of the COST Action CM1105, **2016**.

[6] Cytotoxic Platinum(II) Complexes with Sulfur and Selenium-Containing Natural Products as Ligands

Jana Hildebrandt, Wolfgang Weigand

27th International Symposium on Organic Chemistry of Sulfur, ISOCS, **2016**.

[7] Cytotoxic metal complexes with cinnamic acid derivatives as ligands to overcome Cisplatin resistance

Jana Hildebrandt, Norman Häfner, Daniel Kritsch, Helmar Görls, Giarita Ferraro, Matthias Dürst, Ingo B. Runnebaum, Antonello Merlino, Wolfgang Weigand

13th European Biological Inorganic Chemistry Conference (EuroBIC 13), **2016**.

[8] Cytotoxic metal complexes with cinnamic acid derivatives as ligands to overcome Cisplatin resistance

Jana Hildebrandt, Wolfgang Weigand

Mitteldeutsches Anorganiker Nachwuchssymposium, **2016**.

[9] Cytotoxic Platinum(II) Complexes with Sulfur and Selenium-Containing Natural Products as Ligands

Jana Hildebrandt, Ralf Trautwein, Norman Häfner, Helmar Görls, Marie-Christin Barth, Matthias Dürst, Ingo B. Runnebaum, Wolfgang Weigand

Mitteldeutsches Anorganiker Nachwuchssymposium, **2016**.

[10] Cytotoxic metal complexes to overcome Cisplatin resistance

Jana Hildebrandt, Daniel Kritsch, Norman Häfner, Helmar Görls, Matthias Dürst, Ingo B. Runnebaum, Antonello Merlino, Wolfgang Weigand

Frontiers in Medicinal Chemistry, **2017**.

[11] Cytotoxic Platinum(II) Complexes with Sulfur and Selenium-Containing Natural Products as Ligands

Jana Hildebrandt, Ralf Trautwein, Daniel Kritsch, Norman Häfner, Helmar Görls, Tobias Niksch, Matthias Dürst, Ingo B. Runnebaum, Wolfgang Weigand

GDCh-Wissenschaftsforum Chemie, **2017**.

[12] Cytotoxic metal complexes with cinnamic acid derivatives as ligands to overcome Cisplatin resistance

Jana Hildebrandt, Wolfgang Weigand

Meeting Hebrew University and Vienna University, **2017**.

Prizes regarding to this PhD thesis:

[1] Best Poster Award: Cytotoxic Platinum(II) Complexes with Sulfur and Selenium-Containing Natural Products as Ligands, *Mitteldeutsches Anorganiker Nachwuchssymposium*, **2016**.

[2] Best Poster Award: Cytotoxic metal complexes to overcome Cisplatin resistance, *Frontiers in Medicinal Chemistry*, **2017**.

2. Documentation of Authorship

2.1 **[JH1]** Unusual mode of protein binding by a cytotoxic π-arene ruthenium(II) piano-stool compound containing an O,S-chelating ligand

Jana Hildebrandt,[1] Helmar Görls,[2] Norman Häfner,[3] Giarita Ferraro,[4] Matthias Dürst,[5] Ingo B. Runnebaum,[6] Wolfgang Weigand,[7] Antonello Merlino[8]

Dalton Transactions **2016**, *45*, 12283-12287.

Beteiligt an	**Autoren**							
	1	2	3	4	5	6	7	8
Manuscript preparation	x							x
Discussion of the manuscript	x							x
Synthesis of compounds	x							
Characterization of compounds	x							
MTT-Assays	x							
X-Ray structures	x	x		x				x
UV-Vis spectra				x				x
Strategy of research approach	x						x	
Strategy of investigation	x						x	x
Supervision			x		x	x	x	
Vorschlag Anrechnung Publikationsäquivalente	1,0							

2.2 **[JH2]** Highly cytotoxic Osmium(II) compounds and their Ruthenium(II) Analogues targeting Ovarian Carcinoma cell lines and evading Cisplatin resistance mechanisms

Jana Hildebrandt,[1] Norman Häfner, [2] Daniel Kritsch,[3] Helmar Görls,[4] Matthias Dürst,[5] Ingo B. Runnebaum,[6] Wolfgang Weigand[7]

In preparation

Beteiligt an	**Autoren**						
	1	2	3	4	5	6	7
Manuscript preparation	x	x					
Discussion of the manuscript	x	x	x				
Synthesis of compounds	x						
Charaterization of compounds	x						
Stability Determinations	x						
X-Ray structures	x			x			
MTT-Assays	x						
Cell cycle arrest			x				
Foci analysis	x	x					
Strategy of research approach	x						x
Strategy of research investigation	x	x					x
Supervision		x			x	x	x
Vorschlag Anrechnung Publikationsäquivalente	1,0						

2.3 **[JH3]** Platinum(II) O,S complexes as potential metallodrugs against Cisplatin resistance

Jana Hildebrandt,[1] Norman Häfner,[2] Helmar Görls,[3] Daniel Kritsch,[4] Giarita Ferraro,[5] Matthias Dürst,[6] Ingo B. Runnebaum,[7] Antonello Merlino,[8] Wolfgang Weigand[9]

Dalton Transactions **2016**, *45*, 18876-18891.

Beteiligt an	**Autoren**								
	1	2	3	4	5	6	7	8	9
Manuscript preparation	X								
Discussion of the manuscript	x	X							
Synthesis of compounds	x								
Characterization of compounds	x								
MTT-Assays	x								
X-Ray structures	x		x		x			x	
Stability Determinations	x				x				
DNA-binding behavior	x								
Interactions with proteins		x		x				x	
Strategy of research approach	x								x
Strategy of investigation	x	x							x
Supervision		x				x	x		x
Vorschlag Anrechnung Publikationsäquivalente	1,0								

2.4 **[JH4]** Novel Nickel(II), Palladium(II), and Platinum(II) complexes with O,S-bidendate cinnamic acid ester derivatives: An *in vitro* cytotoxic comparison to Ruthenium(II) and Osmium(II) Analogues

Jana Hildebrandt,[1] Norman Häfner,[2] Helmar Görls,[3] Matthias Dürst,[4] Ingo B. Runnebaum,[5] Wolfgang Weigand[6]

In preparation

Beteiligt an	**Autoren**					
	1	2	3	4	5	6
Manuscript preparation	X					
Discussion of the manuscript	X					
Synthesis of compounds	X					
Characterization of compounds	X					
MTT-Assays	X	x				
X-Ray structures	x		x			
Stability Determinations	x					
Strategy of research apporach	x					x
Strategy of research investigation	x					x
Supervision		x		x	x	x
Vorschlag Anrechnung Publikationsäquivalente	1,0					

2.5 **[JH5]** Synthesis, characterization and biological investigation of platinum(II) complexes with asparagusic acid derivatives as ligands

Jana Hildebrandt,[1] Ralf Trautwein,[2] Daniel Kritsch,[3] Norman Häfner,[4] Helmar Görls,[5] Matthias Dürst,[6] Ingo B. Runnebaum,[7] Wolfgang Weigand[8]

Dalton Transactions **2019**, *48*, 936-944.

Beteiligt an	**Autoren**							
	1	2	3	4	5	6	7	8
Manuscript preparation	x							
Discussion of the manuscript	x							
Synthesis of compounds	x	x						
Characterization of compounds	x	x						
MTT-Assays	x		x					
X-Ray structures	x	x			x			
Supervision				x		x	x	x
Strategy of research approach	x							x
Strategy of investigations	x							x
Vorschlag Anrechnung Publikationsäquivalente	1,0							

2.6 **[JH6]** Asparagusic Acid Derivatives and their Cytotoxic Platinum(II) Complexes

Jana Hildebrandt,[1] Tobias Niksch,[2] Ralf Trautwein,[3] Norman Häfner,[4] Helmar Görls,[5] Marie-Christin Barth,[6] Matthias Dürst,[7] Ingo B. Runnebaum,[8] Wolfgang Weigand[9]

Phosphorous, Sulfur, and Silicon and the Related Elements, **2017**, *192*, 182-186.

Beteiligt an	**Autoren**								
	1	2	3	4	5	6	7	8	9
Manuscript preparation	x	x	x						
Discussion of the manuscript	x	x	x						
Synthesis of compounds	x	x	x						
Characterization of compounds	x	x	x						
MTT-Assays	x								
X-Ray structures		x			x	x			
Strategy of research approach	x	x	x						x
Strategy of investigations	x	x	x						x
Supervision of JH				x			x	x	x
Supervision of MB	x								x
Supervision of TN and RT									x
Vorschlag Anrechnung Pubikationsäquivalente	0,5								

2.7 Declaration

Erklärung zu den Eigenanteilen des Promovenden sowie der weiterer Doktoranden/ Doktorandinnen als Koautoren an den Publikationen und Zweitpublikationsrechten bei einer kumulativen Dissertation.

Für alle in dieser kumulativen Dissertation verwendeten Manuskripte liegen die notwendigen Genehmigungen der Verlage für die Zweitpublikation vor.

Die Ko-Autoren der in dieser kumulativen Dissertation verwendeten Manuskripte sind sowohl über die Nutzung, als auch über die oben angegebenen Eigenanteile informiert und stimmen dem zu.

Ich bin mit der Abfassung der Dissertation als publikationsbasiert, d.h. kumulativ, einverstanden und bestätige die vorstehenden Angaben. Eine entsprechend begründete Befürwortung mit Angabe des wissenschaftlichen Anteils des Doktoranden an den verwendeten Publikationen werde ich parallel an den Rat der Fakultät der Chemisch-Geowissenschaftlichen Fakultät richten.

M.Sc. M.Sc. Jana Hildebrandt Jena, _____

Prof. Dr. Wolfgang Weigand Jena, _____

3. Introduction

3.1 Cancer – Definition and characteristics

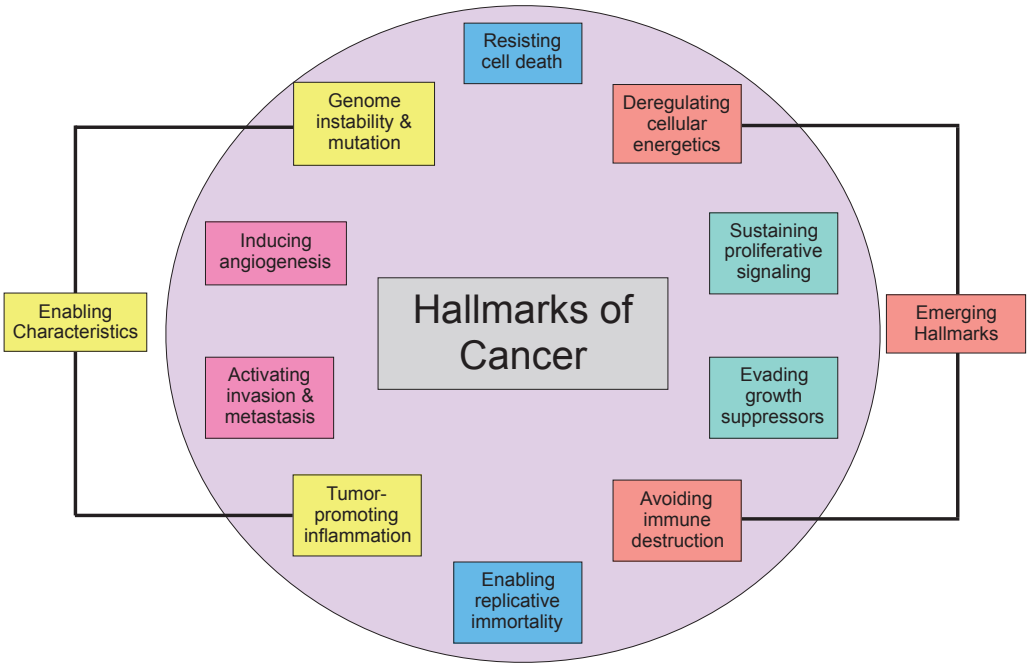

Fig. 3.1-1: Overview of the hallmarks of cancer, six capabilities, two emerging hallmarks and two enabling characteristics which can be observed in most common tumors, described by Weinberg and coworkers.[Hanahan, 2000; Hanahan, 2011]

The hallmarks of cancer describe six main characteristics, two emerging and two enabling characteristics, which have been reported by Weinberg and coworkers in 2000 and 2011 specifying rules that regularly lead to the transformation of normal human cells to malignant ones, Figure 3.1-1.[Hanahan, 2000; Hanahan, 2011] The development of malignant cells and tumors is a multistep process and is based on genetic alterations. Therefore it is known, that cancer cells imply defects in regulatory circuits that govern normal cell proliferation and homeostasis and become 'masters of their own destinies'.[Hanahan, 2000; Hanahan, 2011] Tumors are on one hand side based on genetic alterations and diversity and on the other hand they are able to create their own tumor environment by recruiting other cells around having multiple interaction ways with each other.[Hanahan, 2011] More than 100 different tumor types and subtypes are known pointing to the molecular diversity of cancer.[Hanahan, 2000] Overall six essential alterations occur in cancer cells, which are observable in most types of cancers,

but in different lifetime phases and in various mechanistic strategies:[Hanahan, 2000]

- Self-sufficiency in growth signals

Normal cells proliferate after stimulation *via* mitogenic growth signals (GS). Those signal molecules, *e.g.* diffusible growth factors, extracellular matrix components, cell-to-cell adhesion/ interaction molecules, can bind on transmembrane receptors and start intracellular responses. Most mitogenic growth factors (GFS) are made by one cell type to stimulate another one in the surrounding tissue (paracrine signals).[Hanahan, 2000] GF receptors are overexpressed in many cancer cells, therefore already low levels of GFS in the tissue are able to trigger proliferation of that cells. Next to the overexpression cancer cells are also able to switch the type of extracellular matrix receptors (integrins) favoring receptors which receive pro-growth signals.[Lukasehv, 1998; Giancotti, 1999] Most cancer cells are able to produce GFs to which they are sensitive resulting in an autocrine stimulation. Tumor cells are also able to stimulate their normal neighbor cells to produce growth-stimulating signals as well.[Skobe, 1998] Next to the involved extracellular factors and receptors, growth autonomy may also result from mutations and alterations of intracellular pathways downstream of the extracellular signals. This involves very often the SOS-Ras-Raf-MAPK pathway as in many human tumor cells the Ras oncoprotein is deregulated.[Hanahan, 2000]

- Insensitivity to growth-inhibitory (antigrowth) signals

Antigrowth signals can be recognized by cells *via* transmembrane receptors, similar to growth-stimulating factors also resulting in intracellular signal pathway activation. In normal cells multiple factors control proliferation/ growth- and antigrowth-stimulation, for antigrowth signals soluble growth inhibitors (like TGFβ) and immobilized inhibitors embedded in the extracellular matrix and on surfaces of neighbor cells are involved. In a normal tissue cells monitor their environment and decide to proliferate or to be quiescent.[Hanahan, 2000] The proliferation can be blocked mainly by two mechanisms: entering in a postmitotic state (G_0),

which means a quiescent state for cells, that can be reversible or also irreversible. Cancer cells try to circumvent the irreversible quiescent state using various strategies. Many antiproliferative signals are mediated by the retinoblastoma protein (pRb) which blocks in a hypophosphorylated form the proliferation of a cell. Dysregulation of this protein leads to insensitivity for antigrowth signals, as seen in many cancer cells. The disruption of anti-proliferative-signaling can be very different as for example receptor mutation or downregulation next to alterations in the pathway and pRb itself.[Hanahan, 2000]

- Evasion of programmed cell death (apoptosis)

The resistance to apoptosis is a hallmark of all kinds of cancer cells. Two classes of compounds are involved in apoptosis: sensors, which monitor the conditions in the environment of the cell and effectors, which start the apoptotic program. Abnormality signals can be received from outside the cell *via* death receptors or intracellular, for example after the recognition of DNA-damage, (DNA= Desoxyribonucleic acid). Death receptors can activate intracellular caspases (effectors).[Thornberry, 1998] An important component of the apoptotic cell death program is tumor suppressor protein p53, which is inactivated in more than 50% of all tumors leading to the resistance of cancer cells for death receptor signaling.[Hanahan, 2000] Moreover, p53, the 'guardian of the genome', is the central component for the integration of DNA damage signals eventually triggering apoptosis, if the DNA damage levels reaches a certain threshold.

- Limitless replicative potential

All cells have an intrinsic cell-autonomous program which limits their cell divisions. Therefore, the singular loss of anti-proliferative cell-to-cell signaling cannot lead to expansive tumor growth and disruptions of the limit for the replication of cells is found in many tumors. This results in unlimited replicative potential for cancer cells.[Hanahan, 2000]

- Sustained angiogenesis

The growth of new blood vessels, angiogenesis, to transport essential nutrients and oxygen to the cells in all tissues is normally a strictly regulated process. Caused by the high proliferation rate of cancer cells, their use of nutrients is immense compared to normal cells. Therefore, the induction of angiogenesis is an early to midstage step in the development of tumors. Pro-angiogenetic signals can come from soluble factors and their receptors *e.g.* vascular endothelial growth factor (VEGF) and acidic and basic fibroblast growth factors (FGF1/2). These factors bind to transmembrane tyrosine kinase receptors and activate respective signaling pathways.[Fedi, 1997; Veikkola, 1999] Tumors may overexpress VEGF and FGFs. Signals can be also introduced by cell-to-cell adhesion *via* adhesion molecules and integrins.[Hanahan, 2000]

- Tissue invasion and metastasis

Cells from primary tumors may spread to other tissues in the human body and form new colonies named metastases. This capability enables the cancer to find new spaces and to keep on growing. Many proteins are involved in that process, for example extracellular proteases which are upregulated and their inhibitors are downregulated in cancer cells, or cell-to-cell adhesion molecules (CAMs).[Hanahan, 2000; Coussens, 1996; Chambers, 1997]

Next to the six major hallmarks two enabling characteristics have been reported:[Hanahan, 2000; Hanahan, 2011]

- Genome instability

The genome instability and the resulting heterogeneity are underlying characteristics for all six major hallmarks. All cells develop random mutations which are normally repaired by specific DNA repair programs. Nevertheless, if genes which are involved in sensing or repairing DNA-damage are affected this may result in an increased mutational load and carcinogenesis. Defects in the DNA-maintenance-machinery can involve the detection of DNA-damage and the activation of the repair machine, as well as the repair of damaged DNA itself.[Negrini, 2010;

Jackson, 2009; Kastan, 2008; Harper, 2007; Friedberg, 2006] In many cancer types p53 is mutated because it plays a central role for the genomic integrity.[Hanahan, 2000; Hanahan, 2011]

- Tumor-promoting inflammation

Tumor cells show the capability to involve other cells and turn them into tumor-associated ones. This includes cells of the immune system, which play an essential role in late-state tumors and micrometastases.[Hanahan, 2011]

In 2011 Weinberg and coworkers focused on two emerging hallmarks:[Hanahan, 2011]

- Deprogramming cellular energy metabolism

Normal cells produce carbon dioxide out of pyruvate and glucose under aerobic, and other way round for anaerobic conditions. The anomalous characteristic of cancer cell energy metabolism has been first described by O. Warburg.[Warburg, 1956a; Warburg 1956b] He recognized, that even in the presence of oxygen cancer cells can reprogram their glucose metabolism to 'aerobic glycolysis' and create more energy.[Hanahan, 2011]

- Avoiding immune destruction

Fully established cancer cells are able to escape the recognition by immune cells and therefore inhibit their own destruction and the possibility to be attacked by immune cells.[Hanahan, 2011]

Despite these hallmarks represent basic properties of tumor cells in general, the specific aberrations that lead to malignant cells are variable: both temporal and spatial order of occurring mutations and the specifically affected genes depend on the tumor.[Hanahan, 2000; Hanahan, 2011]

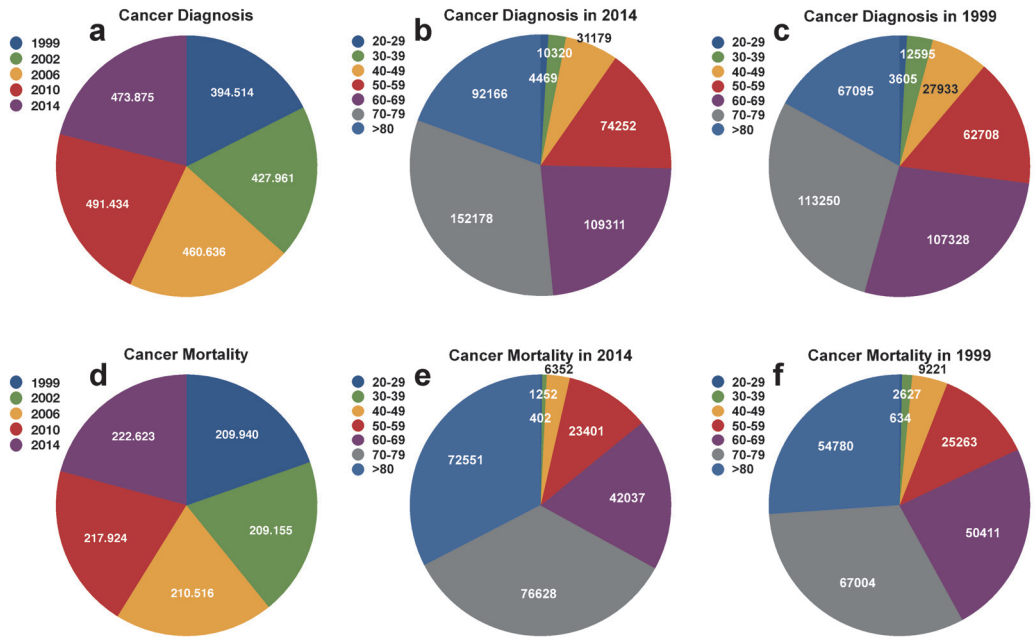

Fig. 3.1-2: Cancer statistics for Germany[1]. **a**: Cancer diagnoses in the years 1999, 2002, 2006, 2010 and 2014, number of patients. **b** and **c**: Total number of cancer diagnoses in the years 2014/ 1999, classified by the age of the patients. **d**: Cancer mortality in the years 1999, 2002, 2006, 2010 and 2014, total number of patients. **e** and **f**: Total number of cancer mortality in the year 2014/ 1999, classified by the age of the patients.

Every year approximately 450.000 people get cancer in Germany (Figure 3.1-2, **a**). The number of new cancer diagnoses is almost stable in the time frame of 16 years (1999-2014) (**b**-**c**). Considering the different ages of patients, most people get cancer in the ages of 70-79. In general, it can be concluded from the Figure 3.1-2 that cancer is an age-depending disease, as the absolute numbers of patients increase with the ages. The same fact can be concluded from the cancer mortality statistics (**d**-**f**). Overall approximately 210.000 patients die because of cancer every year.[1]

The treatment of cancer depends from the tumor entity and different factors of the specific tumor and patient. Very often a drug-based medicinal treatment is chosen, called chemotherapy. In the year 2018 more than 200 anticancer drugs are listed for anti-cancer application in Germany.[Honecker, 2018]

[1] All data are taken from „Zentrum für Krebsregisterdaten“, Robert Koch Institut, www.krebsdaten.de.

3.2 Metal-based anticancer compounds

Metal-based drugs have been discussed for medicinal treatment and analyzed for different pharmacological properties in history. For their anticancer use the development of Cisplatin (discussed in Chapter 3.2.1) enhanced the research intrest.[Frezza, 2010] Using metals for treating diseases must be carefully defined to achive the optimal therapeutic responses, otherwise it results in undesirable toxicity.[Holm, 1996; Mertz, 1993] Nevertheless, there are some essential advantages of metal-based compounds compared to organic carbon-based structures:[Frezza, 2010]

- The ability to coordinate (organic-) ligands: Metal compounds have a wide spectrum of coordination numbers, geometries and kinetic properties which cannot be realized in carbon-based molecules. Usually more than one ligand is coordinated to the central metal ion and these groups can be functionalized making use of their biological functions.[Fricker, 2007; Meggers, 2009; Cohen, 2007; Ott, 2007]
- *d*-orbitals in transition metals: Electronic properties which can be useful for target-structure design.[Hambley, 2007]
- Ligand exchange kinetics: Metal compounds can be activated inside the human body by release of their ligands and binding to their biological targets.
- The charge of the complexes: Metals can form positively charged ions which can bind to negatively charged biomolecules. Moreover, by choosing the ligand the complexes can be neutral, anionic or cationic and therefore interact with different biological targets.[Orvig, 1999]
- The oxidation state of the metal: The exact type and structure of a coordinated ligand can strongly influence the redox chemistry of the metal complex and consequently the biological properties, the optimal doses and the bioavailability.[Orvig, 1999; Thompson, 2003]

The best investigated metal complexes for anticancer treatment are platinum(II)/(IV) and ruthenium(II)/(III), which will be discussed next to osmium and palladium compounds, in Chapters 3.2.1, 3.2.2 and 3.2.3. Furthermore, research focuses on: titanium, copper, gallium, zinc and gold complexes.[Frezza, 2010; Muhammad, 2014]

Titanocene dichloride has been the first molecule after platinum based complexes in clinical trials.[Buettner, 2012; Muhammad, 2014] Current studies focuses on titanium(IV) anticancer compounds which are stable and water-soluble.[Muhammad, 2014; Tshuva, 2009]

Zinc is a key structural component in many proteins and enzymes in the human body. This includes transcription factors, cellular signaling proteins and DNA-repair enzymes.[Frezza, 2010; Prasad, 1995; Prasad, 2002] It is reported, that zinc anticancer compounds can induce apoptosis.[Franklin, 2009]

Next to zinc also copper is an essential trace metal and a driving force in many biochemical reactions, especially because of its redox properties. Inside the human body, copper can be found in oxidation states +I and +II, therefore it is a co-factor in many redox reactions.[Frezza, 2010; Chen, 2009; Tapiero, 2003] High levels of copper have been found in many and various kinds of tumors.[Frezza, 2010]

Increased research is done for gold compounds in oxidation states +I and +III. It was shown, that gold complexes are able to inhibit the thioredoxin reductase (TrxR), they can bind to DNA and proteins, as well as induction of apoptotic events.[Muhammad, 2014; Bindoli, 2009]

3.2.1 Cisplatin and analogues

In 1845 M. Peyrone first synthesized the molecule *cis*-$[Pt(NH_3)_2Cl_2]$, today known as Cisplatin, and called it 'Peyrone's Chlorid'.[Alderden, 2006; Muggia, 2015] Its structure was determined almost 50 years after the synthesis by A. Werner, how got the noble prize as the first inorganic chemist in 1913.[Alderden, 2006; Muggia, 2015] The identification of its antitumor properties have been discovered accidently by B. Rosenberg and coworkers at Michigan State University and first published in 1965.[Rosenberg, 1965] The development of Cisplatin took place during five years in Rosenberg's laboratory and included three steps:[Muggia, 2015]

1. Recognition that *Eschericha coli* (*E.Coli*) cell division was inhibited when the bacteria were exposed to an electric field generated by platinum electrodes.

Long, filamentous strands were formed, up to 300-fold of their normal shape and length.

2. The search for the agent of this bacterial phenomena
3. The discovery of two molecules, Cisplatin and its platinum(IV) analogue *cis*-[$Pt(NH_3)_2Cl_4$], whereas Cisplatin turned out to be the active molecule.[Muggia, 2015]

In 1968 Cisplatin was tested *in vivo* in mice and three years later the first patient was treated with that drug, getting clinical approval by the FDA (Food and Drug Administration) in 1978.[Kelland, 2007; Rosenberg, 1969]

- Mechanisms of action – Interactions with DNA and proteins

Cisplatin is a square-planar platinum(II) compound which can be administered intravenously to the patients.[Jungwirth, 2011] Important for its antitumor activity are the weak platinum-chlorido bonds (less than 100 kJ/mol), compared to other bonds, *e.g.* C-C, C-N or C-O (250-500 kJ/mol).[Frezza, 2010; Kostova, 2006; Reedijk, 2003] Cisplatin is quite polar and enters the cell slowly compared to other small-molecule cancer drugs.[Kelland, 2007] Cellular uptake is concentration-dependent and it is believed to enter mainly *via* passive diffusion, but also active transport-systems are discussed to enhance significantly the uptake, Figure 3.2.1-1.[Dilruba, 2016; Kelland, 2007] It is accepted that the copper transporter CTR1 plays an important role in Cisplatins cellular uptake. This *trans*-membrane protein is involved in copper homeostasis and down-regulation of this transporter is observed in Cisplatin resistant cells as well as in tumors from patients with poor therapeutic responses.[Dilruba, 2016; Kalayda, 2012; Safaei, 2006; Zisowsky, 2007; Yang, 2015] Also involved in Cisplatin-transport are copper-extruding P-type ATPases, ATP7A and ATP7B, whereas ATP7B is also responsible for its efflux, (ATP= Adenosinetriphosphate).[Dilruba, 2016; Safaei, 2006; Kalayda, 2008] The up-regulation of these transporters has been observed in resistant cells.[Samimi, 2004; Dilruba, 2016] The uptake of Cisplatin is influenced by its concentration as well as concentrations of potassium- and sodium-ions, the pH value and the presence of reducing agents.[Kelland, 2007] Ad-

ditionally, inhibition of Na^+/K^+-ATPase leads to a reduction of Cisplatin accumulation and this transporter is also down-regulated in resistant cells. Furthermore, the loss of the LRRC8A- and LRRC8D-subunits of the heteromeric volume-regulated anion channels (VRACs) can lead to resistance.[Dilruba, 2016; Schneider, 2013; Planells-Cases, 2015]

Inside the cell, a rapid hydrolysis takes place ($T_{1/2}$= 2h), resulting in monoaqua $[Pt(NH_3)_2(H_2O)Cl]^+$ and diaqua $[Pt(NH_3)_2(H_2O)_2]^{2+}$ species and loss of its chlorido-ligands.[Brabec, 2017; Dilruba, 2016; Frezza, 2010] The reason for the ligand exchange is a lower intracellular chlorid concentration (4-20 mM) than in the bloodstream (100 mM).[Dilruba, 2016; Wheate, 2010] The aqua complexes of Cisplatin are accepted as the 'active species' responsible for the cytotoxic activity. Early studies identified the nuclear DNA as a target of platinum drugs, and it is still recognized as the primary target of Cisplatin and the main reason for its anticancer activity.[Messori, 2016; Brabec, 2017; Dilruba, 2016] Cisplatin favorable binding site on the DNA is N7 of guanine bases, resulting in cross-links within or between DNA strands (intra- and interstrand adducts).[Dilruba, 2016] It is reported, that 60-65% of the drug bind two guanine bases forming 1,2-d(GpG) intrastrand cross links, 20% bind to guanine and the second purine-base adenine and the 1,3-intrastrand product is formed by approximately 2%.[Brabec, 2017; Lemaire, 1991; Brabec, 2000; Takahara, 1995] Nuclear DNA in eukaryotic cells is wound around histone proteins, which are positively charged building nucleosoms which are compacted to chromatin. Changes of these structure by Cisplatin binding to the DNA leads to distortion of the helical-DNA-structure resulting in effects on DNA associated processes, such as inhibition of replication and transcription.[Jungwirth, 2011; Jung, 2007] Next to that, various signal transduction pathways are activated as DNA-damage recognition and repair, cell cycle arrest and programmed cell death/ apoptosis.[Kelland, 2007] The major pathways which result in apoptosis involves the sequential activation of the ataxia telangiectasia mutated (ATM)- and RAD3-related protein (ATR= sensor of DNA-damage). The substrate CHEK1 (checkpoint kinase 1) phosphorylates p53 (tumor suppressor 53) and allows its stabilization.[Galuzzi, 2012] Activation of p53 leads to

cell death, next to that CHEK1 also activates the mitogen-activated protein kinase system (MAPK), including stress-activated protein kinases.[Galuzzi, 2012; Kroemer, 2007; Galuzzi, 2011; Persons, 2000; Wang, 2000; Dent, 2001; Yeh, 2002] Platinum-DNA-adducts are recognized by several proteins, *e.g.* non-chromosomal high-mobility group protein 1 and 2 (HMG1/ HMG2), nucleotide excision repair proteins (NER) and mismatch repair proteins (MMR).[Dilruba, 2016] Gene-expression regulation and chromatin-structure changes are mediated by HMG-proteins, therefore they contribute to apoptosis induction after Cisplatin binding to DNA and also shield adducts from repair.[Dilruba, 2016; Brown, 1993; Huang, 1994] NER-, MMR- and PAR-proteins (= poly(ADP-ribosyl)ated) are responsible for repair mechanism, and aberrations can result in resistance to Cisplatin.[Dilruba, 2016] NER-proteins remove Cisplatin-adducts from DNA and PARP (= PAR protein) tries to repair these base excisions.[Dilruba, 2016; Michels, 2013] MMR tries to repair adducts but realize also its failing and induces apoptosis of the cell, its mutation leads to resistance in cancer cells.[Vaisman, 1998; Dilruba, 2016]

Although, proteins are not only involved in recognition of DNA-damages and inducing signal pathways, it is also well-known, that only 1% of injected Cisplatin is able to reach and bind the DNA, several other targets are suggested, including different proteins, to which 65-98% of Cisplatin is bound.[Jungwirth, 2011; Messori, 2016; Gullo, 1980] Platinum(II) likely reacts with different donor-atoms, favorable sulfur- and seleno-containing molecules, like the amino acids methionine, cysteine and selenocysteine, but also to N-donor atoms like the amino acid histidine.[Jungwirth, 2011; Dilruba, 2016; Appleton, 1997; Messori, 2016] Therefore it reacts after administration with *e.g.* hemoglobin, serum albumin, transferrin and cysteine-rich proteins.[Messori, 2016; DeConti, 1973; Barnes, 2004a; Kratz, 1993; Khalaila, 2005; Zhao, 2005] Binding to proteins can occur extra- and intracellular and results in different processes*, e.g.* binding to extracellular proteins can result in increased cellular uptake, but also in inactivation.[Messori, 2016] Inside the cell, Cisplatin-aqua-species can bind to cytoplasmic nucleophiles, *e.g.* gluthathione (GSH), methionine, metallothioneins and others. Binding to GSH is discussed as one major cause for the inactivation of this drug, but

GSH is also involved in the oxidative stress response in cells, potentially leading to apoptotic effects.[Dilruba, 2016] Nevertheless, the enzyme glutathione-S-transferase is responsible for binding of Cisplatin to GSH and high levels are observed in Cisplatin resistant cells.[Dilruba, 2016; Galuzzi, 2012] After binding to GSH, the multi-drug-resistant protein (MRP2) is responsible for the efflux of this adduct, therefore overexpression of this transporter correlates with poor therapeutic responses.[Dilruba, 2016; Borst, 2000; Yamasaki, 2011] Different techniques are involved to understand the binding-behavior of Cisplatin to proteins*, e.g.* nuclear magnetic resonance spectroscopy (NMR), which located Cisplatin to HSA (= human serum albumin), CytC (= Cytochrome C), transferrin, CTR1, ATOX-1, ATPase, ATP7A and ATP7B, mass spectrometry/ electrospray ionization mass spectrometry (MS/ESI-MS) and crystal structure analysis.[Messori, 2016; Ivanov, 1998; Jiang, 1997; Beatty, 1996; Calandrini, 2014a; Arnesano, 2011; Pielak, 2009; Ohno, 2011; Ito, 2010; Calandrini, 2014b; Dolgova, 2013]

Nevertheless, by studying interactions with different cellular targets, DNA-interactions and DNA-platination remain as an essential step for the cytotoxic activity of Cisplatin.[Dilruba, 2016; Brabec, 2017] Recently Brabec and coworkers point out five experimental criteria which confirm that:[Brabec, 2017]

1. A drug must bind to its target at pharmacological doses and it was shown, that only DNA contained enough platinum after *in vitro* incubation of cultured cells with Cisplatin.[Pascoe, 1974]
2. Treatment with Cisplatin causes selective and irreversible inhibition of DNA synthesis in the cells.[Howle, 1970; Harder, 1970]
3. Cells which are deficient in DNA repair systems are more sensitive to Cisplatin, as well as enhanced repair-mechanism lead to resistance and poor responses.[Alazard, 1982; Arora, 2010]
4. DNA-adducts of Cisplatin inhibit DNA-synthesis and -transcription more efficient than the inactive analogue Transplatin.[Arora, 2010; Johnson, 1978; Ciccarelli, 1985; Mello, 1995]
5. Antagonists block the formation of cytotoxic platinum-DNA lesions.[Reedijk, 1999]

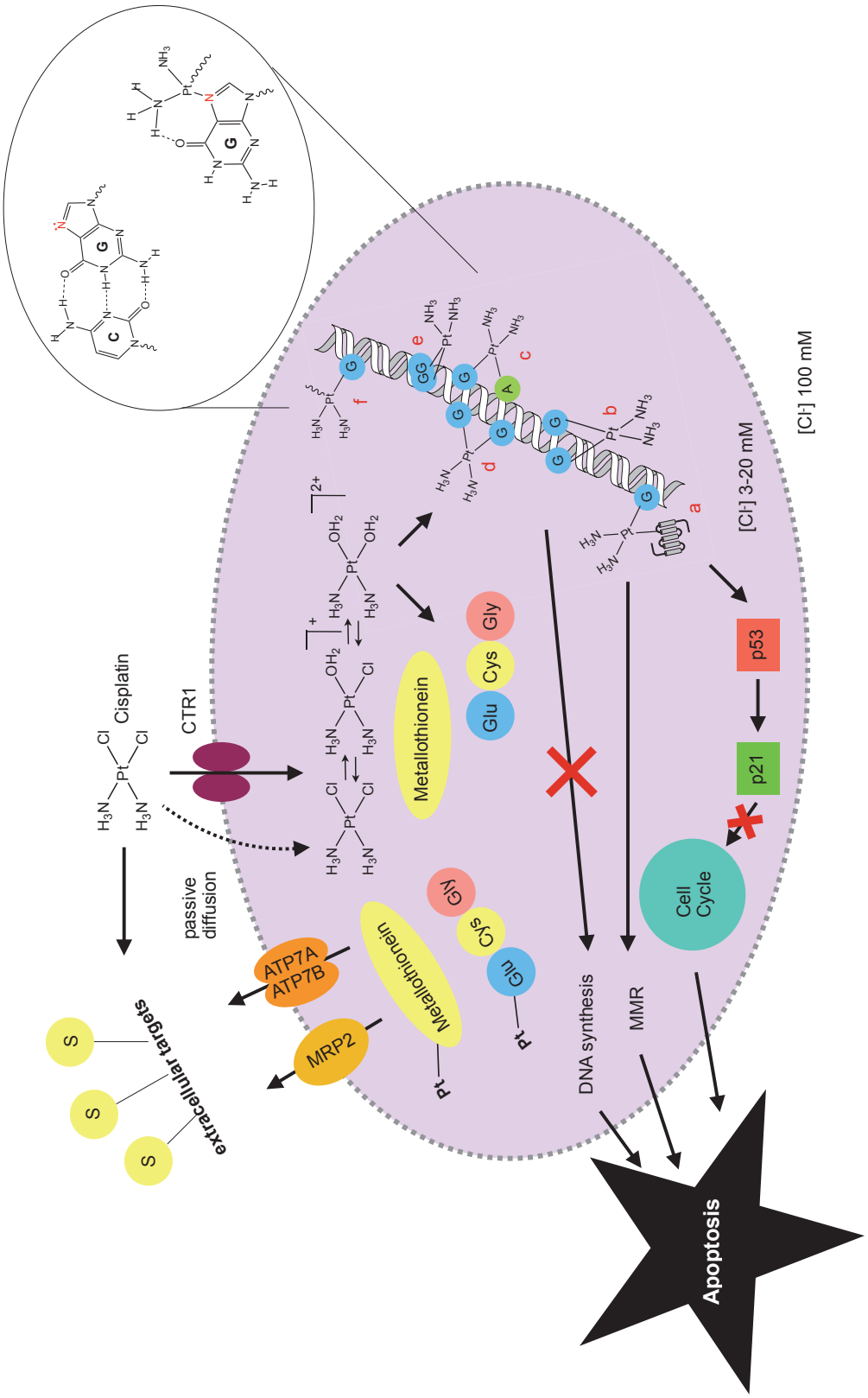

Fig. 3.2.1-1: Mechanism of action for Cisplatin. Cellular uptake by copper-transporter CTR1 or passive diffusion, intracellular hydrolysis to aqua-species, binding to proteins and DNA resulting in the activation of signaling pathways which lead to apoptosis. DNA-binding: **a**: guanine and protein; **b**: two guanines interstrand; **c**: guanine and adenine; **d**: two guanines, intrastrand; **e**: two adjacent guanines

intrastrand; **f**: monofuntional adduct.[Kelland, 2007; Brabec, 2017; Dilruba, 2016]

Additionally, recent studies by Merlino and coworkers focussing on protein-interactions confirm the DNA-binding as Cisplatin's main anticancer mechanism.[Messori, 2016] It was concluded, that the levels of platinum-atoms bound to proteins and RNA (= ribonucleic acid) are too low to exhibit significant inhibitory effects on the targets.[Jung, 2007] Nevertheless, it is well accepted that not all mechanisms and interactions of this drug are understood right now, leading also to unknown resistance mechanisms and lack in therapeutic efficiency.[Dilruba, 2016]

- Side effects and resistance mechanisms

Cisplatin exerts anticancer effects *via* multiple mechanisms, *e.g.* apoptosis *via* DNA-damage and mitochondrial pathway.[Galuzzi, 2012] The clinical success of this drug is limited by several drawbacks and side effects, as well as intrinsic and acquired resistance mechanisms.[Dilruba, 2016] In addition to many tumors being intrinsically resistant to platinum drugs, some sensitive tumors are able to develop resistance mechanisms after first treatment.[Dilruba, 2016; Galuzzi, 2012] As resistance mechanisms are multifarious, researchers try to classify them and distinguish four different kinds:[Galuzzi, 2012; Dilruba, 2016]

1. Pre-target resistance: Involves steps preceding the binding of Cisplatin to its target DNA, *e.g.* transport or inactivation by binding to proteins
2. On-target resistance: Mechanisms that directly relate to Cisplatin-DNA-adducts, *e.g.* repair mechanisms
3. Post-target resistance: Cellular events that take place after DNA-platination, *e.g.* lethal signaling pathways
4. Off-target resistance: Molecular circuits that are not linked with Cisplatin-induced signals, *e.g.* alterations and mutations in signaling pathways.

Two mechanisms of pre-target resistance are known, reduced intracellular accumulation of Cisplatin and inactivation by cytoplasmic 'scavengers' with nucleophilic properties.[Galuzzi, 2012] On-target resistance mechanisms are described above and involve different proteins like PARP and proteins of the NER.[Dilruba, 2016] Defects and mutations in signaling pathways result in post-target resistance, for example mutation and inactivation of p53. HMG1 and HMG2 bind to p53 to induce the activation of essential target genes involved in cell cycle arrest and apoptosis like p21 and Bax, mutations can lead to insufficient binding.[Dilruba, 2016; Kirsch, 1998] Overexpression of some proteins like HER-2, a proto-oncogene and member of epidermal growth factor receptor (EGFR) leads to Cisplatin resistance but is not necessary involved in Cisplatin-binding, therefore an example for off-target resistance.[Galuzzi, 2012] Mainly these mechanisms are known for causing treatment failure in cancer therapy in general, as described by Weinberg and coworkers some years ago.[Hanahan, 2000; Hanahan, 2011] Research attention shifted from determinations of tumor resistance to understand reasons of intrinsic resistance in some tumors.[Kelland, 2007] Overall, it should be mentioned that main knowledge about the numerous interactions, mechanisms of action and resistance mechanisms result from *in vitro* data and the translation and validation for most of these experimental data is still lacking.[Dilruba, 2016; Kelland, 2007]

Next to problems of resistance, dose-limitations are due to toxic side-effects, *e.g.* nephrotoxicity, neuropathy, ototoxicity, nausea and vomiting.[Dilruba, 2016] Therefore, next to understand molecular mechanisms, research is done in developing new platinum based anticancer drugs, started already soon after the improvement of Cisplatin.[Dilruba, 2016]

- Second- and third-generation drugs

Aims and challenges in the improvement of platinum drugs are to enhance therapy efficacy and safety, provide oral bioavailability, reduce toxicity and circumvent tumor resistance.[Kelland, 2007] The development of the second-genera-

tion drug Carboplatin was based on the hypothesis to put a more stable leaving-group to the platinum(II) center and therefore lower toxicity, while retain Cisplatins mechanism of action.[Kelland, 2007; Dilruba, 2016] Due to the bidendate cyclobutane carboxylate ligand the aquation rates of Carboplatin are lower than for Cisplatin.[Dilruba, 2016; Calvert, 1982] It shows less toxic side effects, especially no ototoxicity and neurotoxicity but is limited by its myelosuppression as well as the fact that a 20-40-fold higher concentrations of this drug are needed for forming DNA-adducts as efficient as Cisplatin.[Kelland, 2007; Dilruba, 2016] Carboplatin is therapeutically used worldwide since its first approval by the FDA in 1989 and it belongs to WHOs 'Model list of essential medicines'.[Johnstone, 2016; Muggia, 2015] It is mainly used in lung cancer and ovarian cancer.[Dilruba, 2016; Ozols, 2003] As it shows mainly the same mechanisms of action like Cisplatin, the resistance mechanisms, as known so far, are similar.[Dilruba, 2016; Stewart, 2007]

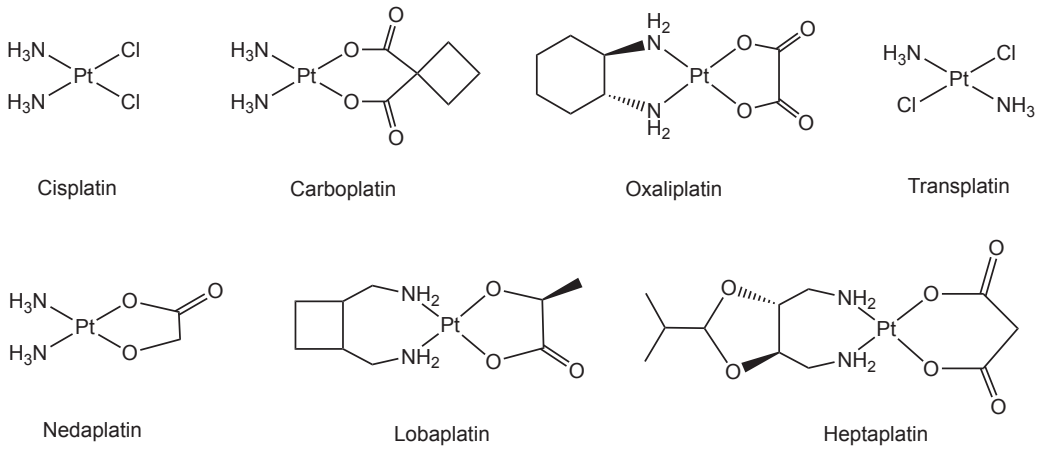

Fig. 3.2.1-2: Cisplatin, its inactive analogue Transplatin and FDA-approved-analogues: Carboplatin and Oxaliplatin, as well as regional-approved drugs: Nedaplatin, Lobaplatin and Heptaplatin.[Dilruba, 2016]

Nedaplatin, a second-generation platinum drug which is accepted in Japan for treatment of small cell lung cancer (SCLC), non-small cell lung cancer (NSCLC), head and neck and esophageal cancers.[Wheate, 2010] The toxicity profile and its pharmacokinetic properties are similar to Cisplatin.[Dilruba, 2016]

Most famous, third-generation drug is Oxaliplatin which is approved worldwide since 2002.[Wheata, 2010; Muggia, 2015] Oxaliplatin has a (1*R*, 2*R*)-1,2-diamino-cyclohexane- (DACH) ligand and oxalate as a leaving group.[Dilruba, 2016] The oxalate limits its reactivity and result in lower toxicity, the DACH-ligand is more lipophilic and increases therefore the passive diffusion. It is also known, that cat-ionic transporters OCT1 and OCT2 (= organic cationic transporter 1 and 2) are involved in cellular uptake of this drug and those receptors are overexpressed in colorectal cancers.[Dilruba, 2016; Zhang, 2006] Oxaliplatin is approved for colon cancer treatment in combination with 5-fluorouracil and folinic acid (FOL-FOX).[Wheate, 2010] Initially it was designed to overcome re-sistance-mechanisms limiting Cisplatin- and Carboplatin-treatment. The bulkier ligand results in enlarged DNA-adducts and inhibits DNA-synthesis more effi-ciently.[Dilruba, 2016]

The other third-generation drugs Lobaplatin and Heptaplatin have only limited and regional approval. Lobaplatin is used in China for treatment of metastatic breast cancer, chronic myelogenous leukemia and SCLC, whereas Heptaplatin is used in the Republic of Korea against gastric tumors and shows less side effects than Cisplatin.[Dilruba, 2016; Wheate, 2010]

3.2.2 Platinum and Palladium based compounds

- Platinum(II) compounds

All six approved platinum(II) drugs are based on the same structure-activity-relationships (SARs), described in 1973.[Cleare, 1973] These complexes exhibit two *cis*-oriented ammine or chelating diamine ligands, and two leaving groups which are two chlorides or a bidendate ligand, bound with two oxygen atoms to the square-planar platinum(II) center.[Gibson, 2016] Their cytotoxic activity is mainly based on the mechanism described for Cisplatin in Figure 3.2.1-1. Due to limitations and side effects of all these approved drugs, research for designing new platinum(II) molecules with anticancer activity increases. Several working groups focus on this, as well as several reviews are written to classify all these compounds.[Johnstone, 2016] Lippard and coworkers reported in 2016 on a classification of new platinum-based drug candidates with separation of three different subgroups for platinum(II) compounds: (1) Classical (which follow the original SARs), (2) Non-classical and (3) Nanodelivery platinum(II) complexes.[Johnstone, 2016] All together, the aim of drug design is to specifically fit them to their selected target, a principle which has been described over 100 years ago by Paul Ehrlich and is known as ‘Magische Kugeln’. Drugs as ‘magic bullets’ seeking out for their target.[Johnstone, 2016; Strebhart, 2008] With the help of the excellent review of Lippard and coworkers in 2016 some examples for this subgroups will be described.

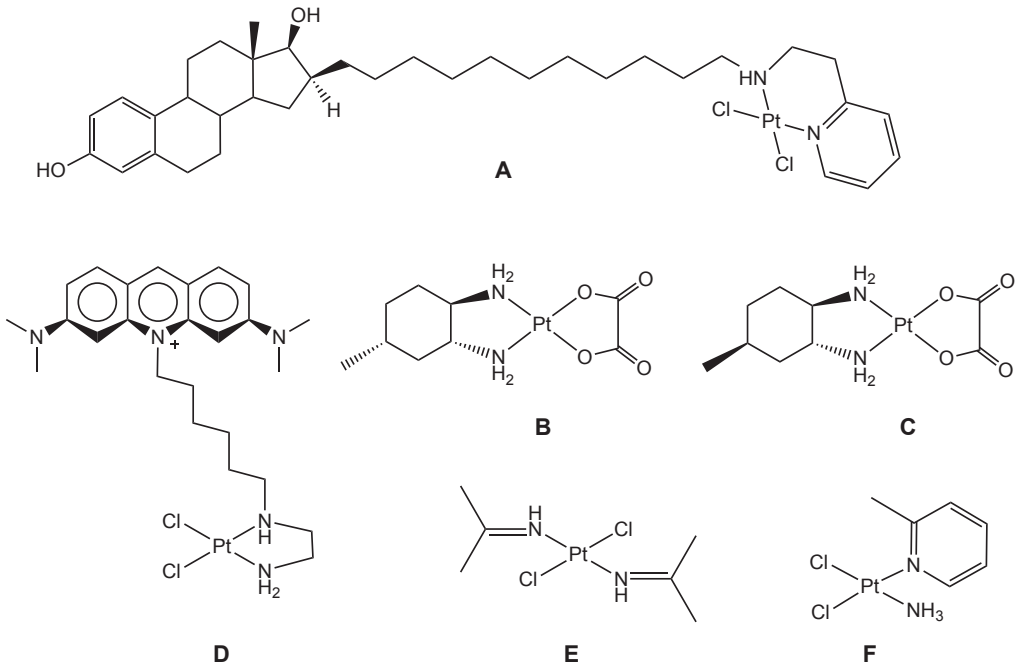

Fig. 3.2.2-1: Different platinum(II) compounds, developed to circumvent Cisplatins' drawbacks: **A**: VP-128, targeting the estrogen-receptor with an estradiol moiety [Dilruba, 2016; Saha, 2012], **B/C**: KP1537/ KP1691, Oxaliplatin-derivatives with promising *in vivo* results [Jungwirth, 2012], **D**: *cis*-$[Pt(AO(CH_2)_6en)Cl_2]^+$, a non-classical platinum(II) complex with intercalating properties [Bowler, 1986], **E**: A *trans*-compound with iminoether-functions as a promising-example for *trans*-platinum(II) compounds [Boccarreli, 2006], and **F**: Picoplatin, an early investigated platinum(II) complex with bulky ligand [Holford, 1998].

(1) Cisplatin- and analogues-like platinum(II) complexes

Recently developed platinum(II) complexes which follows the SARs of the six already approved compounds exhibit very often target molecules to enhance the cellular uptake of this drugs. One early approach is the combination with carbohydrates (sugars) to target for example glucose-transporters (GLUTs).[Johnstone, 2016; Dilruba, 2016] These transporters are overexpressed on many cancer cells due to their increased need for higher doses of glucose (Warburg effect).[Johnstone, 2016] Also it has been shown, that carbohydrates are able to engage extensive hydrogen-bonding interactions on the cell surfaces.[Johnstone, 2016] Sugars can be conjugated to platinum(II) for example by using substituted aminosugars (in case of substituating the ammine ligands).[Johnstone, 2016] Moreover, substituted carbohydrates might change biological and

physiochemical properties of these complexes and could enhance activity, solubility and cellular-uptake.[Ndagi, 2017; Ohi, 2012]

Next to carbohydrates also steroid-targeting is a well-known strategy. Therefore a steroid unit can be placed as a non-leaving group and deliver the platinum(II) directly to the steroid receptor.[Johnstone, 2016] Some tumors overexpress estrogen-receptors and it was shown that estrogen is able to enhance Cisplatin's cytotoxicity by increasing the HMGB1 protein and shielding platinated DNA from repair enzymes.[Dilruba, 2016; Barnes, 2004b] Compound VP-128, **A** Figure 3.2.2-1, which exhibits an estradiol-ligand shows good results like binding affinity to its targeted receptor.[Dilruba, 2016; Saha, 2012] Next to estrogen-, also testosterone-receptors can be used as a target.[Johnstone, 2016]

Malignant cells require high doses of folic acid for rapid cell growth, therefore folate receptors, a glycoprotein, which are overexpressed on many cancer cell surfaces can be targeted as well.[Johnstone, 2016; Weitman, 1992; Sudimack, 2000] Next to this approach also different targeting peptides can be conjugated to platinum(II) with diverese biological functions.[Johnstone, 2016]

The strategy to attach bulky carrier ligands to platinum(II) should reduce the affinity to extracellular molecules, like S-containing proteins, and consequently prevent inactivation of the drugs.[Dilruba, 2016] One early investigated example by Kelland and coworkers is *cis*-[$PtCl_2(NH_3)$(2-methylpyridine)], known as Picoplatin, **F** Figure 3.2.2-1. It was shown, that Picoplatin showed less interaction with thiols and therefore lower inactivation, compared to Cisplatin.[Holford, 1998] In clinical trials, Picoplatin was administered orally and showed synergistic acting with Paclitaxel but unfortunately no advantage in comparison to the control group.[Kelland, 2007; Dilruba, 2016] Some studies on alkyl-substituted Oxaliplatin-derivatives have been carried out by Keppler and coworkers, **B/C** Figure 3.2.2-1.[Buss, 2011; Abramkin, 2010; Jungwirth, 2012] Compounds KP1537, [(1*R*,2*R*,4*R*)-4-methyl-1,2-cyclohexanediamine]oxalatoplatinum(II) and KP1691, [(1*R*,2*R*,4*S*)-4-methyl-1,2-cyclohexanediamine]oxalatoplatinum(II) showed promising *in vivo* results and might be potential candidates for further clinical development.[Jungwirth, 2012]

(2) Non-classical platinum(II) complexes

Next to bulky chain ligands which follow the SARs of Cisplatin and its analogues, one well-established design is to place intercalators as ligands, next to the covalent bonding of the platinum(II), and this π-conjugated heterocyclic ligand can intercalate into the dsDNA. Those intercalators are known to utilize π - π -stacking and dipole-dipole interactions.[Dilruba, 2016; Johnstone, 2016; Jennette, 1974; Long, 1990; Wu, 2005] Metallointercalators are able to unwind, bend and distort the DNA topology and show antineoplastic properties.[Johnstone, 2016; Garbutcheon-Singh, 2013; Krause-Heuer, 2009; Kemp, 2007; Brodie, 2004] One of the first compounds from this subgroup has been described by Lippard and coworkers in 1986, *cis*-$[Pt(AO(CH_2)_6en)Cl_2]^+$, **D** Figure 3.2.2-1.[Bowler, 1986]

The change of the traditional SARs normally leads to a completely different mode of action and therefore a different chemotherapeutic activity overall.[Johnstone, 2016] So-called *trans*-compounds, inspired by Transplatin, Figure 3.2.1-2, cannot form the 1,2-intrastrand cross-links between two adjacent purine bases, the main adduct of Cisplatin. Therefore it is well-accepted that Transplatin shows less anticancer activity than its *cis*-isomer Cisplatin, and therefore for a long time period the *cis*-geometry was thought to be necessary for platinum(II) anticancer drug design.[Johnstone, 2016; Dilruba, 2016] Cisplatin's drawback of repair mechanism after binding to the DNA led to a rethinking of *trans*-compounds.[Dilruba, 2016] Established *trans*-compounds are able to form 1,3-intrastrand cross-links, preferently between guanine and a complementary cytosine, as well as monofunctional adducts.[Johnstone, 2016; Brabec, 1993] Lippard and coworkers devided active *trans*-platinum complexes into three groups, *trans*-platinum(II) complexes with: (i) heteroaromatic ligands, (ii) iminoether ligands (**E**) and (iii) asymmetric aliphatic amine ligands.[Johnstone, 2016] All of these groups exhibit some promising candidates and even though, some investigated complexes are able to circumvent Cisplatin resistance.[Dilruba, 2016; Coluccia, 1995; Ma, 2005; Boccarreli, 2006] One example of promising *trans*-compounds with iminoether-groups compared to their *cis*-analogues have been investigated in 2006 by Natile and coworkers, **E** Figure 3.2.2-1. Whereas the *cis*-analogues have been nearly inactive, the *trans*-compounds show greater activity in

general compared with Cisplatin and circumvent the Cisplatin resistance mechanisms.[Boccarreli, 2006]

Despite *trans*-platinum(II) complexes which are able to form monofunctional DNA-adducts, some compounds are especially designed with just one labile group, so called monofunctional platinum(II) complexes, to create one covalent bond to a DNA-base.[Dilruba, 2016; Johnstone, 2016] Lippard and coworkers prepared some complexes with the general formula: *cis*-$[Pt(NH_3)AmCl]^+$, where Am is a planar aromatic base like pyridine, purine or pyrimidine or an intercalator.[Dilruba, 2016; Johnstone, 2013]

Polynuclear compounds are designed to form lesions that cannot be formed by traditional drugs due to distances. For some dinuclear- and trinuclear-platinum(II) compounds it was shown that their unconventional formed DNA-adducts are able to overcome drug resistance.[Johnstone, 2016; Farrell, 1990; Harris, 2005]

(3) Nanodelivery of platinum(II) complexes

Several publications and reviews recently focused on nanocarriers to deliver platinum(II) drugs.[Johnstone, 2016; Wang, 2013; Gabano, 2009; Haxton, 2009; Bryde, 2009; Liu, 2013; Oberoi, 2013; Zalba, 2013; Kieler-Ferguson, 2013] Most prominent examples are Lipoplatin, a liposomal form of Cisplatin, and ProLindac, an Oxaliplatin-derivative with a hydrophilic poly(*N*-(2-hydroxypropyl)methacrylamide)polymer carrier.[Ndagi, 2017; Johnstone, 2016] ProLindac was designed to target solid tumors with an enhanced retention within the tumor cells and is currently in phase III clinical trials.[Ndagi, 2017; Johnstohne, 2016; Liu, 2014] Lipoplatin was designed to mainly enhance the pharmacological safety profile of Cisplatin and is at the moment developed for different kind of cancers with promising results and might be the next platinum based anticancer drug. [Johnstone, 2016; Ndagi, 2017; Stathopoulos, 2012]

- Platinum(IV) compounds

The drawbacks of Cisplatin and other platinum(II) drugs led to the prodrug-strategy of designing platinum(IV) complexes, an approach which started in the

1990s.[Giandomenico, 1995; Hall, 2002] Compared to platinum(II), platinum(IV) complexes have some advantages:[Gibson, 2009; Gibson, 2016]

- Chemically inert low-spin d^6 octahedral structure which is more inert against substitution
- Due to their inertness they can be administered orally
- Two additional ligands in the axial positions
- Activation by reduction which takes place inside the cancer cell and releases the platinum(II) complex and the two axial ligands.

Preparation of these compounds is based on the square-planar platinum(II) complex and oxidative addition (usually with hydrogen peroxide) leads to a platinum(IV) compound with two hydroxides in the axial positions which can be further substituted to improve the pharmacological/ biological properties.[Gibson, 2016] The reduction by cellular reducing agents, for example ascorbic acid or glutathione in a two electron reductive elimination reaction leads to the intracellular activation.[Gibson, 2016] The axial ligands can be used to enhance the pharmacological properties, *e.g.* increased lipophilicity and cell uptake, selective targeting (passive or active), prodrug linkage to delivery vehicles (polymers, nanoparticles, etc.) and co-administration of bioactive moieties (inhibitors, drugs, p53 activators, etc.).[Hildebrandt, 2016; Gibson, 2016]

Most prominent example is Satraplatin, *ctc*-[Pt(NH_3)(c-hexylamine)(OAc_2)Cl_2] (Figure 3.2.2-2), which finished phase III clinical trials in combination with prednisone against hormone refractory prostate cancer (HRPC) by oral administration. However, Satraplatin was not approved by the FDA because it could not provide a significant enhancement in overall survival.[Gibson, 2016; Petrylak, 2007] Satraplatin is a compound where the axial ligands are simple acetato moieties without any specific biological activity. Consequently, as mentioned above, there are strategies which try to improved this situation:[Hildebrandt, 2016]

(1) Trying to enhance the drug-uptake/ targeting or use delivery agents
(2) Use bioactive ligands to overcome resistance by simultaneous treatment of different targets with different modes of action, which should result in improved anticancer efficacy.

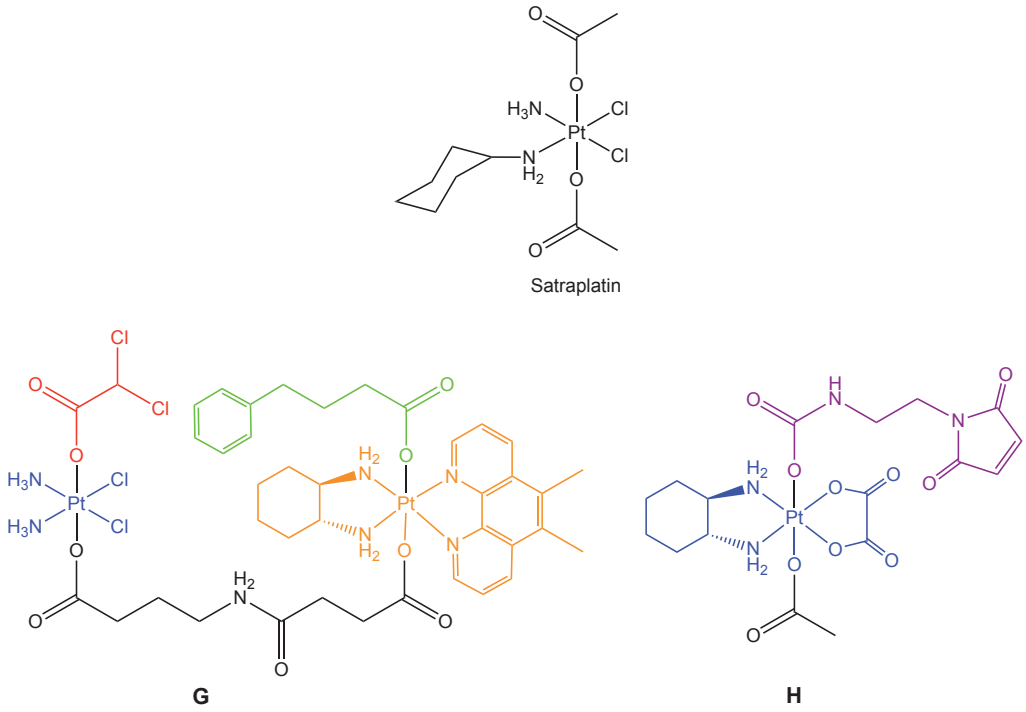

Fig. 3.2.2-2: Examples for platinum(IV) compounds: Satraplatin which finished phase III clinical trials[Gibson, 2016; Petrylak, 2007]; **G**: Quadruple action compound, investigated by Petruzzella and coworkers, and **H**: A promising-candidate for clinical trials, Maleimide-platinum(IV) complex of Mayr and coworkers, both published in 2017.[Petruzzella, 2017; Mayr, 2017] Blue/ Orange: platinum(II) drug(s). Red: DCA. Green: PhB. Purple: Maleimide.

The research approaches for bioactive ligands are based on the knowledge of placing estrogen moieties in the axial positions of a platinum(IV) compound, done by Lippard and coworkers in 2004.[Barnes, 2004b] This molecule targets the estrogen-receptor positive cells [ER(+)] and increases the levels of HMGB1, which are able to mask platinated DNA from repair enzymes, a strategy which is also known for platinum(II) compounds.[Dilruba, 2016] Nevertheless, it has only minor improvements in IC50 values (half maximal inhibitory concentration) in general, due to [ER(-)] cancer cell lines.[Barnes, 2004b]

Whereas the research field of platinum(IV) prodrugs gain high interest in the last years by several working groups, two outstanding results for the two approaches have been published in the last years by Keppler and coworkers, improving the

selectivity with a targeting-approach (1), and Gibson and coworkers, focusing on bioactive ligands (2).

The idea of placing bioactive ligands at axial positions started with so called 'dual-action' compounds, which are molecules based on Cisplatin/ Carboplatin or Oxaliplatin with ligands showing antiproliferative activity itself, potentially enhancing the activity of the platinum(II) drugs or help them to circumvent resistance mechanisms.[Gibson, 2016] Those complexes showed good results in the last years. Examples for bioactive ligands are *e.g.* inhibitors of: Glutathione S-transferase GST (ethacrynic acid), pyruvate dehydrogenase kinase PDK {dichloroacetate (DCA)}, cyclooxigenases COXs {aspirin (Asp), ibuprofen (Ibu), indomethacine} and histone deacetylases HDACs {valoproate (Val), phenylbutyrate (PhB)}; activators of the tumor suppressor p53 (chalcone).[Gibson, 2016; Ang, 2005a; Ang, 2005b; Dhar, 2009; Neumann, 2015; Raveendran, 2016; Ma, 2015; Pathak, 2014; Cheng, 2014]

COX is associated with resistance mechanisms and is involved in tumorigenesis and COXi are used to modulate the cellular response and inducing apoptosis.[Gibson, 2016; Pathak, 2014; Cheng, 2014; Neumann, 2015] It was shown by Hey-Hawkins and coworkers that platinum(IV) complexes with COXi result in IC50 values in nm-range.[Neumann, 2015] HDACis, causing hyperacetylated histones and leading to the growth arrest of cancer cells, are used to loosen the chromatin and enabling an open DNA structure for platination.[Gibson, 2016] It was shown, that platinum(IV) complexes with HDACis result in compounds which are up to 100-fold more potent than Cisplatin itself.[Ravendraan, 2016; Alessio, 2013; Yang, 2012] Mitaplatin, a platinum(IV) compound with two DCA-moieties showed good anticancer results, therefore PDKis are used as ligands which are able to shift the metabolism of the cancer cell towards glycolysis by phosphorylation of the pyruvate dehydrogenase complex (PDHC).[Petruzzella, 2017; Dhar, 2009; Vander Heiden, 2009]

Recently, Gibson and coworkers reported on a series of so called 'triple-action' platinum(IV) molecules with two different bioactive ligands in the axial positions.[Petruzzella, 2017; Petruzzella, 2018] All compounds were more cytotoxic than Cisplatin itself and show good results on KRAS-mutated cells, as well as a

production of reactive oxygen species (ROS).[Petruzzella, 2017; Petruzzella, 2018] However, most promising results were observed for a compound based on Cisplatin and another platinum(II) complex, **G**, [Pt(1*S*,2*S*,diaminocyclohexande)(5,6-dimethyl-1,10-phenanthroline)]$^{2+}$, (Pt56MeSS) with DCA and PhB as ligands in axial positions, Figure 3.2.2-2.[Petruzzella, 2018] This creation of a 'quadruple action' molecule with Pt56MeSS, a potent cytotoxic agent itself, resulted in a more potent compound than the triple action and dual action complexes.[Fisher, 2007; Petruzzella, 2018] Overall, this complexes are designed to inhibit specific enzymes inside the cancer cell upon reduction and to release the platinum(II) moiety. Once inside the cancer cell the bioactive ligands can trigger many different cellular responses.[Gibson, 2016]

Nevertheless, those complexes are based on the hypothesis that the molecules are just activated inside the cancer cell, but it was shown that this activation is not specifically in the tumor tissue, especially in the presence of hemeproteins platinum(IV) molecules can be reduced before they reach their target.[Pichler, 2013; Jungwirth, 2012; Carr, 2002; Carr, 2006]

To enhance the tumor-targeting one approach is to use molecules like vitamins or peptides which target overexpressed receptors on tumor cells (active targeting) or molecules which enhance the permeability and retention (EPR)-effect like nanoparticles and large proteins which are able to accumulate in the tumor tissue (passive targeting).[Mayr, 2017] For that reason Keppler and coworkers prepared some platinum(IV) molecules with maleimide function(s) to bind selectively to HSA as a carrier ligand in the bloodstream.[Pichler, 2013; Mayr, 2017; Legin, 2016] This approach should lead to an increased accumulation of the compound in the tumor tissue and less renal clearance, due to the well-accepted strategy to use albumin, the most abundant protein in HSA, as a carrier.[Pichler, 2013] Because of the EPR, albumin accumulates mainly in malignant and inflammatory tissues and can be also enter cancer cells by endocytosis.[Pichler, 2013; Baban, 1998; Kratz, 2008; Frei, 2011] The properties of the HSA-coupled anticancer-drugs have been already investigated with doxorubicin and paclitaxel.[Pichler, 2013; Mayr, 2017] It was shown by them, that maleimide is a

useful coupling-agent to HSA due a single free thiol-group (cyteine-34) which enables selective and defined binding.[Pichler, 2013] Their *in vitro* results show that the platinum(IV) compounds with maleimides function(s) are stable and bind to albumin in the serum. *In vivo* experiments resulted in better activity than the free drug (oxaliplatin-based molecule; CT-26-bearing mice), as well as the proposed accumulation in the tumor-tissue.[Mayr, 2017] Outstanding results have been reported in 2017 by identifying an oxaliplatin-based platinum(IV) complex with one maleimide-function, **H**, which shows a long-lasting and complete response for more than 70% of female animals, still tumor-free after one year of treatment pointing to a promising candidate for clinical trials, Figure 3.2.2-2.[Mayr, 2017]

- Palladium(II) compounds

Soon after the success of Cisplatin and analogues palladium(II) complexes were investigated due to the similiarities in coordination chemistry between d^8-systems platinum(II) and palladium(II).[Alam, 2016] First researchers focused on the classical SARs of Cisplatin and realized, that the corresponding Pd(II) complexes did not show promising results at all, due to lability of the complexes.[Alam, 2016; Abu-Surrah, 2008; Livingstone, 1970; Cleare, 1974; Durig, 1976; Das, 1978] The palladium analogues of Cisplatin and Carboplatin show no antitumor activity and it was shown, that both compounds hydrolyze very fast *in vivo* followed by various, unspecific interactions with other biomolecules leading to inactivation. Consequently, the palladium(II) complexes cannot reach their target(s).[Abu-Surrah, 2008; Butour, 1997; Wimmer, 1989; Zhao, 1999] The hydrolysis of palladium(II) complexes is known to be 10^5 times faster than for their platinum(II) counterparts. Therefore classical SARs of the compounds cannot be useful for the drug design of palladium complexes.[Abu-Surrah, 2008] The drawbacks in Cisplatin-based therapy and the increasing research activities for non-classical platinum(II) drugs led to a break for the classical, established SARs and new developed palladium(II) complexes.[Abu-Surrah, 2008; Alam, 2016] Next to platinum, copper, gold and ruthenium, palladium is the most widely discussed metal for the development of

metal anticancer drugs.[Alam, 2016] In the last years many palladium(II) complexes have been investigated with significant *in vitro* antitumor activity comparable to Cisplatin.[Alam, 2016] The design of palladium(II) requires more stable ligand systems than for platinum(II) compounds and suitable leaving groups. Many researches focused on bulky and chelating bidendate ligands to stabilize the complexes and avoid *cis-trans*-isomerism with some promising results.[Abu-Surrah, 2008; Churusova, 2017; Abu-Surrah, 2002; Carreira,2012a; Carreira, 2012b]

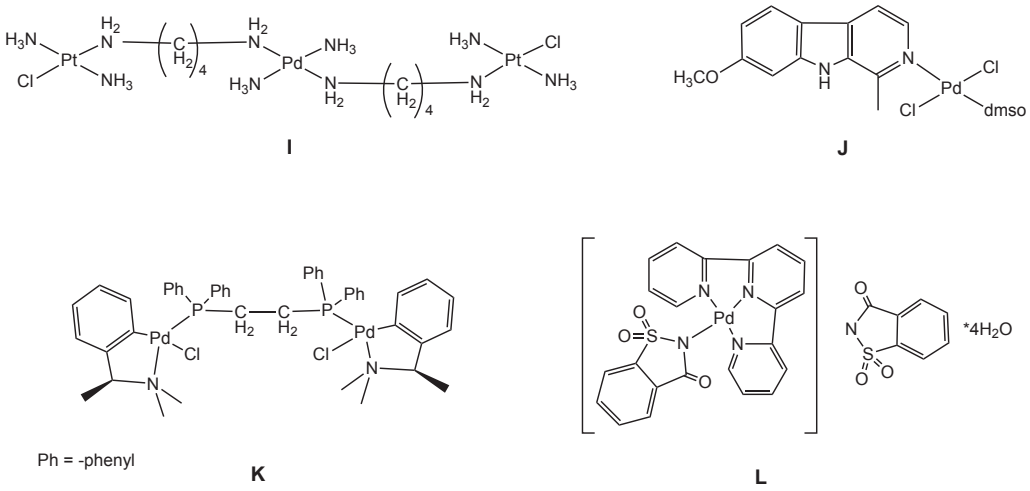

Fig. 3.2.2-3: Examples for palladium(II) complexes with promising cytotoxic results, **I**: Multinuclear compound by Huq and coworkers [Huq, 2004], **J**: *trans*-[Pd(harmine)(DMSO)Cl_2] by Rashan and coworkers [Al-Allaf, 1998], **K**: [Pd_2[$S_{(-)}C^2$,N-dmpa]$_2$(μ-dppe)Cl_2] by Caires and coworkers [Serrano, 2011] and **L**: [Pd(sac)(terpy)](sac)*4H_2O by Yilmaz and coworkers.[Ulukaya, 2011; Alam, 2016]

The first palladium(II) complex with a bulky ligand showing greater antitumor activity than the reference compound Cisplatin (against Sacroma180 cells) has been described in 1984 by Gill, [Pd(bpy)(ONO_2)$_2$], where bpy is 2,2'-bipyridine.[Alam, 2016; Gill, 1984] Most promising results have been reported on *trans*-compounds, normally with bulky, monodendate ligands showing, in general, a better *in vivo* activity than their *cis*-counterparts and the comparable platinum(II) complexes.[Abu-Surrah, 2008; Alam, 2016] In 1998 Rashan and coworkers published the first, active *trans*-palladium(II) complex,

trans-[Pd(harmine)(DMSO)Cl_2], **J**, where harmine is 7-methoxy-1-methyl-9H-pyrido[3,4-b]indole and DMSO is dimethylsulfoxide (Figure 3.2.2-3), with greater activity than Carboplatin and 5-Flourouracil against different cell lines (P_{388}, L_{1210}, K_{562}).[Abu-Surrah, 2008; Alam, 2016; Al-Allaf, 1998] Huq and coworkers reported in the last years on a series of multinuclear active *trans*-palladium(II) complexes against Cisplatin resistant cell lines, **I** Figure 3.2.2.-3.[Alam, 2016] Their compounds showed greater activity on resistant-cells than on their sensitive-counterparts and better results on ovarian-cancer cell line A2780 compared to Cisplatin.[Huq, 2004; Huq, 2007; Daghriri, 2004; Cheng, 2006; Mazumder, 2012]

Next to *trans*- and multinuclear palladium(II) complexes also phosphine ligands gain high interest for the design of palladium(II) drugs.[Abu-Surrah, 2008; Alam, 2016] It was shown by Caires and coworkers, that bisphosphine-based cyclopalladated complexes are more stable, less toxic and show tumor-selectivity, for example bearing 1,2-bis(diphenylphosphino)ethane-ligands (dppe).[Caires, 1999; Abu-Surrah, 2008] Later on, they reported on *in vitro* and *in vivo* results of $[Pd_2[S_{(-)}C^2,N\text{-dmpa}]_2(\mu\text{-dppe})Cl_2]$, where dmpa is *N,N*-dimethyl-1-phenethyl-amine, **K** Figure 3.2.2-3, showing lower IC50 values on a panel of cell lines compared to Cisplatin and good preclinical results against primary and metastatic melanoma tumors with less toxic side effects.[Alam, 2016; Serrano, 2011]

Palladium(II) complexes with bidendate ligands often bear N,N-chelates, but also N,C-, O,O-, N,S- and O,S-chelats have been reported.[Abu-Surrah, 2008; Alam, 2016; Maurya, 2015; Carreira, 2012a] They very often show remarkable *in vitro* results but lower DNA-interactions than platinum(II) complexes, therefore it is accepted that they target other biomolecules.[Abu-Surrah, 2008; Alam, 2016; Carreira, 2012a] Yilmaz and coworkers reported in 2011 on a palladium(II) complex containing terpyridine and saccharinate (sac) ligands, [Pd(sac)(terpy)](sac)*4H_2O where terpy is 2,2':6',2''-terpyridine, **L** Figure 3.2.2-3, with high *in vitro* and *in vivo* activity against breast cancer.[Ulukaya, 2011] Focusing on the mechanism of action for this compound they showed significant changes in protein expression after treatment, affecting a number of cellular pathways, including DNA repair, apoptosis and protein folding.[Adiguzel, 2014]

In 2016 Alam and coworkers summarized 264 research articles based on palladium(II) complexes for anticancer treatment and 847 palladium(II) compounds to establish some general SARs for these compounds, including:[Alam, 2016]

- SARs for platinum(II) complexes should not be used as a guide to design palladium(II) complexes as several investigations showed that the antitumor activity of Pd(II)/Pt(II) counterparts can be very different;
- Bulkly and bidendate ligands which possess cytotoxic activity itself may be a good choice to enhance the stability of the complexes and therefore the anticancer activity;
- Lipophilicity increase the antitumor activity in general;
- *Trans*-complexes are more active than their *cis*-counterparts and some show promising results compared to already clinically used drugs.

Until now some promising *in vitro* and *in vivo* results have been generated with palladium(II) complexes, nevertheless no compound reached clinical trials so far.[Alam, 2016]

As mentioned above often direct analogues of palladium(II) complexes are compared with their platinum(II) counterparts. In contrast, some publications focus on comparison of palladium based complexes with their copper and nickel counterparts. In general, the respective nickel(II) complexes, reveal moderate anticancer activity, whereas very often promising results could be observed for the copper complexes even compared to the palladium complexes.[Dobrova, 2016; Haribabu, 2015]

3.2.3 Ruthenium and Osmium based compounds

Due to resistance and side effect problems for Cisplatin-therapy the search for new metal based anticancer drugs increased. Especially ruthenium based drugs are supposed to be attractive candidates.[Leijen, 2015; Meier-Menches, 2018] More and more research focuses also on its neighbor metal osmium. Ruthenium and osmium have some biochemical properties which are useful for anticancer drug design.[Leijen, 2015]:

- Slow ligand exchange kinetics in general [Antonarakis, 2010; Bloemink, 1996; Reedijk, 2003]
- DNA- and protein-binding as possible mode of actions [Clarke, 2002; Messori, 2014; Merlino, 2016]
- Prodrug systems for metal(III) compounds and the 'activation-by-reduction' strategy, impact selective behavior [Frasca, 1996; Clarke, 2002; Clarke, 1999; Clarke, 1980a]
- Ruthenium can mimic iron and bind to transferrin and/ or albumin [Frasca, 1996; Clarke, 2002; Messori, 2000a; Messori, 2000b]

Possible oxidation states of ruthenium range from -2, 0, +2, +3, +4, +6 to +8, whereas ruthenium(II) and ruthenium(III) are most relevant. Ruthenium complexes can have different coordination environment: tetrahedral, square-planar, and, most prominent, octahedral.[Jungwirth, 2011]

- Ruthenium(III) compounds

Starting with the research for other metal based compounds, the structures of interest were similar to Cisplatin. Therefore first experiments have been carried out with $[Ru(NH_3)_4Cl(OH)]Cl$ by Rosenberg himself.[Meier-Menches, 2018; Rosenberg 1965; Rosenberg, 1969] Some years later, in 1976, first promising results on this kind of compounds show similar effects like Cisplatin for *fac*-$[RuCl_3(NH_3)_3]$ tested on *E.coli*.[Durig, 1976] In that study, Durig and coworkers compared ruthenium and palladium compounds with Cisplatin, concluded that the mechanism of action is similar for Cisplatin, the ruthenium compounds and the ineffi-

ciency of some palladium compounds. Interactions between the DNA and ruthenium(III) compounds have been also reported by Clarke and coworkers in the 1970s.[Clarke, 1974; Clarke 1978] Therefore further developments were carried out investigating metal-nucleic acid interactions and show, that the attack of the ruthenium(III) to different nucleic acids leads to a reduction of the metal.[Clarke, 1980a] They confirmed a binding of the ruthenium to exocyclic nitrogen atoms of DNA bases, *e.g.* binding to N7 of guanine.[Clarke, 1980a; Clarke, 1978] Some $[Ru(NH_3)_5(Pur)]Cl_3$ complexes whereas Pur is purine, have been synthesized and tested for biological activity, showing also interactions with proteins.[Kelman, 1977] For both DNA- and protein-synthesis inhibition it was shown, that ruthenium compounds are already active at very low concentrations.[Meier-Menches, 2018; Kelman, 1977] In 1977 data supporting the 'activation-by-reduction' hypothesis were reported first time, which means, that the ruthenium(III) compounds are widely inactive, but can be reduced to ruthenium(II), the active species.[Meier-Menches, 2018; Kelman, 1977; Clarke, 2003] An advantage of ruthenium(III) compounds, is that their reduction should be facilitated in the hypoxic tumor tissue and therefore result in higher selectivity, compared to Cisplatin.[Meier-Menches, 2018] However, it was also shown in 1980, that some cellular components, *e.g.* GSH are involved in the reduction mechanism.[Clarke, 1980b] Nevertheless Clarke pointed out the potency of ruthenium anticancer agents and this culminated in enhanced interest for those complexes.[Meier-Menches, 2018]

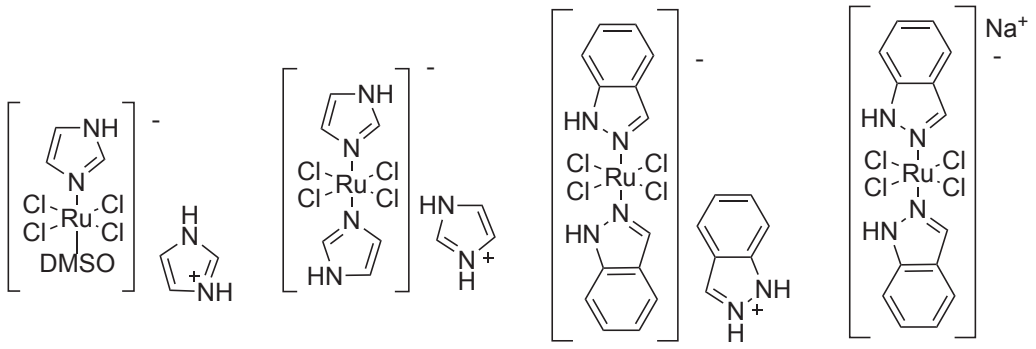

Fig. 3.2.3-1: NAMI-A: Designed for antimetastatic treatment of NSLCL patients by Mestrone/ Alessio and coworkers [*e.g.* Sava, 1994] KP418, KP1019, IT-139: Most promising anticancer drug candidates by Keppler and coworkers.[*e.g.* Meier-Menches, 2018]

Next to the work of Clarke and coworkers, first studies with S-donor ligands have been published in 1975 by Mestroni and coworkers. By testing Cisplatin and other different metal compounds on *E.Coli* they found only [$RuCl_2(DMSO)_4$] as a promising compound with *e.g.* selective toxicity and filamentous growth production similar to Cisplatin.[Monti-Bragadin, 1975] For this ruthenium(II) compound they also observed a reduction of lung metastases in 1989, but also for a ruthenium analogue: *trans*-[$RuCl_4(DMSO)_2$].[Sava, 1989; Alessio, 1991] Structural optimizations, necessary due to the instability of the first compounds, lead to a compound named NAMI (= Novel Anti-Tumor Metastasis Inhibitor), Figure 3.2.3-1.[Meier-Menches, 2018; Sava, 1992; Sava, 1994] Next to the S-donor ligand DMSO, NAMI-A consists of the N-donor ligand imidazole. NAMI-A was designed against metastases and reduced them significantly as well as inhibits the formation of new ones.[Sava, 1994] They observed a different behavior of NAMI-A compared to Cisplatin in mice experiments and proposed that molecule as an effective anticancer agent against lung metastasis in combination with surgery and therefore an advantage in postsurgical prognosis for the patients.[Sava, 1994] NAMI-A was the first ruthenium compound which entered clinical trials and finished phase I studies in 2004.[Meier-Menches, 2018; Rademaker-Lakhai, 2004] In 2015 they reported on phase I/II-studies of NAMI-A in NSCLC patients in combination with gemcitabine.[Leijen, 2015] Results show, that NAMI-A resulted in side effects *e.g.* renal toxicity, nausea, vomiting, neutropenia and anemia, as well as it was less active than gemcitabine alone.[Leijen, 2015] Therefore clinical trials with that compound were stopped.[Meier-Menches, 2018]

Starting in the late 1980s, Keppler reported on ruthenium(III) compounds with imidazole ligands (HIm), Figure 3.2.3-1.[Keppler, 1986; Keppler, 1987] Compound KP418, *trans*-[$RuCl_4(HIm)_2$] was first investigated in 1986, structure-activity-relationships were done with *in vivo* screening, and concluded N-heterocycle-systems as the most efficient one.[Keppler, 1989; Keppler, 1986; Keppler, 1987] KP418 was tested in autochronous colorectal carcinoma model in rats and shows significant tumor inhibition, whereas Cisplatin was inactive.[Berger, 1989] Further experiments showed toxic side effects of KP418 and therefore structure-optimizations led to indazole compounds (HInd), mainly KP1019,

trans-[$RuCl_4(HInd)_2$]. Following its mode of action, it is believed that the tumor-specifity results from interacting with serum proteins in the blood.[Berger, 1989; Chatlas, 1995; Smith, 1996; Trynda-Lemiesz, 1999; Bijelic, 2016; Depenbrock, 1997; Cetinbas, 2010] Binding studies with albumin and transferrin show, that the major amount of the ruthenium is bound to HSA. Binding leads to a structural change of the protein structures.[Trynda-Lemiesz, 1999; Smith, 1996] To understand the pathways and interactions of this ruthenium(III) drug the interactions with serum proteins have been studied, also with X-Ray structure analysis, and it is hypothesized that the transportation to and accumulation in the tumor tissues are associated with binding to these proteins, causing the tumor-specifity.[Bijelic, 2016] It is known, that ruthenium can interact with the iron-transporter transferrin by mimic the iron ion and therefore binding reversible to its transporter.[Bijelic, 2016] Transferrin(Tf)-receptors are overexpressed on cancer cells due to higher iron demand and the Tf-metal complex is delivered in the cell by endocytosis thus the ruthenium compound has a selective vehicle inside the tumor cells.[Bijelic, 2016; Spreckelmeyer, 2014; Kratz, 1994] The HSA-mediated pathway is based on the EPR-effect, in tumor tissues.[Bijelic, 2016] Due to insufficient solubility of KP1019 the counter ion has been changed to sodium, resulting in NKP-1339, also known as IT-139.[Meier-Menches, 2018; Trondl, 2014; Burris, 2016] It is known, that KP418, KP1019 and IT-139 induce apoptosis of the tumor cells *via* the intrinsic mitochondrial pathway and their cytotoxic activity is potentially related to the possibility of inducing oxidative stress rather than DNA damage.[Meier-Menches, 2018; Kapitza, 2005; Bijelic, 2016; Flocke, 2016; Bierle, 2015; Trondl, 2014] The cinical phase-I study for KP1019 was finished in 2006.[Hartinger, 2008; Lentz, 2009] Phase I/II-studies for KP1019 and IT-139 showed disease stabilization in patients with advanced solid tumors and activity against colorectal tumors.[Bijelic, 2016; Lentz, 2009] At the moment, IT-139 is the only ruthenium based anticancer compound in clinical trials.[Meier-Menches, 2018; Fuerder, 2017]

- Ruthenium(II) compounds

The ruthenium(III) compounds are 'activated-by-reduction' to ruthenium(II) species, therefore several compounds have been designed during the last years which do not need this activation step.[Meier-Menches, 2018] Nevertheless, one advantage of the ruthenium(III) compounds is the stability, and first studies of ruthenium(II) complexes have been compromised by their instability.[Meier-Menches, 2018; Monti-Bragadin, 1975; Alessio, 1988; Gopal, 1999] Ruthenium(II) complexes contain in general an η^6-arene ligand which can be substituted *e.g.* η^6-cymene. For that reason they are called 'half-sandwich-complexes' and show a typical 'piano-stool' geometry, Figure 3.2.3-2.[Bruijnincx, 2009] Next to the arene ligand three coordination sites are left X, Y, Z, whereas one is very often an halide and the other two are often occupied by different bidendate ligands.[Bruijnincx, 2009] The ligand exchange kinetics are comparable to platinum(II) complexes, the loss of the -Cl-ligand (Z) is possible in intracellular medium, as described for Cisplatin, therefore they gain high interest in drug research.[Süss-Fink, 2010]

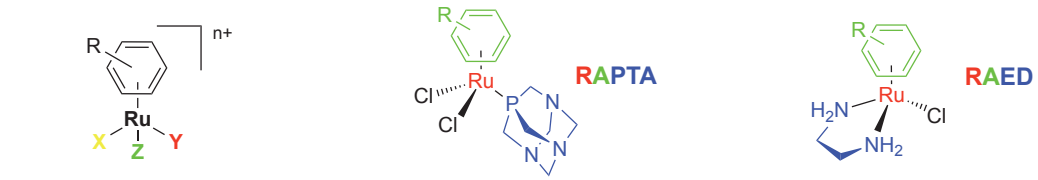

General ruthenium(II) structure | General structure of RAPTA-compounds | General structure of RAED-compounds

Fig. 3.2.3-2: General structure of ruthenium(II) complexes. A η^6-arene ligand which can be substituted (-R); **Z**: normally a halide (*e.g.* -Cl); **X/ Y**: monodendate- or bidendate-system. Some compounds can be charged (n+).[Bruijnincx, 2009] General structure of RAPTA compounds, introduced by Dyson and coworkers and general structure of RAED compounds, introduced by Sadler and coworkers.[Murray, 2016]

Organometallic compounds are often described as unstable (in water/ in air), a fact which is true for a broad range of such complexes, but not for many ruthenium(II) arene complexes. In general, ruthenium(II) complexes are accepted nowadays for showing low toxicity but being selective for cancer

cells.[Süss-Fink, 2010; Allardyce, 2001a; Kostova, 2006] The main reason for the design of ruthenium(II) complexes with substituted-arene ligands is the amphiphilic character of the compounds by placing a hydrophobic arene ligand on a hydrophilic metal center. Numerous substitutions at the arene but also at the bidendate-chelating ligands, proving the possibility for targeted-chemotherapy.[Süss-Fink, 2010; Dyson, 2007]

For ruthenium(II) drug candidates (as well as osmium(II) compounds) research is mainly based on structure-activity relationship determinations. Variations contain:

- Substitution of the η^6-arene ligand,
- Substitution of the leaving group,
- Substitution of the metal (Ru/ Os/ Rh/...),
- Substitution of the bidendate ligands.

Exemplary compounds are depicted in Table 3.2.3-1.[2] Ruthenium(II) compounds can be cationic charged or neutral, mononuclear compounds can be substituted by P- / N-donor ligands or by bidendate ligands, containing different combinations, *e.g.*: N,N; N,O; O,O; C,N; S,N; S,O.[Süss-Fink, 2010; Meier-Menches, 2018] Next to mononuclear compounds, dinuclear complexes with organic linkers, trinuclear clusters, tetranuclear complexes that can be photoactive, and also hexanuclear ruthenium(II) cages which are empty or filled with other molecules can be found in the literature.[Süss-Fink, 2010]

[2] The examples in the table are taken from [Meier-Menches, 2018].

Tab. 3.2.3-1: Some examples for (mainly bidendate) ligand systems of ruthenium(II) /osmium(II) complexes.[Meier-Menches, 2018]

Example No.	**Inert ligand system**	**Coordination mode**	**Metal**	**References**
1	Pta	P	Ru/Os	[Scolaro, 2005], [Dorcier, 2006]
2	Amino acids	N,O	Ru	[Habtemariam, 2006]
3	Picolinates	N,O	Os	[van Rijt, 2010], [Peacock, 2007c], [van Rijt, 2009]
4	N-Phenyl-picolinamides	N,O	Ru/Os	[van Rijt, 2009]
5	Ethylenediamines	N,N	Ru/Os	[Morris, 2001], [Peacock, 2007a]
6	Bipyridines	N,N	Ru	[Habtemariam, 2006]
7	Bipyrimidines	N,N	Ru	[Betanzos-Lara, 2012]
8	N-Phenyl-azopyridines	N,N	Ru/Os	[Dougan, 2006], [Fu, 2011], [Fu, 2012]
9	N-Phenyl-iminopyridines	N,N	Os	[Fu, 2012]
10	6-Paullones	N,N	Ru/Os	[Schmid, 2007a], [Schmid, 2007b]
11	9-Paullones	N,N	Ru/Os	[Schmid, 2007b]
12	2-Indolo-quinolines	N,N	Ru/Os	[Filak, 2013]
13	6-Indolo-quinolines	N,N	Ru/Os	[Filak, 2010]
14	Quinoxalinones	N,N	Ru/Os	[Ginzinger, 2012]
15	Acetylacetonates	O,O	Ru	[van Rijt, 2009]
16	Pyrones	O,O	Ru/Os	[Hanif, 2010], [Peacock, 2007b], [Kandioller, 2009a], [Kandioller, 2009b], [Kandioller, 2009c]
17	Pyridones	O,O	Ru/Os	[Hanif, 2010]
18	Flavonoids	O,O	Ru	[Kurzwernhart, 2012a], [Kurzwernhart, 2012b]
19	Phenyltriazoles	C,N	Ru/Os	[Riedl, 2017]
20	Carbothio-amides	S,N	Ru/Os	[Meier, 2013]
21	Thiopyrones	S,O	Ru/Os	[Hanif, 2010], [Kandioller, 2009a], [Kandioller, 2009c], [Schmidlehner, 2016], [Hackl, 2016]

The first active ruthenium(II) compound has been published in 2000 by Reedijk and coworkers, Figure 3.2.3-3.[Velders, 2000] They reported on three different

isomeric complexes with great changes in *in vitro* cytotoxicity. The most promising compound, α-[Ru(azpy)$_2$Cl$_2$] (azpy = 2-phenylazopyridine), **M**, showed activity against a panel of cancer cell lines.[Velders, 2000] Due to solubility problems, *in vivo* tests as well as binding studies to DNA-bases like guanine were done with α-[Ru(azpy)$_2$(NO$_3$)$_2$].[Hotze, 2000] Initiators of this class of compounds were Dyson and coworkers and Sadler and coworkers both starting in the year 2001.[Allardyce, 2001a; Allardyce, 2001b; Allardyce, 2001c; Morris, 2001] Figure 3.2.3-2 shows the general structure of RAPTA and RAED compounds which have been introduced in 2001.[Murray, 2016]

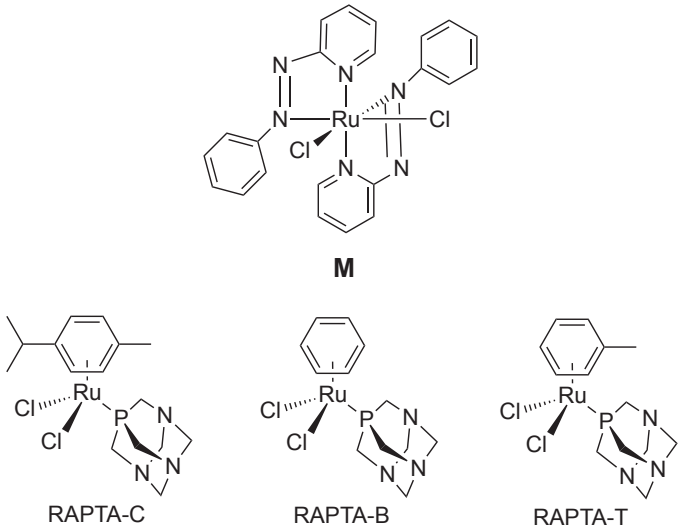

Fig. 3.2.3-3: **M**: Compound [Ru(azpy)$_2$Cl$_2$], introduced 2000 by Reedijk and coworkers and some examples of the RAPTA-family: RAPTA-C, RAPTA-B and RAPTA-T, introduced by Dyson and coworkers.[Allardyce, 2001a; Velder, 2000]

The first compound of the RAPTA-family was [Ru(η^6-*p*-cymene)(pta)Cl$_2$], (pta= 1,3,5-triaza-7-phosphatricyclo-[3.3.1.1]decane) which is called RAPTA-C, Figure 3.2.3-3.[Murray, 2016; Allardyce, 2001a] All RAPTA compounds are characterized by a monodentate 1,3,5-triaza-7-phosphatricyclo-[3.3.1.1]decane ligand (= pta).[Ang, 2011] It was shown by structure-activity-relationship studies, that the pta ligand is essential for the biological activity of this class and structural changes led to a loss of the promising activity.[Ang, 2011] The amphiphilic pta ligand has a positive aspect on water-solubility of the complexes and is steri-

cally less demanding compared to other phosphines.[Murray, 2016; Phillips, 2004] Lead structure, RAPTA-C, is water-soluble and might be applied oral.[Murray, 2016] In general, the RAPTA-structure is stable as the Ru-P and the Ru-arene bond are chemically inert.[Ang, 2011] Hydrolysis studies for RAPTA-C and RAPTA-B, [Ru(η^6-benzene)(pta)Cl_2] show that monoaqua-adducts of these complexes are formed at low [Cl^-]-concentrations (5 mM), comparable to Cisplatin.[Murray, 2016] Additionally the Ru-P- and Ru-arene-bonds can be cleaved by interaction with biomolecules.[Ang, 2011] To identify targets of RAPTA compounds, interactions with DNA and proteins were investigated. First reports show DNA-damages after treatment with RAPTA-C and formations of DNA-adducts, but in general only a low affinity for DNA-binding was observed.[Murray, 2016; Ang, 2011; Allardyce, 2001a] In contrast, a broad range of studies showed a high affinity of RAPTA complexes for specific proteins, which was determined *in vitro* in cell extract analysis after treatment, as well as in different MS studies.[Murray, 2016; Ang, 2011] It is accepted, that interactions with proteins is one of the major modes of action for this compound class.[Murray, 2016] For RAPTA-C one target is cathepsin B (catB), a cysteine protease which is relevant for cancer cells and therefore a good target for anticancer drugs.[Ang, 2011] Some of the effects of RAPTA compounds are their antimetastatic activity, due to intra- and extracellular interactions, especially on the cell membrane and the ability to activate key proteins essential for cellular apoptosis.[Ang, 2011] The alternative mechanism compared to Cisplatin, by addressing proteins as major target, is a good opportunity to circumvent cross-resistance.[Ang, 2011] A special fact while considering the RAPTA-family is their low cytotoxic activity *in vitro*.[Ang, 2011; Murray, 2016] In general, IC50 values are in the range of 50-500 μM for this class of compounds.[Ang, 2011] First *in vitro* experiments were done against TS/A adenocarcinoma and HBL-100 epithelial (non-cancerous) cell lines, showing low cytotoxicity.[Scolaro, 2005] Nevertheless, in different *in vivo* experiments, RAPTA-C and -B were tested against the MCa mammary carcinoma, showing no activity against the primary tumor but reduction of solid lung metastases.[Scolaro, 2005; Murray, 2016] Experiments showing, that RAPTA-C increases significantly the survival of mice bearing a highly proliferative tumor

were later on validated in preclinical models revealing effects on primary tumor growth.[Scolaro, 2005; Chatterjee, 2008; Weiss, 2014] Biological tests show, that interactions with intra- and extracellular targets result in multiple effects on cells, RAPTA-C inhibits the tumor growth by interrupting the cell cycle at G2/M-phase. It up-regulates p21 and p53, which leads to apoptosis by the mitochondrial pathway, and down-regulation of cyclin E.[Ang, 2011] The highest selectivity was shown for compound RAPTA-T, [Ru(η^6-toluene)(pta)Cl_2], Figure 3.2.3-3.[Murray, 2016] Therefore, further experiments were performed with that compound *in vitro* and *in vivo*. In cell culture for MDA-MB-231 and MCF-7 cells a reduced ability to migrate could be observed, and *in vivo* results showed a reduction of lung metastases (35%).[Murray, 2016; Bergamo, 2008] In line with these results a strong anti-angiogenic effect of RAPTA-C and RAPTA-T by decreasing microvessel density was observed.[Nowak-Sliwinska, 2011; Murray, 2016] Comparison studies of RAPTA-C with the highly cytotoxic anticancer drug doxorubicin *in vivo* showed an improved tumor growth inhibition by RAPTA-C, even by using lower doses than for doxorubicin.[Murray, 2016] It can be concluded, that RAPTA compounds show low cytotoxicity *in vitro*, but promising activity *in vivo* by antiangiogenic effects and antimetastatic activity.[Murray, 2016; Wang, 2013] Additionally, they exhibit low toxic side effects in mouse models.[Murray, 2016] Recent studies show that cytotoxicity of RAPTA compounds can be enhanced by tethering to human serum albumin.[Wang, 2013] Most work was focused on optimization of the RAPTA-structure and the determination of structure-activity-relationships. Thus, functionalization of the arene ligand is used for tumor-targeting and synthetic work is done by developing macromolecular compounds based on the general RAPTA-structure.[Wang, 2013; Murray, 2016] *In vitro* results for several RAPTA-structures are published with little changes of the arene ligand and the exchange of pta to pta-Me.[Scolaro, 2005] Nevertheless, at the moment most promising results are shown for RAPTA-C, -B and -T, Figure 3.2.3-3.[Murray, 2016]

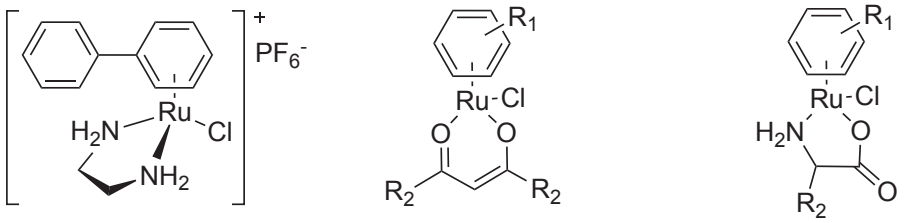

RM175 | General structure of O,O-chelating substances | General structure of N,O-chelating substances

Fig. 3.2.3-4: RM175: A N,N-chelating compound and general structures of O,O- and N,O-chelating substances, introduced by Sadler and coworkers, R_1 is the substituted arene ligand (*e.g. p*-cymene), R_2 can be different substituents.[Habtemariam, 2006]

As mentioned before, early investigations have been done by Sadler and coworkers with X,Y-chelating ruthenium(II) substances, whereas X,Y can be N,N (*e.g.* diamine), N,O (*e.g.* amino acidate), and O,O (β-diketonate), Figure 3.2.3-4.[Habtemariam, 2006].By their structure-activity-relationship studies with overall 13 different ruthenium(II) complexes, they show the impact of the arene and the chelating ligand which playing an important role for anticancer activity.[Habtemariam, 2006] Whereas some of their compounds show significant activity against A2780, as well as against A2780cis proving no cross-resistance to Cisplatin, others are nearly inactive. For example, little variations of the N,N-chelating ligand resulted in shifts of IC50 values for A2780 cells from >100 to 8 μM. Structural changes of the arene ligand enabled IC50 changes for A2780 from >100 to 3 μM, whereas N,O-bidendate substances showed no activity at all. The most active O,O-chelating compound was substituted with two phenyl-rings and a *p*-cymene as arene ligand. After all, they concluded that the most promising candidates overall contain 'en' (= ethylenediamine; N,N) and a polycylic-arene.[Habtemariam, 2006] Based on this publication and earlier work, it was published that [Ru(η^6-arene)(en)Cl]PF_6 complexes show cytotoxic activity *in vitro* and *in vivo*, as well as no cross-resistance to Cisplatin.[Habtemariam, 2006; Morris, 2001; Aird, 2002] By trying to understand the mode of action of these compounds, they concluded, that the hydrolysis of the metal-chlorid bond is an important step. The formed aqua-products are able to bind to the DNA or proteins and result in

monodentate binding products.[Habtemariam, 2006; Wang, 2003] The most famous compound, RM175, [Ru(η^6-biphenyl)(en)Cl]PF_6, Figure 3.2.3-4, show antiproliferative activity comparable to Carboplatin and binds specifically to guanine's N7.[Meier-Menches, 2018; Habtemariam, 2006; Morris, 2001] The guanine-ruthenium adduct is stabilized with hydrogen-bonds between C6O and en-H.[Chen, 2002] Therefore it is likely, that RM175 follows a different mode of action than RAPTA compounds (and ruthenium(III) complexes) because of its affinity to target the DNA, especially guanine.[Meier-Menches, 2018; Morris, 2001; Chen, 2002] RM175 and its analogue HC11, [Ru(η^6-tetrahydroanthracene)(en)Cl]PF_6 have been investigated for cytotoxicity against 13 cell lines, showing good *in vivo* results for A549 by inhibiting tumor growth after *i.p.* single-dose administration.[Meier-Menches, 2018; Guichard, 2006] Compound RM175 has been further investigated *in vivo* against A2780/ A2780cis xenografts and for its antimetastatic effect in MCa mammary carcinoma xenograft models.[Meier-Menches, 2018; Aird, 2002; Bergamo, 2010] Results show, no-cross resistance to Cisplatin, acceptance of higher doses, but only half of the Cisplatin activity (in A2780-studies). Therefore RM175 is introduced as an antimetastatic agent, similar to NAMI-A.[Meier-Menches, 2018] Sadler and coworkers expanded binding-studies to different biomolecules and show, that RM175 and its *p*-cymene analogue, prefers binding to DNA than to molecules like glutathione. GSH, known for binding and inactivating Cisplatin, is not able to capture them efficiently pointing to a big advantage for Sadler's compounds.[Meier-Menches, 2018; Wang, 2005; Adhireksan, 2014]

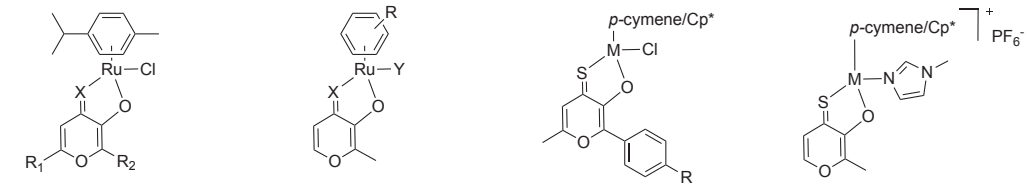

Fig. 3.2.3-5: **N**-**Q**: O,O- and O,S-chelating metal(II) complexes with arene ligands from Keppler and coworkers.[Kandioller, 2009a; Kandioller, 2009b; Hanif, 2010; Schmidlehner, 2016; Hackl, 2016]

Notably, most studies publish results for N,N-, N,O-, and O,O-chelating ruthenium(II) and osmium(II) complexes, only Keppler and coworkers focused also on O,S-chelating systems, **N**-**Q** Figure 3.2.3-5.[Kandioller, 2009a; Kandioller, 2009b; Hanif, 2010; Schmidlehner, 2016; Hackl, 2016] First studies have been done in 2009 with different thiopyrone ligands on ruthenium(II) *p*-cymene complexes.[Kandioller, 2009a; Kandioller, 2009b] It was shown, that changing the O,O-chelating system to an O,S-chelat, **N**, increased stability and show good anticancer results (IC50 values in low micromolar range).[Kandioller, 2009b] In 2010 the *in vitro* comparison of maltol- and thiomaltol-bidendate ruthenium(II) complexes, **O**, confirmed on three different cell lines the increased cytotoxicity for the thiomaltol-derivatives, whereas the maltol-based compounds show only low activity. Furthermore, the authors presented that the aqua-species of these compounds can interact with the DNA-model substance 5'-GMP (= 5'-guanosinemonophosphate).[Hanif, 2010] For ruthenium(II) and rhodium(II) complexes, **P**, the water-solubility was enhanced due to a higher binding affinity to sulfur than to oxygen, resulting in stable complexes for biological experiments. *In vitro* experiments display higher activity for the rhenium complexes than for their ruthenium(II) analogues. In the same study, they reported on the impact of the ligand backbone modification for thiopyrone-based ligands.[Schmidlehner, 2016] A comparison study of ruthenium(II)/ osmium(II)/ rhodium(II) and iridium(II) complexes with thiomaltol ligands, **Q**, have been published 2016.[Hackl, 2016] Results point out the best biological activity for iridium and rhodium complexes as well as the fact, that the ligand itself exhibits the highest cytotoxicity at all. The ruthenium(II) complexes had IC50 values ranging from 12 to 3 μM, the osmium compounds from 4 to 2 μM.[Hackl, 2016]

- Osmium compounds

As Table 3.2.3-1 already shows, osmium compounds cannot be discussed seperately from their ruthenium analogues. Many studies focus on comparisons of ruthenium compounds and their osmium counterparts, as described above for the thiomaltol derivatives.[Hackl, 2016] The first osmium compounds have been an-

alogues of promising ruthenium candidates, *e.g.* RAPTA-C [Dorcier, 2005; Dorcier, 2006], RM175 [Peacock, 2006; Peacock, 2007a-c] and NAMI-A [Cebrian-Losantos, 2007]. All of these compounds have been first described in the years 2005-2007.[Meier-Menches, 2018] Due to the HSAB-principle (= hard and soft acids and bases), osmium is slightly softer than ruthenium, resulting in different coordination spheres to biomolecules.[Meier-Menches, 2018] The change of the metal, from ruthenium to osmium has a great influence on anticancer activity and osmium is more promising due to lower metal-ligand exchange kinetics, including slower hydrolysis of the metal-halide bond.[Paunescu, 2015; Stepanenko, 2013; Bergamo, 2010; Büchel, 2013; Meier-Menches, 2018; van Rijt, 2009; Pizarro, 2010] Therefore, comparison studies show different results for these analogue compounds.[Meier-Menches, 2018; Paunescu, 2015] The osmium analogues of NAMI-A and RM175 (AFAP51) are more inert and stable towards hydrolysis and do not interact with DNA-base models (*e.g.* 9-methyladenine). Furthermore, they result in a different biological activity profile compared to their ruthenium analogues.[Meier-Menches, 2018; Groessl, 2007; Bergamo, 2010] For AFAP51/ RM175, lower IC50 values were observed for the osmium compound on different cell lines.[Bergamo, 2010] One of the most promising candidates is [Os(aspy-NMe_2)(*p*-cymene)I] FY026, where aspy-NMe_2 is *p*-dimethylaminophenylazopyridine investigated by Sadler and coworkers, which was evaluated in the colon adenocarcinoma xenograft model (HCT-116) *in vivo* and show better results than the ruthenium(II) compound, Figure 3.2.3-6.[Meier-Menches, 2018; Shnyder, 2011] Most studies focused on osmium(II) arene compounds and several were already evaluated *in vivo*.[Paunescu, 2015; Schmid, 2007a; Schmid, 2007b; Kilpin, 2014; Peacock, 2007a-c; Fu, 2010; Fu, 2011; Romero-Canelon, 2013; van Rijt, 2009; van Rijt, 2010; Bergamo, 2010; Shnyder, 2011; Filak, 2013] Some of these compounds show activity comparable to Carboplatin and/or Cisplatin, others show significantly lower anticancer activity than their ruthenium counterparts.[Fu, 2011; Fu, 2010; Meier-Menches, 2018] Dyson and coworkers compared metal complexes with O,O-bidendate systems resulting in contradictory results. Some osmium complexes show higher antiproliferative activity than their

ruthenium counterparts and some show more selectivity towards cancer cells, but one ruthenium complex was more active than its osmium analogue. However, the IC50 values were generally high for all investigated complexes. Nevertheless these compounds will be also evaluated in the future *in vivo* due to the fact, that the most promising RAPTA candidates also showed low activity *in vitro*.[Paunescu, 2015; Clavel, 2014]

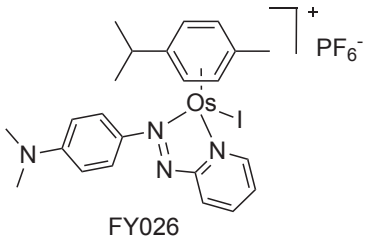

FY026

Fig. 3.2.3-6: Compound FY026, an osmium(II) compound investigated by Sadler and coworkers, showing better *in vivo* results than its ruthenium(II) analogue.[Meier-Menches, 2018; Shnyder, 2011]

Overall, it is well accepted that the biological activity of metal compounds is due to the ligand system, as well as a symbiotic effect of ligand and metal. Thus, next to the ligand system the metal itself and its interactions with the ligand system have a very strong influence. Therefore, there is no real correlation observable and it cannot be concluded overall that osmium compounds are in general more promising candidates than their ruthenium analogues. However, some facts of osmium compounds, *e.g.* their aqueous chemistry is actually not understand.[Meier-Menches, 2018] A structure-activity-relationship study by Keppler and coworkers comparing different published *in vitro* and *in vivo* data on ruthenium and osmium compounds concluded, that osmium compounds bearing a P-monodendate or O,O-bidendate ligand system are less active than the ruthenium compounds and other way round for the bidendate systems with: N,N/ N,O/ C,N and S,N ligands.[Meier-Menches, 2018; Dorcier, 2006; Hanif, 2010; Peacock, 2007a-c; Mendoza-Ferri, 2009; Fu, 2011; Filak, 2011; Filak, 2010; Schmid, 2007a; Schmid, 2007b; Riedl, 2017; Meier, 2013] They also concluded, that the charge of the complex does not correlate with the anticancer activity.[Meier-Menches, 2018; Mendozza-Ferri, 2009] Moreover, it is known

that ruthenium and osmium compounds have different biological targets and do not necessarily interact with the DNA.[Meier-Menches, 2018] It was point out, *e.g.* for RAPTA compounds, that *in vitro* and *in vivo* data do not correlate. Some complexes which exhibit low IC50 values *in vitro* are nevertheless evaluated *in vivo*.[Paunescu, 2015; Weiss, 2014; Scolaro, 2005; Nowak-Sliwinska, 2011; Weiss, 2015] Dyson and coworkers concluded, that osmium compounds tend to be slightly more cytotoxic in general, compared to ruthenium analogues in cell culture assays. But they also mentioned that *in vitro* and *in vivo* data can tell a different story and it might be, that one compound is more active *in vitro* but not *in vivo* and other way round. This was observed for some ruthenium as well as for some osmium complexes.[Paunescu, 2015] So the rational drug design is difficult for these compounds and comparison studies of differently substituted ligand systems using both metals, ruthenium and osmium, is needed to find future promising drug candidates.

3.3 Cinnamic acid and its derivatives

Cinnamic acid is an organic compound occuring in plants, fruits and beverages (*e.g.* tea and coffee).[Sova, 2012; Clifford, 1999; Clifford, 2000; Edreva, 2005] It belongs to the class of auxins, plant hormones which regulate cell growth and differentiation.[De, 2011; Thimann, 1969] Cinnamic acid acts as a key intermediate in the shikimate- and phenylpropanoid-pathways as a precursor of the flavonoids and lignin, the second most abundant biopolymer (after cellulose) which is responsible for plant structures.[De, 2011; Sova, 2012; Edreva, 2005; Hrazdina, 1992; Whetten, 1998] Next to this it is used as a component in scents and flavourings.[De, 2011; Hoskins, 1984]

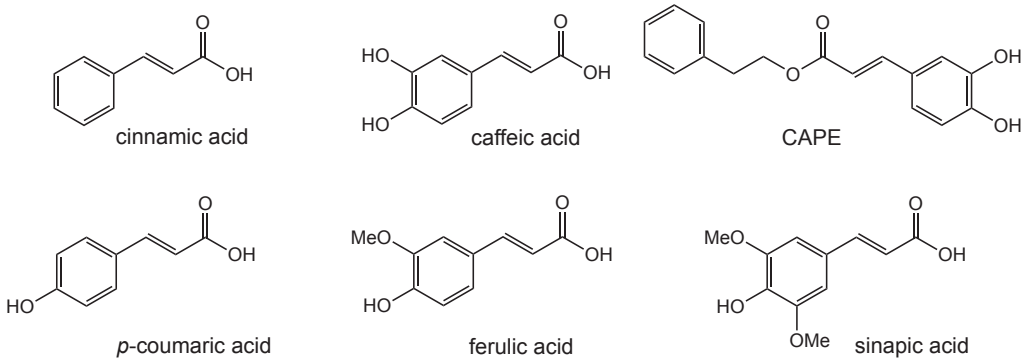

Fig. 3.3-1: Cinnamic acid and its naturally occuring derivatives *p*-coumaric acid, ferulic acid, sinapic acid, caffeic acid and its analogue caffeic acid phenethyl ester (CAPE).[De, 2011; Sova, 2012]

Its chemical structure the 3-Phenylacrylic acid, exhibit three different substitution sides: an α,β-unsaturated double-bond (Michael-acceptor), a phenyl-ring and a carboxylic acid function.[De, 2011] The presence of the benzyl-ring and a short hydrocarbon chain lead to a low polarity of cinnamic acid itself and a low water solubility, but both characteristics can be archived by the synthesis of derivatives.[Sova, 2012] Therefore, numerous naturally and synthetically derivatives are known, most prominent: *p*-coumaric, caffeic, ferulic and sinapic acid (Figure 3.3-1) and its derivatives.[Sova, 2012]

Cinnamic acid itself has a long history in medicinal use especially for anticancer treatment in chinese traditional medicines.[De, 2011] It has been reported, that in 1905 cancer patients were treated with the sodium salt of cinnamic acid and

o-coumaric acid and it was shown, that the natural hydroxy cinnnamates are extremly potent antitumor agents.[De, 2011; Epifano, 2007; Kron, 1999; Prager, 1966] The options to create derivatives, especially using the α,β-unsaturated moiety which acts as a Michael-acceptor, an active moiety used very often in drug synthesis, enhances its use for the design of anticancer drugs.[De, 2011; Ahn, 1996] Cinnamic acid acts as an antiproliferative agent and inhibits DNA synthesis and tumor growth.[De, 2011; Ekmekcioglu, 1998; Liu, 1995] It was shown, that some cinnamyl analogues may act as proteine kinases inhibitors resulting in inhibition of cell growth, as well as some studies suggested that caffeic acid has anticarcinogenic effects.[De, 2011; Shiraishi, 1989] Beside this many biological and synthetical derivatives have been studied to determine their anticancer properties, for example: Prenylated cinnamic acids, *cis*-cinnamic acid derivatives, cinnamoyl esters of cinnamic acid, dicarbonyl cinnamoates, cinnamide derivatives and many more.[De, 2011] Remarkable antitumor effects *in vivo* have been reported for caffeic acid phenethyl ester (CAPE), a natural occuring compound showing *e.g.* apoptotic effects, the ability to modify CYP450 (cytochrom P450) activity and inhibition of NF-κB (nuclear factor 'kappa-light-chain-enhancer' of activated B-cells). Therefore it can control tumor growth.[De, 2011]

Many derivatives, naturally and synthetical ones, have been reported regarding various pharmacological properties.[Sova, 2012] Beside the potential as anticancer drugs, cinnamic acid derivatives are known for low toxicity and a broad spectrum of biological activities and the moiety is very often used as starting material for effective drug design.[Sova, 2012; Simonyan, 1993; De, 2011; Sharma, 2011] Many derivatives show antioxidant properties, especially those with phenolic hydroxyl groups.[Sova, 2012] Several reports focuses on the antioxidant properties of *p*-coumaric, ferulic, caffeic and sinapic acid (and derivatives), showing that hydroxycinnamic acids are more effective antioxidants than the benzoic analogues.[Sova, 2012; Tsao, 2004; Fotti, 1996; Shahidi, 2010; Szwajgier, 2005; Baderschneider, 2001; Natella, 1999] For caffeic, ferulic and sinapic acid very strong reducing abilities have been reported. Moreover, cinnamic, coumaric, ferulic and sinapic acid show inhibition of bacterial growth of several gram-positive and -negative bacteria.[Sova, 2012; Szwajgier, 2005]

Beside the various biological functions of this group of compounds, there is a lack of information considering their mode of action(s), their toxicity and their full pharmacological properties mainly due to limited *in vivo* results until now.[Sova, 2012; De, 2011] This leads to an increasing number of studies and new synthetic derivatives are explored to understand their properties and their biological activities.[De, 2011; Sova, 2012]

3.4 Asparagusic acid and its derivatives

Asparagusic acid, 1,2-dithiolane-4-carboxylic acid, is a disulfur-5-membered heterocyclic ring with carboxylic acid function, isolated only from *Asparagus officinalis*, Figure 3.4-1.[Mitchell, 2014] First isolation from asparagus juice have been done by Jansen and coworkers in 1948.[Salemme, 2016; Jansen, 1948] Early reports describe the growth-inhibitory effects on higher plants and anti-fungal properties.[Mitchell, 2014; Yanagawa, 1972] Therefore it was investigated in early studies for its cytostatic and antineoplastic properties, its antioxidant and vasodilatory capabilities, its inhibitory activity against cyclooxygenases (COX-1 and -2), and to treat acne.[Mitchell, 2014; Kieller, 1962; Jang, 2004] The presence of two sulfur atoms has several chemical and biological useful properties.[Mitchell, 2014] The thiol-function of dihydroasparagusic acid, for example, is able to bind metals, but also different biomolecules and is well-known from antioxidant molecules like GSH.[Salemme, 2016] Research interest of that compound, as well as its reduced form dihydroasparagusic acid (Figure 3.4-1) and other ingredients in general, increased in the last years. Several articles and reviews report on the pharmacological properties of asparagus, *e.g.* Waring and coworkers, 2014, Saito and coworkers 2015, Venditti and coworkers 2016, Imran and coworkers, 2017, Sharma and coworkers, 2017 and Matile and coworkers 2013/ 2017.[Mitchell, 2014; Iqbal, 2017; Salemme, 2016; Nakabayaski, 2015; Sharma, 2017; Abegg, 2017; Carmine, 2013]

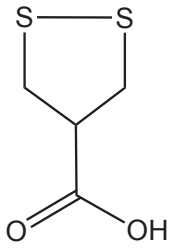

Asparagusic acid

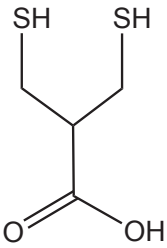

Dihydroasparagusic acid

Fig. 3.4-1[3]: Asparagusic acid, an ingredient of *Asparagus officinalis*, and its reduced form Dihydroasparagusic acid.

The main bioactive ingredients of *Asparagus officinalis* are steroidal glycosides, saponins, inulin, some fructo-oligosaccharide and the asparagusic acid.[Iqbal, 2017] All of this ingredients have been studied for several pharmacological properties. For asparagusic acid the following pharmacological properties have been reported: '*anticancer, antioxidant, antifungal, antibacterial, anti-dysenteric, anti-inflammatory, anti-abortifacient, anti-oxytoxic, anticulcer, hypersensitive and anticoogulant*.'[Iqbal, 2017] Next to this it should reduce the risk of several diseases, for example diabetes.[Iqbal, 2017] Nevertheless, until now it is not commercially available for all these applications.[Mitchell, 2014] Beside its pharmacological properties itself, asparagusic acid is able to enhance cellular uptake of different molecules, like proteins.[Abegg, 2017] It was shown, by Matile and coworkers, that the molecule interacts with transferrin receptor and provides a possibility for thiol-mediated uptake of anticancer compounds which have asparagusic acid as functional group.[Abegg, 2017]

[3] Asparagus picture taken from: https://www.spargelhof-simianer.de.

3.5 Motivation

Since the discovery of its potent anticancer properties, Cisplatin is very well established in clinical cancer treatment (Chapter 3.2.1). However, due to its limitations and drawbacks there is a high research interest on improved compounds and five have been gained approval (three just regionally) so far. Nevertheless, cancer is still one of the most common reasons of death nowadays (Chapter 3.1), its treatment is often difficult because of specific characteristics and a high heterogeneity of tumor cells. As time passes by, the understanding of molecular mechanisms of malignant cells increases, whereas Cisplatin and its two worldwide approved analogues remains important drugs for tumor treatment. Modifying and enhancing their properties is the aim for several researchers worldwide, focusing on different strategies, for example changing the ligands on the platinum(II) (Chapter3.2.2), the oxidation state to platinum(IV) (Chapter 3.2.2) or substitute the metal to *e.g.* ruthenium, osmium or palladium (Chapter 3.2.2 and 3.2.3).

It has been shown, that direct Cisplatin analogues of ruthenium and palladium do not display the same efficiency (Chapter 3.2.2 and 3.2.3) and therefore, the SARs of Cisplatin and analogues cannot be taken as a guide for other metals in anticancer drug design. Additionally, non-classical platinum(II) compounds showed promising results (Chapter 3.2.2) and led to a rethinking of the old proposed SARs for metal drug design in general.

Taking natural compounds for anticancer treatment has a long tradition, one prominent example is the drug Paclitaxel (Taxol), first isolated from the bark of *Taxus brevifola*, approved by the FDA in 1992.[Gordaliza, 2007]

Whereas the research on some molecules increased (*e.g.* curcurmin) in the last years and several derivatives and metal complexes have been generated, focusing on cinnamic acid and asparagusic acid and derivatives can still be identified as a niche strategy.[Gordaliza, 2007]

Cinnamic acid and asparagusic acid are two different natural occurring molecules with promising pharmacological potencies. Therefore, both systems have been

already used in the past to generate a libary of structural analogues and determine of anticancer properties. The increased interest on their biological activities in the last years, as well as the fact that both show a good potential for structural changes and for the coordination to metals are ideal prerequisits to focus on the design of metal complexes with analogues of these natural ligands. Consequently, the development of structural-analogues and their corresponding metal complexes as anticancer agents are the main goal of this thesis.

Although it is known, that the chosen metal and the ligand should interact in a synergistic manner, already small structural changes of organic molecules, can result in significant changes of their chemical and biological behavior *e.g.* anticancer activities. Moreover, SARs can be different, not only for the ligand-metal-synergism, but also in general as shown by the comparison to almost similar molecules. This is exemplified in reviews trying to generalize SARs for a group of compounds and to establish some correlations. However, often the authors already state, that the overall SARs are not easy to determine and add exceptions for their 'rules' (seen for Ru/Os compounds [Meier-Menches, 2018] and Pd(II) complexes [Alam, 2016]).

Cisplatin resistance leads to limitations in cancer treatments. Next to the toxic side effects of this compounds this is the main problem of platinum based therapy. Resistance of tumors can be acquired or intrinsically (Chapter 3.2.1) and caused by numerous aberrations. New anticancer drugs should have more selectivity towards cancer cells (which may result in lower toxic side effects) and should be active against Cisplatin resistant tumors. Those two goals are focused in this thesis by:

- Placing suitable ligands on different metals and study their interactions with biomolecules (proteins and DNA),
- Explore IC50 values for all organic and metal complexes on different cell lines by focusing on ovarian cancers and
- Determine their overall toxicity on non-cancerous cell lines.

This thesis describes three different kinds of designs (Part1, Part2 and Part 3), the Parts 1 and 2 include the overall chemical studies:

- Synthesis of ligands and metal complexes,
- Molecular structures for every described system,
- Stability determinations and
- Full characterization by NMR, MS and elemental analysis.

Next to this the cytotoxic properties of all compounds have been determined with:

- IC50 determinations,
- γH2AX-foci analysis,
- Protein- and DNA-interactions, well selected after initial results.

Part 1: β-Hydroxydithiocinnamic acid derivatives and corresponding Ruthenium(II), Osmium(II), Platinum(II), Palladium(II) and Nickel(II) complexes targeting Cisplatin resistant ovarian cancer cell lines

It was pointed out by Weigand and coworkers that β-Hydroxydithiocinnamic acid esters can be used for ligands of metal complexes as well as some promising results have been shown for some platinum(II) molecules.[Weigand, 1993; Saumweber, 1998; Schubert, 2003; Schubert, 2005; Schubert, 2006; Schubert, 2007; Mügge, 2014; Mügge, 2016] Nevertheless, it is well-known that some ligands exhibit better anticancer activity itself compared to their metal complexes. Therefore, the overall biological activity of the organic molecules to understand their real potential, as well as the influence on the activity of the metal(s), have been missing so far. One aim of this thesis is to show the biological activity of these molecules also with structural changes, which can lead to different chemical and biological behavior for the molecules itself as well as for the corresponding metal complexes.

Chapter 3.2 introduced the different metals in anticancer drugs design, their different properties and the lack of understanding in their biological mechanisms.

It is well-accepted, that the selection of the metal is a key factor in cytotoxic activity and in the biological pathways, which not only lead to their anticancer activity, but also different side effects and varying drug resistances.
This work is based on the proposed hypothesis, that the chosen metal and the ligand should interact in synergism. Therefore, the properties of metal complexes and its ligands can only be significantly determined by an overall comparison of different metals with the same ligand to hopefully find a 'magic bullet'.
Due to different metals, all groups of compounds discussing in this part exhibit different second (and third) ligands which offers variations as well.

Part 2: Chemical and biological investigations of platinum(II) complexes with asparagusic acid derivatives as S/S, Se/Se and S/Se -bidendate ligands

Beside the probably various biological and pharmacological functions, it has been shown that asparagusic acid can act as a ligand for platinum(II) complexes with phosphane ligands by Siemeling and coworkers.[Siemeling, 2010] The synthesis of platinum(II) complexes with sulfur- and selenium-based ligands as well as different phosphane ligands have been explored by several working groups, including Weigand and coworkers.[*e.g.* Rothenburger, 2006; Niksch, 2010; Mügge, 2011] The aim of this part of the thesis is to synthesize new platinum(II) complexes of asparagusic acid derivatives for the development of potential anticancer drugs. The asparagusic acid can be modified to selenium and sulfur/selenium analogues as well as the use of PPh_3 and dppma ligands for the platinum(II) complexes. The IC50 values of these compounds, takes place in Part 2.

Part 3: 'Quadrupole Action' compounds as anticancer agents

Chapter 3.2.2 introduced the potential of a platinum(IV) prodrug system. Part 3 of this thesis discusses two projects focussing on this approach.

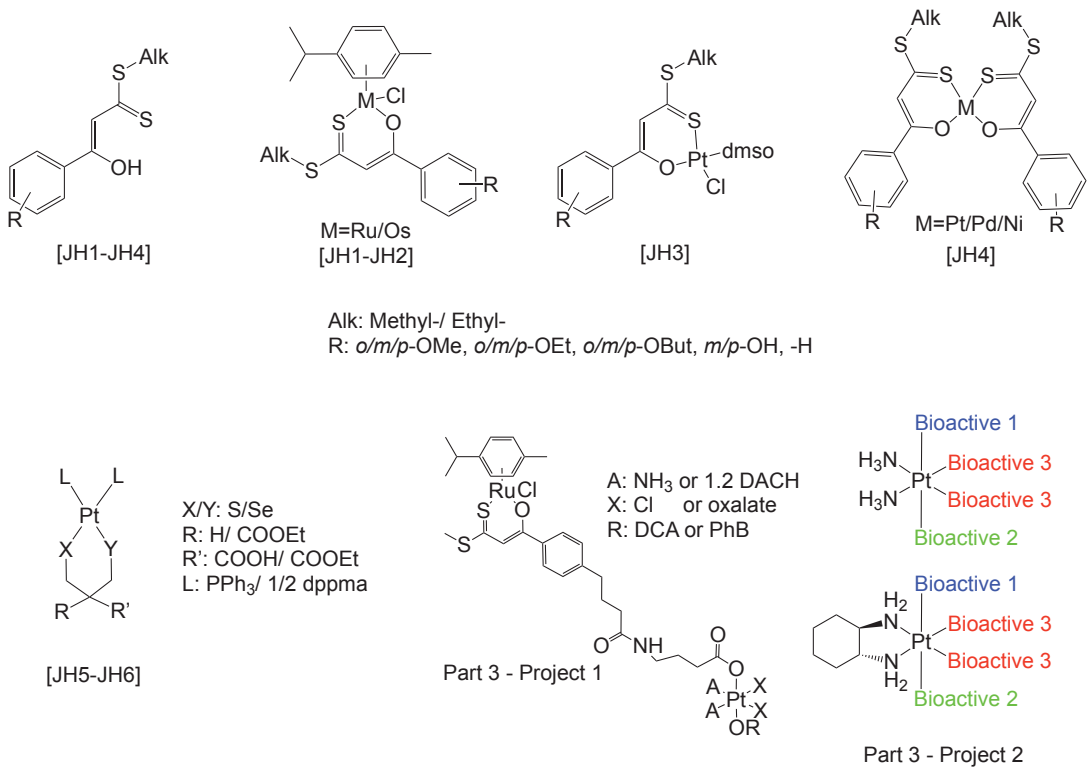

Fig. 3.5-1: Overview of compounds in Part 1: Publication numbers [JH1-4], Part 2: Publication numbers [JH5-6] and Part 3 of this thesis.

Part 1

β-Hydroxydithiocinnamic acid derivatives and corresponding Ruthenium(II), Osmium(II), Platinum(II), Palladium(II) and Nickel(II) complexes targeting Cisplatin resistant ovarian cancer cell lines

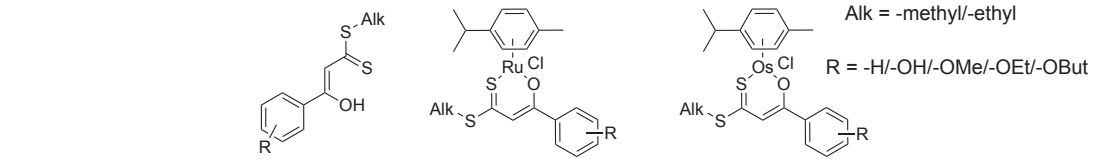

General substance code: Lx Rux Osx

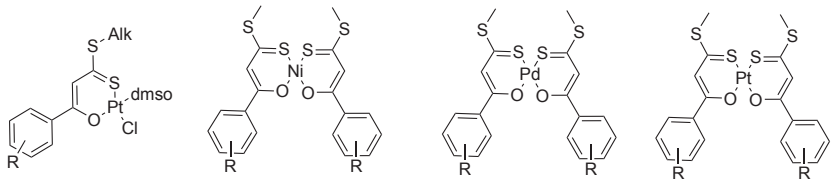

General substance code: Ptdmsox Nix Pdx Ptx

x	1	2	3	4	5	6	7	8	9	10	11	12	13	14	15	16	17	18
R	*o*-O-Me	*m*-O-Me	*p*-O-Me	*o*-O-Et	*m*-O-Et	*p*-O-Et	*o*-O-But	*m*-O-But	*p*-O-But	*m*-OH	*p*-OH	H	*o*-O-Me	*m*-O-Me	*p*-O-Me	*m*-OH	*p*-OH	H
Alk	Me	Me	Me	Me	Me	Me	Me	Me	Me	Me	Me	Me	-Et	-Et	-Et	-Et	-Et	-Et

Part 1 discuss chemical and biological behavior of different metal complexes with O,S-bidendate ligands.[4]

[JH1] Ruthenium(II) complexe (L10, Ru10)

[JH2] Ruthenium(II) and Osmium(II) complexes (Lx, Rux and Osx)

[JH3] Platinum(II) complexes (Lx, Ptdmsox)

[JH4] Platinum(II), Palladium(II) and Nickel(II) complexes (Lx, Ptx, Pdx and Nix)

[4] The general substance code introduced here is used in all discussions in this thesis. Substance code in publications [JH1-JH4] may be different to that.

4. Publications

4.1 [JH1]

Unusual mode of protein binding by a cytotoxic π-arene ruthenium(II) piano-stool compound containing an O,S-chelating ligand

Jana Hildebrandt, Helmar Görls, Norman Häfner, Giarita Ferraro, Matthias Dürst, Ingo B. Runnebaum, Wolfgang Weigand, Antonello Merlino

Dalton Transactions **2016**, *45*, 12283-12287.

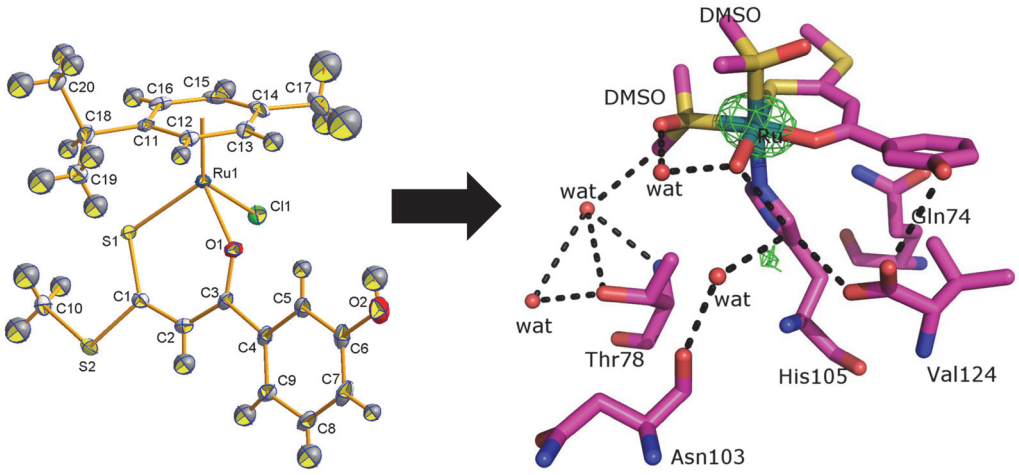

In this publication synthesis, characterization, cytotoxic activity *in vitro*, solution stability *via* UV-Vis spectrometry and interaction with the model protein bovine pancreatic ribonuclease (RNase A) of the π-arene ruthenium(II) complex Ru10 is described. It was shown that Ru10 binds to RNase A through an unusual mode of protein binding that includes ligand exchanges and alteration of coordination sphere geometry that shows similarity to well-known ruthenium(III) compounds NAMI-A and KP1019 after their binding to proteins. IC50 values have been determined with MTT assays on ovarian carcinoma cell lines SKOV3, A2780 as well as their Cisplatin resistant analogues, and lung carcinoma cell line A549. Ru10 exhibits cytotoxic activity in low µM range for cancer cell lines and a low toxicity for non-malignant cell lines.

Dalton Transactions

COMMUNICATION

View Article Online
View Journal | View Issue

Cite this: *Dalton Trans.*, 2016, **45**, 12283

Received 15th June 2016,
Accepted 27th June 2016

DOI: 10.1039/c6dt02380k

www.rsc.org/dalton

Unusual mode of protein binding by a cytotoxic π-arene ruthenium(II) piano-stool compound containing an O,S-chelating ligand†

Jana Hildebrandt,[a] Helmar Görls,[a] Norman Häfner,[b] Giarita Ferraro,[c] Matthias Dürst,[b] Ingo B. Runnebaum,[b] Wolfgang Weigand*[a] and Antonello Merlino*[c,d]

A new pseudo-octahedral π-arene ruthenium(II) piano-stool compound, containing an O,S-bidentate ligand (compound 1) and showing significant cytotoxic activity *in vitro*, was synthesized and characterized. In solution stability and interaction with the model protein bovine pancreatic ribonuclease (RNase A) were investigated by using UV-Vis absorption spectroscopy. Its crystal structure and that of the adduct formed upon reaction with RNase A were obtained by X-ray crystallography. The comparison between the structure of purified compound 1 and that of the fragment bound to RNase A reveals an unusual mode of protein binding that includes ligand exchange and alteration of coordination sphere geometry.

Since the discovery that cisplatin (*cis*-$Pt(NH_3)_2Cl_2$) could be used to treat or even cure several forms of cancer,[1] the use of metal compounds as anticancer drugs has continued to attract the attention of the scientific community.[2] Cisplatin and its second generation derivatives carboplatin and oxaliplatin are currently the most widely used chemotherapeutic drugs.[3] The activity of these anticancer agents is associated with the formation of DNA lesions that interfere with transcription, resulting in cell death by apoptosis.[4] In spite of their success in clinical applications, Pt-based drugs are of limited efficacy due to severe side effects, including toxicity and intrinsic or acquired resistance. These limitations prompted the design and synthesis of novel chemotherapeutic agents based on the use of non-Pt metals, such as gold and ruthenium.[5,6] In this context, Ru compounds have emerged as a promising alternative to Pt drugs, as they show selective activity against specific cancers and low toxicity.[7] Among Ru compounds, indazolium *trans*-[tetrachloridobis(1*H*-indazole)ruthenate(III)] (KP1019) and imidazolium *trans*-[tetrachloride(1*H*-imidazole)(*S*-dimethylsulfoxide)ruthenate(III)] (NAMI-A) have attracted the most attention as potential anticancer agents; both have successfully completed phase I and II clinical trials.[6,8,9] The octahedral geometry of the Ru coordination sphere in these molecules provides a higher degree of binding site selectivity when compared to the square-planar coordination sphere of Pt(II) compounds. This results in low toxicity and good clearance.

Another family of potential Ru drugs consists of pseudo-octahedral π-arene ruthenium(II) piano-stool compounds of the type $[(\eta^6\text{-arene})Ru(chelate)Cl]^+$ where the chelating ligands are N,N– or N,O–.[10,11]

Recently, we have reported the synthesis, structural characterization, binding to biological macromolecules (DNA and proteins) and antitumor activity of Pt(II) compounds containing cinnamic acid derivative ligands.[12–14] Taking advantages of the experience we have gained in this field, we have designed new Ru(II) compounds containing these O,S-chelating ligands. The aim is to provide a new class of π-arene ruthenium(II) piano-stool compounds with potential cytotoxic activity. In particular, we started with the synthesis of compound **1** (Scheme 1). The O,S-bidentate ligand β-hydroxy dithiocinnamic methyl ester, **L**, was chosen because it ensures moderate solubility of metal complexes in mixed organic/aqueous

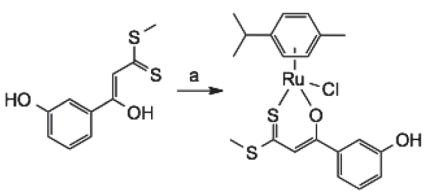

Scheme 1 Reagents and conditions: (a) (i) $[(\eta^6\text{-}p\text{-cymene})RuCl_2]_2$, tetrahydrofuran (THF), room temperature; (ii) 2 equiv. *t*-BuOK, THF, r.t., 0.5 h; (iii) 24 h, r.t.; (iv) H_2SO_4/H_2O, r.t., 0.5 h.

[a]*Department of Inorganic and Analytical Chemistry, University of Jena, Germany. E-mail: wolfgang.weigand@uni-jena.de*
[b]*Department of Gynecology, Jena University Hospital - Friedrich-Schiller-University Jena, Germany*
[c]*Department of Chemical Sciences, University of Naples Federico II, Italy. E-mail: antonello.merlino@unina.it; Fax: +39081674090; Tel: +39081674276*
[d]*Institute of Biostructures and Bioimages, Naples, Italy*

†Electronic supplementary information (ESI) available. CCDC 1476883. For ESI and crystallographic data in CIF or other electronic format see DOI: 10.1039/c6dt02380k

solvents and also because the Pt compounds containing this ligand are stable under different experimental conditions and have been found to bind proteins, as demonstrated by mass spectrometry and X-ray crystallography data.[14] The synthesis of compound **1** was accomplished as reported in Scheme 1. The experimental conditions and details of the protocol used to synthesize compound **1** are reported in the ESI.†

^{1}H NMR and elemental analysis confirm the identity and purity of the compound. Single crystals suitable for X-ray diffraction were obtained by an evaporation method (see the ESI† for details). The structure is reported in Fig. 1.

The antiproliferative activity of compound **1** was evaluated by the MTT assay towards different cell lines, including the cancer cell lines SKOV-3 (human ovarian cancer), A2780 (human ovarian carcinoma) and A549 cells (human lung carcinoma) and cisplatin resistant cancer cells A2780cis and SKOV-3cis. Data were compared with those obtained using **L** or cisplatin and testing the compound against non-cancerous cell lines (Table 1). Compound **1** exhibits significant cytotoxicity against all the five tested cancerous cell lines with IC_{50} values in the low μM range, *i.e.* with values similar to those exhibited by cisplatin (Table 1). Interestingly, lower sensitivity for compound **1** is observed for two of three non-tumorigenic cell cultures. In contrast, cisplatin exerts high activity against all three control cultures comparable to the cancer cell lines. These data point to an increased cancer cell-specificity of compound **1** in comparison with cisplatin.

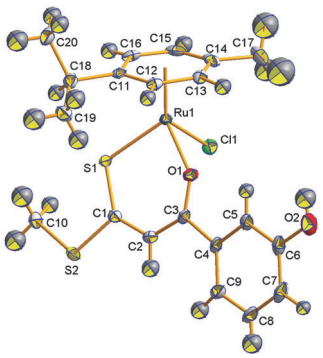

Fig. 1 Molecular structure (50% probability) of compound **1**. Selected bond lengths and angles: the Ru–centroid of the arene ligand (X*) = 1.667(3) Å; Ru–Cl1 = 2.4374(6) Å; Ru–O1 = 2.054(1) Å; Ru–S1 = 2.3415(4) Å; O1–Ru–Cl1 = 83.54(4)°; S1–Ru–Cl1, 88.33(2)°; S1–Ru–O1 = 90.25(4)°; O1–Ru–X* = 125.97(7)°; S1–Ru–X* = 127.97(6); Cl1–Ru–X* = 127.13(6)°. Further details, including the comparison between the structural features of compound **1** and those of L are reported in Tables S1–S3.† The structure has been deposited in the Cambridge Crystallographic Data Centre under the accession code 1476883.

Table 1 IC_{50} values in μM of compound **1** for the antiproliferative effects in cancerous and non-tumorigenic cells compared with the values obtained for ligand **L** and cisplatin. The incubation time was 48 h, and the mean values are from at least three independent experiments. Standard deviations are in parentheses (n.d. – not determined)

Cell line	Compound **1**	**L**	Cisplatin
SKOV-3	18.9 (0.8)	270.1 (18.0)	3.8 (2.8)
SKOV-3cis	12.1 (5.5)	189.5 (15.0)	13.5 (4.4)
A2780	8.7 (3.8)	63.2 (6.3)	1.3 (0.2)
A2780cis	7.4 (0.8)	175 (2.0)	6.1 (2.1)
A549	8.0 (8.5)	201.4 (29.3)	7.6 (2.6)
Keratinocytes	12.3 (6.9)	n.d.	5.7 (3.1)
Fibroblasts	76.4 (23.8)	n.d.	4.1 (1.1)
MCF10A	28.8 (7.1)	n.d.	3.3 (0.6)

The mechanism of action of ruthenium compounds is still debated although it is commonly believed that, at variance with Pt-based antitumor agents, like cisplatin, carboplatin and oxaliplatin that interact with DNA,[2] they preferentially hit protein targets.[15–17] For this reason, to obtain insights into the possible mechanisms of action of compound **1**, we have studied its reactivity with guanine derivative guanosine-5′-monophosphate (5′-GMP) and with the model protein bovine pancreatic ribonuclease (RNase A), which has already been shown to bind both Pt-[18–21] and Ru-based anticancer agents.[22] First, to assess the stability of compound **1** in different solvents, including mixed aqueous/solvent solutions used to test the cytotoxicity of the compound, UV-Vis absorption spectra were collected as a function of time (Fig. 2 and S1†). The changes in the spectral profile of compound **1** were monitored over 24 h at room temperature. The UV-Vis spectra of compound **1** in DMSO show an intense peak at 349 nm, a small peak at 296 nm and a shoulder at 457 nm (Fig. 2 and S1A†). The absorption bands at 296 and 349 nm were assigned to π–π*/n–π* transitions, while the low intense absorption band at approximately 457 nm to metal to ligand charge transfer (MLCT). Within 24 h, the complex seems rather stable, although it experiences a slow red shift of its main band up to 354 nm, accompanied by a progressive slow and very slight decrease in the intensity of all bands of the spectrum. The observed spectral changes reported in Fig. 2A and S1A† are similar to those observed when the compound is dissolved in 50% DMSO and 50% PBS at pH 7.4 (Fig. S1B†) and in 10% DMSO and 90% PBS at pH 7.4 (Fig. 2B). These spectral changes are consistent with those obtained in the case of other Ru–arene compounds[23] and are attributed to the occurrence of a ligand exchange process: for example in aqueous solutions these spectral changes are attributed to conversion of the starting chlorido complex into the corresponding aqua species. This is also demonstrated by the finding that, when dissolved in 1 M NaCl solution, aquation was significantly suppressed (Fig. S2†), due to an increased concentration of Cl^- anions inhibiting hydrolysis of the Ru–chloride bond.

Spectral modifications were observed also when the compound reacts in the presence of 5′-GMP (Fig. S3†). These changes appear even more significant when compound **1** reacts in the presence of RNase A (Fig. 2C) in 10% DMSO and 90% PBS at pH 7.4 or in 10 mM sodium citrate at pH 5.1 (Fig. S1C and D†). The latter condition was chosen since it can be used to test the catalytic activity of RNase A and to crystallize the protein (see below). Under these experimental conditions the behaviour of the compound in the presence of the protein (Fig. S1D†) is different when compared to that of

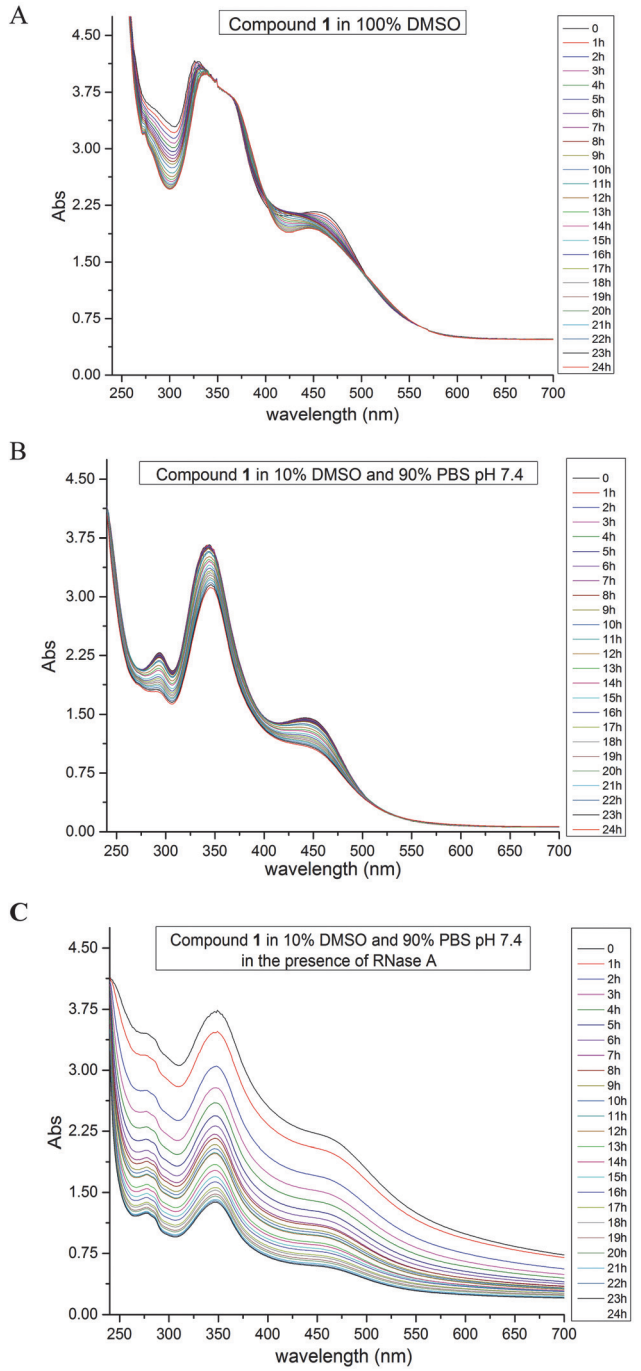

Fig. 2 UV-Vis spectra of 1 mM compound **1** in 100% DMSO (panel A) and in 90% PBS at pH 7.4, 10% DMSO in the absence (panel B) and presence of RNase A (panel C) in a 1 : 3 protein to metal molar ratio, following each 1 h over 24 h.

compound **1** alone (Fig. S1C†). These spectral changes were attributed to interaction of the compound with protein residue side chains and in particular with the side chains of His. This was confirmed by spectra collected in the presence of imidazole (Fig. S1E†) and by crystallographic studies reported below. Notably, RNase A remains active in the presence of compound **1** (Fig. S4†). These data are also consistent with the crystallographic finding that compound **1** does not bind in the enzyme active site (see below).

In order to obtain further information on the interactions that compound **1** can form with proteins, the structure of its adduct with RNase A was then solved by X-ray crystallography. Crystals of RNase A–compound **1** were obtained by soaking experiments where native protein crystals were incubated with an excess of the drug. The representative structure of RNase A–compound **1** is reported in Fig. 3. The model, containing two RNase A molecules (chains A and B hereafter) in the asymmetric unit (a.u), comprises 2373 non-H atoms and is refined to the *R*-factor and R_{free} values of 0.172 and 0.236, respectively. Crystallization, data collection, structure solution and refinement details are reported in the ESI.†

The overall structure of the protein is basically unaffected upon compound **1** binding. The root mean square deviation in the positions of carbon alpha atoms between the adduct and the native proteins is within the range of 0.33–0.60 Å.

The Ru binding sites were identified by analysing the Fourier difference and anomalous electron density maps (Fig. 4, S5 and S6†): the compound **1** fragment binds the side chain of His105 in both molecules of a.u. Unexpectedly, inspection of the e.d. maps reveals a change in the geometry of the coordination sphere of the Ru centre, which binds the imidazole of the His105 side chain, three water molecules and the O,S-chelating ligand in chain A (Fig. S5†), the imidazole of the His105 side chain, two DMSO molecules, the O,S-bidentate ligand and a water molecule in chain B (Fig. 4). These data unambiguously demonstrate that, at least under the investigated experimental conditions, a loss of the more labile η^6-*p*-cymene and chlorido ligands from the Ru centre together with a change in the metal coordination number (and thus in the geometry of the ruthenium coordination sphere) occurs upon protein binding. It is also interesting to note that the two fragments bound to the protein are different; thus the metal complex binds to the protein through two different binding

Fig. 3 Cartoon representation of the RNase A–compound **1** structure (chain B). The compound **1** binding site is also shown along with Ru and its ligands. Structural refinement suggests a partial occupancy of compound **1** equal to 0.40 and 0.50 in chains A and B, respectively. The *B*-factors of Ru atoms and ligand atoms in the A and B chains are 27.7, 15.6 Å^2 and in the range of 12.8–29.7 Å^2, respectively. The structure has been deposited in the Protein Data Bank under the accession code 5JLG.

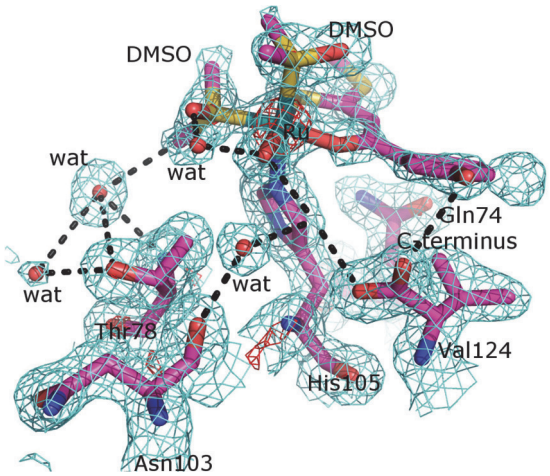

Fig. 4 Details of the compound **1** binding site in the RNase A–compound **1** adduct showing the Ru centre bound to His105. 2Fo–Fc electron density maps are contoured at 5σ (red) and 1σ (cyan) levels.

modes, *i.e.* with different patterns of ligand exchange. The loss of an arene ligand upon protein binding is unusual for a π-arene ruthenium(II) piano-stool compound. It was reported just in one paper, studying the interaction of ubiquitin with Ru(II)(η^6-$C_6H_5CF_3$)(PTA)Cl_2 (PTA = 1,3,5-triaza-7-phosphaadamantane), by mass spectrometry.[24]

To the best of our knowledge there are no other cases, documented with crystallographic data, of this kind of protein binding mode for a π-arene ruthenium(II) piano-stool compound. Interestingly, upon modification of its geometry the Ru centre adopts the octahedral coordination that is typical of the Ru compounds NAMI-A and KP1019 in clinical trials.[5]

In the X-ray structure of the half-sandwich arene Ru(II)–lysozyme complex, solved by Sadler and coworkers, the η^6-*p*-cymene ligand is retained and the geometry around the Ru centre is comparable to that of the [η^6-*p*-cymene Ru(L-His-methyl ester)Cl]Cl compound.[25]

Similarly, the η^6-*p*-cymene ligand is retained upon protein binding in the structures of a "piano-stool" organometallic Ru(II) arene compound encapsulated within the ferritin nanocage, solved by Ueno and coworkers.[26]

The X-ray structure of the adducts that NAMI-A forms with carbonic anhydrase[27] and hen egg white lysozyme[28] indicated that NAMI-A behaves as a prodrug, progressively releasing all Ru ligands, with naked Ru centers that bind the final target protein residues. Overall, the reactivity of compound **1** with proteins reveals the loss of ligands and an octahedral coordination of the Ru centre and thus a behaviour similar to that of NAMI-A.

In conclusion, here we have prepared and fully characterised a new π-arene ruthenium(II) piano-stool compound containing a O,S-chelating ligand. The cytotoxicity data show that it is active against five different cancer cell lines with IC_{50} values ranging from 7.4 μM to 18.9 μM likely with increased selectivity for cancer cells compared to cisplatin. The reactivity of the compound with a guanine derivative 5′-GMP and the model protein RNase A was analysed by UV-Vis absorption spectroscopy. The adduct that the compound forms with RNase A was studied by X-ray crystallography. The structure of the adduct is characterised by the presence of an octahedral Ru complex fragment where the O,S-chelating ligand is retained, whereas the η^6-*p*-cymene and chlorido ligands are lost. The octahedral geometry of the metal is completed by three solvent molecules (DMSO or water molecules) and by an N atom from the side chain of a protein residue. Overall, these observations disclose a peculiar mode of compound **1** binding to the model protein RNase A. This binding mode could be operative also with other proteins. To the best of our knowledge this is the first example of an adduct formed in the reaction between a cytotoxic Ru compound and a protein, where a change in the geometry and coordination number of the Ru centre favoured by protein binding was found.

The authors thank G. Sorrentino and M. Amendola for technical assistance.

Notes and references

1 (*a*) Y. W. Jung and S. J. Lippard, *Chem. Rev.*, 2007, **107**, 1387–1407; (*b*) *Cisplatin – Chemistry and Biochemistry of a Leading Anticancer Drug*, ed. B. Lippert, VCHA, Zürich, Wiley-VCH, Weinheim, 1999, pp. 1–563; (*c*) S. Dasari and P. B. Tchounwou, *Eur. J. Pharmacol.*, 2014, **740**, 364–78.

2 (*a*) G. Sava, A. Bergamo and P. J. Dyson, *Dalton Trans.*, 2011, **40**, 9069–9075; (*b*) C. G. Hartinger and P. J. Dyson, *Chem. Soc. Rev.*, 2009, **38**, 391–401; (*c*) C. G. Hartinger, N. Metzler-Nolte, P. J. Dyson and G. Sava, *Organometallics*, 2012, **31**, 5677–5685; (*d*) *Metal Complexes in Tumor Diagnosis and as Amticancer Agents*, ed. A. Sigel, H. Sigel, M. Dekker, Inc., York & Basel, 2004, pp. 1–534.

3 (*a*) T. C. Johnstone, K. Suntharalingam and S. J. Lippard, *Chem. Rev.*, 2016, **116**(5), 3436–86; (*b*) S. Dilruba and G. V. Kalayda, *Cancer Chemother. Pharmacol.*, 2016, **77**(6), 1103–24.

4 L. Kelland, *Nat. Rev. Cancer*, 2007, **7**, 573–584.

5 (*a*) S. Nobili, E. Mini, I. Landini, C. Gabbiani, A. Casini and L. Messori, *Med. Res. Rev.*, 2010, **30**(3), 550–80; (*b*) B. Bertrand and A. Casini, *Dalton Trans.*, 2014, **43**(11), 4209–19.

6 (*a*) E. Alessio, G. Mestroni, A. Bergamo and G. Sava, *Curr. Top. Med. Chem.*, 2004, **4**(15), 1525–35; (*b*) S. Komeda and A. Casini, *Curr. Top. Med. Chem.*, 2012, **12**(3), 219–35.

7 W. H. Ang, A. Casini, G. Sava and P. J. Dyson, *J. Organomet. Chem.*, 2011, **696**, 989–998.

8 M. Groessl, E. Reisner, C. G. Hartinger, R. Eichinger, O. Semenova, A. R. Timerbaev, M. A. Jakupec, V. B. Arion and B. K. Keppler, *J. Med. Chem.*, 2007, **508**(9), 2185–2193.

9 C. G. Hartinger, M. A. Jakupec, S. Zorbas-Seifried, M. Groessl, A. Egger, W. Berger, H. Zorbas, P. J. Dyson and B. K. Keppler, *Chem. Biodiversity*, 2008, **5**(10), 2140–55.

10 (*a*) A. Bergamo, A. Masi, A. F. A. Peacock, A. Habtemariam, P. J. Sadler and G. Sava, *J. Inorg. Biochem.*, 2010, **104**, 79–86; (*b*) M. Frik, A. Martinez, B. T. Elie, O. Gonzalo, D. R. de Mingo, M. Sanau, R. Sanchez-Delgado, T. Sadhukha, S. Prabha, J. W. Ramos, I. Marzo and M. Contel, *J. Med. Chem.*, 2014, **57**, 9995–10012.

11 (*a*) C. Scolaro, A. Bergamo, L. Brescacin, R. Delfino, M. Cocchietto, G. Laurenczy, T. J. Geldbach, G. Sava and P. J. Dyson, *J. Med. Chem.*, 2005, **48**, 4161–4171; (*b*) A. Bergamo, A. Masi, P. J. Dyson and G. Sava, *Int. J. Oncol.*, 2008, **33**, 1281–1289; (*c*) A. Weiss, R. H. Berndsen, M. Dubois, C. Mueller, R. Schibli, A. W. Griffioen, P. J. Dyson and P. Nowak-Sliwinska, *Chem. Sci.*, 2014, **5**, 4742–4748.

12 C. Mügge, R. Liu, H. Görls, C. Gabbiani, E. Michelucci, N. Rüdiger, J. H. Clement, L. Messori and W. Weigand, *Dalton Trans.*, 2014, **43**(8), 3072–86.

13 C. Mügge, D. Musumeci, E. Michelucci, F. Porru, T. Marzo, L. Massai, L. Messori, W. Weigand and D. Montesarchio, *J. Inorg. Biochem.*, 2016, **160**, 198–209.

14 C. Mügge, T. Marzo, L. Massai, J. Hildebrandt, G. Ferraro, P. Rivera-Fuentes, N. Metzler-Nolte, A. Merlino, L. Messori and W. Weigand, *Inorg. Chem.*, 2015, **54**, 8560–8570.

15 (*a*) L. Messori, P. Orioli, D. Vullo, E. Alessio and E. Iengo, *Eur. J. Biochem.*, 2000, **267**, 1206–1213; (*b*) M. Ravera, S. Baracco, C. Cassino, D. Colangelo, G. Bagni, G. Sava and D. Osella, *J. Inorg. Biochem.*, 2004, **98**, 984–990.

16 (*a*) A. Bergamo, L. Messori, F. Piccioli, M. Cocchietto and G. Sava, *Invest. New Drugs*, 2003, **21**, 401–411; (*b*) G. Sava, F. Frausin, M. Cocchietto, F. Vita, E. Podda, P. Spessotto, A. Furlani, V. Scarcia and G. Zabucchi, *Eur. J. Cancer*, 2004, **40**, 1383–1396.

17 (*a*) F. Frausin, V. Scarcia, M. Cocchietto, A. Furlani, B. Serli, E. Alessio and G. Sava, *J. Pharmacol. Exp. Ther.*, 2005, **313**, 227–233; (*b*) S. Kapitza, M. Pongratz, M. A. Jakupec, P. Heffeter, W. Berger, L. Lackinger, B. K. Keppler and B. Marian, *J. Cancer Res. Clin. Oncol.*, 2005, **131**, 101–110.

18 L. Messori and A. Merlino, *Inorg. Chem.*, 2014, **53**(8), 3929–31.

19 L. Messori, T. Marzo and A. Merlino, *J. Inorg. Biochem.*, 2015, **153**, 136–42.

20 D. Picone, F. Donnarumma, G. Ferraro, I. Russo Krauss, A. Fagagnini, G. Gotte and A. Merlino, *J. Inorg. Biochem.*, 2015, **146**, 37–43.

21 L. Messori, T. Marzo, E. Michelucci, I. Russo Krauss, C. Navarro-Ranninger, A. G. Quiroga and A. Merlino, *Inorg. Chem.*, 2014, **53**(15), 7806–8.

22 A. Vergara, I. Russo Krauss, D. Montesarchio, L. Paduano and A. Merlino, *Inorg. Chem.*, 2013, **52**(19), 10714–6.

23 A. Rilak, I. Bratsos, E. Zangrando, J. Kljun, I. Turel, Z. D. Bugarcic and E. Alessio, *Inorg. Chem.*, 2014, **53**, 6113–6126.

24 A. E. Egger, C. G. Hartinger, A. K. Renfrew and P. J. Dyson, *J. Biol. Inorg. Chem.*, 2010, **15**(6), 919–927.

25 I. W. McNae, K. Fishburne, A. Habtemariam, T. M. Hunter, M. Melchart, F. Wang, M. D. Walkinshawa and P. J. Sadler, *Chem. Commun.*, 2004, 1786–1787.

26 Y. Takezawa, P. Bockmann, N. Sugi, Z. Wang, S. Abe, T. Murakami, T. Hikage, G. Erker, Y. Watanabe, S. Kitagawa and T. Ueno, *Dalton Trans.*, 2011, **40**, 2190–2195.

27 A. Casini, C. Temperini, C. Gabbiani, C. T. Supuran and L. Messori, *ChemMedChem*, 2010, **5**, 1989–1994.

28 L. Messori and A. Merlino, *Dalton Trans.*, 2014, **43**(16), 6128–31.

Supplementary information

Unusual mode of protein binding by a cytotoxic π-arene ruthenium(II) piano-stool compound containing an O,S–chelating ligand

Jana Hildebrandt,[a] Helmar Görls,[a] Norman Häfner,[b] Giarita Ferraro,[c] Matthias Dürst,[b] Ingo B. Runnebaum,[b] Wolfgang Weigand,[a,*] and Antonello Merlino[c,d,*]

Materials and Methods

Materials and Methods

Synthesis and characterization of Compound 1

The β-hydroxy dithiocinnamic methyl ester and $[(\eta^6\text{-}p\text{-cymene})RuCl_2]_2$ were prepared using protocols available in literature, with minor modifications. $[(\eta^6\text{-}p\text{-cymene})RuCl_2]_2$ (0.5 equiv, 500 mg, 0.81 mmol) was dissolved in 50 mL tetrahydrofurane (THF). The β-hydroxy dithiocinnamic methyl ester (1 equiv, 367 mg, 1.62 mmol) was dissolved in 25 mL THF. Potassium-*tert*-butoxylate (*t*-BuOK, 2 equiv, 182 mg, 1.62 mmol) was added to that solution and stirred 30 min at room temperature (r.t.). The solution of the deprotonated ligand was added dropwise to the suspension of $[(\eta^6\text{-}p\text{-cymene})RuCl_2]_2$ and stirred at rt for 24 h. After adding sulfuric acid (H_2SO_4, 20 ml, 2M) to the solution, the mixture was stirred for 30 min and afterwards extracted with dichloromethane (DCM, 3 x 30 mL). The combined organic phases were washed with water (3 x 20 mL) and dried over sodium sulfate. After filtration and evaporation of the solvent, the crude product was purified with column chromatography. Column chromatography mobile phase: DCM - DCM 10:THF 1 – THF. Yield: 190 mg (23.6%) as red crystals. ^{1}H NMR (600 MHz, CD_2Cl_2): δ = 1.26 (d, $^3J_{H\text{-}H}$=6.4 Hz, 6H, -cymene-CH-(CH_3)$_2$); 2.20 (s, 3H, CH_3, -cymene-CH_3); 2.64 (s, 3H, -SCH_3); 2.83 (sp, 1H, -cymene-C*H*-(CH_3)$_2$); 5.33 (m, 2H, -cymene:CH_3-C-C*H*-CH-C-CH-(CH_3)$_2$); 5.52 (m, 2H –cymene:CH_3-C-CH-C*H*-C-CH-(CH_3)$_2$); 6.71 (s, 1H, =C*H*); 6.85 (m, 2H, -Ar-*o*-H); 7.11 (m, 1H, -Ar-*m*-H); 7.23 (m, 3H, =C*H*/ -Ar-*p*-H); 10.1 (s, 1H, -CO*H*). ^{13}C{^{1}H} NMR (101 MHz, CD_2Cl_2): δ = 17.6 (-SCH_3); 18.3 (-cymene-C-*C*H_3); 22.4 (-cymene-CH-(*C*H_3)$_2$); 30.9 (-cymene-*C*H-(CH_3)$_2$); 83.3 (-cymene:CH_3-C-*C*H-CH-C-CH-(CH_3)$_2$); 83.8 (CH_3-C-*C*H-CH-C-CH-(CH_3)$_2$); 85.5 (CH_3-C-CH-*C*H-C-CH-(CH_3)$_2$); 85.6 (CH_3-C-CH-*C*H-C-CH-(CH_3)$_2$); 100.8 (CH_3-*C*-CH-CH-C-CH-(CH_3)$_2$); 102.3 (CH_3-C-CH-CH-*C*-CH-(CH_3)$_2$); 109.2 (=*C*H); 125.2 (-Ar-*m*-C); 129.2 (-Ar-*o*-C); 129.4 (-*C*OH); 156.9 (-Ar-*p*-C); 178.0 (-Ar*C*1); 187.3 (-*C*-O-); 207.2 (-*C*=S). MS (DEI): m/z = 134, 119, 115, 91, 77, 39, 28. Elemental analysis: calculated for $C_{20}H_{23}ClO_2RuS_2$ C: 48.43%; H: 4.67%; S: 12.93%, found: C: 48.33%; H: 4.83%; S: 12.42%.

Crystal structure determination

To obtain single crystals of Compound **1**, the sample was dissolved in a DCM solution after addition of a few drop of methanol. Crystals were grown by slow evaporation of the solvent. X-ray diffraction data were collected at University of Jena using a Nonius KappaCCD diffractometer and graphite-monochromated Mo-Kα radiation. The intensity data were collected on a Nonius KappaCCD diffractometer, using graphite-monochromated Mo-K_α radiation. Data were corrected for Lorentz and polarization effects; absorption was taken into account on a semi-empirical basis using multiple-scans [1-3]. The structure was solved by direct methods (SHELXS [4]) and refined by full-matrix least squares techniques against Fo^2 (SHELXL-97 [4]). All hydrogen atoms were located by difference Fourier synthesis and refined isotropically. All non-hydrogen atoms were refined anisotropically [4]. Crystallographic data and refinement statistics are reported in Table S1. Details on the structure are in Table S2. A comparison of selected bond lengths and angles of Compound **1** with data obtained for the ligand **L** are reported in Table S3.

Crystallographic data for Compound **1** have been deposited at the Cambridge Crystallographic Data Centre under the accession code CCDC-1476883, They contain the supplementary crystallographic data excluding structure factors; these data can be obtained free of charge via www.ccdc.cam.ac.uk/conts/retrieving.html (or from the Cambridge Crystallographic Data Centre, 12, Union Road, Cambridge CB2 1EZ, UK; fax: (+44) 1223-336-033; or deposit@ccdc.cam.ac.uk).

Cytotoxicity

The IC50 values of Compound **1**, L and Cisplatin was determined by means of the colorimetric MTT assay (MTT = 3-(4,5-dimethyl-2-thiazolyl)-2,5-diphenyl-2Htetrazolium bromide), CellTiter96 non-radioactive proliferation assay (Promega) [5]. For this purpose, cancer cell lines were cultured under standard conditions (5 % CO2, 37 °C, 90 % humidity) in RPMI medium supplemented with 10 % FCS, 100 U/ml penicillin and 100 µg/ml streptomycin (Life Technologies, Germany). Cisplatin (Sigma, Germany) was freshly dissolved at 1 mg/ml in 0.9 % NaCl solution and diluted appropriately. Compound 1 and L were dissolved in dmso. After seeding 5000 cells per well in a 96-well plate cells were allowed to attach for 24h and were incubated for 48h with different concentrations of the substances ranging from 0 to 500 µM for Compound 1 and 0 to 1000 µM for L tests. Each measurement was done in triplicate and repeated 3-times. The proportion of live cells was quantified by the MTT assay and after background subtraction relative values compared to the mean of medium controls were calculated. Non-linear regression analyses applying the Hill-slope were run in GraphPad 5.0 software. Platinum-resistant A2780 and SKOV3 cells were established by repeated rounds of three day incubations with increasing amounts of Cisplatin starting with 0.1 µM. The concentration was doubled after three incubations interrupted by recovery phases with normal medium. Cells that survived the third round of 12.8 µM Cisplatin were defined as resistant cultures. Analyzed control samples of non-tumorigenic cells included normal keratinocytes, normal fibroblasts and the immortal non-tumorigenic epithelial mammary gland cell line MCF-10A. Primary keratinocytes and fibroblasts were isolated from two individual human foreskins. Cultures of normal cells were used at early passages still showing cell proliferation.

UV-Vis absorption spectroscopy

UV-vis spectra of Compound **1** were recorded at room temperature on a Varian Cary 5000 UV-Vis-NIR spectrophotometer using 1 cm path length cuvette. The spectra were collected in the 240-700 nm range every 1 nm at a scan rate of 600 nm min^{-1}. The

spectral profile of Compound **1** was analysed under different experimental conditions: in pure DMSO, in a 50% DMSO and 50% PBS pH 7.4 solution and in 10 mM sodium citrate, in the absence and in the presene of RNase A (protein to metal ratio 1:3), that was the condition used to grow protein crystals.

Crystallization, X-ray diffraction data collection, structure resolution and refinement of RNase A-Compound 1 adduct

Crystals of RNase A were obtained as previously described [6]. Crystals of the adduct were obtained by soaking procedure (4 days) as described in previous works [7-8]. Briefly, 1 µL solution of Compound **1** dissolved in DMSO was mixed with an equal amount of precipitant solution. Then, half of the resulting solution was added to the drop containing crystals of RNase A. After four days of soaking, X-ray diffraction data were collected at the CNR Institute of Biostructures and Bioimages, using a Saturn944 CCD detector equipped with CuKα X-ray radiation from a Rigaku Micromax 007 HF generator. Crystals were dehydrated [10] and data collection was performed without addition of cryoprotectants [9]. Data sets were processed, merged and scaled using Mosflm [11]. Data collection statistics are reported in Table S1.

The structure was solved by molecular replacement method, using protein atoms of chain A from pdb file 1JVT [12] as a starting model and the program Phaser [13]. Structure was refined with Refmac5.7 [14]. Model building, addition of ligands and inspection of electron density maps were performed using Coot [15]. The electron density m¸ap is very well definied for all residues of the two molecules in the asymmetric unit with exceptions of the regions encompassing residuies 16-22 that are rather disordered in both the two chains. Model refines against data to 1.79 Å resolution with Rfactor and Rfree values of 17.9 and 23.6 %. The model was also refined against all the data collected with $CC_{1/2}$>0.3 following the indications of Diederichs and Karplus [16-17], up to 1.51 Å resolution, with Rfactor and Rfree values of 17.8 and 23.9 %. However at this resolution the completeness is too low (overal completeness=60.6%), and thus the model refined and the structure factors at 1.79 Å resolution were deposited in the Protein Data Bank (PDB code 5JLG). Refinement statistics are reported in Table S1. Structure validations were carried out using Whatcheck [18]. Final structure has 3 residues in the disallowed region of the Ramachandran plot, which correspond to Ser22 and Gln60 in the chain A, Ser16 in the chain B. In the Fo-.Fc electron density maps there are just five peaks > 5 σ uninterpreted. Four out of these peaks could correspond to solvent molecules alternative to Compound 1 fragment bound to the protein.

References

1. COLLECT, Data Collection Software; Nonius B.V., Nether¬lands, 1998
2. Z. Otwinowski & W. Minor, „Processing of X-Ray Diffraction Data Collected in Oscillation Mode“, in Methods in Enzymology, Vol. 276, Macromolecular Crystallography, Part A, edited by C.W. Carter & R.M. Sweet, pp. 307-326, Academic Press, San Diego, USA, 1997
3. SADABS 2.10, Bruker-AXS inc., 2002, Madison, WI, U.S.A
4. Sheldrick, G. M. Acta Cryst. (2008). A46, 112-122.
5. T. Mosmann. *Journal of Immunological Methods* **65** (1–2): 55–63.
6. L. Vitagliano, A. Merlino, A. Zagari, L. Mazzarella. *Proteins Sci* 2000, **9**, 1217-1225.
7. L. Messori, A. Merlino. *Inorg. Chem*. 2014, **53**, 3929-3931.
8. L. Messori, T. Marzo, E. Michelucci, I. Russo Krauss, C. Navarro-Ranninger, A. G. Quiroga, A. Merlino. *Inorg Chem*. 2014, **53**, 7806-7808.
9. I. Russo Krauss, F. Sica, C.A. Mattia, A. Merlino. *Int J Mol Sci*. 2012, **13**, 3782-3800.
10. E. Pellegrini, D. Piano, M. W. Bowler. *Acta Crystallogr D Biol Crystallogr.* 2011, **67**, 902–906.
11. T. G. G. Battye, L. Kontogiannis, O. Johnson, H. R. Powell, A. G. W. Leslie. *Acta Crystallogr D Biol Crystallogr*. 2011, **67** (Pt 4), 271–281.
12. L. Vitagliano, A. Merlino, A. Zagari, L. Mazzarella. Proteins 2002, **46**, 97-104
13. A. J. McCoy, R.W.Grosse-Kunstleve, P. D. Adams, M. D. Winn, L.C. Storoni, R.J. Read. J *Appl Crystallogr.* 2007, **40**, 658–674.
14. G. N. Murshudov, P. Skubak, A. A. Lebedev, N. S. Pannu, R. A. Steiner, R. A. Nicholls, M. D. Winn, F. Long, A. A. Vagin, *Acta Crystallogr., Sect. D: Biol. Crystallogr*. 2011, **67**, 355-367.
15. P. Emsley, B. Lohkamp, W. G. Scott, K. Cowtan. *Acta Crystallogr D Biol Crystallogr.* 2010, **66**, 486–501.
16. P.A. Karplus, K. Diederichs. *Science* 2012, **336**(6084), 1030-1033.
17. K. Diederichs, P.A. Karplus *Acta Crystallogr D Biol Crystallogr*. 2013, **69** (Pt 7), 1215-1222.
18. R.W.W. Hooft, G. Vriend, C. Sander, E. E. Abola, *Nature* 1996, **381**, 272.
19. M. Kunitz. *J. Biol. Chem*. 1946, **164**, 563–568.

Table S1. Crystal data and structure refinement for Compound **1**.

	Compound **1**
Empirical formula	C20 H23 Cl O2 Ru S2
Formula weight	496.02
Temperature	133(2) K
Wavelength	0.71073 Å
Crystal system	Orthorhombic
Space group	Pna2(1)
Unit cell dimensions	a = 22.1070(4) Å
	b = 11.4122(2) Å
	c = 7.9006(1) Å
Volume	1993.24(6) $Å^3$
Z	4
Density (calculated)	1.653 Mg x m^{-3}
Absorption coefficient	1.142 mm^{-1}
F(000)	1008
Crystal size	0.042 x 0.038 x 0.012 mm3
θ range for data collection	3.27 to 27.49°.
Index ranges	-28<=h<=28, -14<=k<=14, -10<=l<=8
Reflections collected	13265
Independent reflections	4028 [R(int) = 0.0207]
Completeness to θ = 27.49°	99.6 %
Absorption correction	Semi-empirical from equivalents
Max. and min. transmission	0.7456 and 0.6881
Refinement method	Full-matrix least-squares on F2
Data / restraints / parameters	4028 / 1 / 327
Goodness-of-fit on F2	1.070
Final R indices [I>2sigma(I)]	R1 = 0.0149, wR2 = 0.0362
R indices (all data)	R1 = 0.0151, wR2 = 0.0364
Absolute structure parameter	-0.012(18)
Largest diff. peak and hole	0.236 and -0.284 e^- x $Å^{-3}$

Table S2. Bond lengths [Å] and angles [°] for Compound **1.**

Ru(1)-O(1)	2.0538(12)
Ru(1)-C(15)	2.1644(18)
Ru(1)-C(16)	2.1717(19)
Ru(1)-C(12)	2.175(2)
Ru(1)-C(11)	2.1984(19)
Ru(1)-C(13)	2.208(2)
Ru(1)-C(14)	2.2351(19)
Ru(1)-S(1)	2.3415(4)
Ru(1)-Cl(1)	2.4374(6)
S(1)-C(1)	1.6892(19)
S(2)-C(1)	1.7614(19)
S(2)-C(10)	1.800(2)
O(1)-C(3)	1.268(2)
O(2)-C(6)	1.364(3)
O(2)-H(1O2)	0.78(3)
C(1)-C(2)	1.381(2)
C(2)-C(3)	1.407(3)
C(2)-H(2)	0.93(2)
C(3)-C(4)	1.502(2)
C(4)-C(9)	1.389(3)
C(4)-C(5)	1.396(3)
C(5)-C(6)	1.393(2)
C(5)-H(5)	0.94(2)
C(6)-C(7)	1.391(3)
C(7)-C(8)	1.379(3)
C(7)-H(7)	0.94(2)
C(8)-C(9)	1.397(3)
C(8)-H(8)	0.86(3)
C(9)-H(9)	0.99(3)
C(10)-H(10C)	0.94(3)
C(10)-H(10B)	0.95(3)
C(10)-H(10A)	0.94(3)
C(11)-C(12)	1.413(3)
C(11)-C(16)	1.427(3)
C(11)-C(18)	1.513(3)
C(12)-C(13)	1.425(3)
C(12)-H(12)	0.94(2)
C(13)-C(14)	1.397(3)
C(13)-H(13)	0.97(2)
C(14)-C(15)	1.425(3)
C(14)-C(17)	1.507(3)
C(15)-C(16)	1.402(3)
C(15)-H(15)	0.96(3)
C(16)-H(16)	0.90(2)
C(17)-H(17C)	0.94(3)
C(17)-H(17B)	1.02(3)
C(17)-H(17A)	0.92(4)
C(18)-C(19)	1.522(3)
C(18)-C(20)	1.529(3)
C(18)-H(18)	0.96(2)
C(19)-H(19B)	0.91(3)
C(19)-H(19A)	1.00(4)
C(19)-H(19C)	0.91(3)
C(20)-H(20C)	0.92(3)
C(20)-H(20B)	0.94(3)
C(20)-H(20A)	0.96(3)

O(1)-Ru(1)-C(15)	148.69(7)
O(1)-Ru(1)-C(16)	159.40(7)
C(15)-Ru(1)-C(16)	37.74(8)
O(1)-Ru(1)-C(12)	92.70(7)
C(15)-Ru(1)-C(12)	80.20(8)
C(16)-Ru(1)-C(12)	67.69(8)
O(1)-Ru(1)-C(11)	121.59(6)
C(15)-Ru(1)-C(11)	68.81(7)
C(16)-Ru(1)-C(11)	38.11(7)
C(12)-Ru(1)-C(11)	37.70(7)
O(1)-Ru(1)-C(13)	88.70(6)
C(15)-Ru(1)-C(13)	66.97(8)
C(16)-Ru(1)-C(13)	79.60(7)
C(12)-Ru(1)-C(13)	37.92(8)
C(11)-Ru(1)-C(13)	68.36(7)
O(1)-Ru(1)-C(14)	111.41(7)
C(15)-Ru(1)-C(14)	37.76(8)
C(16)-Ru(1)-C(14)	68.07(8)
C(12)-Ru(1)-C(14)	67.76(9)
C(11)-Ru(1)-C(14)	81.28(7)
C(13)-Ru(1)-C(14)	36.63(8)
O(1)-Ru(1)-S(1)	90.25(4)
C(15)-Ru(1)-S(1)	120.41(6)
C(16)-Ru(1)-S(1)	92.71(6)
C(12)-Ru(1)-S(1)	115.64(6)
C(11)-Ru(1)-S(1)	89.84(5)
C(13)-Ru(1)-S(1)	153.39(6)
C(14)-Ru(1)-S(1)	158.17(6)
O(1)-Ru(1)-Cl(1)	83.54(4)
C(15)-Ru(1)-Cl(1)	90.63(6)
C(16)-Ru(1)-Cl(1)	116.90(6)
C(12)-Ru(1)-Cl(1)	155.81(6)
C(11)-Ru(1)-Cl(1)	154.81(5)
C(13)-Ru(1)-Cl(1)	117.93(6)
C(14)-Ru(1)-Cl(1)	91.32(6)
S(1)-Ru(1)-Cl(1)	88.333(19)
C(1)-S(1)-Ru(1)	110.14(7)
C(1)-S(2)-C(10)	104.65(9)
C(3)-O(1)-Ru(1)	134.09(11)
C(6)-O(2)-H(1O2)	113(2)
C(2)-C(1)-S(1)	129.20(15)
C(2)-C(1)-S(2)	113.15(14)
S(1)-C(1)-S(2)	117.59(10)
C(1)-C(2)-C(3)	127.12(17)
C(1)-C(2)-H(2)	115.9(15)
C(3)-C(2)-H(2)	116.8(15)
O(1)-C(3)-C(2)	126.18(15)
O(1)-C(3)-C(4)	113.91(15)
C(2)-C(3)-C(4)	119.90(16)
C(9)-C(4)-C(5)	119.84(17)
C(9)-C(4)-C(3)	123.85(18)
C(5)-C(4)-C(3)	116.28(16)
C(6)-C(5)-C(4)	120.29(18)
C(6)-C(5)-H(5)	117.8(13)
C(4)-C(5)-H(5)	122.0(13)
O(2)-C(6)-C(7)	118.38(17)
O(2)-C(6)-C(5)	121.77(19)

C(7)-C(6)-C(5)	119.84(19)
C(8)-C(7)-C(6)	119.62(18)
C(8)-C(7)-H(7)	120.9(13)
C(6)-C(7)-H(7)	119.5(13)
C(7)-C(8)-C(9)	121.2(2)
C(7)-C(8)-H(8)	120.1(18)
C(9)-C(8)-H(8)	118.7(18)
C(4)-C(9)-C(8)	119.2(2)
C(4)-C(9)-H(9)	124.9(15)
C(8)-C(9)-H(9)	115.5(15)
S(2)-C(10)-H(10C)	114.0(14)
S(2)-C(10)-H(10B)	106.0(18)
H(10C)-C(10)-H(10B)	107(2)
S(2)-C(10)-H(10A)	114.9(17)
H(10C)-C(10)-H(10A)	101(2)
H(10B)-C(10)-H(10A)	114(2)
C(12)-C(11)-C(16)	116.93(18)
C(12)-C(11)-C(18)	123.40(19)
C(16)-C(11)-C(18)	119.61(17)
C(12)-C(11)-Ru(1)	70.23(12)
C(16)-C(11)-Ru(1)	69.93(11)
C(18)-C(11)-Ru(1)	128.16(13)
C(11)-C(12)-C(13)	121.5(2)
C(11)-C(12)-Ru(1)	72.07(12)
C(13)-C(12)-Ru(1)	72.33(13)
C(11)-C(12)-H(12)	118.7(14)
C(13)-C(12)-H(12)	119.7(14)
Ru(1)-C(12)-H(12)	125.0(15)
C(14)-C(13)-C(12)	121.26(19)
C(14)-C(13)-Ru(1)	72.72(12)
C(12)-C(13)-Ru(1)	69.75(12)
C(14)-C(13)-H(13)	121.0(14)
C(12)-C(13)-H(13)	117.6(14)
Ru(1)-C(13)-H(13)	126.6(14)
C(13)-C(14)-C(15)	117.52(18)
C(13)-C(14)-C(17)	120.7(2)
C(15)-C(14)-C(17)	121.6(2)
C(13)-C(14)-Ru(1)	70.65(11)
C(15)-C(14)-Ru(1)	68.43(11)
C(17)-C(14)-Ru(1)	128.30(16)
C(16)-C(15)-C(14)	121.49(19)
C(16)-C(15)-Ru(1)	71.41(11)
C(14)-C(15)-Ru(1)	73.81(11)
C(16)-C(15)-H(15)	120.3(14)
C(14)-C(15)-H(15)	117.6(14)
Ru(1)-C(15)-H(15)	119.9(14)
C(15)-C(16)-C(11)	121.24(18)
C(15)-C(16)-Ru(1)	70.85(11)
C(11)-C(16)-Ru(1)	71.96(10)
C(15)-C(16)-H(16)	120.0(16)
C(11)-C(16)-H(16)	118.5(15)
Ru(1)-C(16)-H(16)	126.0(16)
C(14)-C(17)-H(17C)	108(2)
C(14)-C(17)-H(17B)	112(2)
H(17C)-C(17)-H(17B)	116(3)
C(14)-C(17)-H(17A)	113(2)
H(17C)-C(17)-H(17A)	104(3)
H(17B)-C(17)-H(17A)	103(4)

C(11)-C(18)-C(19)	112.84(17)
C(11)-C(18)-C(20)	109.64(17)
C(19)-C(18)-C(20)	111.1(2)
C(11)-C(18)-H(18)	107.6(14)
C(19)-C(18)-H(18)	109.4(14)
C(20)-C(18)-H(18)	105.9(15)
C(18)-C(19)-H(19B)	109.6(17)
C(18)-C(19)-H(19A)	109.2(14)
H(19B)-C(19)-H(19A)	108(3)
C(18)-C(19)-H(19C)	109.6(18)
H(19B)-C(19)-H(19C)	109(2)
H(19A)-C(19)-H(19C)	112(3)
C(18)-C(20)-H(20C)	109(2)
C(18)-C(20)-H(20B)	108.4(14)
H(20C)-C(20)-H(20B)	112(3)
C(18)-C(20)-H(20A)	110.1(15)
H(20C)-C(20)-H(20A)	107(2)
H(20B)-C(20)-H(20A)	111(2)

Table S3. Selected distances [Å] and angles [°] of Compound **1** compared to those observed for **L**

	L	Compound **1**
O(1)-Ru(1)		2.0538(12)
S(1)-Ru(1)		2.3415(4)
Cl(1)-Ru(1)		2.4374(6)
O(1)-C(3)	1.330(6)	1.268(2)
C(3)-C(4)	1.477(6)	1.502(2)
S(1)-C(1)	1.662(5)	1.6892(19)
O(2)-C(8/6)	1.376(6)	1.364(3)
S(1)-Ru(1)-O(1)		90.25(4)
S(1)-Ru(1)-Cl(1)		88.333(19)
O(1)-Ru(1)-Cl(1)		83.54(4)

Table S4. Data collection and refinement statistics of the RNase A-Compound **1** adduct

	RNase A-Compound **1**
PDB code	5JLG
Data collection temperature (K)	100
Data reduction	
Space group	C2
Unit cell parameters	
a (Å)	100.47
b (Å)	32.74
c (Å)	72.45
β	90.06
Molecules per asymmetric unit	2
Observed reflections	57189
Unique reflections	22643
Resolution (Å)	72.47-1.79 (1.83-1.79)
Completeness (%)	78.7 (70.2)
Rmerge (all I+ and I-)	0.064 (0.242)
Rmerge in top intensity bin	0.047
Rpim	0.050 (0.238)
I/σ(I)	10.5 (2.4)
Multiplicity	2.9 (2.0)
Refinement	
Resolution (Å)	72.47-1.79
number of reflections in working set	16805
number of reflections in test set	906
R-factor/Rfree/Rall (%)	17.2/23.6/17.5
Number of residues	2 x 124
Non-H atoms used in the refinement	2373
Mean B-value (Å^2)	23.6
Ru atom occupancy	0.4, 0.5
Ru atom B-factor (Å^2)	27.7, 15.6
Estimated overall coordinate errors	
Rmsd bonds (Å)	0.015
Rmsd angles (°)	1.74
Ramachandran values (%) from Coot	
Preferred region	95.6
Allowed	2.9 (number of residues:6)
Disallowed	1.9 (number of residues:3)

Parentheses indicate information for highest resolution shell.

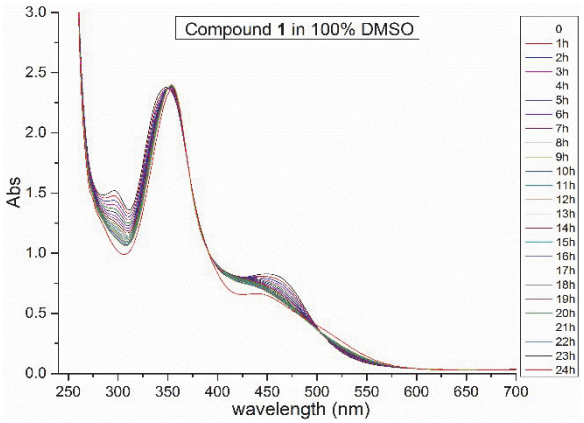

A

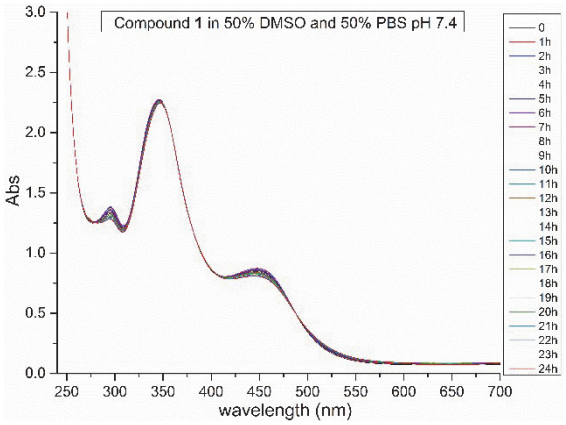

B

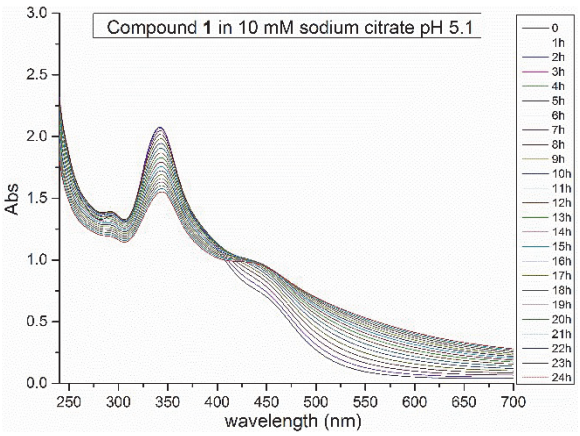

C

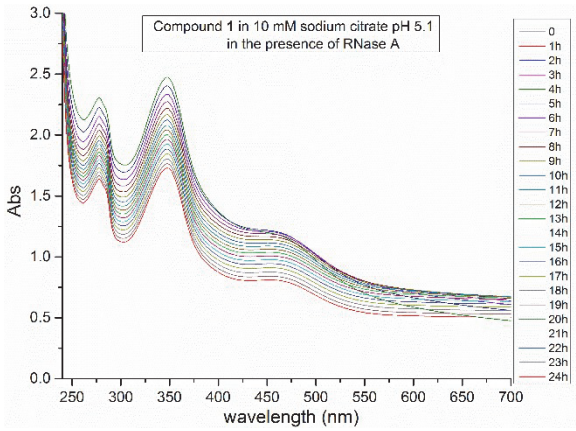

D

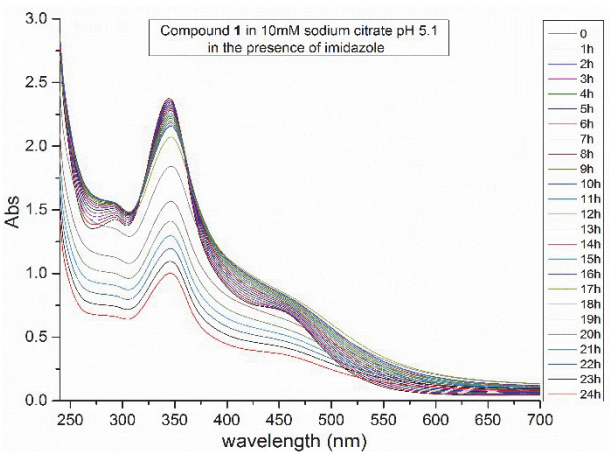

E

Figure S1. UV-Vis spectra of 0.3 mM Compound **1** under different experimental conditions followed each 1 h over 24 h. (A) 100 % DMSO; (B) 50 % DMSO; 50 % PBS pH 7.4. (C) 10 mM sodium citrate pH 5.1; (D) 10 mM sodium citrate pH 5.1, protein:metallodrug ratio 1:3; (E) 10 mM sodium citrate pH 5.1, protein:imidazole ratio 1:3;

UV/Vis spectra of Compound 1 in DMSO show an intense peak at 346 nm, a small peak at 296 nm and a shoulder at 457 nm. The Compound experiences a slow red shift of its main band up to 354 nm, accompained by a progressive slow decrease in intensity of all bands of the spectrum.

UV/Vis spectra of Compound 1 in PBS pH 7.4 show a similar behaviour when compared to the spectra of the compound in DMSO, although changes in the spectra are less pronounced. Peaks are observed at 295 nm and at 345 nm. Shoulder at 450 nm.

UV/Vis spectra of Compound 1 in sodium citrate pH 5.1 show an intense peak at 342 nm, a small peak at 293 nm and a shoulder at 450 nm. Within 24 h, the complex experiences a red shift of its major band up to 346 nm and a blue shift of the band at 293 nm which disappears upon 24 h and of the shoulder to 431 nm. The observed spectral changes are different in the presence of the protein. In fact, Compound 1 spectra in the presence of RNase A show a major peak at 346 nm and a very small peak at 457 nm that decrease their intensity with time. The peak at 293 nm is overlapped with that of the protein at 280 nm. After 24 h a red shift of the band at 346 nm is observed also in this case.

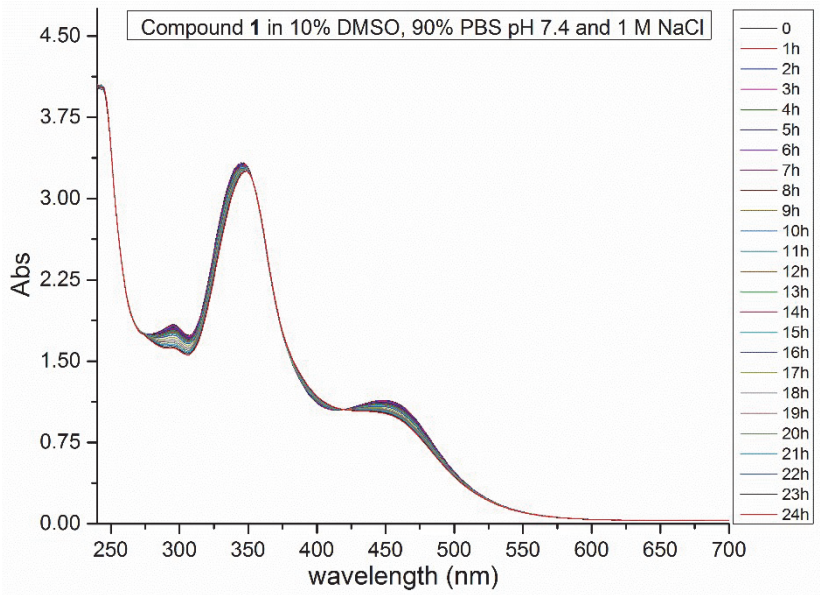

Figure S2. UV-Vis spectra of 1 mM Compound **1** in 90% PBS at pH 7.4, 10% DMSO, 1M NaCl, followed each 1 h over 24 h. These spectra should be compared to those reported in Figure 2B.

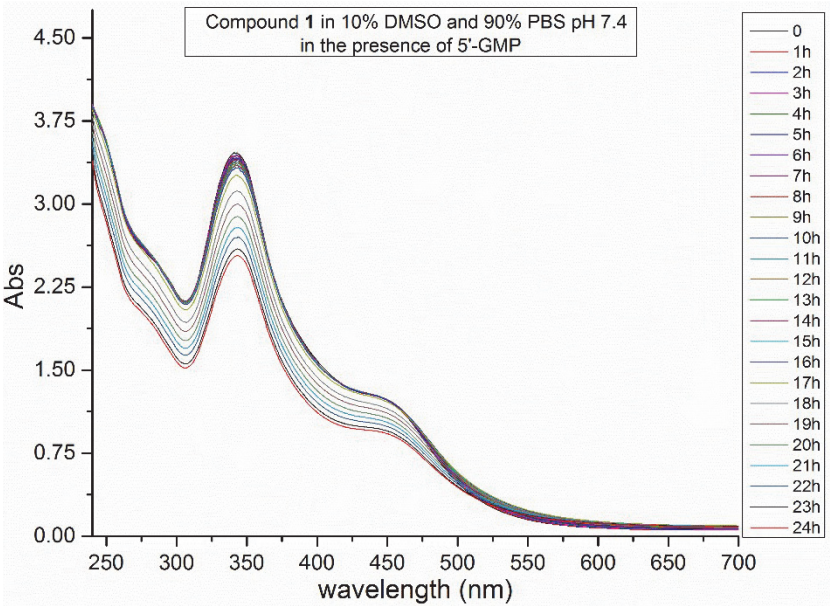

Figure S3. UV-Vis spectra of 1 mM Compound **1** followed each 1 h over 24 h in 10% DMSO and 90% PBS at pH 7.4, in the presence of 5'-GMP.

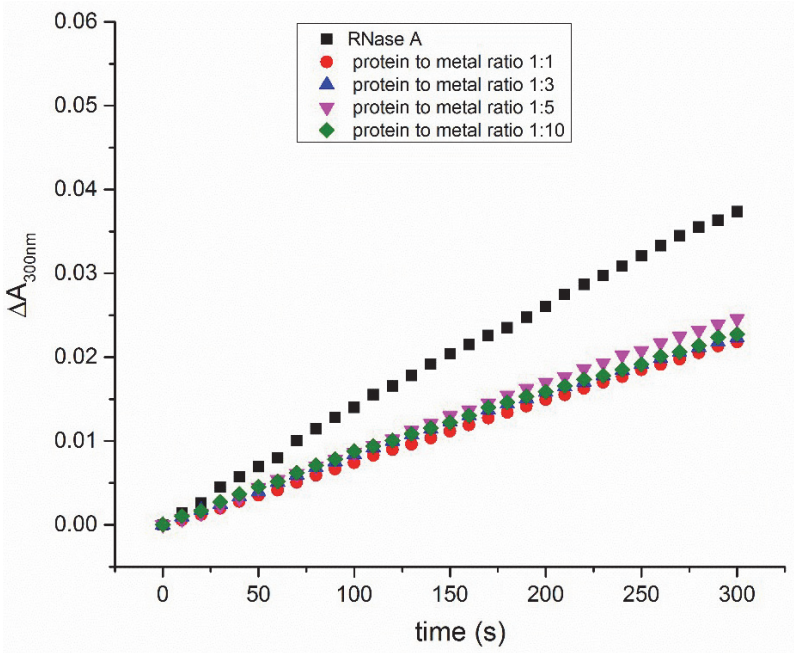

Figure S4. Hydrolysis of yeast RNA (evaluated by measuring the variation of absorbance at 300 nm as function of time upon addition of the protein to the yeast RNA sample) by RNase A (black) and its adducts with Compound **1**. Catalytic activity of RNase A in the presence of Compound 1 at different protein to metal ratio was determined spectrophotometrically by using the Kunitz assay [19]. 0.5 mg x mL^{-1} of RNA and enzyme concetration =0.1 mg x mL^{-1} were used in 50 mM sodium citrate buffer pH 5.1, at 298 K. Spectrophotometric measurements were performed with a Jasco spectrophotometer. Experiments have been performed after 24 h of incubation. Protein remains well active in the presence of the compound.

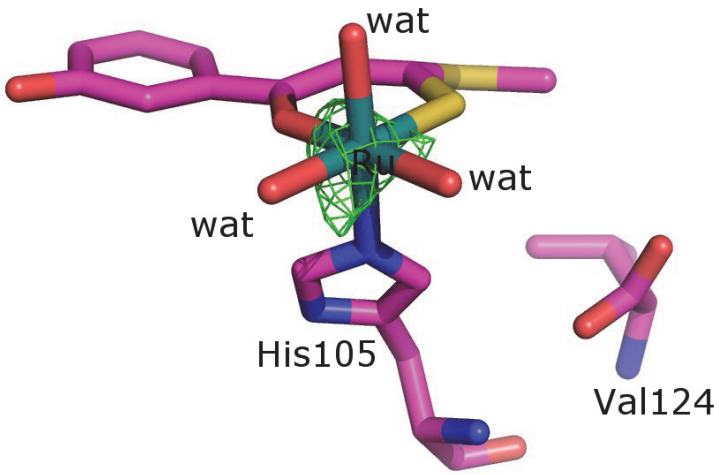

A

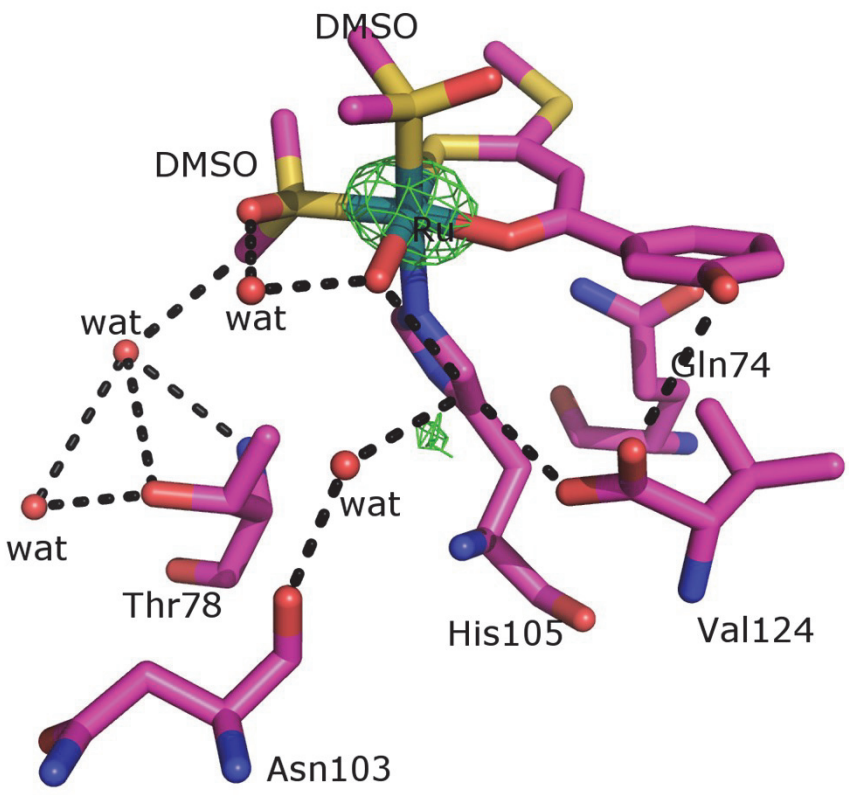

B

Figure S5. Compound **1** binding site in RNase A-Compound **1** adduct showing the Ru centre bound to His105. Anomalous electron density map that allows the identification of Ru centre is shown at 4σ level.

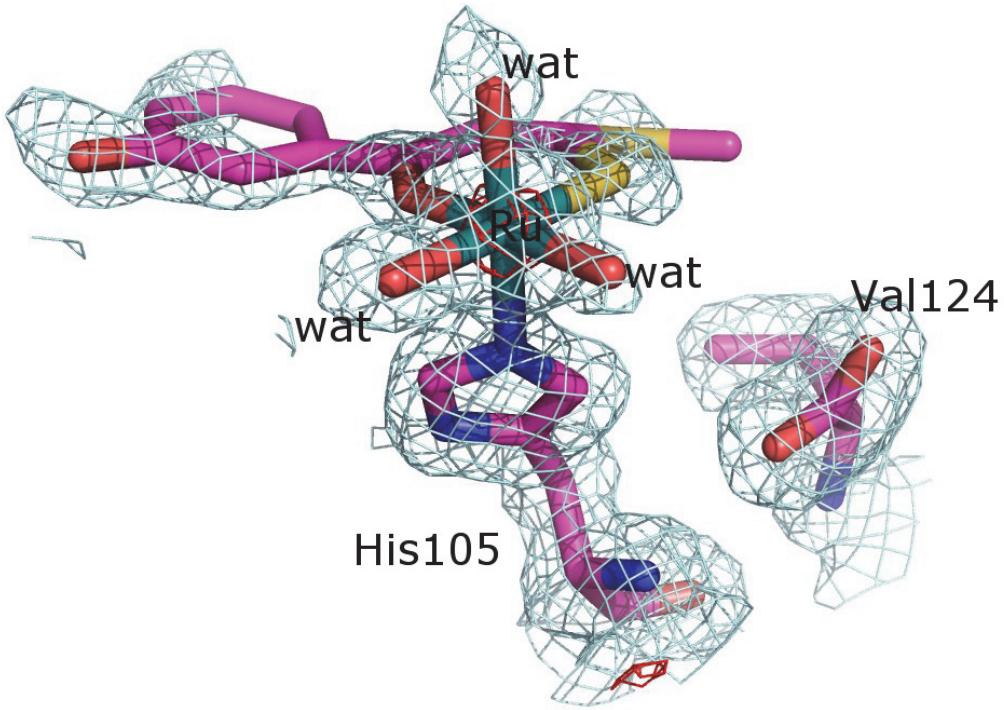

Figure S6. Details of Compound **1** binding site in molecule A of RNase A-Compound **1** adduct showing the Ru centre bound to His105. 2Fo-Fc electron density maps are contoured at 5σ (red) and 0.8σ (cyan) level.

4.2 [JH2]

Highly cytotoxic Osmium(II) compounds and their Ruthenium(II) Analogues targeting Ovarian Carcinoma cell lines and evading Cisplatin resistance mechanisms

Jana Hildebrandt, Norman Häfner, Daniel Kritsch, Helmar Görls, Matthias Dürst, Ingo B. Runnebaum, Wolfgang Weigand

in preparation

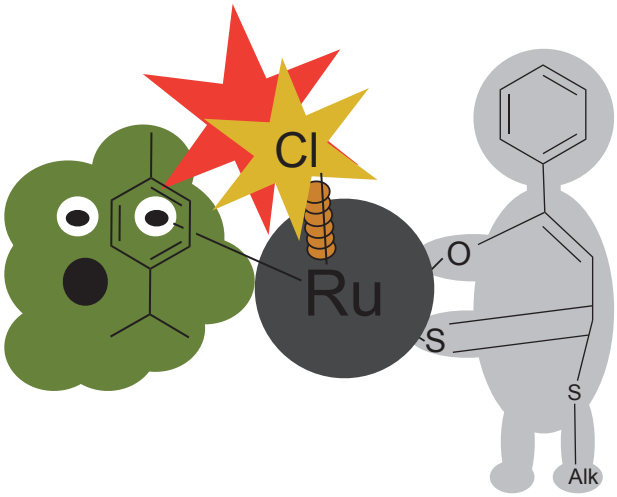

In this publication the determination of structure-activity relationships of 18 β-Hydroxydithiocinnamic acid esters, 17 corresponding ruthenium(II) complexes and their cytotoxic properties are described. Moreover, four osmium(II) complexes were characterized with IC50 values in low µM range. Next to synthesis and characterization of all compounds, stability determinations were done with NMR spectroscopy, giving new insights in the solution behavior of the metal complexes. The molecular structures for ruthenium(II) complexes and some β-Hydroxydithiocinnamic acid esters were discussed in detail. Altogether it could be shown, that the ruthenium(II) complexes exhibit high cytotoxic activity against Cisplatin resistant tumors *in vitro*, resulting in low resistant factors. A different mode of action for ruthenium(II) complexes in comparison to Cisplatin is confirmed by cell cycle arrest data.

Part 1

Highly cytotoxic Osmium(II) compounds and their Ruthenium(II) Analogues targeting Ovarian Carcinoma cell lines and evading Cisplatin resistance mechanisms

Jana Hildebrandt, Norman Häfner, Daniel Kritsch, Helmar Görls, Matthias Dürst, Ingo B. Runnebaum, Wolfgang Weigand

Abstract

Ruthenium and osmium complexes attract increasing interest as next generation anticancer drugs. Focusing on structure-activity-relationships of this class of compounds, we report on 17 different ruthenium(II) complexes and four promising osmium(II) analogues. Structural characterizations and stability determinations have been carried out with standard techniques, including NMR spectroscopy and molecular structures. All complexes and single ligands have been tested for cytotoxic activity on five different cancer cell lines as well as two non-cancerous cell lines *in vitro*. IC50 values for ovarian cancer cell lines A2780/ A2780cis and SKOV3/ SKOV3cis show promising results for most of the compounds. Histon γH2AX-foci and FACS experiments for DNA damage and cell cycle analyses, respectively, using exemplary compounds revealed thus pointing to another mode of action for this class of compounds. Importantly, this seems to be the basis to circumvent resistance mechanisms and for the observed high activity against Cisplatin resistant cell lines.

Introduction

Cisplatin and analogues

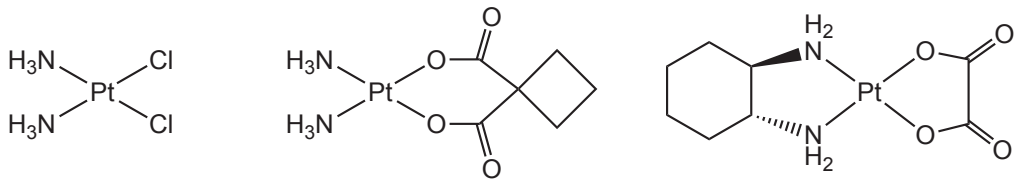

A **B** **C**

Fig. 1: Structures of: Cisplatin, **A**; Carboplatin, **B**; and Oxaliplatin **C**.[Raveendran, 2016]

The development of metals as anticancer agents began with the coincidental discovery of the biology activity of *cis*-[$Pt(NH_3)_2Cl_2$], Cisplatin (Fig. 1, **A**) by Rosenberg in 1965.[Rosenberg, 1965] Cisplatin was clinically approved in 1978 and targets primarily the DNA leading to DNA adducts, DNA damage and apoptosis induction.[Muggia, 2015; Pascoe, 1974] Nowadays, Cisplatin is used in clinical anticancer treatment against: cervical, bladder, head and neck cancers as single agent and in combination therapy against testicular, ovarian, bladder and head and neck cancers.[Meier-Menches, 2018] Unfortunately the chemotherapy is limited by side effects, *e.g.* nephrotoxicity, ototoxicity, neurotoxicity and innate and acquired resistant mechanism, which limit its clinical potencies.[Mayr, 2017; Amable, 2016] Since 1992, the second-generation drug Carboplatin, **B**, is approved worldwide, showing less nephro- and neurotoxicity than Cisplatin.[Meier-Menches, 2018; Muggia, 2015; Lokich, 1998] The third-generation drug Oxaliplatin, **C**, was approved in 2002 and shows different behavior than Cisplatin and Carboplatin, therefore it is used against colon cancers.[Meier-Menches, 2018; Andre, 2004] Since Oxaliplatin, no other platinum based drug could reach a worldwide approval.[Muggia, 2015] The several drawbacks of the three drugs, next to their importance in anticancer treatment, lead to the design of new drug candidates to improve the clinical efficacy of untargeted anticancer treatments.[Raveendran, 2016]

Ruthenium compounds for anticancer treatment

Whereas many research is still focused on platinum based anticancer drugs, the development of potential ruthenium anticancer molecules, started almost same time as the discovery of Cisplatin.[Meier-Menches, 2018] Already 34 years before the discovery of Cisplatins' potential two researchers found the activity of $Cs_2[RuCl_6]$hydrate, a ruthenium(IV) species which shows inhibition of tumor growth.[Collier, 1931] Rosenberg himself discovered the activity of $[Ru(NH_3)Cl(OH)]Cl$, a ruthenium(III) species.[Rosenberg, 1965; Rosenberg, 1969] The first ruthenium compounds were designed to mimic the platinum drugs and therefore had also am(m)ine and chlorido ligands, but the research in the last

years showed that ruthenium based compounds have a different mode of action.[Meier-Menches, 2018]

Ruthenium(III) compounds

As mentioned above, Rosenberg investigated some activity on this class of compounds, in 1976 the compound *fac*-[$RuCl_3(NH_3)_3$] showed similar effects as Cisplatin.[Durig, 1976] At the same time Clarke and coworkers reported interaction studies with [$Ru(NH_3)_5Cl]Cl_2$ and DNA, but later on protein interactions have been monitored for some [$Ru(NH_3)_5(Pur)]Cl_3$ compounds, whereas Pur is a purine.[Clarke, 1974; Clarke, 1978; Kelman, 1977; Clarke, 2003] They introduced the 'activation-by-reduction'-hypothesis, which is well accepted nowadays implying, that the ruthenium(III) drugs act as prodrugs which are reduced to their active species, ruthenium(II).[Meier-Menches, 2018; Kelman, 1977; Clarke, 2003] Two years after the approval of Cisplatin, Clarke and coworkers reported more interesting details on the activity of [$Ru(NH_3)_5Cl]Cl_2$, these milestones lead to increased research on this class of compounds.[Clarke, 1980a; Clarke, 1980b] Promising candidates following the discovery of Clarke and coworkers are tetrachloridobis(indazole)ruthenium(III), known as KP1019, **E**, NKP-1339 or IT-139 ,**D**, and tetrachlorido(dimethylsulfoxide)(imidazole)ruthenium(III), known as NAMI or NAMI-A, **F**, Figure 2.[Meier-Menches, 2018; Berger 1989; Pieper, 1998; Sava, 1992]

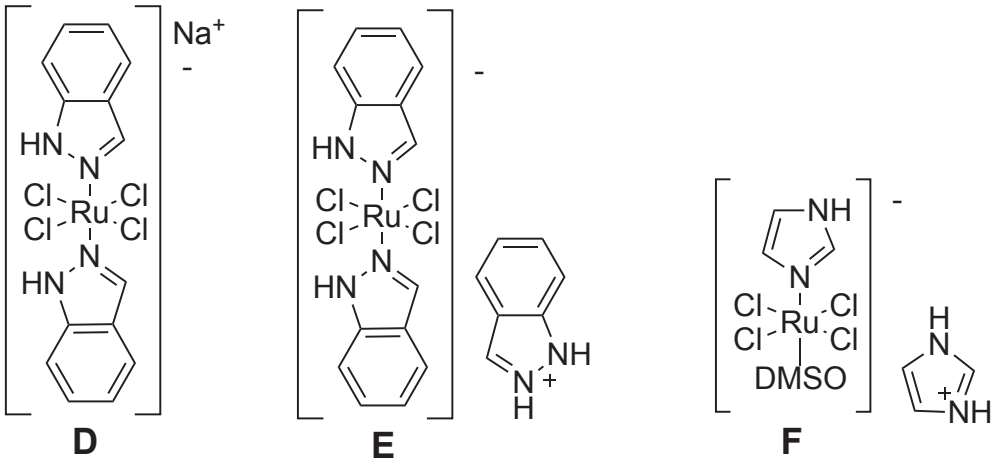

Fig. 2: Overview of most-promising ruthenium(III) drugs, **D**: IT-139 (NKP-1339), **E**: KP1019, **F**: NAMI-A.[Meier-Menches, 2018; Berger, 1989; Pieper, 1998; Sava, 1992]

At the moment, the only drug candidate in clinical development is IT-139, developed by Keppler and coworkers, Figure 2**D**.[Fuereder, 2017; Trondl, 2014] First studies focused on *trans*-[$RuCl_4(HIm)_2$], where Him is imidazole, known as KP418.[Keppler, 1986; Keppler, 1987] This compound shows a significant inhibition of tumour growth.[Berger, 1989] It was shown, that N-heterocyclic systems are the most promising, but side effects of KP418 led to a structural change resulting in KP1019. KP1019, as well as IT-139 show a fast binding to serum proteins in the blood such as transferrin and albumin, which may regulate the tumor-specific activity of these compounds.[Keppler, 1989; Berger, 1989; Dhubhghaill, 1994; Chatlas, 1995; Smith, 1996; Trynda-Lemiesz, 1999; Bijelic, 2016; Depenbrock, 1997; Cetinbas, 2010] Both compounds, KP418 and KP1019 induce apoptosis *via* the mitochondrial pathway. KP1019 as the most promising compound and finished Phase-1 clinical studies.[Kapitza, 2005; Hartinger, 2008; Lentz, 2009] Due to its limited solubility the counter cation has been changed to sodium in IT-139. This drug showed increased solubility and lead to the application of higher drug concentrations and is undergoing Phase I/II-clinical studies.[Meier-Menches, 2018; Pieper, 1998; Trondl, 2014; Burris, 2016]

Beside compounds with N-donor ligands, early investigations were also done with S-donor ligands and first studies were published in 1975.[Monti-Bragadin, 1975] Some years later it was shown that *trans*-[$RuCl_2(DMSO_4)$] and [$RuCl_4(DMSO)_2$], whereas DMSO is dimethylsulfoxide, can reduce the volume of lung metastases.[Sava, 1989; Alessio, 1991] Although, this species haven't been stable in aqueous solution, optimizations lead to *trans*-[$RuCl_4$(DMSO)(HIm)], whereas HIm is imidazole, known as NAMI (= Novel Anti Tumour Metastasis Inhibitor).[Meier-Menches, 2018; Sava, 1992; Sava, 1994] NAMI-A, **F**, was the first ruthenium based compound which entered clinical trials and shows a selective activity against metastatic cells *in vivo*, but due to its poor clinical responses clinical trials were interrupted.[Rademaker-Lakhai, 2004; Bergamo, 2012; Leijen, 2015]

Ru(II) compounds

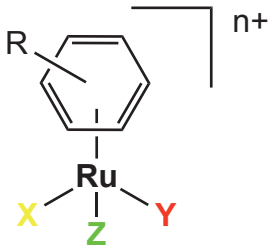

G

Fig. 3: General structure of Ru(II) compounds.[Bruijnincx, 2009]

As mentioned before, ruthenium(III) compounds act as prodrugs which must be reduced inside the body. Therefore, ruthenium(II) compounds were investigated which do not need this step. It is known, that ruthenium(II) compounds are activated by ligand exchange mechanism, especially by hydrolysis of the Ru-Cl bond.[Meier-Menches, 2018; Pizarro, 2010] Ruthenium(II) complexes which are investigated for anticancer activity show in general a typical 'piano-stool' geometry, Figure 3, with an η^6-arene and three open coordination sites X, Y, Z for different ligands, which can lead to a charge of the complex itself. The arene ligand can be substituted (*e.g.* cymene), whereas Z is usually a halide. The positions X and Y can be two different monodentate ligands, but more common are bidentate ligands (e.g. N,N; N,O; O,O or O,S).[Bruijnincx, 2009]

First studies have been done by Reedijk and coworkers with ruthenium(II) compounds containing 2-phenylazopyridine (azpy), like $[Ru(azpy)_2Cl_2]$ and $[Ru(azpy)_2(NO_3)_2]$ which have been tested *in vivo* and *in vitro*.[Meier-Menches, 2018; Velders, 2000; Hotze, 2000]

Considering the general structure of ruthenium(II) complexes for anticancer activity in Figure 3, these organometallic 'half-sandwich piano-stool' compounds were investigated, mainly by Dyson and coworkers and Sadler and coworkers.[Yan, 2005; Allardyce, 2001a; Allardyce, 2001b; Morris, 2001]

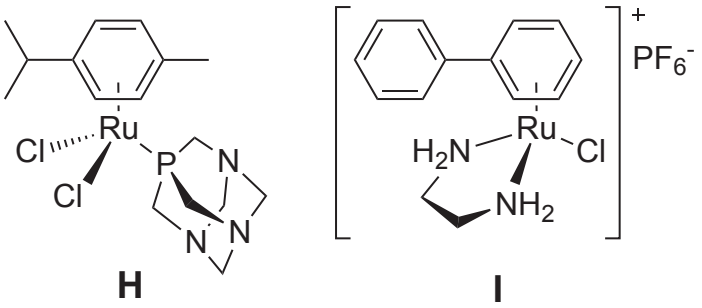

Fig. 4: Structure of **H**: RAPTA-C and **I**: RAED compound.[Murray, 2016; Gasser, 2010]

A great series of compounds, named RAPTA, were investigated by Dyson and coworkers.[Murray, 2016; Scolaro, 2005] Well-known candidates of this compound family are RAPTA-C, $[RuCl_2(cym)(pta)]$, whereas cym is η^6-*p*-cymene and pta is 1,3,5-triaza-7-phosphaadamantane, **H**, Figure 4, and RAPTA-T, with a changed arene-ligand. RAPTA-C was developed as an antimetastatic agent and shows good aqueous solubility, as well as anti-angiogenic properties.[Allardyce, 2001a; Allardyce, 2001b; Bergamo, 2008] It is known, that their primary target is not the DNA as they show interactions with proteins.[Wu, 2008] *In vivo* and *in vitro* studies showed, that the RAPTA compounds are not cytotoxic to normal cells, but active against some tumour cells.[Scolaro, 2005; Hartinger, 2013] A second series, first introduced by Sadler and coworkers, are the RAED compounds.[Morris, 2001; Habtemariam, 2006] The RAED compound **I**, $[(\eta^6\text{-bisp})RuCl(en)]Pf_6$, whereas bisp is η^6-biphenyl, also known as RM175, was first investigated in 2001 and show a mechanism of action similar to Cisplatin by interacting with guanine as well as some compounds show intercalation through the DNA.[Meier-Menches, 2018; Morris, 2001; Habtemariam, 2006] With its halido leaving group it is also thought to have another mechanism of action compared to the ruthenium(III) compounds.[Meier-Menches, 2018; Chen, 2002; Morris, 2001] Both compounds, RAPTA-C and RM175 are in advanced clinical studies due to good *in vivo* results.[Allardyce, 2001a; Peacock, 2006; Peacock, 2008; Renfrew, 2011; Schmidlehner, 2016] It is known, that RM175 acts against primary tumours as well as shows activity against lung metastases and has no cross-resistance to Cisplatin.[Bergamo, 2010; Murray 2016; Aird, 2002; Morris,

2001] It was shown, that RM175 shows antiproliferative activity comparable to Carboplatin and is highly active against human ovarian cancer A2780.[Meier-Menches, 2018; Aird, 2002]

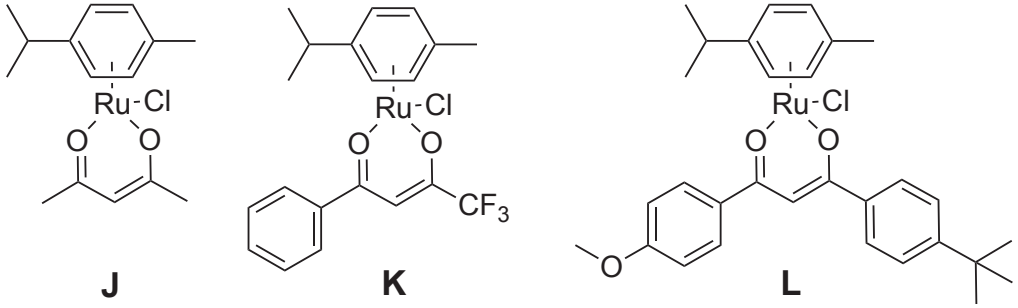

Fig. 5: Three examples for O,O-chelating systems. **J**: Investigated by Sadler and coworkers in 2006; **K**: Investigated by Turel and coworkers in 2013 and **L**: Investigated by Dyson and coworkers in 2016.[Habtemariam, 2006; Sersen, 2013; Pettinari, 2016]

Next to N,N-chelating substances, different chelating ligands *e.g.*: N,O; O,O; C,N and S,N have been reported in the last years. A series of this compounds have been introduced by Sadler and coworkers in 2006.[Habtemariam, 2006; Meier-Menches, 2018] Compound **J,** Figure 5, is one example of these compounds and has been compared to others dealing with the structure-activity-relationships and the biological behavior of this class of compounds. It was shown, that there is no cross-resistant to Cisplatin.[Habtemariam, 2006] O,O-chelating ruthenium(II) complexes with CF_3 groups, like compound **K**, were developed 2013 by Turel and coworkers whereas the biological activity, especially the selective mode of action for different organoruthenium compounds was published in 2015.[Sersen, 2013; Sersen, 2015] Dyson and coworkers published a series of O,O-chelating ruthenium(II) compounds as compound **L** in 2016 which has an avobenzone as chelating ligand which shows cytotoxic activity itself. They investigated IC50 values on A2780 and its resistant analogues for different charged complexes and showed also binding behaviour to DNA and proteins.[Pettinari, 2016]

As well as the known strategy to place bioactive ligands to platinum(IV) compounds,[Raveendran, 2016; Petruzzella, 2017] this is also a strategy for ruthenium(II) complexes, there are several examples in the literature with *e.g.* flavones, naphtoquinones, curcurmin, staurosporine or thiosemicarbazone.[Schmidlehner, 2016; Kurzwernhart, 2013; Schwarz, 2013; Kilpin, 2013; Meggers, 2007; Beckford, 2011]

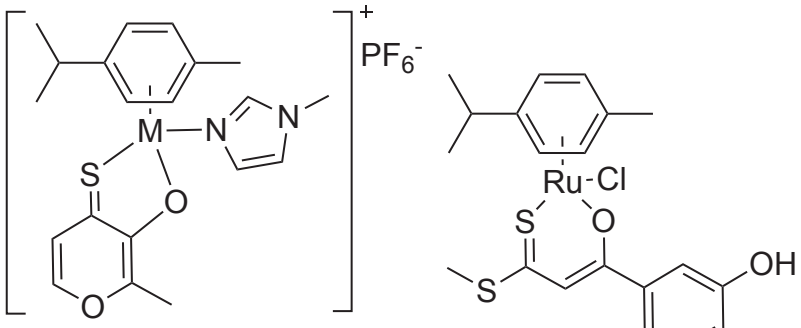

M **N**

Fig. 6: **M**/**N**: Examples for O,S-chelating ruthenium(II)/ osmium(II) complexes known in the literature.[Hildebrandt, 2016b; Hanif, 2010; Hackl, 2016]

Ruthenium(II) compounds with O,S-chelating ligands have been introduced and investigated by Keppler and coworkers, first in 2009.[Kandioller, 2009a; Kandioller 2009b] Further investigations were following 2010 and 2016.[Hanif, 2010; Schmidlehner, 2016; Hackl, 2016] This work is based on the comparison of O,O- and O,S-chelating ligands to mainly ruthenium(II) species. They used maltol/ thiomaltol, compound **M**, Figure 6, [Hanif, 2010; Hackl, 2016] and pyrone/ thiopyrone [Kandioller, 2009a; Kandioller, 2009b; Schmidlehner, 2016] for this structure-activity-relationship experiments and confirm, that the change from O,O to O,S ligands increase the solubility, stability and result in lower IC50 values.[Kandioller, 2009a; Kandioller, 2009b; Hanif, 2010] In 2016 we have shown already the increased biological activity of one ruthenium(II) complex with a cinnamic acid derivative as O,S-chelating ligand, compound **N**, compared to their platinum(II) analogues and analyzed the interaction with proteins.[Hildebrandt, 2016a; Hildebrandt, 2016b] In the same year Keppler and coworkers compared first time ruthenium(II) and osmium(II) analogues with O,S ligands, together with

iridium(II) and rhenium(II) complexes.[Hackl, 2016] They investigated the impact of the leaving group (imidazole vs. chlorido) and the change of the metal, resulting in good IC50 values in general. As the influence of the leaving group is just due to stability changes, the IC50 values of ruthenium(II) and their osmium(II) analogues have been almost in the same range for three different cell lines (Ru: 12-3 µm, Os: 4-2 µm; MTT assays, 96h incubation time).[Hackl, 2016] The best IC50 values were generated by the ligand itself, without any complexation to metals, what shows a great difference to our compound **N**, which results after complexation to the ruthenium(II) in 50-up to more than 200-fold lower IC50 values.[Hildebrandt, 2016a; Hackl, 2016]

Osmium Compounds for Anticancer Treatment

Significant results in the ruthenium drugs have enhanced the interest for osmium compounds to develop anticancer-drugs.[Paunescu, 2015] Therefore, a discussion of osmium compounds can't be separated from their ruthenium analogues, as the first compounds of this class have been analogues of well-known ruthenium complexes, *e.g.* RAPTA-C, RM175, NAMI-A and KP1019.[Meier-Menches, 2018; Paunescu, 2015, Cebrian-Losantos, 2007; Büchel, 2011; Kuhn, 2014; Dorcier, 2005; Dorcier, 2006; Peacock, 2006; Peacock, 2007a-c] The comparison of the osmium compounds to their ruthenium counterparts results very often in different biological behavior, especially in the anticancer-activity.[Paunescu, 2015; Meier-Menches, 2018; Bergamo, 2010; Büchel, 2013] According to the HSAB-principle, osmium is a softer metal compared to ruthenium and therefore results in different coordination preferences to biomolecules. Moreover, it is known that the metal-ligand exchange mechanism are slower for the osmium compounds compared to their ruthenium analogues.[Meier-Menches, 2018; Paunescu, 2015; Pizarro, 2010; Groessl, 2007; van Rijt, 2009] Therefore, many osmium compounds, mostly representing half-sandwich complexes have been investigated for their biological activity *in vitro* and partly *in vivo*.[Paunescu, 2015; Schmid, 2007a; Schmid, 2007b; Kilpin, 2014; Pea-

cock, 2007; Romero-Camelon, 2013; van Rijt, 2009; van Rijt, 2010; Bergamo, 2010; Shnyder, 2011; Filak, 2013] Some osmium(II) compounds show similarities to Cisplatin and Carboplatin.[Paunescu, 2015; Fu, 2011]

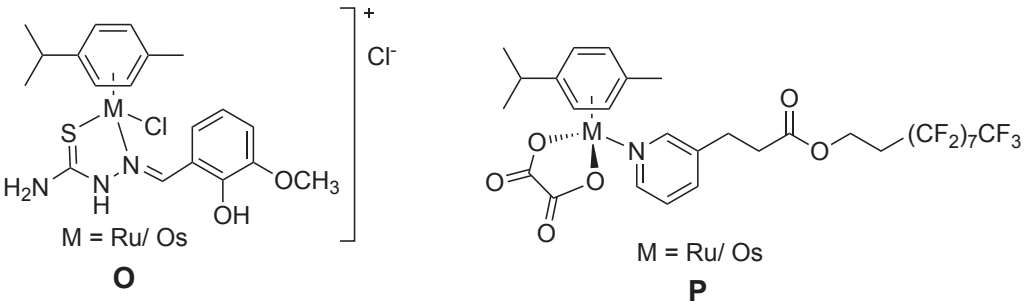

Fig. 7: **O**/**P**: Two examples for osmium(II) complexes and their ruthenium(II) analogues, showing different biological behavior.[Gatti, 2018; Paunescu, 2015]

Several studies focused on comparing ruthenium(II) and their osmium(II) analogues, *e.g.* the study of Keppler and coworkers with the first comparison of O,S-chelating ligands to these metals, as mentioned before (compound **M**).[Hackl, 2016] To point out some other examples, in 2018 Carcelli and coworkers compared ruthenium(II) and osmium(II) thiosemicarbazone, **O**, (S,N-chelating) complexes on different cell lines, *e.g.* A2780 and its resistant-analogue A2780cis, Figure 7.[Gatti, 2018] All of their investigated compounds show lower resistant factors than Cisplatin and again, the ligands itself, without complexation, exhibit lower or comparable IC50 values than the ruthenium(II) and osmium(II) compounds. They concluded that the substitution of the ligands has a great influence of anticancer activity of the compounds and point out one ruthenium complex as a lead compound. All together the ruthenium(II) and osmium(II) analogues show results in the same range.[Gatti, 2018] Dyson and coworkers reported 2015 on the difference of osmium and ruthenium analogues, compound **P**.[Paunescu, 2015] While testing their osmium(II) complexes they recognized a low cytotoxicity on A2780 cell line (38 µM - >100 µM). Nevertheless, some show better results than their ruthenium(II) analogues and two complexes are more selective to cancer cells.[Paunescu, 2015; Clavel, 2014] They continued their biological investigations of these class of compounds, due to the important statement, that ruthenium compounds which show good *in vivo* results (*e.g.* RAPTA-C)

are compounds with low or even no cytotoxic behavior *in vitro*.[Paunescu, 2015; Rademaker-Lakhai, 2004; Leijen, 2015; Hartinger, 2006; Hartinger, 2008; Trondl, 2014; Bergamo, 2007; Weiss, 2014; Scolaro, 2005; Nowak-Sliwinska, 2011; Weiss, 2015] In general, they concluded, that the osmium complexes '*tend to be slightly more cytotoxic than their ruthenium counterparts'[Paunescu, 2015]* but overall it changes from system to system which metal complex is more cytotoxic *in vitro* and/or *in vivo*.[Paunescu, 2015; Bergamo, 2010; Shnyder, 2011; Filak, 2013]

Ruthenium and osmium compounds were investigated to mimic the mode of action of platinum based complexes.[Meier-Menches, 2018] Both metals are the most investigated and advanced non-platinum metallodrugs, but still with the major current challenge to discover their molecular targets.[Meier-Menches, 2018] Several works, ours included, showed that the biological behavior of this class of compounds is different compared to Cisplatin and analogues and that the DNA is not the primary target.[Meier-Menches, 2018; Hildebrandt, 2016b] As well as next to the nature of the ligands, also the change of the metal (from ruthenium to osmium) results in different anticancer activity and biological activity in general.[Paunescu, 2015] Keppler and coworkers investigated some general structure-activity-relationships for osmium(II) and ruthenium(II) complexes, they concluded, that the effect of the chosen metal and its anticancer activity is highly ligand-dependent.[Meier-Menches, 2018] For them, ruthenium(II) complexes are more active than their osmium(II) analogues with O,O-chelating ligand systems, whereas N,O/ N,N/ C,N and S,N osmium(II) compounds show better results.[Meier-Menches, 2018; Mendoza-Ferri, 2009; Peacock, 2007a-c; Fu, 2011; Filak, 2010; Filak, 2011; Schmid, 2007a; Schmid, 2007b; Riedl, 2017; Meier, 2013] As mentioned above, to the best of our knowledge, only one study focuses on comparison of an O,S-chelating system while focusing on leaving groups on the metal center.[Hackl, 2016] In this work we will focus on different ruthenium(II) complexes and some of their osmium(II) counterparts for anticancer properties. Next to compare the influence of the metal-change we

focus on the structure-activity-relationships on different cinnamic acid derivatives as O,S-bidendate ligands. A general structure of the ligand-system and the metal compounds is given in Figure 8.

Substance Code	**-R**	**-Alk**
L/Ru1	-H	-Me
L/Ru2	-H	-Et
L/Ru/Os3	-*m*-OH	-Me
L/Ru4	-*p*-OH	-Me
L/Ru5	-*m*-OH	-Et
L/Ru6	-*p*-OH	-Et
L/Ru/Os7	-*m*-OMe	-Me
L/Ru8	-*p*-OMe	-Me
L/Ru9	-*o*-OMe	-Me
L/Ru10	-*m*-OMe	-Et
L/Ru11	-*p*-OMe	-Et
L/Ru12	-*o*-OMe	-Et
L/Ru/Os13	-*m*-OEt	-Me
L/Ru/Os14	-*p*-OEt	-Me
L/Ru15	-*o*-OEt	-Me
L/Ru16	-*m*-OBut	-Me
L/Ru17	-*p*-OBut	-Me
L18	-*o*-OBut	-Me

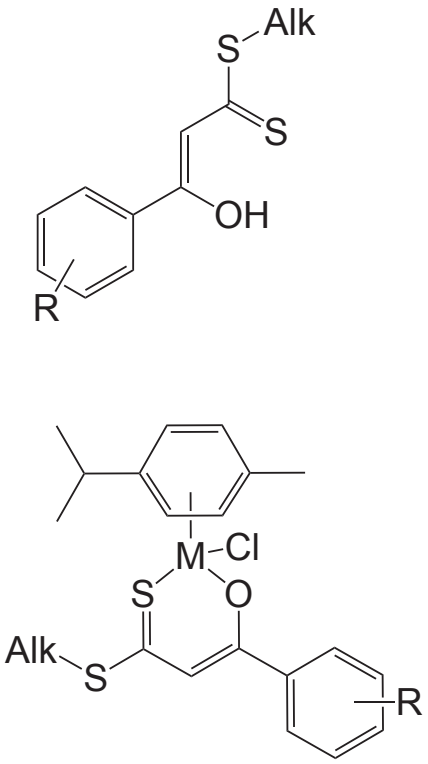

Fig. 8: Overview and substance code of compounds this work is dealing with: β-Hydroxydithiocinnamic acid esters L1-L18 and corresponding Ru complexes Ru1-Ru17 and Os compounds Os3/ Os7/ Os13 and Os14.

Results and Discussion

Synthesis

Cinnamic acid derivatives L1-L18 were synthesized according to published procedures and as described in the Supplementary part.[Hildebrandt, 2016a] For ruthenium(II)/ osmium(II) complexes Ru1-Ru17/ Os3, Os7, Os13 and Os14 (Scheme 1) the corresponding β-Hydroxydithiocinnamic acid ester is deprotonated at the vyniloge acid function with 1 equiv. *t*-BuOK and afterwards given to a 0.5 equiv. $[(\eta^6\text{-}p\text{-cymene})MCl_2]_2$ (M= Ru or Os) suspension in THF. By adding the yellow ester solution to the M(II)-dimer the color turns dark red and is stirring over night at room temperature, following by acidic work up and column chromatography (THF/DCM).

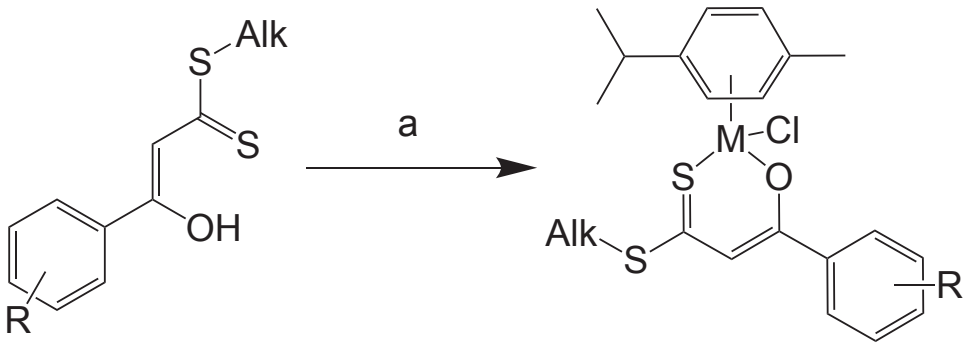

Scheme 1: Reagents and conditions: (a) (i) 1 equiv. *t*-BuOK, THF, rt, 0.5 h; (ii) 0.5 equiv. $[(\eta^6\text{-}p\text{-cymene})MCl_2]_2$, THF, rt; (iii) (i)+(ii), rt, 24 h; (iv) H_2SO_4/H_2O, rt , 0.5 h.

Characterization

All compounds were characterized by NMR spectroscopy, mass spectrometry and elemental analysis (see Experimental part). Results for L13-L18 are in common with those for L1-L12 which were reported earlier (see Supplementary part).[Hildebrandt, 2016a] The chemical shifts in ^1H NMR and $^{13}C\{^1H\}$ NMR spectra show significant changes after complexation to the metal(II) center for both ligand systems, the O,S-chelating and the arene ligand. Specific changes in the NMR spectra have been already discussed previously for corresponding platinum(II) compounds and are in good agreement for the metal(II) compounds this work is dealing with.[Hildebrandt, 2016a] Interestingly the signal of the methine

protons are shifted to high-field as a result of their complexation with ruthenium(II)/ osmium(II) whereas a low-field shift of the corresponding signals for the platinum(II) complexes were observed, Figure 9. A high-field shift for the ^{13}C isotope of the -C=S-group was observed previously in the $^{13}C\{^{1}H\}$ NMR spectra of the platinum(II) compounds after complexation and can be confirmed for the ruthenium(II)/ osmium(II) complexes as well (see Experimental part and Tab. 1). Synthesis for the metal complexes start with the symmetrical bimetallic complex $[(\eta^6\text{-}p\text{-cymene})MCl_2]_2$ and aromatic signals of the cymene ligand are observed as two dubletts, whereas the isopropyl groups resulted in one dublett. Nevertheless, the complexation to the O,S-chelating ligand leads to an unsymmetrical structure and results in chemically non-equivalent aromatic protons and carbons. Thus, four aromatic dubletts for the cymene and two dubletts for the isopropyl-groups in the ^{1}H NMR spectra, as well as four (instead of two) aromatic carbon signals and two (instead of one) signal for the isopropyl groups in the $^{13}C\{^{1}H\}$ NMR spectra are detectable. For the mass spectra in general the molecular peak is not observable, only a $[M\text{-}Cl]^+$ fragment, comparable to literature data,[Schmidlehner, 2016] and a further fragmentation pathway as observed for the β-Hyroxydithiocinnamic acid derivatives itself.

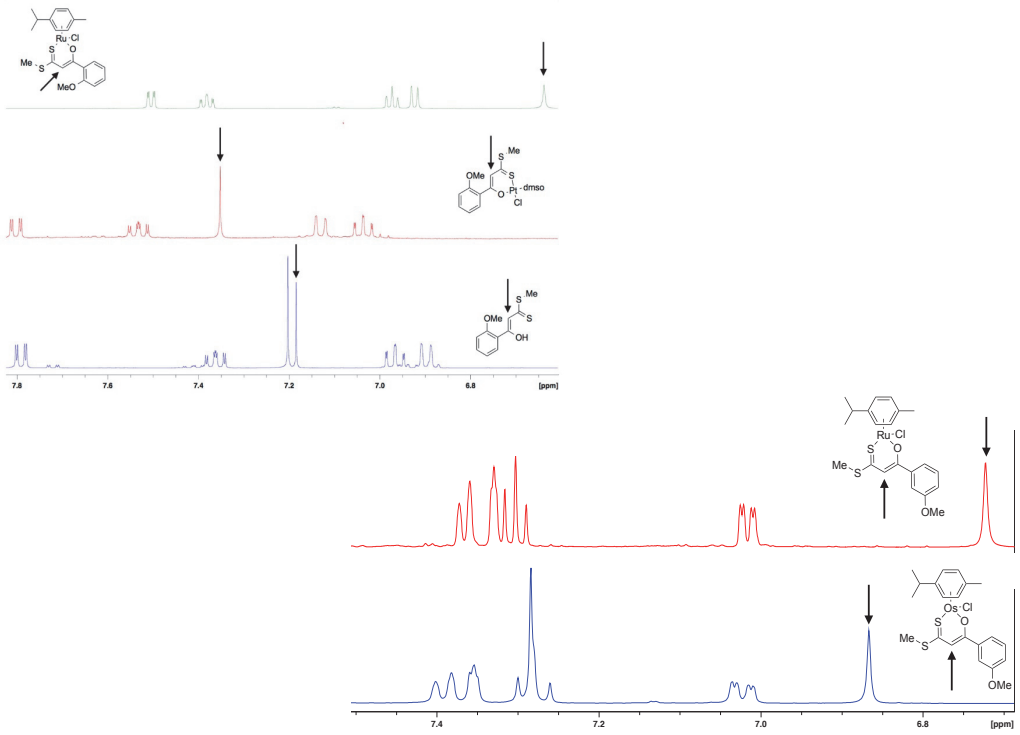

Fig. 9: Left: Part of the ^{1}H NMR spectra for L9/ Ru9 and their corresponding Pt(II) complex, a significant shift of the marked methine proton is observable after

complexation to the metals. Right: Shift of the methine proton for the Ru(II) and the Os(II) compounds, the Os(II) complexes do not shift as much (in comparison to the free ligand) as the Ru(II) analogues.

Tab. 1: Selected NMR signals for L7/ Ru7/ Os7. Ru and Os compounds show similar effects after complexation result in similar NMR pattern and changes. A high-field shift is observable for signals 2 and 4, a low-field shift for signal 1, signal 3 does not show remarkable changes.

Signal no.		**L7**	**Ru7**	**Os7**
1	-C-OH/M	169.1 ppm	179.0 ppm	174.9 ppm
2	-C=S	217.3 ppm	185.9 ppm	186.7 ppm
3	=C-H	112.9 ppm	113.4 ppm	112.7 ppm
4	=C-H	6.97 ppm	6.64 ppm	6.87 ppm

Stability Determination

For the investigation of the in solution behaviour of the ruthenium(II) complexes Ru1, Ru3 and Ru8 we analyzed kinetic measurements *via* ^{1}H NMR spectroscopy (every 0.5 hours one spectra). As mentioned before, NMR signals and behaviour of the ruthenium and osmium compounds is quite similar and osmium(II) compounds show a slower ligand exchange mechanism and a higher stability in general.[Meier-Menches, 2018] The stability determinations for the osmium(II) compounds using NMR spectroscopy show no structural changes (Data for Os3 in Supplementary part, Figure S3). Therefore we will discuss the changes for ruthenium(II). Figure 10 shows the results for measurements at 37 °C in dmso-d_6. All ^{1}H NMR spectra show that the ruthenium(II) molecules are not stable in dmso-d_6 solution. Figure 10, Part I shows the results for Ru1, the blue spectra displays the first measurement at t=0 hours and as shown in picture field (a) the double-dubletts of the cymene ligand changed quickly and already disappeared after

24 hours (red spectra). The detailed part (b) of the picture shows all of the ^{1}H NMR spectra for 72 hours and it is observable that already after 5 hours measurements the signals for the cymene ligand changes to a new signal part resulting in a high-field shift. Part II presents the results for Ru3 including an enlargement of the aromatic region at ~ 7 ppm (c), showing that signals change quickly and the methine proton disappears after 7 hours measurements (d). Part III displays results for Ru8 in detail, which are in common with those for Ru1 and Ru3 and proves again the development of a new species after some hours. The same measurements were done also with dmso at room temperature. It is observable that at room temperature the same changes in the spectra occur and after 15 hours the new species is detectable (examplified for Ru1 in the Supplementary part, Figure S2). As reported earlier dmso molecules are able to bind to the ruthenium(II) center by losing the cymene ligand and changing the structure to an octahedral metal(II) coordination sphere.[Hildebrandt, 2016b] Thus, an explanation for the new species can be the binding of dmso molecules to the ruthenium(II) center and the loss of the cymene ligand representing the new species in the ^{1}H NMR spectra. To support this hypothesis the ruthenium(II) complexes were measured under same conditions (rt, 72 hours) in CD_2Cl_2 and it was shown that the compounds are stable under these conditions in another solvent (see Supplementary Part, Figure S1). In conclusion, it is shown that the analyzed Ru(II) compounds are able to react with dmso at room temperature as well as at 37 °C but not with dichlormethane.

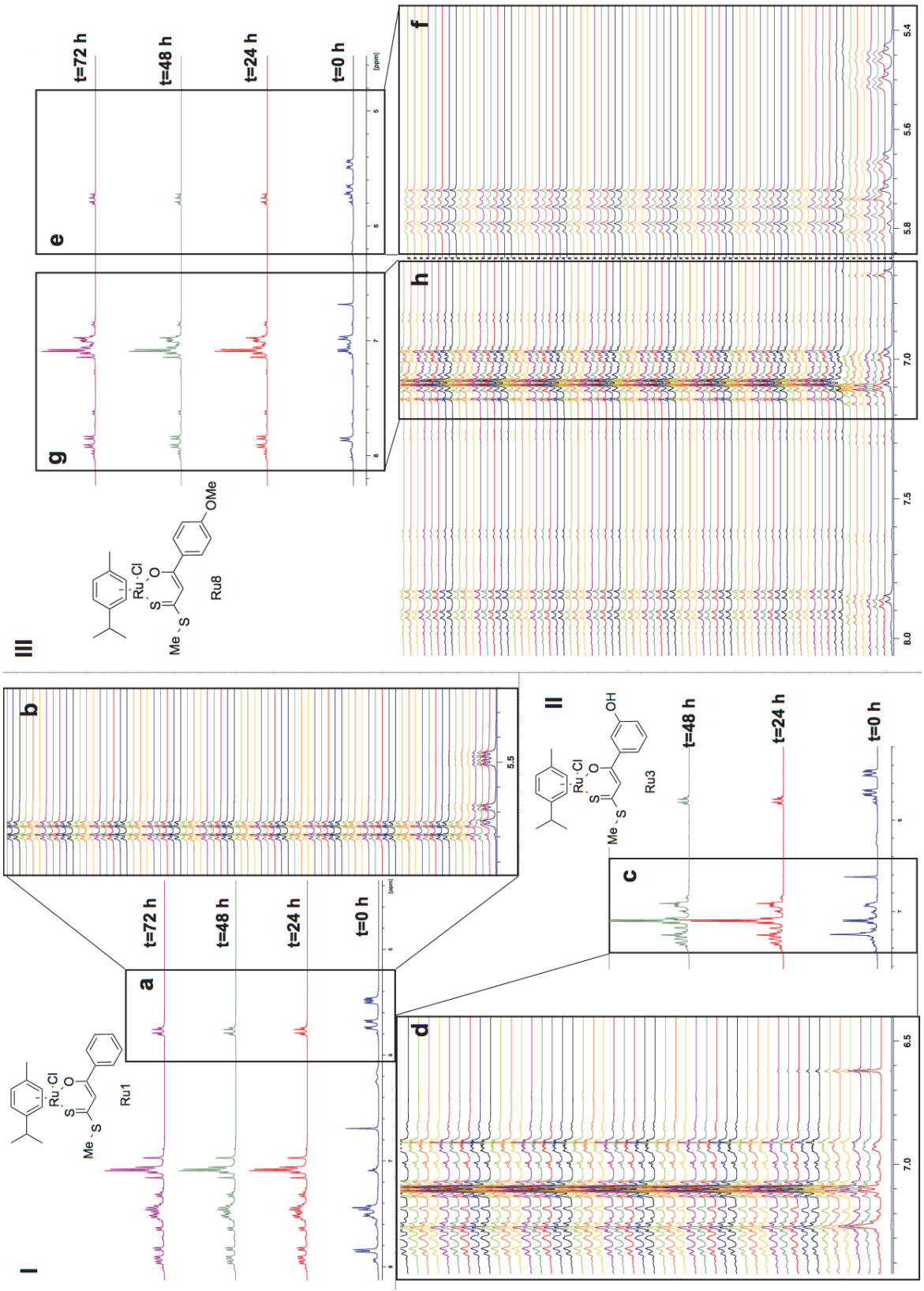

Fig. 10: Overview of stability determination *via* ^{1}H NMR spectroscopy for substances Ru1 (I), Ru3 (II) and Ru8 (III).

Molecular Structures

Ruthenium(II) complexes Ru9, Ru13 and Ru14 as well as L14, L15, L17 and L18 were characterized by means of single crystal X-ray structure determination, whereas the molecular structures of Ru3, L1, L3, L4, L8 and L9 are already known. Figure 11 shows the ruthenium(II) complexes, whereas the molecular structures of the ligands are discussed in the Supplementary part, Figure S4 and Table S1. Results are in good agreement with the values reported earlier.[Hilde-brandt, 2016b]

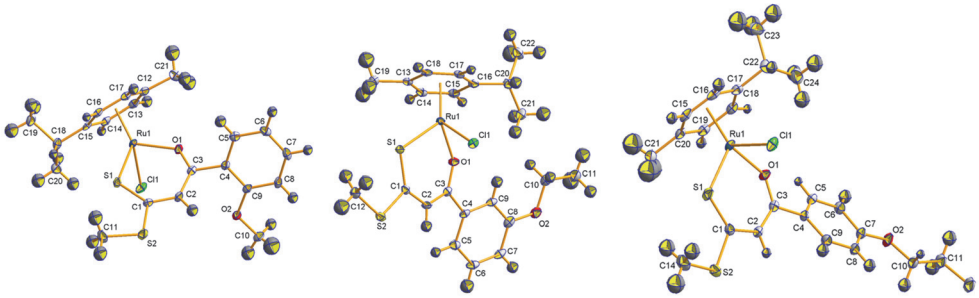

Fig. 11: Molecular structures (50% probability) of Ru9 (left), Ru13 (middle) and Ru14 (right).

Table 2 displays specific bond length and angles for the presented compounds, the ruthenium(II) center shows a tetrahedral structure environment with L-Ru-L angles of around 90°. The bond lengths of ruthenium (here for example Ru9) and their neighbouring atoms are decreasing in the order of S(1)-Ru(1) (2.3544(5)) > Cl(1)-Ru(1) (2.4081(5)) > O(1)-Ru(1) (2.0790 (14) Å). The bond lengths of the oxygen substituted moiety at the aromatic ring O(2)-C(9/8/7) are in the same range, whereas the bond lengths for *ortho*-substituted Ru9 (1.359(3) Å) is the smallest. Coordination of the O,S-chelating ligands to ruthenium(II) results in the elongation of the C(1)-S(1) bond and shortening of the C(3)-O(1) bond, this is comparable to the already discussed platinum(II) complexes.[Hilde-brandt, 2016a]

Tab. 2: Specific bond angles [°] and bond lengths [Å] for all characterized ruthenium(II) compounds.

	Ru9	**Ru13**	**Ru14**
O(1)-Ru(1)	2.0790(14)	2.0822(14)	2.0754(15)
S(1)-Ru(1)	2.3544(5)	2.3498(5)	2.3498(6)
Cl(1)-Ru(1)	2.4081(5)	2.4317(5)	2.4091(6)
O(1)-C(3)	1.266(2)	1.268(2)	1.270(3)
C(3)-C(4)	1.503(3)	1.501(3)	1.492(3)
S(1)-C(1)	1.690(2)	1.699(2)	1.690(2)
O(2)-C(9/8/7)	1.359(3)	1.373(3)	1.372(3)
S(1)-Ru(1)-O(1)	91.85(4)	91.37(4)	92.71(5)
S(1)-Ru(1)-Cl(1)	86.37(2)	87.227(19)	88.09(2)
O(1)-Ru(1)-Cl(1)	85.86(4)	84.43(4)	82.29(5)

Biological Behavior

For investigation of the biological behavior all named substances were characterized for their cytotoxic activity against a panel of cell lines enabling an understanding of the structure-activity relationship. Cytotoxic activity was determined on ovarian carcinoma cell lines SKOV3 and A2780 as well as their special-prepared Cisplatin resistant analogues (SKOV3cis and A2780cis) and lung carcinoma cell line A549. Due to a low solubility in water, dmso is used as a solvent for the preparation of a dilution series in cell culture experiments. The toxic influence of dmso was determined earlier and experiments were carried out with 0.5% dmso in cell culture media and this concentration was used as reference sample in each MTT assay (details: Experimental Part).[Hildebrandt, 2016a] Cisplatin was used as reference substance and a 4.7 or 3.6 times higher IC50 value was observed for resistant cell lines, see Table 3. Resistant factors (RF) were determined for all

substances (for IC50 values and RF of β-Hydroxydithiocinnamic acid esters L1-L18 see Table S2 and S3, Supplementary part). All investigated ruthenium(II) compounds show lower RF values than Cisplatin on ovarian carcinoma cell lines, differing from 0.2 to 1.5 (Table 3). Whereas the IC50 values on the non-resistant cell lines are in most cases higher than for the reference substance no increased IC50 value is observed on the resistant cell lines. Contrary, nine ruthenium complexes show lower IC50 values on SKOV3cis than Cisplatin and four compounds on A2780cis. Thus, it can be concluded that these compounds are able to bypass the Cisplatin resistance mechanism in these cell lines and act by a different mechanism of action.

The osmium compounds show in most cases lower IC50 values than the reference Cisplatin (except for SKOV3 and Os7, 13 and 14, Table 3). To point out, all substances show IC50 values between 0.3-0.4 µM on A2780 whereas Cisplatin has an IC50 value of 1.3 µM. On the resistant analogue of A2780 the activity is more than 5-times higher for Os3 (0.4 µM) and Os13 (0.8 µM) in comparison to Cisplatin (6.1 µM). Albeit only one compound (Os3) exhibits a lower IC50 value for SKOV3 than Cisplatin, all compounds have a higher activity against SKOV3cis. Remarkably, Os7 shows a 13-times lower IC50 value than Cisplatin (0.6 to 13.5 µM). The most promising candidate, Os3, shows IC50 values between 0.4 µM (A2780s) and 2.3 µM (SKOV3cis), whereas the range of Cisplatin is between 1.3 µM (A2780) – 13.5 µM (SKOV3cis). The resistance factors of the ruthenium compounds are in most cases lower than 1 pointing to the targeting of resistant cells, the osmium analogues do not behave the same. This confirms earlier comparison studies in the literature that osmium analogues of ruthenium complexes show different biological behavior *in vitro*, as mentioned in the Introduction part. To conclude, the osmium compounds are in general more active against all five cell lines than Cisplatin and their ruthenium counterparts whereas the ruthenium compounds are able to circumvent the Cisplatin resistance. This shows the enormous potential for osmium compounds as next generation anticancer drugs and the opportunity for ruthenium compounds to be selected for resistant tumors.

Tab. 3: IC50 values in µM of all metal(II) compounds for the antiproliferative effects in cancerous cells.

Substance	SKOV3 [µM]	SKOV3cis [µM]	A2780 [µM]	A2780cis [µM]	A549 [µM]
Ru1	34.7 (±0.2)	18.4 (±5.1)	9.6 (±1.1)	9.6 (±6.4)	28.8 (±5.1)
RF(Ru1)	0.5		1		
Ru2	15.7 (±3.7)	11.1 (±5.6)	4.8 (±7.4)	4.8 (±5.4)	12.2 (±2.8)
RF(Ru2)	0.7		1		
Ru3	18.9 (±0.8)	12.1 (±5.5)	8.7 (±3.8)	7.4 (±0.8)	8.0 (±8.5)
RF(Ru3)	0.6		0.9		
Os3	1.1 (±0.2)	2.3 (±0.2)	0.4 (±0.1)	0.4 (±0.3)	0.7 (±0.1)
RF(Os3)	2.1		0		
Ru4	21.8 (±4.6)	27.9 (±5.6)	21.4 (±7.5)	21.4 (±4.1)	26.3 (±11.8)
RF(Ru4)	1.3		1		
Ru5	15.4 (±4.0)	9.3 (±5.2)	44.9 (±1.3)	8.1 (±5.6)	11.5 (±3.8)
RF(Ru5)	0.6		0.2		
Ru6	28.6 (±4.5)	22.6 (±3.0)	15.4 (±5.6)	15.3 (±0.6)	48.5 (±4.3)
RF(Ru6)	0.8		1		
Ru7	25.3 (±8.6)	12.5 (±5.9)	24.2 (±6.5)	16.4 (±3.7)	39.6 (±2.7)
RF(Ru7)	0.5		0.7		
Ru7	22.4 (±9.6)	17.8 (±0.9)	16.4 (±3.3)	15.0 (±2.9)	15.3 (±8.1)
RF(Ru7)	0.8		0.9		
Os7	8.8 (±4.4)	0.6 (±0.5)	0.4 (±0.1)	2.1 (±1.5)	6.2 (±5.8)

RF(Os7)	0.1		5.3		
Ru8	21.3 (±1.9)	20.3 (±4.9)	14.3 (±7.7)	16.8 (±3.0)	13.7 (±4.6)
RF(Ru8)	1		1.2		
Ru9	25.3 (±8.6)	12.5 (±5.9)	24.2 (±6.5)	16.4 (±3.7)	39.6 (±2.7)
RF(Ru9)	0.5		0.7		
Ru10	27.7 (±5.5)	17.7 (±3.6)	14.6 (±6.2)	11.7 (±2.3)	27.7 (±10.8)
RF(Ru10)	0.6		0.8		
Ru11	17.0 (±1.5)	16.8 (±1.1)	15.6 (±7.1)	11.8 (±4.6)	19.0 (±1.9)
RF(Ru11)	1		0.8		
Ru12	24.0 (±10.4)	12.7 (±7.5)	11.0 (±8.1)	10.1 (±6.8)	6.9 (±0.8)
RF(Ru12)	0.5		0.9		
Ru13	16.9 (±2.2)	17.4 (±3.1)	2.6 (±0.4)	4.8 (±3.9)	28.4 (±4.0)
RF(Ru13)	1		1.8		
Os13	4.1 (±2.1)	7.1 (±1.8)	0.3 (±0.0)	0.8 (±0.4)	3.1 (±1.2)
RF(Os13)	1.7		2.7		
Ru14	3.5 (±2.0)	5.1 (±2.8)	1.9 (±0.5)	2.9 (±0.8)	2.7 (±1.2)
RF(Ru14)	1.5		1.5		
Os14	10.4 (±1.4)	12.1 (±0.7)	0.3 (±0.0)	1.3 (±0.6)	5.5 (±4.0)
RF(Os14)	1.2		4.3		
Ru15	7.4 (±1.4)	3.7 (±0.8)	5.8 (±2.3)	4.4 (±1.4)	16.5 (±1.9)
RF(Ru15)	0.5		0.8		
Ru16	13.2 (±2.9)	13.2 (±4.4)	5.4 (±3.5)	6.8 (±4.6)	4.9 (±0.4)

RF(Ru16)	1		1.3		
Ru17	17.2 (±3.4)	17.5 (±0.6)	14.2 (±2.6)	9.8 (±2.8)	15.1(±0.5)
RF(Ru17)	1		0.7		
CDDP	**3.8 (±2.8)**	**13.5 (±4.4)**	**1.3 (±0.2)**	**6.1 (±2.1)**	**7.6 (±2.6)**
RF(CDDP)	**3.6**		**4.7**		

Tab. 4: IC50 values in μM of Ru14, Os3 and Cisplatin investigated for non-cancerous cell lines.

Cell line	**Ru14**	**Os3**	**Cisplatin**
Keratinocytes	› 100	84.5 (±31.3)	5.7 (±3.1)
Fibroblasts	› 100	› 100	4.1 (±1.1)
MCF10A	16.7 (±4.1)	21.3 (±3.3)	3.3 (±0.6)

Table 4 shows IC50 values for normal primary short-term cell cultures of Keratinocytes and Fibroblasts as well as the non-cancerous breast epithelial cell line MCF10A. As mentioned before Cisplatin shows numerous side effects by its unselective behavior and cytotoxic activity against non-cancerous cell lines. The here investigated IC50 values for non-cancerous cultures confirm that. Despite this, the both most active compounds, Os3 and Ru14, show high IC50 values for these cells. The ruthenium compounds show high cytotoxic activity, especially against Cisplatin resistant cell lines, which means they are able to escape the mechanisms of Cisplatin resistance. Additionally, they do not attack non-cancerous cells potentially leading to lower side effects during the therapy *in vivo*. The osmium compounds show very low IC50 values in general and high IC50 values on non-cancerous cell lines, thus they are more active than Cisplatin and also, comparable to the ruthenium complexes, more specific against cancer cells. Lower side effects may translate into the treatment with higher doses of the drugs resulting in earlier and increased effects. Therefore, acquired drug resistance mechanisms arising after several treatments with suboptimal doses may

be circumvented by drugs like these osmium compounds due to lower toxic side effects.

To conclude, there are possibly two different indication forms for the ruthenium(II) and osmium(II) complexes. The ruthenium(II) compounds should be further developed for a treatment of Cisplatin resistant tumours, whereas the osmium(II) complexes can be an alternative for the first-line therapy due to higher cytotoxic activity compared to Cisplatin.

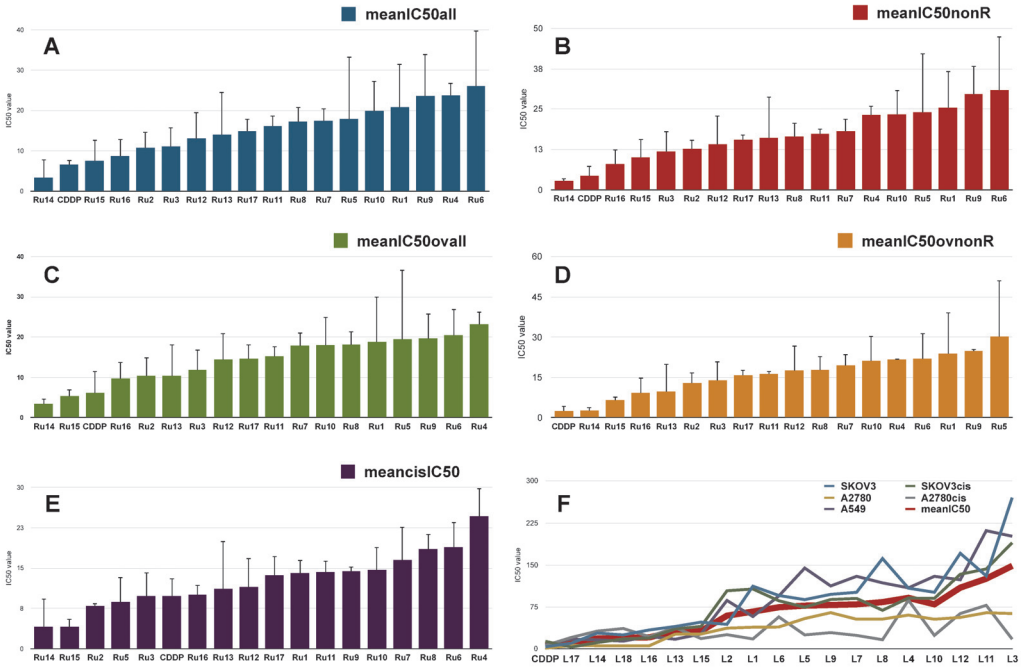

Fig. 12: (**A-E**): Mean IC50 values for all ruthenium(II) complexes. **A**: All 5 investigated cell lines; **B**: SKOV3/ A2780 and A549; **C**: SKOV3/SKOV3cis/A2780 and A2780cis; **D**: SKOV3 and A2780; **E**: SKOV3cis and A2780cis; **F**: Trend of IC50 values for all β-Hydroxydithiocinnamic acid alkyl esters for all investigated cell lines and the meanIC50 value (red line).

A further analysis for the different ruthenium(II) compounds to determine structure-activity-relationships shows that five compounds (Ru14, Ru15, Ru2, Ru5 and Ru3) exhibit lower mean IC50 value on Cisplatin resistant cell lines than Cisplatin itself, Figure 12**E**. Interestingly, compounds Ru14, Ru15 and Ru16 are, all together, the most active compounds in comparison to Cisplatin (Figure 12). The compound Ru14 shows a lower IC50 value when compared to Cisplatin for all cancer cell lines (12**A**), for all ovarian carcinoma cell lines (12**C**), for the Cisplatin

resistant cell lines (12**E**) and for all non-resistant cell lines (12**B**) than Cisplatin. In conclusion, the determined structure-activity-relationship shows that longer alkyl chains at the aromatic ring lead to higher cytotoxic activity. Most active is the compound with an ethoxy-group at *para*-position (Ru14), followed by Ru15 with an ethoxy-group at *ortho*-position. Interestingly, compound Ru16 has a butoxy-substituent at *meta*-position. Thus, it can be concluded that the biological activity is mediated by a longer chain (butoxy) at the *meta*-position, whereas the *ortho*- and *para*-positions are more suitable with a shorter chain (ethoxy). To have a further look at the influence of the different ligand systems and substitution patterns all β-Hydroxydithiocinnamic acid alkyl esters were tested under same conditions as their derived ruthenium(II) complexes (Table S2 Supplementary Part, Figure 12**F**). Figure 12**F** shows the trend of all IC50 values ordered by an increased meanIC50 value (determined for all five cell lines) for the β-Hydroxydithiocinnamic acid alkyl esters. Interestingly the most active compounds are L17, L14, L18, L16, L13 and L15 showing similar low IC50 values on all cell lines. This confirms the results for the corresponding ruthenium(II) complexes proving that the longer alkyl chains on the aromatic positions are the most active compounds and that the IC50 values increase by decreasing lipophilicity. All substances are less cytotoxic than Cisplatin itself and therefore the metal(II) center is necessary for the high cytotoxic activity, what is in clear contrast to the literature.[Hackl, 2016]

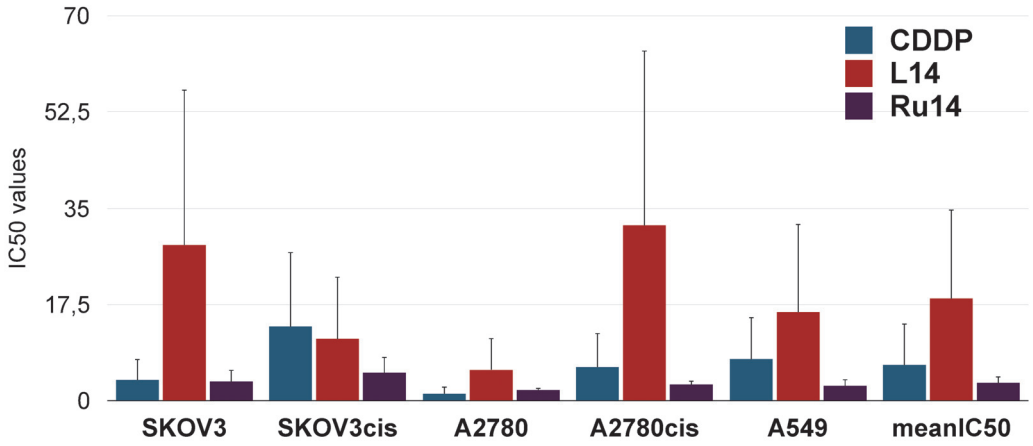

Fig. 13: IC50 values for compounds CDDP/ L14/ Ru14.

Figure 13 shows all IC50 values for the reference substance Cisplatin (CDDP) as well as for L14 and Ru14. It is shown that the ruthenium(II) center decreases the IC50 values in all cases and therefore the metal is the active part, underlined with a suitable fit to the most active ligand system.

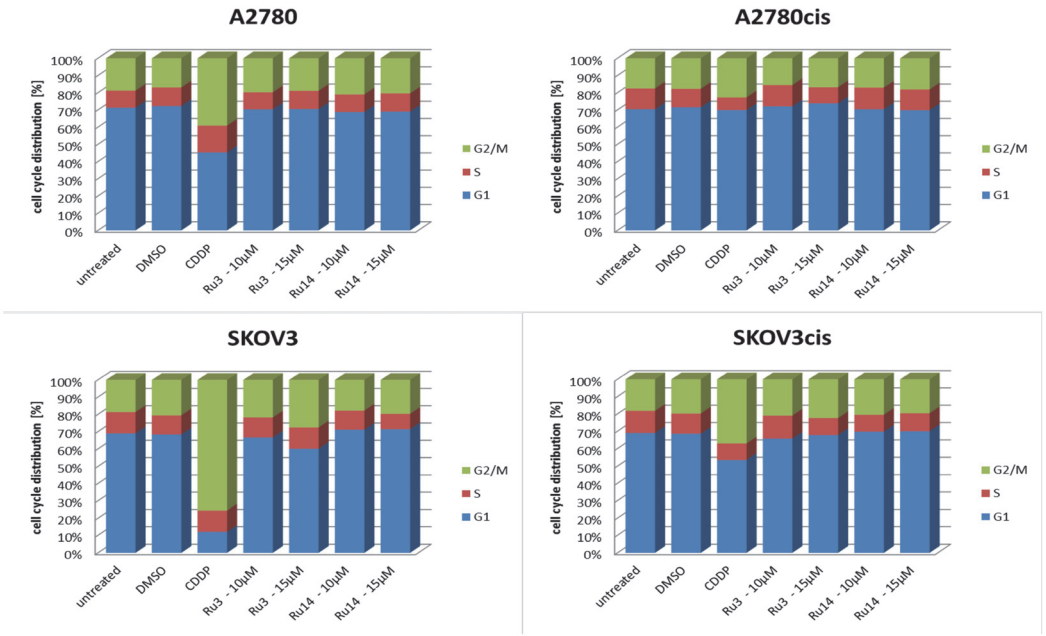

Fig. 14: Cell cycle distribution for CDDP/ Ru3/ Ru14 in A2780 and SKOV3 cells. Cells were incubated for 48h followed by a recovering time of 24h.

The reduced viability can be a result of cell cycle arrest and/or increased apoptosis. To further evaluate the anticancer properties of the ruthenium(II) complexes we therefore measured cell cycle distribution and cell death rates after treatment with Ru3 or Ru14. After seeding and attaching the cells were treated for 48h with different concentrations. For cell cycle distribution measurements a recovery phase of 24h was added after treatment and cells were fixed and stained with PI for the DNA content. Arresting of cells in specific cell cycle phases gives them time to resolve the DNA damage (G1arrest) or is an initial step to apoptosis, if DNA damage is to severe (G2/M arrest).[Čanovic´, 2017] As previously shown CDDP (5 µM) efficiently induces cell cycle arrest in G2/M phase in parental A2780 and SKOV3 cells, whereas resistant cell show only a minor G2/M arrest.[Kritsch, 2017] On the other side, both examined ruthenium complexes show no or only a minor effect on cell cycle distribution (Figure 14). This is in line with some published ruthenium(II) complexes, which do not all induce

cell cycle arrest.[Čanovic, 2017; Sun, 2017] Therefore, one can suggest that these complexes do not induce high DNA damage levels leading to cell cycle arrest. Secondly, for cell death rate analysis alive cells were stained with PI immediately after 48h treatment. Again, it can be seen that 15 µM CDDP efficiently induces cell death in parental ovarian cancer cells, [Kritsch, 2017] where it is 29.9 fold higher for A2780 and 6.3 fold higher for SKOV3 compared to DMSO. Furthermore, resistant cells show much lower cell death rates. Both complexes, Ru3 and Ru14, have a high capacity to induce cell death *in vitro* (Figure 15). In A2780 cells both compounds trigger similar cell death rates in parental and CDDP-resistant cells. Interestingly, CDDP-resistant SKOV3 are much more sensitive to both ruthenium(II) complexes than the parental counterpart, with a median of 3.3 fold higher sensitivity. Interestingly, Ru3, induced a higher cell death rate as Ru14 despite contrary IC50 values.

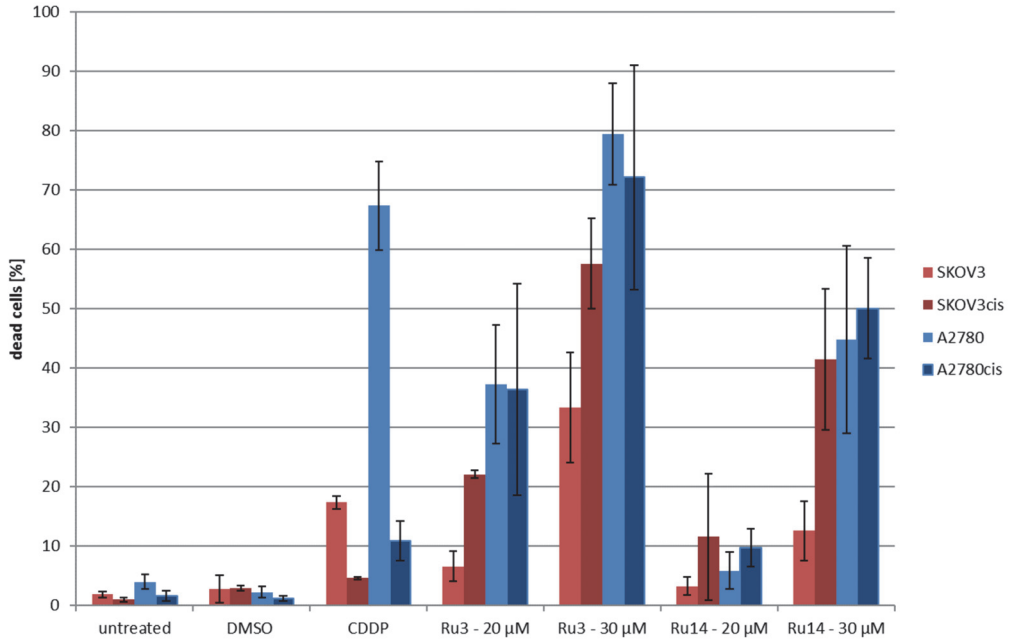

Fig. 15: Cell death rates induced by 15 µM CDDP or 20 µM and 30 µM Ru3/ Ru14 in A2780 and SKOV3 cells. Untreated or DMSO-treated cells served as controls. Cells were incubated for 48h. The amount of dead cells was measured *via* PI staining.

Previous studies showed a direct induction of apoptosis by ruthenium(II) complexes *via* ROS production and activation of pro-apoptotic BCL2-family proteins.[Yang, 2012; Tang, 2017] This might be the case here as well, as we see

efficient cell death- but no cell cycle arrest induction by Ru3/ Ru14. Furthermore, the ruthenium(II) core atom might be responsible for this effect, because of the lack of anticancer behavior of the ligand L14 (Figure 13). Additionally, many ruthenium(II) complexes with different ligands induce intracellular ROS.[Qian, 2013; Zeng, 2016; Kasprzak, 2011; Zhao, 2014]

To further confirm that Ru compounds use another mechanism of action DNA damage analyses were conducted for Ru3 and Ru14 (Figure 16). Both Ru compounds (at IC50 concentration) induced less γH2AX-foci as CDDP after 24h incubation under the same conditions.

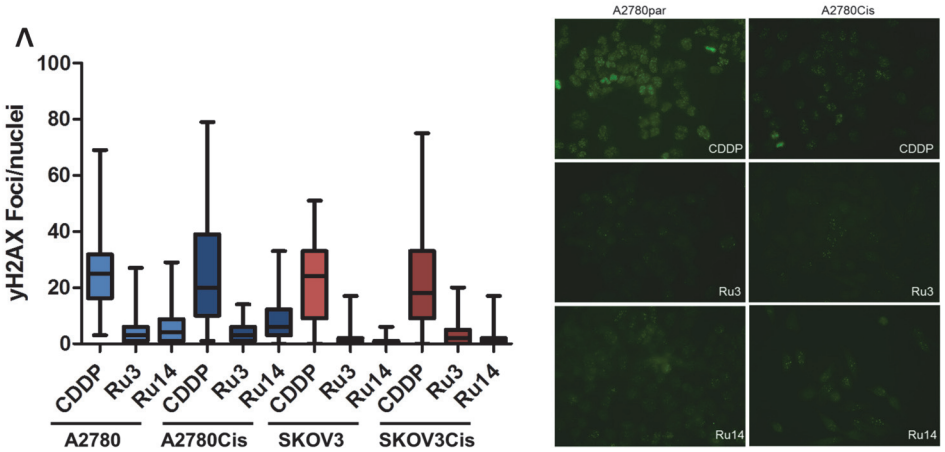

Fig. 16: γH2AX-foci analysis (DNA damage) after 24h incubation with IC50 concentrations for Cisplatin, Ru3 and Ru14.

Conclusion

In this work we investigated 18 cinnamic acid derivatives, 17 ruthenium(II) complexes and 4 osmium(II) complexes, all of these compounds have been characterized by different methods, including X-Ray diffraction analysis. NMR spectra signals have been compared also to previously reported platinum(II) complexes and show significant changes in the ligand systems after complexation to metals. Stability determinations for some ruthenium(II) compounds were done with NMR spectroscopy, showing that these compounds are not stable in the solvent dmso, but in different other organic solvents.

The biological activity of these complexes have been investigated mainly by IC50 measurements for all substances, as well as by cell cycle arrest, cell death and DNA damage analyses for two of the ruthenium(II) complexes.

Regarding the IC50 values, we can add to the previously reported SARs of ruthenium(II) and osmium(II) complexes by Keppler and coworkers, that bearing an O,S-chelating ligand shows lower IC50 values on osmium(II) complexes than on their ruthenium(II) analogues, but the ruthenium(II) compounds show lower resistance factors.[Meier-Menches, 2018] Nevertheless, regarding non-cancerous cell lines and therefore possible toxicity and side effects, both complexes show selective behavior to cancer cell lines and high IC50 values on non-cancerous cells.

Focusing on the structure-activity-relationship of the ruthenium(II) compounds, it is shown that longer alkyl chains at the aromatic ring lead to higher cytotoxic activity of these compounds. For the osmium complexes, most active compound is Os3, with hydroxy-group at *meta*-position. Therefore, some of these compounds will be selected for further development, including *in vivo* experiments.

Experimental Part

Materials and Techniques

All reactions were performed using standard Schlenk and vacuum-line techniques under nitrogen atmosphere. The NMR spectra were recorded with a Bruker Avance 200 MHz, 400 MHz or 600 MHz spectrometer. Chemical shifts are given in ppm with reference to $SiMe_4$. Mass spectra were recorded with a Finnigan MAT SSQ 710 instrument. Elemental analysis was performed with a Leco CHNS-932 apparatus. Silica gel 60 (0.015-0.040 mm) was used for column chromatography and TLC was performed using Merck TLC aluminium sheets (Silica gel 60 F_{254}). Chemicals were purchased from Fisher Scientific, Aldrich or Acros and were used without further purification. All solvents were dried and distilled prior to use according to standard methods.

Synthesis

Different β-Hydroxydithiocinnamic acid alkyl esters and $[(\eta^6\text{-}p\text{-cymene})XCl_2]_2$ (X= Ru or Os) were prepared by modified literature methods.[Hildebrandt, 2016a; Bennett, 1974] New compounds L13-L17 are described in the supplementary information.

General procedure 1: Ruthenium(II) complexes with β-Hydroxydithiocinnamic acid alkyl esters, chlorido and *p*-cymene as ligands (Ru1-Ru17).

$[(\eta^6\text{-}p\text{-cymene})RuCl_2]_2$ (0.5 equiv.) was dissolved in 50 ml tetrahydrofurane (THF). The corresponding ligand L1-L12 (1 equiv.) was solved in 25 ml THF and potassium-*tert*.-butoxylate (*t*-BuOK, 2 equiv.) was added to that solution and stirred 30 min at rt. The solution of the deprotonated ligand was added dropwise to the suspension of $[(\eta^6\text{-}p\text{-cymene})RuCl_2]_2$ and stirred at room temperature for 24 h. After adding sulfuric acid (H_2SO_4, 20 ml, 2M) to the solution, the mixture was stirred for 30 min at rt and afterwards extracted with dichlormethane (DCM, 3 x 30 ml). The combined organic phases were washed with water (3x20 ml), dried over sodium sulfate and after filtration and evaportaion of the solvent the crude product was purified with column chromatography.

General procedure 1: Osmium(II) complexes with β-Hydroxydithiocinnamic acid alkyl esters, chlorido and *p*-cymene as ligands (Os1-Os4).

$[(\eta^6\text{-}p\text{-cymene})OsCl_2]_2$ (0.5 equiv.) was dissolved in 50 ml tetrahydrofurane (THF). The corresponding ligand (1 equiv.) was solved in 25 ml THF and potassium-*tert*.-butoxylate (*t*-BuOK, 2 equiv.) was added to that solution and stirred 30 min at rt. The solution of the deprotonated ligand was added dropwise to the suspension of $[(\eta^6\text{-}p\text{-cymene})RuCl_2]_2$ and stirred at room temperature for 24 h. After adding sulfuric acid (H_2SO_4, 20 ml, 2M) to the solution, the mixture was stirred for 30 min at rt and afterwards extracted with dichlormethane (DCM, 3 x 30 ml), the combined organic phases were washed with water (3x20 ml), dried over sodium sulfate and after filtration and evaporation of the solvent the crude product was purified with column chromatography.

[(n^6-*p*-cymene)Ru(1-phenyl-3-(methylthio)-3-thioxo-prop-1-en-1-olate-*O,S*)Cl] (Ru1)

Synthesis was performed according to general procedure 1. [(η^6-*p*-cymene)$RuCl_2]_2$ (500 mg, 0.81 mmol) was used. L1 (341 mg, 1.62 mmol) was dissolved in THF, *t*-BuOK (182 mg, 1.62 mmol) was added. Column chromatography mobile phase: DCM - DCM 10:THF 1 – THF. Yield: 540 mg (69.5 %) as red crystals. ^{1}H NMR (600 MHz, CD_2Cl_2): δ = 1.29 (dd, $^3J_{H-H}$=5.8 Hz, $^4J_{H-H}$=2.2 Hz, 6H, -cymene-CH-(CH_3)$_2$); 2.20 (s, 3H, -cymene-CH_3); 2.69 (s, 3H, -SCH_3); 2.85 (sp, 1H, -cymene-C*H*-$(CH_3)_2$); 5.29 (d, $^3J_{H-H}$=5.9 Hz, 2H, -cymene:CH_3-C-C*H*-CH-C-CH-$(CH_3)_2$); 5.50 (dd, $^3J_{H-H}$=22.6 Hz, $^4J_{H-H}$=5.9 Hz, 2H –cymene:CH_3-C-CH-C*H*-C-CH-$(CH_3)_2$); 6.76 (s, 1H, =C*H*); 7.40 (t, 2H, -Ar-*m*-H); 7.48 (t, 1H, -Ar-*p*-H); 7.81 (d, $^3J_{H-H}$=7.4 Hz, 2H, -Ar-*o*-H). ^{13}C{^{1}H} NMR (101 MHz, CD_2Cl_2): δ = 17.4 (-SCH_3); 18.1 (-cymene-C-*C*H_3); 22.3 (-cymene-CH-(*C*H_3)$_2$); 30.8 (-cymene-*C*H-$(CH_3)_2$); 83.1 (-cymene:CH_3-C-*C*H-CH-C-CH-$(CH_3)_2$); 83.3 (CH_3-C-*C*H-CH-C-CH-$(CH_3)_2$); 85.5 (CH_3-C-CH-*C*H-C-CH-$(CH_3)_2$); 100.4 (CH_3-*C*-CH-CH-C-CH-$(CH_3)_2$); 102.5 (CH_3-C-CH-CH-*C*-CH-$(CH_3)_2$); 109.1 (=*C*H); 127.4 (-Ar-*o*-C); 131.3 (-Ar-*p*-C); 140.0 (-Ar-C1); 178.0 (-*C*-O-); 187.8 (-*C*=S). MS (DEI): m/z = 444, 438, 399, 394, 317, 315, 280, 274. Elemental analysis: calculated for $C_{20}H_{23}ClORuS_2$ C: 50.04 %; H: 4.83 %, found: C: 49.92 %; H: 4.82 %.

[(η^6-*p*-cymene)Ru(1-phenyl-3-(ethylthio)-3-thioxo-prop-1-en-1-olate-*O,S*)Cl] (Ru2)

Synthesis was performed according to general procedure 1. [(η^6-*p*-cymene)$RuCl_2]_2$ (500 mg, 0.81 mmol) was used. L2 (363 mg, 1.62 mmol) was dissolved in THF, *t*-BuOK (182 mg, 1.62 mmol) was added. Column chromatography mobile phase: DCM - DCM 10:THF 1 – THF. Yield: 460 mg (57.3 %) as red crystals.^{1}H NMR (600 MHz, CD_2Cl_2): δ = 1.29 (dd, $^3J_{H-H}$=7.0 Hz, $^4J_{H-H}$=2.1 Hz, 6H, -cymene-CH-(CH_3)$_2$); 1.40 (t, 3H, -S-CH_2-CH_3); 2.21 (s, 3H, -cymene-CH_3); 2.85 (sp, 1H, -cymene-C*H*-$(CH_3)_2$); 3.28 (q, 2H, -S-CH_2-CH_3); 5.28 (dd, $^3J_{H-H}$=5.8 Hz, 2H, -cymene:CH_3-C-C*H*-CH-C-CH-$(CH_3)_2$); 5.50 (dd, $^3J_{H-H}$=20.7 Hz, $^4J_{H-H}$=5.8 Hz, 2H, –cymene:CH_3-C-CH-C*H*-C-CH-$(CH_3)_2$); 6.75 (s, 1H, =C*H*); 7.40 (t, 2H, -Ar-*m*-H); 7.48 (t, 1H, -Ar-*p*-H); 7.80 (d, $^3J_{H-H}$=7.4 Hz, 2H, -Ar-*o*-H). ^{13}C{^{1}H} NMR (101 MHz,

CD_2Cl_2): δ = 13.9 (-SCH_2CH_3); 18.2 (-cymene-C-CH_3); 22.4 (-cymene-CH-(CH_3)$_2$); 24.2 (-S-CH_2CH_3); 30.9 (-cymene-CH-(CH_3)$_2$); 83.1 (-cymene:CH_3-C-CH-CH-C-CH-(CH_3)$_2$); 83.3 (CH_3-C-CH-CH-C-CH-(CH_3)$_2$); 85.6 (CH_3-C-CH-CH-C-CH-(CH_3)$_2$); 85.6 (CH_3-C-CH-CH-C-CH-(CH_3)$_2$); 100.6 (CH_3-C-CH-CH-C-CH-(CH_3)$_2$); 102.6 (CH_3-C-CH-CH-C-CH-(CH_3)$_2$); 109.4 (=CH); 127.5 (-Ar-*o*-C); 131.4 (-Ar-*p*-C); 140.1 (-Ar-C1); 178.0 (-C-O-); 187.1 (-C=S). MS (DEI): m/z = 458, 456, 399, 393, 311, 297. Elemental analysis: calculated for $C_{20}H_{25}ClORuS_2$ C: 51.05 %; H: 5.10 %, found: C: 50.97 %; H: 5.03 %.

[(η^6-*p*-cymene)Ru(1-(3-hydroxyphenyl)-3-(methylthio)-3-thioxo-prop-1-en-1-olate-*O,S*)Cl] (Ru3)

Synthesis was performed according to general procedure 1. [(η^6-*p*-cymene)$RuCl_2]_2$ (500 mg, 0.81 mmol) was used. L3 (367 mg, 1.62 mmol) was dissolved in THF, *t*-BuOK (182 mg, 1.62 mmol) was added. Column chromatography mobile phase: DCM - DCM 10:THF 1 – THF. Yield: 190 mg (23.6 %) as red crystals. ^{1}H NMR (600 MHz, CD_2Cl_2): δ = 1.26 (d, $^3J_{H-H}$=6.4 Hz, 6H, -cymene-CH-(CH_3)$_2$); 2.20 (s, 3H, CH_3, -cymene-CH_3); 2.64 (s, 3H, -SCH_3); 2.83 (sp, 1H, -cymene-CH-(CH_3)$_2$); 5.33 (m, 2H, -cymene:CH_3-C-CH-CH-C-CH-(CH_3)$_2$); 5.52 (m, 2H –cymene:CH_3-C-CH-CH-C-CH-(CH_3)$_2$); 6.71 (s, 1H, =CH); 6.85 (m, 2H, -Ar-*o*-H); 7.11 (m, 1H, -Ar-*m*-H); 7.23 (m, 3H, =CH/ -Ar-*p*-H); 10.1 (s, 1H, -COH). ^{13}C{^{1}H} NMR (101 MHz, CD_2Cl_2): δ = 17.6 (-SCH_3); 18.3 (-cymene-C-CH_3); 22.4 (-cymene-CH-(CH_3)$_2$); 30.9 (-cymene-CH-(CH_3)$_2$); 83.3 (-cymene:CH_3-C-CH-CH-C-CH-(CH_3)$_2$); 83.8 (CH_3-C-CH-CH-C-CH-(CH_3)$_2$); 85.5 (CH_3-C-CH-CH-C-CH-(CH_3)$_2$); 85.6 (CH_3-C-CH-CH-C-CH-(CH_3)$_2$); 100.8 (CH_3-C-CH-CH-C-CH-(CH_3)$_2$); 102.3 (CH_3-C-CH-CH-C-CH-(CH_3)$_2$); 109.2 (=CH); 125.2 (-Ar-*m*-C); 129.2 (-Ar-*o*-C); 129.4 (-COH); 156.9 (-Ar-*p*-C); 178.0 (-ArC1); 187.3 (-C-O-); 207.2 (-C=S). MS (DEI): m/z = 134, 119, 115, 91, 77, 39, 28. Elemental analysis: calculated for $C_{20}H_{23}ClO_2RuS_2$ C: 48.43 %; H: 4.67 %, found: C: 48.60 %; H: 4.83 %.

[(η^6-*p*-cymene)Ru(1-(4-hydroxyphenyl)-3-(methylthio)-3-thioxo-prop-1-en-1-olate-*O,S*)Cl] (Ru4)

Synthesis was performed according to general procedure 1. [(η^6-*p*-cymene)$RuCl_2]_2$ (500 mg, 0.81 mmol) was used. L4 (367 mg, 1.62 mmol) was dissolved in THF, *t*-BuOK (182 mg, 1.62 mmol) was added. Column chromatography mobile phase: DCM - DCM 6:THF 1 – THF. Yield: 190 mg (23.6 %) as red crystals. ^{1}H NMR (400 MHz, CD_2Cl_2): δ = 1.20 (m, 6H, -cymene-CH-(CH_3)$_2$); 2.10 (s, 3H, -cymene-CH_3); 2.59 (s, 3H, -SCH_3); 2.75 (sp, 1H, -cymene-C*H*-(CH_3)$_2$); 5.45 (dd, $^3J_{H\text{-}H}$=5.7 Hz, 2H, -cymene:CH_3-C-C*H*-CH-C-CH-(CH_3)$_2$); 5.67 (dd, $^3J_{H\text{-}H}$=20.4 Hz, $^4J_{H\text{-}H}$=5.8 Hz, 2H –cymene:CH_3-C-CH-C*H*-C-CH-(CH_3)$_2$); 6.65 (s, 1H, =C*H*); 6.80 (m, 2H, -Ar-*o*-H); 7.76 (m, 2H, -Ar-*m*-H): 10.1 (s, 1H, -CO*H*). ^{13}C{^{1}H} NMR (101 MHz, CD_2Cl_2): δ = 17.5 (-SCH_3); 18.2 (-cymene-C-*C*H_3); 22.2/22.6 (-cymene-CH-(*C*H_3)$_2$); 30.8 (-cymene-*C*H-(CH_3)$_2$); 82.9 (-cymene:CH_3-C-*C*H-CH-C-CH-(CH_3)$_2$); 84.4 (CH_3-C-*C*H-CH-C-CH-(CH_3)$_2$); 85.1 (CH_3-C-C-*C*H-C-CH-(CH_3)$_2$); 85.5 (CH_3-C-CH-*C*H-C-CH-(CH_3)$_2$); 100.6 (CH_3-*C*-CH-CH-C-CH-(CH_3)$_2$); 102.2 (CH_3-C-CH-CH-*C*-CH-(CH_3)$_2$); 108.5 (=*C*H); 125.2 (-Ar-*o*-C); 129.9 (-Ar-C1); 130.9 (-Ar-*m*-C); 160.7 (-*C*OH); 177.8 (-*C*-O-); 185.0 (-*C*=S). MS (ESI): m/z = 463, 461, 415, 315, 281 Elemental analysis: calculated for $C_{20}H_{23}ClO_2RuS_2$ C: 48.43 %; H: 4.67 %, found: C: 48.17 %; H: 4.76 %.

[(η^6-*p*-cymene)Ru(1-(3-hydroxyphenyl)-3-(ethylthio)-3-thioxo-prop-1-en-1-olate-*O,S*)Cl] (Ru5)

Synthesis was performed according to general procedure 1. [(η^6-*p*-cymene)$RuCl_2]_2$ (500 mg, 0.81 mmol) was used. L5 (390 mg, 1.62 mmol) was dissolved in THF, *t*-BuOK (182 mg, 1.62 mmol) was added. Column chromatography mobile phase: DCM - DCM 10:THF 1 – THF. Yield: 340 mg (41.0 %) as red crystals. ^{1}H NMR (600 MHz, CD_2Cl_2): δ = 1.26 (d, $^3J_{H\text{-}H}$=6.9 Hz, 6H, -cymene-CH-(CH_3)$_2$); 1.37 (t, 3H. –SCH_2CH_3); 2.21 (s, 3H, CH_3, -cymene-CH_3); 2.83 (sp, 1H, -cymene-C*H*-(CH_3)$_2$); 3.23 (q, 2H, -SCH_2CH_3); 5.33 (m, 2H, -cymene:CH_3-C-C*H*-CH-C-CH-(CH_3)$_2$); 5.52 (m, 2H –cymene:CH_3-C-CH-C*H*-C-CH-(CH_3)$_2$); 6.68 (s, 1H, =C*H*); 6.83 (m, 2H, -Ar-*o*-H); 7.08 (t, 1H, -Ar-*m*-H); 7.20 (m, 3H, =C*H*/ -Ar-*p*-H). ^{13}C{^{1}H} NMR (101 MHz, CD_2Cl_2): δ = 13.5 (-SCH_2CH_3); 18.0 (-cymene-C-*C*H_3); 22.1 (-cymene-CH-

(CH$_3$)$_2$); 25.6 (-SCH$_2$CH$_3$); 30.5 (-cymene-CH-(CH$_3$)$_2$); 82.9 (-cymene:CH$_3$-C-CH-CH-C-CH-(CH$_3$)$_2$); 83.4 (CH$_3$-C-CH-CH-C-CH-(CH$_3$)$_2$); 85.0 (CH$_3$-C-CH-CH-C-CH-(CH$_3$)$_2$); 85.3 (CH$_3$-C-CH-CH-C-CH-(CH$_3$)$_2$); 100.7 (CH$_3$-C-CH-CH-C-CH-(CH$_3$)$_2$); 101.7 (CH$_3$-C-CH-CH-C-CH-(CH$_3$)$_2$); 109.0 (=CH); 124.8 (-Ar-*m*-C); 129.0 (-COH); 156.5 (-Ar-*p*-C); 177.9 (-ArC1); 187.1 (-C-O-). MS (ESI): m/z = 518, 576, 474, 414, 328, 294, 292. Elemental analysis: calculated for $C_{21}H_{25}ClO_2RuS_2$ C: 49.45 %; H: 4.94 %, found: C: 49.29 %; H: 5.02 %.

[(η^6-*p*-cymene)Ru(1-(4-hydroxyphenyl)-3-(ethylthio)-3-thioxo-prop-1-en-1-olate-*O,S*)Cl] (Ru6)

Synthesis was performed according to general procedure 1. [(η^6-*p*-cymene)RuCl$_2$]$_2$ (385 mg, 0.62 mmol) was used. L6 (300 mg, 1.25 mmol) was dissolved in THF, *t*-BuOK (140 mg, 1.25 mmol) was added. Column chromatography mobile phase: DCM - DCM 6:THF 1 – THF. Yield: 100 mg (15.6 %) as red crystals. ^{1}H NMR (600 MHz, CD$_2$Cl$_2$): δ = 1.22 (d, $^3J_{H\text{-}H}$=6.9 Hz, 6H, -cymene-CH-(CH_3)$_2$); 1.33 (t, 3H, -SCH$_2$CH_3); 2.14 (s, 3H, -cymene-CH_3); 2.79 (sp, 1H, -cymene-CH-(CH$_3$)$_2$); 3.19 (q, 2H, -SCH_2CH$_3$); 5.23 (dd, $^3J_{H\text{-}H}$=5.7 Hz, 2H, -cymene:CH$_3$-C-CH-CH-C-CH-(CH$_3$)$_2$); 5.45 (dd, $^3J_{H\text{-}H}$=17.4 Hz, $^4J_{H\text{-}H}$=5.5 Hz, 2H –cymene:CH$_3$-C-CH-CH-C-CH-(CH$_3$)$_2$); 6.67 (s, 1H, =CH); 6.80 (d, 2H, $^3J_{H\text{-}H}$=8.7 Hz, -Ar-*o*-H); 7.68 (d, $^3J_{H\text{-}H}$=8.4 Hz, 2H, -Ar-*m*-H): 8.62 (s, 1H, -COH). ^{13}C{^{1}H} NMR (101 MHz, CD$_2$Cl$_2$): δ = 13.9 (-SCH$_2$$CH_3$); 18.0 (-cymene-C-$CH_3$); 22.3 (-cymene-CH-($CH_3$)$_2$); 24.1(-S$CH_2CH_3$); 30.8 (-cymene-$C$H-(CH$_3$)$_2$); 83.0 (-cymene:CH$_3$-C-$C$H-CH-C-CH-(CH$_3$)$_2$); 83.1 (CH$_3$-C-$C$H-CH-C-CH-(CH$_3$)$_2$); 85.4 (CH$_3$-C-CH-$C$H-C-CH-(CH$_3$)$_2$); 85.6 (CH$_3$-C-CH-$C$H-C-CH-(CH$_3$)$_2$); 100.4 (CH$_3$-$C$-CH-CH-C-CH-(CH$_3$)$_2$); 102.3 (CH$_3$-C-CH-CH-$C$-CH-(CH$_3$)$_2$); 115.5 (=$C$H); 126.5 (-Ar-*o*-C); 129.2 (-Ar-C1); 131.5 (-Ar-*m*-C); 160.7 (-COH); 177.8 (-C-O-); 185.0 (-C=S). MS (ESI): m/z = 476, 474, 414, 331, 301, 293. Elemental analysis: calculated for $C_{21}H_{25}ClO_2RuS_2$ C: 49.45 %; H: 4.94 %, found: C: 49.40 %; H: 5.00 %.

[(η^6-*p*-cymene)Ru(1-(2-methoxyphenyl)-3-(methylthio)-3-thioxo-prop-1-en-1-olate-*O,S*)] (Ru7)

Synthesis was performed according to general procedure 1. [(η^6-*p*-cymene)$RuCl_2]_2$ (500 mg, 0.81 mmol) was used. L7 (389 mg, 1.62 mmol) was dissolved in THF, *t*-BuOK (182 mg, 1.62 mmol) was added. Column chromatography mobile phase: DCM - DCM 6:THF 1 – THF. Yield: 700 mg (84.6 %) as red crystals. ^{1}H NMR (600 MHz, CD_2Cl_2): δ = 1.23 (dd, $^3J_{H-H}$=6.9 Hz, $^4J_{H-H}$=2.7 Hz, 6H, -cymene-CH-(CH_3)$_2$); 2.19 (s, 3H,-cymene-CH_3); 2.62 (s, 3H, -SCH_3); 2.85 (sp, 1H, -cymene-C*H*-(CH_3)$_2$); 3.83 (s, 3H, -OCH_3); 5.24 (d, $^3J_{H-H}$=6.1 Hz, 2H, -cymene:CH_3-C-C*H*-CH-C-CH-(CH_3)$_2$); 5.46 (dd, $^3J_{H-H}$=23.8 Hz, $^4J_{H-H}$=11.7 Hz, 2H –cymene:CH_3-C-CH-C*H*-C-CH-(CH_3)$_2$); 6.64 (s, 1H, =C*H*); 6.92 (d, $^3J_{H-H}$=8.3 Hz, 1H, -Ar-*o*-H); 6.97 (t, 1H, -Ar-*m*-H); 7.38 (ddd, $^3J_{H-H}$=7.7 Hz, $^4J_{H-H}$=1.8 Hz, 1H, -Ar-*p*-H); 7.50 (dd, $^3J_{H-H}$=7.6 Hz, $^4J_{H-H}$=1.7 Hz, 1H, -Ar-*m*-H). ^{13}C{^{1}H} NMR (101 MHz, CD_2Cl_2): δ = 17.5 (-SCH_3); 18.1 (-cymene-C-*C*H_3); 22.4/22.4 (-cymene-CH-(*C*H_3)$_2$); 30.8 (-cymene-*C*H-(CH_3)$_2$); 56.0 (-O*C*H_3); 82.8 (-cymene:CH_3-C-*C*H-CH-C-CH-(CH_3)$_2$); 83.3 (CH_3-C-*C*H-CH-C-CH-(CH_3)$_2$); 85.4 (CH_3-C-CH-*C*H-C-CH-(CH_3)$_2$); 100.7 (CH_3-*C*-CH-CH-C-CH-(CH_3)$_2$); 102.6 (CH_3-C-CH-CH-*C*-CH-(CH_3)$_2$); 111.9 (-Ar-*o*-C); 113.4 (=*C*H); 120.9 (-Ar-*m*-C); 129.2 (-Ar-C1); 130.6 (-Ar-*m*-C); 131.7 (-Ar-*p*-C); 156.9 (-Ar-*C*-OCH_3); 179.0 (-*C*-O-); 185.9 (-*C*=S). MS (DEI): m/z = 503, 477, 475, 428, 341, 315, 281, 275. Elemental analysis: calculated for $C_{21}H_{25}ClO_2RuS_2$ C: 49.45 %; H: 4.94 %, found: C: 49.79 %; H: 5.13 %.

[(η^6-*p*-cymene)Ru(1-(3-methoxyphenyl)-3-(methylthio)-3-thioxo-prop-1-en-1-olate-*O,S*)] (Ru8)

Synthesis was performed according to general procedure 1. [(η^6-*p*-cymene)$RuCl_2]_2$ (500 mg, 0.81 mmol) was used. L8 (389 mg, 1.62 mmol) was dissolved in THF, *t*-BuOK (182 mg, 1.62 mmol) was added. Column chromatography mobile phase: DCM - DCM 10:THF 1 – THF. Yield: 450 mg (54.5 %) as red crystals. ^{1}H NMR (600 MHz, $CDCl_3$): δ = 1.32 (dd, $^3J_{H-H}$=5.9 Hz, $^4J_{H-H}$=1.7 Hz, 6H, -cymene-CH-(CH_3)$_2$); 2.25 (s, 3H, CH_3, -cymene-CH_3); 2.70 (s, 3H, -SCH_3); 2.91 (sp, 1H, -cymene-C*H*-(CH_3)$_2$); 3.85 (s, 3H, -OCH_3); 5.29 (dd, $^3J_{H-H}$=24.0 Hz, $^4J_{H-H}$=5.7 Hz, 2H, -cymene:CH_3-C-C*H*-CH-C-CH-(CH_3)$_2$); 5.46 (dd, $^3J_{H-H}$=22.1 Hz, $^4J_{H-H}$=6.0 Hz, 2H

–cymene:CH_3-C-CH-C*H*-C-CH-$(CH_3)_2$); 6.76 (s, 1H, =C*H*); 6.99 (m, 1H, -Ar-*o*-H); 7.25-7.31 (m, 2H, -Ar-*m*-H); 7.34-7.40 (m, 2H, -Ar-*p*-H). $^{13}C\{^1H\}$ NMR (101 MHz, CD_2Cl_2): δ = 17.1 (-SCH_3); 17.9 (-cymene-C-*C*H_3); 22.5 (-cymene-CH-(*C*$H_3)_2$); 30.8 (-cymene-*C*H-$(CH_3)_2$); 55.1 (-O*C*H_3); 82.7 (-cymene:CH_3-C-*C*H-CH-C-CH-$(CH_3)_2$); 82.8 (CH_3-C-*C*H-CH-C-CH-$(CH_3)_2$); 85.2 (CH_3-C-CH-*C*H-C-CH-$(CH_3)_2$); 85.7 (CH_3-C-CH-*C*H-C-CH-$(CH_3)_2$; 100.0 (CH_3-*C*-CH-CH-C-CH-$(CH_3)_2$); 102.5 (CH_3-C-CH-CH-*C*-CH-$(CH_3)_2$); 109.7 (=*C*H); 116.7 (-Ar-*o*-C); 120.0 (-Ar-*m*-C); 129.0 (-Ar-*p*-C); (-Ar-C1); 141.4 (-Ar-*m*-C);159.3 (-Ar-O*C*H_3); 177.4 (-*C*-O-); 187.6 (-*C*=S). MS (ESI): m/z = 563, 474, 428. Elemental analysis: calculated for $C_{21}H_{25}ClO_2RuS_2$ C: 49.45 %; H: 4.94 %, found: C: 49.94 %; H: 5.14 %.

[(η^6-*p*-cymene)Ru(1-(4-methoxyphenyl)-3-(methylthio)-3-thioxo-prop-1-en-1-olate-*O,S*)] (Ru9)

Synthesis was performed according to general procedure 1. [(η^6-*p*-cymene)$RuCl_2]_2$ (500 mg, 0.81 mmol) was used. L9 (389 mg, 1.62 mmol) was dissolved in THF, *t*-BuOK (182 mg, 1.62 mmol) was added. Column chromatography mobile phase: DCM - DCM 6:THF 1 – DCM 4:THF 1 - THF. Yield: 240 mg (29.1 %) as red crystals. ^1H NMR (600 MHz, CD_2Cl_2): δ = 1.53 (s, 6H, -cymene-CH-(C$H_3)_2$); 2.20 (s, 3H, CH_3, -cymene-CH_3); 2.67 (s, 3H, -SCH_3); 2.85 (sp, 1H, -cymene-C*H*-$(CH_3)_2$); 3.85 (s, 3H, -OCH_3); 5.27 (dd, $^3J_{H\text{-}H}$=21.6 Hz, $^4J_{H\text{-}H}$=5.0 Hz, 2H, -cymene:CH_3-C-C*H*-CH-C-CH-$(CH_3)_2$); 5.48 (dd, $^3J_{H\text{-}H}$=18.7 Hz, $^4J_{H\text{-}H}$=5.0 Hz, 2H –cymene:CH_3-C-CH-C*H*-C-CH-$(CH_3)_2$); 6.74 (s, 1H, =C*H*); 6.90 (d, $^3J_{H\text{-}H}$=8.8 Hz, 2H, -Ar-H); 7.81 (d, $^3J_{H\text{-}H}$=8.0 Hz, 2H, -Ar-H). $^{13}C\{^1H\}$ NMR (101 MHz, CD_2Cl_2): δ = 18.2 (-SCH_3); 18.2 (-cymene-C-*C*H_3); 22.4/22.4 (-cymene-CH-(*C*$H_3)_2$); 30.9 (-cymene-*C*H-$(CH_3)_2$); 55.8 (-O*C*H_3); 83.1 (-cymene:CH_3-C-*C*H-CH-C-CH-$(CH_3)_2$); 83.3 (CH_3-C-*C*H-CH-C-CH-$(CH_3)_2$); 85.5 (CH_3-C-CH-*C*H-C-CH-$(CH_3)_2$); 100.7 (CH_3-*C*-CH-CH-C-CH-$(CH_3)_2$); 102.6 (CH_3-C-CH-CH-*C*-CH-$(CH_3)_2$); 113.9 (-Ar-*o*-C); 113.4 (=*C*H); 120.9 (-Ar-*m*-C); 129.6 (-Ar-C1); 130.6 (-Ar-*m*-C); 131.7 (-Ar-*p*-C); 156.9 (-Ar-O*C*H_3); 179.0 (-*C*-O-); 185.9 (-*C*=S). MS (ESI): m/z = 503, 477, 475, 429, 315, 281. Elemental analysis: calculated for $C_{21}H_{25}ClO_2RuS_2$ C: 49.45 %; H: 4.94 %, found: C: 49.60 %; H: 5.08 %.

[(η^6-*p*-cymene)Ru(1-(2-methoxyphenyl)-3-(ethylthio)-3-thioxo-prop-1-en-1-olate-*O,S*)] (Ru10)

Synthesis was performed according to general procedure 1. [(η^6-*p*-cymene)$RuCl_2]_2$ (500 mg, 0.81 mmol) was used. L10 (389 mg, 1.62 mmol) was dissolved in THF, *t*-BuOK (182 mg, 1.62 mmol) was added. Column chromatography mobile phase: DCM - DCM 6:THF 1 – THF. Yield: 700 mg (84.6 %) as red crystals. ^{1}H NMR (600 MHz, CD_2Cl_2): δ = 1.23 (dd, $^3J_{H-H}$=6.9 Hz, $^4J_{H-H}$=2.7 Hz, 6H, -cymene-CH-(CH_3)$_2$); 1.38 (t, 3H, -SCH$_2$CH_3); 2.19 (s, 3H, -cymene-CH_3); 2.84 (sp, 1H, -cymene-C*H*-(CH$_3$)$_2$); 3.20 (q, 2H, -SCH_2CH$_3$); 3.83 (s, 3H, -OCH_3); 5.24 (d, $^3J_{H-H}$=6.0 Hz, 2H, -cymene:CH$_3$-C-C*H*-CH-C-CH-(CH$_3$)$_2$); 5.45 (dd, $^3J_{H-H}$=22.3 Hz, $^4J_{H-H}$=11.9 Hz, 2H –cymene:CH$_3$-C-CH-C*H*-C-CH-(CH$_3$)$_2$); 6.63 (s, 1H, =C*H*); 6.92 (d, $^3J_{H-H}$=8.3 Hz, 1H, -Ar-*o*-H); 6.97 (t, 1H, -Ar-*m*-H); 7.38 (ddd, $^3J_{H-H}$=7.8 Hz, $^4J_{H-H}$=1.8 Hz, 1H, -Ar-*p*-H); 7.51 (dd, $^3J_{H-H}$=7.6 Hz, $^4J_{H-H}$=1.8 Hz, 1H, -Ar-*m*-H). ^{13}C{^{1}H} NMR (101 MHz, CD_2Cl_2): δ = 13.9 (-SCH$_2$CH_3); 18.0 (-cymene-C-*C*H$_3$); 22.3/22.4 (-cymene-CH-(*C*H$_3$)$_2$); 25.9 (-S*C*H$_2$CH$_3$); 30.8 (-cymene-*C*H-(CH$_3$)$_2$); 55.9 (-O*C*H$_3$); 82.7 (-cymene:CH$_3$-C-*C*H-CH-C-CH-(CH$_3$)$_2$); 83.2 (CH$_3$-C-*C*H-CH-C-CH-(CH$_3$)$_2$); 85.4 (CH$_3$-C-CH-*C*H-C-CH-(CH$_3$)$_2$); 85.5 (CH$_3$-C-CH-*C*H-C-CH-(CH$_3$)$_2$); 100.8 (CH$_3$-*C*-CH-CH-C-CH-(CH$_3$)$_2$); 102.5 (CH$_3$-C-CH-CH-*C*-CH-(CH$_3$)$_2$); 111.9 (-Ar-*o*-C); 113.6 (=*C*H); 120.8 (-Ar-*m*-C); 129.2 (-Ar-C1); 130.6 (-Ar-*m*-C); 131.7 (-Ar-*p*-C); 156.9 (-Ar-*C*-OCH$_3$); 179.2 (-*C*-O-); 185.0 (-*C*=S). MS (DEI): m/z = 502, 493, 489, 483, 428, 328, 296, 294. Elemental analysis: calculated for $C_{22}H_{27}ClO_2RuS_2$ C: 50.42 %; H: 5.19 %, found: C: 50.74%; H: 5.25 %.

[(η^6-*p*-cymene)Ru(1-(3-methoxyphenyl)-3-(ethylthio)-3-thioxo-prop-1-en-1-olate-*O,S*)] (Ru11)

Synthesis was performed according to general procedure 1. [(η^6-*p*-cymene)$RuCl_2]_2$ (500 mg, 0.81 mmol) was used. L11 (412 mg, 1.62 mmol) was dissolved in THF, *t*-BuOK (182 mg, 1.62 mmol) was added. Column chromatography mobile phase: DCM - DCM 10:THF 1 – THF. Yield: 700 mg (82.4 %) as red crystals. ^{1}H NMR (600 MHz, $CDCl_3$): δ = 1.32 (dd, $^3J_{H-H}$=7.9 Hz, $^4J_{H-H}$=2.9 Hz, 6H, -cymene-CH-(CH_3)$_2$); 1.41 (t, 3H, -SCH$_2$CH_3); 2.91 (sp, 1H, -cymene-C*H*-(CH$_3$)$_2$); 3.01 (q, 2H,

-SC*H*$_2$CH$_3$); 3.85 (s, 3H, -OC*H*$_3$); 5.28 (dd, $^3J_{H\text{-}H}$=22.7 Hz, $^4J_{H\text{-}H}$=5.6 Hz, 2H, -cymene:CH$_3$-C-C*H*-CH-C-CH-(CH$_3$)$_2$); 5.51 (dd, $^3J_{H\text{-}H}$=26.3 Hz, $^4J_{H\text{-}H}$=5.7 Hz, 2H –cymene:CH$_3$-C-CH-C*H*-C-CH-(CH$_3$)$_2$); 6.74 (s, 1H, =C*H*); 6.99 (d, $^3J_{H\text{-}H}$=8.22 Hz, 1H, -Ar-*o*-H); 7.23-7.41 (m, 4H, -Ar-*m/p*-H). ^{13}C{^{1}H} NMR (101 MHz, CDCl$_3$): δ = 13.7 (-SCH$_2$C*H*$_3$); 18.0 (-cymene-C-*C*H$_3$); 22.5 (-cymene-CH-(*C*H$_3$)$_2$); 25.6 (-S*C*H$_2$CH$_3$); 30.5 (-cymene-*C*H-(CH$_3$)$_2$); 55.4 (-O*C*H$_3$); 82.6 (-cymene:CH$_3$-C-*C*H-CH-C-CH-(CH$_3$)$_2$); 82.8 (CH$_3$-C-*C*H-CH-C-CH-(CH$_3$)$_2$); 85.1 (CH$_3$-C-CH-*C*H-C-CH-(CH$_3$)$_2$); 85.6 (CH$_3$-C-CH-*C*H-C-CH-(CH$_3$)$_2$; 100.1 (CH$_3$-*C*-CH-CH-C-CH-(CH$_3$)$_2$); 102.6 (CH$_3$-C-CH-CH-*C*-CH-(CH$_3$)$_2$); 109.7 (=*C*H); 116.8 (-Ar-*o*-C); 119.9 (-Ar-*m*-C); 126.3 (-Ar-*p*-C); 135.2 (-Ar-C1); 141.4 (-Ar-*m*-C);159.4 (-Ar-O*C*H$_3$); 178.0 (-*C*-O-); 186.8 (-*C*=S). MS (ESI): m/z = 490, 488, 458, 428, 294. Elemental analysis: calculated for C$_{22}$H$_{27}$ClO$_2$RuS$_2$ C: 50.42 %; H: 5.19 %, found: C: 50.51%; H: 5.22 %.

[(η^6-*p*-cymene)Ru(1-(4-methoxyphenyl)-3-(ethylthio)-3-thioxo-prop-1-en-1-olate-*O,S*)] (Ru12)

Synthesis was performed according to general procedure 1. [(η^6-*p*-cymene)RuCl$_2$]$_2$ (500 mg, 0.81 mmol) was used. L12 (412 mg, 1.62 mmol) was dissolved in THF, *t*-BuOK (182 mg, 1.62 mmol) was added. Column chromatography mobile phase: DCM - DCM 6:THF 1 – DCM 4:THF 1 - THF. Yield: 790 mg (93.1 %) as red crystals. ^{1}H NMR (600 MHz, CDCl$_3$): δ = 1.32 (dd, $^3J_{H\text{-}H}$=11.9 Hz, $^4J_{H\text{-}H}$=1.7 Hz, 6H, -cymene-CH-(C*H*$_3$)$_2$); 1.41 (t, 3H, -SCH$_2$C*H*$_3$); 2.90 (sp, 1H, -cymene-C*H*-(CH$_3$)$_2$); 3.30 (q, 2H, -SC*H*$_2$CH$_3$); 3.86 (s, 3H, -OC*H*$_3$); 2.85 (sp, 1H, -cymene-C*H*-(CH$_3$)$_2$); 3.85 (s, 3H, -OC*H*$_3$); 5.29 (dd, $^3J_{H\text{-}H}$=25.0 Hz, $^4J_{H\text{-}H}$=5.7 Hz, 2H, -cymene:CH$_3$-C-C*H*-CH-C-CH-(CH$_3$)$_2$); 5.50 (dd, $^3J_{H\text{-}H}$=22.5 Hz, $^4J_{H\text{-}H}$=5.7 Hz, 2H –cymene:CH$_3$-C-CH-C*H*-C-CH-(CH$_3$)$_2$); 6.78 (s, 1H, =C*H*); 6.89 (d, $^3J_{H\text{-}H}$=8.8 Hz, 2H, -Ar-H); 7.80 (d, $^3J_{H\text{-}H}$=8.5 Hz, 2H, -Ar-H). ^{13}C{^{1}H} NMR (101 MHz, CDCl$_3$): δ = 13.8 (-SCH$_2$C*H*$_3$); 18.1 (-cymene-C-*C*H$_3$); 22.4 (-cymene-CH-(*C*H$_3$)$_2$); 25.6 (-S*C*H$_2$CH$_3$); 30.5 (-cymene-*C*H-(CH$_3$)$_2$); 55.4 (-O*C*H$_3$); 82.9 (-cymene:CH$_3$-C-*C*H-CH-C-CH-(CH$_3$)$_2$); 85.0 (CH$_3$-C-*C*H-CH-C-CH-(CH$_3$)$_2$); 85.3 (CH$_3$-C-CH-*C*H-C-CH-(CH$_3$)$_2$); 99.9 (CH$_3$-*C*-CH-CH-C-CH-(CH$_3$)$_2$); 102.3 (CH$_3$-C-CH-CH-*C*-CH-(CH$_3$)$_2$); 113.4 (-Ar-*o*-C); 113.4 (=*C*H); 126.3 (-Ar-*m*-C); 129.5 (-Ar-C1); 132.4 (-Ar-*m*-C); 132.4 (-Ar-*p*-C); 162.1 (-Ar-O*C*H$_3$); 177.7 (-*C*-O-); 184.8 (-*C*=S). MS (ESI): m/z = 490,

488, 482, 428, 294. Elemental analysis: calculated for $C_{22}H_{27}ClO_2RuS_2$ C: 50.42 %; H: 5.19 %, found: C: 50.52%; H: 5.09 %.

[(η^6-*p*-cymene)Ru(1-(2-ethoxyphenyl)-3-(methylthio)-3-thioxo-prop-1-en-1-olate-*O,S*)] (Ru13)

Synthesis was performed according to general procedure 1. [(η^6-*p*-cymene)$RuCl_2]_2$ (500 mg, 0.81 mmol) was used. L13 (412 mg, 1.62 mmol) was dissolved in THF, *t*-BuOK (182 mg, 1.62 mmol) was added. Column chromatography mobile phase: DCM - DCM 10:THF 1 – THF. Yield: 130 mg (23.7 %) as red oil. ^{1}H NMR (600 MHz, $CDCl_3$): δ = 1.23 (d, $^3J_{H-H}$=7.1 Hz, 6H, -cymene-CH-(CH_3)$_2$); 1.35 (t, 3H, -OCH_2CH_3); 2.16 (s, 3H, CH_3, -cymene-CH_3); 2.57 (s, 3H, -SCH_3); 2.82 (sp, 1H, -cymene-C*H*-(CH_3)$_2$); 3.98 (q, 2H, -O$CH_2$$CH_3$); 4.29 (t, 3H, OCH_2CH_3); 5.18 (dd, $^3J_{H-H}$=16.0 Hz, $^4J_{H-H}$=5.8 Hz, 2H, -cymene:CH_3-C-C*H*-CH-C-CH-(CH_3)$_2$); 5.39 (dd, $^3J_{H-H}$=38.8 Hz, $^4J_{H-H}$=5.7 Hz 2H –cymene:CH_3-C-CH-C*H*-C-CH-(CH_3)$_2$); 6.76 (s, 1H, =C*H*); 6.78 (d, $^3J_{H-H}$=8.4 Hz, 1H, -Ar-*o*-H); 6.87 (t, 1H, -Ar-*m*-H); 7.25 (t, 1H, -Ar-*p*-H); 7.57 (dd, $^3J_{H-H}$=7.7 Hz, $^4J_{H-H}$=1.7 Hz, 1H, -Ar-*m*-H). ^{13}C{^{1}H} NMR (101 MHz, $CDCl_3$): δ = 14.9 (-OCH_2*C*H_3); 17.9 (-SCH_3); 17.9 (-cymene-C-*C*H_3); 22.2 (-cymene-CH-(*C*H_3)$_2$); 30.4 (-cymene-*C*H-(CH_3)$_2$); 64.5 (-O*C*$H_2$$CH_3$); 82.6 (-cymene:$CH_3$-C-*C*H-CH-C-CH-($CH_3$)$_2$); 82.7 ($CH_3$-C-*C*H-CH-C-CH-($CH_3$)$_2$); 85.2 ($CH_3$-C-CH-*C*H-C-CH-($CH_3$)$_2$); 85.5 ($CH_3$-C-CH-*C*H-C-CH-($CH_3$)$_2$; 100.2 ($CH_3$-*C*-CH-CH-C-CH-($CH_3$)$_2$); 102.5 ($CH_3$-C-CH-CH-*C*-CH-($CH_3$)$_2$); 112.8 (=*C*H); 113.8 (-Ar-*o*-C); 117.2 (-Ar-*p*-C); 120.5 (-Ar-*o*-C); 130.6 (-Ar-*C*=C); 131.2 (-Ar-*m*-C); 131.4 (-Ar-C1); 155.9 (-*C*-O-); 177.7 (-*C*=S). MS (DEI): m/z = 524, 458, 119. Elemental analysis: calculated for $C_{22}H_{27}ClO_2RuS_2$ C: 50.42 %; H: 5.19 %, found: C: 50.39 %; H: 5.32 %.

[(η^6-*p*-cymene)Ru(1-(3-ethoxyphenyl)-3-(methylthio)-3-thioxo-prop-1-en-1-olate-*O,S*)] (Ru14)

Synthesis was performed according to general procedure 1. [(η^6-*p*-cymene)$RuCl_2]_2$ (500 mg, 0.81 mmol) was used. L14 (412 mg, 1.62 mmol) was dissolved in THF, *t*-BuOK (182 mg, 1.62 mmol) was added. Column chromatography mobile phase: DCM - DCM 10:THF 1 – THF. Yield: 471 mg (55.5 %) as red crystals.

^{1}H NMR (600 MHz, $CDCl_3$): δ = 1.27 (d, $^{3}J_{H\text{-}H}$=10.32 Hz, 6H, -cymene-CH-(CH_3)$_2$); 1.40 (t, 3H, -OCH$_2$CH_3); 2.07 (s, 3H, CH_3, -cymene-CH_3); 2.66 (s, 3H, -SCH_3); 2.86 (sp, 1H, -cymene-C*H*-(CH_3)$_2$); 4.03 (q, 2H, -OCH_2CH$_3$); 5.22 (d, $^{3}J_{H\text{-}H}$=8.8 Hz, 2H, -cymene:CH_3-C-C*H*-CH-C-CH-(CH_3)$_2$); 5.43 (d, $^{3}J_{H\text{-}H}$=8.6 Hz, 2H –cymene:CH_3-C-CH-C*H*-C-CH-(CH_3)$_2$); 6.71 (s, 1H, =C*H*); 6.94 (dd, $^{3}J_{H\text{-}H}$=12.18 Hz, $^{4}J_{H\text{-}H}$=3.0 Hz, 1H, -Ar-*p*-H); 7.22 (t, 1H, -Ar-*m*-H); 7.30 (s, 1H, -Ar-*o*-H); 7.33 (d, 1H, $^{3}J_{H\text{-}H}$=11.7 Hz, -Ar-*o*-H). ^{13}C{^{1}H} NMR (101 MHz, $CDCl_3$): δ = 14.8 (-OCH$_2$CH_3); 17.2 (-SCH_3); 17.9 (-cymene-C-CH_3); 22.2 (-cymene-CH-(CH_3)$_2$); 30.5 (-cymene-C*H*-(CH_3)$_2$); 63.6 (-OCH$_2$CH$_3$); 82.6 (-cymene:CH_3-C-C*H*-CH-C-CH-(CH_3)$_2$); 82.7 (CH_3-C-C*H*-CH-C-CH-(CH_3)$_2$); 85.0 (CH_3-C-CH-C*H*-C-CH-(CH_3)$_2$); 85.5 (CH_3-C-CH-C*H*-C-CH-(CH_3)$_2$; 99.9 (CH_3-C-CH-CH-C-CH-(CH_3)$_2$); 102.5 (CH_3-C-CH-CH-C-CH-(CH_3)$_2$); 109.4 (=C*H*); 113.5 (-Ar-*o*-C); 117.2 (-Ar-*p*-C); 119.7 (-Ar-*o*-C); 128.9 (-Ar-C=C); 129.1 (-Ar-*m*-C); 141.3 (-Ar-C1); 158.7 (-C-O-); 187.4 (-C=S). MS (ESI): m/z = 488, 442, 314, 282. Elemental analysis: calculated for $C_{22}H_{27}ClO_2RuS_2$ C: 50.42 %; H: 5.19 %, found: C: 50.98 %; H: 5.32 %.

[(η^{6}-*p*-cymene)Ru(1-(4-ethoxyphenyl)-3-(methylthio)-3-thioxo-prop-1-en-1-olate-*O,S*)] (Ru15)

Synthesis was performed according to general procedure 1. [(η^{6}-*p*-cymene)$RuCl_2]_2$ (500 mg, 0.81 mmol) was used. L15 (412 mg, 1.62 mmol) was dissolved in THF, *t*-BuOK (182 mg, 1.62 mmol) was added. Column chromatography mobile phase: DCM - DCM 10:THF 1 – THF. Yield: 471 mg (55.5 %) as red crystals. ^{1}H NMR (600 MHz, $CDCl_3$): δ = 1.25 (d, $^{3}J_{H\text{-}H}$=10.26 Hz, 6H, -cymene-CH-(CH_3)$_2$); 1.39 (t, 3H, -OCH$_2$CH_3); 2.19 (s, 3H, CH_3, -cymene-CH_3); 2.64 (s, 3H, -SCH_3); 2.85 (sp, 1H, -cymene-C*H*-(CH_3)$_2$); 4.03 (q, 2H, -OCH_2CH$_3$); 5.21 (d, $^{3}J_{H\text{-}H}$=8.7 Hz, 2H, -cymene:CH_3-C-C*H*-CH-C-CH-(CH_3)$_2$); 5.43 (d, $^{3}J_{H\text{-}H}$=8.7 Hz, 2H –cymene:CH_3-C-CH-C*H*-C-CH-(CH_3)$_2$); 6.79 (s, 1H, =C*H*); 6.81 (d, $^{3}J_{H\text{-}H}$=13.38 Hz, 2H, -Ar-*m*-H); 7.76 (d, $^{3}J_{H\text{-}H}$=13.14 Hz, 2H, -Ar-*o*-H). ^{13}C{^{1}H} NMR (101 MHz, $CDCl_3$): δ = 14.6 (-OCH$_2$CH_3); 17.1 (-SCH_3); 17.9 (-cymene-C-CH_3); 22.2 (-cymene-CH-(CH_3)$_2$); 30.4 (-cymene-C*H*-(CH_3)$_2$); 63.5 (-OCH$_2$CH$_3$); 82.7 (-cymene:CH_3-C-C*H*-CH-C-CH-(CH_3)$_2$); 82.8 (CH_3-C-C*H*-CH-C-CH-(CH_3)$_2$); 84.9 (CH_3-C-CH-C*H*-C-CH-(CH_3)$_2$); 85.2 (CH_3-C-CH-C*H*-C-CH-(CH_3)$_2$; 99.7 (CH_3-C-CH-CH-C-CH-(CH_3)$_2$); 102.2 (CH_3-C-

CH-CH-*C*-CH-(CH_3)$_2$); 108.7 (=*C*H); 113.8 (-Ar-*m*-C); 128.9 (-Ar-*C*=C); 129.1 (-Ar-*o*-C); 132.1 (-Ar-C1); 161.4 (-Ar-*p*-C); 185.3 (-*C*=S). MS (ESI): m/z = 488, 442, 314, 282. Elemental analysis: calculated for $C_{22}H_{27}ClO_2RuS_2$ C: 50.42 %; H: 5.19 %, found: C: 50.67 %; H: 5.32 %.

[(η^6-*p*-cymene)Ru(1-(3-butoxyphenyl)-3-(methylthio)-3-thioxo-prop-1-en-1-olate-*O,S*)] (Ru16)

Synthesis was performed according to general procedure 1. [(η^6-*p*-cymene)$RuCl_2$]$_2$ (500 mg, 0.81 mmol) was used. L14 (458 mg, 1.62 mmol) was dissolved in THF, *t*-BuOK (182 mg, 1.62 mmol) was added. Column chromatography mobile phase: DCM - DCM 10:THF 1 – THF. Yield: 438 mg (49.0 %) as red oil. ^{1}H NMR (600 MHz, $CDCl_3$): δ = 0.92 (t, 3H, -$OCH_2CH_2CH_2CH_3$); 1.28 (d, $^3J_{H\text{-}H}$=7.38 Hz, 6H, -cymene-CH-(CH_3)$_2$); 1.48 (se, 2H, -$OCH_2CH_2CH_2CH_3$); 1.76 (qu, 2H, -$OCH_2CH_2CH_2CH_3$); 2.17 (s, 3H, CH_3, -cymene-CH_3); 2.62 (s, 3H, -SCH_3); 2.87 (sp, 1H, -cymene-CH-(CH_3)$_2$); 3.98 (t, 2H, -$OCH_2CH_2CH_2CH_3$); 5.24 (d, $^3J_{H\text{-}H}$=5.7 Hz, 2H, -cymene:CH_3-C-CH-CH-C-CH-(CH_3)$_2$); 5.43 (d, $^3J_{H\text{-}H}$=5.6 Hz, 2H –cymene:CH_3-C-CH-CH-C-CH-(CH_3)$_2$); 6.72 (s, 1H, =C*H*); 6.95 (dd, $^3J_{H\text{-}H}$=8.16 Hz, $^4J_{H\text{-}H}$=2.2 Hz, 1H, -Ar-*p*-H); 7.23 (t, 1H, -Ar-*m*-H); 7.30 (s, 1H, -Ar-*o*-H); 7.33 (d, 1H, $^3J_{H\text{-}H}$=7.8 Hz, -Ar-*o*-H). ^{13}C{^{1}H} NMR (101 MHz, $CDCl_3$): δ = 13.8 -$OCH_2CH_2CH_2CH_3$); 16.9 (-SCH_3); 17.9 (-cymene-C-CH_3); 19.8 (-$OCH_2CH_2CH_2CH_3$); 22.3 (-cymene-CH-(CH_3)$_2$); 30.5 (-cymene-CH-(CH_3)$_2$); 31.2 (-$OCH_2CH_2CH_2CH_3$); 67.8 (-$OCH_2CH_2CH_2CH_3$); 82.6 (-cymene:CH_3-C-CH-CH-C-CH-(CH_3)$_2$); 82.7 (CH_3-C-CH-CH-C-CH-(CH_3)$_2$); 85.1 (CH_3-C-CH-CH-C-CH-(CH_3)$_2$); 85.5 (CH_3-C-CH-CH-C-CH-(CH_3)$_2$; 99.8 (CH_3-C-CH-CH-C-CH-(CH_3)$_2$); 102.6 (CH_3-C-CH-CH-C-CH-(CH_3)$_2$); 109.4 (=CH); 113.5 (-Ar-*o*-C); 117.3 (-Ar-*p*-C); 119.0 (-Ar-*o*-C); 128.9 (-Ar-*C*=C); 128.9 (-*C*=C-); 129.0 (-Ar-*m*-C); 141.3 (-*C*1); 158.9 (-*C*-O-); 187.3 (-*C*=S). MS (ESI): m/z = 519, 516, 469, 315, 281, 278. Elemental analysis: calculated for $C_{24}H_{31}ClO_2RuS_2$ C: 52.21 %; H: 5.66 %, found: C: 52.60 %; H: 5.62 %.

[(η^6-*p*-cymene)Ru(1-(4-butoxyphenyl)-3-(methylthio)-3-thioxo-prop-1-en-1-olate-*O,S*)] (Ru17)

Synthesis was performed according to general procedure 1. [(η^6-*p*-cymene)$RuCl_2]_2$ (500 mg, 0.81 mmol) was used. L17 (458 mg, 1.62 mmol) was dissolved in THF, *t*-BuOK (182 mg, 1.62 mmol) was added. Column chromatography mobile phase: DCM - DCM 10:THF 1 – THF. Yield: 357 mg (40.0 %) as red crystals. ^{1}H NMR (600 MHz, $CDCl_3$): δ = 0.95 (t, 3H, -$OCH_2CH_2CH_2CH_3$); 1.26 (d, $^3J_{H-H}$=6.96 Hz, 6H, -cymene-CH-(CH_3)$_2$); 1.46 (se, 2H, -$OCH_2CH_2CH_2CH_3$); 1.74 (qu, 2H, -$OCH_2CH_2CH_2CH_3$); 2.19 (s, 3H, CH_3, -cymene-CH_3); 2.64 (s, 3H, -SCH_3); 2.85 (sp, 1H, -cymene-CH-(CH_3)$_2$); 3.96 (t, 2H, -$OCH_2CH_2CH_2CH_3$); 5.25 (d, $^3J_{H-H}$=8.7 Hz, 2H, -cymene:CH_3-C-CH-CH-C-CH-(CH_3)$_2$); 5.47 (d, $^3J_{H-H}$=8.7 Hz, 2H –cymene:CH_3-C-CH-CH-C-CH-(CH_3)$_2$); 6.72 (s, 1H, =CH); 6.81 (d, $^3J_{H-H}$=8.8 Hz, 1H, -Ar-*m*-H); 7.76 (d, $^3J_{H-H}$=8.6 Hz, 2H, -Ar-*o*-H). ^{13}C{^{1}H} NMR (101 MHz, $CDCl_3$): δ = 13.7 (-$OCH_2CH_2CH_2CH_3$); 17.1 (-SCH_3); 17.9 (-cymene-C-CH_3); 19.1 (-$OCH_2CH_2CH_2CH_3$); 22.3 (-cymene-CH-(CH_3)$_2$); 31.1 (-cymene-CH-(CH_3)$_2$); 33.6 (-$OCH_2CH_2CH_2CH_3$); 67.8 (-$OCH_2CH_2CH_2CH_3$); 82.7 (-cymene:CH_3-C-CH-CH-C-CH-(CH_3)$_2$); 82.8 (CH_3-C-CH-CH-C-CH-(CH_3)$_2$); 84.9 (CH_3-C-CH-CH-C-CH-(CH_3)$_2$); 85.2 (CH_3-C-CH-CH-C-CH-(CH_3)$_2$; 99.7 (CH_3-C-CH-CH-C-CH-(CH_3)$_2$); 102.2 (CH_3-C-CH-CH-C-CH-(CH_3)$_2$); 108.7 (=CH); 113.9 (-Ar-*o*-C); 128.9 (-Ar-C=C); 129.4 (-Ar-*o*-C); 132.0 (-Ar-C1); 161.6 (-C-O-); 185.2 (-C=S). MS (ESI): m/z = 519, 516, 469, 315, 281, 278. Elemental analysis: calculated for $C_{24}H_{31}ClO_2RuS_2$ C: 52.21 %; H: 5.66 %, found: C: 52.29 %; H: 5.76 %.

[(η^6-*p*-cymene)Os(1-(3-hydroxyphenyl)-3-(ethylthio)-3-thioxo-prop-1-en-1-olate-*O,S*)Cl] (Os3)

Synthesis was performed according to general procedure 1. [(η^6-*p*-cymene)$OsCl_2]_2$ (500 mg, 0.63 mmol) was used. 3'-Hydroxy-β-Hydroxydithiocinnamic acid methyl ester (286 mg, 1.26 mmol) was dissolved in THF, *t*-BuOK (140 mg, 1.26 mmol) was added. Column chromatography mobile phase: DCM - DCM 10:THF 1 – THF. Yield: 520 mg (54.8 %) as red crystals. ^{1}H NMR (600 MHz, $CDCl_3$): δ = 1.28 (d, $^3J_{H-H}$=6.7 Hz, 6H, -cymene-CH-(CH_3)$_2$); 2.31 (s, 3H, CH_3, -cy-

mene-C*H*$_3$); 2.64 (s, 3H, -SC*H*$_3$); 2.76 (sp, 1H, -cymene-C*H*-(CH$_3$)$_2$); 5.64 (s, 2H, -cymene:CH$_3$-C-C*H*-CH-C-CH-(CH$_3$)$_2$); 5.82 (s, 2H –cymene:CH$_3$-C-CH-C*H*-C-CH-(CH$_3$)$_2$); 6.88 (s, 1H, =C*H*); 6.91 (m, 1H, -Ar-*o*-H); 7.12 (t, 1H, -Ar-*m*-H); 7.26-7.28 (m, 2H, -Ar-*o*-H / -Ar-*p*-H). ^{13}C{^{1}H} NMR (101 MHz, CDCl$_3$): δ = 17.5 (-SCH$_3$); 18.1 (-cymene-C-*C*H$_3$); 22.8 (-cymene-CH-(*C*H$_3$)$_2$); 30.8 (-cymene-*C*H-(CH$_3$)$_2$); 77.2 (-cymene:CH$_3$-C-*C*H-CH-C-CH-(CH$_3$)$_2$); 77.4 (CH$_3$-C-*C*H-CH-C-CH-(CH$_3$)$_2$); 92.9 (CH$_3$-C-CH-*C*H-C-CH-(CH$_3$)$_2$); 93.2 (CH$_3$-*C*-CH-CH-C-CH-(CH$_3$)$_2$); 110.7 (CH$_3$-C-CH-CH-*C*-CH-(CH$_3$)$_2$); 114.4 (=*C*H); 118.3 (-Ar-*m*-C); 118.9 (-Ar-*o*-C); 129.2 (-*C*OH); 156.1 (-Ar-*p*-C); 174.7 (-Ar*C*1); 174.7 (-*C*-O-). MS (DEI): m/z = 586, 408. Elemental analysis: calculated for $C_{20}H_{23}ClO_2OsS_2$ C: 41.05 %; H: 3.96 %, found: C: 41.04 %; H: 4.49 %.

[(η^6-*p*-cymene)Os(1-(2-methoxyphenyl)-3-(methylthio)-3-thioxo-prop-1-en-1-olate-*O,S*)] (Os7)

Synthesis was performed according to general procedure 1. [(η^6-*p*-cymene)OsCl$_2$]$_2$ (140 mg, 0.17 mmol) was used. 3'-Methoxy-β-Hydroxydithiocinnamic acid methyl ester (85 mg, 0.35 mmol) was dissolved in THF, *t*-BuOK (39.7 mg, 0.35 mmol) was added. Column chromatography mobile phase: DCM - DCM 6:THF 1 – THF. Yield: 80 mg (8.2 %) as red crystals. ^{1}H NMR (600 MHz, CDCl$_3$): δ = 1.31 (dd, $^3J_{H\text{-}H}$=7.0 Hz, $^4J_{H\text{-}H}$=1.8 Hz, 6H, -cymene-CH-(C*H*$_3$)$_2$); 2.31 (s, 3H,-cymene-C*H*$_3$); 2.65 (s, 3H, -SC*H*$_3$); 2.80 (sp, 1H, -cymene-C*H*-(CH$_3$)$_2$); 3.85 (s, 3H, -OC*H*$_3$); 5.59 (d, $^3J_{H\text{-}H}$=5.1 Hz, 2H, -cymene:CH$_3$-C-C*H*-CH-C-CH-(CH$_3$)$_2$); 5.80 (m, 2H –cymene:CH$_3$-C-CH-C*H*-C-CH-(CH$_3$)$_2$); 6.87 (s, 1H, =C*H*); 7.02 (dd, $^3J_{H\text{-}H}$=8.2 Hz, $^4J_{H\text{-}H}$=1.9 Hz, 1H, -Ar-*o*-H); 6.97 (t, 1H, -Ar-*m*-H); 7.28 (m, 1H, -Ar-*p*-H); 7.35-7.40 (m, 1H, -Ar-*m*-H). ^{13}C{^{1}H} NMR (101 MHz, CDCl$_3$): δ = 17.4 (-SCH$_3$); 17.9 (-cymene-C-*C*H$_3$); 22.7/22.9 (-cymene-CH-(*C*H$_3$)$_2$); 30.8 (-cymene-*C*H-(CH$_3$)$_2$); 55.4 (-O*C*H$_3$); 73.9 (-cymene:CH$_3$-C-*C*H-CH-C-CH-(CH$_3$)$_2$); 73.9 (CH$_3$-C-*C*H-CH-C-CH-(CH$_3$)$_2$); 76.8 (CH$_3$-C-CH-*C*H-C-CH-(CH$_3$)$_2$); 92.6 (CH$_3$-*C*-CH-CH-C-CH-(CH$_3$)$_2$); 93.7 (CH$_3$-C-CH-CH-*C*-CH-(CH$_3$)$_2$); 110.9 (-Ar-*o*-C); 112.7 (=*C*H); 116.6 (-Ar-*m*-C); 129.3 (-Ar-C1); 141.2 (-Ar-*m*-C); 159.5 (-Ar-*C*-OCH$_3$); 174.9 (-*C*-O-); 186.7 (-*C*=S). MS (ESI): m/z = 565, 517, 371. Elemental analysis: calculated for $C_{21}H_{24}ClO_2OsS_2$ C: 42.09 %; H: 4.21 %, found: C: 42.75 %; H: 4.14 %.

[(η^6-*p*-cymene)Os(1-(2-ethoxyphenyl)-3-(methylthio)-3-thioxo-prop-1-en-1-olate-*O,S*)] (Os13)

Synthesis was performed according to general procedure 1. [(η^6-*p*-cymene)$OsCl_2]_2$ (500 mg, 0.63 mmol) was used. 3'-Ethoxy-β-Hydroxydithiocinnamic acid methyl ester (302 mg, 1.26 mmol) was dissolved in THF, *t*-BuOK (150 mg, 1.26 mmol) was added. Column chromatography mobile phase: DCM - DCM 10:THF 1 – THF. Yield: 720 mg (72.4 %) as red oil. ^{1}H NMR (600 MHz, $CDCl_3$): δ = 1.31 (d, $^3J_{H-H}$=7.0 Hz, $^4J_{H-H}$=2.6 Hz, 6H, -cymene-CH-(CH_3)$_2$); 1.44 (t, 3H, -OCH_2CH_3); 2.31 (s, 3H, CH_3, -cymene-CH_3); 2.66 (s, 3H, -SCH_3); 2.80 (sp, 1H, -cymene-C*H*-$(CH_3)_2$); 4.08 (q, 2H, -OCH_2CH_3); 4.37 (t, 3H, OCH_2CH_3); 5.59 (dd, $^3J_{H-H}$=15.0 Hz, $^4J_{H-H}$=5.3 Hz, 2H, -cymene:CH_3-C-C*H*-CH-C-CH-$(CH_3)_2$); 5.80 (m, 2H, –cymene:CH_3-C-CH-C*H*-C-CH-$(CH_3)_2$); 6.87 (s, 1H, =C*H*); 7.01 (dd, $^3J_{H-H}$=8.1 Hz, $^4J_{H-H}$=2.4 Hz, 1H, -Ar-*o*-H); 7.25-7.39 (m, 3H, -Ar-*m*-H/ -Ar-*p*-H). ^{13}C{^{1}H} NMR (101 MHz, $CDCl_3$): δ = 14.8 (-OCH_2CH_3); 17.4 (-SCH_3); 17.9 (-cymene-C-CH_3); 22.8 (-cymene-CH-(CH_3)$_2$); 30.8 (-cymene-*C*H-$(CH_3)_2$); 63.6 (-OCH_2CH_3); 73.8 (-cymene:CH_3-C-*C*H-CH-C-CH-$(CH_3)_2$); 73.9 (CH_3-C-*C*H-CH-C-CH-$(CH_3)_2$); 76.7 (CH_3-C-CH-*C*H-C-CH-$(CH_3)_2$); 77.2 (CH_3-C-CH-*C*H-C-CH-$(CH_3)_2$; 92.6 (CH_3-*C*-CH-CH-C-CH-$(CH_3)_2$); 92.6 (CH_3-C-CH-CH-*C*-CH-$(CH_3)_2$); 111.0 (=*C*H); 113.3 (-Ar-*o*-C); 117.2 (-Ar-*p*-C); 119.5 (-Ar-*o*-C); 129.2 (-Ar-*C*=C); 141.2 (-Ar-C1); 158.9 (-*C*-O-); 175.1 (-*C*=S). MS (EI): m/z = 614, 579. Elemental analysis: calculated for $C_{22}H_{27}ClO_2OsS_2$ C: 43.09 %; H: 4.44 %, found: C: 43.20 %; H: 4.38 %.

[(η^6-*p*-cymene)Os(1-(3-ethoxyphenyl)-3-(methylthio)-3-thioxo-prop-1-en-1-olate-*O,S*)] (Os14)

Synthesis was performed according to general procedure 1. [(η^6-*p*-cymene)$OsCl_2]_2$ (500 mg, 0.63 mmol) was used. 4'-Ethoxy-β-Hydroxydithiocinnamic acid methyl ester (302 mg, 1.26 mmol) was dissolved in THF, *t*-BuOK (150 mg, 1.26 mmol) was added. Column chromatography mobile phase: DCM - DCM 10:THF 1 – THF. Yield: 160 mg (16.1 %) as red crystals. ^{1}H NMR (600 MHz, $CDCl_3$): δ = 1.31 (d, $^3J_{H-H}$=6.5 Hz, 6H, -cymene-CH-(CH_3)$_2$); 1.57 (t, 3H, -OCH_2CH_3); 2.31 (s, 3H, CH_3, -cymene-CH_3); 2.58 (s, 3H, -SCH_3); 2.80 (sp, 1H, -cymene-C*H*-$(CH_3)_2$); 4.10 (q, 2H, -OCH_2CH_3); 5.59 (dd, $^3J_{H-H}$=17.1 Hz, $^4J_{H-H}$=5.2 Hz, 2H, -cymene:CH_3-C-

C*H*-CH-C-CH-(CH_3)$_2$); 5.79 (t, 2H –cymene:CH_3-C-CH-C*H*-C-CH-(CH_3)$_2$); 6.85-6.95 (m, 3H, =C*H*/ -Ar-*m*-H); 7.81-7.96 (m, 3H, -Ar-*p*-H/ s, 1H, -Ar-*o*-H). $^{13}C\{^1H\}$ NMR (101 MHz, $CDCl_3$): δ = 14.7 (-OCH_2CH_3); 17.9 (-SCH_3); 22.8 (-cymene-CH-(CH_3)$_2$); 30.8 (-cymene-*C*H-(CH_3)$_2$); 63.6 (-O*C*H_2CH_3); 73.8 (-cymene:CH_3-C-*C*H-CH-C-CH-(CH_3)$_2$); 74.0 (CH_3-C-*C*H-CH-C-CH-(CH_3)$_2$); 76.7 (CH_3-C-CH-*C*H-C-CH-(CH_3)$_2$); 77.0 (CH_3-C-CH-*C*H-C-CH-(CH_3)$_2$; 114.1 (-Ar-*o*-C); 114.1 (-Ar-*p*-C); 129.3 (-Ar-*C*=C); 130.6 (-Ar-C1). MS (DEI): m/z = 614, 579. Elemental analysis: calculated for $C_{22}H_{27}ClO_2OsS_2$ C: 43.09 %; H: 4.44 %, found: C: 42.82 %; H: 4.28 %.

Structure determination

The intensity data for the compounds were collected on a Nonius KappaCCD diffractometer using graphite-monochromated Mo-K_α radiation. Data were corrected for Lorentz and polarization effects; absorption was taken into account on a semi-empirical basis using multiple-scans.[Data Collection Software; Otwinowski, 1997; Sadabs, 2015]

The structures were solved by direct methods (SHELXS [Sheldrick, 2015]) and refined by full-matrix least squares techniques against Fo^2 (SHELXL-97 [Sheldrick, 2015]). All hydrogen atoms (with exception of the methyl-group at C13 of **Ru14** and the methylene-group at C11 of **L18** were located by difference Fourier synthesis and refined isotropically. All other hydrogen atoms were included at calculated positions with fixed thermal parameters.

Crystallographic data as well as structure solution and refinement details are summarized in Table 4. MERCURY was used for structure representations.[Mercury, 2006]

Supporting Information available: Crystallographic data (excluding structure factors) has been deposited with the Cambridge Crystallographic Data Centre as supplementary publication CCDC-1446182 for **L14**, CCDC-1446183 for **L15**, CCDC-1446184 for **L17**, CCDC-1446185 for **L18**, CCDC-1446186 for **Ru9**, CCDC-1446190 for **Ru13**, and CCDC-1446191 for **Ru14**. Copies of the data can be obtained free of charge on application to CCDC, 12 Union Road, Cambridge CB2 1EZ, UK [E- mail: deposit@ccdc.cam.ac.uk].

Stability determinations

NMR spectra were measured *via* NMR spectroscopy on Bruker Avance 400 MHz. Substances were solved in dmso-d_6 or CD_2Cl_2 and measured directly at 37 °C or room temperature for 72 hours. NS=128 scans, t=709 seconds/2891 seconds break, 72 measurements.

Biological Assays

Ovarian cancer cell lines were cultured under standard conditions (5 % CO2, 37 °C, 90 % humidity) in RPMI medium supplemented with 10 % FCS, 100 U/ml penicillin and 100 µg/ml streptomycin (Life Technologies, Germany). Cisplatin (Sigma, Germany) was freshly dissolved at 1 mg/ml in 0.9 % NaCl solution and diluted appropriately. New ruthenium(II) complexes and ligands were dissolved in dmso. Platinum-resistant A2780 and SKOV3 cells were established by repeated rounds of 3 day incubations with increasing amounts of Cisplatin starting with 0.1 µM. The concentration was doubled after 3 incubations interrupted by recovery phases with normal medium. Cells that survived the third round of 12.8 µM Cisplatin were defined as resistant cultures. Determinations of IC50 values were carried out using the CellTiter96 non-radioactive proliferation assay (MTT assay, Promega). After seeding 5000 cells per well in a 96-well plate cells were allowed to attach for 24h and were incubated for 48h with different concentrations of the substances ranging from 0 to 500 µM for Ruthenium and 0 to 1000 µM for ligand tests (0, 1, 10, 50, 100, 500, 1000 µm), for Cisplatin from 0 to 100 µM (0.1, 1, 5, 10, 50, 100 µM). Each measurement was done in triplicate and repeated 3-times. The proportion of viable cells was quantified by the MTT assay and after background subtraction relative values compared to the mean of medium controls were calculated. Non-linear regression analyses applying the Hill-slope were run in GraphPad 5.0 software.

To examine cell cycle distribution and cell death rates 30.000 cells were seeded in 12 well plates. After attaching for 24 h cells were treated with CDDP, Ru3 and Ru14 for 48 h at various concentrations for cell cycle and cell death analyses. For cell death analysis, immediately after treatment cells were stained with Propidium Iodid (PI) (1 µg/ml) on ice and the amount of dead cells was measured using

BD Canto II. For cell cycle distribution, cells recovered for 24 h after treatment. Afterwards cells were fixed in ice-cold, 50 % EtOH for 24 h at -20 °C. For DNA staining fixed cells were incubated in PBS with 0.05 % Triton-X, 0.1 µg/ml RNaseA and 50 µg/ml PI for 1 h at 4 °C in dark. DNA content was measured using BD Canto II.

For the determination of DNA damage induced by the treatment with different substances histone γH2AX-foci were visualized by immunocytochemical staining. Cells were seeded on coverslips to reach 60-70% confluence after 24h. After incubation (24h) with different substances at IC_{50} concentrations for the resistant cells, cells were washed 3x with PBS and fixed for 10min in 4% paraformaldehyde. Cells were again washed 3-times and then permeabilised by incubation with 0.25% Triton-X in PBS for 5min. Primary antibody against γH2AX (clone JBW301, Millipore, diluted 1:2000) was incubated for 1h at RT and coverslips were washed 3-times afterwards. Alexa488-labelled secondary anti-mouse antibody (life technologies) was used in a 1:1000 dilution in PBS and applied for 1h at RT. Cells were washed 3-times, counterstained with DAPI, washed again and embedded in mounting medium (Vectorshield, Vector Systems). Slides were stored at 4°C in darkness until microscopic evaluation was done using a Zeiss LSM 710 laser scanning microscope. Image analysis was done using ImageJ and the FindFoci PlugIn.

Acknowledgements

The authors would like to thank P. Bellstedt, B. Rambach and G. Sentis for the helpful measurements of the NMR spectra.

References

A

[Aird, 2002] R. E. Aird, J. Cummings, A. A. Ritchie, M. Muir, R. E. Morris, H. Chen, P. J. Sadler and D. I. Jodrell, *Br. J. Cancer*, **2002**, 86, 1652-1657.

[Alessio, 1991] E. Alessio, G. Balducci, M. Calligaris, G. Costa, W. M. Attia and G. Mestroni, *Inorg. Chem.*, **1991**, 30, 609-618.

[Allardyce, 2001a] C. S. Allardyce and P. J. Dyson, *Platinum Met. Rev*., **2001**, 45, 62-69.

[Allardyce, 2001b] C. S. Allardyce, P. J. Dyson, D. J. Ellis and S. L. Heath, *Chem. Commun*., **2001**, 1396-1397.

[Amable, 2016] L. Amable, *Pharmacol. Res*., **2016**, 106, 27-36.

[Andre, 2004] T. Andre, C. Boni, L. Mounedji-Boudiaf, M. Navarro, J. Tabernero, T. Hickish, C. Topham, M. Zaninelli, P. Clingan, J. Bridgewater, I. Tabah-Fisch, A. de Gramont and I. Multicenter, International Study of Oxaliplatin/ 5-Fluorouracil/Leucovorin in the Adjuvant Treatment of Colon Cancer, *N. Engl. J. Med*., **2004**, 350, 2343-2351.

B

[Beckford, 2011] F. Beckford, D. Dourth, M. Shaloski Jr., J. Didion, J. Thessing, J. Woods, V. Crowell, N. Gerasimchuk, A. Gonzalez-Sarrías and N. P. Seeram, *J. Inorg. Biochem*., **2011**, 105, 1019-1029.

[Bennett, 1974] M. A. Bennett and A. K. Smith, *J. Chem. Soc., Dalton Trans*., **1974**, 233-241.

[Bergamo, 2007] A. Bergamo and G. Sava, *Dalton Trans*., **2007**, 13, 1267-1272.

[Bergamo, 2008] A. Bergamo, A. Masi, P. J. Dyson and G. Sava*, Int. J. Oncol*., **2008**, 33, 1281-1289.

[Bergamo, 2010] A. Bergamo, A. Masi, A. F. A. Peacock, A. Habtemariam, P. J. Sadler and G. Sava, *J. Inorg. Biochem*., **2010**, 104, 79-86.

[Bergamo, 2012] A. Bergamo, C. Gaiddon, J. H. M. Schellens, J. H. Beijnen and G. Sava, *J. Inorg. Biochem*., **2012**, 106, 90-99.

[Berger, 1989] M. R. Berger, F. T. Garzon, B. K. Keppler and D. Schmahl, *Anticancer Res*., **1989**, 9, 761-765.

[Bijelic, 2016] A. Bijelic, S. Theiner, B. K. Keppler and A. Rompel, *J. Med. Chem*., **2016**, 59, 5894-5903.

[Bruijnincx, 2009] P. C. A. Bruijnincx and P. J. Sadler, *Adv. Inorg. Chem*. **2009**, 61, 1-62.

[Burris, 2016] H. A. Burris, S. Bakewell, J. C. Bendell, J. R. Infante, S. F. Jones, D. R. Spigel, G. J. Weiss, R. K. Ramanathan, A. Ogden and D. D. Von Hoff, *ESMO Open,* **2016**, 1, e000154.

[Büchel, 2011] G. E. Büchel, I. N. Stepanenko, M. Hejl, M. A. Jakupec, B. K. Keppler and V. B. Arion, *Inorg. Chem*. **2011**, 50, 7690-7697.

[Büchel, 2013] G. E. Büchel, A. Gavriluta, M. Novak, S. M. Meier, M. A. Jakupec, O. Cuzan, C. Turta, J. B. Tommasino, E. Jeanneau, G. Novitchi, D. Luneau and V. B. Arion, *Inorg. Chem*. **2013**, 52, 6273-6285.

C

[Čanovic´, 2017] P. Čanovic´, A. R. Simovic´, S. Radisavljevic´, I. Bratsos, N. Demiri, M. Mitrovic´, I. Zelen and Z. D. Bugarcic´, *J. Biol. Inorg. Chem.,* **2017**, DOI 10.1007/s00775-017-1479-7.

[Cebrian-Losantos, 2007] B. Cebrian-Losantos, A. A. Krokhin, I. N. Stepanenko, R. Eichinger, M. A. Jakupec, V. B. Arion and B. K. Keppler, *Inorg. Chem*., **2007**, 46, 5023-5033.

[Cetinbas, 2010] N. Cetinbas, M. I. Webb, J. A. Dubland and C. J. Walsby, *J. Biol. Inorg. Chem*., **2010**, 15, 131-145.

[Chatlas, 1995] J. Chatlas, R. Vaneldik and B. K. Keppler*, Inorg. Chim. Acta*, **1995**, 233, 59-63.

[Chen, 2002] H. M. Chen, J. A. Parkinson, S. Parsons, R. A. Coxall, R. O. Gould and P. J. Sadler, *J. Am. Chem. Soc*., **2002**, 124, 3064-3082.

[Clarke, 1974] M. J. Clarke and H. Taube, *J. Am. Chem. Soc*., **1974**, 96, 5413-5419.

[Clarke, 1978] M. J. Clarke, *J. Am. Chem. Soc*., **1978**, 100, 5068-5075.

[Clarke, 1980a] M. J. Clarke, S. Bitler, D. Rennert, M. Buchbinder and A. D. Kelman, *J. Inorg. Biochem*., **1980**, 12, 79-87.

[Clarke, 1980b] M. J. Clarke, *Inorg. Chem*., **1980**, 19, 1103-1104.

[Clarke, 2003] M. J. Clarke, *Coord. Chem. Rev*., **2003**, 236, 209-233.

[Clavel, 2014] C. M. Clavel, E. Pă unescu, P. Nowak-Sliwinska and P. J. Dyson, *Chem. Sci*. **2014**, 5, 1097-1101.

[Collier, 1931] W. A. Collier and F. Krauss, *Z. Krebsforsch*., **1931**, 34, 526-530.

D

[Data Collection Software] COLLECT, Data Collection Software; Nonius B.V., Netherlands, **1998**.

[Depenbrock, 1997] H. Depenbrock, S. Schmelcher, R. Peter, B. K. Keppler, G. Weirich, T. Block, J. Rastetter and A. R. Hanauske, *Eur. J. Cancer*, **1997**, 33, 2404-2410.

[Dhubhghaill, 1994] O. M. N. Dhubhghaill, W. R. Hagen, B. K. Keppler, K. G. Lipponer and P. J. Sadler, *J. Chem. Soc., Dalton Trans*., **1994**, 3305-3310.

[Dorcier, 2005] A. Dorcier, P. J. Dyson, C. Gossens, U. Rothlisberger, R. Scopelliti and I. Tavernelli, *Organometallics*, **2005**, 24, 2114-2123.

[Dorcier, 2006] A. Dorcier, W. H. Ang, S. Bolano, L. Gonsalvi, L. Juillerat-Jeannerat, G. Laurenczy, M. Peruzzini, A. D. Phillips, F. Zanobini and P. J. Dyson, *Organometallics*, **2006**, 25, 4090-4096.

[Durig, 1976] J. R. Durig, J. Danneman, W. D. Behnke and E. E. Mercer, *Chem.-Biol. Interact*., **1976**, 13, 287-294.

F

[Filak, 2010] L. K. Filak, G. Muhlgassner, M. A. Jakupec, P. Heffeter, W. Berger, V. B. Arion and B. K. Keppler, *J. Biol. Inorg. Chem*., **2010**, 15, 903-918.

[Filak, 2011] L. K. Filak, G. Muhlgassner, F. Bacher, A. Roller, M. Galanski, M. A. Jakupec, B. K. Keppler and V. B. Arion, *Organometallics*, **2011**, 30, 273-283.

[Filak, 2013] L. K. Filak, S. Göschl, P. Heffeter, K. Ghannadzadeh Samper, A. E. Egger, M. A. Jakupec, B. K. Keppler, W. Berger and V. B. Arion, *Organometallics*, **2013**, 32, 903-914.

[Fu, 2011] Y. Fu, A. Habtemariam, A. M. B. H. Basri, D. Braddick, G. J. Clarkson and P. J. Sadler*, Dalton Trans*., **2011**, 40, 10553-10562.

[Fuereder, 2017] T. Fuereder and W. Berger, *ESMO Open*, **2017**, 2, e000239.

G

[Gasser, 2010] G. Gasser, I. Ott, N. Metzler-Nolte, *J. Med. Chem*, **2011**, 54(1), 3-25.

[Gatti, 2018] A. Gatti, A. Habtemariam, I. Romero-Canelon, J.I. Song, B. Heer, G. J. Clarkson, D. Rogolino, P. J. Sadler and M. Carcelli, *Organometallics*, **2018**, 37, 891-899.

[Groessl, 2007] M. Groessl, E. Reisner, C. G. Hartinger, R. Eichinger, O. Semenova, A. R. Timerbaev, M. A. Jakupec, V. B. Arion and B. K. Keppler, *J. Med. Chem*., **2007**, 50, 2185-2193.

H

[Habtemariam, 2006] A. Habtemariam, M. Melchart, R. Fernandez, S. Parsons, I. D. H. Oswald, A. Parkin, F. P. A. Fabbiani, J. E. Davidson, A. Dawson, R. E. Aird, D. I. Jodrell and P. J. Sadler, *J. Med. Chem*., **2006**, 49, 6858-6868.

[Hackl, 2016] C. M. Hackl, M. S. Legina, V. Pichler, M. Schmidlehner, A. Roller, O. Domotor, E. A. Enyedy, M. A. Jakupec, W. Kandioller and B. K. Keppler, *Chem. – Eur. J.*, **2016**, 22, 17269-17281.

[Hanif, 2010] M. Hanif, P. Schaaf, W. Kandioller, M. Hejl, M. A. Jakupec, A. Roller, B. K. Keppler and C. G. Hartinger, *Aust. J. Chem*., **2010**, 63, 1521-1528.

[Hartinger, 2006] C. G. Hartinger, S. Zorbas-Seifried, M. A. Jakupec, B. Kynast, H. Zorbas and B. K. Keppler, *J. Inorg. Biochem*. **2006**, 100, 891-904.

[Hartinger, 2008] C. G. Hartinger, M. A. Jakupec, S. Zorbas-Seifried, M. Groessl, A. Egger, W. Berger, H. Zorbas, P. J. Dyson and B. K. Keppler, *Chem. Biodiversity*, **2008**, 5, 2140-2155.

[Hartinger, 2013] C. G. Hartinger, M. Groessl, S. M. Meier, A. Casini and P. J. Dyson, *Chem. Soc. Rev*., **2013**, 42, 6186-6199.

[Hildebrandt, 2016a] J. Hildebrandt, N. Häfner, H. Görls, D. Kritsch, G. Ferraro, M. Dürst, I. B. Runnebaum, A. Merlino and W. Weigand, *Dalton Trans.* **2016**, 45, 18876-18891.

[Hildebrandt, 2016b] J. Hildebrandt, H. Görls, N. Häfner, G. Ferraro, M. Dürst, I. B. Runnebaum, W. Weigand and A. Merlino, *Dalton Trans.* **2016**, 45, 12283-12287.

[Hotze, 2000] A. C. G. Hotze, A. H. Velders, F. Ugozzoli, M. Biagini-Cingi, A. M. Manotti-Lanfredi, J. G. Haasnoot and J. Reedijk, *Inorg. Chem.,* **2000**, 39, 3838-3844.

K

[Kandioller, 2009a] W. Kandioller, C. G. Hartinger, A. A. Nazarov, M. L. Kuznetsov, R. O. John, C. Bartel, M. A. Jakupec, V. B. Arion and B. K. Keppler, *Organometallics*, **2009**, 28, 4249-4251.

[Kandioller 2009b] W. Kandioller, C. G. Hartinger, A. A. Nazarov, J. H. Kasser, R. O. John, M. Jakupec, V. Arion, P. J. Dyson and B. K. Keppler, *J. Organomet. Chem*., **2009**, 694, 922-929.

[Kapitza, 2005] S. Kapitza, M. Pongratz, M. A. Jakupec, P. Heffeter, W. Berger, L. Lackinger, B. K. Keppler and B. Marian*, J. Cancer Res. Clin. Oncol*., **2005**, 131, 101-110.

[Kasprzak, 2011] M. M. Kasprzak, L. Szmigiero, E. Zyner and J. Ochocki, *J. Inorg. Biochem.*, **2011**, 105(4), 518-524.

[Kelman, 1977] A. D. Kelman, M. J. Clarke, S. E. Edmonds and H. J. Peresie, *J. Clin. Hematol. Oncol*., **1977**, 7, 274-288.

[Keppler, 1986] B. K. Keppler and W. Rupp, *J. Cancer Res. Clin. Oncol*., **1986**, 111, 166-168.

[Keppler, 1987] B. K. Keppler, W. Rupp, U. M. Juhl, H. Endres, R. Niebl and W. Balzer, *Inorg. Chem*., **1987**, 26, 4366-4370.

[Keppler, 1989] B. K. Keppler, M. Henn, U. M. Juhl, M. R. Berger, R. Niebl and F. E. Wagner, *Prog. Clin. Biochem. Med*., **1989**, 10, 41-69.

[Kilpin, 2013] K. J. Kilpin and P. J. Dyson, *Chem. Sci.,* **2013**, 4, 1410-1419.

[Kilpin, 2014] K. J. Kilpin, S. Crot, T. Riedel, J. A. Kitchen and P. J. Dyson, *Dalton Trans*. **2014**, 43, 1443-1448.

[Kritsch, 2017] D. Kritsch, F. Hoffmann, D. Steinbach, L. Jansen, S. M. Photini, M. Gajda, A. S. Mosig, J. Sonnemann, S. Peters, M. Melnikova, J. Thomale, M. Dürst, I. B. Runnebaum and N. Häfner, *Mol. Cancer Biol.*, **2017**, 141(8), 1600-1614.

[Kuhn, 2014] K. J. Kilpin, S. Crot, T. Riedel, J. A. Kitchen and P. J. Dyson, *Dalton Trans*. **2014**, 43, 1443-1448.

[Kurzwernhart, 2013] A. Kurzwernhart, W. Kandioller, É. A. Enyedy, M. Novak, M. A. Jakupec, B. K. Keppler and C. G. Hartinger, *Dalton Trans*., **2013**, 42, 6193-6202.

L

[Leijen, 2015] S. Leijen, S. A. Burgers, P. Baas, D. Pluim, M. Tibben, E. van Werkhoven, E. Alessio, G. Sava, J. H. Beijnen and J. H. Schellens, *Invest. New Drugs,* **2015**, 33, 201-214.

[Lentz, 2009] F. Lentz, A. Drescher, A. Lindauer, M. Henke, R. A. Hilger, C. G. Hartinger, M. E. Scheulen, C. Dittrich, B. K. Keppler and U. Jaehde, *Anti-Cancer Drugs*, **2009**, 20, 97-103.

[Lokich, 1998] J. Lokich and N. Anderson, *Ann. Oncol*., **1998**, 9, 13-21.

M

[Mayr, 2017] J. Mayr, P. Heffeter, D. Groza, L. Galvez, G. Koellensperger, A. Roller, B. Alte, M. Haider, W. Berger, C. R. Kowol and B. K. Keppler, *Chem. Sci.*, **2017**, 8, 2241-2250.

[Meggers, 2007] E. Meggers, G. Atilla-Gokcumen, H. Bregman, J. Maksimoska, S. Mulcahy, N. Pagano and D. Williams, *Synlett*, **2007**, 1177-1189.

[Meier, 2013] S. M. Meier, M. Novak, W. Kandioller, M. A. Jakupec, V. B. Arion, N. Metzler-Nolte, B. K. Keppler and C. G. Hartinger, *Chem. – Eur. J.,* **2013**, 19, 9297-9307.

[Meier-Menches, 2018] S. M. Meier-Menches, C. Gerner, W. Berger, C. G. Hartinger and B. K. Keppler, *Chem. Soc. Rev.,* **2018**, 47, 909-928.

[Mendoza-Ferri, 2009] M. G. Mendoza-Ferri, C. G. Hartinger, A. A. Nazarov, R. E. Eichinger, M. A. Jakupec, K. Severin and B. K. Keppler, *Organometallics*, **2009**, 28, 6260-6265.

[Mercury, 2006] MERCURY, C. F. Macrae, P. R. Edgington, P. McCabe, E. Pidcock, G. P. Shields, R. Taylor , M. Towler and J. van de Streek, *J. Appl. Cryst.,* **2006**, 39:453.

[Monti-Bragadin, 1975] C. Monti-Bragadin, L. Ramani, L. Samer, G. Mestroni and G. Zassinovich, *Antimicrob. Agents Chemother*., **1975**, 7, 825-827.

[Morris, 2001] R. E. Morris, R. E. Aird, P. D. Murdoch, H. M. Chen, J. Cummings, N. D. Hughes, S. Parsons, A. Parkin, G. Boyd, D. I. Jodrell and P. J. Sadler, *J. Med. Chem*., **2001**, 44, 3616-3621.

[Muggia, 2015] F. M. Muggia, A. Bonetti, J. D. Hoeschele, M. Rozencweig and S. B. Howell, *J. Clin. Oncol*., **2015**, 35(33), 4219-4226.

[Murray, 2016] B. S. Murray, M. V. Babak, C. G. Hartinger and P. J. Dyson, *Coord. Chem. Rev*., **2016**, 306, 86-114.

N

[Nowak-Sliwinska, 2011] P. Nowak-Sliwinska, J. R. van Beijnum, A. Casini, A. A. Nazarov, G. Wagnieres, H. van den Bergh, P. J. Dyson and A. W. Griffioen, *J. Med. Chem*., **2011**, 54, 3895-3902.

O

[Otwinowski, 1997] 'Processing of X-Ray Diffraction Data Collected in Oscillation Mode':Otwinowski, Z.; Minor, W. in Carter, C. W.; Sweet, R. M. (eds.): *Methods in Enzymology, Vol. 276, Macromolecular Crystallography, Part A*, pp. 307-326, Academic Press **1997**.

P

[Pascoe, 1974] J. M. Pascoe and J. J. Roberts, *Biochem. Pharmacol*., **1974**, 23, 1345-1357.

[Paunescu, 2015] E. Paunescu, P. Nowak-Sliwinsky, C. M. Clavel, R. Scopelliti, A. W. Griffioen and P. J. Dyson*, ChemMedChem*., **2015**, 10, 1539-1547.

[Peacock, 2006] A. F. A. Peacock, A. Habtemariam, R. Fernandez, V. Walland, F. P. A. Fabbiani, S. Parsons, R. E. Aird, D. I. Jodrell and P. J. Sadler, *J. Am. Chem. Soc*., **2006**, 128, 1739-1748.

[Peacock, 2007a] A. F. A. Peacock, A. Habtemariam, S. A. Moggach, A. Prescimone, S. Parsons and P. J. Sadler, *Inorg. Chem*., **2007**, 46, 4049-4059.

[Peacock, 2007b] A. F. Peacock, M. Melchart, R. J. Deeth, A. Habtemariam, S. Parsons and P. J. Sadler, *Chem. – Eur. J.,* **2007**, 13, 2601-2613.

[Peacock, 2007c] A. F. A. Peacock, S. Parsons and P. J. Sadler, *J. Am. Chem. Soc*., **2007**, 129, 3348-3357.

[Peacock, 2008] A. F. A. Peacock and P. J. Sadler, *Chem. – Asian J*., **2008**, 3, 1890-1899.

[Petruzzella, 2017] E. Petruzzella, J. P. Braude, J. R. Aldrich-Wright, V. Gandin and D. Gibson, *Angew. Chem. Int. Ed.,* **2017**, 56, 11539-11544.

[Pettinari, 2016] R. Pettinari, F. Marchetti, A. Petrini, C. Pettinari, G. Lupidi, P. Smolenski, R. Scopelliti, T. Riedel and P. J. Dyson, *Organometallics,* **2016**, 35(21), 3734-3742.

[Pieper, 1998] T. Pieper and B. K. Keppler, *Analysis*, **1998**, 26, 84-87.

[Pizarro, 2010] A. M. Pizarro, A. Habtemariam and P. J. Sadler, in *Medicinal Organometallic Chemistry*, ed. G. Jaouen and N. Metzler-Nolte, Springer, Heidelberg, **2010**, pp. 21-56, DOI: 10.1007/978-3- 642-13185-1_2.

Q

[Qian, 2013] C. Qian, J. Q. Wang, C. L. Song, L. L. Wang, L. N. Ji and H. Chao, *Metallomics,* **2013**, 5, 844-854.

R

[Rademaker-Lakhai, 2004] J. M. Rademaker-Lakhai, D. van den Bongard, D. Pluim, J. H. Beijnen and J. H. Schellens, *Clin. Cancer Res*., **2004**, 10, 3717-3727.

[Raveendran, 2016] R. Raveendran, J. P. Braude, E. Wexselblatt, V. Novohradsky, O. Stuchlikova, V. Brabec, V. Gandin and D. Gibson, *Chem. Sci*. **2016**, 7, 2381-2391.

[Renfrew, 2011] A. K. Renfrew, L. Juillerat-Jeanneret and P. J. Dyson, *J. Organomet. Chem*., **2011**, 696, 772-779.

[Riedl, 2017] C. A. Riedl, L. S. Flocke, M. Hejl, A. Roller, M. H. Klose, M. A. Jakupec, W. Kandioller and B. K. Keppler, *Inorg. Chem*., **2017**, 56, 528-541.

[Romero-Camelon, 2013] I. Romero-Canelon and P. J. Sadler, *Inorg. Chem*., **2013**, 52, 12276-12291.

[Rosenberg, 1965] B. Rosenberg, L. Vancamp and T. Krigas, *Nature*, **1965**, 205, 698-699.

[Rosenberg, 1969] B. Rosenberg, L. Vancamp, J. E. Trosko and V. H. Mansour, *Nature*, **1969**, 222, 385-386.

S

[Sadabs, 2015] SADABS 2016/2: L. Krause, R. Herbst-Irmer, G. M. Sheldrick and D. Stalke, *J. Appl. Cryst.*, **2015**, 48, 3-10.

[Sava, 1989] G. Sava, S. Pacor, S. Zorzet, E. Alessio and G. Mestroni, *Pharmacol. Res.*, **1989**, 21, 617-628.

[Sava, 1992] G. Sava, S. Pacor, G. Mestroni and E. Alessio, *Anti-Cancer Drugs*, **1992**, 3, 25-31.

[Sava, 1994] G. Sava, S. Pacor, M. Coluccia, M. Mariggio, M. Cocchietto, E. Alessio and G. Mestroni, *Drug Invest*., **1994**, 8, 150-161.

[Schmid, 2007a] W. F. Schmid, R. O. John, G. Muhlgassner, P. Heffeter, M. A. Jakupec, M. Galanski, W. Berger, V. B. Arion and B. K. Keppler, *J. Med. Chem*., **2007**, 50, 6343-6355.

[Schmid, 2007b] W. F. Schmid, R. O. John, V. B. Arion, M. A. Jakupec and B. K. Keppler, *Organometallics*, **2007**, 26, 6643-6652.

[Schmidlehner, 2016] M. Schmidlehner, L. S. Flocke, A. Roller, M. Hejl, M. A. Jakupec, W. Kandioller and B. K. Keppler, *Dalton Trans*., **2016**, 45, 724-733.

[Schwarz, 2013] M. B. Schwarz, A. Kurzwernhart, A. Roller, W. Kandioller, B. K. Keppler and C. G. Hartinger*, Z. Anorg. Allg. Chem*., **2013**, 639, 1648-1654.

[Scolaro, 2005] C. Scolaro, A. Bergamo, L. Brescacin, R. Delfino, M. Cocchietto, G. Laurenczy, T. J. Geldbach, G. Sava and P. J. Dyson, *J. Med. Chem*. **2005**, 48, 4161-4171.

[Sersen, 2013] S. Sersen, J. Kljun, F. Pozgan, B. Stefane and I. Turel, *Organometallics*, **2013**, 32(2), 609-616.

[Sersen, 2015] S. Sersen, J. Kljun, K. Kryeziu, R. Panchuk, B. Alte, W. Körner, P. Heffeter, W. Berger and I. Turel, *J. Med. Chem.*, **2015**, 58(9), 3984-3996.

[Sheldrick, 2015] G. M. Sheldrick, *Acta Cryst.*, **2015**, C71, 3-8.

[Shnyder, 2011] S. D. Shnyder, Y. Fu, A. Habtemariam, S. H. van Rijt, P. A. Cooper, P. M. Loadman and P. J. Sadler, *MedChem- Comm*, **2011**, 2, 666-668.

[Smith, 1996] C. A. Smith, A. J. SutherlandSmith, B. K. Keppler, F. Kratz and E. N. Baker, *J. Biol. Inorg. Chem*., **1996**, 1, 424-431.

[Sun, 2017] D. Sun, Z. Mou, N. Li, W. Zhang, Y. Wang, E.Yang and W. Wang, *JBIC*, **2016**, 21(8), 945-956.

T

[Tang, 2017] B. Tang, D. Wan, S. H. Lai, H. H. Yang, C. Zhang, X. Z. Wang, C. C. Zeng and Y. J. Liu, *J. Inorg. Biochem.*, **2017**, 173, 93-104.

[Trondl, 2014] R. Trondl, P. Heffeter, C. R. Kowol, M. A. Jakupec, W. Berger and B. K. Keppler, *Chem. Sci*., **2014**, 5, 2925-2932.

[Trynda-Lemiesz, 1999] L. Trynda-Lemiesz, B. K. Keppler and H. Kozlowski, *J. Inorg. Biochem*., **1999**, 73, 123-128.

V

[van Rijt, 2009] S. H. van Rijt, A. F. A. Peacock and P. J. Sadler, *in Platinum and Other Heavy Metal Compounds in Cancer Chemotherapy – Molecular Mechanisms and Clinical Applications*, ed. A. Bonetti, R. Leone, F. M. Muggia and S. B. Howell, Humana Press, New York, **2009**, pp. 73-79, DOI: 10.1007/ 978-1-60327-459-3_10.

[van Rijt, 2010] S. H. van Rijt, A. Mukherjee, A. M. Pizarro and P. J. Sadler, *J. Med. Chem*., **2010**, 53, 840-849.

[Velders, 2000] A. H. Velders, H. Kooijman, A. L. Spek, J. G. Haasnoot, D. de Vos and J. Reedijk, *Inorg. Chem.,* **2000**, 39, 2966-2967.

W

[Weiss, 2014] A. Weiss, R. H. Berndsen, M. Dubois, C. M¸ller, R. Schibli, A. W. Griffioen, P. J. Dyson and P. Nowak-Sliwinska, *Chem. Sci*. **2014**, 5, 4742-4748.

[Weiss, 2015] A. Weiss, D. Bonvin, R. H. Berndsen, E. Scherrer, T. J. Wong, P. J. Dyson, A. W. Griffioen and P. Nowak-Sliwinska, *Sci. Rep*. **2015**, 5 (8990), doi: 10.1038/srep08990.

[Wu, 2008] B. Wu, P. Droge and C. A. Davey, *Nat. Chem. Biol*., **2008**, 4, 110-112.

Y

[Yan, 2005] Y. K. Yan, M. Melchart, A. Habtemariam and P. J. Sadler, *Chem. Commun*., **2005**, 4764-4776.

[Yang, 2012] X. Yang, L. Chen, Y. Liu, Y. Yang, T. Chen, W. Zheng, J. Liu and Q. Y. He, *Biochimie,* **2012**, 94(2), 345-353.

Z

[Zhao, 2014] Z. Zhao, Z. Luo, Q. Wu, W. Zheng, Y. Feng and T. Chen, *Dalton Trans.*, **2014**, 43, 17017-17028.

[Zeng, 2016] C. C. Zeng, S. H. Lai, J. H. Yao, C. Zhang, H. Yin, W. Li, B. J. Han and Y. J. Liu, *Eur. J. Med. Chem.*, **2016**, 122, 118-126.

Supplementary Information

Highly cytotoxic Osmium(II) compounds and their Ruthenium(II) Analogues targeting Ovarian Carcinoma cell lines and evading Cisplatin resistance mechanisms

Jana Hildebrandt, Norman Häfner, Daniel Kritsch, Helmar Görls, Matthias Dürst, Ingo B. Runnebaum, Wolfgang Weigand

[1] Institut für Anorganische und Analytische Chemie Friedrich-Schiller Universität Jena, Humboldtstraße 8, 07743 Jena, Germany

[2]Department of Gynecology, Jena University Hospital – Friedrich-Schiller University Jena

Additional Stability determination

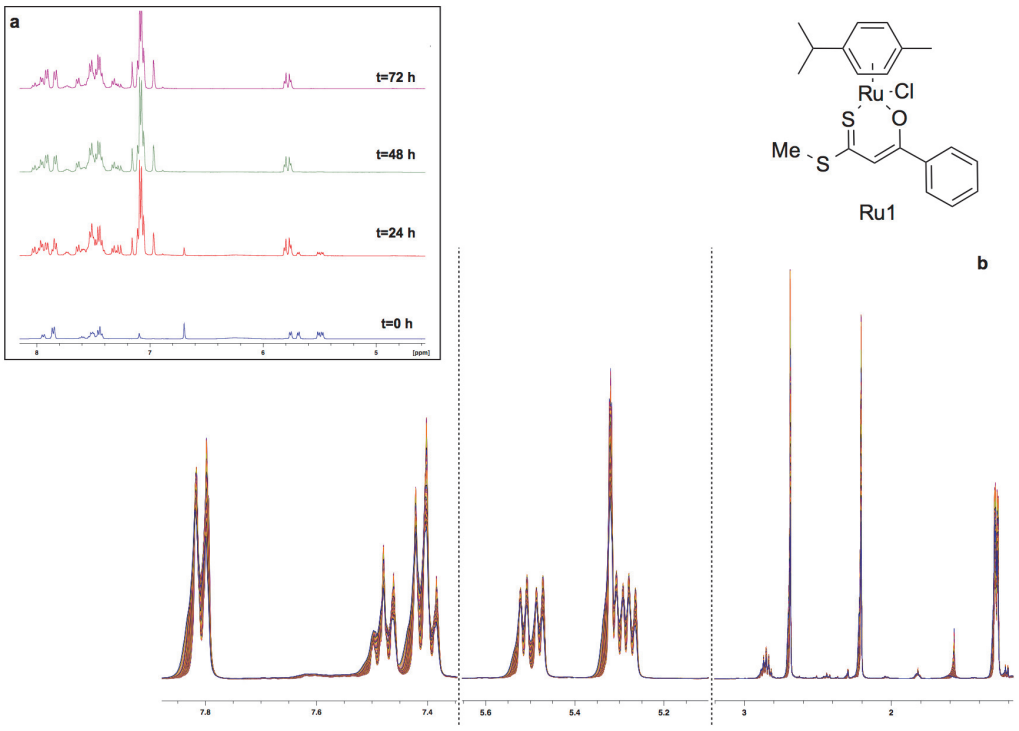

Fig. S1: Stability determination for Ru1, and solvent CD_2Cl_2.

Figure S1 shows the stability for Ru1 at room temperature in d_2-dichlormethane for 72 hours, there are no structural changes observable. Figure S2 shows changes of Ru1 in dmso-d_6 for 72 hours measurement at room temperature. As already discussed in the main part, structural changes are observable (see Fig. 10 and discussion).

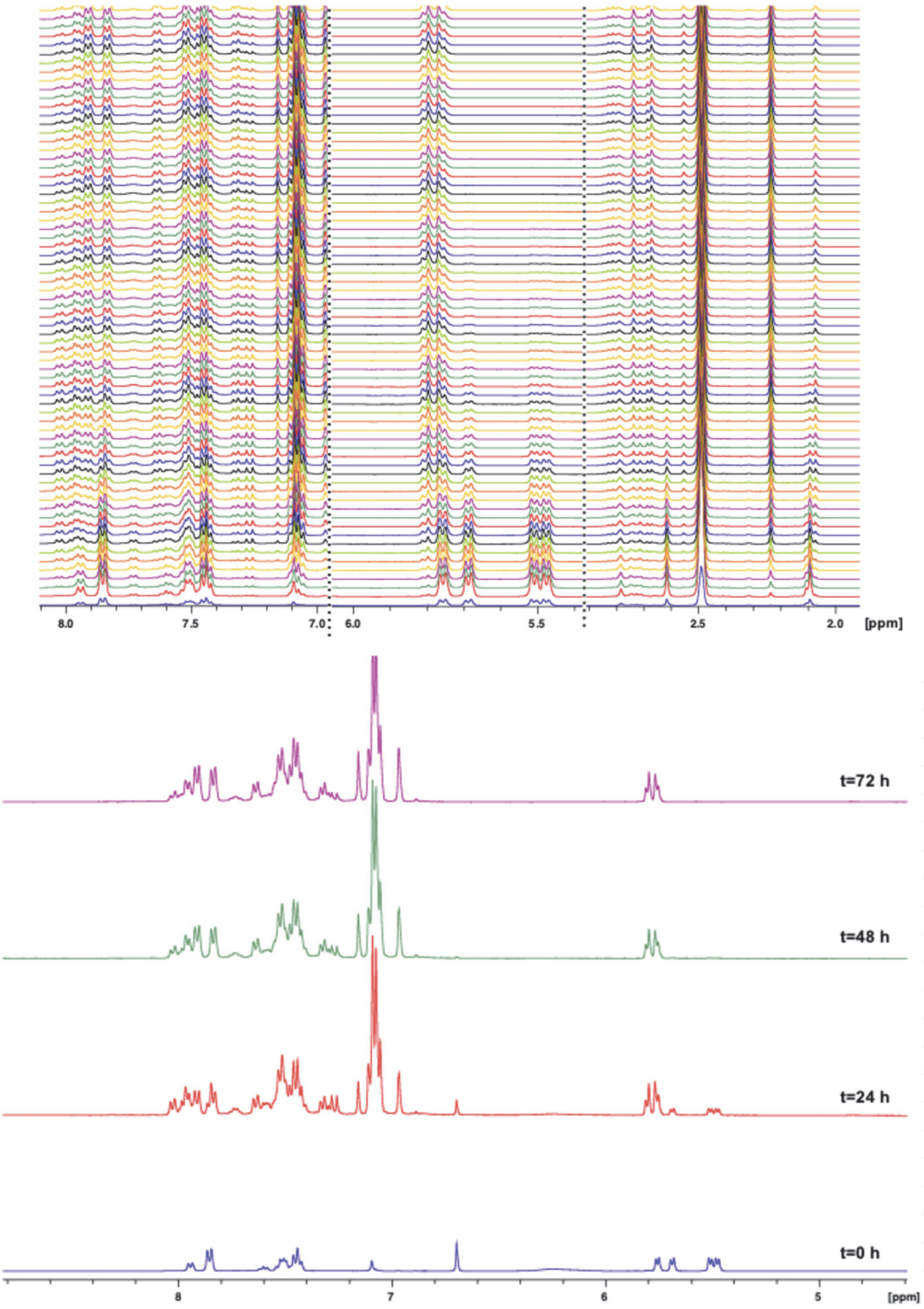

Fig. S2: ^{1}H NMR spectra for Ru1 and dmso at room temperature.

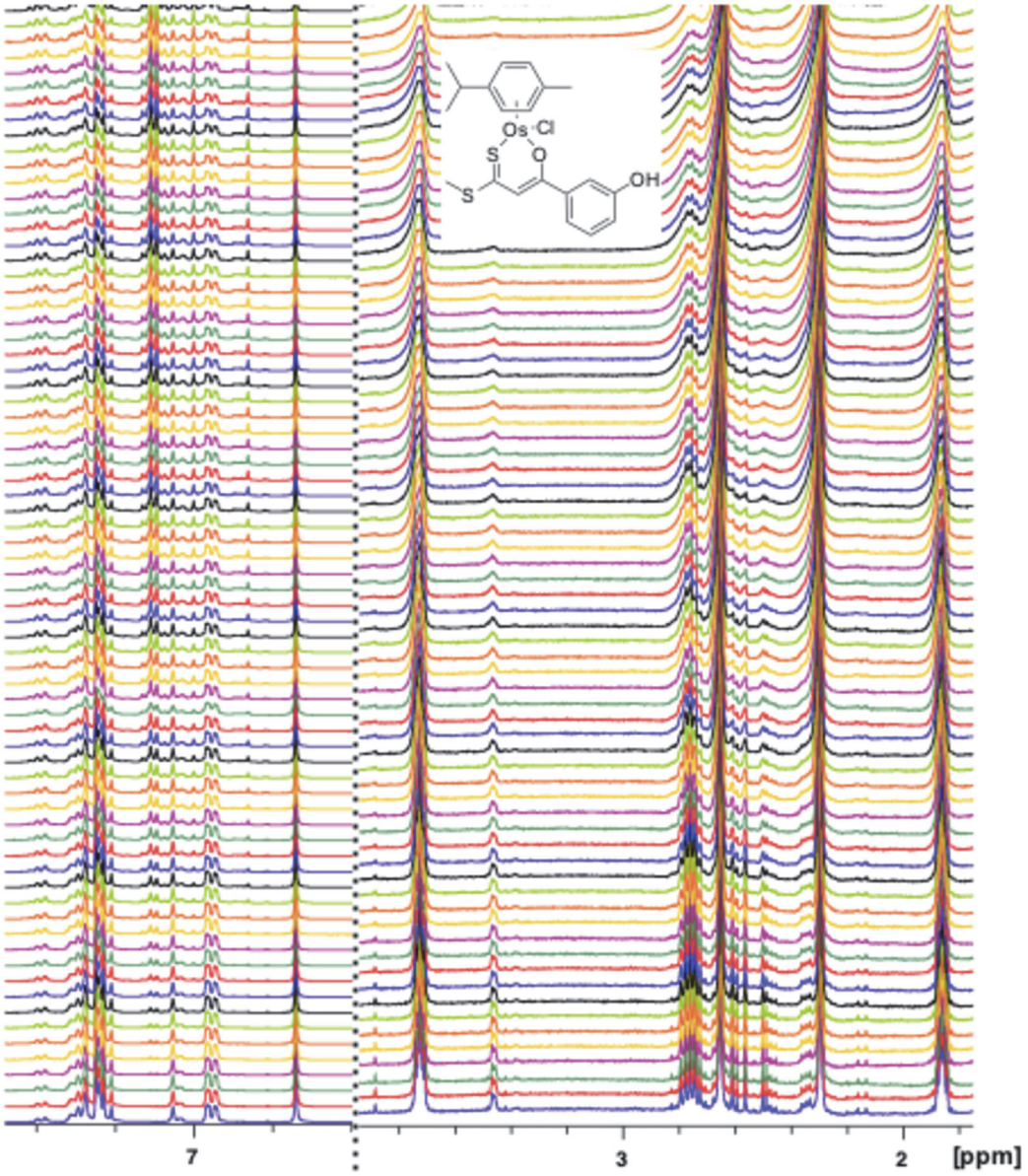

Fig. S3: Stability determination for Os3, 72 hours measurement, 37 °C, dmso-d_6 as solvent.

Figure S3 shows no structural changes for Os3 in dmso-d_6 and 37 °C for 72 hours. Therefore it can be concluded, that the osmium(II) compounds are more stable than the ruthenium(II) analogues.

Additional Molecular structures

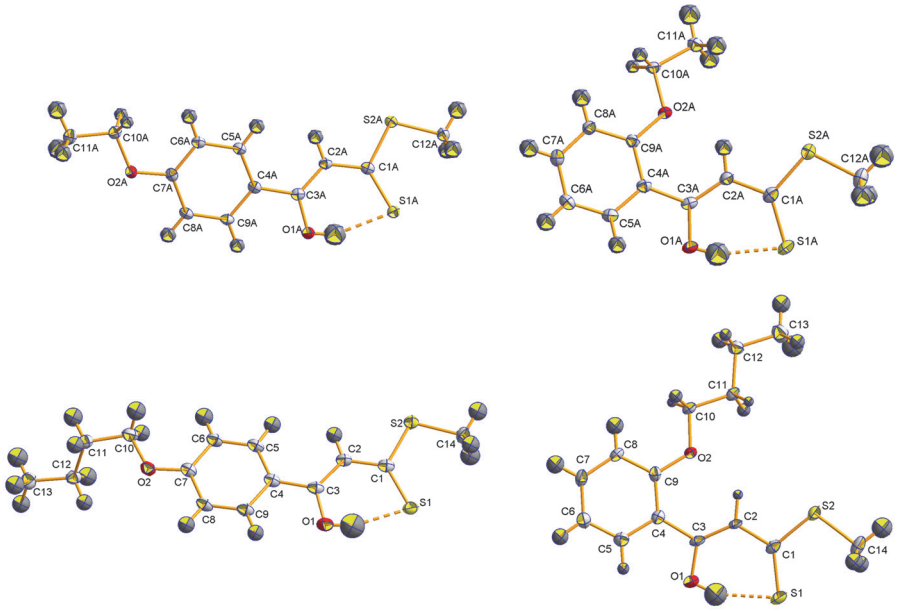

Fig. S2: Molecular structures (50% probability) of L14, L15, L17 and L18.

Tab. S1: Specific bond angles [°] and bond lengths [Å] for all characterized β-Hydroxydithiocinnamic alkyl esters.

	L14	**L15**	**L17**	**L18**
C(1)-S(1)	1.6848(15)	1.6764(16)	1.6816(13)	1.664(3)
C(3)-O(1)	1.3326(18)	1.3449(18)	1.3303(16)	1.334(4)
C(1)-C(2)	1.416(2)	1.431(2)	1.4215(18)	1.434(4)
C(2)-C(3)	1.377(2)	1.370(2)	1.3783(18)	1.363(4)
C(7/9)-O(2)	1.3604(18)	1.3559(18)	1.3603(16)	1.363(3)
O(2)-C(10)	1.4456(18)	1.4428(18)	1.4408(16)	1.443(4)
C(3)-C(4)	1.469(2)	1.482(2)	1.4715(18)	1.485(4)
C(1)-S(2)	1.7527(15)	1.7516(18)	1.7480(13)	1.740(3)
C(2)-H(2)	0.95(2)	0.96(2)	0.933(16)	0.95(3)
S(1)-C(1)-C(2)	126.21(12)	126.37(13)	122.46(8)	122.92(18)
O(1)-C(3)-C(2)	123.08(14)	122.32(14)	122.81(13)	122.7(3)

Figure S2 and Table S1 show molecular structures and characteristics of four different β-Hydroxydithiocinnamic alkyl esters. The data confirm what was reported and discussed earlier.[Hildebrandt, 2016a; Hildebrandt, 2016b]

Tab. S2. Crystal data and refinement details for the X-ray structure determinations of the compounds **L14 - L18**.

Compound	**L14**	**L15**	**L17**	**L18**
formula	$C_{12}H_{14}O_2S_2$	$C_{12}H_{14}O_2S_2$	$C_{14}H_{18}O_2S_2$	$C_{14}H_{18}O_2S_2$
fw ($g \cdot mol^{-1}$)	254.35	254.35	282.40	282.40
°C	-140(2)	-140(2)	-140(2)	-140(2)
crystal system	triclinic	triclinic	monoclinic	triclinic
space group	P $\bar{1}$	P $\bar{1}$	P $2_1/c$	P $\bar{1}$
a/ Å	9.9229(2)	7.7917(2)	18.8992(5)	7.6708(7)
b/ Å	10.1348(2)	10.3986(3)	7.6290(2)	10.2407(8)
c/ Å	24.5662(5)	16.4384(5)	10.0683(2)	10.8263(8)
α/°	98.033(1)	74.505(1)	90	116.040(4)
β/°	97.519(1)	84.461(1)	100.053(2)	90.738(6)
γ/°	90.383(1)	74.706(2)	90	107.985(5)
V/Å^3	2424.48(8)	1237.54(6)	1429.38(6)	715.74(10)
Z	8	4	4	2
ρ ($g \cdot cm^{-3}$)	1.394	1.365	1.312	1.310
μ (cm^{-1})	4.21	4.12	3.64	3.64
measured data	17911	9439	10168	6491
data with I > 2σ(I)	9829	4917	3006	2243
unique data (R_{int})	10644/0.0174	5511/0.0201	3248/0.0228	3102/0.0387
wR_2 (all data, on F^2)[a)]	0.0748	0.0862	0.0766	0.1246
R_1 ($I > 2\sigma(I)$) [a)]	0.0315	0.0363	0.0289	0.0608
S [b)]	1.068	1.108	1.070	1.068
Res. dens./e·Å^{-3}	0.364/-0.218	0.361/-0.206	0.306/-0.194	0.386/-0.358
absorpt method	multi-scan	multi-scan	multi-scan	multi-scan
absorpt corr T_{min}/T_{max}	0.7117/0.7456	0.7123/0.7456	0.7016/0.7456	0.6155/0.7456
CCDC No.	1446182	1446183	1446184	1446185

cont. Tab. S2. Crystal data and refinement details for the X-ray structure determinations of the compounds **Ru9 - Ru14**.

Compound	**Ru9**	**Ru13**	**Ru14**
formula	$C_{21}H_{25}ClO_2RuS_2$	$C_{22}H_{27}ClO_2RuS_2$	$C_{24}H_{31}ClO_2RuS_2$
fw ($g \cdot mol^{-1}$)	510.05	524.08	552.13
°C	-140(2)	-140(2)	-140(2)
crystal system	monoclinic	triclinic	monoclinic
space group	P 2_1/c	P $\bar{1}$	P 2_1/c
a/ Å	10.5639(2)	7.9324(2)	14.8040(3)
b/ Å	10.1107(2)	8.9961(3)	17.9489(4)
c/ Å	19.6796(3)	15.6809(4)	9.3794(2)
α/°	90	93.071(2)	90
β/°	92.098(1)	99.722(2)	96.407(1)
γ/°	90	97.455(1)	90
V/Å^3	2100.54(7)	1090.34(5)	2476.69(9)
Z	4	2	4
ρ ($g \cdot cm^{-3}$)	1.613	1.596	1.481
μ (cm^{-1})	10.86	10.49	9.27
measured data	16140	7983	17923
data with I > 2σ(I)	4325	4639	5020

unique data (R_{int})	4812/0.0328	4865/0.0182	5623/0.0352
wR_2 (all data, on F^2)[a)]	0.0550	0.0553	0.0647
R_1 ($I > 2\sigma(I)$) [a)]	0.0265	0.0250	0.0294
S [b)]	1.111	1.074	1.081
Res. dens./e·Å^{-3}	0.526/-0.425	0.368/-0.426	0.541/-0.452
absorpt method	multi-scan	multi-scan	multi-scan
absorpt corr $T_{min}/_{max}$	0.6910/0.7456	0.7069/0.7456	0.6873/0.7456
CCDC No.	1446187	1446188	1446189

[a)] Definition of the *R* indices: $R_1 = (\Sigma \mid\mid F_o \mid - \mid F_c \mid\mid)/\Sigma \mid F_o \mid$; $wR_2 = \{\Sigma[w(F_o^2-F_c^2)^2]/\Sigma[w(F_o^2)^2]\}^{1/2}$ with $w^{-1} = \sigma^2(F_o^2) + (aP)^2+bP$; $P = [2F_c^2 + \mathrm{Max}(F_O^2]/3$;

[b)] $s = \{\Sigma[w(F_o^2-F_c^2)^2]/(N_o-N_p)\}^{1/2}$.

Additional Biological behaviour

Table S3 shows IC50 values for all 18 β-Hydroxydithiocinnamic alkyl esters on ovarian carcinoma cell lines SKOV3 and A2780, as well as their Cisplatin resistant analogues SKOV3cis and A2780cis and on A549. In general, most compounds do not show cytotoxic properties, but as already mentioned for the ruthenium(II) compounds the resistant factors for the single ligands are lower than Cisplatin. Therefore it can be concluded that the circumvention of the Cisplatin resistance due to the ligand system. Compounds L14 and L17 shows lower IC50 values on SKOV3cis than reference substance Cisplatin. Corresponding ruthenium(II) complex, Ru14 is also most promising candidate in that group of compounds, see Figure 12.

Table S4 shows IC50 values for L14 on non-cancerous cell lines up to 100 µM.

Tab. S3: IC50 values in µM of all β-Hydroxydithiocinnamic alkyl esters for the antiproliferative effects in cancerous cells.

Sustances	**SKOV3 [µM]**	**SKOV3cis [µM]**	**A2780 [µM]**	**A2780cis [µM]**	**A549 [µM]**
L1	112.0 (±11.1)	107.1 (±7.5)	38.8 (±2.5)	17.7 (±1.0)	57.9 (±7.3)
RF(L1)	0.5		1		
L2	43.9 (±14.7)	103.9 (±17.8)	37.1 (±2.5)	25.4 (±7.6)	86.6 (±10.6)
RF(L2)	0.7		1		
L3	270.1 (±18.0)	189.5 (±15.0)	63.2 (±6.3)	17.5 (±2.0)	201.4 (±29.3)
RF(L3)	0.6		0.9		

L4	108.5 (±11.8)	91.0 (±0.7)	60.4 (±5.7)	87.1 (±3.0)	109.1 (±20.1)
RF(L4)	1.3		1		
L5	88.0 (±5.6)	74.6 (±5.9)	54.3 (±7.9)	25.0 (±4.6)	144.5 (±31.4)
RF(L5)	0.6		0.2		
L6	95.4 (±6.1)	86.0 (±11.4)	39.1 (±0.7)	57.1 (±4.5)	94.6 (±2.7)
RF(L6)	0.8		1		
L7	101.2 (±9.2)	90.2 (±3.1)	53.0 (±12.4)	24.1 (±7.2)	129.7 (±13.6)
RF(L7)	0.5		0.7		
L8	161.5 (±24.2)	69.0 (±2.2)	53.3 (±6.2)	16.4 (±3.7)	118.0 (±26.8)
RF(L8)	1		1.2		
L9	97.5 (±12.6)	88.3 (±18.3)	64.8 (±4.1)	29.1 (±6.8)	112.5 (±34.8)
RF(L9)	0.5		0.7		
L10	101.2 (±9.2)	90.2 (±3.1)	53.0 (±12.4)	24.1 (±7.2)	129.7 (±13.6)
RF(L10)	0.6		0.8		
L11	130.5 (±12.9)	142.8 (±23.8)	64.6 (±7.9)	77.9 (±6.2)	211.3 (±63.5)
RF(L11)	1		0.8		
L12	170.9 (±20.0)	133.4 (±26.2)	56.3 (±10.4)	63.2 (±11.3)	123.5 (±1.9)

RF(L12)	0.5		0.9		
L13	40.0 (±23.2)	35.7 (±29.1)	26.3 (±39.3)	38.1 (±28.0)	17.3 (±11.0)
RF(L13)	1		1.8		
L14	28.3 (±27.2)	11.3 (±7.1)	5.7 (±1.2)	31.8 (±25.4)	16.1 (±10.1)
RF(L14)	1.5		1.5		
L15	47.8 (±33.2)	40.2 (±25.2)	26.6 (±39.1)	18.5 (±10.1)	26.6 (±16.6)
RF(L15)	0.5		0.8		
L16	33.8 (±15.9)	19.4 (±2.8)	5.5 (±2.7)	22.1 (±9.5)	22.1 (±5.7)
RF(L16)	1		1.3		
L17	10.2 (±5.9)	3.2 (±2.3)	5.9 (±1.2)	20.5 (±11.2)	17.6(±05.0)
RF(L17)	1		0.7		
L18	25.0 (±19.5)	17.7 (±8.3)	5.6 (±2.0)	36.4 (±21.9)	13.9(±11.2)
RF(L18)	0.7		6.5		
CDDP	**3.8 (±2.8)**	**13.5 (±4.4)**	**1.3 (±0.2)**	**6.1 (±2.1)**	**7.6 (±2.6)**
RF (CDDP)	**3.6**		**4.7**		

Tab. S4: IC50 values in μM for L14 on non-cancerous cell lines.

Cell line	L14
Keratino-cytes	› 100
Fibroblasts	› 100
MCF10A	› 100

Additional Experimental part

General procedure 1: Alkoxyacetophenone

The corresponding hydroxy-substituted acetophenone derivative (8.31g, 61 mmol, 1 equiv.) and potassium carbonate (12.57 g, 91 mmol, 1.5 equiv.) were dissolved in dimethylformamide (DMF) at room temperature and alkyl halide (1.1 equiv.) was added dropwise. After stirring for 12 hours under reflux, solvent was removed and sodium hydroxide solution (80 ml, 2M) was added followed by extraction with ethylacetate (3x50 ml). The combined organic phases were dried over sodium sulfate and solvent was removed under reduced pressure.

General procedure 2: β-Hydroxydithiocinnamic acid alkyl esters (L1-L18)

To a solution of potassium-*tert.*-butoxylate (*t*-BuOK, 2 equiv.) in diethyl ether (250 ml), cooled down at -70°C, was dropped the corresponding acetophenone derivate (1 equiv.) in diethyl ether (50 ml). Carbon disulfide (CS_2, 1.4 equiv.) was dropped to the solution and stirred one hour at -70°C. After warming up to room temperature the reaction mixture was stirred for additional two hours at room temperature. Alkyl halide (1 equiv.) was added and the mixture stirred for 15 h. Solvent was removed and dichlormethane (100 ml) was added to the oil. Sulfuric acid (aqueous solution, 2M, 100 ml) was added to the suspension and stirred for 30 minutes at room temperature. The two-phased system was separated and the aqueous phase extracted with dichlormethane (3x35 ml). The combined organic phases were washed with water (3x20 ml), dried with sodium sulfate, followed by filtration and evaporation of the solvent. The crude product was purified with column chromatography.

3'-Ethoxyacetophenone

Synthesis was performed according to general procedure 1. Ethyliodide (10.41 g) was added as alkyl halide.

Yield: 8.11 g (81.0%) as yellow solid. ^{1}H NMR (400 MHz, $CDCl_3$): δ = 1.41 (t, 3H, -OCH$_2$C*H*$_3$); 2.57 (s, 3H, -CH$_3$); 4.06 (q, 2H, -OC*H*$_2$CH$_3$); 7.07 (d, 1H, $^{3}J_{H\text{-}H}$=8.2 Hz, -Ar-*p*-H); 7.33 (t, 1H, -Ar-*m*-H); 7.45 (t, 1H, -Ar-*o*-H); 7.50 (d, 1H, $^{3}J_{H\text{-}H}$=7.7 Hz, -Ar-*o*-H). ^{13}C{^{1}H} NMR (101 MHz, $CDCl_3$): δ = 14.7 (-OCH$_2$*C*H$_3$); 26.7 (-*C*H$_3$); 63.7 (-O*C*H$_2$CH$_3$); 113.1 (-Ar-*o*-C); 120.0 (-Ar-*p*-C); 121.0 (-Ar-*o*-C); 129.5 (-Ar-*m*-C); 138.5 (qC, -Ar-*m*-C); 159.2 (-Ar-C1); 198.0 (-*C*=S). MS (ESI): m/z = 164.

4'-Ethoxyacetophenone

Synthesis was performed according to general procedure 1. Ethyliodide (10.41 g) was added as alkyl halide.

Yield: 7.50 g (75.0%) as yellow solid. ^{1}H NMR (400 MHz, $CDCl_3$): δ = 1.41 (t, 3H, -OCH$_2$C*H*$_3$); 2.52 (s, 3H, -CH$_3$); 4.06 (q, 2H, -OC*H*$_2$CH$_3$); 6.88 (d, 2H, $^{3}J_{H\text{-}H}$=8.4 Hz, -Ar-*m*-H); 7.89 (d, 2H, $^{3}J_{H\text{-}H}$=8.8 Hz, -Ar-*o*-H). ^{13}C{^{1}H} NMR (101 MHz, $CDCl_3$): δ = 14.6 (-OCH$_2$*C*H$_3$); 26.3 (-*C*H$_3$); 63.7 (-O*C*H$_2$CH$_3$); 114.1 (2C, -Ar-*m*-C); 130.1 (qC, -Ar-*p*-C); 130.5 (2C, -Ar-*o*-C); 162.9 (-Ar-C1); 196.7 (-*C*=S). MS (ESI): m/z = 164.

2'-Ethoxyacetophenone

Synthesis was performed according to general procedure 1. Ethyliodide (10.41 g) was added as alkyl halide.

Yield: 10.57 g (90.0%) as brown solid. ^{1}H NMR (400 MHz, $CDCl_3$): δ = 1.43 (t, 3H, -OCH$_2$C*H*$_3$); 2.62 (s, 3H, -CH$_3$); 4.11 (q, 2H, -OC*H*$_2$CH$_3$); 6.97-6.90 (m, 2H, -Ar-*m*-H); 7.41 (t, 1H, -Ar-*p*-H); 7.72 (dd, 1H, $^{3}J_{H\text{-}H}$=7.7 Hz, $^{4}J_{H\text{-}H}$=1.9 Hz, -Ar-*o*-H). ^{13}C{^{1}H} NMR (101 MHz, $CDCl_3$): δ = 14.7 (-OCH$_2$*C*H$_3$); 32.0 (-*C*H$_3$); 64.0 (-O*C*H$_2$CH$_3$); 112.3 (-Ar-*m*-C); 120.4 (-Ar-*m*-C); 128.3 (qC, -Ar-*o*-C); 130.3 (-Ar-*o*-C); 133.6 (-Ar-*p*-C); 158.4 (-Ar-C1); 200.0 (-*C*=S). MS (ESI): m/z = 164.

3'-Butoxyacetophenone

Synthesis was performed according to general procedure 1. Butyliodide (9.18 g) was added as alkyl halide.

Yield: 9.90 g (84.0%) as orange solid. ^{1}H NMR (400 MHz, $CDCl_3$): δ = 0.97 (t, 3H, -$OCH_2CH_2CH_2CH_3$); 1.48 (sex, 2H, -$OCH_2CH_2CH_2CH_3$); 1.76 (qui, 2H, -$OCH_2CH_2CH_2CH_3$); 2.56 (s, 3H, -CH_3); 3.98 (t, 2H, -$OCH_2CH_2CH_2CH_3$); 7.07 (d, 1H, $^{3}J_{H-H}$=8.2 Hz, -Ar-*p*-H); 7.33 (t, 1H, -Ar-*m*-H); 7.45 (t, 1H, -Ar-*o*-H); 7.48 (d, 1H, $^{3}J_{H-H}$=7.6 Hz, -Ar-*o*-H). ^{13}C{^{1}H} NMR (101 MHz, $CDCl_3$): δ = 13.8 (-$OCH_2CH_2CH_2CH_3$); 19.2 (-$OCH_2CH_2CH_2CH_3$); 26.7 (-$OCH_2CH_2CH_2CH_3$); 31.2 (-CH_3); 67.9 (-$OCH_2CH_2CH_2CH_3$); 113.1 (-Ar-*o*-C); 120.0 (-Ar-*p*-C); 120.9 (-Ar-*o*-C); 129.5 (-Ar-*m*-C); 138.5 (qC, -Ar-*m*-C); 159.4 (-Ar-C1); 198.0 (-*C*=S). MS (ESI): m/z = 192.

4'-Butoxyacetophenone

Synthesis was performed according to general procedure 1. Butyliodide (9.18 g) was added as alkyl halide.

Yield: 10.62 g (91.0%) as orange solid. ^{1}H NMR (400 MHz, $CDCl_3$): δ = 0.95 (t, 3H, -$OCH_2CH_2CH_2CH_3$); 1.46 (sex, 2H, -$OCH_2CH_2CH_2CH_3$); 1.76 (qui, 2H, -$OCH_2CH_2CH_2CH_3$); 2.52 (s, 3H, -CH_3); 3.99 (t, 2H, -$OCH_2CH_2CH_2CH_3$); 6.88 (d, 2H, $^{3}J_{H-H}$=8.9 Hz, -Ar-*m*-H); 7.88 (d, 2H, $^{3}J_{H-H}$=8.9 Hz, -Ar-*o*-H). ^{13}C{^{1}H} NMR (101 MHz, $CDCl_3$): δ = 13.8 (-$OCH_2CH_2CH_2CH_3$); 19.2 (-$OCH_2CH_2CH_2CH_3$); 26.3 (-$OCH_2CH_2CH_2CH_3$); 31.1 (-CH_3); 67.9 (-$OCH_2CH_2CH_2CH_3$); 114.1 (2C, -Ar-*m*-C); 130.1 (qC, -Ar-*p*-C); 130.6 (2C, -Ar-*o*-C); 163.1 (-Ar-C1); 196.8 (-*C*=S). MS (ESI): m/z = 192.

2'-Butoxyacetophenone

Synthesis was performed according to general procedure 1. Butyliodide (9.18 g) was added as alkyl halide.

Yield: 7.06 g (70.0%) as brown solid. ^{1}H NMR (400 MHz, $CDCl_3$): δ = 0.98 (t, 3H, -$OCH_2CH_2CH_2CH_3$); 1.50 (sex, 2H, -$OCH_2CH_2CH_2CH_3$); 1.81 (qui, 2H, -$OCH_2CH_2CH_2CH_3$); 2.60 (s, 3H, -CH_3); 4.02 (t, 2H, -$OCH_2CH_2CH_2CH_3$); 6.95-6.90 (m, 2H, -Ar-*m*-H); 7.35 (t, 1H, -Ar-*p*-H); 7.71 (dd, 1H, $^{3}J_{H-H}$=5.9 Hz, $^{4}J_{H-H}$=1.8 Hz, -Ar-*o*-H). ^{13}C{^{1}H} NMR (101 MHz, $CDCl_3$): δ = 13.7 (-$OCH_2CH_2CH_2CH_3$);

19.3 (-$OCH_2CH_2\mathit{C}H_2CH_3$); 31.2 (-$OCH_2\mathit{C}H_2CH_2CH_3$); 31.9 (-$\mathit{C}H_3$); 68.1 (-$O\mathit{C}H_2CH_2CH_2CH_3$); 112.2 (-Ar-*m*-C); 120.2 (-Ar-*m*-C); 129.5 (-Ar-*m*-C); 128.1 (qC, -Ar-*o*-C); 130.2 -Ar-*o*-C); 133.5 (-Ar-*p*-C); 158.4 (-Ar-C1); 199.8 (-*C*=S). MS (ESI): m/z = 192.

3'-Ethoxy-β-Hydroxydithiocinnamic methyl ester

Synthesis was performed according to general procedure 2. 3'-Ethoxyacetophenone (2.5 g) was used. Column chromatography mobile phase: DCM:hexane 1:1. Yield: 2.56 g (66.0%) as yellow crystals. ^{1}H NMR (400 MHz, $CDCl_3$): δ = 1.43 (t, 3H, -$OCH_2C\mathit{H}_3$); 2.64 (s, 3H, -CH_3); 4.08 (q, 2H, -$OC\mathit{H}_2CH_3$); 6.93 (s, 1H, =C*H*); 7.03 (dd, 1H, $^3J_{H\text{-}H}$=10.8 Hz, $^4J_{H\text{-}H}$=3.4 Hz, -Ar-*p*-H); 7.33 (t, 1H, -Ar-*m*-H); 7.39 (t, 1H, -Ar-*o*-H); 7.43 (d, 1H, $^3J_{H\text{-}H}$=10.4 Hz, -Ar-*o*-H); 15.03 (s, 1H, O*H*). ^{13}C{^{1}H} NMR (101 MHz, $CDCl_3$): δ = 14.7 (-$OCH_2\mathit{C}H_3$); 17.1 (-$\mathit{C}H_3$); 63.7 (-$O\mathit{C}H_2CH_3$); 108.0 (=*C*H); 112.4 (-Ar-*o*-C); 118.3 (-Ar-*p*-C); 118.9 (-Ar-*o*-C); 129.7 (-Ar-*m*-C); 135.6 (-*C*-OH); 159.2 (qC, -Ar-*m*-C); 169.1 (Ar-C1); 217.2 (-*C*=S). MS (ESI): m/z = 254. Elemental analysis: calculated for $C_{12}H_{14}O_2S_2$ C: 56.66%; H: 5.55%; S: 25.21%, found: C: 57.06%; H: 5.36%; S: 25.01%.

4'-Ethoxy-β-Hydroxydithiocinnamic methyl ester

Synthesis was performed according to general procedure 2. 4'-Ethoxyacetophenone (2.5 g) was used. Column chromatography mobile phase: DCM:hexane 1:1. Yield: 1.84 g (48.0%) as yellow crystals. ^{1}H NMR (400 MHz, $CDCl_3$): δ = 1.43 (t, 3H, -$OCH_2C\mathit{H}_3$); 2.64 (s, 3H, -CH_3); 4.08 (q, 2H, -$OC\mathit{H}_2CH_3$); 6.92 (d, 2H, $^3J_{H\text{-}H}$=12.0 Hz, -Ar-*m*-H); 6.92 (s, 1H, =C*H*); 7.84 (d, 2H, $^3J_{H\text{-}H}$=12.0 Hz, -Ar-*o*-H); 15.11 (s, 1H, O*H*). ^{13}C{^{1}H} NMR (101 MHz, $CDCl_3$): δ = 14.7 (-$OCH_2\mathit{C}H_3$); 17.0 (-$\mathit{C}H_3$); 63.8 (-$O\mathit{C}H_2CH_3$); 107.1 (=*C*H); 114.6 (-Ar-*m*-C); 126.0 (-*C*-OH); 128.7 (-Ar-*o*-C); 162.3 (qC, -Ar-*p*-C); 169.7 (-Ar-C1); 215.5 (-*C*=S). MS (ESI): m/z = 254. Elemental analysis: calculated for $C_{12}H_{14}O_2S_2$ C: 56.66%; H: 5.55%; S: 25.21%, found: C: 57.03%; H: 5.37%; S: 25.05%.

2'-Ethoxy-β-Hydroxydithiocinnamic methyl ester

Synthesis was performed according to general procedure 2. 2'-Ethoxyacetophenone (2.5 g) was used. Column chromatography mobile phase: DCM:hexane 1:1. Yield: 1.01 g (26.0%) as yellow crystals. ^{1}H NMR (400 MHz, $CDCl_3$): δ = 1.50 (t, 3H, -OCH_2CH_3); 2.63 (s, 3H, -CH_3); 4.12 (q, 2H, -OCH_2CH_3); 6.93 (dd, 1H, $^{3}J_{H-H}$=12.5 Hz, -Ar-*m*-H); 7.01 (t, 1H, -Ar-*m*-H); 7.39 (t, 1H, -Ar-*p*-H); 7.50 (s, 1H, =C*H*); 7.90 (dd, 1H, $^{3}J_{H-H}$=11.0 Hz, $^{4}J_{H-H}$=2.7 Hz, -Ar-*o*-H); 15.10 (s, 1H, O*H*). ^{13}C{^{1}H} NMR (101 MHz, $CDCl_3$): δ = 14.7 (-OCH_2CH_3); 17.0 (-CH_3); 64.5 (-OCH_2CH_3); 112.7 (-Ar-*m*-C); 113.1 (=*C*H); 120.7 (-Ar-*m*-C); 123.0 (=*C*-OH); 130.2 (-Ar-*o*-C); 132.6 (-Ar-*p*-C); 157.4 (qC, -Ar-*o*-C); 167.3 (Ar-C1); 217.1 (-*C*=S). MS (ESI): m/z = 254. Elemental analysis: calculated for $C_{12}H_{14}O_2S_2$ C: 56.66%; H: 5.55%; S: 25.21%, found: C: 57.09%; H: 5.63%; S: 26.04%.

3'-Butoxy-β-Hydroxydithiocinnamic methyl ester

Synthesis was performed according to general procedure 2. 3'-Butoxyacetophenone (2.92 g) was used. Column chromatography mobile phase: DCM:hexane 1:1. Yield: 3.21 g (73.0%) as yellow crystals. ^{1}H NMR (400 MHz, $CDCl_3$): δ = 0.98 (t, 3H, -$OCH_2CH_2CH_2CH_3$); 1.50 (sex, 2H, -$OCH_2CH_2CH_2CH_3$); 1.78 (qui, 2H, -$OCH_2CH_2CH_2CH_3$); 2.64 (s, 3H, -CH_3); 4.00 (t, 2H, -$OCH_2CH_2CH_2CH_3$); 6.93 (s, 1H, -=C*H*); 7.02 (t, 1H, -Ar-*m*-H); 7.32 (t, 1H, -Ar-*p*-H); 7.39 (t, 1H, -Ar-*o*-H); 7.42 (dd, 1H, $^{3}J_{H-H}$=7.8 Hz, $^{4}J_{H-H}$=1.3 Hz, -Ar-*o*-H); 15.07 (s, 1H, O*H*). ^{13}C{^{1}H} NMR (101 MHz, $CDCl_3$): δ = 13.9 (-$OCH_2CH_2CH_2CH_3$); 17.1 (-CH_3); 19.3 (-$OCH_2CH_2CH_2CH_3$); 31.3 (-$OCH_2CH_2CH_2CH_3$); 67.9 (-$OCH_2CH_2CH_2CH_3$); 108.2 (=*C*H); 112.5 (-Ar-*o*-C); 118.3 (-Ar-*m*-C); 118.8 (-Ar-*o*-C); 129.7 (-Ar-*m*-C); 159.5 (qC, -Ar-*m*-C); 169.2 (Ar-C1); 217.2 (-*C*=S). MS (ESI): m/z = 282. Elemental analysis: calculated for $C_{14}H_{18}O_2S_2$ C: 59.52%; H: 6.42%; S: 22.70%, found: C: 59.85%; H: 6.43%; S: 22.93%.

4'-Butoxy-β-Hydroxydithiocinnamic methyl ester

Synthesis was performed according to general procedure 2. 4'-Butoxyacetophenone (2.92 g) was used. Column chromatography mobile phase: DCM:hexane 1:1. Yield: 3.05 g (71.0%) as yellow crystals. ^{1}H NMR (400 MHz, $CDCl_3$): δ = 0.97

(t, 3H, -$OCH_2CH_2CH_2CH_3$); 1.43 (sex, 2H, -$OCH_2CH_2CH_2CH_3$); 1.78 (qui, 2H, -$OCH_2CH_2CH_2CH_3$); 2.63 (s, 3H, -CH_3); 4.00 (t, 2H, -$OCH_2CH_2CH_2CH_3$); 6.91 (d, 2H, -Ar-*m*-H); 6.92 (s, 1H, =C*H*); 7.73 (d, 2H, -Ar-*o*-H); 15.17 (s, 1H, O*H*). $^{13}C\{^1H\}$ NMR (101 MHz, $CDCl_3$): δ = 13.8 (-$OCH_2CH_2CH_2CH_3$); 17.0 (-CH_3); 19.2 (-$OCH_2CH_2CH_2CH_3$); 31.2 (-$OCH_2CH_2CH_2CH_3$); 68.0 (-$OCH_2CH_2CH_2CH_3$); 107.1 (=*C*H); 114.7 (-Ar-*m*-C); 125.9 (-*C*-OH); 128.7 (-Ar-*o*-C); 162.5 (qC, -Ar-*p*-C); 169.7 (Ar-C1); 215.5 (-*C*=S). MS (ESI): m/z = 282. Elemental analysis: calculated for $C_{14}H_{18}O_2S_2$ C: 59.52%; H: 6.42%; S: 22.70%, found: C: 59.83%; H: 6.42%; S: 23.15%.

2'-Butoxy-β-Hydroxydithiocinnamic methyl ester

Synthesis was performed according to general procedure 2. 2'-Butoxyacetophenone (2.92 g) was used. Column chromatography mobile phase: DCM:hexane 1:1. Yield: 2.69 g (62.0%) as yellow crystals. ^1H NMR (400 MHz, $CDCl_3$): δ = 1.00 (t, 3H, -$OCH_2CH_2CH_2CH_3$); 1.59 (sex, 2H, -$OCH_2CH_2CH_2CH_3$); 1.85 (qui, 2H, -$OCH_2CH_2CH_2CH_3$); 2.63 (s, 3H, -CH_3); 4.05 (t, 2H, -$OCH_2CH_2CH_2CH_3$); 6.93 (dd, 1H, $^3J_{H\text{-}H}$=12.5 Hz, -Ar-*m*-H); 7.05 (t, 1H, -Ar-*m*-H); 7.39 (t, 1H, -Ar-*p*-H); 7.50 (s, 1H, =C*H*); 7.92 (dd, 1H, $^3J_{H\text{-}H}$=11.8 Hz, $^4J_{H\text{-}H}$=2.6 Hz, -Ar-*o*-H); 15.11 (s, 1H, O*H*). $^{13}C\{^1H\}$ NMR (101 MHz, $CDCl_3$): δ = 13.8 -$OCH_2CH_2CH_2CH_3$); 17.0 (-CH_3); 19.5 (-$OCH_2CH_2CH_2CH_3$); 31.2 (-$OCH_2CH_2CH_2CH_3$); 68.4 (-$OCH_2CH_2CH_2CH_3$); 112.4 (-Ar-*m*-C); 113.2 (=*C*H); 120.6 (-Ar-*m*-C); 122.8 (=*C*-OH); 130.2 (-Ar-*o*-C); 157.6 (qC, -Ar-*o*-C); 167.1 (Ar-C1); 217.1 (-*C*=S). MS (ESI): m/z = 282. Elemental analysis: calculated for $C_{14}H_{18}O_2S_2$ C: 59.52%; H: 6.42%; S: 22.70%, found: C: 59.71%; H: 6.45%; S: 22.83%.

References:

[Hildebrandt, 2016a] J. Hildebrandt, N. Häfner, H. Görls, D. Kritsch, G. Ferraro, M. Dürst, I. B. Runnebaum, A. Merlino and W. Weigand, *Dalton Trans.* **2016**, 45, 18876-18891.

[Hildebrandt, 2016b] J. Hildebrandt, H. Görls, N. Häfner, G. Ferraro, M. Dürst, I. B. Runnebaum, W. Weigand and A. Merlino, *Dalton Trans.* **2016**, 45, 12283-12287.

4.3 [JH3]

Platinum(II) O,S complexes as potential metallodrugs against Cisplatin resistance

Jana Hildebrandt, Norman Häfner, Helmar Görls, Daniel Kritsch, Giarita Ferraro, Matthias Dürst, Ingo B. Runnebaum, Antonello Merlino, Wolfgang Weigand

Dalton Transactions **2016**, *45*, 18876-18891.

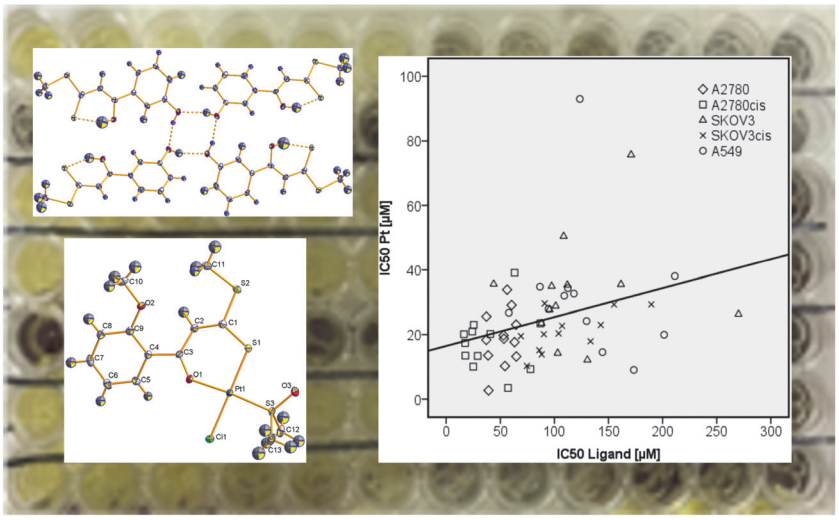

In this publication we report on novel platinum(II) complexes with β-Hydroxydithiocinnamic acid esters as O,S-chelating ligands, dmso and chlorid as additional ligands and their comparison to the free β-Hydroxydithiocinnamic acid esters in relation to the chemical behavior by *e.g.* NMR spectroscopy, stability determinations and molecular structures. The biological behavior *e.g.* IC50 values, the DNA-binding and the protein-binding behavior were determined on a panel of cell lines, for 9-methylguanine and for the model protein hen egg white lysozyme, respectively. It was shown that different ligands and their complexation to platinum(II) resulted in characteristic changes for NMR spectra and molecular structures. Compared to the anticancer drug Cisplatin, our compounds showed high activity against Cisplatin resistant ovarian cancer cell lines. Moreover, a different mode of action can be proposed due to low interactions with DNA, proved by NMR experiments and γH2AX-foci analysis.

Dalton Transactions

PAPER

View Article Online
View Journal | View Issue

Cite this: *Dalton Trans.*, 2016, **45**, 18876

Platinum(II) O,S complexes as potential metallodrugs against Cisplatin resistance†‡

Jana Hildebrandt,[a] Norman Häfner,[b] Helmar Görls,[a] Daniel Kritsch,[b] Giarita Ferraro,[c] Matthias Dürst,[b] Ingo B. Runnebaum,*[b] Antonello Merlino*[c,d] and Wolfgang Weigand*[a]

Received 10th April 2016,
Accepted 10th August 2016

DOI: 10.1039/c6dt01388k

www.rsc.org/dalton

We report on platinum(II) complexes with different cinnamic acid derivatives as ligands with cytotoxic activity against Cisplatin resistant ovarian cancer cell line subcultures of SKOV3 and A2780. A typical mechanism of action for platinum(II) complexes as Cisplatin itself is binding to the DNA and inducing double-strand breaks. We examined the biological behavior of these potential drugs with 9-methylguanine using NMR spectroscopic methods and their DNA damage potential including γH2AX-foci analyses. X-ray diffraction methods have been used to elucidate the molecular structures of the platinum(II) complexes. Interactions with the model protein lysozyme have been evaluated by different techniques including UV-Vis absorption spectroscopy, fluorescence and X-ray crystallography.

Introduction

Cisplatin was first synthesized by Michele Peyrone in 1845 and its square planar configuration was demonstrated by Alfred Werner *ca.* 50 years later.[1–4] Its mechanism of action results in binding to the DNA, especially guanine, introducing strand crosslinks and causing DNA breaks during replication in proliferating cells (Fig. 1). This results in an arrest of the cell cycle and apoptosis of the affected cells as one of the main effects.[5–10] After intravenous application of the drug, delivery into the cells can be achieved by active transport *via* a copper transporter or by passive diffusion.[11–13]

The lower intracellular chloride concentration compared to blood plasma leads to ligand exchange reactions, in which the chlorido ligands of Cisplatin are substituted by aqua ligands.[14] This reaction generates active platinum(II) species being able to bind to the DNA (Fig. 1).[15,16] Nevertheless, there are certain drawbacks in the anticancer therapy using Cisplatin:[17–27]

- low selectivity of this drug for tumor cells, resulting in severe side effects;
- binding to extracellular albumin that leads to inactivation of the drug;
- activity of DNA repair mechanisms may destroy the DNA Cisplatin adduct;
- further principles of drug resistance of tumor cells.

The drug resistance, especially if caused by *p*-glycoprotein, is a major problem in treating diseases by pharmacological therapy.[28,29] Moreover, it has been shown that epigenetic changes in the cancer cells, if treated with sublethal concentrations of Cisplatin may contribute to the resistance phenotype.[30] All resistance mechanisms result in the lowering of Cisplatin effects and, in most cases, reduce the efficacy of a second treatment using Cisplatin. To solve these problems many substances of biological or synthetic origin were investigated concerning their use in cancer therapy. Targeted therapeutics offers an increased selectivity, but they are only suitable for specific cancers harboring the target. For other types of cancer, especially those that occur rarely, the use of Cisplatin is still the best way to treat them. It is noteworthy that even more selective drugs can lose their selectivity by changes in the genetic material of the tumor or of the tumor environment.[21,26]

This work deals with the design of platinum(II) based drugs to circumvent Cisplatin resistance. One problem that has to be solved is the inactivation of Cisplatin by binding to sulfur-containing molecules like albumin in blood plasma. It is known that platinum(II) exhibits a high affinity to sulfur atoms in organic molecules.[20,31,32] By binding to these sulfur sites, the drug molecules are excreted before they can bind to the DNA or

[a]*Institut für Anorganische und Analytische Chemie Friedrich-Schiller-Universität Jena Humboldtstraße 8, 07743 Jena, Germany. E-mail: wolfgang.weigand@uni-jena.de; Fax: +49 3641 948102; Tel: +49 3641 948160*
[b]*Department of Gynecology, Jena University Hospital - Friedrich Schiller University Jena, Germany*
[c]*Department of Chemical Sciences, University of Naples Federico II, Complesso Universitario di Monte Sant' Angelo, Via Cintia, I-80126 Napoli, Italy*
[d]*CNR Institute of Biostructures and Bioimages, Via Mezzocannone 16, I-80100 Napoli, Italy. E-mail: antonello.merlino@unina.it; Fax: +39 081674090; Tel: +39 081674276*

†Dedicated to Professor Heinrich Lang – chair of inorganic chemistry at TU Chemnitz – on the occasion of his 60th birthday.

‡Electronic supplementary information (ESI) available. CCDC 1446182 for **L1**, 1446183 for **L7**, 1446184 for **Pt1**, 1446185 for **Pt2**, 1446186 for **Pt3**, 1446187 for **Pt5**, 1446188 for **Pt6**, 1446189 for **Pt7**, 1446190 for **Pt9** and 1446191 for **Pt10**. For ESI and crystallographic data in CIF or other electronic format see DOI: 10.1039/c6dt01388k

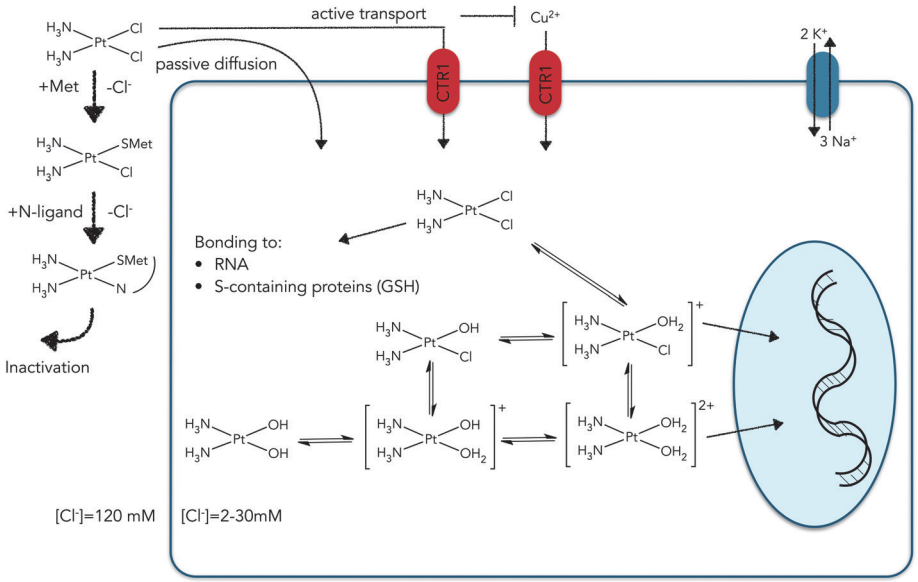

Fig. 1 Behavior of Cisplatin after i.v. application: extracellular inactivation *via* binding to proteins (like albumin), active transport *via* a copper transporter (CTR1) or passive diffusion into the cell and activation inside depending on lower Cl^- concentration [Cl^-] to cationic aqua species which bind to genomic DNA.[4–12]

even before they can pass the cell wall. For this reason, there is a necessity to investigate the interactions of new platinum based drugs with proteins as well as the interactions with the DNA.[33]

Different types of β-hydroxy-dithiocinnamic acid derivatives were used as ligands. The properties of this class of compounds can be modified by changing the substitution pattern as well as the chain length of the alkyl substituent. As substituents for the aromatic moiety, hydroxy and methoxy groups were used to vary the polarity of the ligand as well as of the platinum(II) complex. To investigate the effect of Cisplatin resistance, the cytotoxic activity of all compounds (β-hydroxy dithiocinnamic acid derivatives and the corresponding platinum(II) complexes) was tested with normal and Cisplatin resistant cell lines.

Fig. 2 shows the used β-hydroxy dithiocinnamic acid derivatives and their corresponding platinum(II) complexes. Ligands **L1–L12** can be found in the literature, but their cytotoxic effects have not been determined until now.[33–39] Platinum(II) complexes **Pt7–Pt12** have been reported earlier, and this work presents the biological significance of these compounds depending on their antitumor activity for the first time and reinvestigates what has been reported earlier.[33,40]

Results and discussion

Synthesis

Cinnamic acid derivatives **L1–L12** were synthesized according to the modified literature methods.[34,37–39] A general pathway is shown in Scheme 1.

Substance Code	Rest -R	Alkylgroup -Alk
L1/Pt1	-*o*-OCH_3	-methyl
L2/Pt2	-*m*-OCH_3	-methyl
L3/Pt3	-*p*-OCH_3	-methyl
L4/Pt4	-*o*-OCH_3	-ethyl
L5/Pt5	-*m*-OCH_3	-ethyl
L6/Pt6	-*p*-OCH_3	-ethyl
L7/Pt7	-*m*-OH	-methyl
L8/Pt8	-*p*-OH	-methyl
L9/Pt9	-*m*-OH	-ethyl
L10/Pt10	-*p*-OH	-ethyl
L11/Pt11	-H	-methyl
L12/Pt12	-H	-ethyl

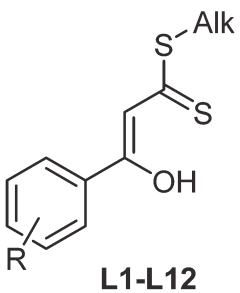

L1-L12

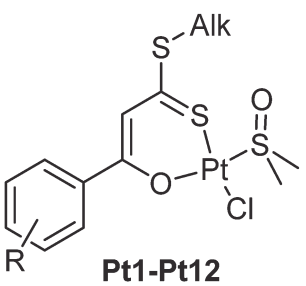

Pt1-Pt12

Fig. 2 Scheme of synthesized ligands and platinum(II) complexes and their substance codes with new platinum(II) complexes **Pt1–Pt6**.

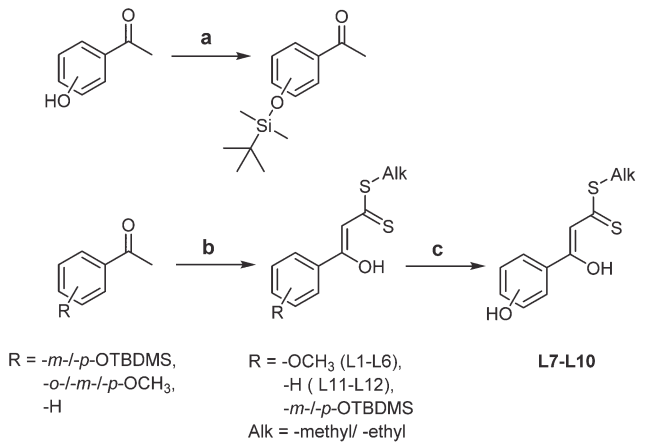

Scheme 1 Reagents and conditions: (a) (i) 2 equiv. imidazole, 1 equiv. TBDMS, DMF, rt, 24 h; (ii) $H_2O/NaHCO_3$; (b) (i) 2 equiv. *t*-BuOK, Et_2O, −70 °C, 0.5 h; (ii) 1.4 equiv. CS_2, −70 °C, 1 h; (iii) rt, 1.5 h; (iv) 1 equiv. Alk-I, rt, 24 h; (v) H_2SO_4/H_2O, rt, 0.5 h; (c) (i) 2 equiv. TBAF, THF, rt, 72 h; (ii) H_2SO_4/H_2O, rt, 0.5 h.

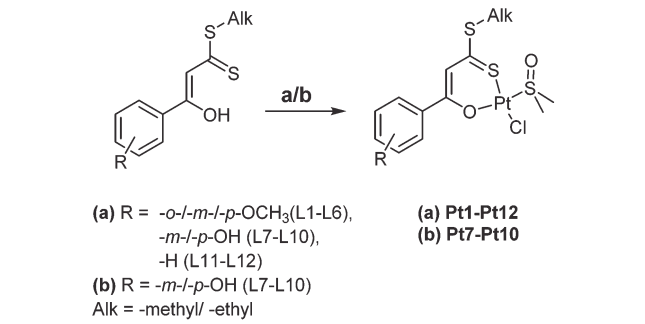

Scheme 2 Reagents and conditions: (a) (i) 1 equiv. *t*-BuOK, THF, rt, 0.5 h; (ii) 1.1 equiv. K[$PtCl_3$(dmso)], rt, H_2O/THF, 96 h; (b) (i) 2 equiv. *t*-BuOK, THF, rt, 0.5 h; (ii) 1.1 equiv. K[$PtCl_3$(dmso)], rt, H_2O/THF, 96 h; (iii) H_2SO_4/H_2O, rt, 0.5 h.

For the synthesis of the platinum(II) complexes (Scheme 2) two pathways differing in the amount of *t*-BuOK can be applied. In the absence of an aromatic –OH substituent one equivalent is used to deprotonate the cinnamic acid derivative. This intermediate is reacted with an *in situ* generated K[$PtCl_3$(dmso)] complex (prepared from K_2PtCl_4 and dmso).[33,40–43] In the presence of an aromatic –OH substituent the use of two equivalents of a base results in a higher yield of the desired platinum(II) complexes. This pathway needs an additional protonation step in the end.

Molecular structures

Platinum(II) complexes **Pt1–Pt3**, **Pt5–Pt7**, **Pt9** and **Pt10** as well as ligands **L1** and **L7** were characterized by means of single crystal X-ray structure determination, whereas the molecular structures of **Pt12**, **L3**, **L8** and **L11** are already known.[32,36,43] For compounds **Pt2**, **Pt3**, **Pt6**, **Pt9** and **L7** there are at least two independent molecules in their unit cells, but just one is shown. Bond lengths and angles are very similar for the molecules in a unit cell so that only one molecule is discussed below. All molecular structures are displayed in the ESI (Fig. S1‡), Fig. 3 shows an example of **Pt1** and **Pt7**.

In Fig. 4 selected bond lengths and angles of the ligands **L1** and **L7** are presented. Both compounds offer a *cis* enol configuration due to their intramolecular hydrogen bonding between the OH group and the adjacent thiocarbonyl moiety. Ligand **L1** displays a OH···S distance of 2.08 Å, which is quite similar to that of ligand **L7** with 2.05 Å. These results confirm data that were reported earlier.[36,43] The C(1)–S(1) distance is a bit longer than that of a typical –C═S double bond (1.61 Å), C(2)–C(3) shows a typical double bond character, whereas the C(1)–C(2) distance is typical of a single bond. The bond lengths C(3)–O(1) are determined as 1.334(3) for **L1** and 1.3308(6) for **L7**. For the *meta* hydroxy substituted ligand **L7** the formation of intermolecular hydrogen bondings can be assumed (2.77 Å for molecule A, 2.74 Å for molecule B) (Fig. 5). Furthermore in the molecular structure of **L1** an interaction of the methoxy substituent and the methine proton can be detected, which is expressed by a short distance (2.33 Å) of the oxygen atom of the methoxy-group and the methine proton.

This proves an intramolecular interaction which results in a low field shift of the resonance signal of the methine proton in the ^{1}H NMR spectra in contrast to other β-hydroxy dithiocinnamic acid alkyl esters. Due to the steric demand of the

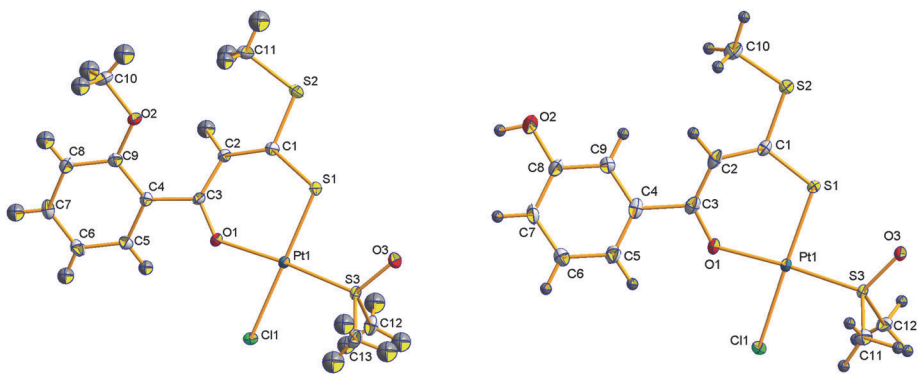

Fig. 3 Molecular structures (50% probability) of **Pt1** (left) and **Pt7** (right).

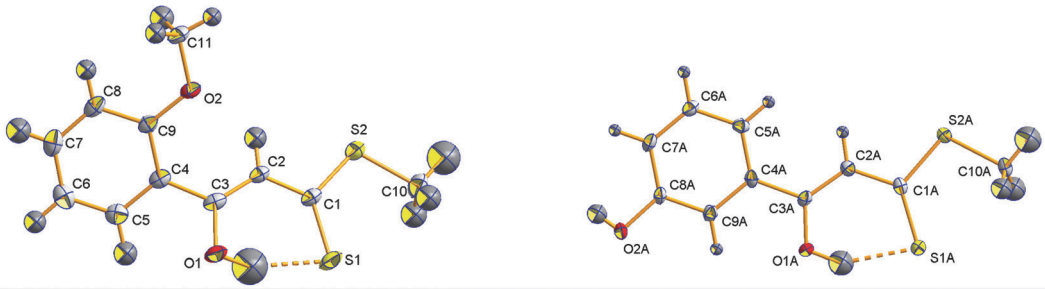

	L1	L7
C(1)-S(1)	1.681(2)	1.662(5)
C(3)-O(1)	1.334(3)	1.330(6)
C(1)-C(2)	1.424(3)	1.435(6)
C(2)-C(3)	1.368(3)	1.361(6)
C(9/8)-O(2)	1.364(3)	1.376(6)
O(1)-C(11)	1.439(3)	
C(3)-C(4)	1.476(3)	1.477(6)
C(1)-S(2)	1.739(3)	1.746(5)
C(2)-H(2)	0.94(3)	0.950(0)
S(1)-C(1)-C(2)	126.29(19)	125.2(4)
O(1)-C(3)-C(2)	123.2(2)	123.4(4)

Fig. 4 Molecular structures (50% probability) of **L1** (left) and **L7** (right) with specific bond angles [°] and bond lengths [Å].

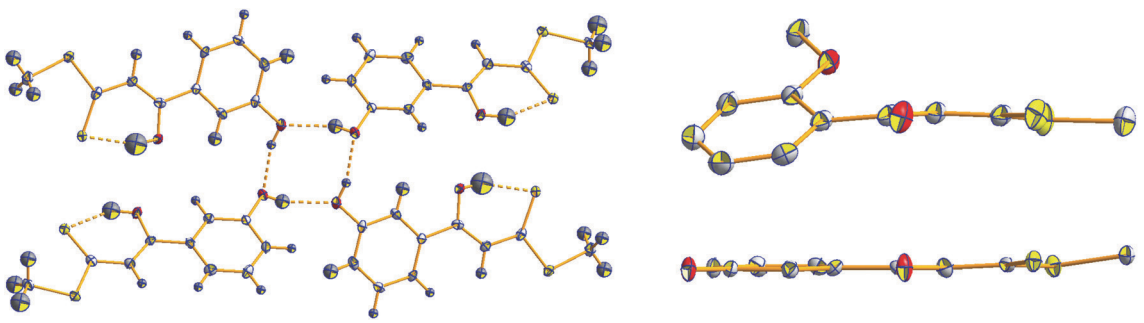

Fig. 5 Left: molecular packing of **L7**, intermolecular hydrogen-bonding; right: steric demand of the methoxy-group resulting in non-planarity behaviour of **L1** (top) in comparison with the planar molecule **L7** (below).

meta-methoxy substituent in **L1** a torsion angle between the aryl ring and the planar enol moiety (C3/C2/C1/O1/S1/S2/C10) of 29° is detected, whereas in **L7** the same angle was determined as 4° (Fig. 5).

The bond lengths and angles in the platinum(II) complexes **Pt1–Pt3**, **Pt5–Pt7**, **Pt 9** and **Pt10** are in good agreement with the values reported earlier.[33] The platinum(II) center shows a distorted square planar environment with L–Pt–L angles of around 90° (see also Fig. 3 and Table 1). The dmso coordination of *cis* to the sulfur atom of the bidendate *O*,*S*-ligand is because of the π-donor-function of the sulfur atom. The bond lengths of platinum (here for example **Pt7**) and their four neighboring atoms are decreasing in the order of Cl(1)–Pt(1) (2.347(2)) > S(1)–Pt(1) (2.234(2)) ≈ S(3)–Pt(1) (2.189(2)) > O(1)–Pt(1) (2.014(6)). Moreover, the angles of these coordination spheres are in the range of 90°. The bond lengths of the oxygen substituted moiety at the aromatic ring O(2)–C(9/8/7) are in the same range.

Table 2 shows torsion angles (aryl planes and C(1)–C(2)–C(3) planes) which are resulting from the steric claim of different substitution patterns at the aromatic ring. The values show clearly that the smallest angle can be observed in the case of the *para* substituted molecules.

Coordination of all *O*,*S*-chelating ligands to platinum(II) results in the elongation of the C(1)–S(1) bond and shortening of the C(3)–O(1) bond. This tendency can also be observed in $^{13}C\{^{1}H\}$-NMR spectra resulting in a high field shift of the signal of the –C=S-resonance and a low field shift of the –C–O-group. For **Pt1** an interaction between the methoxy group and the methine proton is observed as for **L1**. The short O(2)–H(2) distance of 2.20 Å is indicative of the intramolecular relationship in these *ortho* substituted molecules.

Table 1 Specific bond angles [°] and bond lengths [Å] for all characterized platinum(II) compounds

	Pt1	Pt2	Pt3	Pt5
O(1)–Pt(1)	2.015(7)	1.985(10)	1.998(3)	2.007(4)
S(1)–Pt(1)	2.251(6)	2.251(3)	2.2556(13)	2.2520(14)
Cl(1)–Pt(1)	2.347(6)	2.338(3)	2.3595(13)	2.3463(13)
S(3)–Pt(1)	2.195(6)	2.198(3)	2.1846(12)	2.1934(14)
O(1)–C(3)	1.274(3)	1.282(18)	1.283(6)	1.287(7)
S(1)–C(1)	1.710(3)	1.690(14)	1.694(5)	1.701(6)
O(2)–C(9/8/7)	1.363(3)	1.298(17)	1.355(6)	1.368(7)
O(1)–Pt(1)–S(3)	175.10(5)	174.9(3)	174.44(11)	175.75(12)
S(3)–Pt(1)–Cl(1)	91.20(2)	90.05(12)	89.98(5)	89.84(5)
Cl(1)–Pt(1)–O(1)	84.13(5)	85.3(3)	84.48(11)	84.91(12)
S(1)–Pt(1)–S(3)	89.51(2)	89.10(13)	90.11(5)	89.84(5)
	Pt6	**Pt7**	**Pt9**	**Pt10**
O(1)–Pt(1)	2.003(5)	2.014(6)	2.017(3)	2.011(4)
S(1)–Pt(1)	2.2521(17)	2.234(2)	2.2439(10)	2.449(13)
Cl(1)–Pt(1)	2.3430(17)	2.347(2)	2.3520(10)	2.3359(13)
S(3)–Pt(1)	2.1865(17)	2.189(2)	2.1900(10)	2.1985(13)
O(1)–C(3)	1.280(8)	1.278(11)	1.284(5)	1.286(7)
S(1)–C(1)	1.700(7)	1.704(9)	1.700(4)	1.696(6)
O(2)–C(9/8/7)	1.361(8)	1.362(12)	1.351(6)	1.362(7)
O(1)–Pt(1)–S(3)	174.14(15)	174.97(19)	176.34(9)	175.11(11)
S(3)–Pt(1)–Cl(1)	90.08(6)	90.21(7)	90.96(4)	90.48(5)
Cl(1)–Pt(1)–O(1)	84.28(14)	85.96(17)	85.77(8)	84.99(11)
S(1)–Pt(1)–S(3)	89.63(6)	88.77(8)	87.96(4)	88.62(5)

Table 2 Torsion angles: angles between the aryl planes and C(1)–C(2)–C(3) planes in dependence of the substitution pattern

	Pt1	Pt2	Pt3	Pt5	Pt6	Pt7	Pt9	Pt10
Torsion angle	30°	24°	17°	35°	7°	21°	31°	16°

The molecular structure of **L7** reveals that the four molecules are connected through the four hydrogen bonds forming an almost perfect square **Pt10** is able to form an intermolecular hydrogen bonding system (Fig. 6). In the crystal there is a short contact between the hydroxy-group of one molecule and the oxygen of the dmso ligand of another molecule with a O–O distance of 2.73 Å.

Spectroscopic characterization

All compounds were characterized by NMR spectroscopy, mass spectrometry and elemental analysis (see Experimental part). The chemical shifts in ^{1}H NMR and ^{13}C{^{1}H} NMR spectra for ligands **L1–L12** are in good agreement with the values reported earlier, Table 3.[37] Interestingly the interaction between the *ortho* methoxy substituent and the methine proton that was found in the molecular structure of **L1** can also be detected in the ^{1}H NMR spectrum. The resonance signal of this proton is shifted to a low field compared to those resonances of all other ligands, in which such interactions are not possible due to steric reasons. Another characteristic resonance signal in the ^{1}H NMR spectra of this class of compounds is caused by the enolic OH group and can be observed in some cases at very low frequencies at around 15 ppm. This also indicates the intramolecular hydrogen bondings to the sulfur atom of the thiocarbonyl moiety.

Specific shifts of ^{13}C{^{1}H} NMR and ^{1}H NMR resonance signals observable for the platinum(II) complexes are shown in Table 3. After complexation of the ligands *via* oxygen and sulfur atoms to platinum(II) the enolic OH signals in the ^{1}H NMR spectra disappear. Interestingly the signals of the methine protons are shifted to low frequencies as a result of their complexation to platinum(II). In the ^{13}C{^{1}H} NMR spectra the ^{13}C signal of the –C=S group can be observed at high frequencies for the platinum(II) compounds compared to those of the ligands. The protons of the dmso ligand are observed as a singlet accompanied by ^{195}Pt satellites in the ^{1}H NMR spectra. The averages for these signals, which are presented with respect to the carbon side chains are shown in the ESI (Table S2‡).

Mass spectra are in agreement with earlier reported results.[33,37,40]

Stability determination

The stability of compounds **Pt7** and **L8** in dmso as a solvent was determined using ^{1}H NMR spectroscopy. For biological testing compounds were dissolved in dmso (see Experimental part). Fig. 7 shows exemplary aromatic signals for compound

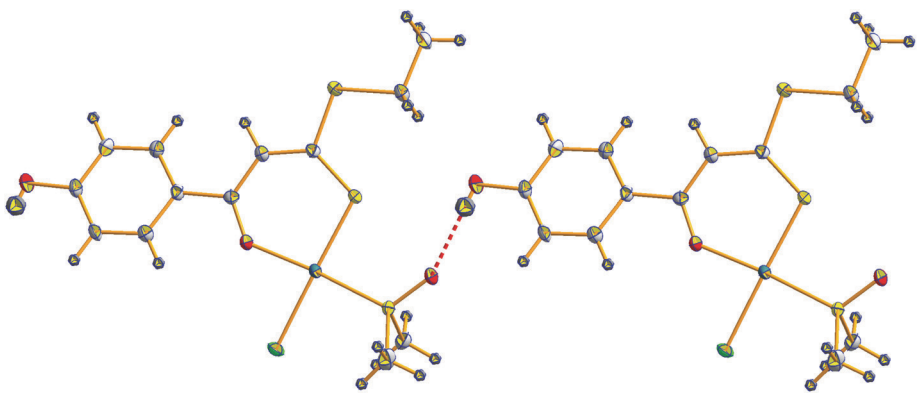

Fig. 6 Intermolecular hydrogen-bonding observed in the crystals of **Pt10**.

Table 3 Specific signals in NMR spectra of **L1–L12** and **Pt1–Pt12** in ppm

^{1}H NMR	L1 Pt1	L2 Pt2	L3 Pt3	L4 Pt4	L5 Pt5	L6 Pt6	L7 Pt7	L8 Pt8	L9 Pt9	L10 Pt10	L11 Pt11	L12 Pt12
–C–O*H*	15.08		15.21	15.21	15.18	15.21	15.09		15.14	15.20	15.02	15.16
–C–*H*	7.20	6.97	6.98	7.23	6.91	6.91	6.96	6.88	6.91	6.91	6.89	6.90
	7.35	7.35	7.04	7.35	7.06	7.07	7.15	7.16	7.15	7.16	7.28	7.27

^{3}C{^{1}H} NMR	L1 Pt1	L2 Pt2	L3 Pt3	L4 Pt4	L5 Pt5	L6 Pt6	L7 Pt7	L8 Pt8	L9 Pt9	L10 Pt10	L11 Pt11	L12 Pt12
–*C*–OH	167.6	169.1	169.6	167.8	169.4	169.9	169.3	169.2	169.6	170.1	169.2	169.4
–C–*C*–H	112.9	112.9	107.1	112.8	112.9	106.8	113.8	106.8	113.8	106.9	107.8	107.7
	116.3	112.9	111.0	116.5	112.9	111.0	110.8	109.9	111.0	110.3	111.6	111.8
–*C*=S	217.2	217.3	215.7	216.3	217.3	214.9	217.8	215.8	217.1	215.2	217.3	216.3
	199.0	180.9	177.9	199.0	177.6	177.9	177.6	178.7	196.8	177.6	177.6	181.5

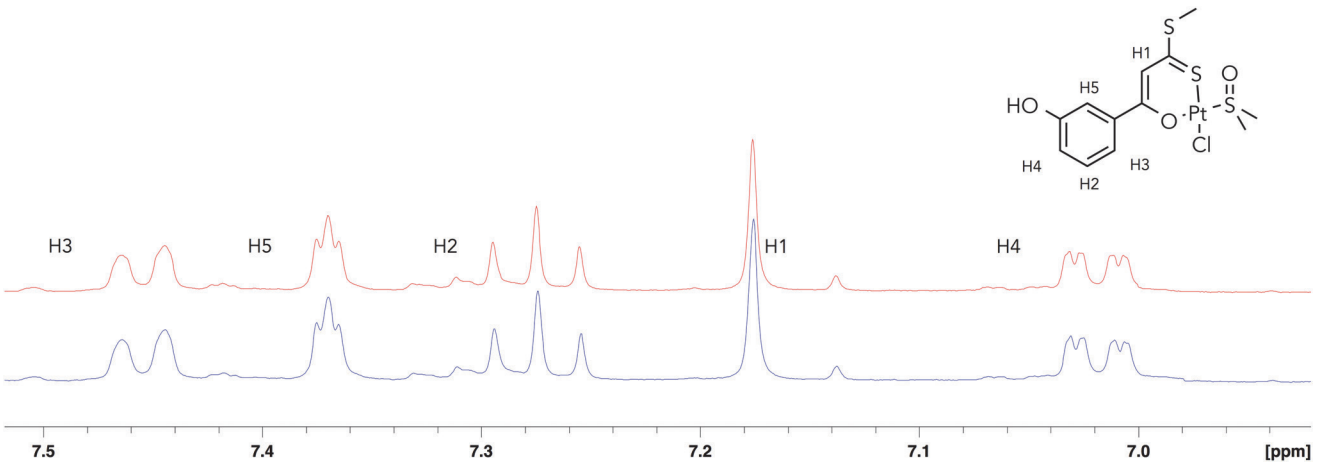

Fig. 7 Stability determination of **Pt7** using ^{1}H NMR spectroscopy, conditions: 600 MHz, 37 °C, dmso-d_6. Blue: first measurement (starting point), red: after 48 h. All compounds are stable under these conditions.

Pt7 from the start point (blue) and after 48 hours (red). It was observed that all compounds are stable under these conditions (for **L8**: Fig. S2 in the ESI‡).

However, since it is well known that the behavior of metal based drugs in organic solvents like dmso could be different when compared to that observed in the solutions used for biological studies, the stability of the platinum complexes studied here was assessed also in aqueous solutions (from 10 to 100% dmso) using UV–Vis absorption spectroscopy.[44] In particular, the spectra of the compounds **Pt1–Pt6** were collected at t = 0 h and after 24 h. Analyses of the spectra show that the compounds **Pt1–Pt6** with the exception of **Pt2**, are highly stable in pure dmso (Fig. S3A‡), and rather stable in 70–90% dmso. The reason why **Pt2** is not so stable in pure dmso is unknown. On the contrary, they are less stable at low dmso concentrations (Fig. S3C‡). For example **Pt1** is stable in 70–90% and pure dmso, in agreement with NMR data, whereas it presents a significant decrease in the intensity of the UV-Vis absorption bands after 24 h in aqueous solutions with dmso ranging from 10 to 60%. This decrease is coincident with the precipitation of the sample.

The stability of Pt complexes **Pt1–Pt6** was also assessed in a saline solution (0.9% NaCl, 1% < [dmso] < 2%), and in the reference physiological buffer solution (10 mM PBS, pH 7.4) (Fig. S4‡). Under these experimental conditions, these complexes seem only marginally stable, since they rapidly precipitate, as occurs in aqueous solutions containing low dmso concentrations. These findings indicate that under these experimental conditions the integrity of the compounds could be compromised.

DNA-binding behavior

The cytotoxic behavior of Cisplatin and its analogues is a result of binding to DNA bases, *i.e.* guanine, influencing the DNA structure and causing DNA damage during genome replication. The preferred binding position is N7 of guanine because of a stabilization effect *via* hydrogen-bonding of the Cisplatin –NH_3 group and the –C=O-group of the DNA base (Fig. 8).[5,31] As shown in Fig. 1, the mechanism of activation contains a ligand-exchange of the chlorido ligands. Using ^{1}H NMR spectroscopy the binding properties of a 3.23-fold stoichiometric excess of the model base 9-methylguanine to plati-

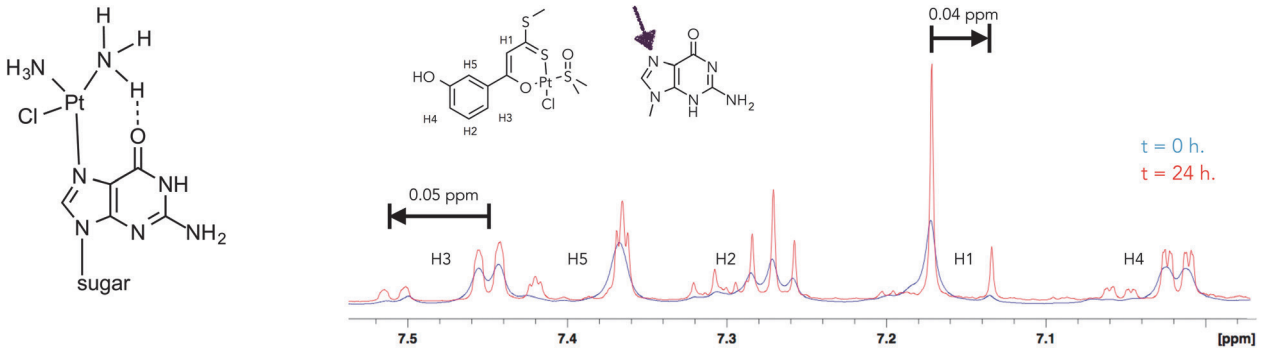

Fig. 8 DNA-binding behaviour of **Pt7** with model base 9-methylguanine shows formation of a new compound after 24 h, 37 °C, 600 MHz, dmso-d_6; blue: start of measurement, red: after 24 h.

num(II) compounds should be investigated. As shown in Fig. 7, platinum(II) complexes are stable under these conditions, so all changes in the NMR spectra result from the interactions with the model base. This NMR spectroscopic experiment carried out for compound **Pt7** and monitored over 24 h at 37 °C in dmso-d_6 showed significant changes in the spectra. After 24 h, the ^{1}H NMR spectra show in the aromatic region that a new compound is generated slowly, which can be seen by the occurrence of a new set of proton signals for the methine proton as well as for all aromatic protons. The spectra show after 24 h a second proton group high field shifted (red spectrum, 0.05 ppm) compared to the signal set at $t = 0$ h (blue spectrum). In contrast, a down field shift (red spectrum) can be observed for the methine proton of **Pt7** after 24 h. These results give hint for a successful reaction of **Pt7** with 9-methylguanine; however, it seems that the reaction is slow and not completed after 24 h.

Biological behavior

A further aim of our investigations was to characterize all of these compounds for their cytotoxic activity against a panel of cell lines enabling an understanding of the structure–activity relationship. The used cell lines differed in their sensitivity against Cisplatin. Therefore candidate platinum(II) complexes potentially effective against Cisplatin resistant cells could be identified.

The analyzed ligands as well as platinum(II) complexes exhibit a low solubility in water independent of the ligand structure. DMSO is used as a solvent for preparation of a dilution series in cell culture experiments. The toxic influence of a range of dmso concentrations was measured *via* MTT assay under identical conditions as for substance tests (Fig. 9). The results show that concentrations of dmso down to 1% have high cytotoxic effects. Therefore a dmso concentration as low as possible to reach the required Pt(II) complex concentration was used in the experiments and was identical for each substance and concentration (0.5% dmso in cell culture media). To exclude side effects from this dmso concentration all IC_{50} determination experiments used 0.5% dmso as reference samples. Additional experimental conditions can bias

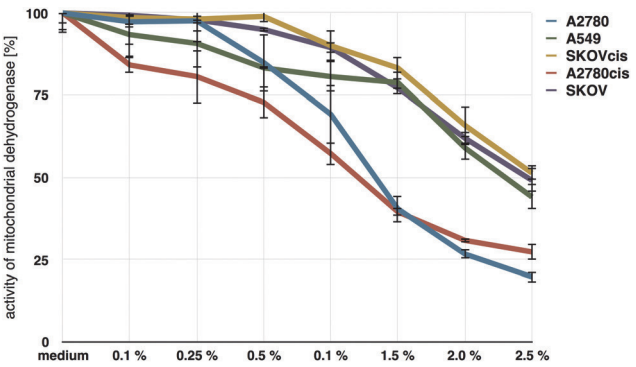

Fig. 9 Influence of dmso depending on % per well for each cell line.

cell cultivation based IC_{50} determinations, *i.e.* cell density, cultivation time and drug exposure time influence measured effects. High cell numbers (>5000 cells per well in 96-well plate) combined with long cultivation times (>72 h) may result in the inhibitory effects on cell proliferation for samples with a low drug concentration and for control cells. Importantly any bias for cells even treated with drug concentrations different from IC_{50} will affect IC_{50} determination because regression analyses will probe all data. Thus we measured the drug effects for 48 h exposure time after 24 h seeding of 5000 cells per well resulting in unsaturated cell density and absorbance measurements for untreated cells (data not shown). Both constantly low dmso concentrations and controlled cultivation procedures represent important improvements in comparison with earlier data.[33,40] Detailed experimental procedures are described in the Experimental part.

The tested cell line panel consisted of A549 (lung cancer) and two pairs of isogenic ovarian cancer cell lines with different Cisplatin sensitivity.[30]

Resistant ovarian cancer cells derived from A2780 and SKOV3 exhibited a 4.7 and 3.6 times higher IC_{50} value for Cisplatin, respectively. These cell cultures were established by repeated rounds of incubation with increasing Cisplatin concentrations starting with non-lethal concentrations.[30] Table 4 shows that the new substances show cytotoxic activity against

Table 4 IC_{50} values and resistance factors (RF) for all substances

Data	SKOV		SKOVcis		RF	A2780		A2780cis		RF	A549	
	IC_{50}		IC_{50}		SKOV	IC_{50}		IC_{50}		A2780	IC_{50}	
Substance code	L	Pt	L	Pt	L Pt	L	Pt	L	Pt	L Pt	L	Pt
1	97.5 (+/−12.6)	35.0 (+/−6.5)	88.3 (+/−18.3)	13.9 (+/−4.4)	0.9 0.4	64.8 (+/−4.1)	13.2 (+/−4.3)	29.1 (+/−6.8)	13.4 (+/−8.6)	0.4 1.0	112.5 (+/−34.8)	34.4 (+/−5.7)
2	101.2 (+/−9.2)	28.8 (+/−4.9)	90.2 (+/−3.1)	20.1 (+/−3.0)	0.9 0.7	53.0 (+/−12.4)	19.8 (+/−1.6)	24.1 (+/−7.2)	21.0 (+/−3.3)	0.5 1.1	129.7 (+/−13.6)	24.2 (+/−2.0)
3	161.5 (+/−24.2)	35.5 (+/−4.7)	69.0 (+/−2.2)	19.5 (+/−0.6)	0.5 0.4	53.3 (+/−6.2)	18.7 (+/−3.1)	16.4 (+/−3.7)	20.1 (+/−5.8)	0.3 1.1	118.0 (+/−26.8)	32.7 (+/−5.7)
4	170.9 (+/−20.0)	75.7 (+/−19.5)	133.4 (+/−26.2)	17.9 (+/−3.7)	0.8 0.2	56.3 (+/−10.4)	33.9 (+/−4.2)	63.2 (+/−11.3)	39.1 (+/−0.5)	1.1 1.2	123.5 (+/−1.9)	93.0 (+/−2.1)
5	103.1 (+/−10.5)	14.3 (+/−3.5)	155.1 (+/−41.6)	29.3 (+/−2.2)	1.5 2.0	37.1 (+/−8.5)	25.6 (+/−2.4)	40.8 (+/−8.5)	20.2 (+/−5.6)	1.1 0.8	173.4 (+/−8.6)	9.1 (+/−3.4)
6	130.5 (+/−12.9)	12.2 (+/−1.5)	142.8 (+/−23.8)	23.0 (+/−5.8)	1.1 1.9	64.6 (+/−7.9)	23.1 (+/−6.7)	77.9 (+/−6.2)	9.3 (+/−1.2)	1.2 0.4	211.3 (+/−63.5)	38.1 (+/−7.5)
7	270.1 (+/−18.0)	26.3 (+/−7.0)	189.5 (+/−15.0)	29.3 (+/−7.8)	0.8 1.1	63.2 (+/−6.3)	17.7 (+/−1.5)	17.5 (+/−2.0)	17.4 (+/−1.1)	0.3 1.0	201.4 (+/−29.3)	20.0 (+/−1.7)
8	108.5 (+/−11.8)	50.5 (+/−10.8)	91.0 (+/−0.7)	29.6 (+/−7.7)	0.8 0.6	60.4 (+/−5.7)	29.1 (+/−8.6)	87.1 (+/−3.0)	23.5 (+/−9.2)	1.4 0.8	109.1 (+/−20.1)	32.0 (+/−2.3)
9	88.0 (+/−5.6)	23.5 (+/−3.7)	74.6 (+/−5.9)	10.3 (+/−5.9)	0.8 0.4	54.3 (+/−7.9)	10.3 (+/−5.5)	25.0 (+/−4.6)	10.1 (+/−4.6)	0.5 1.0	144.5 (+/−31.4)	14.6 (+/−8.1)
10	95.4 (+/−6.1)	27.7 (+/−6.4)	86.0 (+/−11.4)	15.2 (+/−2.7)	0.9 0.5	39.1 (+/−0.7)	2.7 (+/−0.6)	57.1 (+/−4.5)	3.5 (+/−0.7)	1.5 1.3	94.6 (+/−2.7)	28.0 (+/−5.5)
11	112.0 (+/−11.1)	35.3 (+/−6.4)	107.1 (+/−7.5)	22.7 (+/−4.3)	1.0 0.6	38.8 (+/−2.5)	13.6 (+/−3.5)	17.7 (+/−1.0)	13.5 (+/−6.1)	0.5 1.0	57.9 (+/−7.3)	26.8 (+/−0.5)
12	43.9 (+/−14.7)	35.6 (+/−1.5)	103.9 (+/−17.8)	20.4 (+/−3.3)	2.4 0.6	37.1 (+/−2.5)	18.4 (+/−4.1)	25.4 (+/−7.6)	23.0 (+/−6.4)	0.7 1.3	86.6 (+/−10.6)	34.8 (+/−4.0)
CDDP	3.8 (+/−2.8)		13.5 (+/−4.4)		3.6	1.3 (+/−0.2)		6.1 (+/−2.1)		4.7	7.6 (+/−2.6)	

all cell lines, not only for ovarian carcinoma cell lines SKOV and A2780. Determination for all pairs of ligands and platinum(II) complexes proves that dithiocinnamic acid derivatives show low cytotoxic behavior itself and corresponding platinum(II) complex elevated cytotoxicity. It can be concluded that the increased cytotoxic behavior of platinum(II) complexes is a result of the metal itself. An exception seems to be the cell line A2780cis exhibiting IC_{50} values similar between some ligands and their complexes (Table 4). Moreover a significant but weak correlation was identified between the IC_{50} of the ligand and the complex (Pearson correlation coefficient 0.301; $p < 0.01$; Fig. 10).

Thus a limited part of the platinum(II) complexes activity maybe directly contributing to the ligand properties. One aim of the present study was to analyze structure–activity-relationships (SAR). The two structures within the analyzed ligands were systematically changed to vary complex properties (substituent at the benzyl ring (–R) and the alkyl-chain at the sulfur residue (–Alk)). Plotting the IC_{50} values for all substances of each cell line in the order of increasing mean IC_{50} enabled the identification of SAR (Fig. 11). Interestingly most active complexes exhibited an increased polarity of –R (–OH > $-OCH_3$ > –H) but increased lipophilicity at the alkyl chain (Et > Me). The exceptional cases of *ortho*-OCH_3 may be explained by intramolecular interactions between the methoxy group and the methine proton influencing the complex structures (see the molecular structures section). The increased activity of complexes with longer alkyl chains confirms earlier studies.[33,40] Nevertheless differences in the mean IC_{50} were small and the substances exhibited cell line specific activities (*i.e.* **Pt9**, Fig. 11). Interestingly, we did observe an inverse association between the platinum(II) complex stability and the cytotoxic activity. **Pt1** exhibiting a lower stability in aqueous solutions showed a higher cytotoxicity than **Pt4** (Fig. 11, Table 4). Nevertheless the general impact should be determined in the *in vivo* situation taking effects of the bioavailability into account.

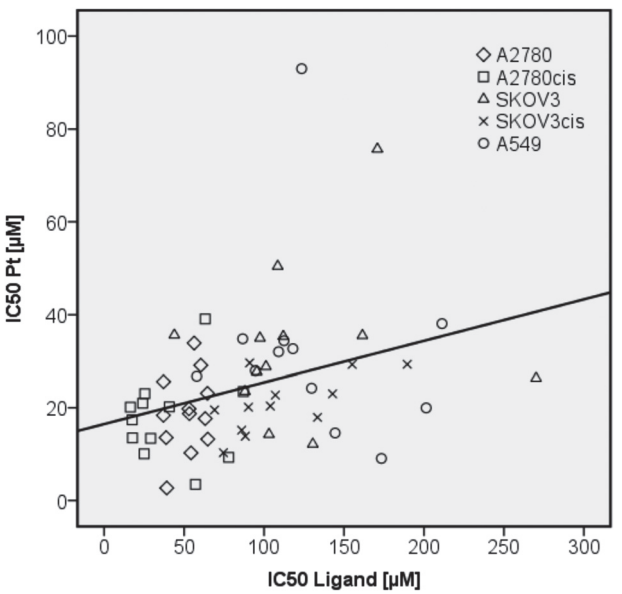

Fig. 10 Correlation of ligand and platinum(II) complex IC_{50} values in all cell lines. The weak but significant correlation (Pearson $r = 0.301$, $p < 0.001$) is depicted by the regression line.

The second aim was to test new platinum(II) complexes on Cisplatin-resistant cell lines to evaluate the possibility to overcome the resistance phenotype. The two most active platinum(II) complexes (**Pt9**, **Pt10**) showed an increased or at least equal cytotoxic activity against the Cisplatin-resistant ovarian cancer cell lines (Table 4). Moreover the activity was similar or even higher against the resistant cell lines in comparison with the parental cells. Calculated resistance factors between parental and resistant ovarian cancer cell lines (Table 4) illustrate clear differences between Cisplatin and some of the new platinum(II) complexes (*i.e.* RF Cisplatin 4.7 and 3.6; **Pt9** 1.0 and 0.4 for A2780 and SKOV3, respectively). These data let us assume that the mechanism of action is different between the new compounds and Cisplatin. Moreover, a different kinetic cannot be excluded and is already seen within the guanine binding studies (see the DNA bonding behavior section). Albeit we detected a high cytotoxic activity of the new complexes *in vitro* an inactivation mechanism by binding to the tripeptide glutathione could not be excluded – for more information see the ESI (Fig. S10‡). To gain insights into the mode of action we exemplarily analyzed **Pt9** and **Pt10** for the induction of DNA damage in the ovarian cancer cell line pairs in two independent experiments. Cells were incubated with IC_{50} concentrations of the resistant cell culture of A2780 or SKOV3 for 24 hours on cover slips. Afterwards cells were washed, fixed and antibody-stained for γH2AX histone. Nuclear foci of γH2AX are indicative of dsDNA break regions.[45] Cisplatin

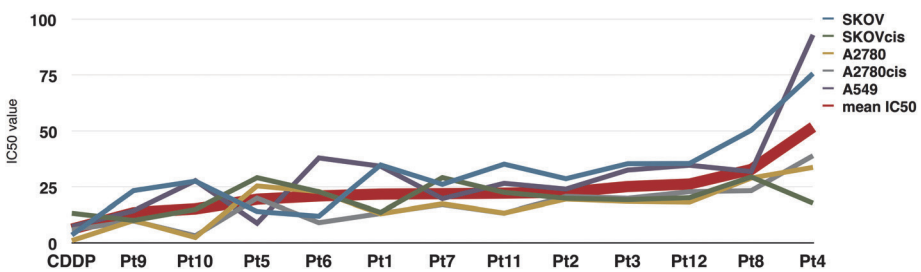

Fig. 11 Structure activity relationship for analyzed platinum(II) complexes. Substances were ordered with increasing mean IC_{50} values.

induced DNA damage and γH2AX foci formation clearly correlate with the cytotoxic effects (Fig. 12). Resistant cells showed decreased numbers of γH2AX foci. SKOV3 cells that are more resistant to Cisplatin than A2780 as illustrated by different IC_{50} values of 13.5 μM and 6.1 μM for the resistant cells, respectively, can tolerate increased γH2AX foci. The amount of γH2AX foci after treatment with **Pt9** or **Pt10** was much lower in comparison with the Cisplatin treatment despite the fact that all the substances were used with IC_{50} concentrations (Fig. 12). Therefore a different mode of action for the new platinum(II) complexes is likely and may include non-genomic targets. Otherwise it cannot be excluded that the platinum(II) complexes show different kinetic behavior or target DNA differently from Cisplatin leading to other DNA damage responses not including γH2AX.

In conclusion, platinum(II) complexes were proven to exhibit cytotoxic activities partially correlated to the ligand properties. The small differences in mean IC_{50} values enable a selection of the best candidates with both cytotoxic activity and superior bioavailability in future experiments (*i.e. in vivo*). Furthermore, a high activity was detected for some substances against Cisplatin-resistant cell lines. Additional experiments will clarify the underlying mode of action for these platinum(II) complexes. If general differences to Cisplatin can be detected the efficacy of a combination treatment should be evaluated.

Interactions with proteins

Previous data show that the here investigated compounds show cytotoxic activity, especially **Pt9** and **Pt10** circumvent Cisplatin resistance (Table 4) but show decreased DNA damage (Fig. 12). For this reason the discovery of other targets for their mechanism of action is necessary. The interaction of metallodrugs with proteins is very important, since it affects their pharmacokinetics, toxicity and tissue distribution. The binding of metal-based drugs with transferrin for example is directly involved in the transport of drugs into the cell. We have already demonstrated that compounds **Pt7** and **Pt9** are able to bind the model protein hen egg white lysozyme (HEWL) and the X-ray structure determinations of the adducts forming upon drug–protein interaction have been determined.[40] The structures demonstrate that the compounds can act as monofunction drugs, retaining a dmso ligand upon macromolecule binding. To further characterize the binding

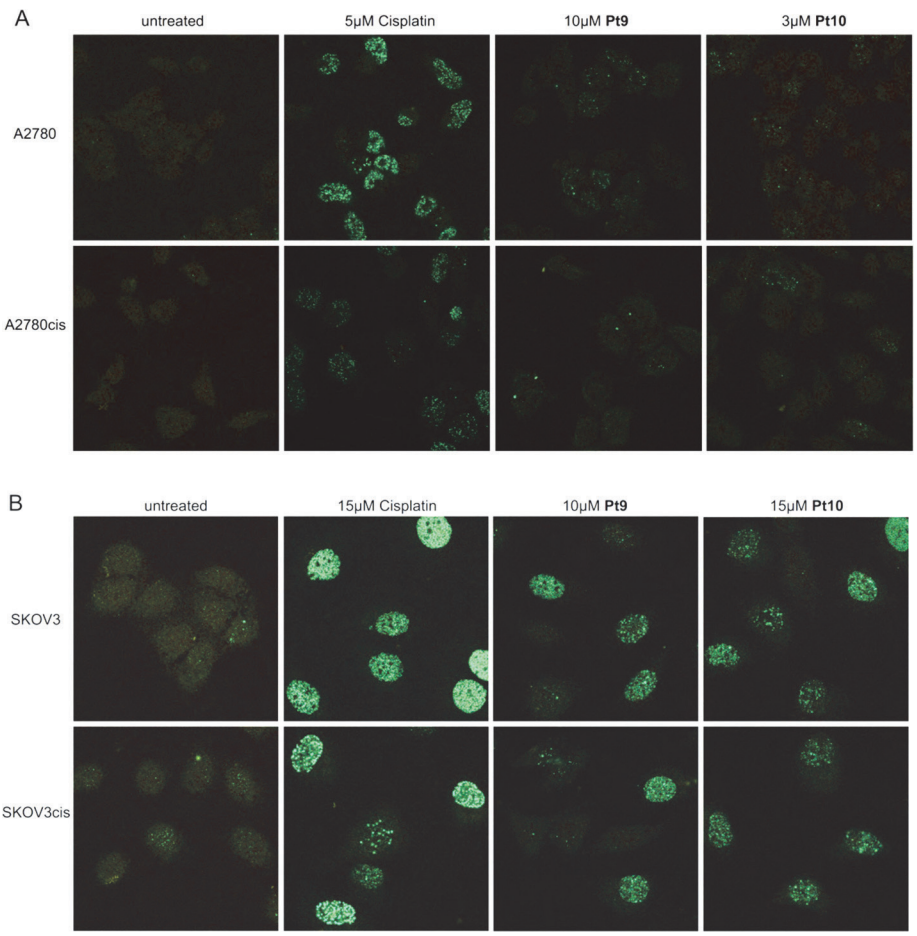

Fig. 12 Detection of γH2AX foci in parental and Cisplatin resistant A2780 (A) and SKOV3 (B) after mock treatment or incubation with Cisplatin, **Pt9** or **Pt10** at IC_{50} concentrations for the resistant cells. Identical results were obtained in an independent experiment.

properties of the compounds here studied with proteins, we have investigated the reactivity of compounds **Pt1–Pt6** with hen egg white lysozyme (HEWL), a protein that is very frequently used as a prototype for protein metalation studies.[46,47]

First, fluorescence spectra of HEWL in the presence of different concentrations of the platinum complexes were collected. Intrinsic fluorescence of HEWL arise from the intrinsic structural features of the protein and is mainly due to the presence of six tryptophan residues. Fig. S5 and S6‡ show the modifications to the fluorescence emission of HEWL, upon excitation at 280 and 295 nm, respectively, when the **Pt1–Pt6** concentrations were increased. The binding of the drugs to the protein induces a significant quenching of the emission. Differences in the fluorescence quenching are probably related to different solubility of the samples rather than to differences in the binding properties of the compounds.

Finally, to identify the type of interaction that occurs between HEWL and the Pt compounds we have tried to obtain structural information on the adducts formed by the protein with **Pt1–Pt4** by X-ray crystallography. Attempts to crystallize the adducts formed upon the binding of the compounds to the protein under the same conditions used to crystallize the HEWL–**Pt7** and HEWL–**Pt9** adducts failed.[40] This is probably due to the lower solubility of **Pt1**, **Pt2**, **Pt3**, and **Pt4** in ethylene glycol when compared to the compounds **Pt7** and **Pt9**, which present a-OH in the *meta* position. Thus, the reactivity of the compounds with HEWL was explored under different experimental conditions and the structures of some adducts formed in the presence of concentrated NaCl solutions were solved (see ESI Fig. S7–S9‡). Under these experimental conditions Pt compounds degrade and the products of this degradation react with the protein forming an adduct with a Pt atom bound to an ND1 atom of a His15 side chain (see for example Fig. S8‡), as in the case of many Pt compounds, including Cisplatin, **Pt7** and **Pt9** (see the ESI‡ for further details).[40,48–51]

Conclusion

The mechanism of action for the standard drug Cisplatin is realized by DNA binding and induction of replicative stress resulting in DNA damage. This mechanism can be disturbed especially by the activity of DNA repair mechanisms and also other mechanisms ending in the resistance of cancer cells. To circumvent Cisplatin resistance by the use of an effective Pt(II) pharmacophore was one aim of this work. Different ligands with varying properties and corresponding Pt(II) complexes were tested on several cell lines. The results show that the platinum(II) center is necessary for an effective anticancer activity. An examination of the mechanism of action shows that the typical DNA-binding behavior of Cisplatin and analogues and the induction of the DNA damage are decreased for the new Pt(II) complexes. Nevertheless some compounds have a high activity against Cisplatin resistant cell lines.

In summary, this work presents new platinum(II) complexes with *O*,*S*-bidendate ligands which are well characterized by different analytical techniques, especially with X-ray structure determinations. These complexes show cytotoxic activity partially overcoming Cisplatin resistance of cell lines which may be explained by a different mechanism of action – specifically the bonding to proteins.

Experimental part

Materials and techniques

All reactions were performed using standard Schlenk and vacuum-line techniques under a nitrogen atmosphere. The NMR spectra were recorded with a Bruker Avance 200 MHz, 400 MHz or 600 MHz spectrometer. Chemical shifts are given in ppm with reference to $SiMe_4$. Mass spectra were recorded with a Finnigan MAT SSQ 710 instrument. Elemental analysis was performed with a Leco CHNS-932 apparatus. Silica gel 60 (0.015–0.040 mm) was used for column chromatography and TLC was performed using Merck TLC aluminium sheets (Silica gel 60 F_{254}). Chemicals were purchased from Fisher Scientific, Aldrich or Acros and were used without further purification. All solvents were dried and distilled prior to use according to standard methods.

Synthesis

General procedure 1: platinum(II)-complexes with β-hydroxy dithiocinnamic acid alkyl esters, chlorido and dmso as ligands (Pt1–Pt12). Pathway A: β-hydroxy dithiocinnamic acid alkyl ester (1 equiv.) was dissolved in tetrahydrofurane (THF, 20 ml) and *t*-BuOK (1 equiv.) was added to the solution and stirred for one hour at room temperature. Potassium tetrachloroplatinate (K_2PtCl_4, 1.1 equiv.) was dissolved in degassed water (10 ml) and dimethylsulfoxide (dmso, 2 equiv.) was added, the mixture was stirred for 30 minutes at room temperature. The solution of the deprotonated ligand was added dropwise to the suspension of the platinum complex and stirred at room temperature for 4 days. After adding water (25 ml) to the solution, the mixture was extracted with dichloromethane (DCM, 3 × 30 ml), the combined organic phases were washed with water (3 × 20 ml), dried over sodium sulfate and after filtration and evaporation of the solvent the crude product was purified with column chromatography. Pathway B: the experimental procedure is similar to pathway A, for deprotonation 2 equiv. of *t*-BuOK was used. Before extracting with DCM, sulfuric acid (20 ml, 2 M) was added and the mixture was stirred for one hour at room temperature followed by extraction and purification.

Chloro-(1-(2-methoxyphenyl)-3-(methylthio)-3-thioxo-prop-1-en-1-olate-*O*,*S*)-(dimethylsulfoxide-*S*)-platinum(II) (Pt1). Synthesis was performed according to general procedure 1, pathway A. **L1** (367 mg, 1.53 mmol) was dissolved in THF and *t*-BuOK (172 mg, 1.53 mmol) was added. K_2PtCl_4 (700 mg, 1.69 mmol) was dissolved in water and dmso (220 μL, 3.07 mmol) was added. Column chromatography mobile phase: DCM 4 : hexane 1–DCM–acetone. Yield: 520 mg (62.1%) as red crystals. ^{1}H NMR (600 MHz, acetone-d_6): δ = 2.65 (s, 3H,

–S–CH_3); 3.66 (s w/Pt satellites $^3J_{Pt–H}$ = 22.5 Hz, 6H, CH_3 (DMSO)); 3.94 (s, 3H, –OCH_3); 7.04 (ddd, $^3J_{H–H}$ = 7.6 Hz, $^4J_{H–H}$ = 1.0 Hz, 1H, –Ar–*m*-H); 7.13 (d, $^3J_{H–H}$ = 8.4 Hz, 1H, –Ar–*o*-H); 7.35 (s, 1H, =CH); 7.53 (ddd, $^3J_{H–H}$ = 7.6 Hz, $^4J_{H–H}$ = 1.0 Hz, 1H, –Ar–*p*-H); 7.80 (dd, $^3J_{H–H}$ = 7.8 Hz, $^4J_{H–H}$ = 1.8 Hz, 1H, Ar–*m*-H). $^{13}C\{^1H\}$ NMR (101 MHz, acetone-d_6): δ = 17.7 (–S–CH_3); 46.7 (DMSO); 56.4 (–OCH_3); 113.3 (–Ar–*o*-C); 116.3 (=CH); 121.7 (–Ar–*m*-C); 128.0 (–Ar–C1); 132.1 (–Ar–*m*-C); 133.8 (–Ar–*p*-C); 158.3 (–Ar–OCH_3); 175.0 (–C–O–); 199.0 (–C=S). MS (DEI): *m*/*z* = 548, 546, 386, 341, 284, 152, 135, 105, 78, 63. Elemental analysis: calculated for $C_{13}H_{17}ClO_3PtS_3$·2/3 acetone C: 30.71%; H: 3.60%; S: 16.40%, found: C: 30.82%; H: 3.32%; S: 16.71%.

Chloro-(1-(3-methoxyphenyl)-3-(methylthio)-3-thioxo-prop-1-en-1-olate-*O*,*S*)-(dimethylsulfoxide-*S*)-platinum(II) (Pt2). Synthesis was performed according to general procedure 1, pathway A. **L2** (367 mg, 1.53 mmol) was dissolved in THF and *t*-BuOK (172 mg, 1.53 mmol) was added. K_2PtCl_4 (700 mg, 1.69 mmol) was dissolved in water and dmso (220 μL, 3.07 mmol) was added. Column chromatography mobile phase: DCM 4 : hexane 1–DCM–acetone. Yield: 350 mg (41.8%) as orange crystals. ^1H NMR (400 MHz, $CDCl_3$): δ = 2.70 (s, 3H, –S–CH_3); 3.68 (s w/Pt satellites $^3J_{Pt–H}$ = 22.5 Hz, 6H, CH_3 (DMSO)); 3.88 (s, 3H, –OCH_3); 7.10 (dd, $^3J_{H–H}$ = 8.2 Hz, $^4J_{H–H}$ = 0.8 Hz, 1H, –Ar–*p*-H); 7.28 (s, 1H, =CH); 7.32 (t, 1H, –Ar–*m*-H); 7.54 (m, 2H, –Ar–*o*-H). $^{13}C\{^1H\}$ NMR (101 MHz, $CDCl_3$): δ = 17.6 (–S–CH_3); 46.9 (DMSO); 55.5 (–OCH_3); 112.9 (=CH); 118.3 (–Ar–*o*-C); 129.7 (–Ar–*m*-C/–Ar–C1); 135.7 (–Ar–*p*-H); 159.9 (–Ar–OCH_3); 174.2 (–C–O–); 180.9 (–C=S). MS (ESI): *m*/*z* = 565, 536, 512, 445, 101. Elemental analysis: calculated for $C_{13}H_{17}ClO_3PtS_3$·1/5 acetone C: 29.19%; H: 3.27%; S: 17.19%, found: C: 29.46%; H: 2.90%; S: 17.10%.

Chloro-(1-(4-methoxyphenyl)-3-(methylthio)-3-thioxo-prop-1-en-1-olate-*O*,*S*)-(dimethylsulfoxide-*S*)-platinum(II) (Pt3). Synthesis was performed according to general procedure 1, pathway A. **L3** (367 mg, 1.53 mmol) was dissolved in THF and *t*-BuOK (172 mg, 1.53 mmol) was added. K_2PtCl_4 (700 mg, 1.69 mmol) was dissolved in water and dmso (220 μL, 3.07 mmol) was added. Column chromatography mobile phase: DCM 4 : hexane 1–DCM–acetone. Yield: 350 mg (41.8%) as orange crystals. ^1H NMR (600 MHz, $CDCl_3$): δ = 2.60 (s, 3H, –S–CH_3); 3.59 (s w/Pt satellites $^3J_{Pt–H}$ = 22.5 Hz, 6H, CH_3 (DMSO)); 3.78 (s, 3H, –OCH_3); 6.84 (d, $^3J_{H–H}$ = 9.0 Hz, 2H, –Ar–*o*-H); 7.04 (s, 1H, =CH); 7.91 (d, $^3J_{H–H}$ = 9.0 Hz, 2H, –Ar–*m*-H). $^{13}C\{^1H\}$ NMR (101 MHz, $CDCl_3$): δ = 22.3 (–S–CH_3); 46.8 (DMSO); 55.5 (–OCH_3); 111.0 (=CH); 114.1 (–Ar–*o*-C); 129.4 (–Ar–*m*-C); 130.3 (–Ar–*m*-C); 163.0 (–Ar–OCH_3); 174.2 (–C–O–); 177.9 (–C=S). MS (ESI): *m*/*z* = 565, 536, 512, 445, 101. Elemental analysis: calculated for $C_{13}H_{17}ClO_3PtS_3$·1/2 acetone C: 30.18%; H: 3.49%; S: 16.67%, found: C: 30.57%; H: 3.18%; S: 16.18%.

Chloro-(1-(2-methoxyphenyl)-3-(ethylthio)-3-thioxo-prop-1-en-1-olate-*O*,*S*)-(dimethylsulfoxide-*S*)-platinum(II) (Pt4). Synthesis was performed according to general procedure 1, pathway A. **L4** (389 mg, 1.53 mmol) was dissolved in THF and *t*-BuOK (172 mg, 1.53 mmol) was added. K_2PtCl_4 (700 mg, 1.69 mmol) was dissolved in water and dmso (220 μL, 3.07 mmol) was added. Column chromatography mobile phase: DCM 4 : pentane 1–DCM–DCM 2 : acetone 1–acetone. Yield: 516 mg (60.0%) as red oil. ^1H NMR (600 MHz, acetone-d_6): δ = 1.43 (t, 3H, –S–CH_2–CH_3); 3.23 (q, 2H, –S–CH_2–); 3.65 (s w/Pt satellites $^3J_{Pt–H}$ = 22.5 Hz, 6H, CH_3 (DMSO)); 3.94 (s, 3H, –OCH_3); 6.99 (ddd, $^3J_{H–H}$ = 7.6 Hz, $^4J_{H–H}$ = 1.0 Hz, 1H, –Ar–*m*-H); 7.14 (d, $^3J_{H–H}$ = 8.4 Hz, 1H, –Ar–*o*-H); 7.35 (s, 1H, =CH); 7.50 (ddd, $^3J_{H–H}$ = 7.6 Hz, $^4J_{H–H}$ = 1.0 Hz, 1H, –Ar–*p*-H); 7.62 (dd, $^3J_{H–H}$ = 7.8 Hz, $^4J_{H–H}$ = 1.8 Hz, 1H, Ar–*m*-H). $^{13}C\{^1H\}$ NMR (101 MHz, acetone-d_6): δ = 13.7 (–S–CH_2–CH_3); 26.1 (–S–CH_2–); 46.7 (DMSO); 56.4 (–OCH_3); 112.9 (–Ar–*o*-C); 116.5 (=CH); 121.7 (–Ar–*m*-C); 129.3 (–Ar–C1); 130.6 (–Ar–*m*-C); 133.8 (–Ar–*p*-C); 158.3 (–Ar–OCH_3); 175.3 (–C–O–); 199.0 (–C=S). MS (ESI): *m*/*z* = 525, 448, 393, 337, 331, 245, 205, 173, 151.

Elemental analysis: calculated for $C_{14}H_{19}ClO_3PtS_3$·2/3 pentane C: 33.62%; H: 5.86%; S: 15.54%, found: C: 33.23%; H: 5.39%; S: 15.25%.

Chloro-(1-(3-methoxyphenyl)-3-(ethylthio)-3-thioxo-prop-1-en-1-olate-*O*,*S*)-(dimethylsulfoxide-*S*)-platinum(II) (Pt5). Synthesis was performed according to general procedure 1, pathway A. **L5** (389 mg, 1.53 mmol) was dissolved in THF and *t*-BuOK (172 mg, 1.53 mmol) was added. K_2PtCl_4 (700 mg, 1.69 mmol) was dissolved in water and dmso (220 μL, 3.07 mmol) was added. Column chromatography mobile phase: DCM 4 : hexane 1–DCM–DCM 2 : acetone1–acetone. Yield: 160 mg (18.6%) as yellow crystals. ^1H NMR (400 MHz, $CDCl_3$): δ = 1.43 (t, 3H, –S–CH_2–CH_3); 3.26 (q, 2H, –S–CH_2–); 3.64 (s w/Pt satellites $^3J_{Pt–H}$ = 22.5 Hz, 6H, CH_3 (dmso)); 3.84 (s, 3H, –OCH_3); 7.06 (m, 2H, –Ar–*p*-H/=CH); 7.29 (t, 1H, –Ar–*m*-H); 7.50 (m, 2H, –Ar–*o*-H). $^{13}C\{^1H\}$ NMR (400 MHz, $CDCl_3$): δ = 14.0 (–S–CH_2–CH_3); 22.3 (–S–CH_2–); 46.9 (dmso); 55.4 (–OCH_3); 112.9 (=CH); 118.3 (–Ar–*o*-C); 129.7 (–Ar–*m*-C/–Ar–C1); 135.7 (–Ar–*p*-C); 159.9 (–Ar–OCH_3); 174.5 (–C–O–); 177.6 (–C=S). MS (ESI): *m*/*z* = 579, 413, 393, 301. Elemental analysis: calculated for $C_{14}H_{19}ClO_3PtS_3$·1/2 acetone C: 31.5%; H: 3.75%; S: 16.27%, found: C: 32.02%; H: 3.75%; S: 16.76%.

Chloro-(1-(4-methoxyphenyl)-3-(ethylthio)-3-thioxo-prop-1-en-1-olate-*O*,*S*)-(dimethylsulfoxide-*S*)-platinum(II) (Pt6). Synthesis was performed according to general procedure 1, pathway A. **L6** (389 mg, 1.53 mmol) was dissolved in THF and *t*-BuOK (172 mg, 1.53 mmol) was added. K_2PtCl_4 (700 mg, 1.69 mmol) was dissolved in water and dmso (220 μL, 3.07 mmol) was added. Column chromatography mobile phase: DCM 4 : pentane 1–DCM–DCM 2 : acetone1–acetone. Yield: 150 mg (17.5%) as yellow crystals. ^1H NMR (400 MHz, $CDCl_3$): δ = 1.42 (t, 3H, –S–CH_2–CH_3); 3.24 (q, 2H, –S–CH_2–); 3.63 (s w/Pt satellites $^3J_{Pt–H}$ = 22.5 Hz, 6H, CH_3 (dmso)); 3.83 (s, 3H, –OCH_3); 6.89 (d, $^3J_{H–H}$ = 9.0 Hz, 2H, –Ar–*o*-H); 7.07 (s, 1H, =CH); 7.95 (d, $^3J_{H–H}$ = 9.0 Hz, 2H, –Ar–*m*-H).

$^{13}C\{^1H\}$ NMR (101 MHz, $CDCl_3$): δ = 13.3 (–S–CH_2–CH_3); 22.3 (–S–CH_2–); 46.8 (dmso); 55.5 (–OCH_3); 111.0 (=CH); 114.1 (–Ar–*o*-C); 129.4 (–Ar–C1); 130.2 (–Ar–*m*-C); 163.0 (–Ar–OCH_3); 174.2 (–C–O–); 177.9 (–C=S). MS (ESI): *m*/*z* = 579, 413, 393, 301. Elemental analysis: calculated for $C_{14}H_{19}ClO_3PtS_3$·1/3 pentane C: 32.11%; H: 3.96%; S: 16.41%, found: C: 32.43%; H: 3.73%; S: 16.52%.

Chloro-(1-(3-hydroxyphenyl)-3-(methylthio)-3-thioxo-prop-1-en-1-olate-*O*,*S*)-(dimethylsulfoxide-*S*)-platinum(II) (Pt7). Synthesis was performed according to general procedure 1, pathways A and B. **L7** (350 mg, 1.53 mmol) was dissolved in THF and *t*-BuOK (172 mg, 1.53 mmol) was added. K_2PtCl_4 (700 mg, 1.70 mmol) was dissolved in water and dmso (220 μL, 3.07 mmol) was added. Column chromatography mobile phase: DCM–acetone 20 : DCM 1–acetone 10 : DCM 1—acetone 2 : DCM 1. Yield: 380 mg (46.4%) as orange crystals.

^{1}H NMR (600 MHz, acetone-d_6): δ = 2.63 (s, 3H, –S–CH_3); 3.61 (s w/Pt satellites $^3J_{Pt-H}$ = 22.5 Hz, 6H, CH_3 (dmso)); 7.02 (dd, $^3J_{H-H}$ = 8.2 Hz, $^4J_{H-H}$ = 0.8 Hz, 1H, –Ar–*p*-H); 7.15 (s, 1H, ═CH); 7.24 (t, 1H, –Ar–*m*-H); 7.47 (m, 2H, –Ar–*o*-H); 8.73 (s, 1H, –Ar–OH). ^{13}C{^{1}H} NMR (101 MHz, acetone-d_6): δ = 16.7 (–S–CH_3); 45.9 (dmso); 110.8 (═CH); 114.6 (–Ar–*o*-C); 118.6 (–Ar–*o*-C); 119.3 (–Ar–C1); 130.1 (–Ar–*m*-C); 138.6 (–Ar–*p*-C); 157.9 (–Ar–OH); 174.2 (–C–O–); 177.6 (–C═S). MS (ESI): *m*/*z* = 516, 471, 413, 359, 301, 215. MS (DEI): *m*/*z* = 279, 167, 149, 121, 113, 83, 71, 57, 43. Elemental analysis: calculated for $C_{12}H_{17}ClO_3PtS_3$·1/3 acetone C: 28.22%; H: 3.09%; S: 17.38%, found: C: 28.53%; H: 2.82%; S: 17.95%.

Chloro-(1-(4-hydroxyphenyl)-3-(methylthio)-3-thioxo-prop-1-en-1-olate-*O*,*S*)-(dimethylsulfoxide-*S*)-platinum(II) (Pt8). Synthesis was performed according to general procedure 1, pathways A and B. **L8** (248 mg, 1.10 mmol) was dissolved in THF and *t*-BuOK (123 mg, 1.10 mmol) was added. K_2PtCl_4 (500 mg, 1.21 mmol) was dissolved in water and dmso (160 μL, 2.20 mmol) was added. Column chromatography mobile phase: DCM 2 : pentane 1–DCM 1–acetone 20 : DCM 1–acetone 10 : DCM 1–acetone 2 : DCM 1. Yield: 210 mg (35.8%) as yellow crystals. ^{1}H NMR (600 MHz, acetone-d_6): δ = 2.61 (s, 3H, –S–CH_3); 3.60 (s w/Pt satellites $^3J_{Pt-H}$ = 22.5 Hz, 6H, CH_3 (dmso)); 6.85 (d, $^3J_{H-H}$ = 9.0 Hz, 2H, –Ar–*o*-H); 7.16 (s, 1H, ═CH); 7.95 (d, $^3J_{H-H}$ = 9.0 Hz, 2H, –Ar–*m*-H).

^{13}C{^{1}H} NMR (101 MHz, acetone-d_6): δ = 16.7 (–S–CH_3); 45.9 (dmso); 109.9 (═CH); 115.7 (–Ar–*o*-C); 128.3 (–Ar–C1); 130.5 (–Ar–*m*-C); 161.7 (–Ar–C–OH); 174.2 (–C–O–); 178.7 (–C═S). MS (ESI): *m*/*z* = 530, 471, 413, 359, 301, 194, 121. MS (DEI): *m*/*z* = 528, 382, 327, 279, 194, 179, 167, 136, 121, 78. Elemental analysis: calculated for $C_{12}H_{17}ClO_3PtS_3$·1/3 pentane C: 29.42%; H: 3.43%; S: 17.24%, found: C: 29.93%; H:3.01%; S: 16.80%.

Chloro-(1-(3-hydroxyphenyl)-3-(ethylthio)-3-thioxo-prop-1-en-1-olate-*O*,*S*)-(dimethylsulfoxide-*S*)-platinum(II) (Pt9). Synthesis was performed according to general procedure 1, pathways A and B. **L9** (369 mg, 1.53 mmol) was dissolved in THF and *t*-BuOK (172 mg, 1.53 mmol) was added. K_2PtCl_4 (700 mg, 1.70 mmol) was dissolved in water and dmso (220 μL, 3.07 mmol) was added. Column chromatography mobile phase: DCM 2 : pentane 1–DCM 1–acetone 20 : DCM 1–acetone 10:DCM 1–acetone 2 : DCM 1. Yield: 130 mg (15.5%) as yellow crystals. ^{1}H NMR (600 MHz, acetone-d_6): δ = 1.37 (t, 3H, –S–CH_2–CH_3); 3.22 (q, 2H, –S–CH_2–); 3.61 (s w/Pt satellites $^3J_{Pt-H}$ = 22.5 Hz, 6H, CH_3 (dmso)); 7.03 (d, $^3J_{H-H}$ = 8.1 Hz, 1H, –Ar–*p*-H); 7.15 (s, 1H, ═CH); 7.24 (t, 1H, –Ar–*m*-H); 7.46 (m, 2H, –Ar–*o*-H); 8.74 (s, 1H, Ar–C–OH). ^{13}C{^{1}H} NMR (101 MHz, acetone-d_6): δ = 12.8 (–S–CH_2–CH_3); 25.9 (–S–CH_2–); 45.9 (dmso); 111.0 (═CH); 114.4 (–Ar–*o*-C); 119.6 (–Ar–C1); 120.2 (–Ar–*o*-C); 129.7 (–Ar–*m*-C); 138.8 (–Ar–*p*-C); 156.9 (–Ar–C–OH); 174.5 (–C–O–); 196.8 (–C═S). MS (ESI): *m*/*z* = 510, 434, 359, 301, 289, 197, 78. MS (DEI): *m*/*z* = 298, 268, 239, 213, 208, 181, 179, 167, 138, 136, 98, 93, 78, 63, 61, 29. Elemental analysis: calculated for $C_{12}H_{17}ClO_3PtS_3$·1/10 pentane C: 29.2%; H: 3.30%; S: 17.33%, found: C: 29.44%; H: 3.02%; S: 17.38%.

Chloro-(1-(4-hydroxyphenyl)-3-(ethylthio)-3-thioxo-prop-1-en-1-olate-*O*,*S*)-(dimethylsulfoxide-*S*)-platinum(II) (Pt10). Synthesis was performed according to general procedure 1, pathways A and B. **L10** (369 mg, 1.53 mmol) was dissolved in THF and *t*-BuOK (172 mg, 1.53 mmol) was added. K_2PtCl_4 (700 mg, 1.70 mmol) was dissolved in water and dmso (220 μL, 3.07 mmol) was added. Column chromatography mobile phase: DCM 1–acetone 20 : DCM 1–acetone 10 : DCM 1–acetone 2 : DCM 1. Yield: 130 mg (15.5%) as yellow crystals.

^{1}H NMR (600 MHz, acetone-d_6): δ = 1.35 (t, 3H, –S–CH_2–CH_3); 3.20 (q, 2H, –S–CH_2–); 3.60 (s w/Pt satellites $^3J_{Pt-H}$ = 22.5 Hz, 6H, CH_3 (dmso)); 6.85 (m, 2H, –Ar–*o*-H); 7.16 (s, 1H, ═CH); 7.82 (d, $^3J_{H-H}$ = 9.0 Hz, 2H, –Ar–*m*-H); 9.24 (s, 1H, Ar–C–OH). ^{13}C{^{1}H} NMR (101 MHz, acetone-d_6): δ = 12.9 (–S–CH_2–CH_3); 28.1 (–S–CH_2–); 45.9 (dmso); 110.3 (═CH); 115.0 (–Ar–*o*-C); 128.4 (–Ar–C1); 129.7 (–Ar–*m*-C); 161.7 (–Ar–C–OH); 174.5 (–C–O–); 177.6 (–C═S). MS (ESI): *m*/*z* = 471, 413, 359, 301, 194, 139. MS (DEI): *m*/*z* = 530, 359, 267, 167, 149, 136, 121, 93, 78, 63, 45, 29. Elemental analysis: calculated for $C_{12}H_{17}ClO_3PtS_3$·2.5 acetone C: 35.52%; H: 4.65%; S: 13.88%, found: C: 35.71%; H: 4.08%; S: 14.68%.

Chloro-(1-phenyl-3-(methylthio)-3-thioxo-prop-1-en-1-olate-*O*,*S*)-(dimethylsulfoxide-*S*)-platinum(II) (Pt11). Synthesis was performed according to general procedure 1, pathway A. **L11** (322 mg, 1.53 mmol) was dissolved in THF and *t*-BuOK (172 mg, 1.53 mmol) was added. K_2PtCl_4 (700 mg, 1.69 mmol) was dissolved in water and dmso (220 μL, 3.07 mmol) was added. Column chromatography mobile phase: DCM 4 : hexane 1–DCM–DCM 1 : acetone 1–acetone. Yield: 330 mg (41.5%) as yellow crystals. ^{1}H NMR (600 MHz, acetone-d_6): δ = 2.70 (s, 3H, –S–CH_3); 3.68 (s w/Pt satellites $^3J_{Pt-H}$ = 22.5 Hz, 6H, CH_3 (dmso)); 7.28 (s, 1H, ═CH); 7.49 (m, 2H, –Ar–*o*-H); 7.62 (m, 1H, –Ar–*p*-H); 8.08 (m, 2H, –Ar–*m*-H). ^{13}C{^{1}H} NMR (101 MHz, acetone-d_6): δ = 17.8 (–S–CH_3); 46.9 (dmso); 111.6 (═CH); 128.2 (–Ar–*m*-C/–Ar–*p*-C); 128.8 (–Ar–*o*-C); 133.0 (–Ar–C1); 175.1 (–C–O–); 177.6 (–C═S). MS (DEI): *m*/*z* = 518, 517, 504, 341, 209, 207, 105, 78, 63, 45. Elemental analysis: calculated for $C_{12}H_{15}ClO_2PtS_3$·1/3 acetone/1/3 $CHCl_3$ C: 27.75%; H: 3.02%; S: 16.67%, found: C: 27.88%; H: 2.72%; S: 17.02%.

Chloro-(1-phenyl-3-(ethylthio)-3-thioxo-prop-1-en-1-olate-*O*,*S*)-(dimethylsulfoxide-*S*)-platinum(II) (Pt12). Synthesis was performed according to general procedure 1, pathway A. **L12** (343 mg, 1.53 mmol) was dissolved in THF and *t*-BuOK (172 mg, 1.53 mmol) was added. K_2PtCl_4 (700 mg, 1.69 mmol) was dissolved in water and dmso (220 μL, 3.07 mmol) was added. Column chromatography mobile phase: DCM 4 : hexane 1–DCM–DCM 1 : acetone 1–acetone. Yield: 470 mg (57.5%) as red crystals. ^{1}H NMR (600 MHz, acetone-d_6): δ = 1.43 (t, 3H, –CH_2–CH_3); 3.29 (q, 2H, –S–CH_2–); 3.67 (s w/Pt

satellites $^{3}J_{Pt-H}$ = 22.5 Hz, 6H, CH_3 (dmso)); 7.27 (s, 1H, =CH); 7.49 (m, 2H, –Ar–*o*-H); 7.62 (m, 1H, –Ar–*p*-H); 8.07 (m, 2H, –Ar–*m*-H). $^{13}C\{^{1}H\}$ NMR (101 MHz, acetone-d_6): δ = 13.7 (–S–CH_2–CH_3); 29.2 (–S–CH_2–); 46.8 (dmso); 111.8 (=CH); 128.1 (–Ar–*o*-C); 128.7 (–Ar–*m*-C/–Ar–*p*-C); 138.2 (–Ar–C1); 175.3 (–C–O–); 181.5 (–C=S). MS (DEI): *m*/*z* = 518, 517, 504, 341, 209, 207, 105, 78, 63, 45. Elemental analysis: calculated for $C_{12}H_{15}ClO_3PtS_3$·2/3 acetone/1/3 $CHCl_3$ C: 30.17%; H: 3.52%; S: 15.76%, found: C: 30.38%; H: 2.93%; S: 15.68%.

Crystal structure determination

The intensity data for the compounds were collected on a Nonius KappaCCD diffractometer using graphite-monochromated Mo-K_α radiation. Data were corrected for Lorentz and polarization effects; absorption was taken into account on a semi-empirical basis using multiple-scans.[52–54]

The structures were solved by direct methods (SHELXS) and refined by full-matrix least squares techniques against F_o^2 (SHELXL-97).[55] All hydrogen atoms of compound **L1**, **Pt1** and molecule B of **L7**, the hydrogen atoms bound to the hydroxy-groups of molecule A of **L7** and **Pt10** were located by difference Fourier synthesis and refined isotropically. All other hydrogen atoms were included at calculated positions with fixed thermal parameters. The crystal of **Pt7** was a non-merohedral twin. The twin law was determined by PLATON to (1.0 0.0 0.129) (0.0 −1.0 0.0) (0.0 0.0 1.0).[56] The contribution of the main component was refined to 0.776(1). Crystallographic data as well as structure solution and refinement details are summarized in Table S1.‡ XP (SIEMENS Analytical X-ray Instruments, Inc.) was used for structure representations.

Stability determinations

NMR-spectra were recorded *via* NMR-spectroscopy on a Bruker Avance 600 MHz. Substances were dissolved in dmso-d_6 and measured directly at 37 °C. NMR tubes were incubated at 37 °C and after 24 hours measured again under the same conditions.

UV–vis spectra of the compounds at different dmso concentrations and under the conditions used to obtain crystals of HEWL–Pt compounds adducts were registered using a Jasco spectrophotometer at room temperature in a cuvette with an optical length of 0.1 cm. Spectra of the compounds in 10 mM PBS pH 7.4 and 0.9% NaCl were registered using a Cary-win 50 spectrophotometer in a cuvette with an optical length of 1 cm.

DNA-binding behavior

DNA-binding behavior was measured *via* NMR-spectroscopy on a Bruker Avance 600 MHz at 37 °C. Model base 9-methylguanine was supplied by Sigma Aldrich, both compounds (a model base as well as a platinum(II)-complex) were dissolved separately in dmso-d_6, quickly mixed and quickly transferred into an NMR tube. Measurements were started directly after the transfer of the single molecules for 24 hours and 30 minutes (NS = 64 (3 minutes and 38 seconds), pause: 390 seconds, 145 experiments). We used 6 mg of the complex as well as of the model base, which resulted in a high molecular excess of the 9-methylguanine, to imitate excesses in the biological system and because of the intensity of the signals.

Biological assays

Ovarian cancer cell lines were cultured under standard conditions (5% CO2, 37 °C, 90% humidity) in RPMI medium supplemented with 10% FCS, 100 U ml^{-1} penicillin and 100 μg ml^{-1} streptomycin (Life Technologies, Germany). Cisplatin (Sigma, Germany) was freshly dissolved at 1 mg ml^{-1} in 0.9% NaCl solution and diluted appropriately. New platinum(II) complexes and ligands were dissolved in dmso. Platinum-resistant A2780 and SKOV3 cells were established by repeated rounds of 3 day incubations with increasing amounts of Cisplatin starting with 0.1 μM. The concentration was doubled after 3 incubations interrupted by recovery phases with normal medium. Cells that survived the third round of 12.8 μM Cisplatin were defined as resistant cultures. Determinations of IC_{50} values were carried out using the CellTiter96 non-radioactive proliferation assay (MTT assay, Promega). After seeding 5000 cells per well in a 96-well plate cells were allowed to attach for 24 h and were incubated for 48 h with different concentrations of the substances ranging from 0 to 1000 μM for Platinum and 0 to 1000 μM for ligand tests (0, 1, 10, 50, 100, 500, 1000 μm), for Cisplatin from 0 to 100 μM (0.1, 1, 5, 10, 50, 100 μM). Each measurement was done in triplicate and repeated 3-times. The proportion of live cells was quantified by the MTT assay and after background subtraction relative values compared to the mean of medium controls were calculated. Non-linear regression analyses applying the Hill-slope were run in the GraphPad 5.0 software.

For the determination of DNA damage induced by the treatment with different substances histone γH2AX foci were visualized by immunocytochemical staining. Cells were seeded on coverslips to reach 60–70% confluence after 24 h. After incubation (24 h) with different substances at IC_{50} concentrations for the resistant cells, cells were washed 3× with PBS and fixed for 10 min in 4% paraformaldehyde. Cells were again washed 3-times and then permeabilised by incubation with 0.25% Triton-X in PBS for 5 min. The primary antibody against γH2AX (clone JBW301, Millipore, diluted 1 : 2000) was incubated for 1 h at RT and coverslips were washed 3-times afterwards. Alexa488-labelled secondary anti-mouse antibody (life technologies) was used in a 1 : 1000 dilution in PBS and applied for 1 h at RT. Cells were washed 3-times, counterstained with DAPI, washed again and embedded in mounting medium (Vectorshield, Vector Systems). Slides were stored at 4 °C in the dark until microscopic evaluation was done using a Zeiss LSM 710 laser scanning microscope.

Fluorescence

Intrinsic fluorescence spectra of HEWL (0.1 mg × mL^{-1}) in the presence of increasing concentrations of the Pt compounds, at a fixed dmso concentration (1.4%), were recorded at 25 °C with a Horiba Fluoromax 4, using 5 nm per 5 nm slit widths. The excitation wavelength was 280 nm, and the emission wave-

length was read at 295–450 nm. The temperature of the sample was maintained by a Peltier-thermostat.

Crystallization of protein–Pt compound adducts

Crystals of hen egg white lysozyme (HEWL)–Pt compound adducts appeared in solutions consisting of 1.1 M NaCl, 0.1 M sodium acetate, pH 4.4. Single crystals suitable for X-ray experiments were grown by the hanging drop vapor-diffusion method using a 1 : 1 ratio of reservoir solution and protein adducts solution with a protein concentration of ~15 mg ml^{-1}.

Data collection, structure determination and refinement

Crystals were flask-cooled in nitrogen in the absence of a cryoprotectant, as done in other studies (see for example ref. 57) and then screened for diffraction quality. X-ray data were collected at ~100 K at the CNR Institute of Biostructure and Bioimages. Data were indexed, integrated and scaled with HKL2000.[52] Details of data processing are reported in Table S3.‡

The structures were solved using the coordinates from PDB code 4J1A, without water and ligands and the molecular-replacement method as implemented in Phaser.[47,58] All the models were refined independently using Refmac of the CCP4 suite (see Table 1).[59,60] Model building and electron density map fitting were performed using WinCoot.[61] Structural figures were prepared using PyMOL (http://www.pymol.org/) and the structures were deposited in the Protein Data Bank.

Acknowledgements

The authors would like to thank Ralf Trautwein for fruitful discussions. A. M. would like to thank G. Sorrentino and M. Amendola at the CNR Institute of Biostructures and Bioimages for technical assistance.

Notes and references

1 B. Rosenberg, L. Van Camp and T. Krigas, *Nature*, 1965, **205**, 698–699.
2 B. Rosenberg, *Interdiscip. Sci. Rev.*, 1978, **3**, 134.
3 M. Galanski and B. K. Keppler, *Anti-Cancer Agents Med. Chem.*, 2007, **7**, 55–73.
4 R. A. Alderden, M. D. Hall and T. W. Hambley, *J. Chem. Educ.*, 2006, **83**, 728–734.
5 J. Reedijk, *Inorg. Chim. Acta*, 1992, **198–200**, 873–881.
6 E. R. Jamieson and S. J. Lippard, *Chem. Rev.*, 1999, **99**, 2467–2498.
7 A. Gadducci, S. Cosio, S. Muraca and A. R. Genazzani, *Eur. J. Gynaecol. Oncol.*, 2002, **23**, 390–396.
8 M. A. Fuertes, J. Castilla, C. Alonso and J. M. Perez, *Curr. Med. Chem.*, 2003, **10**, 257–266.
9 J. Reedijk, *Proc. Natl. Acad. Sci. U. S. A.*, 2003, **100**, 3611–3616.
10 D. Wang and S. J. Lippard, *Nat. Rev. Drug Discovery*, 2005, **4**, 307–320.
11 S. Ishida, J. Lee, D. J. Thiele and I. Herskowitz, *Proc. Natl. Acad. Sci. U. S. A.*, 2002, **99**, 14298–14302.
12 X. Lin, T. Okuda, A. Holzer and S. B. Howell, *Mol. Pharmacol.*, 2002, **62**, 1154–1159.
13 N. D. Eljack, H.-Y. M. Ma, J. Drucker, C. Shen, T. W. Hambley, E. J. New, T. Friedrich and R. J. Clarke, *Metallomics*, 2014, **6**, 2126–2133.
14 S. E. Miller and D. A. House, *Inorg. Chim. Acta*, 1989, **166**, 189–197.
15 D. Steinhilber, M. Schubert-Zsilavecz and H. J. Roth, *Medizinische Chemie: Targets, Arzneistoffe, Chemische Biologie*, Deutscher Apotheker Verlag, 2010.
16 G. Gasser, I. Ott and N. Metzler-Nolte, *J. Med. Chem.*, 2011, **54**, 3–25.
17 D. D. Von Hoff, R. Schilsky, C. M. Reichert, R. L. Reddick, M. Rozencweig, R. C. Young and F. M. Muggia, *Cancer Treat. Rep.*, 1979, **63**, 1527–1531.
18 M. Dabholkar, F. Bostick-Bruton, C. Weber, V. A. Bohr, C. Egwuagu and E. Reed, *J. Natl. Cancer Inst.*, 1992, **84**, 1512–1517.
19 D. Fink, S. Nebel, S. Aebi, H. Zheng, B. Cenni, A. Nehme, R. D. Christen and S. B. Howell, *Cancer Res.*, 1996, **56**, 4881–4886.
20 A. I. Ivanov, J. Christodoulou, J. A. Parkinson, K. J. Barnham, A. Tucker, J. Woodrow and P. J. Sadler, *J. Biol. Chem.*, 1998, **273**, 14721–14730.
21 D. Hanahan and R. A. Weinberg, *Cell*, 2000, **100**, 57–70.
22 E. Reed, *Clin. Cancer Res.*, 2005, **11**, 6100–6102.
23 J. Helleman, S. I. L. van, W. N. M. Dinjens, K. P. F. van, K. Ritstier, P. C. Ewing, D. B. M. E. L. van, G. Stoter and E. M. J. J. Berns, *BMC Cancer*, 2006, **6**, 201.
24 L. Kelland, *Nat. Rev. Cancer*, 2007, **7**, 573–584.
25 M. Yu, J. Han, P. Cui, M. Dai, H. Li, J. Zhang and R. Xiu, *Cancer Sci.*, 2008, **99**, 391–397.
26 D. Hanahan and R. A. Weinberg, *Cell*, 2011, **144**, 646–674.
27 G. Ciarimboli, *Anticancer Res.*, 2014, **34**, 547–550.
28 C. G. Hartinger and P. J. Dyson, *Chem. Soc. Rev.*, 2009, **38**, 391–401.
29 G. Suess-Fink, *Dalton Trans.*, 2010, **39**, 1673–1688.
30 N. Hafner, D. Steinbach, L. Jansen, H. Diebolder, M. Durst and I. B. Runnebaum, *Int. J. Cancer*, 2016, **138**, 217–228.
31 S. S. G. E. van Boom and J. Reedijk, *J. Chem. Soc., Chem. Commun.*, 1993, 1397–1398.
32 J. Reedijk, *Chem. Rev.*, 1999, **99**, 2499–2510.
33 C. Muegge, R. Liu, H. Goerls, C. Gabbiani, E. Michelucci, N. Ruediger, J. H. Clement, L. Messori and W. Weigand, *Dalton Trans.*, 2014, **43**, 3072–3086.
34 F. C. V. Larsson and S. O. Lawesson, *Tetrahedron*, 1972, **28**, 5341–5357.
35 W. Weigand, R. Saumweber and P. Schulz, *Z. Naturforsch., B: Chem. Sci.*, 1993, **48**, 1080–1088.
36 R. Saumweber, C. Robl and W. Weigand, *Inorg. Chim. Acta*, 1998, **269**, 83–90.

37 K. Schubert, R. Saumweber, H. Goerls and W. Weigand, *Z. Anorg. Allg. Chem.*, 2003, **629**, 2091–2096.
38 K. Schubert, T. Alpermann, T. Niksch, H. Goerls and W. Weigand, *Z. Anorg. Allg. Chem.*, 2006, **632**, 1033–1042.
39 K. Schubert, H. Goerls and W. Weigand, *Z. Naturforsch., B: Chem. Sci.*, 2007, **62**, 475–482.
40 C. Muegge, T. Marzo, L. Massai, J. Hildebrandt, G. Ferraro, P. Rivera-Fuentes, N. Metzler-Nolte, A. Merlino, L. Messori and W. Weigand, *Inorg. Chem.*, 2015, **54**, 8560–8570.
41 H. Motschi, P. S. Pregosin and H. Ruegger, *J. Organomet. Chem.*, 1980, **193**, 397–405.
42 S. F. Kaplan, V. Y. Kukushkin and A. J. L. Pombeiro, *J. Chem. Soc., Dalton Trans.*, 2001, 3279–3284.
43 D. J. Aitken, A. Albinati, A. Gautier, H.-P. Husson, G. Morgant, D. Nguyen-Huy, J. Kozelka, P. Lemoine, S. Ongeri, S. Rizzato and B. Viossat, *Eur. J. Inorg. Chem.*, 2007, 3327–3334.
44 M. Patra, T. Joshi, V. Pierroz, K. Ingram, M. Kaiser, S. Ferrari, B. Spingler, J. Keiser and G. Gasser, *Chem. – Eur. J.*, 2013, **19**, 14768–14772.
45 E. P. Rogakou, C. Boon, C. Redon and W. M. Bonner, *J. Cell Biol.*, 1999, **146**, 905–915.
46 L. Messori, F. Scaletti, L. Massai, M. A. Cinellu, C. Gabbiani, A. Vergara and A. Merlino, *Chem. Commun.*, 2013, **49**, 10100–10102.
47 A. Vergara, I. Russo Krauss, D. Montesarchio, L. Paduano and A. Merlino, *Inorg. Chem.*, 2013, **52**, 10714–10716.
48 A. Casini, G. Mastrobuoni, C. Temperini, C. Gabbiani, S. Francese, G. Moneti, C. T. Supuran, A. Scozzafava and L. Messori, *Chem. Commun.*, 2007, 156–158.
49 L. Messori, T. Marzo, E. Michelucci, I. Russo Krauss, C. Navarro-Ranninger, A. G. Quiroga and A. Merlino, *Inorg. Chem.*, 2014, **53**, 7806–7808.
50 S. W. M. Tanley, K. Diederichs, L. M. J. Kroon-Batenburg, C. Levy, A. M. M. Schreurs and J. R. Helliwell, *Acta Crystallogr., Sect. F: Struct. Biol. Cryst. Commun.*, 2014, **70**, 1135–1142.
51 D. Marasco, L. Messori, T. Marzo and A. Merlino, *Dalton Trans.*, 2015, **44**, 10392–10398.
52 Z. Otwinowski and W. Minor, *Methods Enzymol.*, 1997, **276**, 307–326.
53 COLLECT, Data Collection Software, Nonius B.V., Netherlands, 1998.
54 SADABS 2.10, Bruker-AXS inc., Madison, WI, U.S.A., 2002.
55 G. M. Sheldrick, *Acta Crystallogr., Sect. A: Found. Crystallogr.*, 2008, **64**, 112–122.
56 A. L. Spek, *Acta Crystallogr., Sect. D: Biol. Crystallogr.*, 2009, **65**, 148–155.
57 I. Russo Krauss, L. Messori, M. A. Cinellu, D. Marasco, R. Sirignano and A. Merlino, *Dalton Trans.*, 2014, **43**, 17483–17488.
58 A. J. McCoy, R. W. Grosse-Kunstleve, P. D. Adams, M. D. Winn, L. C. Storoni and R. J. Read, *J. Appl. Crystallogr.*, 2007, **40**, 658–674.
59 G. N. Murshudov, P. Skubak, A. A. Lebedev, N. S. Pannu, R. A. Steiner, R. A. Nicholls, M. D. Winn, F. Long and A. A. Vagin, *Acta Crystallogr., Sect. D: Biol. Crystallogr.*, 2011, **67**, 355–367.
60 M. D. Winn, C. C. Ballard, K. D. Cowtan, E. J. Dodson, P. Emsley, P. R. Evans, R. M. Keegan, E. B. Krissinel, A. G. W. Leslie, A. McCoy, S. J. McNicholas, G. N. Murshudov, N. S. Pannu, E. A. Potterton, H. R. Powell, R. J. Read, A. Vagin and K. S. Wilson, *Acta Crystallogr., Sect. D: Biol. Crystallogr.*, 2011, **67**, 235–242.
61 P. Emsley, B. Lohkamp, W. G. Scott and K. Cowtan, *Acta Crystallogr., Sect. D: Biol. Crystallogr.*, 2010, **66**, 486–501.

Supporting Information

Platinum(II) O,S complexes as potential metallodrugs against Cisplatin resistance

Jana Hildebrandt,[a] Norman Häfner,[b] Helmar Görls,[a] Daniel Kritsch,[b] Giarita Ferraro,[c] Matthias Dürst,[b] Ingo B. Runnebaum,[b] * Antonello Merlino,[c,d] * and Wolfgang Weigand[a] *

* Prof. Dr. W. Weigand E-Mail: wolfgang.weigand@uni-jena.de

* Prof. Dr. A. Merlino E-Mail: antonello.merlino@unina.it

[a] Institut für Anorganische und Analytische Chemie Friedrich-Schiller-Universität Jena Humboldtsrasse8, 07743 Jena, Germany

[b]Department of Gynecology, Jena University Hospital - Friedrich Schiller University Jena

[c]Department of Chemical Sciences, University of Naples Federico II, Complesso Universitario di Monte Sant' Angelo, Via Cintia, I-80126, Napoli, Italy

[d]CNR Institute of Biostructures and Bioimages, Via Mezzocannone 16, I-80100, Napoli, Italy

Synthesis and Spectroscopic Data of Compounds **L1-L12**

General procedure 1: β-hydroxy dithiocinnamic acid alkyl esters (L1-L12).
In case of a hydroxy-β-hydroxy dithiocinnamic acid alkyl ester, a mixture of the hydroxy-acetophenone derivate (1 equiv) and imidazole (2 equiv) in dimethylformamide (DMF, 50 ml) was dropped to a solution of *tert.*-butyldimethylchlorosilan (1 equiv) in DMF (25 ml). After stirring for 20 h at room temperature an aqueous solution of sodium hydrogen carbonate (200 ml) was added to the reaction mixture and the evolving two-phased system was seperated. The aquatic phase was extracted with hexane (3x20 ml) and the combined organic solutions washed with water (3x20 ml) followed by drying with sodium sulfate, filtration and evaporation of the solvent.
In a second step to a solution of potassium-*tert.*-butoxylate (*t*-BuOK, 2 equiv) in diethyl ether (250 ml), cooled down at -70°C, was dropped the corresponding acetophenone derivate (1 equiv) in diethyl ether (50 ml). Carbon disulfide (CS_2, 1.4 equiv) was dropped to the solution and stirred one hour at -70°C. After warming up the reaction mixture was stirred two hours at room temperature. Alkyl halide (1 equiv) was added and the mixture stirred for 15 h. Solvent was removed and dichlormethane (100 ml) was added to the oil. Sulfuric acid (aqueous solution, 2M, 100 ml) was added to the suspension and stirred for 30 minutes at room temperature. The two-phased system was seperated and the aqueous phase extracted with dichlormethane (3x35 ml). The combined organic phases were washed with water (3x20 ml), dried with sodium sulfate, followed by filtration and evaporation of the solvent. The crude product was purified with column cromatography.
Last step is the deprotection of the TBDMS-protection group in case of hydroxy-β-hydroxy dithiocinnamic acid alkyl esters. The β-hydroxy dithiocinnamic alkyl ester (1equiv) is solved in tetrahydrofurane (THF, 60 ml) and tetra-n-butylammonium flouride (TBAF, 2 equiv, 1M in THF) was dropped to the solution. After stirring for three days at room temperature sulfuric acid (50 ml, 2M) was added and stirred for four hours, followed by seperating the two phases. The aqueous phase was extracted with DCM (3x35 ml), combined organic phases were washed with water (3x20 ml), dried over sodium sulfate and filtrated. The crude product was purified with column cromatography.
Ligands **L1-L12** were prepared as described above or have been reported earlier.[1-2]

2'-Methoxy-β-hydroxy dithiocinnamic methyl ester (L1)
Synthesis was performed according to general procedure 1. The 2'-methoxyacetophenone (1.8 ml, 13.32 mmol) and CS_2 (1.13 ml, 18.64 mmol) was dropped to the *t*-BuOK (3.0 g, 27.00 mmol) solution. Methyliodide (0.83 ml, 27.00 mmol) was used. Column chromatography mobile phase: DCM 1:hexane 1. Yield: 1.21 g (37.8%) as yellow crystals. ^{1}H NMR (400 MHz, $CDCl_3$): δ = 2.57 (s, 3H, -S-CH_3); 3.85 (s, 3H, -OCH_3); 6.90 (d, $^3J_{H-H}$=8.4 Hz, 1H, -Ar-*o*-H); 6.96 (ddd, $^3J_{H-H}$=7.6 Hz, $^4J_{H-H}$=1.0 Hz, 1H, -Ar-*m*-H); 7.20 (s, 1H, =CH); 7.36 (ddd, $^3J_{H-H}$=7.6 Hz, $^4J_{H-H}$=1.0 Hz, 1H, -Ar-*p*-H); 7.79 (dd, $^3J_{H-H}$=7.8 Hz, $^4J_{H-H}$=1.8 Hz, 1H, Ar-*m*-H); 15.08 (s, 1H, -C-OH). ^{13}C{^{1}H} NMR (101 MHz, $CDCl_3$): δ = 17.1 (-S-CH_3); 55.8 (-OCH_3); 111.7 (-Ar-*o*-C); 112.9 (=CH); 120.8 (-Ar-*m*-C); 123.2 (-Ar-C1); 130.2 (-Ar-*m*-C); 133.8 (-Ar-*p*-C); 157.8 (-Ar-OCH_3); 167.6 (-C-OH); 217.2 (-C=S). MS (DEI): m/z = 242, 240, 209, 193, 135, 121, 92, 77. Elemental analysis: calculated for $C_{11}H_{12}O_2S_2$ C: 54.97%; H: 5.03%; S: 26.68%, found: C: 55.13%; H: 5.03%; S: 27.11%.

3'-Methoxy-β-hydroxy dithiocinnamic methyl ester (L2)
Synthesis was performed according to general procedure 1. The 3'-methoxyacetophenone (1.8 ml, 13.32 mmol) and CS_2 (1.13 ml, 18.64 mmol) were dropped to the *t*-BuOK (3.0 g, 27.00 mmol) solution. Methyliodide (0.83 ml, 27.00 mmol) was used. Column chromatography mobile phase: DCM 1:hexane 1. Yield: 2.14 g (66.9%) as yellow crystals. ^{1}H NMR (400 MHz, $CDCl_3$): δ = 2.68 (s, 3H, -S-CH_3); 3.89 (s, 3H, -OCH_3); 6.97 (s, 1H, =CH); 7.08 (dd, $^3J_{H-H}$=8.2 Hz, $^4J_{H-H}$=0.8 Hz, 1H, -Ar-*p*-H); 7.38 (t, 1H, -Ar-*m*-H); 7.44 (m, 1H, -Ar-*o*-H); 7.48 (m, 1H, -Ar-*o*-H). ^{13}C{^{1}H} NMR (101 MHz, $CDCl_3$): δ = 17.2 (-S-CH_3); 55.5 (-OCH_3); 111.8 (-Ar-*o*-C); 112.9 (=CH); 117.9 (-Ar-*o*-C); 120.3 (-Ar-*m*-C); 121.6 (-Ar-C1); 135.7 (-Ar-*p*-C); 159.9 (-Ar-OCH_3); 169.1 (-C-OH); 217.3 (-C=S). MS (DEI): m/z = 240, 225, 209, 193, 135, 121, 92, 77. Elemental analysis: calculated for $C_{11}H_{12}O_2S_2$ C: 54.97%; H: 5.03%; S: 26.68%, found: C: 55.23%; H: 5.07%; S: 27.01%.

4'-Methoxy-β-hydroxy dithiocinnamic methyl ester(L3).
Synthesis was performed according to general procedure 1. The 4'-methoxyacetophenone (2 g, 13.32 mmol) and CS_2 (1.13 ml, 18.64 mmol) were dropped to the *t*-BuOK (3.0 g, 27.00 mmol) solution. Methyliodide (0.83 ml, 13.32 mmol) was used. Column chromatography mobile phase: DCM 1:hexane 1. Yield: 1.26 g (39.4%) as yellow crystals. ^{1}H NMR (600 MHz, $CDCl_3$): δ = 2.68 (s, 3H, -S-CH_3); 3.89 (s, 3H, -OCH_3); 6.98 (m, 3H, -Ar-*o*-H/=CH); 7.89 (d, $^3J_{H-H}$=9.0 Hz, 2H, -Ar-*m*-H); 15.21 (-C-OH). ^{13}C{^{1}H} NMR (101 MHz, $CDCl_3$): δ = 17.0 (-S-CH_3); 55.5 (-OCH_3); 107.1 (=CH); 126.2 (-Ar-*o*-C); 128.7 (-Ar-C1); 129.0 (-Ar-*m*-C); 131.4 (-Ar-*m*-C); 157.8 (-Ar-OCH_3); 169.6 (-C-OH); 215.7 (-C=S).MS (DEI): m/z = 241, 240, 225, 193, 135, 121, 92.
Elemental analysis: calculated for $C_{11}H_{12}O_2S_2$ C: 54.97%; H: 5.03%; S: 26.68%, found: C: 55.25%; H: 5.08%; S: 27.13%.

2'-Methoxy-β-hydroxy dithiocinnamic ethyl ester (L4).
Synthesis was performed according to general procedure 1. The 2'-methoxyacetophenone (2.3 ml, 16.65 mmol) and CS_2 (1.40 ml, 23.31 mmol) were dropped to the *t*-BuOK (3.7 g, 33.23 mmol) solution. Ethyliodide (1.34 ml, 16.65 mmol) was used. Column chromatography mobile phase: DCM 1:hexane 1. Yield: 2.51 g (59.3%) as orange oil. ^{1}H NMR (400 MHz, $CDCl_3$): δ = 1.36 (t, 3H, -S-CH_2-CH_3); 3.24 (q, 2H, -S-CH_2-); 3.88 (s, 3H, -OCH_3); 6.94 (d, $^3J_{H-H}$=8.5 Hz, 1H, -Ar-*o*-H); 6.96 (ddd, $^3J_{H-H}$=7.6 Hz, $^4J_{H-H}$=1.0 Hz, 1H, -Ar-*m*-H); 7.23 (s, 1H, =CH); 7.41 (ddd, $^3J_{H-H}$=7.96 Hz, $^4J_{H-H}$=1.0 Hz, 1H, -Ar-*p*-H); 7.79 (dd, $^3J_{H-H}$=7.8 Hz, $^4J_{H-H}$=1.8 Hz, 1H, Ar-*m*-H); 15.21 (s, 1H, -C-OH). ^{13}C{^{1}H} NMR (101 MHz, $CDCl_3$): δ = 12.8 (-S-CH_2-CH_3); 27.7 (-S-CH_2-); 55.6 (-OCH_3); 111.6 (-Ar-*o*-C); 112.8 (=CH); 120.7 (-Ar-*m*-C); 123.1 (-Ar-C1); 130.0 (-Ar-*m*-C); 132.5 (-Ar-*p*-C); 157.7 (-Ar-OCH_3); 167.8 (-C-OH); 216.3 (-C=S). MS (DEI): m/z = 256, 254, 223, 193, 135, 121, 92, 77. Elemental analysis: calculated for $C_{11}H_{14}O_2S_2$ C: 56.66%; H: 5.55%; S: 25.21%, found: C: 57.02%; H: 5.60%; S: 25.68%.

3'-Methoxy-β-hydroxy dithiocinnamic ethyl ester (L5).
Synthesis was performed according to general procedure 1. The 3'-methoxyacetophenone (1.8 ml, 13.32 mmol) and CS_2 (1.13 ml, 18.65 mmol) were dropped to the *t*-BuOK (3.0 g, 27.00 mmol) solution. Ethyliodide (1.07 ml, 13.32 mmol) was used. Column chromatography mobile phase: DCM 1:hexane 1. Yield: 2.89 g (85.5%) as orange oil.^{1}H NMR (400 MHz, $CDCl_3$): δ = 1.40 (t, 3H, -S-CH_2-CH_3); 3.29 (q, 2H, -S-CH_2-); 3.86 (s, 3H, -OCH_3); 6.91 (s, 1H, =CH); 7.06 (dd, $^3J_{H-H}$=8.2 Hz, $^4J_{H-H}$=0.8 Hz, 1H, -Ar-*p*-H); 7.38 (t, 1H, -Ar-*m*-H); 7.44 (m, 2H, -Ar-*o*-H); 15.18 (s, 1H, -C-OH). ^{13}C{^{1}H} NMR (101 MHz, $CDCl_3$): δ = 12.8 (-S-CH_2-CH_3); 27.9 (-S-CH_2-); 55.4 (-OCH_3); 111.8 (-Ar-*o*-C); 112.9 (=CH); 117.8 (-Ar-*o*-C); 120.2 (-Ar-*m*-C); 121.6 (-Ar-C1); 135.7 (-Ar-*p*-C); 159.9 (-Ar-OCH_3); 169.4 (-C-OH); 217.3 (-C=S). MS (DEI): m/z = 255, 254, 225, 193, 135, 121, 92, 77. Elemental analysis: calculated for $C_{11}H_{14}O_2S_2$ C: 56.66%; H: 5.55%; S: 25.21%, found: C: 56.53%; H: 5.48%; S: 25.26%.

4'-Methoxy-β-hydroxy dithiocinnamic ethyl ester (L6).
Synthesis was performed according to general procedure 1. The 4'-methoxyacetophenone (2.0 g, 13.32 mmol) and CS_2 (1.13 ml, 18.65 mmol) were dropped to the *t*-BuOK (3.0 g, 27.00 mmol) solution. Ethyliodide (1.07 ml, 13.32 mmol) was used. Column chromatography mobile phase: DCM 1:hexane 1. Yield: 2.64 g (78.1%) as yellow crystals. ^{1}H NMR (600 MHz, $CDCl_3$): δ = 1.40 (t, 3H, -S-CH_2-CH_3); 3.29 (q, 2H, -S-CH_2-); 3.89 (s, 3H, -OCH_3); 6.91 (s, 1H, =CH); 6.97 (d, $^3J_{H-H}$=9.0 Hz, 2H, -Ar-*o*-H); 7.88 (d, $^3J_{H-H}$=9.0 Hz, 2H, -Ar-*m*-H); 15.21 (-C-OH). ^{13}C{^{1}H} NMR (101 MHz, $CDCl_3$): δ = 13.1 (-S-CH_2-CH_3); 27.7 (-S-CH_2-); 55.5 (-OCH_3); 107.1 (=CH); 126.3 (-Ar-*o*-C); 128.7 (-Ar-C1); 129.0 (-Ar-*m*-C); 131.4 (-Ar-*m*-C); 157.8 (-Ar-OCH_3); 169.9 (-C-OH); 214.9 (-C=S). MS (DEI): m/z = 254, 226, 193, 135, 92, 77. Elemental analysis: calculated for $C_{11}H_{14}O_2S_2$ C: 56.66%; H: 5.55%; S: 25.21%, found: C: 56.93%; H: 5.62%; S: 25.56%.

3'-Hydroxy-β-hydroxy dithiocinnamic methyl ester(L7).
Synthesis was performed according to general procedure 1. 3'-Hydroxy-acetophenone (8.2 g, 59.90 mmol) was protected with TBDMS (9.0 g, 59.90 mmol) and imidazole (8.16 g, 119.89 mmol) was used. Yield: 11.91 g (79.4%) as white oil. ^{1}H NMR (400 MHz, $CDCl_3$): δ = 0.1 (s, 6H, -Si-$(CH_3)_2$); 0.78 (s, 9H, -C-$(CH_3)_3$); 2.34 (s, 3H -CH_3); 6.81 (dd, $^3J_{H-H}$=8.1 Hz, 1H, -Ar-*p*-H); 6.82 (t, ^{1}H, -Ar-*m*-H); 7.07 (s, 1H, -Ar-*o*-H); 7.11 (d, $^3J_{H-H}$=7.7 Hz 1H, -Ar-*o*-H). ^{13}C{^{1}H} NMR (101 MHz, $CDCl_3$): δ = -4.6 (-Si-$(CH_3)_2$); 18.0 (q, -C-

$(CH_3)_3$); 25.5 (-C-$(CH_3)_3$); 26.5 (-CH_3); 119.3 (-Ar-*o*-C); 121.4 (-Ar-*o*-C); 124.8 (-Ar-*p*-C); 129.4 (-Ar-*m*-C); 138.5 (-Ar-C1); 155.8 (-Ar-*m*-C-O-); 197.5 (-C=O). MS (ESI): m/z = 216, 184.

The 3'-TBDMS-acetophenone (5.0 g, 19.97 mmol) and CS_2 (1.70 ml, 27.95 mmol) were dropped to the *t*-BuOK (4.5 g, 39.93 mmol) solution. Methyliodide (1.30 ml, 19.97 mmol) was used. Column chromatography mobile phase: DCM 2:hexane 1. Yield: 3.52 g (51.7%) as green crystals. ^{1}H NMR (600 MHz, $CDCl_3$): δ = 0.21 (s, 6H, -Si-$(CH_3)_2$); 0.98 (s, 9H, -C-$(CH_3)_3$); 2.64 (s, 3H, -S-CH_3); 6.90 (s, 1H, =CH); 6.96 (dd, $^3J_{H\text{-}H}$=8.1 Hz, 1H, -Ar-*p*-H); 7.28 (t, 1H, -Ar-*m*-H); 7.33 (s, 1H, -Ar-*o*-H); 7.43 (d, $^3J_{H\text{-}H}$=7.7 Hz, 1H, -Ar-*o*-H); 15.05 (s, 1H, -C-OH). ^{13}C{^{1}H} NMR (101 MHz, $CDCl_3$): δ = -4.2 (-Si-$(CH_3)_2$); 17.1 (q, -C-$(CH_3)_3$); 18.2 (-C-$(CH_3)_3$); 31.6 (-CH_3); 107.9 (=CH); 118.3 (-Ar-*o*-C); 119.6 (-Ar-*o*-C); 123.6 (-Ar-*p*-C); 129.7 (-Ar-*m*-C); 135.7 (-Ar-C1); 156.1 (-Ar-*m*-C-O-); 169.1 (-C-OH); 217.2 (-C=S). MS (DEI): m/z = 341, 340, 293, 235.

The 3'-TBDMS-β-hydroxy dithiocinnamic methyl ester (3.5 g, 10.3 mmol) was deprotected with TBAF (20.7 ml, 20.7 mmol). Column chromatography mobile phase: hexane 2:DCM 1 - hexane 1 : DCM 1 - hexane 1 : DCM 3. Yield: 1.89 g (81.1%) as yellow crystals. ^{1}H NMR (400 MHz, CD_2Cl_2): δ = 2.65 (s, 3H, -S-CH_3); 6.96 (s, 1H, =CH); 7.03 (dd, $^3J_{H\text{-}H}$=8.2 Hz, $^4J_{H\text{-}H}$=0.8 Hz, 1H, -Ar-*p*-H); 7.29 (t, 1H, -Ar-*m*-H); 7.33 (s, 1H, -Ar-*o*-H); 7.39 (d, $^3J_{H\text{-}H}$=8.2 Hz, 1H, -Ar-*o*-H); 15.09 (s, 1H, -C-OH). ^{13}C{^{1}H} NMR (101 MHz, CD_2Cl_2): δ = 17.4 (-CH_3); 108.2 (-Ar-*o*-C); 113.8 (=CH); 118.8 (-Ar-*o*-C); 119.5 (-Ar-C1); 130.3 (-Ar-*m*-C); 135.9 (-Ar-*p*-C); 157.1 (-Ar-C-OH); 169.3 (-C-OH); 217.8 (-C=S). MS (DEI): m/z = 226, 179, 121.Elemental analysis: calculated for $C_{10}H_{10}O_2S_2$ C: 53.07%; H: 4.45%; S:28.34%, found: C: 52.99%; H: 4.55%; S: 27.74%.

4'-Hydroxy-β-hydroxy dithiocinnamic methyl ester(L8).

Synthesis was performed according to general procedure 1. 4'-Hydroxy-acetophenone (8.2 g, 59.90 mmol) was protected with TBDMS (9.0 g, 59.90 mmol) and imidazole (8.16 g, 119.89 mmol) was used.

Yield: 18.73 g (100%) as white crystals. ^{1}H NMR (400 MHz, $CDCl_3$): δ = 0.21 (s, 6H, -Si-$(CH_3)_2$); 0.96 (s, 9H, -C-$(CH_3)_3$); 2.52 (s, 3H -CH_3); 8.84 (d, $^3J_{H\text{-}H}$=8.8 Hz, 2H, -Ar-*o*-H); 7.85 (d, $^3J_{H\text{-}H}$= 8.8 Hz 2H, -Ar-*m*-H).

^{13}C{^{1}H} NMR (101 MHz, $CDCl_3$): δ = -4.1 (-Si-$(CH_3)_2$); 18.2 (q, -C-$(CH_3)_3$); 25.6 (-C-$(CH_3)_3$); 26.3 (-CH_3); 119.8 (-Ar-*o*-C); 130.5 (-Ar-*m*-C); 130.8 (-Ar-C1); 160.2 (-Ar-*p*-C-O-); 196.8 (-C=O). MS (ESI): m/z = 250, 193, 151.

The 4'-TBDMS-acetophenone (5.0 g, 19.97 mmol) and CS_2 (1.70 ml, 27.95 mmol) were dropped to the *t*-BuOK (4.5 g, 39.93 mmol) solution. Methyliodide (1.00 ml, 19.97 mmol) was used. Column chromatography mobile phase: DCM 2:hexane 1. Yield: 3.25 g (47.8%) as green crystals. ^{1}H NMR (600 MHz, $CDCl_3$): δ = 0.21 (s, 6H, -Si-$(CH_3)_2$); 0.97 (s, 9H, -C-$(CH_3)_3$); 2.63 (s, 3H, -S-CH_3); 6.87 (d, $^3J_{H\text{-}H}$=8.8 Hz, 2H, -Ar-*o*-H); 6.91 (s, 1H, =CH); 7.78 (d, $^3J_{H\text{-}H}$=8.8 Hz, 2H, -Ar-*m*-H); 15.15 (s, 1H, -C-OH). ^{13}C{^{1}H} NMR (101 MHz, $CDCl_3$): δ = -4.4 (-Si-$(CH_3)_2$); 16.9 (-CH_3); 18.2 (q, -C-$(CH_3)_3$); 25.6 (-C-$(CH_3)_3$); 107.2 (=CH); 120.3 (-Ar-*m*-C); 126.8 (-Ar-*o*-C); 128.6 (-Ar-C1); 159.5 (-Ar-*p*-C-O-); 196.6 (-C-OH); 215.7 (-C=S). MS (EI): m/z = 341, 293, 235.

The 4'-TBDMS-β-hydroxy dithiocinnamic methyl ester (3.25 g, 9.54 mmol) was deprotected with TBAF (19.1 ml, 19.1 mmol). Column chromatography mobile phase: hexane 2:DCM 1 - hexane 1 : DCM 1 - hexane 1 : DCM 3. Yield: 2.16 g (90.7%) as yellow crystals. ^{1}H NMR (400 MHz, CD_2Cl_2): δ = 2.60 (s, 3H, -S-CH_3); 6.82 (d, $^3J_{H\text{-}H}$=9.0 Hz, 2H, -Ar-*o*-H); 6.88 (s, 1H, =CH); 7.75 (d, $^3J_{H\text{-}H}$=9.0 Hz, 2H, -Ar-*m*-H). ^{13}C{^{1}H} NMR (101 MHz, CD_2Cl_2): δ = 16.7 (-CH_3); 106.8 (=CH); 115.5 (-Ar-*o*-C); 126.1 (-Ar-C1); 128.7 (-Ar-*m*-C); 158.9 (-Ar-C-OH); 169.2 (-C-OH); 215.8 (-C=S). MS (DEI): m/z = 226, 179, 121. Elemental analysis: calculated for $C_{10}H_{10}O_2S_2$ C: 53.07%; H: 4.45%; S:28.34%, found: C: 53.52%; H: 4.52%; S: 28.27%.

3'-Hydroxy-β-hydroxy dithiocinnamic ethyl ester (L9).

Synthesis was performed according to general procedure 1, first step is similar to L7.

The 3'-TBDMS-acetophenone (5.0 g, 19.97 mmol) and CS_2 (1.70 ml, 27.95 mmol) was dropped to the *t*-BuOK (4.5 g, 39.93 mmol) solution. Ethyliodide (1.61 ml, 19.97 mmol) was used. Column chromatography mobile phase: DCM 2:hexane 1. Yield: 4.67 g (66.7%) as brown oil. ^{1}H NMR (600 MHz, $CDCl_3$): δ = 0.22 (s, 6H, -Si-$(CH_3)_2$); 0.99 (s, 9H, -C-$(CH_3)_3$); 1.37 (t, 3H, -S-CH_2-CH_3); 3.25 q, 2H, -S-CH_2-); 6.85 (s, 1H, =CH); 6.96 (dd, $^3J_{H\text{-}H}$=8.1 Hz, 1H, -Ar-*p*-H); 7.27 (t, 1H, -Ar-*m*-H); 7.34 (s, 1H, -Ar-*o*-H); 7.43 (d, $^3J_{H\text{-}H}$=7.9 Hz, 1H, -Ar-*o*-H); 15.11 (s, 1H, -C-OH). ^{13}C{^{1}H} NMR (101 MHz, $CDCl_3$): δ = -4.4 (-Si-$(CH_3)_2$); 12.9 (-S-CH_2-CH_3); 18.2 (q, -C-$(CH_3)_3$); 25.6 (-C-$(CH_3)_3$); 27.8 (-S-CH_2-); 107.9 (=CH); 118.2 (-Ar-*o*-C); 119.5 (-Ar-

o-C); 123.5 (-Ar-*p*-C); 129.6 (-Ar-*m*-C); 135.7 (-Ar-C1); 156.0 (-Ar-*m*-C-O-); 169.0 (-C-OH); 216.4 (-C=S). MS (EI): m/z = 354, 293, 235, 211.
The 3'-TBDMS-β-hydroxy dithiocinnamic ethyl ester (4.7 g, 13.2 mmol) was deprotected with TBAF (26.3 ml, 26.3 mmol). Column chromatography mobile phase: hexane 2:DCM 1 - hexane 1 : DCM 1 - hexane 1 : DCM 3. Yield: 3.14 g (81.1%) as brown oil. ^{1}H NMR (400 MHz, CD_2Cl_2): δ = 1.37 (t, 3H, -S-CH_2-CH_3); 3.26(q, 2H, -S-CH_2-); 6.91 (s, 1H, =CH); 7.04 (d, $^{3}J_{H-H}$=8.2 Hz, 1H, -Ar-*p*-H); 7.32 (t, 1H, -Ar-*m*-H); 7.34 (s, 1H, -Ar-*o*-H); 7.42 (d, $^{3}J_{H-H}$=8.2 Hz, 1H, -Ar-*o*-H); 15.14 (s, 1H, -C-OH). ^{13}C{^{1}H} NMR (101 MHz, CD_2Cl_2): δ = 13.0 (-S-CH_2-CH_3); 28.3 (-S-CH_2-); 108.2 (-Ar-*o*-C); 113.8 (=CH); 118.9 (-Ar-*o*-C); 119.5 (-Ar-C1); 130.3 (-Ar-*m*-C); 136.0 (-Ar-*p*-C); 156.9 (-Ar-C-OH); 169.6 (-C-OH); 217.1 (-C=S). MS (DEI): m/z = 301, 214, 211, 179. Elemental analysis: calculated for $C_{11}H_{12}O_2S_2$ C: 54.97%; H: 5.03%; S: 26.68%, found: C: 55.25%; H: 5.02%; S: 27.02%.

4'-Hydroxy-β-hydroxy dithiocinnamic ethyl ester (L10).
Synthesis was performed according to general procedure 1, first step is similar to L8.
The 4'-TBDMS-acetophenone (5.0 g, 19.97 mmol) and CS_2 (1.70 ml, 27.95 mmol) were dropped to the *t*-BuOK (4.5 g, 39.93 mmol) solution. Ethyliodide (1.60 ml, 19.97 mmol) was used. Column chromatography mobile phase: DCM 2:hexane 1. Yield: 3.47 g (48.9%) as green oil. ^{1}H NMR (400 MHz, $CDCl_3$): δ = 0.22 (s, 6H, -Si-$(CH_3)_2$); 0.97 (s, 9H, -C-$(CH_3)_3$); 1.36 (q, 2H, -S-CH_2-CH_3); 3.25(q, 2H, -S-CH_2-); 6.86 (d, $^{3}J_{H-H}$=8.9 Hz, 2H, -Ar-*o*-H); 6.87 (s, 1H, =CH); 7.78 (d, $^{3}J_{H-H}$=8.8 Hz, 2H, -Ar-*m*-H); 15.19 (s, 1H, -C-OH). ^{13}C{^{1}H} NMR (101 MHz, $CDCl_3$): δ = -4.4 (-Si-$(CH_3)_2$); 13.0 (-S-CH_2-CH_3); 18.2 (q, -C-$(CH_3)_3$); 25.6 (-C-$(CH_3)_3$); 27.6 (-S-CH_2-); 107.2 (=CH); 120.3 (-Ar-*m*-C); 126.9 (-Ar-*o*-C); 128.6 (-Ar-C1); 159.5 (-Ar-*p*-C-O-); 196.9 (-C-OH); 214.9 (-C=S). MS (EI): m/z = 354, 293.
The 4'-TBDMS-β-hydroxy dithiocinnamic methyl ester (3.02 g, 8.52 mmol) was deprotected with TBAF (17.1 ml, 17.1 mmol). Column chromatography mobile phase: hexane 2:DCM 1 - hexane 1 : DCM 1 - hexane 1 : DCM 3. Yield: 2.05 g (91.2%) as brown oil. ^{1}H NMR (400 MHz, CD_2Cl_2): δ = 1.37 (t, 3H, -S-CH_2-CH_3); 3.26 (q, 2H, -S-CH_2-); 6.91 (s, 1H, =CH); 6.92 (d, $^{3}J_{H-H}$=9.0 Hz, 2H, -Ar-*o*-H); 7.81 (d, $^{3}J_{H-H}$=9.0 Hz, 2H, -Ar-*m*-H); 15.20 (s, 1H, -C-OH). ^{13}C{^{1}H} NMR (101 MHz, CD_2Cl_2): δ = 13.9 (-S-CH_2-CH_3); 27.8 (-CH_2-); 106.9 (=CH); 115.8 (-Ar-*o*-C); 126.0 (-Ar-C1); 128.9 (-Ar-*m*-C); 159.8 (-Ar-C-OH); 170.1 (-C-OH); 215.2 (-C=S). MS (DEI): m/z = 240, 179, 121. Elemental analysis: calculated for $C_{11}H_{12}O_2S_2$ C: 54.97%; H: 5.03%; S: 26.68%, found: C: 55.06%; H: 4.97%; S: 26.73%.

β-Hydroxy dithiocinnamic methyl ester (L11).
Synthesis was performed according to general procedure 1. Acetophenone (2.0 ml, 16.65 mmol) and CS_2 (1.41 ml, 23.30 mmol) were dropped to the *t*-BuOK (3.7 g, 33.23 mmol) solution. Methyliodide (1.04 ml, 17.00 mmol) was used. Column chromatography mobile phase: DCM 1:hexane 1.5. Yield: 0.19 g (5.4%) as yellow crystals. ^{1}H NMR (400 MHz, $CDCl_3$): δ = 2.59 (s, 1H, -S-CH_3); 6.89 (s, 1H, =CH); 7.38 (m, 3H, -Ar-*o*-H/ -Ar-*p*-H); 7.80 (m, 2H, -Ar-*m*-H); 15.02 (s, 1H, -C-OH). ^{13}C{^{1}H} NMR (101 MHz, $CDCl_3$): δ = 17.1 (-S-CH_3); 107.8 (=CH); 126.7 (-Ar-C1); 128.7 (-Ar-*o*-C); 131.9 (-Ar-*m*-C); 135.0 (-Ar-*p*-C); 169.2 (-C-OH); 217.3 (-C=S). MS (EI): m/z = 240, 211, 210, 163, 135, 105, 91, 85, 77, 51, 45. Elemental analysis: calculated for $C_{11}H_{10}OS_2$ C: 57.11%; H: 4.79%; S: 30.49%, found: C: 57.50%; H: 4.77%; S: 31.01%.

β-Hydroxy dithiocinnamic ethyl ester (L12).
Synthesis was performed according to general procedure 1. Acetophenone (2.4 ml, 20.81 mmol) and CS_2 (1.80 ml, 29.13 mmol) were dropped to the *t*-BuOK (4.7 g, 41.62 mmol) solution. Ethyliodide (1.70 ml, 20.81 mmol) was used. Column chromatography mobile phase: DCM 1:hexane 1. Yield: 3.15 g (67%) as green oil. ^{1}H NMR (400 MHz, $CDCl_3$): δ = 1.38 (-S-CH_2-CH_3); 3.27 (q, 2H, -S-CH_2-); 6.90 (s, 1H, =CH); 7.46 (m, 3H, -Ar-*o*-H/ -Ar-*p*-H); 7.86 (m, 2H, -Ar-*m*-H); 15.16 (s, 1H, -C-OH). ^{13}C{^{1}H} NMR (101 MHz, $CDCl_3$): δ = 12.8 (-S-CH_2-CH_3); 27.8 (-S-CH_2-); 107.7 (=CH); 126.5 (-Ar-C1); 128.6 (-Ar-*o*-C); 131.7 (-Ar-*m*-C); 134.1 (-Ar-*p*-C); 169.4 (-C-OH); 216.3 (-C=S).MS (EI): m/z = 227, 224, 196, 163, 134, 105, 91, 85, 77, 51. Elemental analysis: calculated for $C_{11}H_{12}OS_2$ C: 58.89%; H: 5.39%; S: 28.58%, found: C: 58.69%; H: 5.30%; S: 28.60%.

Additional molecular structures

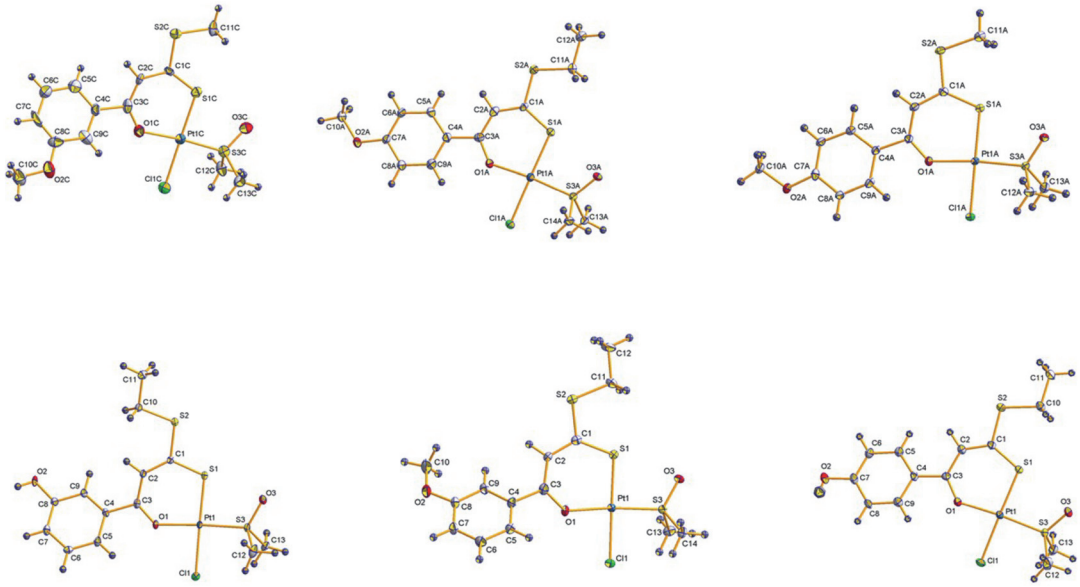

Figure S1. Molecular strucutres (50% propability) for **Pt2, Pt3, Pt5, Pt6, Pt9, Pt10**

Additional stability determinations

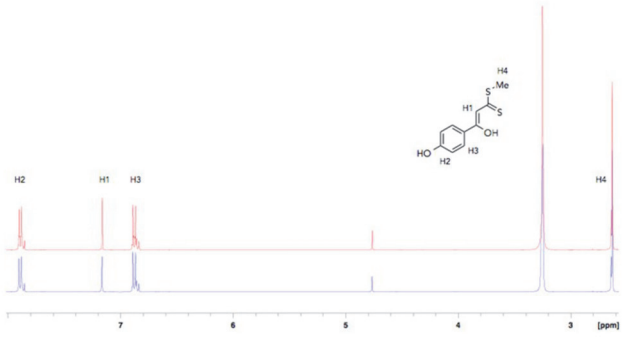

Figure S2. Stability determination of **L8** using ^{1}H NMR spectroscopy, Conditions: 600 MHz, 37 °C, dmso-d_6. Blue: first measurement (starting point), red: after 48 h. All compounds are stable under this conditions.

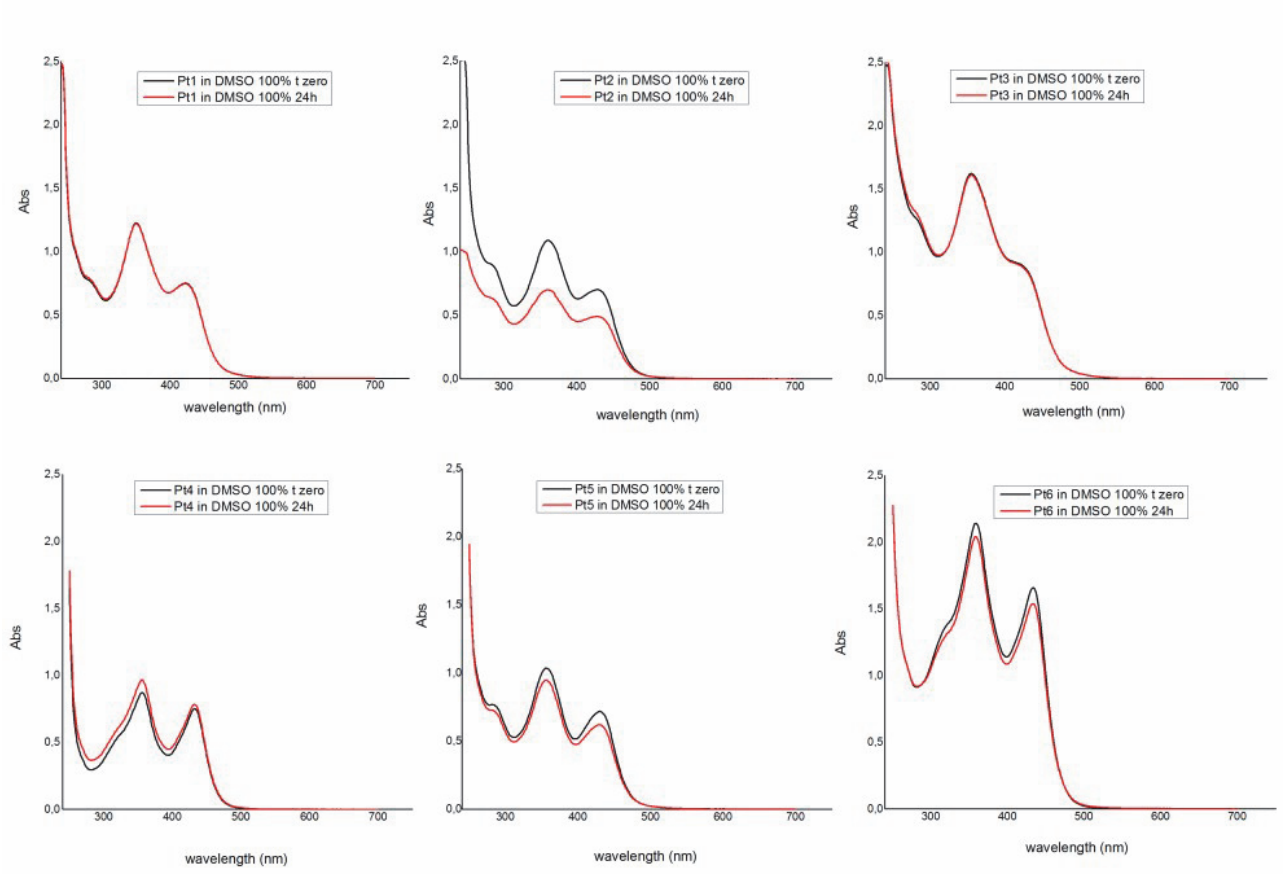

A

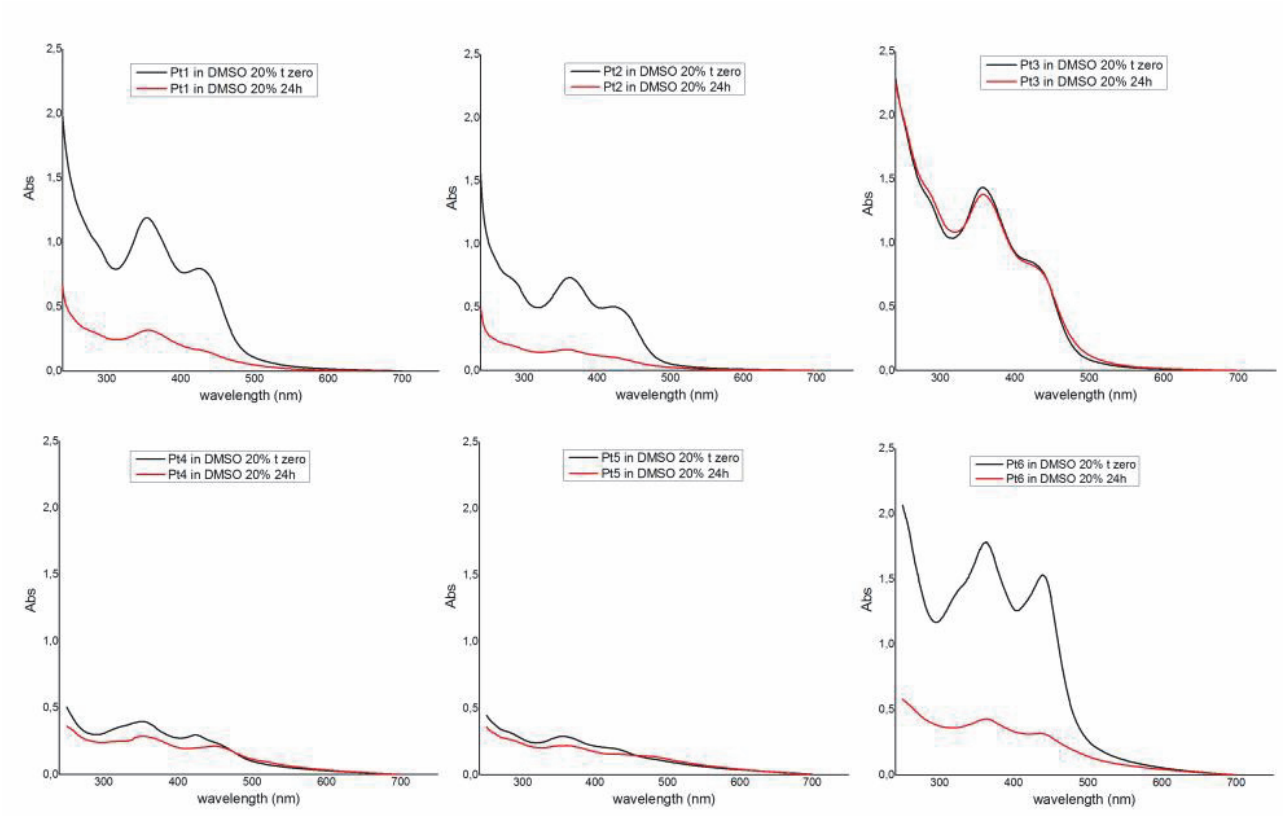

B

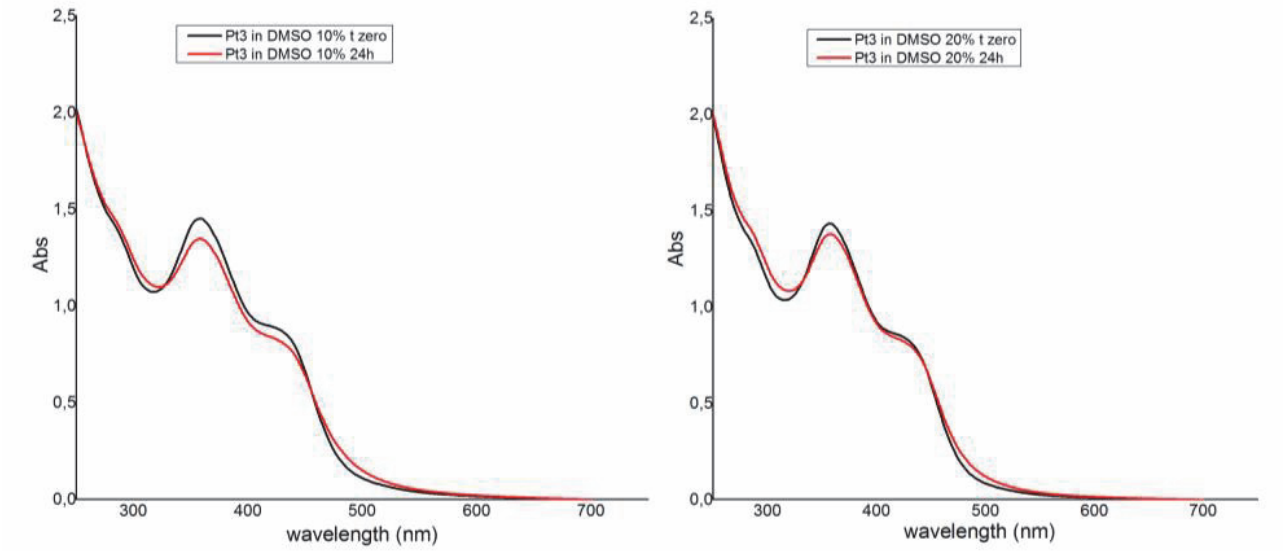

C

Figure S3. UV–visible spectra of compound **Pt1-Pt6** (1mM) in pure dmso (A) and in aqueous solutions containing 10% and 20% dmso (B). In panel C UV-Visible spectra of **Pt3** (1mM) in solution containing 10% and 20% dmso are reported. All spectra were collected after dissolution (black) and after 24 h of incubation (red).

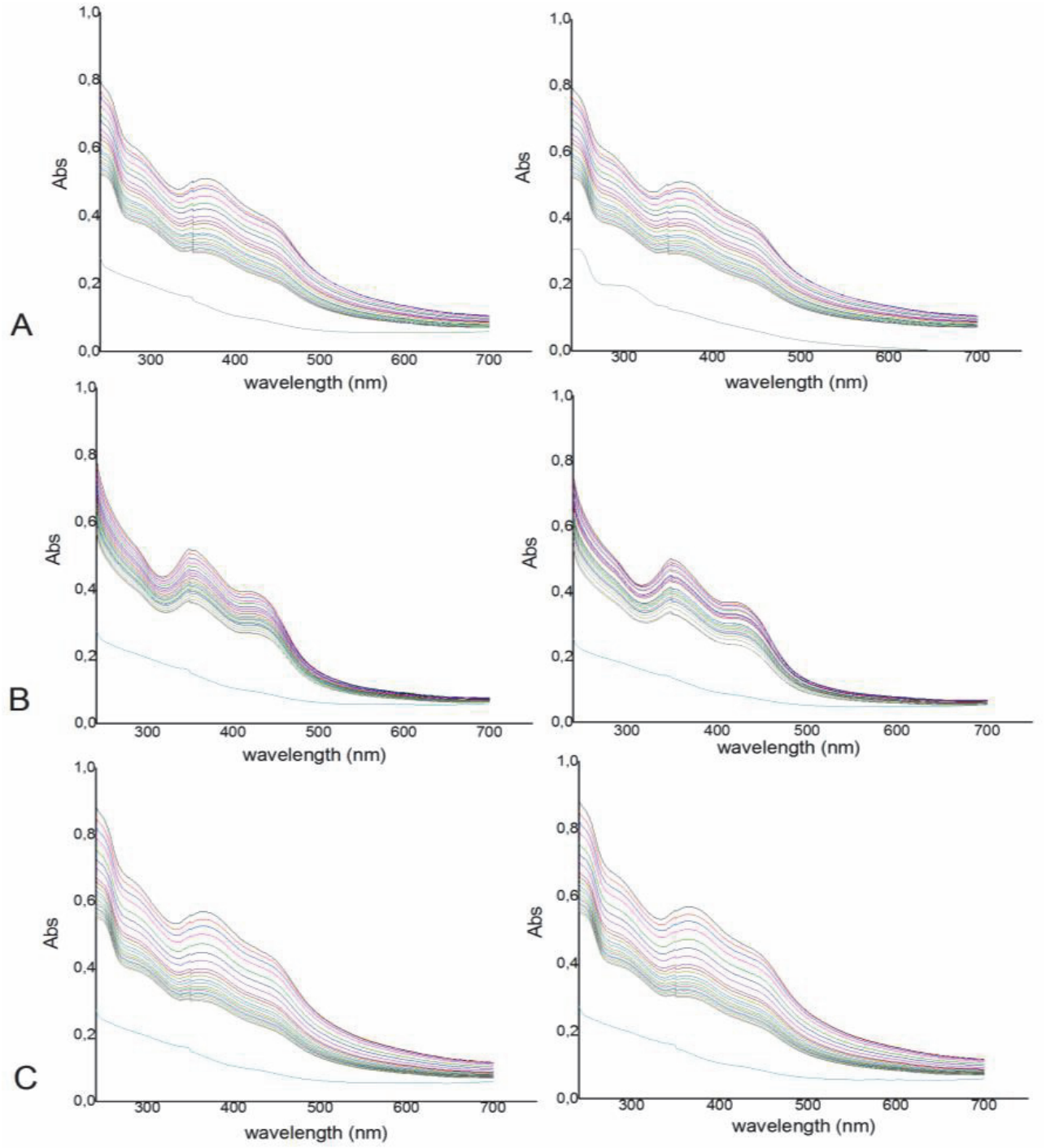
A
B
C
Abs
wavelength (nm)
1,0
0,8
0,6
0,4
0,2
0,0
300
400
500
600
700

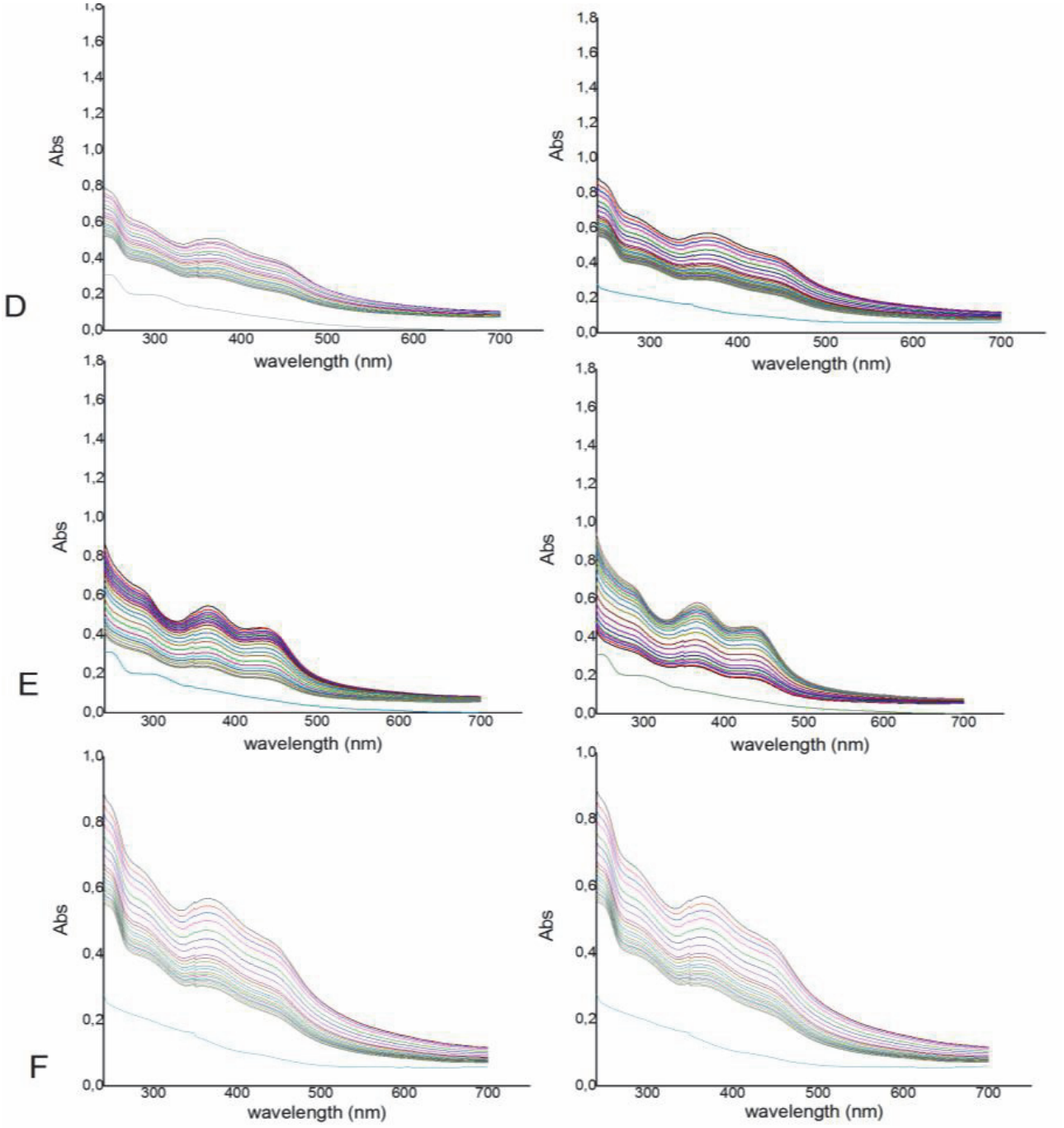

Figure S4. UV–visible spectra of 0.04 mM **Pt1-Pt6** (panels A…F) in 10 mM PBS pH 7.4 (left) and 0.9% NaCl (right) followed each 10 minutes for 3 hours and upon 24 h.

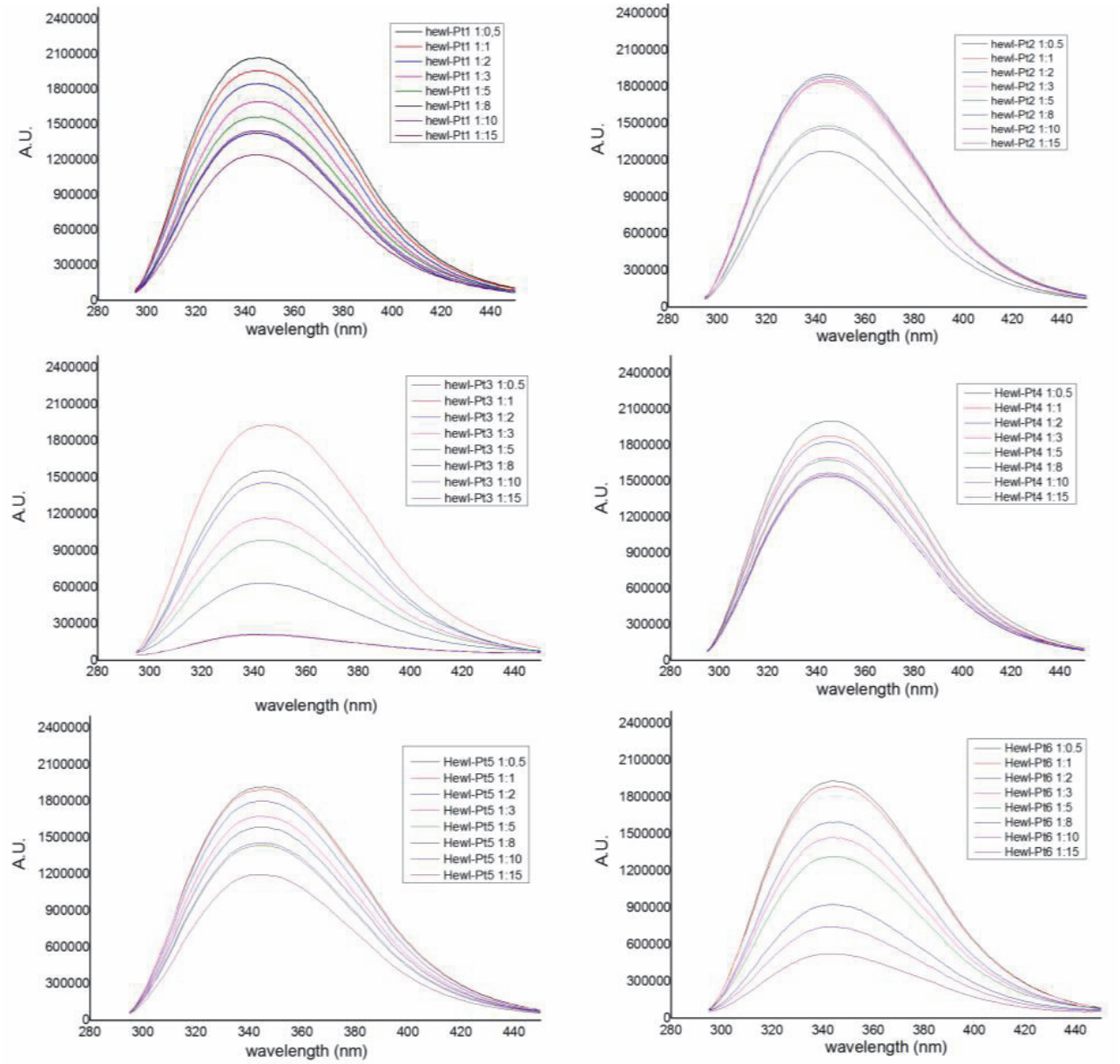

Figure S5. Fluorescence quenching spectra of HEWL (0.1 mg x mL-1) with different concentrations of **Pt1-Pt6** upon excitation at λ=280 nm at 300 K in 10 mM sodium acetate pH 4.4 (1.4% dmso) Spectra collected after excitation at λ=295 nm are reported in Figure S6.

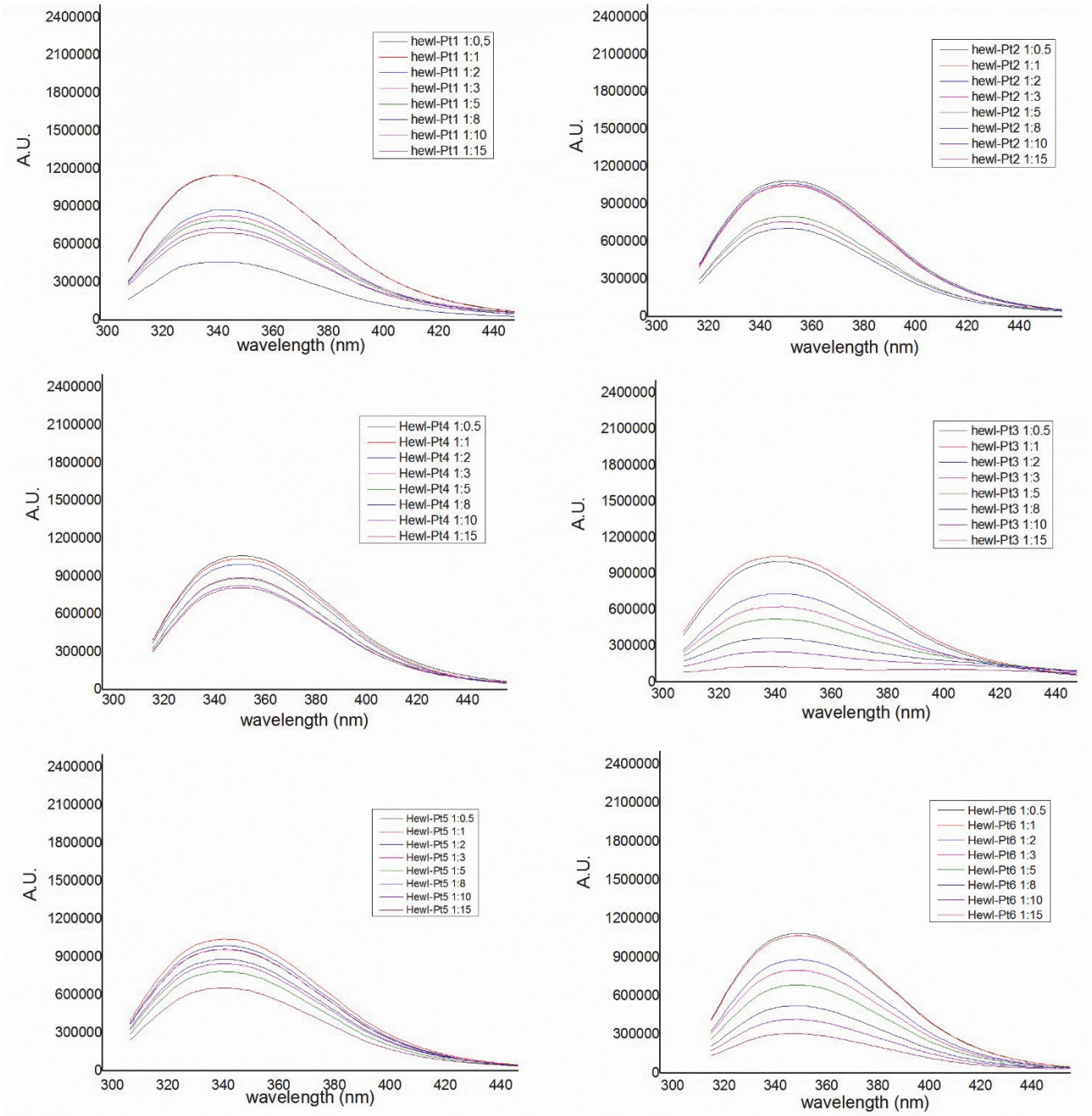

Figure S6. Fluorescence quenching spectra of HEWL (o.1 mg x mL -1) with different concentrations of Pt1-Pt6 upon excitation at 295 nm at 300 K in 10 mM sodium actetate pH 4.4 (1.4% dmso).

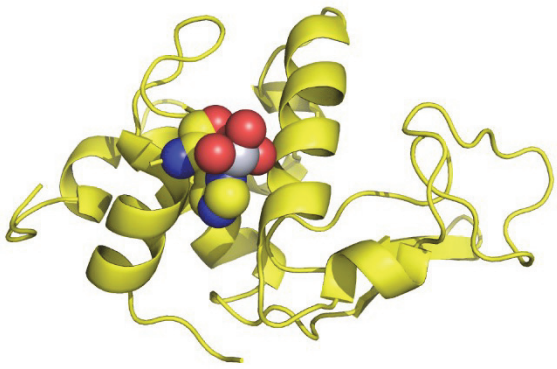

Figure S7. Cartoon representation of the HEWL-**Pt1** structure. The side chain of His15 and the Pt centre with its ligands are also shown as sphere.

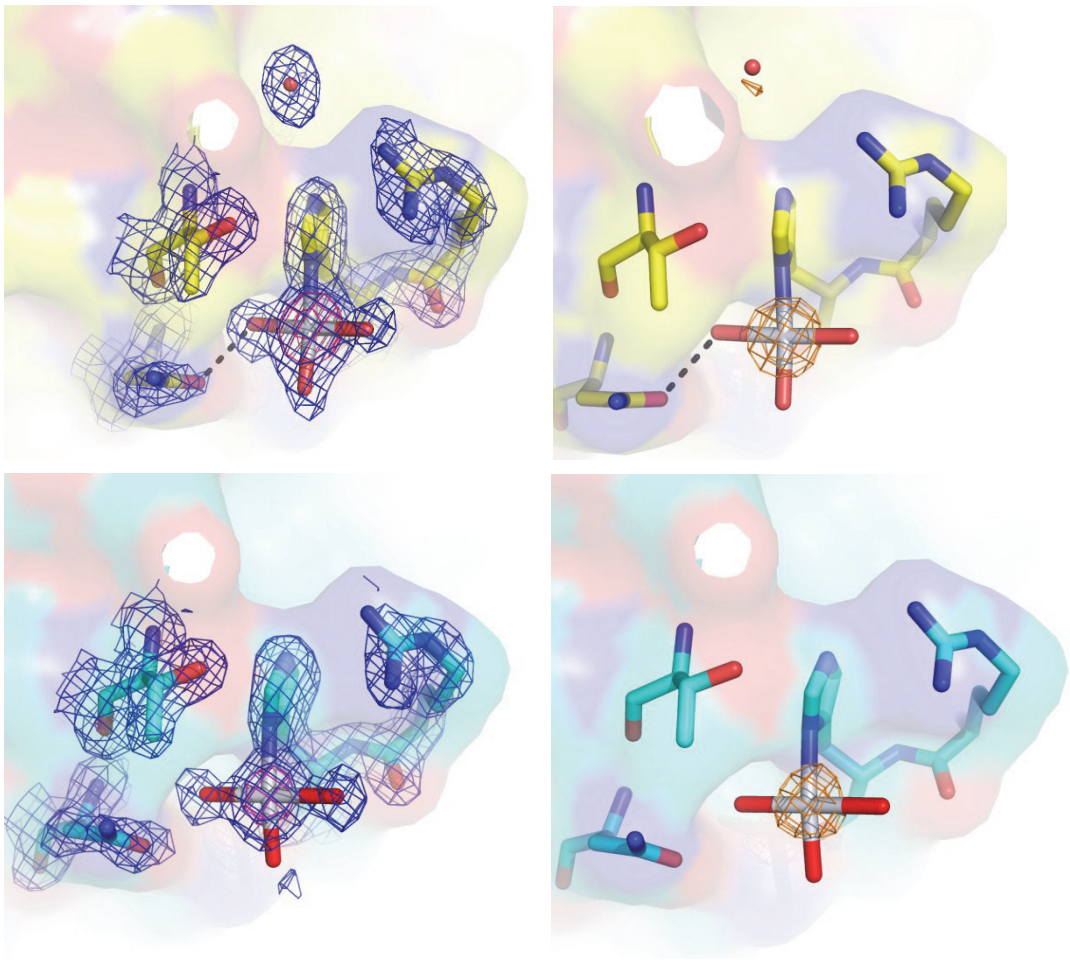

Figure S8. 2Fo – Fc electron density maps of the Pt binding sites in the HEWL-**Pt1** (panel A) and HEWL-**Pt2** (panel B) structures contoured at 1 σ (blue) and 4 σ (purple) obtained after model building and refinement. In panel C and D, anomalous electron density map of the Pt binding site in the two structures (contoured at 4.0 σ, gray) are also reported.

To verify the behavior of the compounds in the solution used to crystallize the adducts with HEWL, the absorption spectra of **Pt1**, in the absence and in the presence of HEWL, were registered in 1.1 M NaCl, 0.1 M sodium acetate pH 4.0 (Figure S9). In these solutions, the concentration of dmso is less than 1%. Under these experimental conditions, the compounds completely degrade: when spectra collected after 24 h were compared to those obtained at t = 0 h, significant changes were observed. In the presence of the protein (Figure S9), the degradation process is even more rapid.

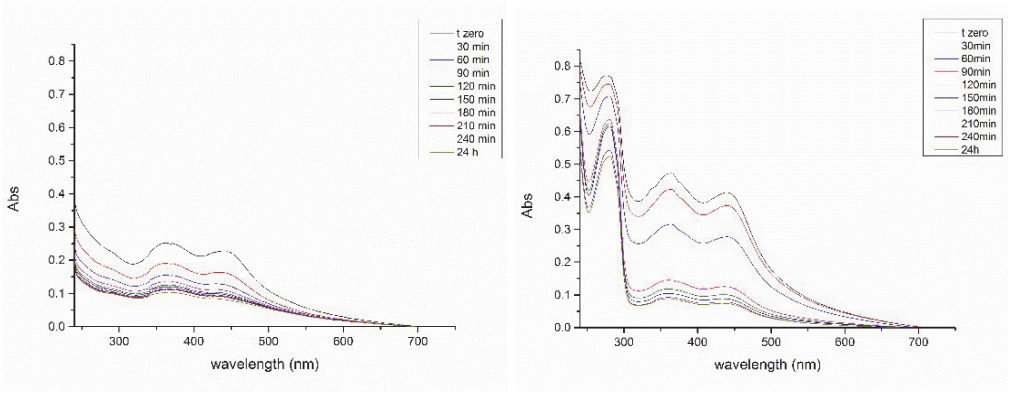

Figure S9. UV–visible time-course spectra of compound **Pt1** (0.6 mM) in the crystallization conditions in the absence (left) and in the presence of HEWL (right) over 4 h and upon 24 h. The Pt/HEWL ratio was 3:1

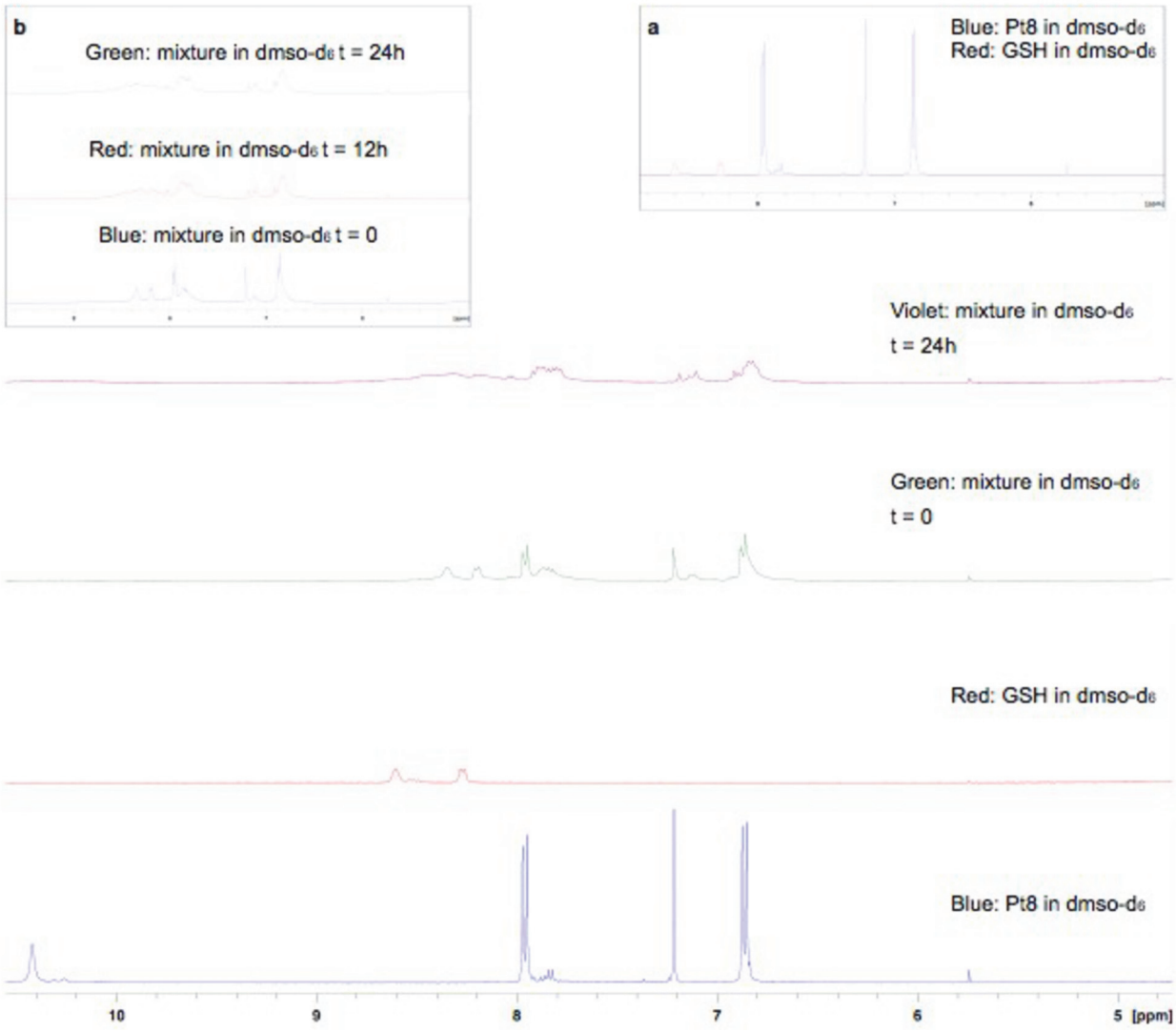

Figure S10. ^{1}H NMR spectroscopic investigation studying the interaction of Pt8 with glutathione

Table S1: Crystal data and refinement details for the X-ray structure determinations of the compounds **L1 - Pt3.**

Compound	**L1**	**L7**	**Pt1**	**Pt2**	**Pt3**
formula	$C_{11}H_{12}O_2S_2$	$C_{10}H_{10}O_2S_2$	$C_{13}H_{17}ClO_3PtS_3$	$C_{13}H_{17}ClO_3PtS_3$	$C_{13}H_{17}ClO_3PtS_3$
fw ($g \cdot mol^{-1}$)	240.33	226.30	547.99	547.99	547.99
°C	-140(2)	-140(2)	-140(2)	20(2)	-140(2)
crystal system	monoclinic	triclinic	monoclinic	trigonal	triclinic
space group	P 2_1/c'	P $\bar{1}$	P 2_1/c	P 3 c 1	P $\bar{1}$
a/ Å	10.4024(4)	3.9126(1)	10.9758(2)	34.3480(5)	7.2182(3)
b/ Å	14.0954(6)	11.6243(5)	19.2769(4)	34.3480(5)	10.6518(4)
c/ Å	7.7684(3)	22.2479(9)	8.0124(2)	7.2750(1)	22.3309(7)
α/°	90	98.186(2)	90	90	93.262(2)
β/°	92.530(2)	90.339(2)	96.398(1)	90	97.228(2)
γ/°	90	94.310(2)	90	120	100.948(2)
V/Å^3	1137.94(8)	998.58(6)	1684.70(6)	7433.04(18)	1666.54(11)
Z	4	4	4	18	4
ρ ($g \cdot cm^{-3}$)	1.403	1.505	2.161	2.204	2.184
μ (cm^{-1})	4.44	5.01	88.64	90.4	89.6
measured data	8017	6425	13229	64398	20804

data with $I > 2\sigma(I)$	2245	3245	3691	8758	6602
unique data (R_{int})	2583/0.0410	4098/0.0475	3830/0.0254	11219/0.0559	7539/0.0365
wR_2 (all data, on F^2)[a)]	0.1145	0.1506	0.0371	0.1397	0.0695
R_1 ($I > 2\sigma(I)$) [a)]	0.0493	0.0737	0.0162	0.0548	0.0296
S [b)]	1.166	1.169	1.098	1.064	1.041
Res. dens./e·Å^{-3}	0.467/-0.261	0.482/-0.432	0.548/-0.851	1.691/-1.083	1.127/-1.131
Flack-parameter	-	-	-	0.131(9)	-
absorpt method	multi-scan	multi-scan	multi-scan	multi-scan	multi-scan
absorpt corr $T_{min/max}$	0.6615/0.7456	0.6831/0.7456	0.5485/0.7456	0.0047/0.0206	0.6358/0.7456
CCDC No.	1446182	1446183	1446184	1446185	1446186

cont. Table S1: Crystal data and refinement details for the X-ray structure determinations of the compounds **Pt5 - Pt10.**

Compound	**Pt5**	**Pt6**	**Pt7**	**Pt9**	**Pt10**
formula	$C_{14}H_{19}ClO_3PtS_3$	$C_{14}H_{19}ClO_3PtS_3$	$C_{12}H_{15}ClO_3PtS_3$	$C_{13}H_{17}ClO_3PtS_3$	$C_{13}H_{17}ClO_3PtS_3$

fw ($g \cdot mol^{-1}$)	562.01	562.01	533.96	547.99	547.99
°C	-140(2)	-140(2)	-140(2)	-140(2)	-140(2)
crystal system	orthorhombic	monoclinic	monoclinic	monoclinic	monoclinic
space group	P b c n	C 2/c	P 2_1/c	P 2_1/c	P 2_1/c
a/ Å	18.6150(6)	22.8319(7)	12.8077(4)	12.8292(3)	5.6743(3)
b/ Å	7.3343(2)	7.1574(2)	16.5312(5)	17.2475(5)	10.8876(5)
c/ Å	27.2528(8)	43.9897(13)	7.3048(2)	7.3364(2)	28.1150(14)
α/°	90	90	90	90	90
β/°	90	96.662(1)	92.120(2)	92.953(2)	94.890(1)
γ/°	90	90	90	90	90
V/Å^3	3720.77(19)	7140.1(4)	1545.56(8)	1621.18(7)	1730.61(15)
Z	8	16	4	4	4
ρ ($g \cdot cm^{-3}$)	2.007	2.091	2.295	2.245	2.103
μ (cm^{-1})	80.29	83.68	96.58	92.11	86.29
measured data	21956	42371	3469	11189	9805
data with I > 2σ(I)	3588	7346	2718	3382	3257
unique data (R_{int})	4083/0.0728	8138/0.0457	3469/0.0211	3691/0.0385	3467/0.0401

wR_2 (all data, on F^2)[a)]	0.0825	0.0918	0.0512	0.0566	0.0690
R_1 ($I > 2\sigma(I)$) [a)]	0.0378	0.0426	0.0281	0.0248	0.0313
S [b)]	1.157	1.073	1.022	1.076	1.139
Res. dens./e·Å^{-3}	2.083/-1.628	1.192/-1.264	1.355/-1.039	0.874/-1.330	2.890/-1.026
absorpt method	multi-scan	multi-scan	multi-scan	multi-scan	'multi-scan'
absorpt corr $T_{min}/_{max}$	0.5777/0.7456	0.6226/0.7456	0.6128/0.7456	0.5549/0.7456	0.5413/0.7456
CCDC No.	1446187	1446188	1446189	1446190	1446191

[a)] Definition of the *R* indices: $R_1 = (\Sigma\,||F_o|-|F_c||)/\Sigma|F_o|$;
$wR_2 = \{\Sigma[w(F_o^2-F_c^2)^2]/\Sigma[w(F_o^2)^2]\}^{1/2}$ with $w^{-1} = \sigma^2(F_o^2) + (aP)^2+bP$; $P = [2F_c^2 + Max(F_O^2]/3$;
[b)] $s = \{\Sigma[w(F_o^2-F_c^2)^2]/(N_o-N_p)\}^{1/2}$.

Additional NMR Data

Table S2 shows the averages for these signals which are presented with respect to carbon side chain. It doesn't matter if aromatic-substitution is a hydroxy-group in case of compounds **7-10** or a methoxy-group in same position **2-6**. Compounds **11/12** just showing multipletts for their aromatic signals. For *para*-substituted compounds (**3/6,8/10**) there are two dubletts observed, because of symmetric substitution of these molecules. For *meta*-substituted molecules (**2/5, 7/9**) different signals are observed for protons in *ortho*-position. Compounds **1/4** which have an *ortho*-methoxy group show signals as proposed for these types of compounds with $^4J_{H\text{-}H}$ coupling.

Table S2. ^{1}H NMR spectroscopy data: Average chemical shifts for all aromatic proton signals. Platinum(II) complexes show same pattern as their corresponding ligands, also alkyl-substitution makes no differences so substance code is shown averages for all four substances.

^{1}H NMR Ar	**1/4**	**2/5**	**3/6**	**7/9**	**8/10**	**11/12**
ortho-postition	1. d (1H) δ~7.0 2. -OMe	1. m (1H) δ~7.5 2. m (1H) δ~7.5	d (2H) δ~6.9	1. s (1H) δ~7.4 2. d (1H) δ~7.4	d (2H) δ~6.8	m (2H) δ~7.5
meta-position	1. dd (1H) δ~7.8 2. ddd (1H) δ~7.0	1. t (1H) δ~7.3 2. -OCH_3	d (2H) δ~7.9	1. t (1H) δ~7.3 2. -OH	d (2H) δ~7.8	m (2H) δ~8.0
para-position	ddd (1H) δ~7.5	dd (1H) δ~7.1	-OCH_3	d/dd (1H) δ~7.0	-OH	m (1H) δ~7.5

Table S3. Data collection and refinement statistics.

Data collection	***Pt1***	***Pt2***	***Pt3***	***Pt4***
PDB code	5IHG	5ILC	5II3	5ILF
Space group	$P4_32_12$	$P4_32_12$	$P4_32_12$	$P4_32_12$
Unit cell parameter				
a=b (Å)	77.575	77.407	78.208	77.983
c (Å)	37.253	37.347	37.005	37.281
Observed reflections	71098	76725	79606	52253
Unique reflections	11472	11233	11254	10170
Resolution (Å)	54.85-1.75 (1.78-1.75)	54.74-1.75 (1.78-1.75)	55.30-1.78 (1.81-1.78)	55.14-1.85 (1.88-1.85)
Completeness (%)	95.3 (64.2)	93.7 (70.7)	97.6 (81.4)	98.6 (90.4)
Rmerge	0.058 (0.507)	0.040 (0.220)	0.052 (0.231)	0.042 (0.134)
I/σ(I)	44.1 (2.3)	7.6 (6.1)	49.1 (6.4)5	9.1 (5.1)
Multiplicity	6.2 (2.9)	6.8 (3.1)	7.1 (3.8)	5.1 (2.8)
Refinement				
Resolution (Å)	54.85-1.75	54.74-1.75	55.30-1.78	55.14-1.85
N. of reflections in working set	10868	10646	10677	9669
N. of reflections in test set	580	556	546	478
R factor (%)	16.1	15.8	15.3	16.6
Rfree (%)	20.3	21.1	19.0	23.3
Rall (%)	16.3	16.1	15.5	17.0
Number of non-H atoms	1176	1219	1172	1178

Mean B-value (Å)	29.9	25.6	21.3	24.2
Ramachandran values				
Most favoured (%)	97.4	91.3	97.6	95.0
Additional allowed (%)	2.6	8.7	2.4	5.0
Generously allowed (%)	0	0	0	0
Disallowed (%)	0	0	0	0
R.m.s.d. bonds (Å)	0.015	0.020	0.015	0.020
R.m.s.d. angles (°)	1.82	1.92	1.68	1.73

References

[1] K. Schubert, T. Alpermann, T. Niksch, H. Goerls and W. Weigand, *Z. Anorg. Allg. Chem.* **2006**, *632*, 1033-1042.
[2] R. Saumweber, C. Robl and W. Weigand, *Inorg. Chim. Acta* **1998**, *269*, 83-90.
[3] K. Schubert, R. Saumweber, H. Goerls and W. Weigand, *Z. Anorg. Allg. Chem.* **2003**, *629*, 2091-2096.
[4] K. Schubert, H. Goerls and W. Weigand, *Z. Naturforsch., B: Chem. Sci.* **2007**, *62*, 475-482.

4.4 [JH4]

Novel Nickel(II), Palladium(II), and Platinum(II) complexes with O,S-bidendate cinnamic acid ester derivatives: An *in vitro* cytotoxic comparison to Ruthenium(II) and Osmium(II) Analogues

Jana Hildebrandt, Norman Häfner, Helmar Görls, Matthias Dürst, Ingo B. Runnebaum, Wolfgang Weigand

in preparation

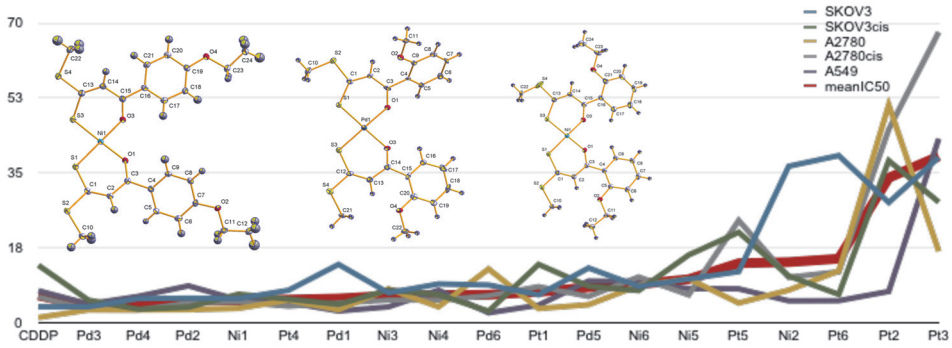

In this publication we report on 18 novel metal(II) complexes, with nickel(II), palladium(II) and platinum(II). All compounds have been synthesized, characterized with standard methods, *e.g.* NMR spectroscopy and X-ray structures and have been compared to their corresponding β-Hydroxydithiocinnamic acid esters which act as O,S-bidendate ligands. IC50 values of the compounds show promising results especially for the palladium(II) molecules which are in general more active on different cancer cell lines than the reference substance Cisplatin. Additionally, it is shown that the most active complexes show low activity on non-cancerous cell lines and are specifically active on Cisplatin resistant cell lines compared to the sensitive counterparts. Next to the investigation of the new compounds comparisons to Ptdmso, Ru and Os compounds, for the chemical and structural characteristics as well as the IC50 values have been carried out.

Part 1

Novel Nickel(II), Palladium(II), and Platinum(II) complexes with O,S-bidendate cinnamic acid ester derivatives: An *in vitro* cytotoxic comparison to Ruthenium(II) and Osmium(II) Analogues

Jana Hildebrandt[1,2], Norman Häfner[2], Helmar Görls[1], Matthias Dürst[2], Ingo B. Runnebaum[2], Wolfgang Weigand[1]

[1] Institut für Anorganische und Analytische Chemie Friedrich-Schiller Universität Jena, Humboldtstraße 8, 07743 Jena, Germany

[2]Department of Gynecology, Jena University Hospital – Friedrich-Schiller University Jena

Abstract

Since the discovery of Cisplatins' cytotoxic properties, platinum(II) compounds gain high interest for anticancer drug development. During the last years, classical structure-activity relationships have been broken by some promising new platinum based compounds. Next to this, other metals as an alternative to platinum are analyzed, mainly ruthenium, copper, gold and palladium. In this study we focus on 18 different complexes with β-Hydroxydithiocinnamic acid esters as O,S-bidendate ligands for nickel(II), palladium(II) and platinum(II) complexes. These compounds are discussed for their chemical characteristics as well as their cytotoxic potential *in vitro* cell culture assays. Next to this we compare our new data with recently reported different platinum(II), ruthenium(II) and osmium(II) complexes based on the same main ligand system. Results show a promising new palladium(II) candidate for further studies, Pd3.

Introduction

Cisplatin was first synthesized by M. Peyrone in 1845, while its anticancer properties have been discovered by accident of B. Rosenberg and coworkers in 1965.[Kelland, 2007; Rosenberg, 1965] Rosenbergs' discovery led to the ap-

proval of the drug by the FDA in 1979.[Dilruba, 2016] The proposed mechanism of action involves binding to its main target, the DNA through DNA-bases especially guanine and formation of intra- and interstrand adducts which lead to an activation of several intracellular signal pathways including apoptosis and the distortion of the helical DNA structure.[Kelland, 2007; Brabec, 2017; Jungwirth, 2012; Messori, 2016] Unfortunately, Cisplatins' therapy is limited by toxic side effects, unselectivity of the drug and resistance mechanisms.[Dilruba, 2016; Gibson, 2016; Kelland, 2007] Therefore soon after Cisplatins' development, the design of new platinum(II) drugs have been started, leading to the worldwide approval of Carboplatin and Oxaliplatin.[Kelland, 2007; Dilruba, 2016] Both drugs follow the structure-activity-relationships (SARs) of Cisplatin, they are square-planar neutral *cis*-platinum(II) complexes with inert ammine or chelating diamine ligands and two semilabile chlorids or oxygen-coordinated bidendate ligands, which lead again to resistances and side effects.[Dilruba, 2016; Gibson, 2016] This fact led to a rethinking of the traditional SARs for platinum based drug design and to several new compounds which do not follow this rules.[Johnstone, 2016; Abu-Surrah, 2008] Several reviews in the last years resume the tries of researches for new metal-based drug design*, e.g.* ruthenium and osmium based compounds by Keppler and coworkers in 2018, platinum(II) complexes by Lippard and coworkers in 2016, platinum(IV) prodrugs by Gibson and coworkers in 2016, and palladium based molecules by Huq and coworkers in 2016.[Meier-Menches, 2018; Johnstone, 2016; Gibson, 2016; Alam, 2016]

Platinum based molecules still gain high research interest and many new complexes are designed and developed for their cytotoxic activities using platinum(II) or platinum(IV) as a core of the drug.[Mayr, 2017; Gibson, 2016; Petruzzella, 2017; Petruzzella, 2018; Johnstone, 2016] An excellent review written by Lippard and coworkers classifies new platinum(II) {and platinum(IV)} molecules in three classes: Classical, non-classical and nanodelivery molecules.[Johnstone, 2016] Classical platinum(II) molecules are normally designed to follow SARs of Cisplatin and analogues while targeting for example overexpressed receptors on cancer cell surfaces and therefore enhance the

cellular uptake and the selectivity of the drugs.[Johnstone, 2016] Non-classical compounds are designed to focus on different mechanism of actions, for example *trans*-compounds or monofunctional complexes as well as platinum(II) molecules which do not bind covalent to the DNA, for example metallointercalators which are able to intercalate through the DNA-bases.[Johnstone, 2016; Dilruba, 2016; Johnstone, 2013] We recently reported on platinum(II) complexes bearing an O,S-bidendate ligand, dmso (dimethylsulfoxide) and as a leaving group one chlorid with promising results on Cisplatin resistant cell lines and for their interaction with other targets than the DNA.[Hildebrandt, 2016a; Mügge, 2014; Mügge, 2016]

Beside the intensive research on new compounds with the metals platinum, copper, gold, ruthenium and osmium, palladium complexes are among the most widely investigated molecules for anticancer-drug design.[Alam, 2016] Palladium(II) is a d^8-system similar to platinum(II) and therefore structural analogues of platinum(II) complexes have been synthesized and explored regarding their anticancer properties.[Alam, 2016; Livingstone, 1970; Durig, 1976] However, those analogues do not show an activity comparable to their promising platinum(II) counterparts as the ligand exchange kinetics for palladium(II) complexes are 10^5 times faster and so those compounds do not reach their finally target, hydrolyze quickly after injection and interact with several biomolecules leading to inactivation.[Alam, 2016; Abu-Surrah, 2008; Butour, 1997; Wimmer, 1989; Zhao, 1999] It is accepted, that the palladium analogues of Cisplatin and Carboplatin show no antitumor activity.[Abu-Surrah, 2008] Therefore changing the traditional Cisplatin-based SARs are crucial for the design of probably potent palladium(II) complexes. Huq and coworkers reported in 2016 a SARs guide for palladium(II) complexes while comparing 847 palladium complexes.[Alam, 2016] They concluded that palladium(II) compounds follow different rules than platinum(II) complexes and most promising candidates often show specific structural characteristics, such as: Bulky ligands - often chelating-ones; Lipophilicity enhances antitumor-activity; *ortho*-substituted benzyl-rings on ligands show better cytotoxic properties than their *meta*-/ *para*-substituted analogues.[Alam, 2016] In 2015 Azam and coworkers

reported on O,S-bidendate palladium(II) complexes with low cytotoxic activity but promising antiamoebic activity.[Maurya, 2015]

On the well-accepted approach of designing potential metal-based anticancer drugs on other SARs than Cisplatin and analogues, focusing on new mechanism of actions, we report on new platinum(II), palladium(II) and nickel(II) complexes with β-Hydroxydithiocinnamic acid esters as two bidendate, O,S-chelating ligands. We previously reported on the synthesis of this group of compounds in general and add now new insights in their cytotoxic activity, as well as their characterization with *e.g.* molecular structures, and stability determinations in this work.[Weigand, 1993; Saumweber, 1998; Schubert, 2003; Schubert, 2005; Schubert, 2006; Schubert, 2007]

Whereas some studies focus on the comparison of nickel(II) complexes with their platinum/ palladium and copper analogues, most show acceptable but no outstanding cytotoxic activity for nickel complexes.[Haribabu, 2015; Dobrova, 2016] Many classes of metalloproteins exhibit nickel-ions, therefore nickel has some pharmacological properties which may be useful for anticancer drug design.[Haribabu, 2015] Our aim was to determine mainly the activity of non-classical platinum(II) and palladium(II) complexes and compare their activity to their structural nickel(II) analogues and get more information for the most suitable β-Hydroxydithiocinnamic acid ester as ligand. Although, we always compare the metal complexes to the ligand itself for structural and biological interpretations placing nickel as metal lead to a better comparison for the other two metals than compared with their free ligand.

The choose of the β-Hydroxydithiocinnamic acid ester as ligand system is based on our previously described promising results for ruthenium(II) and osmium(II) complexes bearing this as O,S-bidendate ligand as well.[Hildebrandt, 2016b; Hildebrandt, 2018]

Figure 1 shows an overview of compounds discussed in this work.

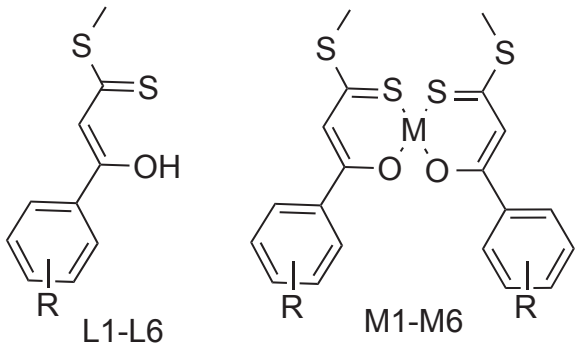

-R	L	Ni	Pd	Pt
-***o*-OMe**	L1	Ni1	Pd1	Pt1
-***m*-OMe**	L2	Ni2	Pd2	Pt2
-***p*-OMe**	L3	Ni3	Pd3	Pt3
-***o*-OEt**	L4	Ni4	Pd4	Pt4
-***m*-OEt**	L5	Ni5	Pd5	Pt5
-***p*-OEt**	L6	Ni6	Pd6	Pt6

Fig. 1: Overview and substance code of compounds this work is dealing with: β-Hydroxydithiocinnamic acid esters L1-L6 and corresponding metal complexes M1-M6 (M= Ni/Pd/Pt).

Results and Discussion

Synthesis and Characterization

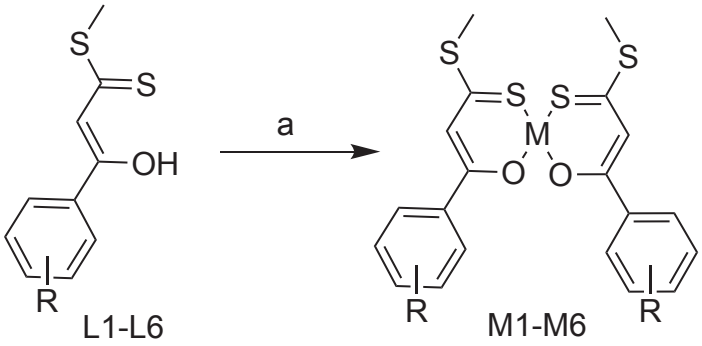

Scheme 1: Reagents and conditions: (a) 2 equiv. L1-L6, 2 equiv. sodiumacetate, 1 equiv. $NiCl_2$* 6 H_2O for Ni1-6, $(PhCN)_2PdCl_2$ for Pd1-6, $(PhCN)_2PtCl_2$ for Pt1-6; acetonitrile; 15 h, rt.

All β-Hydroxydithiocinnamic acid esters L1-L6 have been synthesized and characterized as described previously.[Hildebrandt, 2018; Hildebrandt, 2016a] In a flask, L1-L6 were diluted in 15 ml acetonitrile, deprotonated with sodiumacetate and the corresponding metal salt was added. The reaction mixture was stirred for 15 hours at room temperature, followed by filtration and washing steps with pentane and acetonitrile.

Tab. 1: Selected NMR signals for compounds 2 in [ppm]. Ni, Pd and Pt complexes show similar behavior compared to Ptdmso complex for signals 1-4.[Hildebrandt, 2016a] Different behavior is observed compared to Ru and Os compounds.[Hildebrandt, 2018] A high-field shift is observable for signal 2, a low-field shift for signals 1 and 4, signal 3 does not show remarkable changes.

No.	**Signal**	**L2[5]**	**Ni2**	**Pd2**	**Pt2**	**Ptdmso2[5]**	**Ru2[6]**	**Os2[6]**
1	=C-*H*	6.97	7.16	7.16	7.14	7.35	6.64	6.87
2	-*C*=S	217.3	181.4			180.9	185.9	186.7
3	=*C*-H	112.9	115.1	113.0	112.5	112.9	113.4	112.7
4	-*C*-O-	169.1	178.1	178.1		174.2	179.0	174.9

Characterization with ^{1}H and $^{13}C\{^{1}H\}$ NMR spectroscopy shows in general results compared to those published previously for comparable Ni, Pd and Pt complexes.[Schubert, 2007] Table 1 displays compounds 2 as an example, for all three metal complexes the four chosen signals are in the same range. Compared to L2 there is a high-field shift observable for ^{13}C signal 2 due to the complexation to the metal *via* the thiocarbonyl carbon and the resulting shield of the carbon atom. For ^{13}C signal 4 complexation results in a low-field shift as the oxygen atom exhibit a σ-donor character. Interesting changes are observable for the methine proton, signal 1. Whereas compared to L2, Ni2, Pd2, Pt2 and Ptdmso2 show a shift to higher ppm values, opposite is shown

[5] Signals/ values taken from [Hildebrandt, 2016a]
[6] Signals/ values taken from [Hildebrandt, 2018]

compared to Ru2 and Os2.[Hildebrandt, 2016a; Hildebrandt, 2018] Chemical structures of Ru2, Os2 and Pt2 are shown in the Supplementary Part, Figure S1. Although compared to Ptdmso2, which shows a platinum(II) complex with one L2 as bidendate, dmso and a labile chlorid as ligands, the ^{1}H methine signal for Ni2, Pd2 and Pt2 are around 0.2 ppm up to higher field.[Hildebrandt, 2016a]

The MS spectra for all nickel, palladium, and platinum complexes show the molecular peak and some characteristic patterns for the β-Hydroxydithiocinnamic acid esters as described previously.[Hildebrandt, 2016a]

With the help of ^{1}H NMR spectroscopy stability of the complexes have been studied, showing good results for Ni and Pd complexes and acceptable stability for Pt complexes. Experiments have been carried out once at room temperature and dmso-d_6 or dichloromethane as solvents and once at 37 °C in dmso-d_6 showing same results. Examples (37 °C, dmso-d_6, 48 h measurements) are shown in the Supplementary Part, Figure S2.

Molecular Structures

Nickel(II) complexes Ni1, Ni3, Ni4 and Ni6, as well as palladium(II) complex Pd1 have been characterized by means of single crystal X-ray structure determination, Figure 2 and Table 2 shows molecular structures and characteristics of Ni1 and Pd1. Data for the other nickel(II) complexes and more specific bond lengths and angles, as well as for Ptdmso8 are shown in the Supplementary Part, Figure S3 and S4, Table S1 and Table S2.

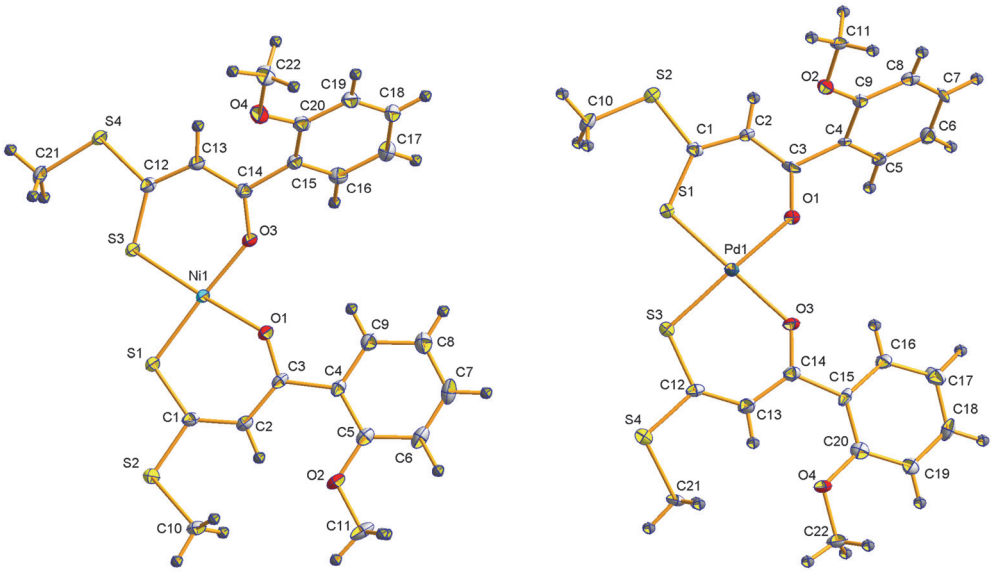

Fig. 2: Molecular structures (50% probability) of Ni1 (left) and Pd1 (right). Molecular structures of Ni3, Ni4 and Ni6 are shown in Figure S3.

The bond lengths and angles of the nickel(II) and palladium(II) complexes are in good agreement with the values reported earlier.[Schubert, 2007; Hildebrandt, 2016a] As the structures are quite symmetric, all bond lengths and angles are in the same range for both β-Hydroxydithiocinnamic acid esters surrounding *cis*-orientated the square-planar metal(II)-center, therefore only one value is chosen for each discussion. The coordination bond lengths of the heteroatoms (O and S) to the metal center are increasing in the order Ni1 {O(1)-M(1): 1.8466(17), S(1)-M(1): 2.1429(7)} < Pd1 {O(1)-M(1): 2.023(4), S(1)-M(1): 2.2307(16)} < Ptdmso1 {O(1)-M(1): 2.015(7), S(1)-M(1): 2.251(6) Å}, Table 2. The L-M-L angles are around 90° and therefore show a slightly distorted square-planar environment for the nickel(II) and palladium(II), resulting in diamagnetic complexes. Bond angles O(1)-M(1)-S(3) and S(1)-M(1)-O(3) show almost 180°, characteristic for the square-planar coordination-sphere.[Schubert, 2007]

Tab. 2: Specific bond angles [°] and bond lengths [Å] for all characterized nickel(II) and palladium(II) complexes. More data is shown in Table S1.

	Ni1	**Ni3**	**Ni4**	**Ni6**	**Pd1**
O(1)-M(1)	1.8466(17)	1.8492(12)	1.8695(17)	1.8720(16)	2.023(4)
O(3)-M(1)	1.8584(17)	1.8512(12)	1.8668(18)	1.8827(15)	2.049(4)
S(1)-M(1)	2.1429(7)	2.1434(4)	2.1309(7)	2.1426(6)	2.2307(16)
S(3)-M(1)	2.1426(7)	2.1406(5)	2.1396(7)	2.1510(6)	2.2348(16)
O(1)-C(3)	1.258(3)	1.270(2)	1.277(3)	1.269(3)	1.271(7)
O(3)-C(14)	1.264(3)	1.278(2)	1.279(3)	1.268(3)	1.254(7)
C(1)-S(1)	1.698(2)	1.7075(18)	1.708(3)	1.711(2)	1.703(6)
C(12)-S(3)	1.696(2)	1.7085(18)	1.704(3)	1.720(2)	1.707(6)
O(1)-M(1)-S(1)	96.42(6)	95.47(4)	95.22(6)	96.44(5)	96.78(13)
O(3)-M(1)-S(3)	97.07(5)	95.76(4)	95.96(6)	95.37(5)	94.93(13)
O(1)-M(1)-	176.48(6)	176.99(5)	177.73(6)	177.53(5)	176.20(13)

S(3) S(1)-M(1)-O(3)	175.71(6)	176.90(4)	177.55(7)	179.16(6)	179.22(13)
O(1)-M(1)-O(3)	80.14(7)	81.43(5)	84.06(8)	83.38(7)	83.26(17)
S(1)-M(1)-S(3)	86.46(3)	87.334(17)	84.86(3)	84.84(2)	85.08(6)

The molecular structure of L1 has been discussed previously, as well as changes in bond length and angles while coordination to its corresponding Ptdmso1.[Hildebrandt, 2016a] Changes for bischelating Ni1 and Pd1 complexes in bond lengths and angles are comparable to the changes for Ptdmso1, Table 3. Coordination of L1 to M1 (M= Ni, Pd, Pt) results in an elongation for the C(1)-S(1)-bonds, increasing in the order of Ni1 < Pd1 < Ptdmso1, this tendency has been already observed in a high-field shift for the -C=S-group in the $^{13}C\{^{1}H\}$ NMR spectra. For the C(3)-O(1)-bond a shortening can be observed following the same order as the elongation described before and the described low-field shift in the corresponding $^{13}C\{^{1}H\}$ NMR spectra.

Tab. 3: Specific bond angles [°] and bond lengths [Å] for compounds 1, data from L1 and Ptdmso1 has been taken from [Hildebrandt, 2016a].

	L1[5]	Ni1	Pd1	Ptdmso1[5]
C(1)-S(1)	1.681(2)	1.698(2)	1.703(6)	1.710(3)
C(3)-O(1)	1.334(3)	1.2583(3)	1.271(7)	1.274(3)
O(1)-M(1)		1.8466(17)	2.023(4)	2.015(7)
S(1)-M(1)		2.1429(7)	2.2307(16)	2.251(6)

Biological Behavior

A further aim of this study is to characterize all metal complexes for their cytotoxic properties *in vitro* and to determine structure-activity-relationships. Therefore, all compounds have been tested against a panel of cell lines, ovarian cancer cell lines SKOV3/SKOV3cis and A2780/A2780cis and lung cancer cell line A549, as well as non-cancerous cells Keratinocytes, Fibroblasts and MCF10A. The used cell lines differed in their sensitivity against Cisplatin. Due to a low solubility in water, dmso was used as a solvent. The toxic influence of dmso was determined earlier and experiments were carried out with 0.5% dmso in cell culture media and used as a reference in MTT assays (see Experimental Part).[Hildebrandt, 2016a] Conditions of these experiments are the same as for Ptdmso, Ru(II), and Os(II) which has been published previously.[Hildebrandt, 2016a; Hildebrandt, 2016b; Hildebrandt, 2018] So next to a comparison of different metals and different substitution patterns of the ligands also the comparison to the other systems is possible. IC50 values of the different β-Hydroxydithiocinnamic acid esters have been evaluated before.[Hildebrandt, 2018]

All IC50 values for the 18 metall(II) complexes as well as reference Cisplatin (CDDP) are displayed in Table 4. Resistant factors (RF) for the ovarian cancer cell lines have been determined. For Cisplatin IC50 values in resistant cell lines (SKOV3cis and A2780cis) are increased compared to the sensitive ones (3.8 µM vs. 13.5 µM and 1.3 µM vs. 6.1 µM) resulting in high resistance factors (3.6 and 4.7). For new metall(II) complexes resistant factors lower than 1 show that compounds activity is not affected by the Cisplatin induced resistance. For cell line SKOV3 this is shown for: Ni2, Ni4, Ni6, Pd1, Pd2, Pd4, Pd5, Pd6, Pt3, Pt4 and Pt6 (total: 11 of 18 compounds), for A2780 this can be observed for: Ni3, Ni5, Pd6, Pt2 and Pt4 (total: 5 of 18 compounds) although it is shown that most resistance factors are much lower than Cisplatins'. Regarding just the ability to circumvent the Cisplatin resistance, Pd6 and Pt4 displays best results as they have lower resistant factors on both cell pairs. The comparison of the IC50 values for each cell line shows best results for compound Pd3 as this compound is more active than reference Cisplatin on four

of the five mentioned cell lines and results in the lowest mean IC50 value (IC50 value of all five cell lines), Figure 3. In Table 4 all IC50 values lower than reference Cisplatin are marked red, this shows that especially palladium complexes show good results. Figure 3 analyses all compounds by increasing mean IC50 values, it can be concluded, that Pd3, Pd4 and Pd1 are the most active compounds of this study, followed by Ni1 and Pt4. For Pd compounds, it is shown in Figure 4A that the mean IC50 values (all six compounds, all five cell lines) are lower compared to Cisplatin (all five cell lines), what shows a general higher cytotoxic activity of these complexes than the reference substance. Although it is shown in Figure 4B that the mean IC50 values on both resistant cell lines for Ni and Pd complexes are lower than the one on the sensitive cell lines, this means that those compounds act especially on the resistant cell lines and may be an alternative in anticancer therapy for Cisplatin resistant tumors.

As mentioned above (see Introduction Part) Huq and coworkers reported in 2016 some general structure-activity relationships (SARs) for palladium(II) complexes.[Alam, 2016] They proposed higher activity for *ortho*-substituted phenyl rings. The top five compounds (regarding the mean IC50 values) of this work are: Pd3 (-*p*-OMe), Pd4 (-*o*-OEt), Pd2 (-*m*-OMe), Ni1 (-*o*-OMe) and Pt4 (-*o*-OEt), what is in a good agreement with the hypothesis as it shows three times an *ortho*-substituted metall(II)-complex. Considering the top 10 compounds of this work it is even more clear, number 6-10 are: Pd1 (-*o*-OMe), Ni3 (-*p*-OMe), Ni4 (-*o*-OEt), Pd6 (-*p*-OEt) and Pt1 (-*o*-OMe), what shows six times *ortho*-substituted, three *para*-substituted molecules and one *meta*-substituted position. For the length of the chain (methoxy- vs. ethoxy-group) there is no correlation observable from the data for the 18 metal complexes. Compared to the results of the β-Hydroxydithiocinnamic acid esters 1-6 it seems that compounds 4-6 (ethoxy-group) are in general more active than 1-3 (methoxy-group), Figure 4C. Nevertheless, most promising candidate compared to Cisplatin is Pd3, bearing a *para*-methoxy-group at the phenyl ring.

Tab. 4: IC50 values [µM] for ovarian cancerous cell lines SKOV3 and A2780 and their resistant analogues (-cis) and lung cancer cell line A549 for all compounds M1-6.

Substances	SKOV3 [µM]	SKOV3cis [µM]	A2780 [µM]	A2780cis [µM]	A549 [µM]
Ni1	5.8(±0.6)	6.8(±3.0)	3.5(±0.3)	5.0(±1.1)	5.4(±0.1)
RF(Ni1)	1.2		1.4		
Ni2	36.6(±9.3)	11.0(±2.1)	7.7(±2.0)	10.7(±6.0)	5.2(±1.0)
RF(Ni2)	0.3		1.4		
Ni3	7.1(±3.7)	7.8(±3.4)	8.0(±4.8)	5.4(±0.8)	3.8(±0.0)
RF(Ni3)	1.1		0.7		
Ni4	9.2(±5.1)	6.7(±2.0)	3.8(±0.1)	5.4(±1.0)	7.7(±2.2)
RF(Ni4)	0.7		1.4		
Ni5	10.3(±5.0)	15.9(±2.3)	10.4(±0.8)	6.6(±0.3)	8.1(±3.9)
RF(Ni5)	1.5		0.6		
Ni6	8.6(±4.6)	7.6(±0.2)	8.8(±8.1)	10.8(±6.5)	9.7(±6.3)
RF(Ni6)	0.9		1.2		
Pd1	13.7(±8.2)	4.4(±1.3)	3.1(±0.0)	4.7(±2.3)	2.8(±1.2)
RF(Pd1)	0.3		1.5		
Pd2	5.8(±4.1)	3.7(±0.8)	3.1(±0.6)	4.7(±2.3)	8.7(±8.2)
RF(Pd2)	0.6		1.5		
Pd3	3.8(±1.0)	5.4(±3.1)	3.1(±0.0)	3.2(±0.1)	4.5(±1.7)
RF(Pd3)	1.4		1.0		
Pd4	5.7(±2.5)	3.3(±0.2)	3.1(±0.0)	3.1(±0.0)	6.3(±2.4)
RF(Pd4)	0.6		1.0		
Pd5	12.9(±7.1)	8.6(±3.4)	4.3(±0.5)	6.2(±2.0)	9.8(±1.3)
RF(Pd5)	0.7		1.4		
Pd6	8.9(±1.0)	2.8(±0.2)	12.7(±1.0)	6.4(±0.4)	2.4(±0.4)
RF(Pd6)	0.3		0.5		
Pt1	6.6(±2.1)	13.7(±7.5)	3.4(±0.0)	8.5(±3.4)	4.2(±0.7)
RF(Pt1)	2.1		2.5		

Pt2	28.2(±7.3)	37.9(±0.6)	50.9(±15.4)	45.2(±9.6)	7.4(±2.5)
RF(Pt2)	1.3		0.9		
Pt3	38.7(±5.1)	28.2(±6.6)	16.8(±18.9)	67.9(±28.4)	43.0(±2.9)
RF(Pt3)	0.7		4.0		
Pt4	7.7(±0.6)	5.6(±1.2)	5.4(±3.0)	4.0(±0.9)	4.8(±1.3)
RF(Pt4)	0.7		0.7		
Pt5	12.0(±7.2)	21.2(±8.0)	4.7(±1.0)	24.0(±0.6)	8.0(±0.8)
RF(Pt5)	1.8		5.1		
Pt6	39.1(±5.3)	6.7(±0.9)	12.2(±13.0)	12.0(±8.7)	5.2(±1.5)
RF(Pt6)	0.2		1.0		
CDDP	**3.8(±2.8)**	**13.5(±4.4)**	**1.3(±0.2)**	**6.1(±2.1)**	**7.6(±2.6)**
RF(CDDP)	**3.6**		**4.7**		

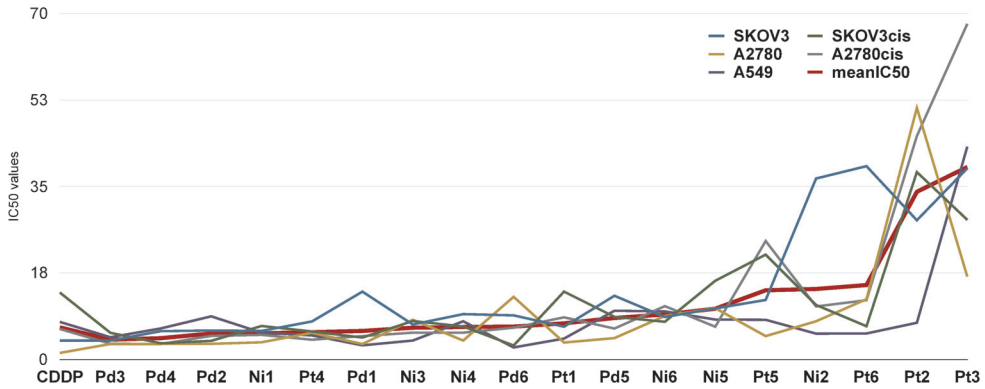

Fig. 3: Structure-activity relationship for analyzed metal complexes. Substances were ordered with increasing mean IC50 values.

The most active compounds for each metal, Pd3, Ni1 and Pt4 have been tested against non-cancerous cell lines Keratinocytes, Fibroblasts and MCF10a to evaluate their toxicity in general, Table 5. It is known for Cisplatin, that it shows toxic side effects by interacting with normal proliferating cells. This is proven by our experiments showing low IC50 values for CDDP on these cells. To point out, the most active metal(II) complexes of this work do not attack those cells, so it can be concluded that these complexes may show higher selectivity for cancer cells.

Tab. 5: IC50 values [µM] on non-cancerous cell lines Keratinocytes, Fibroblasts and MCF10A for most active compounds of each metal-class Ni1, Pd3, Pt4 and their reference Cisplatin.

Cell line	**Ni1** [µM]	**Pd3** [µM]	**Pt4** [µM]	**CDDP** [µM]
Keratino-cytes	87.0(±0)	55.0(±6.7)	› 100	5.7(±3.1)
Fibroblasts	84.3(±8.9)	42.9(±10.2)	› 100	4.1(±1.1)
MCF10A	19.6(±2.6)	28.3(±16.8)	41.5(±25.8)	3.3(±0.6)

The IC50 values for all β-Hydroxydithiocinnamic acid esters have been published before. As experiments have been carried out under same conditions those values are comparable to the ones mentioned in this study.[Hildebrandt, 2016a; Hildebrandt, 2018] Figure 4C displays the comparison of IC50 values of the free β-Hydroxydithiocinnamic acid esters 1-6 and corresponding metal complexes (for all three metals) 1-6 on their mean IC50 values for ovarian cancer cell lines sensitive vs. resistant. It is shown, that those compounds bearing an ethoxy-group at the phenyl-ring are the most active ones, in general. A second correlation can be seen for comparison of the sensitive and resistant values in general, it seems that β-Hydroxydithiocinnamic acid esters and their complexes are more active on Cisplatin resistant cell lines than on sensitive ones what again shows the possibility for the treatment of resistant tumors with those systems.

For compound 2 (-*meta*-OMe) a comparison of the β-Hydroxydithiocinnamic acid ester (L2), the nickel(II), palladium(II) and platinum(II) complexes of this work (Ni2, Pd2, Pt2), the previously reported platinum(II) complex with one O,S-bidendate ligand, dmso and chlorid as additional ligands (Ptdmso2) and the corresponding ruthenium(II) and osmium(II) complexes could be done (structures of Ptdmso2, Ru2 and Os2 is shown in Figure S1).[Hildebrandt, 2016a; Hildebrandt, 2018] Table 6 shows the IC50 values for all compounds as well as reference Cisplatin on the five cell lines. For SKOV3cis Ni2, Pd2, Ru2 and Os2 are more active compared to Cisplatin, even though resulting in lower resistant factors. For A2780cis the two most active compounds Os2 and Pd2

show lower IC50 values than the reference substance. Again, it can be concluded that the resistant factors for all substances are lower than for Cisplatin, showing the correlation that the β-Hydroxydithiocinnamic acid esters and their metal complexes are able to circumvent Cisplatin resistance *in vitro* in ovarian cancer cell lines.

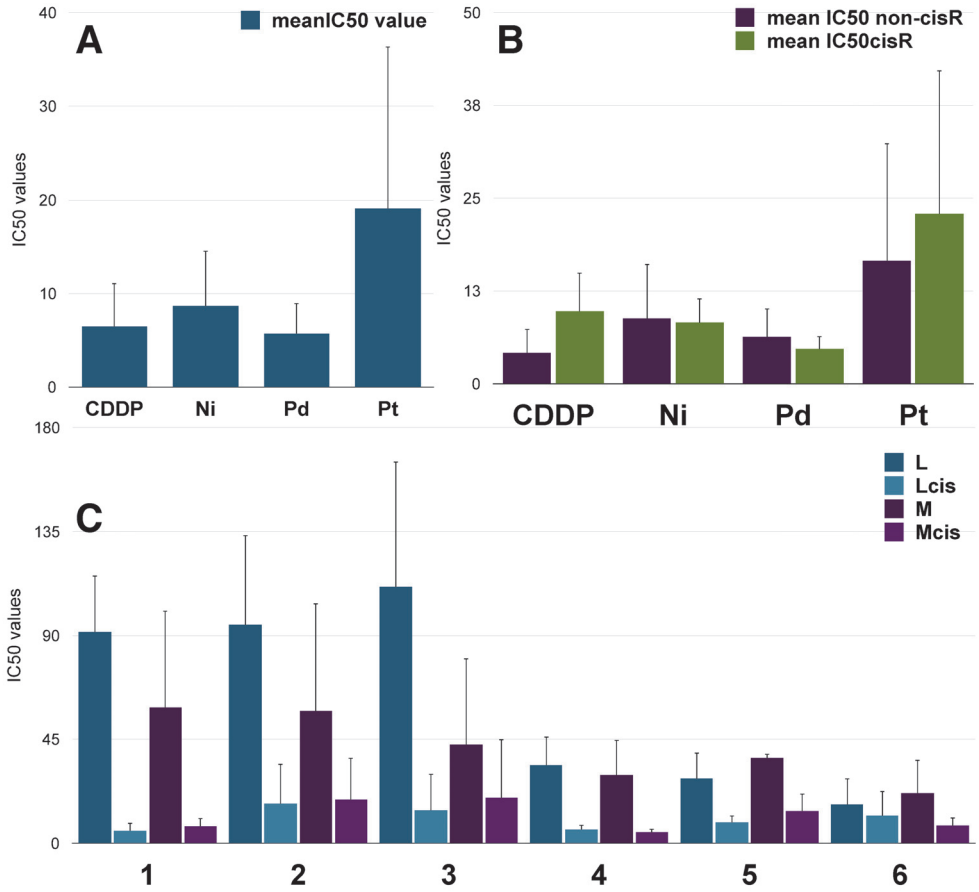

Fig. 4: **A**: Comparison for mean IC50 value (on all five cell lines) for different metals (determined for M1-6) and Cisplatin (CDDP), showing Pd complexes as most active molecules in general. **B**: Mean IC50 values for sensitive and resistant ovarian cancer cell lines SKOV3 and A2780, compared for different metals and Cisplatin, showing promising results for Pd complexes and special activity on resistant cell lines compared to sensitive ones. **C**: Comparison of β-Hydroxydithiocinnamic acid esters and their corresponding metal complexes on ovarian cancer cell lines. All values in [µM].

Tab. 6: IC50 values [µM] for ovarian cancerous cell lines SKOV3 and A2780 and their resistant analogues (-cis) and lung cancer cell line A549 for all compounds 2.

Substance	SKOV3 [µM]	SKOV3cis [µM]	A2780 [µM]	A2780cis [µM]	A549 [µM]
L2[1]	101.2 (±9.2)	90.2 (±3.1)	53.0 (±12.4)	24.1 (±7.2)	129.7 (±13.6)
RF(L2)[1]	0.9		0.5		
Ni2	36.6 (±9.3)	11.0 (±2.1)	7.7 (±2.0)	10.7 (±6.0)	5.2 (±1.0)
RF(Ni2)	0.3		1.4		
Pd2	5.8 (±4.1)	3.7 (±0.8)	3.1 (±0.6)	4.7 (±2.3)	8.7 (±8.2)
RF(Pd2)	0.6		1.5		
Pt2	28.2 (±7.3)	37.9 (±0.6)	50.9 (±15.4)	45.2 (±9.6)	7.4 (±2.5)
RF(Pt2)	1.3		0.9		
Ptdmso2[1]	28.8 (±4.9)	20.1 (±3.0)	19.8 (±1.6)	21.0 (±3.3)	24.2 (±2.0)
RF(Ptdmso2)[1]	0.7		1.1		
Ru2[2]	22.4 (±9.6)	12.5 (±5.9)	24.2 (±6.5)	16.4 (±3.7)	39.6 (±2.7)
RF(Ru2)[2]	0.5		0.7		
Os2[2]	8.8 (±4.4)	0.6 (±0.5)	0.4 (±0.1)	2.1 (±1.5)	6.2 (±5.8)
RF(Os2)[2]	0.1		5.3		
CDDP	**3.8 (±2.8)**	**13.5 (±4.4)**	**1.3 (±0.2)**	**6.1 (±2.1)**	**7.6 (±2.6)**
RF(CDDP)	**3.6**		**4.7**		

Figure 5 shows the order of the compounds by increasing mean IC50 values. All metal(II) compounds show lower IC50 values than the free β-Hydroxydithiocinnamic acid ester L2, Os2 and Pd2 show best results in lower IC50 values than Cisplatin. For platinum(II) complexes bearing a β-Hydroxydithiocinnamic acid ester as ligand it can be concluded, that they show none activity or comparable results to the reference. The advantage of the platinum(II) complexes is the lower RF in general, but it seems that this effect is caused by the β-Hydroxydithiocinnamic acid ester itself, due to lower IC50 values on resistant cell lines in general for this class of compounds. The ability to circumvent the Cisplatin resistance can be seen for all substances.

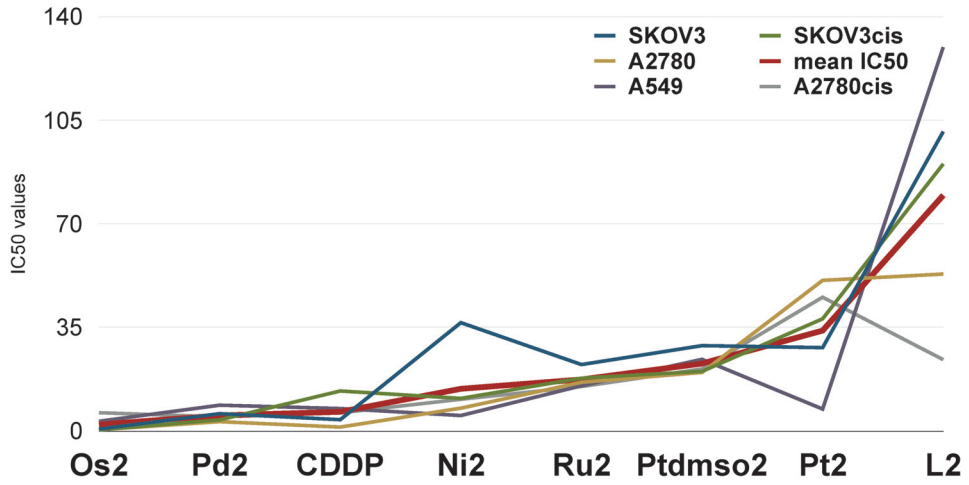

Fig. 5: Influence of the metal for compounds number 2. Substances were ordered with increasing mean IC50 values.

Conclusion

Overall we reported on 18 novel different metal complexes with O,S ligand, including previously reported results on other platinum(II) molecules as well as ruthenium(II) and osmium(II) counterparts.[Hildebrandt, 2016a; Hildebrandt, 2016b; Hildebrandt, 2018] The bidendate compounds have been characterized with classical methods, including NMR spectroscopy, MS spectrometry, elemental analysis and some molecular structures. Stability determinations show good results for palladium(II) and nickel(II) complexes, molecular structures show a *cis*-geometry for all square-planar measured metal(II) complexes. The comparison of NMR spectra and molecular structures show both

characteristic changes after complexation of the β-Hydroxydithiocinnamic acid esters to the metal(II) center, resulting in an elongation of the -C-S bonds of the thiocarbonyl groups and a shortening of the -C-O-bonds. The analysis of IC50 values shows promising results for the palladium(II) complexes, as some of them show low values comparable to Cisplatin and are able to circumvent Cisplatin resistance in ovarian cancer cell lines. Therefore, most active compound Pd3 will be further investigated *in vivo*.

Experimental Part

Materials and Techniques

All reactions were performed using standard conditions. The NMR spectra were recorded with a Bruker Avance 200 MHz, 400 MHz or 600 MHz spectrometer. Chemical shifts are given in ppm with reference to $SiMe_4$. Mass spectra were recorded with a Finnigan MAT SSQ 710 instrument. Elemental analysis was performed with a Leco CHNS-932 apparatus. Silica gel 60 (0.015-0.040 mm) was used for column chromatography and TLC was performed using Merck TLC aluminium sheets (Silica gel 60 F_{254}). Chemicals were purchased from Fisher Scientific, Aldrich or Acros and were used without further purification. All solvents were dried and distilled prior to use according to standard methods.

Synthesis

Different β-Hydroxydithiocinnamic acid alkyl esters were prepared as described before.[Hildebrandt, 2016a; Hildebrandt, 2018] The $(PhCN)_2PtCl_2$/ $(PhCN)_2PdCl_2$ as starting materials were prepared with modified literature methods.[Eysel, 1983; Doyle, 1960]

General procedure 1: Metal(II) complexes with β-Hydroxydithiocinnamic acid alkyl esters as ligands (M1-M6).

The corresponding ligand L1-L6 (2 equiv.), corresponding metal salt (1 equiv.) and sodiumactetate (2 equiv.) was solved in 15 ml acetonitrile and stirred

15 hours at rt. The precipitated red crystals were filtered, washed with acetonitrile and pentane and dried under reduced pressure.

[Ni(1-(2-methoxyphenyl)-3-(methylthio)-3-thioxo-prop-1-en-1-olate-*O,S*)] (Ni1)

Synthesis was performed according to general procedure 1. $NiCl_2 \cdot 6H_2O$ (250 mg, 1 mmol) and L1 (506 mg, 2 mmol) were used. Yield: 240 mg (44.8 %) as red crystals. ^{1}H NMR (400 MHz, $CDCl_3$): δ = 2.59 (s, 6H, -SC*H*$_3$); 3.88 (s, 6H, -OC*H*$_3$); 6.89-6.97 (m, 4H, -Ar-*m*-H); 7.28 (s, 2H, =C*H*); 7.40 (t, 2H, -Ar-*p*-H); 7.34 (d, $^3J_{H\text{-}H}$=7.4 Hz, 2H, -Ar-*o*-H). ^{13}C{^{1}H} NMR (101 MHz, $CDCl_3$): δ = 16.9 (-S*C*H$_3$); 55.8 (-O*C*H$_3$); 111.7 (-Ar-*m*-C); 115.1 (=*C*H); 120.8 (-Ar-*m*-C); 127.9 (-Ar-C1); 131.4 (-Ar-*m*-C); 132.2 (-Ar-*o*-C); 157.2 (-Ar-*C*-OCH$_3$); 178.1 (-*C*-O-); 181.4 (-*C*=S). MS (DEI): m/z = 536, 135. Elemental analysis: calculated for $C_{22}H_{22}O_4NiS_4$ C: 49.18 %; H: 4.13 %, found: C: 49.36 %; H: 4.14 %.

[Ni(1-(3-methoxyphenyl)-3-(methylthio)-3-thioxo-prop-1-en-1-olate-*O,S*)] (Ni2)

Synthesis was performed according to general procedure 1. $NiCl_2 \cdot 6H_2O$ (250 mg, 1 mmol) and L2 (506 mg, 2 mmol) were used. Yield: 300 mg (56.0 %) as red crystals. ^{1}H NMR (400 MHz, $CDCl_3$): δ = 2.65 (s, 6H, -SC*H*$_3$); 3.86 (s, 6H, -OC*H*$_3$); 7.10 (d, $^3J_{H\text{-}H}$=8.8 Hz, 2H, -Ar-*o*-H); 7.16 (s, 2H, =C*H*); 7.40 (t, 2H, -Ar-*p*-H); 7.34 (t, 2H, -Ar-*m*-H); 7.47 (t, 2H, -Ar-*p*-H). ^{13}C{^{1}H} NMR (101 MHz, $CDCl_3$): δ = 16.9 (-S*C*H$_3$); 55.8 (-O*C*H$_3$); 111.7 (-Ar-*m*-C); 115.1 (=*C*H); 120.8 (-Ar-*m*-C); 127.9 (-Ar-C1); 131.4 (-Ar-*m*-C); 132.2 (-Ar-*o*-C); 157.2 (-Ar-*C*-OCH$_3$); 178.1 (-*C*-O-); 181.4 (-*C*=S). MS (DEI): m/z = 536, 135. Elemental analysis: calculated for $C_{22}H_{22}O_4NiS_4$ C: 49.18 %; H: 4.13 %, found: C: 49.45 %; H: 4.15 %.

[Ni(1-(4-methoxyphenyl)-3-(methylthio)-3-thioxo-prop-1-en-1-olate-*O,S*)] (Ni3)

Synthesis was performed according to general procedure 1. $NiCl_2 \cdot 6H_2O$ (250 mg, 1 mmol) and L3 (506 mg, 2 mmol) were used. Yield: 350 mg (65.3 %) as red crystals. ^{1}H NMR (400 MHz, $CDCl_3$): δ = 2.63 (s, 6H, -SC*H*$_3$); 3.89 (s,

6H, -OC*H*$_3$); 6.92 (d, $^3J_{H-H}$=8.8 Hz, 4H, -Ar-*o*-H); 7.10 (s, 2H, =C*H*); 7.88 (d, $^3J_{H-H}$=8.9 Hz, 4H, -Ar-*m*-H). $^{13}C\{^1H\}$ NMR (101 MHz, $CDCl_3$): δ = 16.6 (-S*C*H$_3$); 55.5 (-O*C*H$_3$); 110.0 (=*C*H); 113.8 (-Ar-*o*-C); 129.4 (-Ar-*m*-C); 130.3 (-Ar-C1); 162.5 (-Ar-*C*-OCH$_3$); 177.8 (-*C*-O-); 181.6 (-*C*=S). MS (DEI): m/z = 536, 135. Elemental analysis: calculated for $C_{22}H_{22}O_4NiS_4$ C: 49.18 %; H: 4.13 %, found: C: 49.26 %; H: 4.10 %.

[Ni(1-(2-ethoxyphenyl)-3-(methylthio)-3-thioxo-prop-1-en-1-olate-*O,S*)] (Ni4)

Synthesis was performed according to general procedure 1. $NiCl_2{\cdot}6H_2O$ (250 mg, 1 mmol) and L4 (540 mg, 2 mmol) were used. Yield: 250 mg (44.3 %) as red crystals. ^1H NMR (400 MHz, $CDCl_3$): δ = 1.48 (m, 6H, -OCH$_2$C*H*$_3$); 2.61 (s, 6H, -CH$_3$); 4.11 (q, 4H, -OC*H*$_2$CH$_3$); 6.90-6.96 (m, 4H, -Ar-*m*-H); 7.28-7.46 (m, 2H, -Ar-*p*-H); 7.79-7.81 (m, 2H, -Ar-*o*-H). $^{13}C\{^1H\}$ NMR (101 MHz, $CDCl_3$): δ = 14.9 (-OCH$_2$*C*H$_3$); 16.7 (-*C*H$_3$); 64.5 (-O*C*H$_2$CH$_3$); 112.8 (-Ar-*m*-C); 115.0 (=*C*H); 120.7 (-Ar-*m*-C); 127.8 (=*C*-OH); 131.6 (-Ar-*o*-C); 132.3 (-Ar-*p*-C); 156.7 (qC, -Ar-*o*-C); 177.9 (Ar-C1); 181.1 (-*C*=S). MS (DEI): m/z = 564. Elemental analysis: calculated for $C_{24}H_{26}O_4NiS_4$ C: 50.98 %; H: 4.64 %, found: C: 50.99 %; H: 4.63 %.

[Ni(1-(3-ethoxyphenyl)-3-(methylthio)-3-thioxo-prop-1-en-1-olate-*O,S*)] (Ni5)

Synthesis was performed according to general procedure 1. $NiCl_2{\cdot}6H_2O$ (250 mg, 1 mmol) and L5 (540 mg, 2 mmol) were used. Yield: 200 mg (35.5 %) as red crystals. ^1H NMR (400 MHz, $CDCl_3$): δ = 1.57 (m, 6H, -OCH$_2$C*H*$_3$); 2.66 (s, 6H, -CH$_3$); 4.07 (q, 4H, -OC*H*$_2$CH$_3$); 7.08 (d, 2H, $^3J_{H-H}$=8.0 Hz, -Ar-*p*-H); 7.15 (s, 2H, =C*H*); 7.33 (t, 2H, -Ar-*m*-H); 7.41 (s, 2H, -Ar-*o*-H); 7.47 (d, 2H, $^3J_{H-H}$=7.8 Hz, -Ar-*o*-H). $^{13}C\{^1H\}$ NMR (101 MHz, $CDCl_3$): δ = 14.7 (-OCH$_2$*C*H$_3$); 17.1 (-*C*H$_3$); 63.7 (-O*C*H$_2$CH$_3$); 108.0 (=*C*H); 112.4 (-Ar-*o*-C); 118.3 (-Ar-*p*-C); 118.9 (-Ar-*o*-C); 129.7 (-Ar-*m*-C); 159.2 (qC, -Ar-*m*-C); 169.1 (Ar-C1); 217.2 (-*C*=S). MS (DEI): m/z = 564. Elemental analysis: calculated for $C_{24}H_{26}O_4NiS_4$ C: 50.98 %; H: 4.64 %, found: C: 51.08 %; H: 4.63 %.

[Ni(1-(4-ethoxyphenyl)-3-(methylthio)-3-thioxo-prop-1-en-1-olate-*O,S*)] (Ni6)

Synthesis was performed according to general procedure 1. $NiCl_2 \cdot 6H_2O$ (250 mg, 1 mmol) and L6 (540 mg, 2 mmol) were used. Yield: 190 mg (33.7 %) as red crystals. ^{1}H NMR (400 MHz, $CDCl_3$): δ = 1.37 (t, 6H, -OCH$_2$C*H*$_3$); 2.53 (s, 6H, -CH$_3$); 4.02 (q, 4H, -OC*H*$_2$CH$_3$); 6.81 (d, 4H, $^3J_{H\text{-}H}$=8.6 Hz, -Ar-*m*-H); 7.01 (s, 2H, =C*H*); 7.78 (d, 4H, $^3J_{H\text{-}H}$=8.6 Hz, -Ar-*o*-H). ^{13}C{^{1}H} NMR (101 MHz, $CDCl_3$): δ = 14.7 (-OCH$_2$*C*H$_3$); 16.6 (-*C*H$_3$); 63.7 (-O*C*H$_2$CH$_3$); 110.0 (=*C*H); 114.2 (-Ar-*m*-C); 130.1 (-Ar-C1); 162.0 (-Ar-*C*-OCH$_3$); 177.8 (-*C*-O-); 181.5 (-*C*=S). MS (DEI): m/z = 564. Elemental analysis: calculated for $C_{24}H_{26}O_4NiS_4$ C: 50.98 %; H: 4.64 %, found: C: 50.91 %; H: 4.60 %.

[Pd(1-(2-methoxyphenyl)-3-(methylthio)-3-thioxo-prop-1-en-1-olate-*O,S*)] (Pd1)

Synthesis was performed according to general procedure 1. $(PhCN)_2PdCl_2$ (399 mg, 1 mmol) and L1 (500 mg, 2 mmol) were used. Yield: 120 mg (20.5 %) as red crystals. ^{1}H NMR (400 MHz, $CDCl_3$): δ = 2.66 (s, 6H, -SC*H*$_3$); 3.90 (s, 6H, -OC*H*$_3$); 6.93-7.01 (m, 4H, -Ar-*m*-H/-Ar-*o*-H); 7.19 (s, 2H, =C*H*); 7.42 (t, 2H, -Ar-*p*-H); 7.79 (d, $^3J_{H\text{-}H}$=7.6 Hz, $^4J_{H\text{-}H}$=1.8 Hz, 2H, -Ar-*m*-H). ^{13}C{^{1}H} NMR (101 MHz, $CDCl_3$): δ = 17.5 (-S*C*H$_3$); 55.9 (-O*C*H$_3$); 111.8 (-Ar-*m*-C); 115.3 (=*C*H); 120.7 (-Ar-*m*-C); 129.0 (-Ar-C1); 130.4 (-Ar-*m*-C); 131.2 (-Ar-*o*-C); 157.4 (-Ar-*C*-OCH$_3$); 179.2 (-*C*-O-); 180.2 (-*C*=S). MS (EI): m/z = 584, 135. Elemental analysis: calculated for $C_{22}H_{22}O_4PdS_4$ C: 45.16 %; H: 3.79 %, found: C: 45.23 %; H: 3.72 %.

[Pd(1-(3-methoxyphenyl)-3-(methylthio)-3-thioxo-prop-1-en-1-olate-*O,S*)] (Pd2)

Synthesis was performed according to general procedure 1. $(PhCN)_2PdCl_2$ (399 mg, 1 mmol) and L2 (500 mg, 2 mmol) were used. Yield: 150 mg (25.7 %) as red crystals. ^{1}H NMR (400 MHz, $CDCl_3$): δ = 2.71 (s, 6H, -SC*H*$_3$); 4.09 (s, 6H, -OC*H*$_3$); 7.09 (dd, $^3J_{H\text{-}H}$=8.1 Hz, $^4J_{H\text{-}H}$=2.4 Hz, 2H, -Ar-*o*-H); 7.16 (s, 2H, =C*H*); 7.34 (t, 2H, -Ar-*m*-H); 7.54-7.57 (m, 2H, -Ar-*p*-H); 7.65 (t, 2H, -Ar-*o*-H). ^{13}C{^{1}H} NMR (101 MHz, $CDCl_3$): δ = 17.5 (-S*C*H$_3$); 55.4 (-O*C*H$_3$); 110.8 (-Ar-*m*-C); 113.0 (=*C*H);

117.9 (-Ar-*m*-C); 120.0 (-Ar-C1); 129.4 (-Ar-*m*-C); 139.7 (-Ar-*o*-C); 159.8 (-Ar-*C*-OCH_3); 178.1 (-*C*-O-). MS (DEI): m/z = 584, 240, 135. Elemental analysis: calculated for $C_{22}H_{22}O_4PdS_4$ C: 45.16 %; H: 3.79 %, found: C: 45.40 %; H: 3.75 %.

[Pd(1-(4-methoxyphenyl)-3-(methylthio)-3-thioxo-prop-1-en-1-olate-*O,S*)] (Pd3)

Synthesis was performed according to general procedure 1. $(PhCN)_2PdCl_2$ (399 mg, 1 mmol) and L3 (500 mg, 2 mmol) were used. Yield: 60 mg (10.3 %) as red crystals. ^{1}H NMR (400 MHz, $CDCl_3$): δ = 2.70 (s, 6H, -SC*H*$_3$); 3.91 (s, 6H, -OC*H*$_3$); 6.97 (d, $^3J_{H-H}$=8.7 Hz, 4H, -Ar-*o*-H); 7.13 (s, 2H, =C*H*); 8.02 (d, $^3J_{H-H}$=9.1 Hz, 4H, -Ar-*m*-H). ^{13}C{^{1}H} NMR (101 MHz, $CDCl_3$): δ = 17.4 (-S*C*H$_3$); 55.5 (-O*C*H$_3$); 110.5 (=*C*H); 113.9 (-Ar-*o*-C); 130.0 (-Ar-*m*-C); 130.3 (-Ar-C1); 162.7 (-Ar-*C*-OCH$_3$); 178.1 (-*C*-O-); 180.4 (-*C*=S). MS (DEI): m/z = 583, 135. Elemental analysis: calculated for $C_{22}H_{22}O_4PdS_4$ C: 45.16 %; H: 3.79 %, found: C: 45.23 %; H: 3.80 %.

[Pd(1-(2-ethoxyphenyl)-3-(methylthio)-3-thioxo-prop-1-en-1-olate-*O,S*)] (Pd4)

Synthesis was performed according to general procedure 1. $(PhCN)_2PdCl_2$ (600 mg, 1.5 mmol) and L4 (700 mg, 2.9 mmol) were used. Yield: 80 mg (13.1 %) as red crystals. ^{1}H NMR (400 MHz, $CDCl_3$): δ = 1.28 (m, 6H, -OCH$_2$C*H*$_3$); 2.66 (s, 6H, -CH$_3$); 4.17 (q, 4H, -OC*H*$_2$CH$_3$); 6.95-7.02 (m, 4H, -Ar-*m*-H); 7.44-7.61 (m, 4H, -Ar-*p*-H/=C*H*); 7.75-7.84 (m, 2H, -Ar-*o*-H). ^{13}C{^{1}H} NMR (101 MHz, $CDCl_3$): δ = 14.9 (-OCH$_2$*C*H$_3$); 16.7 (-*C*H$_3$); 64.5 (-O*C*H$_2$CH$_3$); 112.8 (-Ar-*m*-C); 115.0 (=*C*H); 120.7 (-Ar-*m*-C); 127.8 (=*C*-OH); 131.6 (-Ar-*o*-C); 132.3 (-Ar-*p*-C); 156.7 (qC, -Ar-*o*-C); 177.9 (Ar-C1); 181.1 (-*C*=S). MS (EI): m/z = 164. Elemental analysis: calculated for $C_{24}H_{26}O_4PdS_4$ C: 47.02 %; H: 4.26 %, found: C: 47.41 %; H: 4.26 %.

[Pd(1-(3-ethoxyphenyl)-3-(methylthio)-3-thioxo-prop-1-en-1-olate-*O,S*)] (Pd5)

Synthesis was performed according to general procedure 1. $(PhCN)_2PdCl_2$ (399 mg, 1 mmol) and L5 (500 mg, 2.1 mmol) were used. Yield: 120 mg (16.6 %) as red crystals. ^{1}H NMR (400 MHz, $CDCl_3$): δ = 1.46 (t, 6H, -OCH$_2$C*H*$_3$); 2.71 (s, 6H, -CH$_3$); 4.13 (q, 4H, -OC*H*$_2$CH$_3$); 7.07-7.09 (m, 2H, -Ar-*p*-H); 7.13 (s, 2H, =C*H*); 7.32 (t, 2H, -Ar-*m*-H); 7.54-7.58 (m, 4H, -Ar-*o*-H). ^{13}C{^{1}H} NMR (101 MHz, $CDCl_3$): δ = 14.8 (-OCH$_2$*C*H$_3$); 17.5 (-*C*H$_3$); 63.6 (-O*C*H$_2$CH$_3$); 110.9 (=*C*H); 113.5 (-Ar-*o*-C); 118.5 (-Ar-*p*-C); 120.0 (-Ar-*o*-C); 129.4 (-Ar-*m*-C); 159.1 (qC, -Ar-*m*-C); 178.4 (Ar-C1); 182.6 (-*C*=S). MS (DEI): m/z = 613, 254. Elemental analysis: calculated for $C_{24}H_{26}O_4PdS_4$ C: 47.02 %; H: 4.27 %, found: C: 46.68 %; H: 4.24 %.

[Pd(1-(4-ethoxyphenyl)-3-(methylthio)-3-thioxo-prop-1-en-1-olate-*O,S*)] (Pd6)

Synthesis was performed according to general procedure 1. $(PhCN)_2PdCl_2$ (399 mg, 1 mmol) and L6 (500 mg, 2.1 mmol) were used. Yield: 100 mg (16.3 %) as red crystals. ^{1}H NMR (400 MHz, $CDCl_3$): δ = 1.47 (t, 6H, -OCH$_2$C*H*$_3$); 2.70 (s, 6H, -CH$_3$); 4.14 (q, 4H, -OC*H*$_2$CH$_3$); 6.95 (d, 4H, $^3J_{H\text{-}H}$=8.8 Hz, -Ar-*m*-H); 7.13 (s, 2H, =C*H*); 8.00 (d, 4H, $^3J_{H\text{-}H}$=8.9 Hz, -Ar-*o*-H). ^{13}C{^{1}H} NMR (101 MHz, $CDCl_3$): δ = 14.7 (-OCH$_2$*C*H$_3$); 17.4 (-*C*H$_3$); 63.7 (-O*C*H$_2$CH$_3$); 110.0 (=*C*H); 114.3 (-Ar-*m*-C); 130.0 (-Ar-C1). MS (DEI): m/z = 614, 254. Elemental analysis: calculated for $C_{24}H_{26}O_4PdS_4$ C: 47.02 %; H: 4.27 %, found: C: 47.35 %; H: 4.32 %.

[Pt(1-(2-methoxyphenyl)-3-(methylthio)-3-thioxo-prop-1-en-1-olate-*O,S*)] (Pt1)

Synthesis was performed according to general procedure 1. $(PhCN)_2PtCl_2$ (492 mg, 1 mmol) and L1 (500 mg, 1 mmol) were used. Yield: 60 mg (8.9 %) as red crystals. ^{1}H NMR (400 MHz, $CDCl_3$): δ = 2.63 (s, 6H, -SC*H*$_3$); 3.89 (s, 6H, -OC*H*$_3$); 6.92-7.11 (m, 4H, -Ar-*m*-H/-Ar-*o*-H); 7.20 (s, 2H, =C*H*); 7.43-7.54 (m, 2H, -Ar-*p*-H); 7.82 (dd, $^3J_{H\text{-}H}$=7.6 Hz, $^4J_{H\text{-}H}$=1.7 Hz, 2H, -Ar-*m*-H). ^{13}C{^{1}H} NMR (101 MHz, $CDCl_3$): δ = 17.5 (-S*C*H$_3$); 55.8 (-O*C*H$_3$); 111.9 (-Ar-*m*-C); 117.1 (=*C*H);

120.4 (-Ar-*m*-C); 129.1 (-Ar-C1); 130.4 (-Ar-*m*-C); 131.9 (-Ar-*o*-C). MS (DEI): m/z = 672, 149. Elemental analysis: calculated for $C_{22}H_{22}O_4PtS_4$ C: 39.22 %; H: 3.29 %, found: C: 39.36 %; H: 3.32 %.

[Pt(1-(3-methoxyphenyl)-3-(methylthio)-3-thioxo-prop-1-en-1-olate-*O,S*)] (Pt2)

Synthesis was performed according to general procedure 1. $(PhCN)_2PtCl_2$ (470 mg, 1 mmol) and L2 (506 mg, 1 mmol) were used. Yield: 290 mg (43.1 %) as red crystals. ^{1}H NMR (400 MHz, $CDCl_3$): δ = 2.66 (s, 6H, -SC*H*$_3$); 3.91 (s, 6H, -OC*H*$_3$); 7.12 (dd, $^3J_{H\text{-}H}$=8.4 Hz, $^4J_{H\text{-}H}$=2.5 Hz, 2H, -Ar-*o*-H); 7.14 (s, 2H, =C*H*); 7.32 (t, 2H, -Ar-*m*-H); 7.59 (d, $^3J_{H\text{-}H}$=7.8 Hz, 2H, -Ar-*p*-H); 7.67 (t, 2H, -Ar-*o*-H). ^{13}C{^{1}H} NMR (101 MHz, $CDCl_3$): δ = 17.6 (-S*C*H$_3$); 55.4 (-OCH$_3$); 112.5 (-Ar-*m*-C); 112.5 (=*C*H); 117.5 (-Ar-*m*-C); 119.4 (-Ar-C1); 129.6 (-Ar-*m*-C); 140.3 (-Ar-*o*-C); 160.0 (-Ar-*C*-OCH$_3$). MS (DEI): m/z = 674, 240, 135. Elemental analysis: calculated for $C_{22}H_{22}O_4PtS_4$ C: 39.22 %; H: 3.29 %, found: C: 39.11 %; H: 3.25 %.

[Pt(1-(4-methoxyphenyl)-3-(methylthio)-3-thioxo-prop-1-en-1-olate-*O,S*)] (Pt3)

Synthesis was performed according to general procedure 1. $(PhCN)_2PtCl_2$ (470 mg, 1 mmol) and L3 (506 mg, 1 mmol) were used. Yield: 210 mg (31.2 %) as red crystals. ^{1}H NMR (400 MHz, $CDCl_3$): δ = 2.72 (s, 6H, -SC*H*$_3$); 3.90 (s, 6H, -OC*H*$_3$); 7.00 (d, $^3J_{H\text{-}H}$=9.0 Hz, 4H, -Ar-*o*-H); 7.02 (s, 2H, =C*H*); 8.04 (d, $^3J_{H\text{-}H}$=8.9 Hz, 4H, -Ar-*m*-H). ^{13}C{^{1}H} NMR (101 MHz, $CDCl_3$): δ = 17.5 (-S*C*H$_3$); 55.5 (-OCH$_3$); 112.0 (=*C*H); 114.1 (-Ar-*o*-C); 129.3 (-Ar-*m*-C); 131.4 (-Ar-C1); 162.3 (-Ar-*C*-OCH$_3$); 173.6 (-*C*-O-). MS (DEI): m/z = 674, 135. Elemental analysis: calculated for $C_{22}H_{22}O_4PtS_4$ C: 39.22 %; H: 3.29 %, found: C: 39.29 %; H: 3.32 %.

[Pt(1-(2-ethoxyphenyl)-3-(methylthio)-3-thioxo-prop-1-en-1-olate-*O,S*)] (Pt4)

Synthesis was performed according to general procedure 1. $(PhCN)_2PtCl_2$ (700 mg, 1.5 mmol) and L4 (700 mg, 2.9 mmol) were used. Yield: 120 mg (17.1 %) as red crystals. ^{1}H NMR (400 MHz, $CDCl_3$): δ = 1.28 (m, 6H, -OCH$_2$C*H*$_3$);

2.66 (s, 6H, -CH_3); 4.17 (q, 4H, -OC*H*$_2$$CH_3$); 6.95-7.02 (m, 4H, -Ar-*m*-H); 7.44-7.50 (m, 4H, -Ar-*p*-H/=C*H*); 7.75-7.83 (m, 2H, -Ar-*o*-H). $^{13}C\{^1H\}$ NMR (101 MHz, $CDCl_3$): δ = 14.9 (-OCH$_2$*C*H$_3$); 16.7 (-*C*H$_3$); 64.5 (-O*C*H$_2$CH$_3$); 112.3 (-Ar-*m*-C); 115.0 (=*C*H); 120.7 (-Ar-*m*-C); 127.8 (=*C*-OH); 131.6 (-Ar-*o*-C); 132.3 (-Ar-*p*-C); 156.7 (qC, -Ar-*o*-C); 177.9 (Ar-C1); 181.1 (-*C*=S). MS (EI): m/z = 121. Elemental analysis: calculated for $C_{24}H_{26}O_4PtS_4$ C: 41.08 %; H: 3.73 %, found: C: 41.18 %; H: 3.25 %.

[Pt(1-(3-ethoxyphenyl)-3-(methylthio)-3-thioxo-prop-1-en-1-olate-*O,S*)] (Pt5)

Synthesis was performed according to general procedure 1. $(PhCN)_2PtCl_2$ (470 mg, 1 mmol) and L5 (510 mg, 2 mmol) were used. Yield: 210 mg (30.0 %) as red crystals. ^1H NMR (400 MHz, $CDCl_3$): δ = 1.45 (t, 6H, -OCH$_2$C*H*$_3$); 2.65 (s, 6H, -CH_3); 4.13 (q, 4H, -OC*H*$_2$$CH_3$); 7.09-7.13 (m, 4H, -Ar-*p*-H/ =C*H*); 7.31 (t, 2H, -Ar-*m*-H); 7.58-7.60 (m, 4H, -Ar-*o*-H). $^{13}C\{^1H\}$ NMR (101 MHz, $CDCl_3$): δ = 14.8 (-OCH$_2$*C*H$_3$); 17.6 (-*C*H$_3$); 63.6 (-O*C*H$_2$CH$_3$); 112.5 (=*C*H); 112.9 (-Ar-*o*-C); 118.0 (-Ar-*p*-C); 119.4 (-Ar-*o*-C); 129.5 (-Ar-*m*-C); 159.3 (qC, -Ar-*m*-C); 177.8 (Ar-C1). MS (DEI): m/z = 702, 254. Elemental analysis: calculated for $C_{24}H_{26}O_4PtS_4$ C: 41.08 %; H: 3.73 %, found: C: 41.03 %; H: 3.78 %.

[Pt(1-(4-ethoxyphenyl)-3-(methylthio)-3-thioxo-prop-1-en-1-olate-*O,S*)] (Pt6)

Synthesis was performed according to general procedure 1. $(PhCN)_2PtCl_2$ (470 mg, 1 mmol) and L6 (510 mg, 2 mmol) were used. Yield: 140 mg (20.0 %) as red crystals. ^1H NMR (400 MHz, $CDCl_3$): δ = 1.47 (t, 6H, -OCH$_2$C*H*$_3$); 2.64 (s, 6H, -CH_3); 4.16 (q, 4H, -OC*H*$_2$$CH_3$); 6.95 (d, 4H, $^3J_{H\text{-}H}$=9.1 Hz, -Ar-*m*-H); 7.12 (s, 2H, =C*H*); 8.03 (d, 4H, $^3J_{H\text{-}H}$=8.7 Hz, -Ar-*o*-H). $^{13}C\{^1H\}$ NMR (101 MHz, $CDCl_3$): δ = 14.7 (-OCH$_2$*C*H$_3$); 17.5 (-*C*H$_3$); 63.7 (-O*C*H$_2$CH$_3$); 109.1 (=*C*H); 114.5 (-Ar-*m*-C); 161.7 (-Ar-C1). MS (DEI): m/z = 701, 149. Elemental analysis: calculated for $C_{24}H_{26}O_4PtS_4$ C: 41.08 %; H: 3.73 %, found: C: 41.77 %; H: 3.72 %.

Crystal structure determination

The intensity data for the compounds were collected on a Nonius KappaCCD diffractometer using graphite-monochromated Mo-K_α radiation. Data were corrected for Lorentz and polarization effects; absorption was taken into account on a semi-empirical basis using multiple-scans.[Data Collection Software; Otwinowski, 1997; Sadabs, 2015]

The structures were solved by direct methods (SHELXS [Sheldrick, 2015]) and refined by full-matrix least squares techniques against Fo^2 (SHELXL-97 [Sheldrick, 2015]). The hydrogen atoms of **Ni6** were located by difference Fourier synthesis and refined isotropically. All other hydrogen atoms were included at calculated positions with fixed thermal parameters.

Crystallographic data as well as structure solution and refinement details are summarized in Table 4. MERCURY was used for structure representations.[Mercury, 2006]

Supporting Information available: Crystallographic data (excluding structure factors) has been deposited with the Cambridge Crystallographic Data Centre as supplementary publication CCDC-XXXXXXX for **Ni1**, CCDC- XXXXXXX for **Ni3**, CCDC- XXXXXXX for **Ni4**, CCDC- XXXXXXX for **Ni6**, and CCDC- XXXXXXX for **Pd1**, and CCDC- XXXXXXX for **Ptdmso8**. Copies of the data can be obtained free of charge on application to CCDC, 12 Union Road, Cambridge CB2 1EZ, UK [E- mail: deposit@ccdc.cam.ac.uk].

Stability determinations

NMR spectra were measured *via* NMR spectroscopy on Bruker Avance 400 MHz. Substances were solved in dmso-d_6 or CD_2Cl_2 and measured directly at 37 °C or room temperature for 72 hours. NS=128 scans, t=709 seconds/2891 seconds break, 72 measurements.

Biological Assays

Cancer cell lines were cultured under standard conditions (5 % CO2, 37 °C, 90 % humidity) in RPMI medium supplemented with 10 % FCS, 100 U/ml penicillin and 100 µg/ml streptomycin (Life Technologies, Germany). Cisplatin (Sigma, Germany) was freshly dissolved at 1 mg/ml in 0.9 % NaCl solution and diluted appropriately. New Metal(II) complexes and ligands were dissolved in dmso. Platinum-resistant A2780 and SKOV3 cells were established by repeated rounds of 3 day incubations with increasing amounts of Cisplatin starting with 0.1 µM. The concentration was doubled after 3 incubations interrupted by recovery phases with normal medium. Cells that survived the third round of 12.8 µM Cisplatin were defined as resistant cultures. Determinations of IC50 values were carried out using the CellTiter96 non-radioactive proliferation assay (MTT assay, Promega). After seeding 5000 cells per well in a 96-well plate cells were allowed to attach for 24h and were incubated for 48h with different concentrations of the substances ranging from 0 to 1000 µM for Metal complexes and 0 to 1000 µM for ligand tests (0, 1, 10, 50, 100, 500, 1000 µm), for Cisplatin from 0 to 100 µM (0.1, 1, 5, 10, 50, 100 µM). Each measurement was done in triplicate and repeated 3-times. The proportion of live cells was quantified by the MTT assay and after background subtraction relative values compared to the mean of medium controls were calculated. Non-linear regression analyses applying the Hill-slope were run in GraphPad 5.0 software.

Acknowledgements

The authors would like to thank P. Bellstedt, B. Rambach and G. Sentis for the helpful measurements of the NMR spectra.

Notes and References

[Abu-Surrah, 2008] A. S. Abu-Surrah, H. H. Al-Sa'doni and M. Y. Abdalla, *Cancer Therapy*, **2008**, 6, 1-10.

[Alam, 2016] M. D. Alam and F. Huq, *Coord. Chem. Rev.,* **2016**, 316, 36-67.

[Brabec, 2017] V. Brabec, O. Hrabina and J. Kasparkova, *Coord. Chem. Rev.*, **2017**, 351, 2-31.

[Butour, 1997] S. Butour, F. Wimmer, F. Wimmer and P. Castan, *Chemico- Biological Interactions*, **1997**, 104, 165-178.

[Data Collection Software] COLLECT, Data Collection Software; Nonius B.V., Nethlands, **1998**.

[Dilruba, 2016] S. Dilruba and G. V. Kalayda, *Cancer Chemother. Pharmacol.*, **2016**, 77, 1103-1124.

[Dobrova, 2016] A. Dobrova, S. Platzer, F. Bacher, M. M. Milunovic, A. Drobrov, G. Spengler, E. A. Enyedy, G. Novitchi and V. B. Arion, *Dalton Trans*., **2016**, 45, 13427-13439.

[Doyle, 1960] J. R. Doyle, P. E. Slade and H. B. Jonassen, *Inorg. Synth.*, **1960**, 6, 218-220.

[Durig, 1976] J. R. Durig, J. Danneman, W. D. Behnke and E. E. Mercer, *Chem.-Biol. Interact*., **1976**, 13, 287-294.

[Eysel, 1983] H. H. Eysel, E. Guggolz, M. Kopp and M. L. Ziegler, *Z. Anorg. Allg. Chem.*, **1983**, 499, 31-43.

[Gibson, 2016] D. Gibson, *Dalton Trans.*, **2016**, 45, 12983-12991.

[Haribabu, 2015] J. Haribabu, K. Jeyalakshmi, Y. Arun, N. S. P. Bhuvanesh, P. T. Perumal and R. Karvembu, *RSC Adv.*, **2015**, 5, 46031-46049.

[Hildebrandt, 2016a] J. Hildebrandt, N. Hafner, H. Görls, D. Kritsch, G. Ferraro, M. Dürst, I. B. Runnebaum, A. Merlino and W. Weigand, *Dalton Trans.,* **2016**, 45, 18876-18891.

[Hildebrandt, 2016b] J. Hildebrandt, H. Görls, N. Häfner, G. Ferraro, M. Dürst, I. B. Runnebaum, W. Weigand and A. Merlino, *Dalton Trans.,* **2016**, 45, 12283-12287.

[Hildebrandt, 2018] J. Hildebrandt, N. Häfner, D. Kritsch, H. Görls, M. Dürst, I. B. Runnebaum and W. Weigand, *in preparation*.

[Johnstone, 2013] T. C. Johnstone, J. J. Wilson and S. J. Lippard, *Inorg. Chem.*, **2013**, 52, 12234-12249.

[Johnstone, 2016] T. C. Johnstone, K. Suntharalingam and S. J. Lippard, *Chem. Rev.*, **2016**, 116, 3436-3486.

[Jungwirth, 2012] U. Jungwirth, D. N. Xanthos, J. Gojo, A. K. Bytzek, W. Korner, P. Heffeter, S. A. Abramkin, M. A. Jakupec, C. G. Hartinger, U. Windberger, M. Galanski, B. K. Keppler and W. Berger, *Mol. Pharmacol*., **2012**, 81, 719-728.

[Kelland, 2007] L. Kelland, *Nat. Rev. Cancer*, **2007**, 7, 573-584.

[Livingstone, 1970] S. E. Livingstone and A. E. Mihkelson, *Inorg. Chem*., **1970**, 9, 2545-2551.

[Maurya, 2015] M. R. Maurya, B. Uprety, F. Avecilla, S. Tariq and A. Azam, *Eur. J. Med. Chem.*, **2015**, 98, 54-60.

[Mayr, 2017] J. Mayr, P. Heffeter, D. Groza, L. Galvez, G. Koellensperger, A. Roller, B. Alte, M. Haider, W. Berger, C. R. Kowol and B. K. Keppler, *Chem. Sci.*, **2017**, 8, 2241-2250.

[Meier-Menches, 2018] S. M. Meier-Menches, C. Gerner, W. Berger, C. G. Hartinger and B. K. Keppler, *Chem. Soc. Rev.,* **2018**, 47, 909-928.

[Mercury, 2006] MERCURY, C. F. Macrae, P. R. Edgington, P. McCabe, E. Pidcock, G. P. Shields, R. Taylor , M. Towler and J. van de Streek, *J. Appl. Cryst.,* **2006**, 39:453.

[Messori, 2016] L. Messori and A. Merlino, *Coord. Chem. Rev.,* **2016**, 315, 67-89.

[Mügge, 2014] C. Mügge, R. Liu, H. Goerls, C. Gabbiani, E. Michelucci, N. Ruediger, J. H. Clement, L. Messori and W. Weigand, *Dalton Trans*., **2014**, 43, 3072-3086.

[Mügge, 2016] C. Mügge, T. Marzo, L. Massai, J. Hildebrandt, G. Ferraro, P. Rivera-Fuentes, N. Metzler-Nolte, A. Merlino, L. Messori and W. Weigand, *Inorg. Chem*., **2015**, 54, 8560-8570.

[Otwinowski, 1997] „Processing of X-Ray Diffraction Data Collected in Oscillation Mode“:Otwinowski, Z.; Minor, W. in Carter, C. W.; Sweet, R. M. (eds.): *Methods in Enzymology, Vol. 276, Macromolecular Crystallography, Part A*, pp. 307-326, Academic Press **1997**.

[Petruzzella, 2017] E. Petruzzella, J. P. Braude, J. R. Aldrich-Wright, V. Gandin and D. Gibson, *Angew. Chem., Int. Ed*., **2017**, 56, 11539-11544.

[Petruzzella, 2018] E. Petruzzella, R. Sirota, I. Solazzo, V. Gardin and D. Gibson, *Chem. Sci.*, **2018**, 9, 4299-4307.

[Rosenberg, 1965] B. Rosenberg, L. Vancamp and T. Krigas, *Nature*, **1965**, 205, 698-699.

[Sadabs, 2015] SADABS 2016/2: L. Krause, R. Herbst-Irmer, G. M. Sheldrick and D. Stalke, *J. Appl. Cryst.*, **2015**, 48, 3-10.

[Saumweber, 1998] R. Saumweber, C. Robl and W. Weigand, *Inorg. Chim. Acta,* **1998**, 269, 83-90.

[Schubert, 2003] K. Schubert, R. Saumweber, H. Görls and W. Weigand, *Z. Anorg. Allg. Chem.*, **2003**, 629, 2091-2096.

[Schubert, 2005] K. Schubert, H. Görls and W. Weigand, *Heteroatom. Chemistry*, **2005**, 16(5), 369-378.

[Schubert, 2006] K. Schubert, T. Alpermann, T. Niksch, H. Görls and W. Weigand, *Z. Anorg. Allg. Chem.*, **2006**, 632, 1033-1042.

[Schubert, 2007] K. Schubert, H. Görls and W. Weigand, *Z. Naturforsch.*, **2007**, 62b, 475-482.

[Sheldrick, 2015] G. M. Sheldrick, *Acta Cryst.*, **2015**, C71, 3-8.

[Weigand, 1993] W. Weigand, R. Saumweber and P. Schulz, *Z. Naturforsch.*, **1993**, 48b, 1080-1088.

[Wimmer, 1989] F. Z. Wimmer, S. Wimmer, P. Castan, S. Cros, N. Johnson and E. Colacio- Rodrigez, *Anticancer Res.,* **1989**, 9, 791-794.

[Zhao, 1999] G. Zhao, H. Lin, P.Yu, H. Sun, S. Zhu, X. Su and Y. Chen, *J. Inorg. Biochem.*, **1999**, 73, 145-149.

Supplementary Part

Novel Nickel(II), Palladium(II), and Platinum(II) complexes with O,S-bidendate cinnamic acid ester derivatives: An *in vitro* cytotoxic comparison to Ruthenium(II) and Osmium(II) Analogues

Jana Hildebrandt[1,2], Norman Häfner[2], Helmar Görls[1], Matthias Dürst[2], Ingo B. Runnebaum[2], Wolfgang Weigand[1]

[1] Institut für Anorganische und Analytische Chemie Friedrich-Schiller Universität Jena, Humboldtstraße 8, 07743 Jena, Germany

[2]Department of Gynecology, Jena University Hospital – Friedrich-Schiller University Jena

Additional Characterization

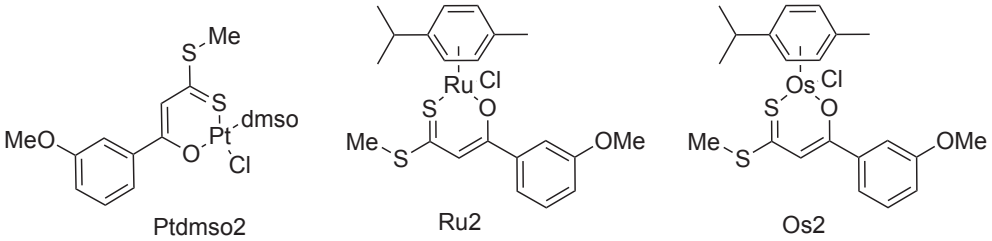

Fig. S1: Overview of compounds compared with Ni, Pd, and Pt complexes for NMR spectra characterization and IC50 comparison.[Hildebrandt, 2016a; Hildebrandt, 2018]

Stability Determination

Figure S2 shows stability investigations for Ni2, Pd3 and Pt6 as examples for all discussed metal complexes. During the time of the measurements, nothing changed for Ni and Pd compounds at all discussed conditions. For the platinum(II) complexes there is a formation of a side product observable in dmso-d_6.

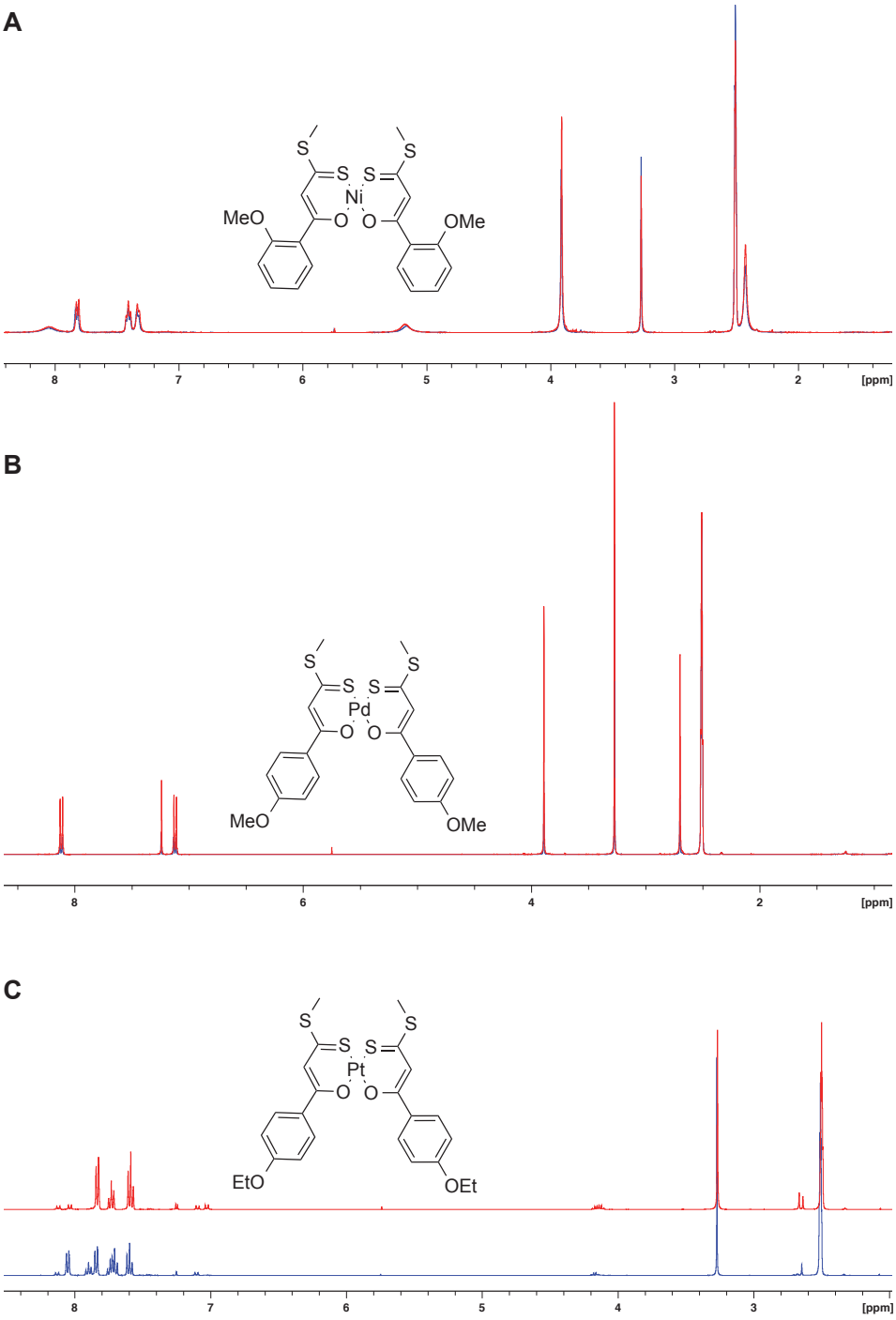

Fig. S2: Stability determinations for Ni1, Pd3 and Pt6 as examples for all complexes discussed in this work. Conditions: dmso-d_6 as solvent, 48 h measurements (red: t=0, blue: t= 48 h) at 37 °C.

Additional Molecular Structures

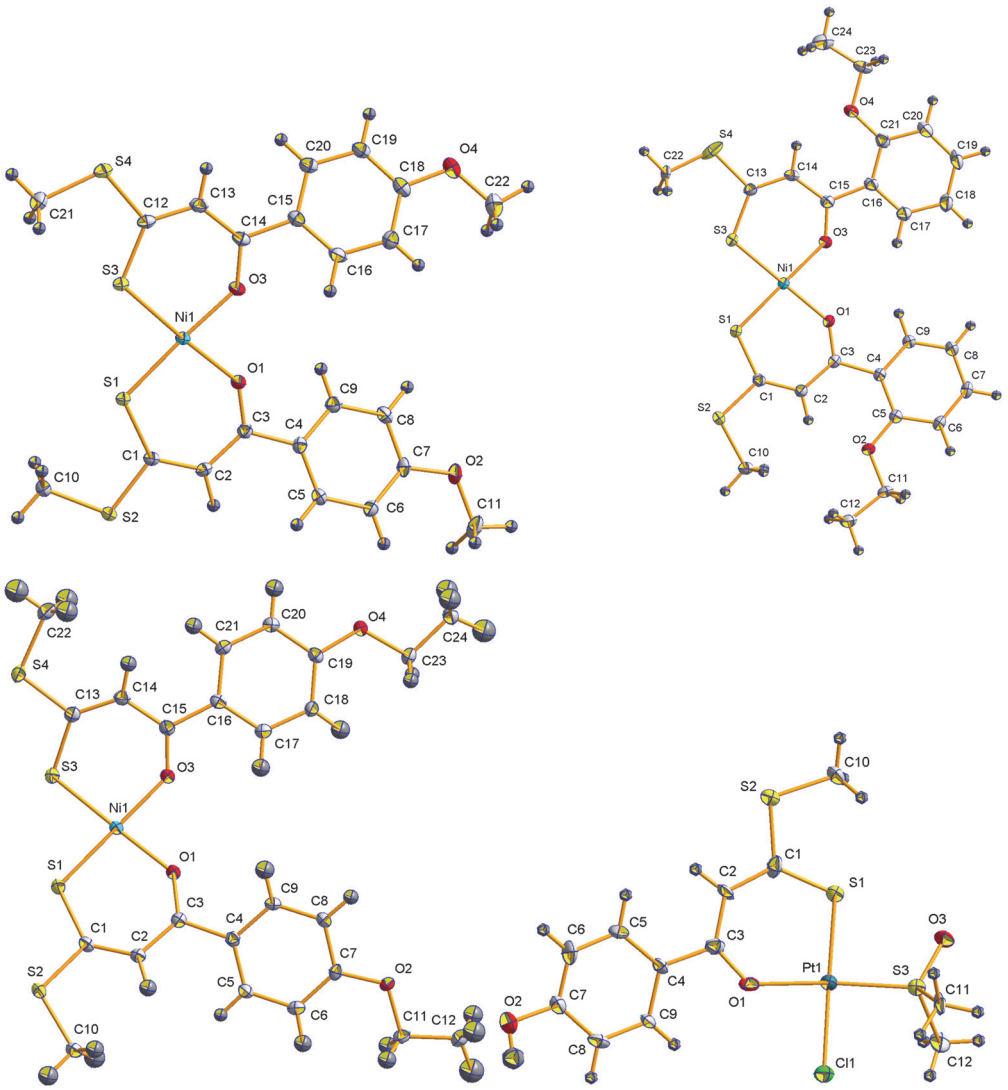

Fig. S3: Molecular structures (50% probability) of Ni3, Ni4, Ni6 and Ptdmso8.

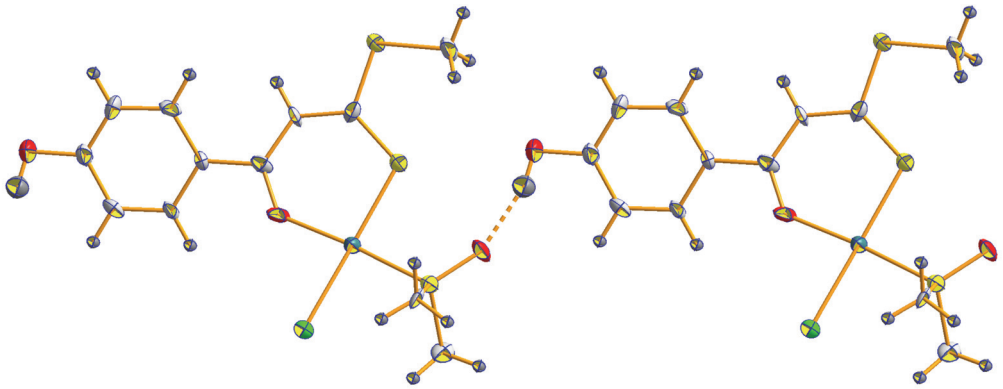

Fig. S4: Intermolecular hydrogen-bonding observed in the crystals of Ptdmso8.

Tab. S1: Specific bond angles [°] and bond lengths [Å] for all characterized nickel(II) and palladium(II) compounds.

	Ni1	**Ni3**	**Ni4**	**Ni6**	**Pd1**
O(1)-C(3)	1.258(3)	1.270(2)	1.277(3)	1.269(3)	1.271(7)
C(3)-C(2)	1.398(3)	1.416(2)	1.415(3)	1.417(3)	1.400(9)
C(2)-C(1)	1.378(3)	1.374(2)	1.374(3)	1.366(3)	1.369(9)
C(1)-S(1)	1.698(2)	1.7075(18)	1.708(3)	1.711(2)	1.703(6)
O(1)-M(1)	1.8466(17)	1.8492(12)	1.8695(17)	1.8720(16)	2.023(4)
S(1)-M(1)	2.1429(7)	2.1434(4)	2.1309(7)	2.1426(6)	2.2307(16)
O(3)-C(14/15)	1.264(3)	1.278(2)	1.279(3)	1.268(3)	1.254(7)
C(14/15)-C(13/14)	1.386(3)	1.401(3)	1.411(4)	1.420(3)	1.510(9)
C(13/14)-C(12/13)	1.383(3)	1.386(3)	1.379(4)	1.367(3)	1.415(9)
C(12/13)-S(3)	1.696(2)	1.7085(18)	1.704(3)	1.720(2)	1.707(6)
O(3)-M(1)	1.8584(17)	1.8512(12)	1.8668(18)	1.8827(15)	2.049(4)
S(3)-M(1)	2.1426(7)	2.1406(5)	2.1396(7)	2.1510(6)	2.2348(16)
O(1)-C(3)-C(2)	123.5(2)	124.45(16)	123.5(2)	125.2(2)	127.0(6)
C(3)-C(2)-C(1)	125.7(2)	124.65(16)	124.5(2)	125.3(2)	128.0(6)

C(2)-C(1)-S(1)	128.83(19)	128.24(13)	129.1(2)	128.21(17)	130.4(5)
S(3)-C(12/13)-C(13/14)	128.19(19)	128.26(14)	128.9(2)	127.31(18)	131.5(5)
C(12/13)-C(13/14)-C(14/15)	125.3(2)	124.91(17)	125.2(2)	125.4(2)	121.1(5)
C(13/14)-C(14/15)-O(3)	126.0(2)	124.35(17)	123.8(2)	124.9(2)	124.8(6)
M(1)-O(1)-C(3)	136.99(17)	136.96(11)	137.39(16)	134.51(14)	129.9(4)
O(1)-M(1)-S(1)	96.42(6)	95.47(4)	95.22(6)	96.44(5)	96.78(13)
S(3)-M(1)-O(3)	97.07(5)	95.76(4)	95.96(6)	95.37(5)	94.93(13)
C(14/15)-O(3)-M(1)	133.89(17)	36.84(12)	136.51(17)	133.55(15)	132.9(4)
M(1)-S(3)-C(12/13)	108.84(9)	109.84(7)	109.60(9)	108.49(8)	107.5(2)
O(1)-M(1)-O(3)	80.14(7)	81.43(5)	84.06(8)	83.38(7)	83.26(17)
S(1)-M(1)-S(3)	86.46(3)	87.334(17)	84.86(3)	84.84(2)	85.08(6)

O(1)-M(1)-S(3)	176.48(6)	176.99(5)	177.73(6)	177.53(5)	176.20(13)
S(1)-M(1)-O(3)	175.71(6)	176.90(4)	177.55(7)	179.16(6)	179.22(13

Tab. S2: Specific bond angles [°] and bond lengths [Å] for Ptdmso8.

O(1)-Pt(1)	2.014(10)
S(1)-Pt(1)	2.258(3)
Cl(1)-Pt(1)	2.337(3)
S(3)-Pt(1)	2.215(3)
O(1)-C(3)	1.291(15)
S(1)-C(1)	1.692(13)
O(2)-C(7)	1.365(17)
O(1)-Pt(1)-S(3)	174.9(3)
S(3)-Pt(1)-Cl(1)	90.56(12)
Cl(1)-Pt(1)-O(1)	84.9(3)
S(1)-Pt(1)-S(3)	88.75(12)

Table S1 displays an overview of characteristic bond lengths and angles for bischelating compounds, Figure S3.

Table S2, Figure S3 and Figure S4 shows compound Ptdmso8. All data is in good agreement with those reported earlier for similar complexes and those which has been discussed in the main part of the manuscript.[Hildebrandt, 2016a] Compound Ptdmso8 shows intermolecular hydrogen bonding, as it has been already shown for Ptdmso10.[Hildebrandt, 2016a]

Tab. S3. Crystal data and refinement details for the X-ray structure determinations of the compounds **Ni1 - Ni4**.

Compound	**Ni1**	**Ni3**	**Ni4**
formula	$C_{22}H_{22}NiO_4S_4$	$C_{22}H_{22}NiO_4S_4$	$C_{24}H_{26}NiO_4S_4$
fw (g·mol^{-1})	537.35	537.35	565.40
°C	-140(2)	-140(2)	-140(2)
crystal system	triclinic	monoclinic	triclinic
space group	P $\bar{1}$	P 2_1	P $\bar{1}$
a/ Å	8.9141(6)	12.0833(2)	8.1607(2)
b/ Å	11.1045(8)	7.0305(2)	10.4617(4)
c/ Å	11.9011(9)	13.5338(4)	15.0239(5)
α/°	84.903(4)	90	78.659(1)
β/°	84.716(3)	97.701(1)	88.945(2)
γ/°	71.651(2)	90	74.336(2)
V/Å^3	1111.17(14)	1139.35(5)	1210.09(7)
Z	2	2	2
ρ (g·cm^{-3})	1.606	1.566	1.552
μ (cm^{-1})	12.77	12.45	11.77
measured data	14108	8607	15199
data with I > 2σ(I)	3432	4989	4661
unique data (R_{int})	3691/0.0496	5079/0.0227	5524/0.0341
wR_2 (all data, on F^2)[a]	0.1030	0.0569	0.0897
R_1 (I > 2σ(I)) [a]	0.0402	0.0235	0.0432
S [b]	1.067	1.064	1.075
Res. dens./e·Å^{-3}	0.741/-0.749	0.378/-0.201	0.737/-0.785
Flack-parameter	-	0.152(10)	-
absorpt method	multi-scan	multi-scan	multi-scan
absorpt corr $T_{min}/_{max}$	0.5782/0.7456	0.6651/0.7456	0.6506/0.7456

cont. Tab. S3. Crystal data and refinement details for the X-ray structure determinations of the compounds **Ni6 - Ptdmso8**.

Compound	**Ni6**	**Pd1**	**Ptdmso8**
formula	$C_{24}H_{26}NiO_4S_4$	$C_{22}H_{22}O_4PdS_4$	$C_{12}H_{15}ClO_3PtS_3$
fw ($g \cdot mol^{-1}$)	565.40	585.04	533.96
°C	-140(2)	-140(2)	-140(2)
crystal system	monoclinic	triclinic	monoclinic
space group	P $2_1/n$	P $\bar{1}$	P $2_1/c$
a/ Å	10.0852(2)	7.1500(3)	5.7783(6)
b/ Å	22.9804(6)	10.8504(5)	10.9133(12)
c/ Å	10.6285(3)	15.5213(7)	25.682(3)
α/°	90	78.967(2)	90
β/°	92.662(1)	85.536(3)	92.801(2)
γ/°	90	76.541(2)	90
V/Å^3	2460.62(11)	1148.73(9)	1617.6(3)
Z	4	2	4
ρ ($g \cdot cm^{-3}$)	1.526	1.691	2.193
μ (cm^{-1})	11.57	11.99	92.28
measured data	17207	8764	12971
data with I > 2σ(I)	4850	3852	3295
unique data (R_{int})	5545/0.0465	5013/0.0466	3606/0.0508
wR_2 (all data, on F^2)[a)]	0.0775	0.1387	0.2394

R_1 ($I > 2\sigma(I)$) [a]	0.0366	0.0612	0.0745
S [b]	1.061	1.152	1.090
Res. dens./e·Å^{-3}	0.400/-0.321	0.751/-0.884	4.599/-3.298
absorpt method	multi-scan	multi-scan	multi-scan
absorpt corr $T_{min}/_{max}$	0.6697/0.7456	0.6207/0.7456	0.5337/0.7456
CCDC No.	XXXXXXX	XXXXXXX	XXXXXXX

[a] Definition of the *R* indices: $R_1 = (\Sigma \mid\mid F_o \mid - \mid F_c \mid\mid)/\Sigma \mid F_o \mid$;

$wR_2 = \{\Sigma[w(F_o^2-F_c^2)^2]/\Sigma[w(F_o^2)^2]\}^{1/2}$ with $w^{-1} = \sigma^2(F_o^2) + (aP)^2+bP$; $P = [2F_c^2 + Max(F_O^2]/3$; [b] $s = \{\Sigma[w(F_o^2-F_c^2)^2]/(N_o-N_p)\}^{1/2}$.

Part 2

Chemical and biological investigations of platinum(II) complexes with asparagusic acid derivatives as S/S, Se/Se and S/Se -bidendate ligands

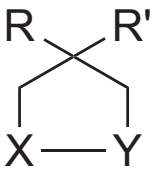

L1-L4

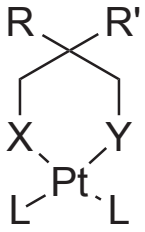

Pt1-Pt7

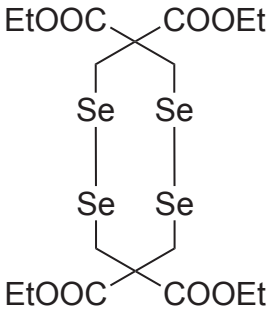

L5

	L1/Pt1	Pt2	L2/Pt3	Pt4	L3/Pt5	Pt6	L4/Pt7
X	S	S	S	S	Se	Se	Se
Y	S	S	Se	Se	Se	Se	Se
R	H	H	H	H	H	H	COOEt
R'	COOH	COOH	COOH	COOH	COOH	COOH	COOEt
L	PPh_3	½ dppma	PPh_3	½ dppma	PPh_3	½ dppma	PPh_3

Part 2 of this thesis discuss platinum(II) complexes Pt1-Pt7 with asparagusic acid derivatives as ligands L1-L4.

[JH5] Pt1-7

[JH6] L1-5 and Pt1-7

4.5 [JH5]

Synthesis, characterization and biological investigation of platinum(II) complexes with asparagusic acid derivatives as ligands

Jana Hildebrandt, Ralf Trautwein, Daniel Kritsch, Norman Häfner, Helmar Görls, Matthias Dürst, Ingo B. Runnebaum, Wolfgang Weigand

Dalton Transactions **2019**, *48*, 936-944.

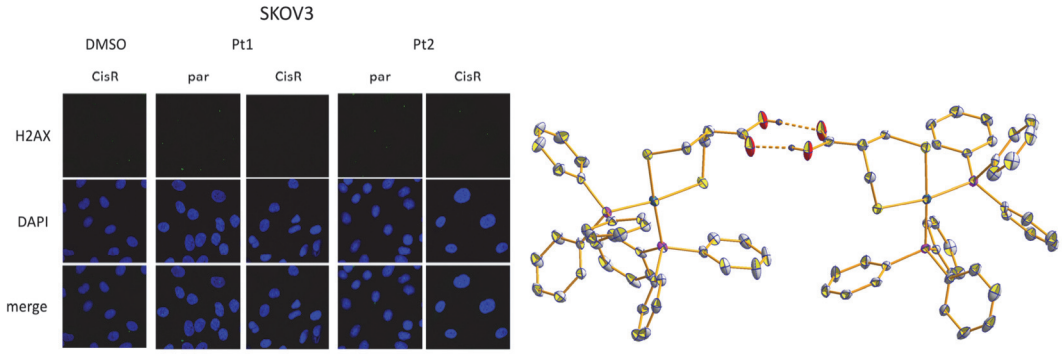

In this publication we report on novel platinum(II) complexes which do not follow the classical SARs of Cisplatin and analogues by bearing different asparagusic acid derivatives as ligands. The platinum(II) complexes have been synthesized and characterized, including molecular structures for Pt1 and Pt7. IC50 values determinations points out that especially Pt6 and Pt7, two selenium-containing derivatives, show good activity on Cisplatin resistant ovarian cancer cell lines. Overall, for most compounds RFs are lower than for Cisplatin itself.

Dalton Transactions

PAPER

View Article Online
View Journal | View Issue

Cite this: *Dalton Trans.*, 2019, **48**, 936

Synthesis, characterization and biological investigation of platinum(II) complexes with asparagusic acid derivatives as ligands†

Jana Hildebrandt,[a,b] Ralf Trautwein,[a] Daniel Kritsch,[b] Norman Häfner,[b] Helmar Görls,[a] Matthias Dürst,[b] Ingo B. Runnebaum*[b] and Wolfgang Weigand *[a]

Received 22nd June 2018,
Accepted 5th December 2018

DOI: 10.1039/c8dt02553c

rsc.li/dalton

After more than 50 years of platinum-based anticancer research only three compounds are in clinical use worldwide. The use of the well-known lead compound of this class of anticancer agents, cisplatin, is limited by its side effects and varying resistance mechanisms. Therefore, we report on platinum(II) compounds with asparagusic acid derivatives as ligands which show interesting anticancer results on cisplatin resistant cell lines.

Introduction

Cisplatin and analogues

Since its first description as a molecule with anticancer activity in the 1960s, cisplatin has acted as one of the major drugs in chemotherapeutic treatment.[1,2] The compound is mainly used in the treatment of lung, head and neck, ovarian, bladder and testicular cancer types.[2–6] The drug application is limited by several side effects *e.g.* hepato-, nephro-, neuro- and ototoxicity as well as several resistance mechanisms inside the human body.[3,7–10] Although there is a great research community working on improving platinum(II) cancer agents, only two additional molecules are approved worldwide, namely carboplatin and oxaliplatin.[3,7,10,11] Carboplatin, developed in 1989, is clinically used against advanced ovarian carcinomas, whereas oxaliplatin has been well-implemented against metastatic colorectal cancers since 2002.[10,12,13] All three complexes contain a square-planar platinum(II) core and on one side, amine-ligands.[11,13,14] The rational design of platinum(II) anticancer agents putting effective leaving groups on the other two coordination sides seems to be an important characteristic. In the case of cisplatin the molecule exhibits two chlorido ligands, whereas carboplatin and oxaliplatin have *O*,*O*-bidentate ligands. Inside the cell, these ligands can be substituted with aqua-complexes which are able to bind to the genomic DNA.[9,15–17] This interaction with the DNA results in a distortion of the dsDNA structure and erroneous DNA replication and leads to apoptosis of the proliferating cells.[9] Although this previously described mechanism is well accepted as the mechanism of action, more and more publications additionally concentrate on the understanding of the bioavailability of the drug after i.v. application. Importantly, the potential interaction with other molecules will just lead to the inactivation of cisplatin.[18–20] Many compounds are designed to follow cisplatin's mechanism of action and target the DNA, although the effectiveness of compounds is likely reduced by resistance mechanisms *i.e.* those mediated by the DNA repair enzymes removing the platinum-adducts from the DNA.[9] Additionally, more than 50 years of research did not identify a drug superior to cisplatin. Thus, new strategies for drug design should be investigated.[3,10] Therefore, other researchers developed compounds for interaction with other, so-called non-classical targets, *e.g.* proteins and enzymes.[6,7,14,21] These complexes do not follow the "basic rules" for platinum-based anticancer compounds but some of them exhibit acceptable anticancer activity.[6,7,22,23]

Asparagusic acid

Natural products are of high interest for medicinal applications. Sulfur-containing metabolites exemplify one group of such compounds with biological activities influencing human health.[24] Next to metabolites, small sulfur-containing compounds like glutathione also have important physiological roles.[25] Asparagusic acid is a sulfur-containing five membered heterocyclic ring (1,2-dithiolane-4-carboxylic acid) with a carboxylic acid function which is unique to asparagus from which it was isolated first in 1948.[26–28] The structure is close to that of α-lipoic acid which can act as a co-factor for *e.g.* pyruvate

[a]*Institut für Anorganische und Analytische Chemie Friedrich-Schiller-Universität Jena, Humboldstraße 8, 07743 Jena, Germanywolfgang.weigand@uni-jena.de; Fax: +49 3641 948102; Tel: +49 3641 948160*
[b]*Klinik für Frauenheilkunde und Fortpflanzungsmedizin, Universitätsklinikum Jena Friedrich-Schiller-Universität Jena, Am Klinikum 1, 07747 Jena, Germany*

†CCDC 1514265 for **Pt1** and 1514266 for **Pt7** (excluding structure factors). For crystallographic data in CIF or other electronic format see DOI: 10.1039/C8DT02553C

multienzyme and is often compared regarding its activity and chemical behavior to this molecule.[27,29,30] The reactivity of the disulfide moieties is essential for mechanisms in biology, biochemistry, medicinal chemistry, organic synthesis, catalysis, coordination chemistry and materials science.[29–38] This contemplation supplemented with the wide range of observed medicinal properties for this compound leads to high interest in asparagusic acid and its analogues for medicinal chemists. The pharmacological properties of ingredients of asparagus are numerous and the research on that increased in the last few years.[24,25,27,28,39,40] Concentrating on asparagusic acid itself, several useful characteristics have been observed: anticancer, antioxidant, antifungal, antibacterial, anti-dysenteric, anti-inflammatory, anti-abortifacient, anti-oxytocic, antiulcer and anticoagulant activities, and it should reduce the risk of rheumatism and diabetes.[27,39] These observations are based on the knowledge that asparagusic acid acts as a growth-inhibitor on higher plants as well as it prevents plants from fungal-growth, which has been observed already in the 1970s.[27,41] Important for medicinal applications of asparagusic acid and its analogues or modified compounds is the cellular uptake which is well-identified as a thiol-mediated mechanism. Asparagusic acid uptake is mediated by binding to a cysteine molecule on the surface of the transferrin receptor.[42,43] These facts and the ability to synthesize metal-complexes with dithiolato and diselenolato ligands (see below) form the basis for the design of our compounds discussed in this publication.

Platinum(II) complexes with S/Se and P containing ligands

In 2010 Siemeling *et al.* reported on the oxidative addition of platinum(0) complexes to asparagusic acid along the sulfur–sulfur bond.[36] We reported previously and later on this kind of reaction to build dithiolato platinum(II) compounds with phosphane ligands.[44–50] Because it is already well-known how to synthesize platinum(II) complexes with sulfur and selenium based ligands some researchers focus on the anticancer activity of these groups of metal complexes.[51–61] In general, most researchers found high IC_{50} values for sulfur-containing platinum(II) complexes in comparison to cisplatin, but results proving higher cytotoxic activity were identified for the selenium-containing species.[52,55,57,62] Fuks *et al.* reported in 2010 on a comparison study between platinum(II) complexes with sulfur or selenium containing ligands showing that the selenium compound was the most promising on HeLa cervical carcinoma cells.[55] Next to sulfur phosphor donor ligands also form strong and inert bonds with the platinum(II) ion.[59,63] Therefore, several phosphane containing platinum(II) complexes are known in the literature.[64–74] Several publications examine the cytotoxic activity of these kinds of compounds, and most of them have a higher IC_{50} value compared to cisplatin.[67,69,70,74] Nevertheless, some publications show lower IC_{50} values for their compounds compared to that of cisplatin on resistant-cell lines pointing to a different mechanism of action overcoming the resistance mechanisms.[65,66,70,75] Concentrating on the structure–activity-relationships of these compounds Ramos-Lima *et al.* found that the replacement of amine ligands by phosphanes results in lower IC_{50} values. Moreover the PPh_3 containing complexes are more active than those with PMe_2Ph-ligands because of their steric effects.[73] In 2011 the synthesis and cytotoxic activity of 14 different platinum(II) compounds with the PtP_2S_2 pharmacophore have been published.[59] Researchers observed high IC_{50} values on the cell line A2780 in comparison to cisplatin for their phosphane platinum(II) complexes. Also the simple $PtCl_2(PPh_3)_2$ which acts as a starting compound for many platinum(II) complexes exhibits very low cytotoxic activity.[59,67] Interestingly, the resistance ratio for these PtP_2S_2 complexes was much lower than that for cisplatin, caused by lower IC_{50} values on resistant cell lines compared to cisplatin itself. To point out, the IC_{50} value for cisplatin on A2780cis/r is 17.1 whereas the average resistant ratio of all eight analyzed compounds is 1.9 (range from 1.5 to 3.0).[59] This may be a consequence of circumventing the resistance mechanisms proving the relevance of this group of compounds despite the fact that their IC_{50} values are in general very high. The most promising phosphane ligand in this previous work has been PPh_3, because of the best resistance factor. Therefore, we focus in our work on the $(PPh_3)_2Pt$ group with dichalcogenolato ligands. Due to the biological relevance of asparagusic acid, this kind of structure completes our platinum-complexes to generate compounds with lower IC_{50} values than cisplatin. It can be expected that they have the same effects on the resistance factors, as previously described by Mügge *et al.* In addition, as described above, selenium containing complexes result in low IC_{50} values in comparison to sulfur containing ones. Thus, the aim of this study was to compare sulfur and selenium containing compounds as well as the mixed ones. To the best of our knowledge, this has not been discussed before. To shed light on the biological activity of the above discussed complexes we designed seven platinum(II) compounds with four different asparagusic acid derivatives and dppma, whereas dppma is bis(diphenylphosphino)methylamine or PPh_3 ligands. These compounds were tested on cisplatin sensitive and resistant cell lines.

Results and discussion

Synthesis and characterization

For **Pt2**, **Pt4** and **Pt6**, the first step is the preparation of $(dppma)PtCl_2$ starting from $(COD)PtCl_2$ which was prepared by adding COD (1,5-cyclooctadiene) to K_2PtCl_4 as described in the literature.[76,77] General synthesis of **Pt1–Pt7** is described in Scheme 1. For the dithiolate compounds **Pt1** and **Pt2** (Scheme 1a), the first step is the deprotonation of both SH groups at the dihydroasparagusic acid with K_2CO_3. In a next step the corresponding $PtCl_2L_2$ (L = PPh_3 or $\frac{1}{2}$ dppma, for more information see Scheme 1) component is added to the solution of the deprotonated diasparagusic acid in $CHCl_3$/EtOH, followed by stirring at room temperature for 16 hours. After the addition of an aqueous solution of $KHSO_4$ (c = 2 mol L^{-1}), the crude product is purified by column chromatography (see

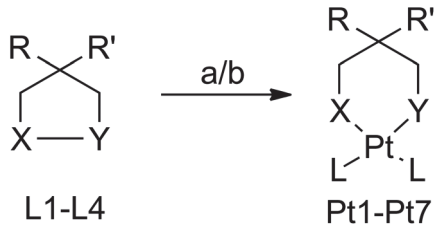

Scheme 1 Synthesis and overview of the platinum(II) complexes **Pt1–Pt7** with their corresponding asparagusic acid derivatives as ligands L1–L7. **Pt1** was first published by Siemeling *et al.*[36] Reagents and conditions: a (for **Pt1**/**Pt2**): (i) 1 equiv. dihydroasparagusic acid, 4 equiv. K_2CO_3, 10 ml EtOH, r.t.; (ii) 1 equiv. $PtCl_2L_2$, 10 ml $CHCl_3$, r.t., 16 h; (iii) $KHSO_4$; b (for **Pt1–Pt7**): (i) 1.05 equiv. corresponding ligand, 3.15 equiv. $NaBH_4$, 10 ml EtOH, r.t., 10 min; (ii) 0.5 M HCl, r.t., 5 min; (iii) K_2CO_3, 1 equiv. $PtCl_2L_2$, 10 ml $CHCl_3$, r.t., 16 h; (iv) $KHSO_4$.

the Experimental section). Another option for the preparation of **Pt1**/**Pt2** as well as for all other Pt(II) compounds (**Pt3–Pt7**) is to start with the asparagusic acid derivatives L1–L4. The first step is reduction to a dianionic species using $NaBH_4$ followed by removal of unreacted $NaBH_4$ with an aqueous solution of HCl and addition of K_2CO_3 to adjust the pH value. Next steps are similar to those described above: addition of $PtCl_2L_2$ (L = PPh_3, dppma), stirring overnight and work up steps (see the Experimental section).

The compounds are characterized by NMR spectroscopy, mass spectrometry and elemental analysis (see the Experimental section). The $^{31}P\{^1H\}$NMR spectrum of **Pt1** shows one singlet at 26.3 ppm with the corresponding ^{195}Pt-satellites as well as for **Pt6** at 34.0 ppm with ^{195}Pt- as well as ^{77}Se-satellites ($^2J_{Se-P}$ = 34.6 Hz). The unsymmetrically substituted S/Se platinum(II) compounds **Pt3** and **Pt4** show a typical AB spin system in the $^{31}P\{^1H\}$ NMR spectra. Mass spectra show the molecular peak as well as the characteristic isotopic pattern for compounds **Pt1**, **Pt3**, **Pt5** and **Pt7** with the PPh_3 ligand. All of them show the fragment m/z = 720 in the Micro-ESI pos. spectrum, which can be detected as a loss of the asparagusic acid derivative. For the dppma containing compounds **Pt2** and **Pt6** their molecular peaks are observed as well as characteristic isotopic patterns. Compound **Pt4** has been characterized only by NMR spectroscopic methods.

Platinum(II) complexes **Pt1** and **Pt7** (Fig. 1) are characterized by means of single crystal X-ray structure determination. Molecular structures of the ligands L2 and L3 were discussed previously.[78] For compound **Pt7** are at least two independent molecules in the unit cell but just one is shown and discussed because bond lengths and angles are very similar. All of them are in the same range like those reported earlier.[36,44,59] In both structures platinum(II) atoms reside in a slightly distorted square-planar coordination sphere similar to those reported previously.[44,59] Because of the steric demand of the PPh_3 ligands the P1–Pt–P2 angle is, in both cases, larger than 90° (99.96°(5) for **Pt1** and 97.38°(5) for **Pt7**), contrary to angles reported for the platinum(II) compounds by Mügge *et al.*, which show P–Pt angles typically for the dppe ligand of ~85°. The S1/Se1–Pt–S2/Se2 angles are close to 90°. The two Pt–P bond lengths are slightly longer (~2.28 Å) than those which were published previously (~2.25 Å).[59] The angles P1–Pt–S1, P2–Pt–S2, P1–Pt–Se1, are P2–Pt–Se2 are between 81° and 90°. The bond lengths of the corresponding X/Y to platinum(II) are longer for **Pt7** than for **Pt1** (for example S1–Pt 2.3375(13) and Se1–Pt 2.4427(5)). The carboxylic function of **Pt1** forms intermolecular hydrogen bonds with another unit (Fig. 1) leading to a dimeric structure in the crystal.

Biological activity

The IC_{50} values of all platinum(II) complexes were determined with the MTT-assay (see the Experimental section for further conditions) on two different ovarian carcinoma cell lines SKOV3 and A2780 (par – parental) as well as on their cisplatin-resistant analogues (SKOV3cis and A2780cis; see the Experimental section for preparation details).[79] Cisplatin acts as a reference and IC_{50} values were determined under the same conditions for platinum(II) compounds. Determined IC_{50} values (Table 1) for cisplatin confirmed significantly higher

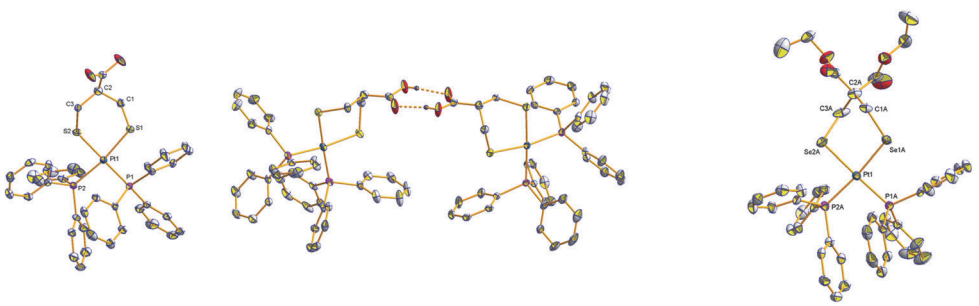

Fig. 1 Left: Molecular structures of **Pt1** in the crystal. Middle: Dimeric unit of **Pt1** in the crystal, displaying intermolecular hydrogen bonding. Ellipsoids are drawn at 50% probability level, hydrogen atoms have been omitted for clarity. Selected bond lengths (Å) and angels (°): P1–Pt 2.2847(13), P2–Pt 2.2925(12), S1–Pt 2.3375(13), S2–Pt 2.3472(13), C1–S1 1.818(6), C3–S2 1.822(5), P1–Pt–P2 99.96(5), P1–Pt–S1 88.75(5), S1–Pt–S2 90.09(4), P2–Pt–S2 81.09(5), C1–S1–Pt 107.60(19), C3–S2–Pt 103.09(19). Right: Molecular structures of **Pt7** in the crystal. Only one of the two individual molecules present in the asymmetric unit is shown. Ellipsoids are drawn at 50% probability level, and hydrogen atoms have been omitted for clarity. Selected bond lengths (Å) and angels (°): P1–Pt 2.2351(14), P2–Pt 2.2866(13), Se1–Pt 2.4427(5), Se2–Pt 2.4733(6), C1–Se1 1.962(5), C3–Se2 1.971(6), P1–Pt–P2 97.38(5), P1–Pt–Se1 88.32(3), Se1–Pt–Se2 90.23(2), P2–Pt–Se2 84.12(4), C1–Se1–Pt 107.02(16), C3–Se2–Pt 101.09(19).

Table 1 IC_{50} values for **Pt1–Pt7** on ovarian carcinoma cell lines SKOV3, A2780 and their cisplatin-resistant analogues SKOV3cis and A2780Cis. Resistant factors (RF) were calculated for each substance[78]

Substance	SKOV3par [μM]	SKOV3cis [μM]	A2780par [μM]	A2780cis [μM]
Pt1	5.5 (±1.3)	23.5 (±1.8)	9.8 (±1.6)	11.8 (±0.9)
RF(**Pt1**)	4.3		1.2	
Pt2	22.0 (±0.2)	12.2 (±2.3)	11.7 (±1.6)	16.1 (±1.7)
RF(**Pt2**)	0.6		1.4	
Pt3	17.8 (±5.2)	18.7 (±3.7)	9.7 (±2.7)	16.0 (±1.9)
RF(**Pt3**)	1.1		1.6	
Pt4	n.m.	n.m.	n.m.	n.m.
RF(**Pt4**)	—		—	
Pt5	13.7 (±6.6)	15.9 (±2.1)	5.4 (±2.4)	17.0 (±4.5)
RF(**Pt5**)	1.2		3.1	
Pt6	9.8 (±1.8)	12.2 (±6.4)	5.0 (±3.5)	5.4 (±1.9)
RF(**Pt6**)	1.2		1.1	
Pt7	6.3 (±0.9)	4.3 (±1.4)	7.8 (±0.9)	5.9 (±1.6)
RF(**Pt7**)	0.7		0.8	
CDDP	**3.8 (±2.8)**	**13.5 (±4.4)**	**1.3 (±0.2)**	**6.1 (±2.1)**
RF (CDDP)	**3.6**		**4.7**	

values for the cisplatin-resistant analogues of both cell lines. Parental SKOV3 and A2780 show higher cytotoxic activity of cisplatin in comparison to **Pt1–Pt7**. Interestingly, whereas IC_{50} values for cisplatin increase in SKOV3cis and A2780cis cells, IC_{50} is not increasing for most of the platinum(II) complexes with asparagusic acid derivatives. Contrarily, in some cases IC_{50} values decrease in a significant way. Similar results have been shown under the same conditions for our latest published platinum(II) complexes with sulfur- and oxygen-containing ligands.[80] Compound **Pt2** shows for SKOV3 an IC_{50} value of 22.0 (±0.2) μM but SKOV3cis exhibits a significantly lower IC_{50} value of 12.2 (±2.3) μM. Also compound **Pt7** has an increased influence on SKOV3cis and A2780cis in comparison to SKOV3 and A2780 (see Table 1). This results in improved resistant factors (RF). Cisplatin shows RF 3.6 (SKOV3) and 4.7 (A2780) whereas the investigated compounds resulted in a RF near to 1, Table 1. Previously reported results of sulfur containing platinum(II) compounds showed for A2780 and its resistant-analogue that these molecules exhibit a higher IC_{50} value on the resistant cell line than on the sensitive one.[59] This is also observable for **Pt1** and **Pt2** (Table 1). IC_{50} values for most of our compounds are in the same range than those already reported.[59] Nevertheless, herein we used different incubation times (48 h to 72 h) pointing to a higher cytotoxic activity of our complexes. The best results are detected for selenium-containing compounds **Pt6** and **Pt7**, both of them show lower IC_{50} values on resistant cell lines than cisplatin and **Pt7** shows lower IC_{50} values for the resistant cell lines than for the sensitive ones. This means that complex **Pt7** exhibits an increased cytotoxic activity for resistant tumour cells in comparison to the parental, sensitive carcinoma cells. To conclude, we can confirm from the previously published results that these kinds of compounds show good RF, that Se/Se-containing platinum(II) complexes show a higher activity than sulfur containing ones and we can add the fact that especially **Pt7** is a promising candidate to target resistant cell lines.[55,59]

An overview of all IC_{50} values, the mean IC_{50} for the compounds and their properties are given in Fig. 2. This overview depicts some SARs of the compounds. As mentioned before **Pt7**, with a Se–Se ligand, is the most active compound and has a mean IC_{50} value of 6.09 μM which is comparable to that of cisplatin (mean IC_{50} value 6.18 μM). Interestingly, also the second most active compound **Pt6** contains a Se/Se ligand. Moreover, the hydrophobicity of the residue R may play an important role. **Pt7** is more active than **Pt5** despite the identical structure except the residues (–COO–Et *vs.* –H and –COOH).

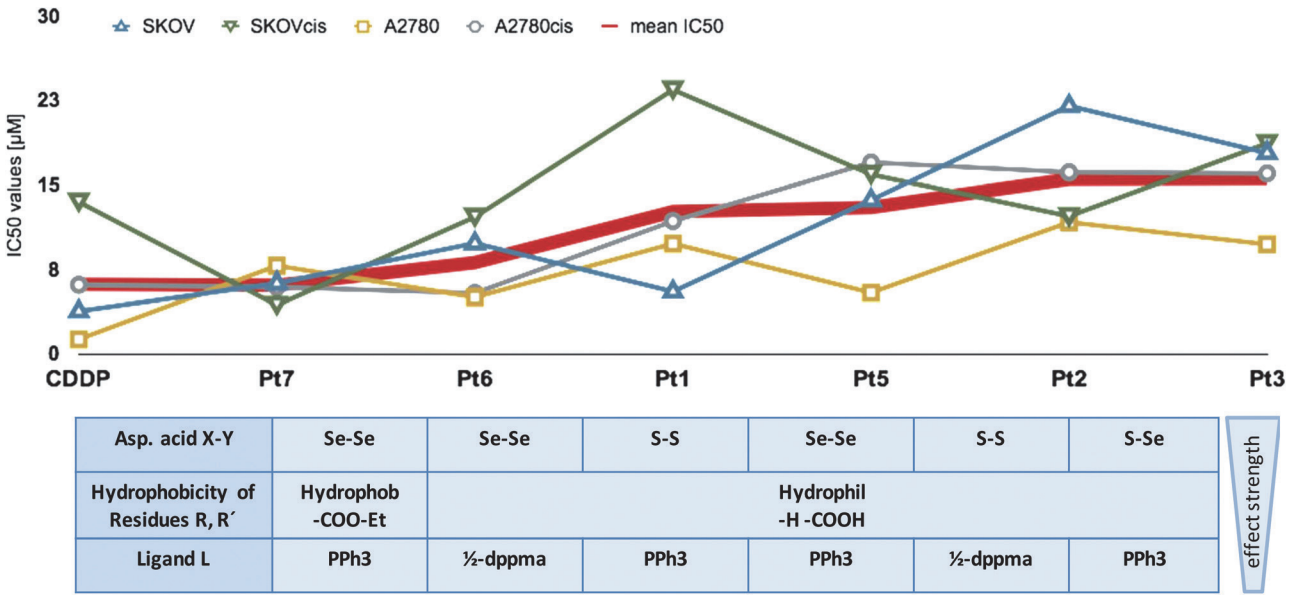

Fig. 2 IC_{50} values for the platinum(II) complexes ordered by rising mean IC_{50} (calculated with all four IC_{50} values per substance) and the characteristics of the compounds. The strength of the SARs for the different characteristics is depicted on the right.

The most active compounds harbour either PPh_3 (**Pt7**) or dppma (**Pt6**) as ligands pointing to a slightly higher activity of PPh_3. Nevertheless, the ligand seems not to be able to break the superior role of the asparagusic acid structure (Se *vs.* S) as **Pt1** (PPh3, S–S) is less active compared to **Pt6** (1/2 dppma, Se–Se).

Conclusions

The investigated platinum(II) complexes containing dichalcogenolato ligands were all characterized using NMR spectroscopy, MS spectrometry and elemental analysis. **Pt1** and **Pt7** were characterized in addition to X-ray diffraction analysis showing a slightly distorted square-planar coordination sphere for the platinum(II) atom. All of these compounds were tested with MTT-assays for their cytotoxic behaviour. Albeit the compounds do not show a higher activity as Cisplatin against the tested sensitive ovarian cancer cell lines, the data suggest that some compounds are able to specifically target resistant cell lines under the tested conditions. For the cell line SKOV3cis the compounds **Pt2**, **Pt6** and **Pt7** have a lower IC_{50} value than cisplatin; for A2780cis this is observable for the compounds **Pt6** and **Pt7**. To point out **Pt7** shows a high cytotoxic activity on all four cancer cell lines and lower IC_{50} values for the two cisplatin-resistant cell lines. In SKOV3cis for example the IC_{50} is significantly lower than that for cisplatin (4.3 ± 1.4 μM in comparison to 13.5 ± 4.4 μM, respectively). Therefore, this compound should be validated as a substitute for cisplatin in the treatment of resistant tumours. High resistance factors (RF IC_{50} resistant/IC_{50} sensitive) for CDDP (3.6 and 4.7 for A2780 and SKOV3) reflect the resistance status for cisplatin, whereas the RF values for substances **Pt1–Pt7** are lower. For **Pt7** and **Pt2** it is, as described above, lower than 1. This indicates that the platinum(II) compounds with asparagusic acid derivatives as ligands are not detoxified by the same resistance mechanisms as cisplatin in the resistant cell lines. Moreover, some platinum(II) compounds (*i.e.* **Pt7**) may specifically target cells with cisplatin resistance associated aberrations because of lower IC_{50} values on resistant cell lines than on sensitive ones.

Experimental section

General

If not otherwise mentioned, all reactions were carried out under a dry nitrogen or argon atmosphere using standard Schlenk techniques. The reagents were purchased from Acros, Fisher Scientific, Merck, Umicore or Aldrich and were used without further purification. Solvents were dried according to common procedures prior to use. ^1H, $^{13}C\{^1H\}$ and $^{31}P\{^1H\}$ NMR spectra were recorded on either a Bruker Avance 200, Bruker Avance 400 or Bruker Avance 600 NMR spectrometer. $^1H^{77}Se$ HMBC NMR measurements were performed on a Bruker Avance 400 NMR spectrometer. The NMR spectra were calibrated with respect to the signal of the residual protons (^1H) or the signal of the deuterated solvent (^{13}C). For $^{31}P\{^1H\}$ and ^1H ^{77}Se HMBC NMR spectra 85% H_3PO_4 and Me_2Se was used as an external standard, respectively. Mass spectra were recorded with a Finnigan MAT SSQ 710 instrument. Elemental analysis was performed with a Leco CHNS-932 apparatus. Silica gel 60 (0.015–0.040 mm) was used for column chromatography and TLC was performed using Merck TLC aluminium sheets (Silica Gel 60 F_{254}).

Preparation of the platinum(II) complexes

Method A. One equivalent of dihydroasparagusic acid was dissolved in ethanol (10 ml for 0.1 mmol) and a fourfold excess of an aqueous solution of K_2CO_3 was added. After stirring for 5 minutes one equivalent of a $[PtP_2Cl_2]$ suspension in chloroform was added and stirred overnight. The resulting yellow solution was acidified with an aqueous $KHSO_4$ solution and extracted with $CHCl_3$ three times. Before removal of the solvent, the combined organic phases were washed with water and dried with Na_2SO_4. Purification of the crude product by column chromatography using dichloromethane/acetone (5 : 1) gave the complexes after precipitation from chloroform/hexane as slight yellow solids.

Method B. The cyclic 1,2-dichalcogenolane derivatives (1.05 equivalents) were suspended in ethanol (10 ml for 0.1 mmol). After addition of 3.15 equivalents $NaBH_4$ and stirring for 10 minutes the resulting clear solution was acidified with diluted hydrochloric acid and then treated with aqueous K_2CO_3 to deprotonate the intermediately occurring dichalcogenolate. To this solution a suspension of $[PtCl_2L_2]$ (one equivalent) in chloroform was added and stirred overnight. After treatment with aqueous $KHSO_4$ the mixture was extracted with chloroform three times and the combined organic phases were washed with water and dried with Na_2SO_4, followed by removal of the solvent under reduced pressure. Subsequent column chromatography with dichloromethane/acetone (5 : 1) as the mobile phase and precipitation from chloroform/*n*-hexane gave the complexes as yellow powders.

[Pt(dppma)Cl$_2$][81]

In a Schlenk flask 0.498 g (1.331 mmol) of $[Pt(cod)Cl_2]$ was dissolved in 70 mL of $CHCl_3$ and 532 mg (1.331 mmol) dppma was added. The mixture was stirred overnight at room temperature and reduced to 5 mL, resulting in the formation of a white precipitate. This was filtered off, washed with a small amount (1 mL) of $CHCl_3$ and dried *in vacuo*. Yield: 0.610 g (69%) white powder.

[Pt(1,2-dithio-4-carboxylic acid)(PPh$_3$)$_2$] (Pt1)

This compound was prepared according to method A using 30 mg (0.20 mmol) dihydroasparagusic acid and 111 mg (0.80 mmol) $[Pt(PPh_3)Cl_2]$. Yield: 50 mg (0.057 mmol, 29%) ^1H-NMR (400 MHz, $CDCl_3$): δ = 3.02–3.44 (m, 5 H, HOOC–C*H* and S–CH_2), 7.14 (m, 12 H, *o*-C*H*), 7.28 (m, 6 H, *p*-C*H*), 7.40 (m, 12 H; *m*-C*H*) ppm; $^{13}C\{^1H\}$-NMR (100.6 MHz, $CDCl_3$): δ = 25.79 (s, S–CH_2), 46.38 (s, HOOC–*C*H), 127.69 (m, *m*-*C*H), 130.41 (s, *p*-*C*H), 134.69 (m, *o*-*C*H), 177.52 (s, *C*OOH) ppm, i-*C*H not detected; $^{31}P\{^1H\}$-NMR (81 MHz, $CDCl_3$): δ = 26.26 (s with

^{195}Pt-satellites, $^{1}J_{Pt-P}$ = 2887 Hz) ppm; MS (ESI): 892 $[M + Na]^+$ 870 $[M + H]^+$ 720 $[M - Asp]^+$; $C_{40}H_{36}O_2P_2PtS_2$ (869.868 g mol^{-1}): calcd C 55.23, H 4.17, S 7.37; found C 54.36, H 4.39, S 7.34.

[Pt(1,2-dithio-4-carboxylic acid)(dppma)] (Pt2)

This compound was prepared according to method A using 30 mg (0.20 mmol) dihydroasparagusic acid and 122 mg (0.20 mmol) [Pt(dppma)Cl_2]. Yield: 28 mg (0.038 mmol, 19%) ^{1}H-NMR (400 MHz, $CDCl_3$): δ = 2.42 (t, $^{3}J_{P-H}$ = 10.2 Hz; 3 H; N–C*H*$_3$), 2.91–3.37 (m, 5 H, HOOC–C*H* and S–C*H*$_2$), 7.42–7.53 (m, 12 H, *o*-C*H* and *p*-C*H*), 7.66 (m, 8 H, *m*-C*H*) ppm; ^{13}C{^{1}H}-NMR (100.6 MHz, $CDCl_3$): δ = 24.19 (s, S–*C*H$_2$), 33.10 (s, N–*C*H$_3$), 49.56 (s, HOOC–*C*H), 129.11 (m, *m*-*C*H), 132.31 (s, *p*-*C*H), 132.44 (s, *p*-*C*′H), 132.77 (m, *o*-*C*H), 133.10 (m, *o*-*C*′H), 177.54 (s, *C*OOH) ppm, i-*C*H not detected; ^{31}P{^{1}H}-NMR (81 MHz, $CDCl_3$): δ = 37.19 (s with ^{195}Pt-satellites, $^{1}J_{Pt-P}$ = 2478 Hz) ppm; MS (ESI): 767 $[M + Na]^+$ 745 $[M + H]^+$; $C_{29}H_{29}NO_2P_2PtS_2$ (744.702 g mol^{-1}): calcd C 46.77, H 3.93, N 1.88; S 8.61; found C 46.87, H 3.95, N 1.88; S 8.73.

[Pt(1,2-Thiaselenolane-4-carboxylic acid)(PPh_3)$_2$] (Pt3)

This compound was prepared according to method B using 41 mg (0.21 mmol) monoselenoasparagusic acid, 24 mg (0.63 mmol) $NaBH_4$ and 158 mg (0.20 mmol) [Pt(PPh_3)Cl_2]. Yield: 56 mg (0.061 mmol, 31%) ^{1}H-NMR (400 MHz, $CDCl_3$): δ = 3.12–3.46 (m, 5 H, HOOC–C*H*, S–C*H*$_2$ and Se–C*H*$_2$), 7.15 (m, 12 H, *o*-C*H*), 7.29 (m, 6 H, *p*-C*H*), 7.43 (m, 12 H, *m*-C*H*) ppm; ^{13}C{^{1}H}-NMR (100.6 MHz, $CDCl_3$): δ = 17.10 (s, Se–*C*H$_2$), 29.29 (s, S–*C*H$_2$), 45.59 (s, HOOC–*C*H), 127.51 (m, *m*-*C*H), 127.72 (m; *m*-*C*H), 130.38 (s, *p*-*C*H), 134.4–134.9 (m, *o*-*C*H), 177.21 (s, *C*OOH) ppm, i-*C*H not detected; ^{31}P{^{1}H}-NMR (81 MHz, $CDCl_3$): δ = 22.53 (d with ^{195}Pt-satellites, $^{2}J_{P-P}$ = 19.4 Hz, $^{1}J_{Pt-P}$ = 2896 Hz), 24.89 (d with ^{195}Pt-satellites, $^{2}J_{P-P}$ = 19.5 Hz, $^{1}J_{Pt-P}$ = 2907 Hz) ppm; ^{1}H–^{77}Se-HMBC (400/76.3 MHz, $CDCl_3$): 67 (m; 1 Se; Pt–*Se*); MS (ESI): 917 $[M]^+$ 720 $[M - Asp]^+$; $C_{40}H_{36}O_2P_2PtSeS$ (916.763 g mol^{-1}) calcd C 52.40, H 3.96, S 3.50; found C 51.33, H 4.38, S 4.04.

[Pt(1,2-Thiaselenolane-4-carboxylic acid)(dppma)] (Pt4)

This compound was prepared according to method B using 41 mg (0.21 mmol) monoselenoasparagusic acid, 24 mg (0.63 mmol) $NaBH_4$ and 133 mg (0.20 mmol) [Pt(dppma)Cl_2]. ^{1}H-NMR (400 MHz, $CDCl_3$): δ = 2.46 (t, $^{3}J_{P-H}$ = 10.2 Hz, 3 H, N–C*H*$_3$), 3.07–3.38 (m, 5 H, HOOC–C*H*, S–C*H*$_2$ and Se–C*H*$_2$), 7.45–7.58 (m, 12 H, *o*-C*H* and *p*-C*H*), 7.70 (m, 8 H, *m*-C*H*) ppm; ^{13}C{^{1}H}-NMR (100.6 MHz, $CDCl_3$): δ = 13.21 (s, Se–*C*H$_2$), 26.50 (s, S–*C*H$_2$), 48.41 (s, HOOC–*C*H), 129.0 (m, *m*-*C*H), 130.38 (s, *p*-*C*H), 132.2–133.2 (m, *o*-*C*H), 177.29 (s, *C*OOH) ppm, i-*C*H not detected; ^{31}P{^{1}H}-NMR (81 MHz, $CDCl_3$): δ = 33.87 (d with ^{195}Pt-satellites, $^{2}J_{P-P}$ = 50.3 Hz, $^{1}J_{Pt-P}$ = 2503 Hz), 37.21 (d with ^{195}Pt-satellites, $^{2}J_{P-P}$ = 50.3 Hz, $^{1}J_{Pt-P}$ = 2439 Hz) ppm; ^{1}H–^{77}Se-HMBC (400/76.3 MHz, $CDCl_3$): 573.5 (m; 1 Se; Pt–*Se*).

[Pt(1,2-Diselenolane-4-carboxylic acid)(PPh_3)$_2$] (Pt5)

This compound was prepared according to method B using 51 mg (0.21 mmol) diselenoasparagusic acid, 24 mg (0.63 mmol) $NaBH_4$ and 158 mg (0.20 mmol) [Pt(PPh_3)Cl_2]. Yield: 63 mg (0.065 mmol, 33%); ^{1}H-NMR (200 MHz, $CDCl_3$): δ = 3.10–3.45 (m, 5 H, HOOC–C*H* and Se–C*H*$_2$), 7.15 (m, 12 H, *o*-C*H*), 7.29 (m, 6 H, *p*-C*H*), 7.45 (m, 12 H, *m*-C*H*) ppm; ^{13}C{^{1}H}-NMR (50.3 MHz, $CDCl_3$): δ = 25.79 (s, Se–*C*H$_2$), 44.54 (s, HOOC–*C*H), 127.52 (m, *m*-*C*H), 130.31 (s, *p*-*C*H), 134.73 (m, *o*-*C*H); 177.28 (s, *C*OOH) ppm, *iC*H not detected, Se*C*H$_2$: n.z.; ^{1}P{^{1}H}-NMR (81 MHz, $CDCl_3$): δ = 21.51 (s with ^{195}Pt-satellites and ^{77}Se-satellites; $^{1}J_{Pt-P}$ = 2923 Hz, $^{2}J_{Se-P}$ = 49.3 Hz) ppm; MS (DEI): 961 $[M]^+$ 719 $[M - Asp]^+$; $C_{40}H_{36}O_2P_2PtSe_2 \cdot \frac{1}{4}$ $CHCl_3$ (993 503 g mol^{-1}) calcd C 48.66, H 3.68; found C 48.58, H 3.51.

[Pt(1,2-Diselenolane-4-carboxylic acid)(dppma)] (Pt6)

This compound was prepared according to method B using 51 mg (0.21 mmol) diselenoasparagusic acid, 24 mg (0.63 mmol) $NaBH_4$ and 133 mg (0.20 mmol) [Pt(dppma)Cl_2]. Yield: 85 mg (0.101 mmol, 51%); ^{1}H-NMR (400 MHz, $CDCl_3$): δ = 2.44 (t, $^{3}J_{P-H}$ = 10.4 Hz, 3 H, N–C*H*$_3$), 3.10–3.35 (m, 5 H, HOOC–C*H* and Se–C*H*$_2$), 7.49 (m, 8 H, *o*-C*H*), 7.55 (m, 4 H, *p*-C*H*), 7.71 (m, 8 H, *m*-C*H*) ppm; ^{13}C{^{1}H}-NMR (100.6 MHz, $CDCl_3$): δ = 16.31 (s, Se–*C*H$_2$), 33.28 (s, N–*C*H$_3$), 47.57 (s, HOOC–*C*H), 129.07 (m, *m*-*C*H), 132.28 (s, *p*-*C*H), 132.34 (s, *p*-*C*′H), 132.81 (m, *o*-*C*H), 132.98 (m, *o*-*C*′H), 177.54 (s, *C*OOH) ppm, i-*C*H not detected; ^{31}P{^{1}H}-NMR (81 MHz, $CDCl_3$): δ = 33.98 (s with ^{195}Pt-satellites and ^{77}Se-satellites, $^{1}J_{Pt-P}$ = 2465 Hz, $^{2}J_{Se-P}$ = 34.6 Hz) ppm; MS (ESI): 839 $[M]^+$; $C_{29}H_{29}NO_2P_2PtSe_2 \cdot \frac{1}{4}$ $CHCl_3$ (868.336 g mol^{-1}) calcd C 40.46, H 3.40, N 1.61; found C 40.85, H 3.28, N 1.19.

[Pt(1,2-Diselenolane-diethylester)(PPh_3)$_2$] (Pt7)

This compound was prepared according to method B using 110 mg of the ligand mixture, 18 mg (0.47 mmol) $NaBH_4$ and 119 mg (0.15 mmol) [Pt(PPh_3)Cl_2]. Yield: 86 mg (0.081 mmol, 54%); ^{1}H-NMR (200 MHz, $CDCl_3$): δ = 1.11 (t, $^{3}J_{H-H}$ = 7.2 Hz, 6 H, CH_2–C*H*$_3$), 3.59 (d with ^{195}Pt-satellites, $^{3}J_{Pt-H}$ = 46 Hz, 4 H, Se–C*H*$_2$), 7.09 (m, 12 H, *o*-C*H*), 7.23 (m, 6 H, *p*-C*H*), 7.41 (m, 12 H, *m*-C*H*) ppm; ^{13}C-NMR (100.6 MHz, $CDCl_3$): 13.95 (s, *C*H$_3$), 23.55 (s, Se*C*H$_2$), 58.97 (s, SeCH$_2$–*C*), 60.89 (s, CH$_3$–*C*H$_2$), 127.30 (m, *m*-*C*H), 129.94 (s, *p*-*C*H), 130.80 (m, i-*C*), 134.66 (m; *o*-*C*H) ppm; ^{31}P{^{1}H}-NMR (81 MHz, $CDCl_3$): δ = 22.09 (s with ^{195}Pt-satellites and ^{77}Se-satellites, $^{1}J_{Pt-P}$ = 2902 Hz, $^{2}J_{Se-P}$ = 47.5 Hz) ppm; ^{1}H–^{77}Se-HMBC (400/76.3 MHz, $CDCl_3$): δ = 85.5 (m, *Se*–CH$_2$) ppm; MS (ESI): 1063 $[M]^+$, 719 $[M - Asp]^+$; $C_{45}H_{44}O_4P_2PtSe_2$ (1063.75 g mol^{-1}) calcd C 50.81, H 4.17; found C 50.78, H 4.24.

Crystal structure determination

The intensity data were collected on a Nonius KappaCCD diffractometer, using graphite-monochromated Mo-K$_\alpha$ radiation. Data were corrected for Lorentz and polarization effects; absorption was taken into account on a semi-empirical basis using multiple-scans.[82–84]

The structure was solved by direct methods (SHELXS[83]) and refined by full-matrix least squares techniques against F_o^2 (SHELXL-97[83]).

The hydrogen atoms bonded to the sulfur ligand of **Pt1** were located by difference Fourier synthesis and refined isotropically. All other hydrogen atoms were included at calculated positions with fixed thermal parameters. All non-hydrogen atoms were refined anisotropically.[85]

Crystal data for Pt1. $C_{40}H_{36}O2P_2PtS_2$, $CHCl_3$, M_r = 989.21 g mol^{-1}, colourless prism, size 0.122 × 0.112 × 0.108 mm^3, monoclinic, space group $C2/c$, a = 27.8130(5), b = 19.4794(3), c = 19.1878(3) Å, β = 130.220(1)°, V = 7937.8(2) Å^3, T = −140 °C, Z = 8, ρ_{calcd} = 1.655 g cm^{-3}, μ (Mo-K$_\alpha$) = 39.59 cm^{-1}, multi-scan, transmin: 0.5671, transmax: 0.7456, F(000) = 3920, 23 970 reflections in h(−36/28), k(−25/25), l(−24/24), measured in the range 2.09° ≤ Θ ≤ 27.48°, completeness Θ_{max} = 99.7%, 9075 independent reflections, R_{int} = 0.0526, 7484 reflections with $F_o > 4\sigma(F_o)$, 484 parameters, 0 restraints, R_{1obs} = 0.0425, wR_{2obs} = 0.0799, R_{1all} = 0.0591, wR_{2all} = 0.0864, GOOF = 1.085, largest difference peak and hole: 1.136/−1.364 e Å^{-3}.

Crystal data for Pt7. $C_{45}H_{44}O_4P_2PtSe_2$, $0.5{\cdot}C_7H_8$, M_r = 1109.82 g mol^{-1}, yellow prism, size 0.05 × 0.05 × 0.05 mm^3, monoclinic, space group $P2_1/n$, a = 21.7853(3), b = 15.5909(3), c = 26.9714(4) Å, β = 105.2560(10)°, V = 8838.1(2) Å^3, T = −90 °C, Z = 8, ρ_{calcd} = 1.668 g cm^{-3}, μ (Mo-K$_\alpha$) = 49.38 cm^{-1}, multi-scan, transmin: 0.6571, transmax: 0.7456, F(000) = 4376, 63 123 reflections in h(−28/28), k(−20/16), l(−34/35), measured in the range 2.04° ≤ Θ ≤ 27.48°, completeness Θ_{max} = 99.8%, 20 228 independent reflections, R_{int} = 0.0864, 11 743 reflections with $F_o > 4\sigma(F_o)$, 1041 parameters, 0 restraints, R_{1obs} = 0.0434, wR_{2obs} = 0.0764, R_{1all} = 0.1080, wR_{2all} = 0.0928, GOOF = 0.935, largest difference peak and hole: 1.212/−1.288 e Å^{-3}.

MTT assays

Ovarian cancer cell lines were cultured under standard conditions (5% CO_2, 37 °C, 90% humidity) in RPMI medium supplemented with 10% FCS, 100 U ml^{-1} penicillin and 100 μg ml^{-1} streptomycin (Life Technologies, Germany). Cisplatin (Sigma, Germany) was freshly dissolved at 1 mg ml^{-1} in 0.9% NaCl solution and diluted appropriately. New platinum(II) complexes and ligands were dissolved in dmso. Platinum-resistant A2780 and SKOV3 cells were established by repeated rounds of 3 day incubations with increasing amounts of cisplatin starting with 0.1 μM. The concentration was doubled after 3 incubations interrupted by recovery phases with normal medium. The cells that survived the third round of 12.8 μM cisplatin were defined as resistant cultures. Determinations of IC_{50} values were carried out using the CellTiter96 non-radioactive proliferation assay (MTT assay, Promega). After seeding 5000 cells per well in a 96-well plate the cells were allowed to attach for 24 h and were incubated for 48 h with different concentrations of the substances ranging from 0 to 1000 μM for platinum and 0 to 1000 μM for ligand tests. Each measurement was done in triplicate and repeated 3-times. The proportion of live cells was quantified by the MTT assay and after background subtraction relative values compared to the mean of medium controls were calculated. Non-linear regression analyses applying Hill-slope were run in GraphPad 5.0 software.

Conflicts of interest

There are no conflicts to declare.

Acknowledgements

Umicore AG & Co. KG is acknowledged for a generous gift of K_2PtCl_4.

Notes and references

1 B. Rosenberg, L. Van Camp and T. Krigas, *Nature*, 1965, **205**, 698–699.
2 L. Amable, *Pharmacol. Res.*, 2016, **106**, 27–36.
3 S. Dilruba and G. V. Kalayda, *Cancer Chemother. Pharmacol.*, 2016, **77**, 1103–1124.
4 M. Galanski, *Recent Pat. Anti-Cancer Drug Discovery*, 2006, **1**, 285–295.
5 D. Lebwohl and R. Canetta, *Eur. J. Cancer*, 1998, **34**, 1522–1534.
6 J. Mayr, P. Heffeter, D. Groza, L. Galvez, G. Koellensperger, A. Roller, B. Alte, M. Haider, W. Berger, C. R. Kowol and B. K. Keppler, *Chem. Sci.*, 2017, **8**, 2241–2250.
7 P. C. Bruijnincx and P. J. Sadler, *Curr. Opin. Chem. Biol.*, 2008, **12**, 197–206.
8 L. Galluzzi, L. Senovilla, I. Vitale, J. Michels, I. Martins, O. Kepp, M. Castedo and G. Kroemer, *Oncogene*, 2012, **31**, 1869–1883.
9 Y. Jung and S. J. Lippard, *Chem. Rev.*, 2007, **107**, 1387–1407.
10 F. M. Muggia, A. Bonetti, J. D. Hoeschele, M. Rozencweig and S. B. Howell, *J. Clin. Oncol.*, 2015, **33**, 4219–4226.
11 L. Bai, C. Gao, Q. Liu, C. Yu, Z. Zhang, L. Cai, B. Yang, Y. Qian, J. Yang and X. Liao, *Eur. J. Med. Chem.*, 2017, **140**, 349–382.
12 K. R. Harrap, *Cancer Treat. Rev.*, 1985, **12**(Suppl A), 21–33.
13 A. M. Montana and C. Batalla, *Curr. Med. Chem.*, 2009, **16**, 2235–2260.
14 S. Komeda and A. Casini, *Curr. Top. Med. Chem.*, 2012, **12**, 219–235.
15 V. Brabec, O. Hrabina and J. Kasparkova, *Coord. Chem. Rev.*, 2017, **351**, 2–31.
16 N. P. Farrell, *Chem. Soc. Rev.*, 2015, **44**, 8773–8785.
17 E. R. Jamieson and S. J. Lippard, *Chem. Rev.*, 1999, **99**, 2467–2498.
18 U. Jungwirth, C. R. Kowol, B. K. Keppler, C. G. Hartinger, W. Berger and P. Heffeter, *Antioxid. Redox Signaling*, 2011, **15**, 1085–1127.
19 L. Messori and A. Merlino, *Coord. Chem. Rev.*, 2016, **315**, 67–89.
20 A. Terenzi, C. Pirker, B. K. Keppler and W. Berger, *J. Inorg. Biochem.*, 2016, **165**, 71–79.

21 G. Palermo, A. Magistrato, T. Riedel, T. von Erlach, C. A. Davey, P. J. Dyson and U. Rothlisberger, *ChemMedChem*, 2016, **11**, 1199–1210.
22 W. H. Ang and P. J. Dyson, *Eur. J. Inorg. Chem.*, 2006, 4003–4018.
23 M. A. Jakupec, V. B. Arion, S. Kapitza, E. Reisner, A. Eichinger, M. Pongratz, B. Marian, N. Graf von Keyserlingk and B. K. Keppler, *Int. J. Clin. Pharmacol. Ther.*, 2005, **43**, 595–596.
24 R. Nakabayashi, Z. Yang, T. Nishizawa, T. Mori and K. Saito, *J. Nat. Prod.*, 2015, **78**, 1179–1183.
25 A. Salemme, A. R. Togna, A. Mastrofrancesco, V. Cammisotto, M. Ottaviani, A. Bianco and A. Venditti, *Brain Res. Bull.*, 2016, **120**, 151–158.
26 E. F. Jansen, *J. Biol. Chem.*, 1948, **176**, 657–664.
27 S. C. Mitchell and R. H. Waring, *Phytochemistry*, 2014, **97**, 5–10.
28 A. Sharma and D. N. Sharma, *Am. J. PharmTech Res.*, 2017, **7**, 1–19.
29 A. Carmine, Y. Domoto, N. Sakai and S. Matile, *Chemistry*, 2013, **19**, 11558–11563.
30 N. Chuard, G. Gasparini, D. Moreau, S. Lorcher, C. Palivan, W. Meier, N. Sakai and S. Matile, *Angew. Chem., Int. Ed.*, 2017, **56**, 2947–2950.
31 D. W. Essex, *Antioxid. Redox Signaling*, 2009, **11**, 1191–1225.
32 G. Fortman, T. Kégl and C. Hoff, *Curr. Org. Chem.*, 2008, **12**, 1279–1297.
33 T. Kondo and T. A. Mitsudo Ta, *Chem. Rev.*, 2000, **100**, 3205–3220.
34 T. Kondo, S. Y. Uenoyama, K. Fujita and T. A. Mitsudo, *J. Am. Chem. Soc.*, 1999, **121**, 482–483.
35 J. C. Love, L. A. Estroff, J. K. Kriebel, R. G. Nuzzo and G. M. Whitesides, *Chem. Rev.*, 2005, **105**, 1103–1169.
36 U. Siemeling, F. Bretthauer and C. Bruhn, *J. Organomet. Chem.*, 2010, **695**, 626–629.
37 X. Wang and Z. Guo, *Dalton Trans.*, 2008, 1521–1532.
38 N. Yamagiwa, Y. Suto and Y. Torisawa, *Bioorg. Med. Chem. Lett.*, 2007, **17**, 6197–6201.
39 M. Iqbal, Y. Bibi, N. Iqbal Raja, M. Ejaz, M. Hussain, F. Yasmeen, H. Saira and M. Imran, *J. Plant Biochem. Physiol.*, 2017, **5**, DOI: 10.4172/2329-9029.1000180.
40 D. S. Jang, M. Cuendet, H. H. Fong, J. M. Pezzuto and A. D. Kinghorn, *J. Agric. Food Chem.*, 2004, **52**, 2218–2222.
41 H. Yanagawa, N. Takahash, T. Kato, Y. Kato and Y. Kitahara, *Tetrahedron Lett.*, 1972, 2549–2552.
42 D. Abegg, G. Gasparini, D. G. Hoch, A. Shuster, E. Bartolami, S. Matile and A. Adibekian, *J. Am. Chem. Soc.*, 2017, **139**, 231–238.
43 N. Chuard, A. I. Poblador-Bahamonde, L. L. Zong, E. Bartolami, J. Hildebrandt, W. Weigand, N. Sakai and S. Matile, *Chem. Sci.*, 2018, **9**, 1860–1866.
44 T. Niksch, H. Görls, M. Friedrich, R. Oilunkaniemi, R. Laitinen and W. Weigand, *Eur. J. Inorg. Chem.*, 2010, 74–94.
45 H. Petzold, T. Weisheit, S. Brautigam, H. Görls, G. Mloston and W. Weigand, *Eur. J. Inorg. Chem.*, 2010, 3636–3641.
46 W. Weigand, G. Bosl, C. Robl and W. Amrein, *Chem. Ber./Recl.*, 1992, **125**, 1047–1051.
47 W. Weigand, G. Bosl, C. Robl and J. Kroner, *Z. Naturforsch., B: J. Chem. Sci.*, 1993, **48**, 627–635.
48 W. Weigand, S. Brautigam and G. Mloston, *Coord. Chem. Rev.*, 2003, **245**, 167–175.
49 R. Wunsch, G. Bosl, C. Robl and W. Weigand, *J. Organomet. Chem.*, 2001, **621**, 352–358.
50 R. Wunsch, W. Weigand and G. Nuspl, *J. Prakt. Chem./Chem.-Ztg.*, 1999, **341**, 768–772.
51 E. Amtmann, M. Zoller, H. Wesch and G. Schilling, *Cancer Chemother. Pharmacol.*, 2001, **47**, 461–466.
52 S. M. Chopade, P. P. Phadnis, A. S. Hodage, A. Wadawale and V. K. Jain, *Inorg. Chim. Acta*, 2015, **427**, 72–80.
53 D. Dolfen, K. Schottler, S. M. Valiahdi, M. A. Jakupec, B. K. Keppler, E. R. T. Tiekink and F. Mohr, *J. Inorg. Biochem.*, 2008, **102**, 2067–2071.
54 P. K. Dutta, A. K. Asatkar, S. S. Zade and S. Panda, *Dalton Trans.*, 2014, **43**, 1736–1743.
55 L. Fuks, E. Anuszewska, H. Kruszewska, A. Krowczynski, J. Dudek and N. Sadlej-Sosnowska, *Transition Met. Chem.*, 2010, **35**, 639–647.
56 A. Ishii, S. Kashiura, Y. Hayashi and W. Weigand, *Chemistry*, 2007, **13**, 4326–4333.
57 F. Li, T. Li, X. Han, H. Zhuang, G. Nie and H. Xu, *ACS Biomater. Sci. Eng.*, 2018, **4**, 1954–1962.
58 V. Lingen, A. Luning, A. Krest, G. B. Deacon, J. Schur, I. Ott, I. Pantenburg, G. Meyer and A. Klein, *J. Inorg. Biochem.*, 2016, **165**, 119–127.
59 C. Mügge, C. Rothenburger, A. Beyer, H. Görls, C. Gabbiani, A. Casini, E. Michelucci, I. Landini, S. Nobili, E. Mini, L. Messori and W. Weigand, *Dalton Trans.*, 2011, **40**, 2006–2016.
60 A. Muscella, N. Calabriso, S. A. De Pascali, L. Urso, A. Ciccarese, F. P. Fanizzi, D. Migoni and S. Marsigliante, *Biochem. Pharmacol.*, 2007, **74**, 28–40.
61 L. W. Zeng, Y. Li, T. Y. Li, W. Cao, Y. Yi, W. J. Geng, Z. W. Sun and H. P. Xu, *Chem. – Asian J.*, 2014, **9**, 2295–2302.
62 C. Rothenburger, M. Galanski, V. B. Arion, H. Görls, W. Weigand and B. K. Keppler, *Eur. J. Inorg. Chem.*, 2006, 3746–3752.
63 R. G. Pearson, *J. Am. Chem. Soc.*, 1963, **85**, 3533–3539.
64 D. B. D. Amico, M. Colalillo, L. Labella, F. Marchetti and S. Samaritani, *Inorg. Chim. Acta*, 2018, **470**, 181–186.
65 P. Bergamini, V. Bertolasi, L. Marvelli, A. Canella, R. Gavioli, N. Mantovani, S. Manas and A. Romerosa, *Inorg. Chem.*, 2007, **46**, 4267–4276.
66 P. Bergamini, V. Ferretti, P. Formaglio, A. Marchi, L. Marvelli and F. Sforza, *Polyhedron*, 2014, **78**, 54–61.
67 S. Bombard, M. B. Gariboldi, E. Monti, E. Gabano, L. Gaviglio, M. Ravera and D. Osella, *JBIC, J. Biol. Inorg. Chem.*, 2010, **15**, 841–850.
68 M. M. Dell'Anna, V. Censi, B. Carrozzini, R. Caliandro, N. Denora, M. Franco, D. Veclani, A. Melchior, M. Tolazzi and P. Mastrorilli, *J. Inorg. Biochem.*, 2016, **163**, 346–361.
69 A. R. Khokhar, Q. Y. Xu and Z. H. Siddik, *J. Inorg. Biochem.*, 1990, **39**, 117–123.

70 J. Kozelka, E. Segal and C. Bois, *J. Inorg. Biochem.*, 1992, **47**, 67–80.
71 A. Medrano, S. M. Dennis, A. Alvarez-Valdes, J. Perles, T. McGregor Mason and A. G. Quiroga, *Dalton Trans.*, 2015, **44**, 3557–3562.
72 A. Messere, E. Fabbri, M. Borgatti, R. Gambari, B. Di Blasio, C. Pedone and A. Romanelli, *J. Inorg. Biochem.*, 2007, **101**, 254–260.
73 F. J. Ramos-Lima, A. G. Quiroga, B. Garcia-Serrelde, F. Blanco, A. Carnero and C. Navarro-Ranninger, *J. Med. Chem.*, 2007, **50**, 2194–2199.
74 M. Ravera, E. Gabano, M. Sardi, E. Monti, M. B. Gariboldi and D. Osella, *Eur. J. Inorg. Chem.*, 2012, 3441–3448.
75 L. Dalla Via, A. N. Garcia-Argaez, A. Adami, S. Grancara, P. Martinis, A. Toninello, D. B. Dell'Amico, L. Labella and S. Samaritani, *Bioorg. Med. Chem.*, 2013, **21**, 6965–6972.
76 J. Chatt, L. M. Vallarino and L. M. Venanzi, *J. Chem. Soc.*, 1957, 3413–3416.
77 V. Gallo, P. Mastrorilli, C. F. Nobile, P. Braunstein and U. Englert, *Dalton Trans.*, 2006, 2342–2349.
78 J. Hildebrandt, T. Niksch, R. Trautwein, N. Häfner, H. Görls, M. C. Bartha, M. Durst, I. B. Runnebaum and W. Weigand, *Phosphorus Sulfur Relat. Elem.*, 2017, **192**, 182–186.
79 K. Heinze, D. Kritsch, A. S. Mosig, M. Dürst, N. Häfner and I. B. Runnebaum, *Int. J. Mol. Sci.*, 2018, **19**, DOI: 10.3390/ijms19010253.
80 J. Hildebrandt, N. Häfner, H. Görls, D. Kritsch, G. Ferraro, M. Durst, I. B. Runnebaum, A. Merlino and W. Weigand, *Dalton Trans.*, 2016, **45**, 18876–18891.
81 A. Romerosa, P. Bergamini, V. Bertolasi, A. Canella, M. Cattabriga, R. Gavioli, S. Manas, N. Mantovani and L. Pellacani, *Inorg. Chem.*, 2004, **43**, 905–913.
82 *COLLECT, Data Collection Software*, Nonius B.V., Netherlands, 1998.
83 *SADABS 2.10*, Bruker-AXS Inc., Madison, WI, USA, 2002.
84 Z. Otwinowski and W. Minor, *Methods Enzymol.*, 1997, **276**, 307–326.
85 G. M. Sheldrick, *Acta Crystallogr., Sect. A: Found. Crystallogr.*, 2008, **64**, 112–122.

Part 2

4.6 [JH6]

Asparagusic Acid Derivatives and their Cytotoxic Platinum(II) Complexes

Jana Hildebrandt, Tobias Niksch, Ralf Trautwein, Norman Häfner, Helmar Görls, Marie-Christin Barth, Matthias Dürst, Ingo B. Runnebaum, Wolfgang Weigand

Phosphorous, Sulfur, and Silicon and the Related Elements **2017**, *192*, 182-186.

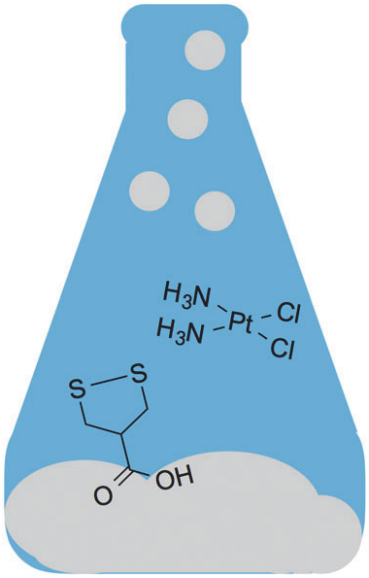

In this publication we reported the first time on platinum(II) complexes with asparagusic acid derivatives as ligands. A general overview of seven different platinum(II) complexes and five different asparagusic acid derivatives is given. Molecular structures of L2, L3 and L5 are shown and discussed. First mentioned IC50 values on all seven platinum(II) complexes prove the relevance of this class of compounds for Cisplatin resistant cell lines.

This publication can be seen as an addition for [JH5] and includes, next to the work of this thesis, results of the PhD thesis of Dr. T. Niksch (molecular structures of L2 and L3, first synthesis and part of discussion), the diploma thesis of Dr. R. Trautwein (idea of the design and first synthesis of Pt compounds) and the bachelor thesis (molecular structure of L5) of M. Barth (supervision by J. Hildebrandt).

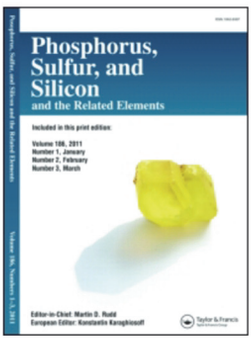

Taylor & Francis
Taylor & Francis Group

Phosphorus, Sulfur, and Silicon and the Related Elements

ISSN: 1042-6507 (Print) 1563-5325 (Online) Journal homepage: http://www.tandfonline.com/loi/gpss20

Asparagusic acid derivatives and their cytotoxic platinum(II) complexes

Jana Hildebrandt, Tobias Niksch, Ralf Trautwein, Norman Häfner, Helmar Görls, Marie-Christin Barth, Matthias Dürst, Ingo B. Runnebaum & Wolfgang Weigand

To cite this article: Jana Hildebrandt, Tobias Niksch, Ralf Trautwein, Norman Häfner, Helmar Görls, Marie-Christin Barth, Matthias Dürst, Ingo B. Runnebaum & Wolfgang Weigand (2017) Asparagusic acid derivatives and their cytotoxic platinum(II) complexes, Phosphorus, Sulfur, and Silicon and the Related Elements, 192:2, 182-186, DOI: 10.1080/10426507.2016.1250760

To link to this article: https://doi.org/10.1080/10426507.2016.1250760

Accepted author version posted online: 21 Oct 2016.
Published online: 21 Oct 2016.

PHOSPHORUS, SULFUR, AND SILICON
2017, VOL. 192, NO. 2, 182–186
http://dx.doi.org/10.1080/10426507.2016.1250760

Taylor & Francis
Taylor & Francis Group

Asparagusic acid derivatives and their cytotoxic platinum(II) complexes

Jana Hildebrandt[a,b], Tobias Niksch[a], Ralf Trautwein[a], Norman Häfner[b], Helmar Görls[a], Marie-Christin Barth[a], Matthias Dürst[b], Ingo B. Runnebaum[b], and Wolfgang Weigand[a]

[a]Institute of Inorganic and Analytical Chemistry, Friedrich-Schiller University Jena, Germany; [b]Department for Gynecology, Jena University Hospital - Friedrich-Schiller University Jena, Germany

ABSTRACT

This work presents platinum(II) compounds with asparagusic acid and derivatives as ligands. Examples of these derivatives were characterized using X-ray diffraction methods and the cytotoxic activity of corresponding platinum(II) complexes was measured in vitro against ovarian cancer cell lines SKOV3 and A2780 and their specially prepared cisplatin-resistant analogues.

ARTICLE HISTORY
Received 17 October 2016
Accepted 17 October 2016

KEYWORDS
Asparagusic acid; cisplatin; anticancer therapy

GRAPHICAL ABSTRACT

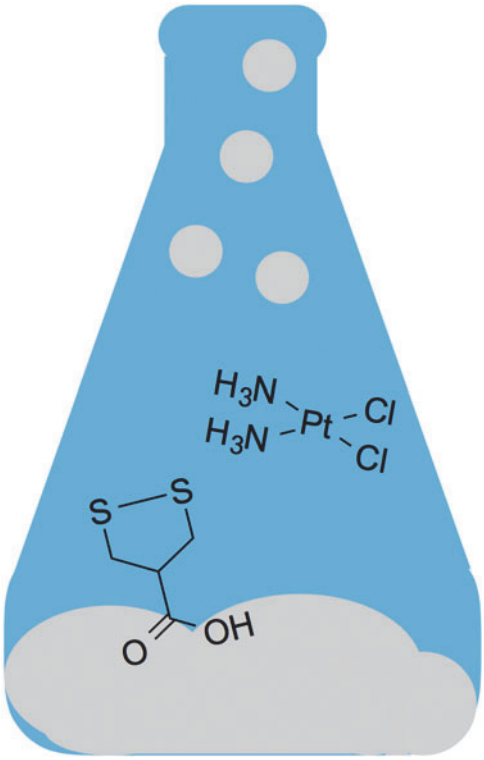

Introduction

Asparagus "*have been on the culinary menu for over two thousand years.*"[1] One of the constituents, the asparagusic acid, shows a 1,2-dithiolane ring system similar to the α-lipoic acid, which acts as a cofactor for pyruvate and α-ketoglutarate multi-enzyme dehydrogenase complexes. For that reason asparagusic acid is of high biological interest. It is known that asparagusic acid shows growth inhibitory effects on fungals and higher plants, a characteristic of high interest for anticancer compounds.[1,2]

Since its discovery cisplatin *cis*-$Cl_2Pt(NH_3)_2$ is one of the most used anticancer drugs worldwide.[3] The square-planar cisplatin acts by distortion of the dsDNA structure after *i.v.*

CONTACT Wolfgang Weigand wolfgang.weigand@uni-jena.de Institute of Inorganic and Analytical Chemistry, Friedrich-Schiller University Jena, Humboldt Strasse 8, 07743 Jena, Germany.
Color versions of one or more of the figures in the article can be found online at www.tandfonline.com/gpss.
Crystallographic data for the structural analysis of compound xx has been deposited at the Cambridge Crystallographic Data Center (CCDC numbers: 1509351 for L2, 1509352 for L3, 1509353 for L5). Copies of the information may be obtained free of charge from The Director, CCDC, 12 Union Road, Cambridge CB2 1 EZ, UK (Fax: + 44-1223-336033; email: deposit@ccdc.cam.ac.uk or www.ccdc.can.ac.uk).

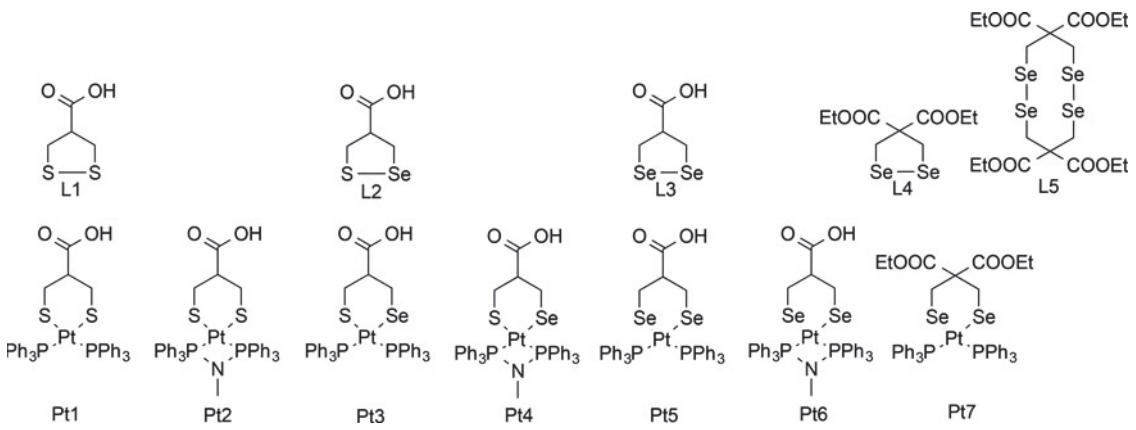

Figure 1. Asparagusic acid derivatives L1–L4, compound L5 and Pt(II) complexes P1–P7.

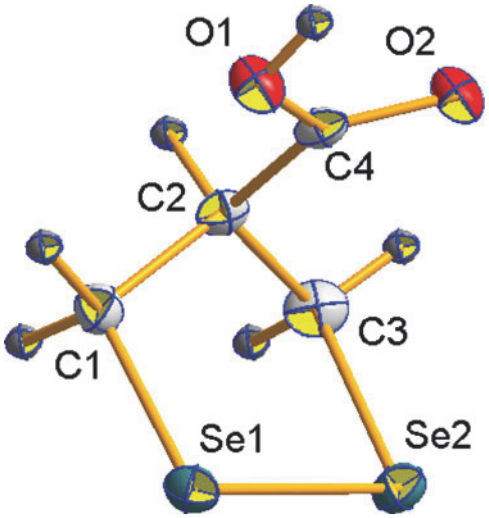

Figure 2. Molecular structure of L3. Selected bond lengths (Å) and angles (°): Se1—Se2 2.3762(5), C1—Se1 1.969(4), C3—Se2 1.967(4), C4—O1 1.283(5), C4—O2 1.260(5), O1···O2^{i} 2.625, Se1···Se2^{ii} 3.622, Se2···Se2^{iii} 3.552; C1—Se1—Se2 91.81(11), C3—Se2—Se1 91.71(12); torsion angle C1—Se1—Se2—C3 −0.3°; i: 1−x, 1 −y, 1−z; ii:1.5 −x, −0.5+y, 0.5 −z; iii: 1−x, 1−y, −z. Ellipsoids are drawn at 50% probability level, hydrogen atoms have been omitted for clarity.

application and the uptake in the cancer cells. Side effects due to its highly toxic properties as well as numerous resistance mechanisms of cancer cells lead to a limitation of the drug dose and reduced clinical efficacy.[4,5] For that reason the design and biological investigations of cisplatin analogues attract great attention in the recent literature. Recent results reporting on overcoming cisplatin-resistance in cancer cell lines showed good activity for different metal-complexes containing derivatives of natural products as ligands.[6,7]

Results and discussion

Design of the asparagusic acid derivatives and their platinum(II) complexes

Figure 1 shows the compounds used for this work. Asparagusic acid and its derivatives have been discussed in literature for several years.[8-15] Crystals suitable for X-ray diffraction analysis have been obtained from compounds L2, L3, and L5.

X-ray structure analysis

Results of the X-ray structure analysis are similar to what was reported earlier.[16]

The molecular structure of L3 reveals that two molecules form a dimeric aggregate via hydrogen bridges between their

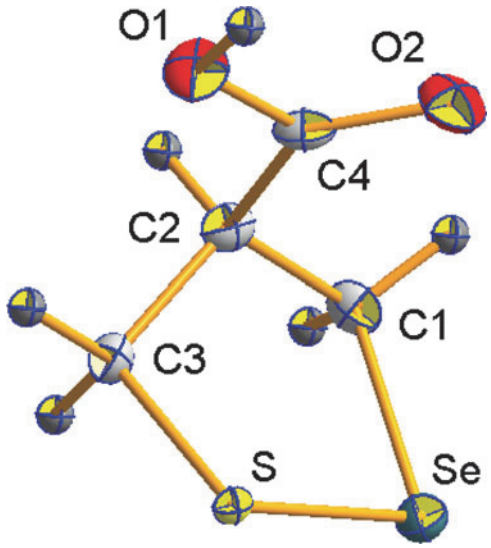

Figure 3. Molecular structure of L2. Selected bond lengths (Å) and angles (°): S—Se 2.2331(15), C1—Se 1.972(6), C3—S 1.838(6), C4—O1 1.322(7), C4—O2 1.229(8), O1···O2^{i} 2.674, Se···Se^{ii} 3.616, Se···Se^{iii} 3.616, Se···Se^{iv} 3.570, Se···Se^{v} 3.601, Se···Se^{vi} 3.601, S···S^{v} 3.723, S···S^{vi} 3.723; C1—Se—S 93.27(18), C3—S—Se 91.39(18); torsion angle C1—Se—S—C3 −20.4°; i: 1−x, −y, −z; ii: 1.5−x, y, 0.5+z; iii: 1.5−x, y, −0.5+z; iv: 1.5−x, 0.5−y, z; v: x, 0.5−y, −0.5+z; vi: x, 0.5−y, 0.5+z. Ellipsoids are drawn at 50% probability level, hydrogen atoms have been omitted for clarity.

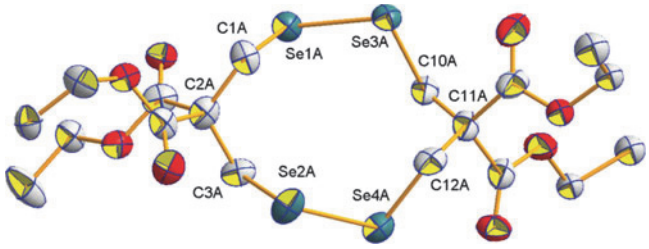

Figure 4. Molecular structure of L5. Selected bond lengths (Å) and angles (°): Se1—Se3 2.3250(15), Se2—Se4 2.3289(16), C1—Se1 1.974(9), C3—Se2 1.966(10), C10—Se3 1.986(9), C12—Se4 1.962(10), C1—C2 1.527(14), C2—C3 1.534(14), C10—C11 1.487(15), C11—C12 1.579(15), C1—Se1—Se3 101.5(3), C10—Se3—Se1 101.0(3); C3—Se2—Se4 101.0(3); C12—Se4—Se2 100.7(3); C1—C2—C3 115.2(9); C10—C11—C12 113.1(9); Ellipsoids are drawn at 50% probability level, hydrogen atoms have been omitted for clarity.

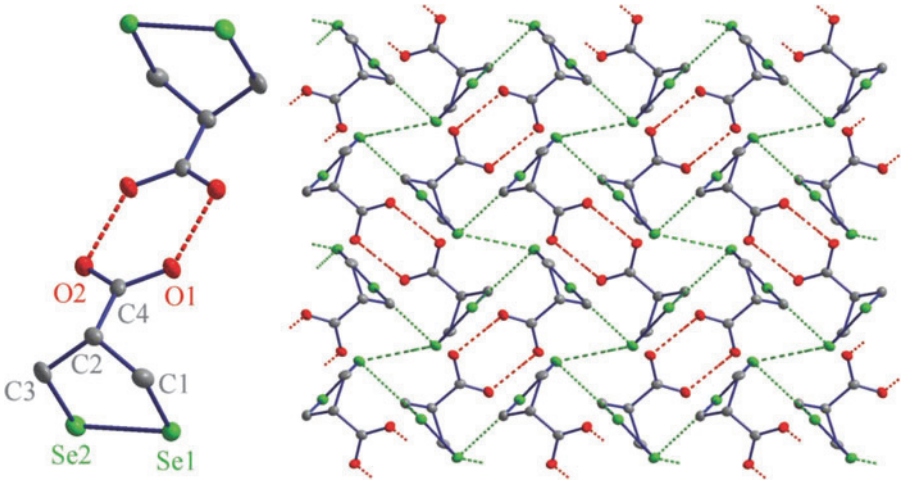

Figure 5. Molecular structure of L3 in the crystal. Left: Aggregated dimeric unit formed via hydrogen bridges. Right: View along the a–axis showing the supramolecular arrangement due to strong hydrogen bridges and non-bonding intermolecular selenium–selenium interactions.

carboxyl groups (Figures 2 and 5, left). The lone pairs at the selenium atoms are forced in eclipsed conformation, as can be read from the torsion angle C1—Se1—Se2—C3 that is determined to −0.28°. Thus, the diselenolane ring can be described as an envelope structure. Expectedly, 1,2-diselenolane-4-carboxylic acid L3 shows a complex supramolecular arrangement (Figures 5, right and 6). Short contacts between selenium atoms of neighboring molecules are observed, being 3.552 Å and 3.622 Å, respectively. The alignment of L3 in the solid state shows that all diselenide moieties arrange in well separated selenium layers, which are connected via a system of hydrogen bridges and therewith building a complex three-dimensional network (Figure 6). The layers are separated by approximately 9 Å, as determined from atom positions.

Even more astonishing is the molecular structure of L2 (Figures 3, 7 and 8). As a consequence of the exchange of a selenium atom by a smaller sulphur atom, the 1,2-thiaselenolane ring is distorted from the envelope conformation that was observed in the molecular structure of L3. This fact is underlined by the torsion angle C1—Se—S—C3 that is −20.4°, while the bond angles at Se and S are close to 90°, being 93.27(18)° and 91.39(18)° for C1—Se—S and C3—S—Se, respectively. Expectedly, the supramolecular arrangement of L2 is determined by hydrogen bridges and non-bonding intermolecular chalcogen–chalcogen interactions. As shown in Figure 7, right, a complex network of interactions between selenium atoms of neighboring molecules is detected. Each selenium atom has not less than five short contacts to adjacent molecules, all intermolecular Se···Se distances are in the range of 3.580—3.616 Å and thus clearly shorter than the sum of their van der Waals radii. These interactions align the selenium atoms in strings along the *c*–axis that can be described as edge-associated tetrahedral strands (Figures 7, right and 8). As can be seen from the Se···Se distances, the tetrahedrons are only slightly distorted. Regarding comparable interactions between sulphur atoms, the shortest contacts were determined to be 3.723 Å and thus are slightly longer than the sum of their van der Waals radii (3.6 Å). (a complete list of van der Waals radii is available at: http://www.ccdc.cam.ac.uk/products/csd/radii/.)

Figure 4 shows compound L5 as a formal dimer of L4, which results in a ten-membered distorted ring structure with six carbon and four selenium atoms. Different bond lengths and angles of C11 and its neighbour atoms show significant differences whereas the values of its analogue C2 resulting in nearly the same ranges.

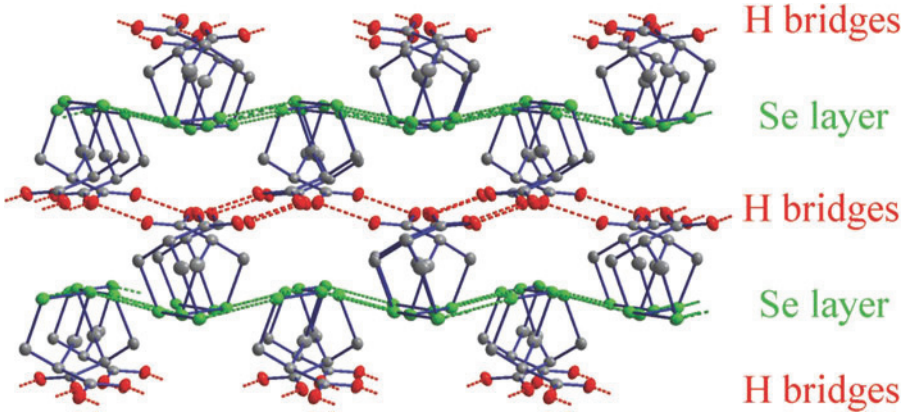

Figure 6. Supramolecular arrangement of L3 displaying the clearly separated selenium layers that are connected via a hydrogen bonding system. Ellipsoids are drawn at 50% probability level, hydrogen atoms have been omitted for clarity.

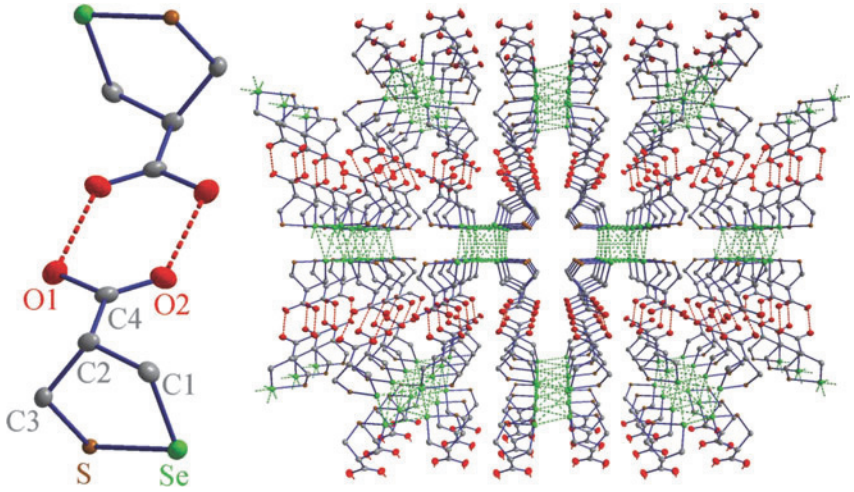

Figure 7. Molecular structure of L2 in the crystal. Left: Dimeric unit due to aggregation via intermolecular hydrogen bridges between the carboxyl groups. Right: Supramolecular arrangement caused by hydrogen bridging system and complex non-bonding chalcogen–chalcogen intermolecular interactions.

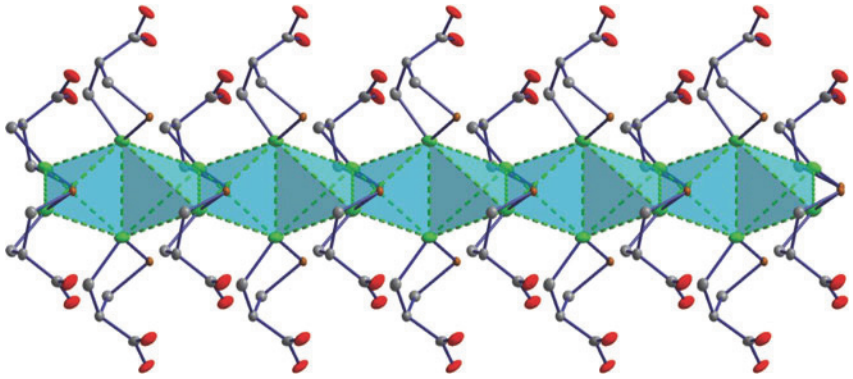

Figure 8. Supramolecular assembly of L2 in the solid state displaying the several short selenium selenium contacts. The selenium atoms form tetrahedrons, which are edge-associated resulting in strands along the *c*–axis of the crystal. Ellipsoids are drawn at 50% probability level, hydrogen atoms have been omitted for clarity.

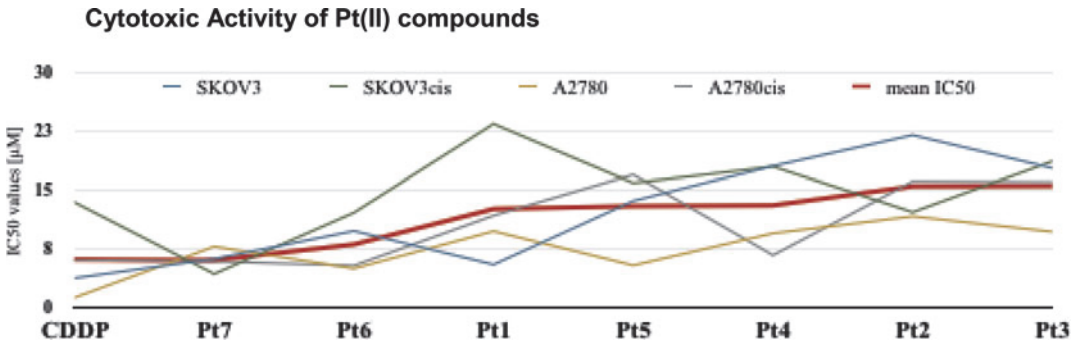

Figure 9. Overview of all IC50 values and the mean IC50 value in comparison to cisplatin. Substances were sorted by their mean IC50 values.

Cytotoxic activity of Pt(II) compounds

The cytotoxic activities of the compounds Pt1-Pt7 were determined on two ovarian carcinoma cell lines SKOV3 and A2780 as well as on their special-prepared cisplatin-resistant analogues (SKOV3cis and A2780cis). It was observed that the platinum(II) complexes, except Pt6 and Pt7, show higher or equal IC50 value in comparison to cisplatin as a reference standard, Figure 9.

First investigations of the structure-activity-relationships (SARs) show the best results for two of the Se/Se-containing compounds Pt6 and Pt7, Table 1. Both compounds show lower

Table 1. IC50 values for all compounds were measured in triplicates with MTT-Assays under same conditions (37°C, 48 h incubation time).

	SKOV3 [μM]	SKOV3cis [μM]	A2780 [μM]	A2780cis [μM]
Pt1	5.5 (±1.3)	23.5 (±1.8)	9.8 (±1.6)	11.8 (±0.9)
Pt2	22.0 (±0.2)	12.2 (±2.3)	11.7 (±1.6)	16.1 (±1.7)
Pt3	17.8 (±5.2)	18.7 (±3.7)	9.7 (±2.7)	16.0 (±1.9)
Pt4	18.1 (±3.1)	18.0 (±2.7)	9.5 (±1.4)	6.7 (±4.0)
Pt5	13.7 (±6.6)	15.9 (±2.1)	5.4 (±2.4)	17.0 (±4.5)
Pt6	9.8 (±1.8)	12.2 (±6.4)	5.0 (±3.5)	5.4 (±1.9)
Pt7	6.3 (±0.9)	4.3 (±1.4)	7.8 (±0.9)	5.9 (±1.6)
CDDP	**3.8 (±2.8)**	**13.5 (±4.4)**	**1.3 (±0.2)**	**6.1 (±2.1)**

IC50 values than cisplatin on cisplatin-resistant cell lines which results in a possibility to circumvent cisplatin-resistance.

Conclusions

In this work we investigated platinum(II) complexes with asparagusic acid and its S/Se and Se/Se derivatives. L2 and L3 as well as the dimeric structure L5 were characterized using X-ray diffraction analysis showing an unsymmetrically coordination sphere. All of the platinum(II) compounds Pt1-Pt7 were tested with MTT-Assay and the IC50 values were determined for ovarian carcinoma cell lines SKOV3 and A2780. The results show higher or equal IC50 values for most of the novel platinum(II) compounds with the exception of Pt6 and Pt7, which show lower IC50 values on cisplatin-resistant cell lines SKOV3cis and A2780cis. In conclusion the described platinum(II) complexes are potentially able to circumvent the cisplatin-resistance in ovarian carcinoma cell lines.

References

1. Mitchel, C. S.; Waring, R. H. *Phytochemistry* **2014,** 97, 5-10.
2. Siemeling, U.; Bretthauer, F.; Bruhn, C. *J. Organomet. Chem.* **2010,** 695, 626-629.
3. Rosenberg, B.; *Interdiscip. Sci. Rev.* **1978,** 3, 134-147.
4. Reedijk, J.; *J. Inorg. Chim. Acta* **1992,** 873, 198-200.
5. Fink, D.; *Cancer Res*. **1996,** 56, 4881-4886.
6. Hildebrandt, J., Görls, H., Häfner, N., Ferraro, G., Dürst, M., Runnebaum, I. B., Weigand, W., Merlino, A., *Dalton Trans*. **2016,** 45, 12283-12287.
7. Hildebrandt, J., Häfner, N., Görls, H., Kritsch, D., Ferraro, G., Dürst, M., Runnebaum, I. B., Merlino, A., Weigand, W., *Dalton Trans*. **2016,** DOI: 10.1039/C6DT01388K.
8. Sato, R., Kimura, T., *Science of Synthesis* **2007,** 39, 1097–1107.
9. Nygrad, B., Olofsson, J., Bergson, G., *Arkiv foer Kemi* **1967,** 28, 41–51.
10. Krackov, M. H., Bergson, G., Biezais, A., Mautner, H. G., *J. Am.Chem. Soc.* **1966,** 88(8), 1759-1762.
11. Bergson, G., Claeson, G., Schotte, L., *Acta Chem. Scand.* **1962,** 16, 1159-1174.
12. Bergson, G., *Acta Chem. Scand.* **1961,** 15, 1611-1613.
13. Bergson, G., *Arkiv foer Kemi* **1962,** 19(15), 195-214.
14. Bergson, G., Biezais, A., *Arkiv foer Kemi* **1961,** 18, 143-149.
15. Wrixon, J. D., Hayward, J. J., Raza, O., Rawson, J. M. *Dalton Trans*. **2014,** 43, 2134-2139.
16. Niksch, T., Görls, H., Friedrich, M., Oilunkaniemi, R., Laitinen, R., Weigand, W., *Eur. J. Inorg. Chem*. **2010,** 74-94.

Part 2

Part 3

‘Quadrupole Action’ compounds as anticancer agents

Two additional projects have been done next to the two main parts of this thesis focusing on so called ‘quadrupole-action’ compounds. Both projects have been carried out at the Hebrew University Jerusalem under supervsion of Prof. D. Gibson and will be continued there.

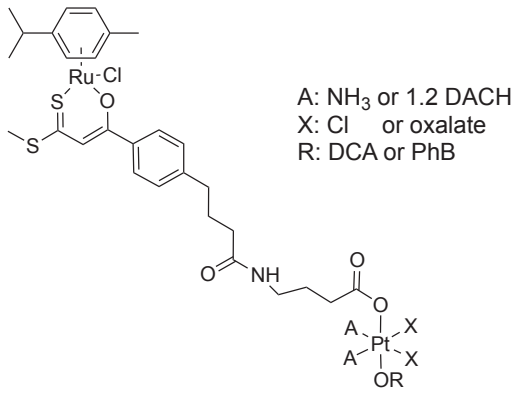

Bimetallic Ru-Pt complexes
Project 1

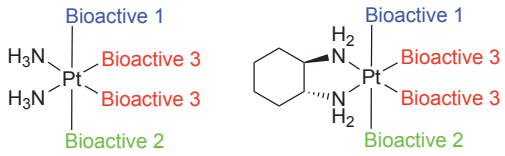

Quadrupole action platinum(IV) prodrugs
Project 2

Project 1:

Novel bimetallic Ru-Pt complexes as potential anticancer agents

Project 2:

‘Quadrupole Action’ Platinum(IV) prodrugs as anticancer agents

4.7 Project 1: Novel bimetallic Ru-Pt complexes as potential anticancer agents[7]

- Scientific aim

Since its discovery Cisplatin as well as its analogues Carboplatin and Oxaliplatin, are used in anticancer therapy. There are several side effects caused by the treatment with these drugs. Their high toxicity limits the drug dose. Platinum(II) compounds undergo a high extracellular inactivation due to their binding to sulfur-containing molecules. Moreover, cancer cells are able to acquire drug resistance after the first treatment.[Rosenberg, 1969; Muggia, 2015] For this reason several platinum(IV) compounds with a chemical inert low-spin d^6 octahedral structure were established in the literature as pro-drugs which are less likely to undergo extracellular inactivation. The axial positions of these compounds can be modified with different bioactive ligands, for example dichloroactetate and phenylbutyrate.[Wexselblatt, 2012; Dhar, 2009] A second option to generate metal drugs as anticancer agents is to change the metal. For that reason cytotoxic ruthenium(III) as well as different ruthenium(II) compounds are well known in the literature.[Hartinger, 2008; Soldevila-Barreda, 2015] Ruthenium(III) compounds are less cytotoxic than Cisplatin is, but they do not have the DNA as a primary target. It is known that they are able to interact with different biomolecules, for example transferrin, and for that reason they have optimal cell-uptake. Following the cell-uptake they undergo reduction to the active species with oxidation stage +II. Several ruthenium(II) compounds have a higher cytotoxicity than Cisplatin or the Ruthenium(III) compounds. Different molecules like the RAPTA compounds, or different molecules with chelating ligands are known, all of them have an arene ligand mostly *para*-cymene at one position.[Allardyce, 2016; Hartinger, 2008; Soldevila-Barreda, 2015] Different Platinum(IV) complexes with bioactive ligands in the axial positions were synthesized by the working group of Prof. D. Gibson in Jerusalem. It was shown that they have cytotoxic behaviour against tumor cell lines by reduction to the platinum(II) inside the cell by the loss of the ligands in axial position which can act against cancer cells as well.[Raveendran, 2016] It was

[7] Results and discussions are taken from Final Report of STSM Fellowship, COST Action CM1105, written in 2016 by J. Hildebrandt.

shown that ruthenium(II) compounds with O,S-chelating ligands can overcome Cisplatin resistance in cancer cell lines and interact with different model proteins. For that reason the purpose of the project was to combine the described advantages of the single compounds and to generate a bimetallic complex with a platinum(IV) as well as a ruthenium(II) center which could be more cytotoxic than the two single complexes.

- Description of the work

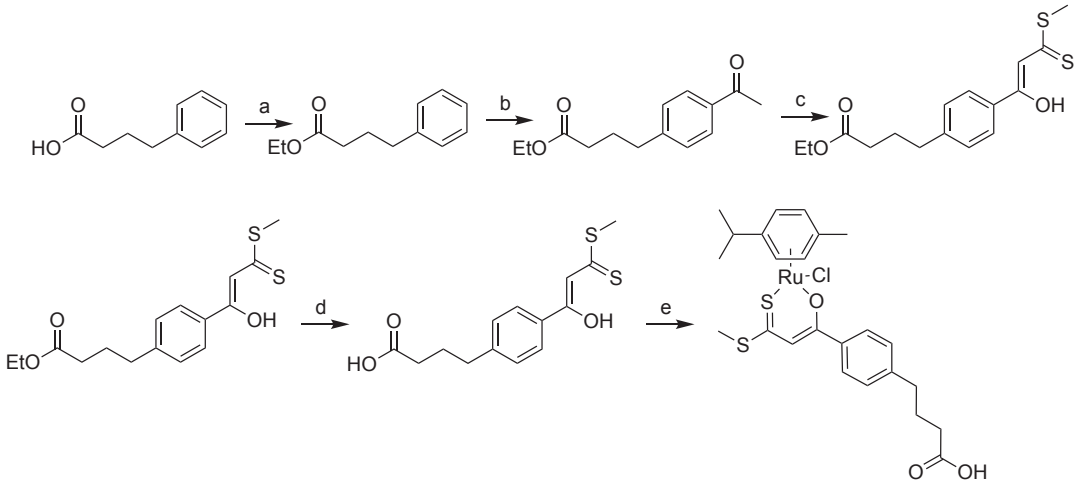

Fig. 4.7-1: Synthesis of the β-Hydroxydithiocinnamicacidmethylester and corresponding ruthenium(II) complex: **a**: Sulfuric acid, ethanol; 5 h; 78 °C; **b**: 4.42 equiv. $AlCl_3$, 2.07 equiv. acetylchloride; dichloromethane (dcm); 0.25 h; r t; **c**: 2 equiv. *t*-BuOK, 1.4 equiv. CS_2, 1. equiv. methyliodide; diethylether; 1 h; -70 °C; **d**: 3 equiv. $LiOH*3H_2O$; tetrahydrofurane (thf)/ methanol/ water; 16 h, r t; **e**: 2 equiv. *t*-BuOK, 0.5 equiv. $[(\eta^6\text{-}p\text{-cymene})RuCl_2]_2$; thf; 12 h, r t.

The different steps of the synthesis of the O,S-chelating ligand (step a-d) are known in the literature, Figure 4.7-1.[Patent: US 2012/0071461 A1] The terminal carboxylic acid group which is essential for the coupling reaction to the platinum(IV) compound was in a first step protected with an ethylester. Step b is a Friedel-Crafts-Acylation to place an acetyl-group in *para*-position to the protected acid, followed by step c, the synthesis of the thioester and the deprotection step d in the end. The *cis*-configurated enol-structure of the thioester is stabelized by an intramolecular hydrogen bond. The methine proton of the free ligand has a chemical shift in the ^1H NMR spectrum

at 6.98 ppm, this signal changes characteristically by the complexation to a metal like ruthenium(II). For the ruthenium(II) compounds we have a high-field shift to 6.79 ppm in the ^{1}H NMR spectrum. As well as the fact that the *para*-cymene ligand shows an unsymmetrical behaviour in comparison to the starting material. This is observable by two double dubletts in the ^{1}H NMR spectrum at 5.33-5.55 ppm The MS spectrum (Figure 4.7-2) shows the molepeak of the ruthenium(II) compound minus the chloride $[530]^{+}$.

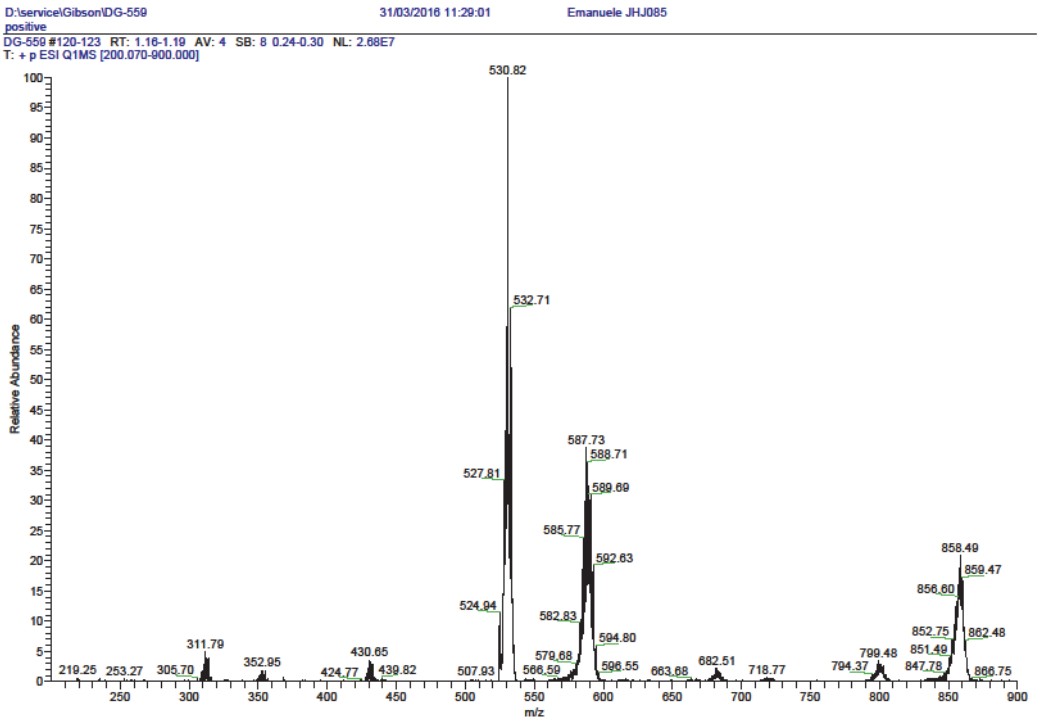

Fig. 4.7-2: MS spectrum of the single ruthenium(II) compound.

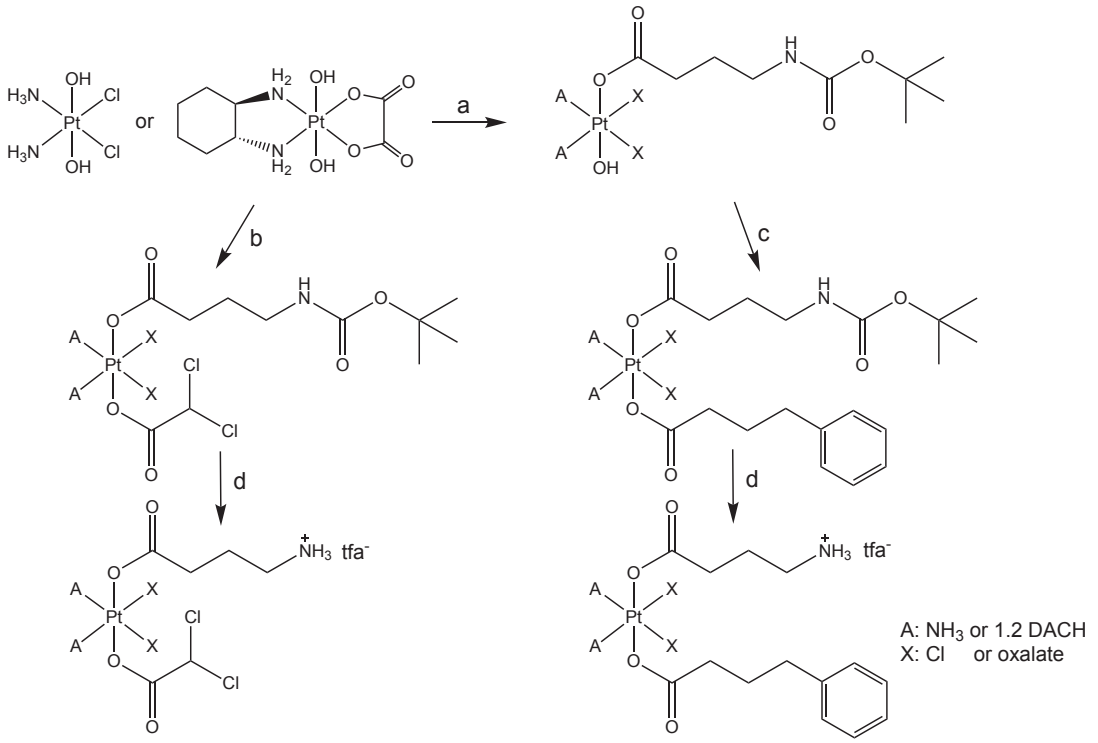

Fig. 4.7-3: Scheme of the synthesis for the different platinum(IV) moieties: **a**: 1.1 equiv. GABA-anhydride; dmso; 12 h, r t; **b/c**: 2 equiv. corresponding anhydride; dimethylformamide (dmf); 12h; r t; **d**: dcm / trifluoroacetic acid (tfa); 0.5 h; r t.

The different platinum(IV) moieties were synthesized starting with two different platinum(IV) complexes (Figure 4.7-3) which have two hydroxyl groups in the axial positions as well as the ligands of Cisplatin or Oxaliplatin. In a first step (a) the protected GABA-group (GABA= Gamma amino-butyric acid) as an anhydride was added to the first axial position followed by step b/c the addition of the second anhydride to place dichloroacetate (option 1) or phenylbutyrate (option 2) in the axial position. The GABA-group is essential for the coupling reaction to the ruthenium(II) moiety, for that reason the last step is the deprotection of the GABA (d).

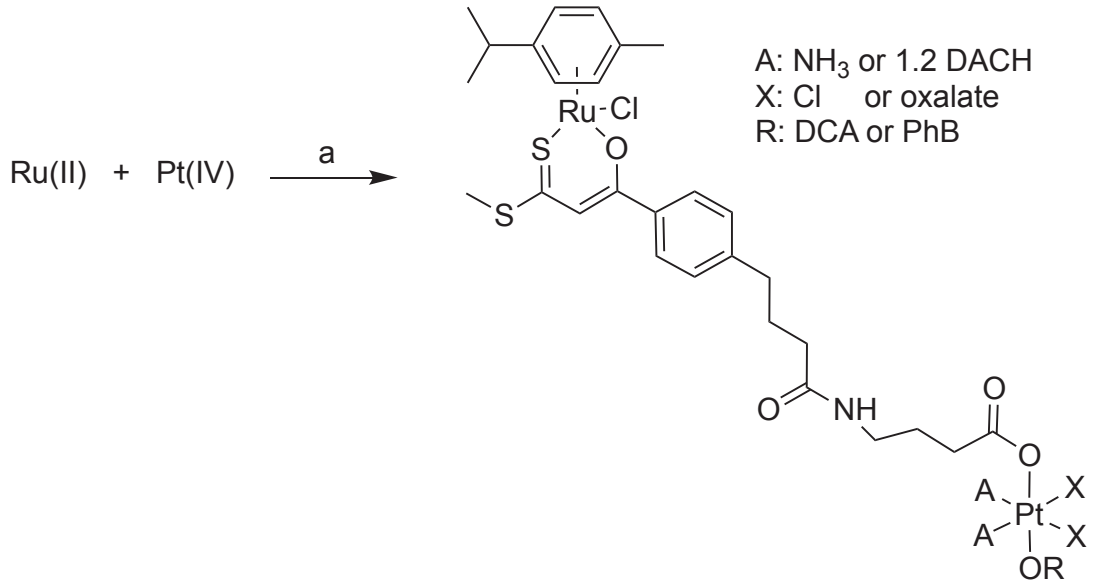

Fig. 4.7-4: Coupling reaction of the bimetallic compounds: **a**: (I) 1 equiv. Ru(II), 2 equiv. EDC, 2 equiv. NHS; 0.5h, dmso, r t; 1 equiv. Pt(IV), 2 equiv. trimethylamine, 0.25 h, dmso, r t; (II) 3 h, r t.

The ruthenium(II) compound is incubated with EDC (= 1-Ethyl-3-(3-dimethylaminopropyl)carbodiimide) and NHS (= N-Hydroxysuccinimide) as well as in a second flask the platinum(IV) single complex is incubated with trimethylamine and given to the ruthenium(II) flask. Both molecules are connected with an amide bond. For that reason the characterization of the successful synthesis of the bimetallic complex in comparison to both single compounds with NMR spectroscopy is not easy. Upon conjugation, the solubility of the platinum(IV) complexes change. The single compounds are not soluble in chloroforme, whereas the bimetallic product as well as the ruthenium(II) single complex are. The ^{195}Pt NMR spectra show the platinum(IV) signal at 1119 ppm in $CDCl_3$. The MS spectra for all compounds show the molecular peak minus the chloride. As shown before for the single ruthenium(II) compound, the chloride is lost during ionization. In Figure 4.7-5 it is shown for the bimetallic compound with Cisplatin and penylbutyrate as ligands on the platinum(IV) moiety m/z = 1078.

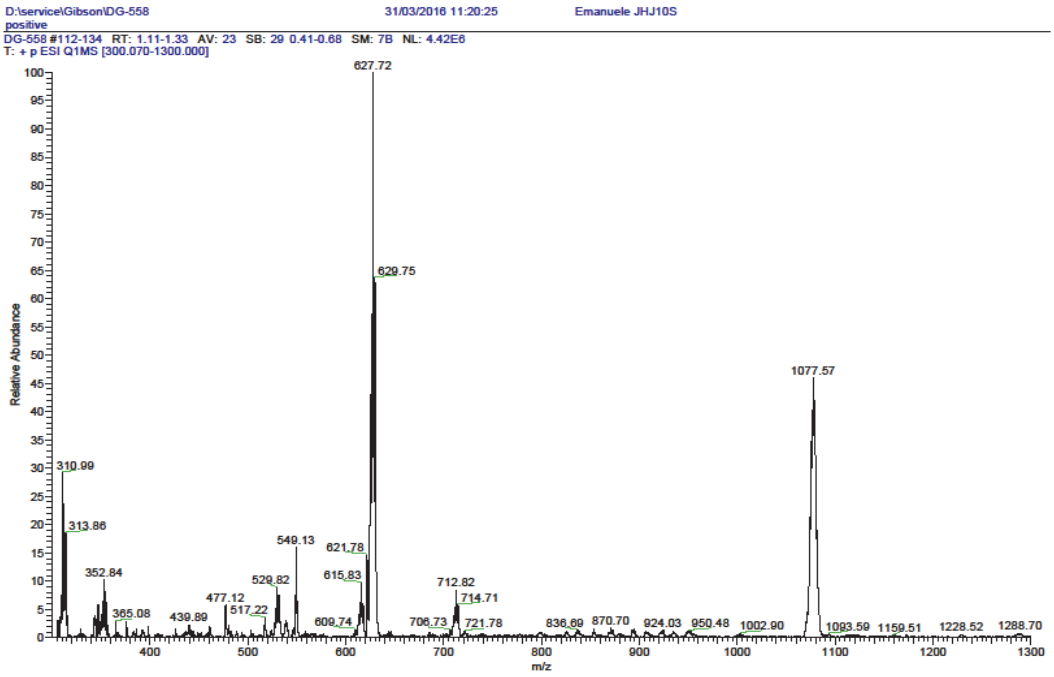

Fig. 4.7-5: MS spectrum for the bimetallic compound with Cisplatin-based platinum(IV) compound and penylbutyrate as ligand in one of the axial positions.

- Conclusion and outlook

During this project we successfully designed and synthesized new Pt(IV)/Ru(II) bimetallic compounds with bioactive ligands in the axial position of the platinum(IV) complex. Due to solubility and purification problems of the compounds this project was not continued.

4.8 Project 2: 'Quadrupole Action' Platinum(IV) prodrugs as anticancer agents[8]

- Scientific aim

This Project is part of the paradigm shift of moving from a 'magic bullet' approach to a 'cluster bomb' approach where several bioactive moieties, that showed synergism with Cisplatin, will be released inside the cancer cell. In Prof. Gibson's lab they already prepared 'triple action' platinum(IV) prodrugs. These prodrugs are platinum(IV) derivatives of Cisplatin or oxaliplatin that have two different bioactive moieties as axial ligands. For instance, one axial position can be an HDACi and in the other COXi (*e.g.* aspirin/ ibuprofen), or one HDACi (*e.g.* phenylbutyrate/ valprate) and one PDKi (*e.g*. dichloroacetate) etc. In this particular project the goal is to expand this concept to 'quadrupole action' mononuclear platinum(IV) prodrugs. Figure 4.8-1 shows examples of the general structures of the target molecules. All the bioactive ligands are attached to the platinum by carboxylate bonds. Following the loss of the two axial ligands by reduction, the semilabile diamminedicarboxylateplatinum(II) will release the bioactive 3 ligands through aquation. Thus, four bioactive moieties, each with a different cellular target, will be released into the same cancer cell.

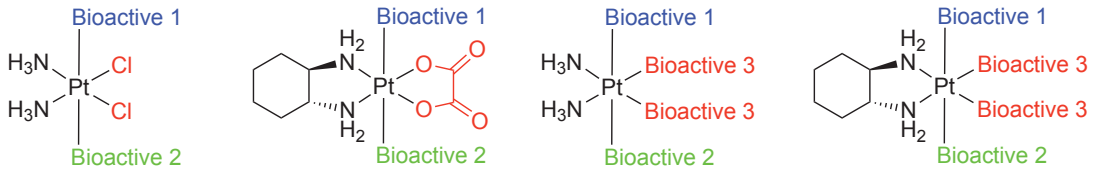

Triple action platinum(IV) prodrugs Quadrupole action platinum(IV) prodrugs

Fig. 4.8-1: General structures of 'triple action' prodrugs and 'quadrupole action' platinum(IV) molecules.

- Description of the work

With the motivation to create new 'quadrupole action' platinum(IV) prodrugs, the project started with the synthesis of those compounds. First we focused on four dif-

[8] Results and discussions are taken from Proposals for Minerva Fellowship, written in 2016 and 2017 by J. Hildebrandt.

ferent platinum(II) compounds (Figure 4.8-2) I-IV with different ligands in the equatorial position. Synthesis started for compounds I/III with $Pt(NH_3)_2I_2$ and for compounds II/IV with $Pt(NH_3)_2Cl_2$ (Cisplatin) by removing the corresponding halide atoms with the help of $AgNO_3$ and afterwards adding the deprotonated acid to the platinum(II). While the synthesis of all complexes was in the end successful, handling the compounds is very difficult. The fast hydrolysis of the platinum(II) complexes is a major problem, therefore several attempts to isolate and purify them were not successful.

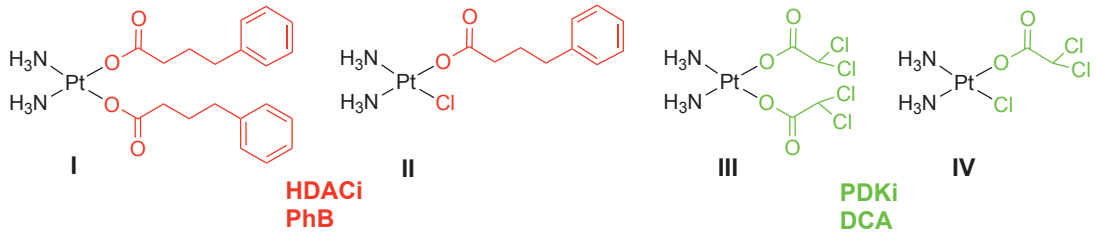

Fig. 4.8-2: New platinum(II) complexes with different bioactive ligands 3, I-IV.

First analytical results for compound I show the product peak in the HPLC chromatogram and the M+1 peak in the MS spectrum for the collected sample, Figure 4.8-3. As an example, the corresponding spectra of the synthetic route I-V-IX is shown in Figures 4.8-3 and 4.8-5. The other platinum complexes could not been analyzed further.

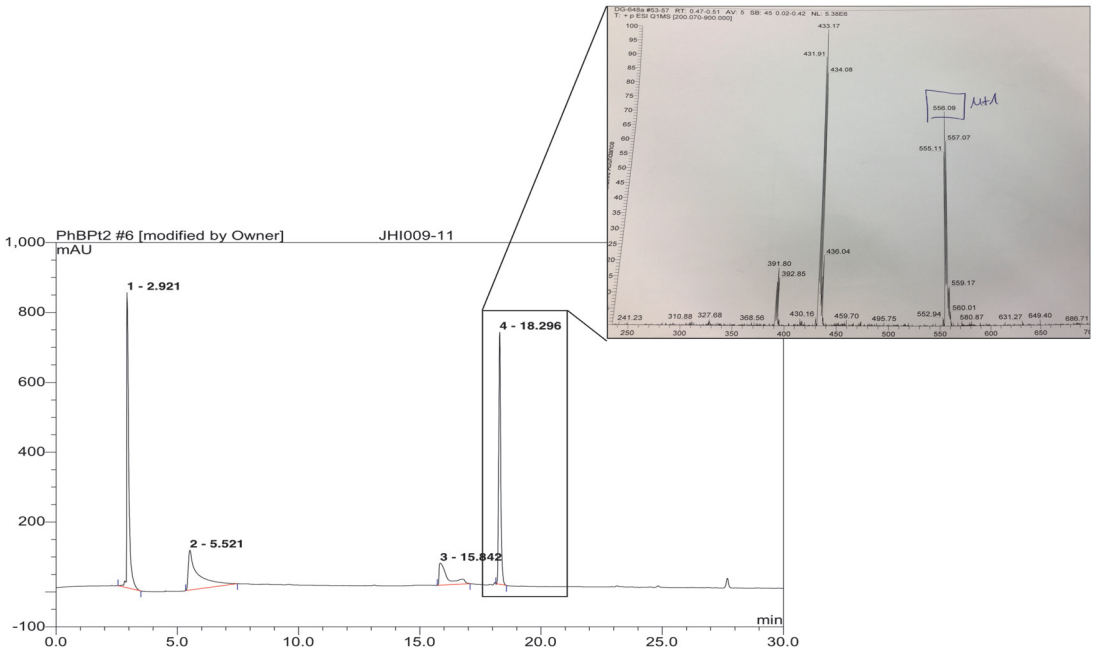

Fig. 4.8-3: HPLC chromatogram before purification of compound I, product peak at rt= 18.296 min. MS spectra of the collected sample shows the M+1 peak.

For compounds II/IV, synthesis started with the removal of one chloride of Cisplatin. The reactions were monitored with ^{195}Pt NMR and a monoaqua product peak at -1803 ppm. After that one equivalent of the deprotonated acid was added and stirred over night at room temperature. Due to the instability of the compounds and the unsuccessful isolation they were oxidized immediately to the platinum(IV) complexes with H_2O_2 (Figure 4.8-4). Compound V shows a platinum(IV) peak at 1869 ppm and compound VI at 1378 ppm in the NMR spectra, for both compounds the M+1 peak in the MS spectra was observable. Compounds VII and VIII show several platinum(IV) peaks in the NMR spectra as well as a lot of products in the HPLC.

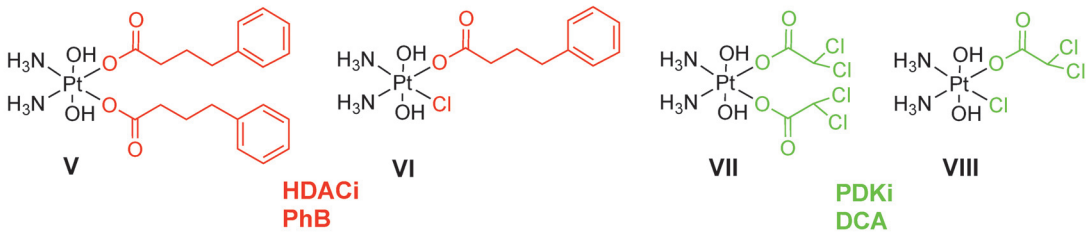

Fig. 4.8-4: New platinum(IV) complexes with different bioactive ligands 3, V-VIII.

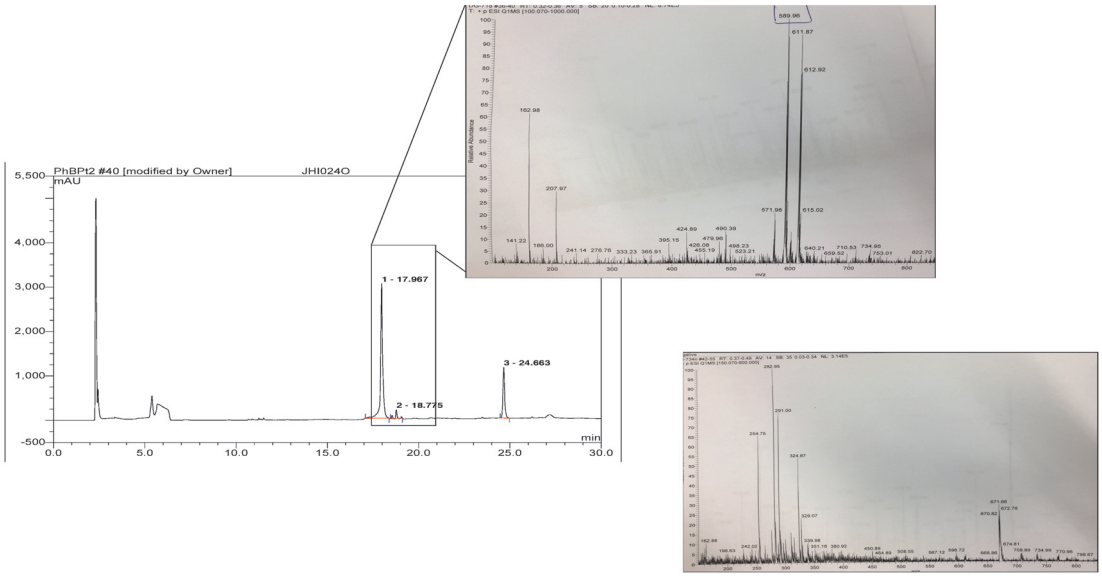

Fig. 4.8-5: Results for compound V (HPLC chromatogram before purification and MS spectra of collected sample) and MS spectra of the crude product of compound IX, showing the molecular peak.

After purification and preparation of higher amounts of compound V preparation of compounds IX and X started (Figure 4.8-6). For complex IX, compound V was incubated with two equivalents of acetic anhydride. Whereas acetic anhydride has no known biological function compound IX should act as a reference for the quadrupole action target molecules. These compounds could not been purified and analyzed further.

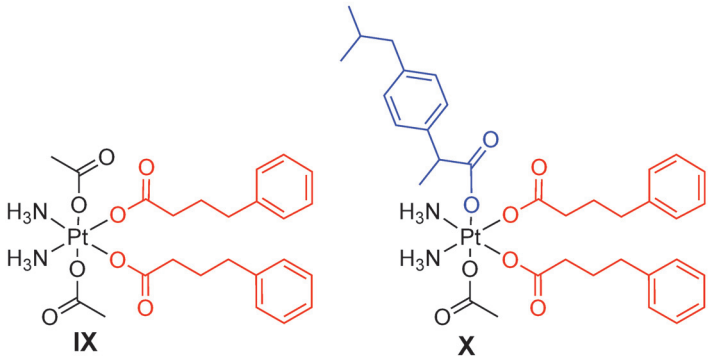

Fig. 4.8-6: General structure of compounds IX and X.

- Conclusion and outlook

First analytical results show that synthesis of compound I-IX was successful. Unfortunately, most synthesis (including the first successful oxidation of a platinum(II) complex) could not been reproduced and due to the instability of the compounds and problems with the oxidation to platinum(IV) the compounds have not been analyzed further. The main problems of these compounds are the instability and therefore isolation and purification as well as difficulties during the oxidation.

5. Summary

Part 1: β-Hydroxydithiocinnamic acid derivatives and corresponding Ruthenium(II), Osmium(II), Platinum(II), Palladium(II) and Nickel(II) complexes targeting Cisplatin resistant ovarian cancer cell lines

Cinnamic acid itself and its derivatives are under discussion for their anticancer properties. As it has been shown, that β-Hydroxydithiocinnamic acid esters can coordinate to platinum(II), nickel(II) and palladium(II), investigation of this synthetical derivative of the cinnamic acid and different metal complexes has been one aim of this thesis. Therefore, a series of β-Hydroxydithiocinnamic acid esters have been synthesized and their chemical and biological behavior were compared to each other as well as to their corresponding metal(II) complexes (including also ruthenium(II) and osmium(II)). Especially those metals are discussed to follow different mode of actions compared to Cisplatin and may be an alternative for the next generation of anticancer drugs.

Preparation of the β-Hydroxydithiocinnamic acid esters started with the corresponding acetophenone, deprotonation, addition of carbon disulfide (CS_2) and alkylation with methyliodide or ethyliodide followed by column chromatography.

For all metal(II) complexes, synthesis started with deprotonation of the β-Hydroxydithiocinnamic acid ester and preparation of the starting metal compound in another flask. The corresponding metal compound was given to the dithioester. The work up and conditions of the reaction depend on the metal, for Ni, Pd, Pt compounds, the reaction was stirred at room temperature for 15 hours and work up was done with filtration and washing steps. For all others (Ru, Os, Ptdmso) reactions have been carried out under nitrogen atmosphere and multiple work up steps, including column chromatography. Figure 5-1 shows a general scheme for synthesis of different substance classes this work is dealing with.

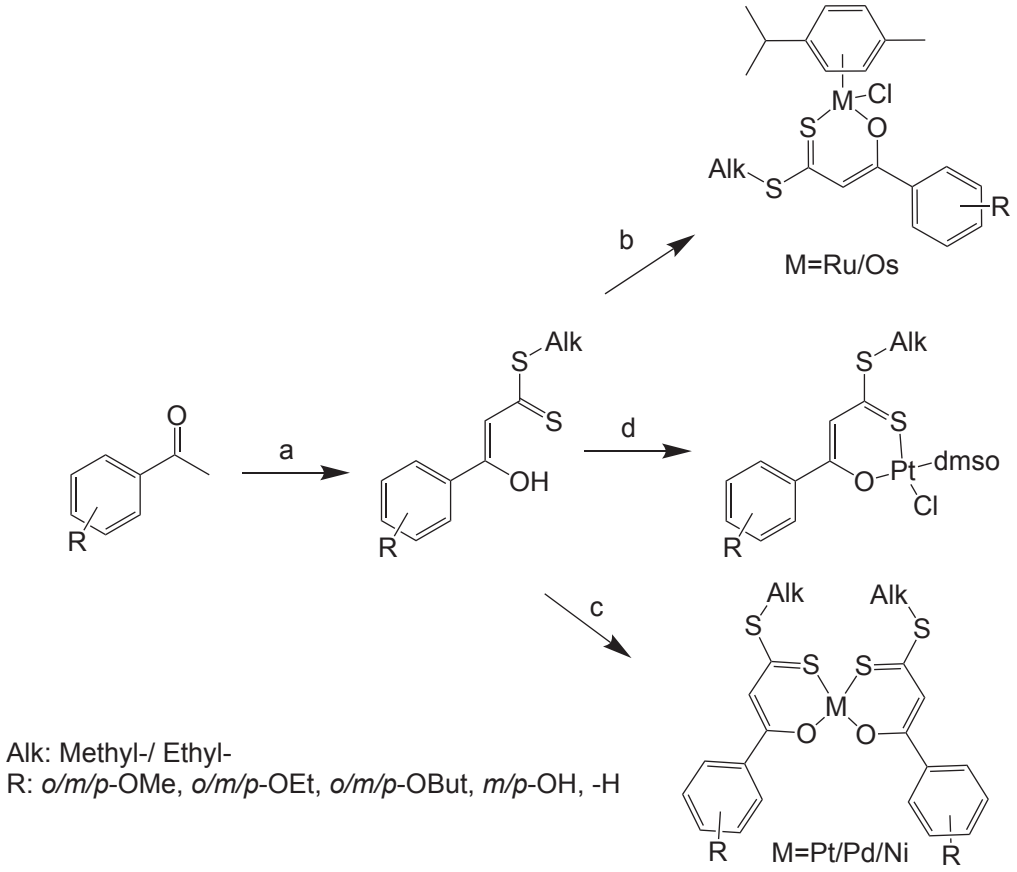

Fig. 5-1: Overview of synthesis of metal(II) compounds with β-Hydroxydithiocinnamic acid esters as ligands. This Figure depicts the general scheme, exact conditions have been discussed in [JH1-JH4]. For a: Deprotonation with *t*-BuOK, addition of CS_2 and alkylation were done. For b: $[(\eta^6\text{-}p\text{-cymene})MCl_2]_2$ was added. For c: $NiCl_2$* 6 H_2O / $(PhCN)_2PdCl_2$ or $(PhCN)_2PtCl_2$ have been added. For d: $K[PtCl_3(dmso)]$ has been added.

All compounds show characteristic patterns and signals in spectroscopy and spectrometry experiments. Therefore, all have been analyzed with NMR spectroscopy, MS spectrometry and elemental analysis. Especially in the NMR spectra characteristics have been discussed for all compounds. For the β-Hydroxydithiocinnamic acid esters different substitution patterns at the benzyl-ring can be observed in the ^{1}H NMR spectra at around 7 ppm. The ^{1}H NMR signal of the methine proton of the -C=C-H double bond is also at around 7 ppm. Those signals can be observed in the spectra of all metal(II) complexes with some characteristic changes due to their chemical shift as a result of complexation to a metal(II) center. To point out some example, Table 5-1 shows compounds number 2 in

$^{13}C\{^{1}H\}$ and ^{1}H NMR spectra. The methine proton (signal No. 1) shows a high-field shift after complexation to ruthenium(II) and osmium(II) compounds but a low-field shift for d^8 complexes with nickel(II), palladium(II) and platinum(II). The corresponding ^{13}C signal (signal No. 3) does not show any significant correlation, compared to the free β-Hydroxydithiocinnamic acid esters it shifts in slightly different directions of the spectra. The ^{13}C signal of the -C-O-group shows a low-field shift for all complexes, the thiocarbonyl-group a high-field shift. These changes can be confirmed with the X-Ray structures which show elongation for the thiocarbonyl-group and shortening for the C-O-bond lengths. These characteristics prove the successful complexation of the β-Hydroxydithiocinnamic acid esters to different metal(II) centers.

Tab. 5-1: Characteristic NMR spectra signals for compounds 2.

No.	Signal	L2	Ni2	Pd2	Pt2	Ptdmso2	Ru2	Os2
1	=C-*H*	6.97	7.16	7.16	7.14	7.35	6.64	6.87
2	-*C*=S	217.3	181.4			180.9	185.9	186.7
3	=*C*-H	112.9	115.1	113.0	112.5	112.9	113.4	112.7
4	-*C*-O-	169.1	178.1	178.1		174.2	179.0	174.9

Due to the variable other ligands some characteristics for each class of compounds can be observed. The ruthenium(II) and osmium(II) compounds start with the symmetrical bimetallic complexes $[(\eta^6\text{-}p\text{-cymene})MCl_2]_2$ (M=Ru/ Os) which show for the cymene ligand two dubletts in ^{1}H NMR spectra for all aromatic protons and one dublett for the isopopyl-groups. Complexation to the O,S-bidendate ligand leads to an unsymmetrical structure and results in chemical non-equivalent aromatic protons and carbons resulting in four aromatic dubletts and two dubletts for the isopropyl-groups in the ^{1}H NMR spectra and four aromatic carbons (instead of two) and two isopropyl-carbon signals (instead of one signal) in the $^{13}C\{^{1}H\}$ NMR spectra. For the platinum(II) compounds of the Ptdmso-group, protons of the dmso-group are observed as a singlet accompanied by ^{195}Pt satellites in the ^{1}H NMR spectra.

Tab. 5-2: Compounds 1 in comparison for some characteristics bond lengths [Å].

Signal	L1	Ru1	Ni1	Pd1	Ptdmso1
C(1)-S(1)	1.681(2)	1.690(2)	1.698(2)	1.703(6)	1.710(3)
C(3)-O(1)	1.334(3)	1.266(2)	1.2583(3)	1.271(7)	1.274(3)
O(1)-M(1)		2.0790(14)	1.8466(17)	2.023(4)	2.015(7)
S(1)-M(1)		2.3544(5)	2.1429(7)	2.2307(16)	2.251(6)

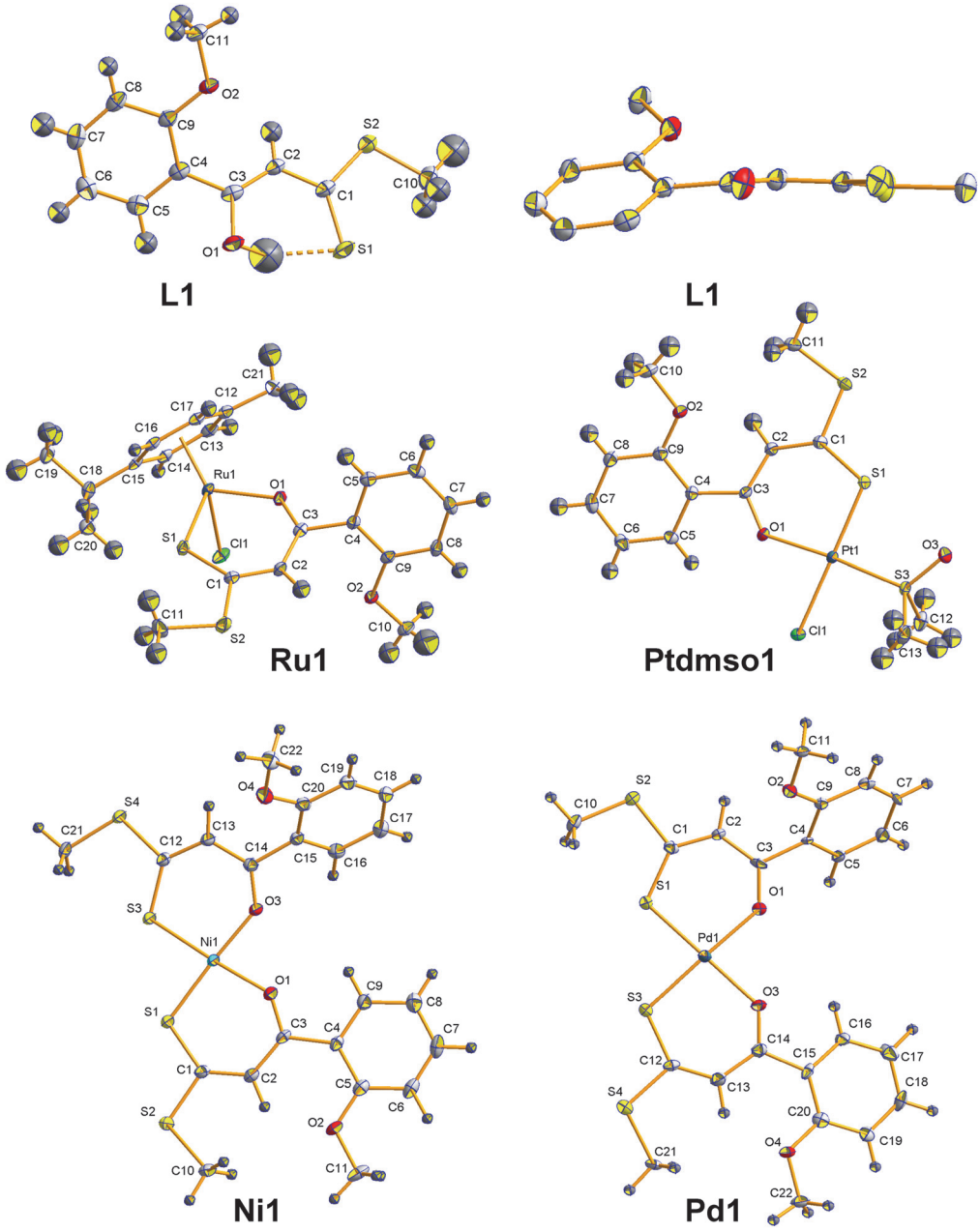

Fig. 5-2: Molecular structures (50% probability) of L1, Ru1, Ptdmso1, Ni1 and Pd1.

As described previously for the NMR spectra signals, the elongation of the C(1)-S(1)- and the shortening of the C(3)-O(1)-bonds after complexation to the different metals can be observed in the molecular structures. Table 5-2 shows some characteristic bond lengths of compounds 1. The bond lengths of the C(1)-S(1)-bonds increase in the order: L1 (1.681(2) Å) < Ru1 (1.690(2) Å) < Ni1 (1.698(2) Å) < Pd1 (1.703(6) Å) < Ptdmso1 (1.710(3) Å). The bond lengths of the C(3)-O(1)-bond decrease in the order: L1 (1.334(3) Å) > Ptdmso1 (1.274 (3) Å) > Pd1 (1.271 (7) Å) > Ru1 (1.266(2) Å) > Ni1 (1.2583(3) Å). Figure 5-2 shows the molecular structures of the discussed compounds. For metal(II) complexes with nickel, palladium and platinum (Ni1, Pd1, Ptdmso1) a slightly distorted square-planar coordination sphere can be observed, what is typical for d^8 complexes. For the ruthenium(II) complex (Ru1) a tetrahedral structure is observed.

Solubility behavior and stability determinations for all compounds have been done with different techniques, *e.g.* UV-Vis spectroscopy and ^{1}H NMR spectroscopy under different conditions and in different solvents. In general, all compounds show stability and solubility in organic solvents like dichloromethane and chloroform. The water-solubility increases with polar substituents on the aromatic ring of the β-Hydroxydithiocinnamic acid esters, but for biological investigations dimethylsulfoxide (dmso) was needed to solve the samples. Therefore, stability determinations have been done *e.g.* in dmso-d_6 under varying conditions and followed by ^{1}H NMR spectroscopy. In general, compounds: L, Os, Ni, Pd and Ptdmso are stable under all tested conditions. Platinum(II) complexes (Pt) show some unspecific changes after 48 hours what may be explained by their generally low solubility in that solvent. For ruthenium(II) compounds changes can be explained with the coordination of dmso molecules to the ruthenium(II) center and the loss of the arene ligand. Nevertheless, even if the ruthenium(II) compounds change their structure during their experiments, biological data shows some promising results.

The investigation of the described metal(II) complexes as potential anticancer drugs is the main aim of these thesis. Therefore, all mentioned compounds have been tested under identical conditions together with the reference Cisplatin in *in vitro* cell culture MTT assays against two ovarian cancer cell lines SKOV3 and

A2780, as well as their Cisplatin resistant analogues SKOV3cis and A2780cis and the lung cancer cell line A549 for comparison. As mentioned before, dmso was used to solve the samples and therefore the influence of dmso was determined and always added as control. The toxic influence of 0.5% dmso was considered as acceptably low for the overall results. Considering structure-activity relationships the results are very different and no general correlation can be seen for all classes. Nevertheless, SARs were identified for the substances of each class and similarities were seen between specific classes. The β-Hydroxydithiocinnamic acid esters show low activity on all cancer cell lines, SARs for those compounds show better results for the ones with longer alkyl-chains at the benzyl-ring, most active compound is L9 (Table 5-3). The most active compounds in general are the osmium(II) complexes which show low IC50 values on all cell lines, most active compound of this class is Os10, which bears a hydroxy-group in *meta*-position and is the most polar-complex of this study (Table 5-3). Therefore, the SARs of the Os compounds do not follow the same rules as for the β-Hydroxydithiocinnamic acid esters L. The same, considering the SARs, is shown for the Ptdmso compounds, which show in general lower IC50 values with increased polarity, most active compound is Ptdmso16 (Table 5-3). Beside the Os complexes most promising candidates of this work are Pd and Ru compounds. Both systems follow in general SARs as for β-Hydroxydithiocinnamic acid esters having good results with increased lipophilicity, Ru6 and Pd3 are the most active complexes of this class. In general, Ni and Pt compounds are comparable with the SARs to their Pd analogues, but with lower activity in general (Table 5-3). Table 5-3 shows the most active compounds of each class, their mean IC50 value (for all five cell lines) and reference Cisplatin. Especially Ru6, Pd3 and Os10 are promising candidates for *in vivo* studies.

Tab. 5-3: Substitution pattern and mean IC50 value [µM] for most active compounds and Cisplatin.

	L9	**Ru6**	**Os10**	**Ni1**	**Pd3**	**Pt4**	**Ptdmso16**	**CDDP**
-R	*p*-OBut	*p*-OEt	*m*-OH	*o*-OMe	*p*-OMe	*o*-OEt	*m*-OH	
-Alk	-Me	-Me	-Me	-Me	-Me	-Me	-Et	
Mean IC50	11.49	3.22	0.97	5.26	3.98	5.49	13.75	6.5

In Figure 5-3 mean IC50 values for all substance classes are shown (purple), as well as the mean IC50 values on the sensitive- (blue) and resistant- (red) ovarian cancer cell lines. It can be concluded, that in general palladium(II) and osmium(II) complexes show promising results and lower IC50 values compared to Cisplatin. Moreover, for all compounds (except for Pt) the mean IC50 values for the Cisplatin resistant cell lines are lower than the values for the sensitive one, proving an activity against the Cisplatin resistant tumors. As this is already shown for the β-Hydroxydithiocinnamic acid esters L this effect is potentially caused by the O,S-bidendate ligand. Nevertheless, the metal(II) decreases the values in general and in all cases.

To determine the activity on resistant tumors, resistant factors (RF) have been determined for all substances. Table 5-4 shows the proportion of substances with RF ≤ 1 (a higher activity on resistant cell lines than on their sensitive counterparts) for all classes on the ovarian cancer cell lines. Especially for SKOV3/ SKOV3cis there are remarkable results, 67% of the L, 65% of all Ru, 83% of all Pd and 75% of all Ptdmso compounds show better activity on the resistant cell line SKOV3cis. Also, it has to be mentioned, that in most cases RF are much lower compared to Cisplatin, showing that those molecules are not only able to circumvent the mechanisms leading to Cisplatin resistance, but they are also more active on resistant cell lines and this effect is likely caused by the β-Hydroxydithiocinnamic acid esters itself.

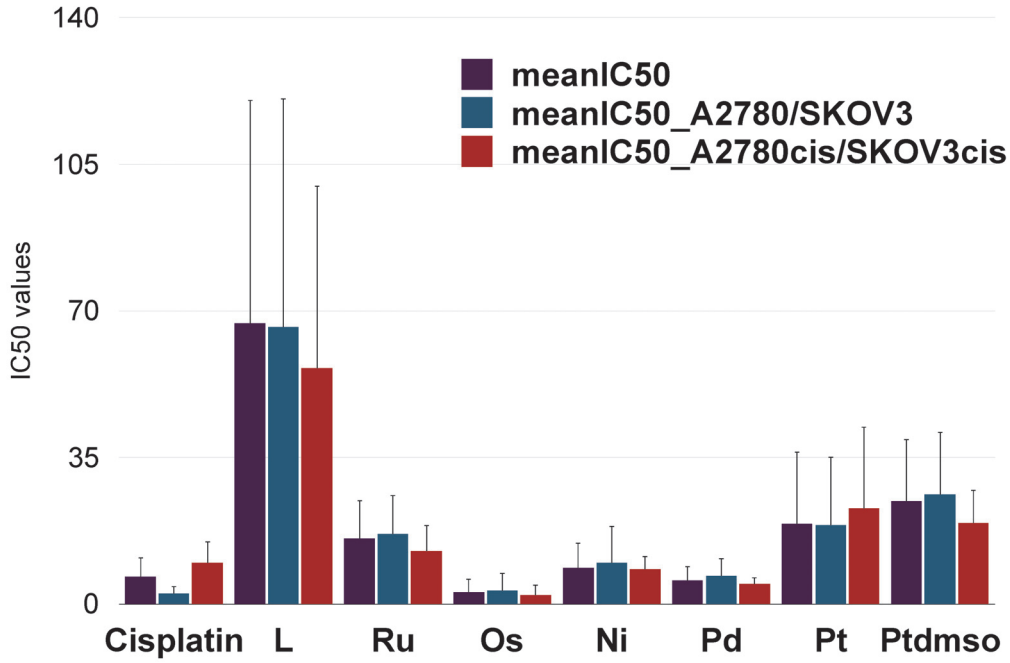

Fig. 5-3: Overview of mean IC50 values [µM] for all substances of each molecule class and reference Cisplatin (purple), meanIC50 for Cisplatin sensitive cell lines SKOV3 and A2780 (blue) and for their Cisplatin resistant counterparts (red).

Tab. 5-4: Percentages of RF ≤ 1 on ovarian cancer cell lines for all classes of compounds.

RF ≤ 1	L	Ru	Os	Ni	Pd	Pt	Ptdmso
SKOV3/ SKOV3cis	67%	65%	25%	50%	83%	50%	75%
A2780/ A2780cis	50%	59%	25%	33%	17%	33%	50%

Focusing on the resistant cell lines this work is dealing with, overall 22 compounds show a lower mean IC50 value than Cisplatin, Figure 5-4. Even though, again Os, Pd and Ru compounds show best results.

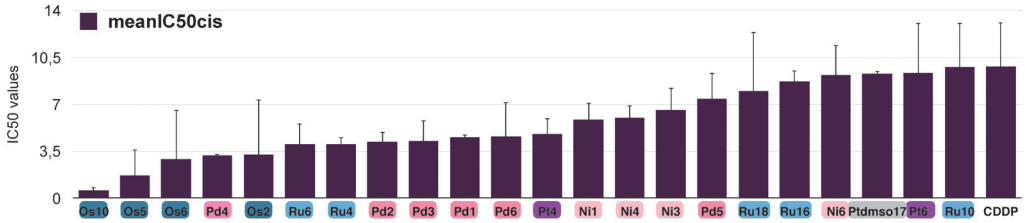

Fig. 5-4: Mean IC50 values [µM] on SKOV3cis and A2780cis for all compounds which show lower values than reference compound Cisplatin.

Next to the high potential and promising results (low IC50 values) for Os and Pd compounds, the Ru complexes are good candidates for further developments, as it has been shown in the literature (especially for RAPTA complexes) that they gain high *in vivo* potential, even if the *in vitro* results are just comparable to Cisplatin.

Tab. 5-5: IC50 values for some of the most active compounds on non-cancerous cell lines to determine selectivity and toxic side effects: Keratinocytes (1), Fibroblasts (2) and MCF10A (3), all values are in [µM].

Cell-line	L6	Ru10	Os10	Ni1	Pd3	Pt4	Ptdmso16	CDDP
1	>100	>100	84.5 (±31.3)	87.0 (±0)	55.0 (±6.7)	>100	72.4 (±17.9)	5.7 (±3.1)
2	>100	>100	>100	84.3 (±8.9)	42.9 (±10.2)	>100	52.4 (15.8)	4.1 (±1.1)
3	>100	16.7 (±4.1)	21.3 (±3.3)	19.6 (±2.6)	28.3 (±16.8)	41.5 (±25.8)	42.6 (±13.5)	3.3 (±0.6)

Additionally, some of the most active compounds have been tested against three non-cancerous cell lines: Keratinocytes (1), Fibroblasts (2) and MCF10A (3) under the same conditions as for reference Cisplatin. As it is known, that Cisplatin shows toxic side effects IC50 values are in the range of 3.3 to 5.7 µM. All investigated compounds show higher IC50 values on these non-cancerous cell lines than Cisplatin, therefore it can be concluded, that these compounds show higher

activity (especially against resistant cell lines) than Cisplatin but lower cytotoxic activity to non-cancerous cell lines, what leads to a higher selectivity for cancer cells and a success for these complexes.

For Ptdmso and Ru compounds the mechanism of action was further investigated with different techniques, including X-Ray structures and NMR studies. It was shown, for both systems that their binding to Cisplatins' main target, the DNA, is reduced. This was evaluated and proved with γH2AX-foci analyses, 9-methylguanine binding studies and cell cycle arrest analyses. The search for other targets, led to two crystal structures monitoring binding of A) ruthenium(II) compounds to RNAse A by losing the arene ligand and B) platinum(II) complex binding to HEWL by losing all coordinated ligands. So, the higher *in vitro* activity of these compounds compared to Cisplatin, especially on resistant cell lines may be defined with a different mode of action and their interactions with proteins.

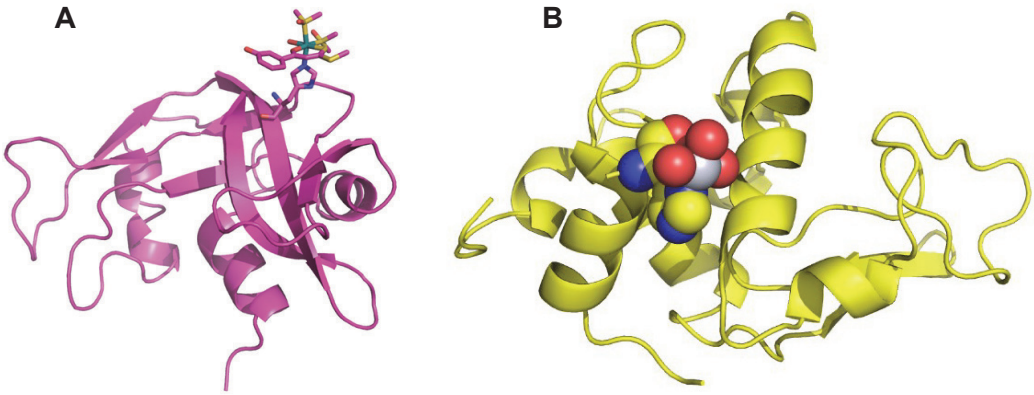

Fig. 5-5: **A**: Interaction of Ru10 and RNAse A. **B**: Interaction of Pt1 with HEWL.

In summary, this works presents new metal(II) complexes with promising cytotoxic activity against Cisplatin resistant cell lines by following a different mechanism of action and showing higher cancer selectivity *in vitro*.

Part 2: Chemical and biological investigations of platinum(II) complexes with asparagusic acid derivatives as S/S, Se/Se and S/Se -bidendate ligands

Asparagusic acid as a constituent of asparagus is a 1,2-dithiolane ring system similar to the α-lipoic acid, which acts as a cofactor for *e.g.* pyruvate dehydrogenase complex. Therefore, it has been discussed for numerous pharmacological properties, as well, as it was shown for asparagusic acid itself and its Se/Se analogue that it may lead to an enhanced uptake of drugs. As it is known, that asparagusic acid is able to coordinate to platinum(II), the design of its derivatives and the biological investigation of these complexes are part of this thesis. The main aim of this Part 2 was to determine the anticancer properties for this class of compounds, especially on Cisplatin resistant cell lines, as shown for the complexes of cinnamic acid derivatives (Part 1).

Preparation of the platinum(II) complexes starts with L1-L4 synthesis and for Pt2, Pt4 and Pt6 with the synthesis of the corresponding platinum(II) starting compound, (dppma)$PtCl_2$. Next step is the reduction of L1-L4 and addition of $PtCl_2L_2$ (L= dppma or PPh_3). For the preparation of Pt1 and Pt2 another route is possible, starting with the deprotonation of the dihydroasparagusic acid.

Characterization of all compounds have been carried out with different spectroscopic and spectrometric techniques, including NMR spectroscopy. Characteristic ^{195}Pt- and ^{77}Se-satellites in the $^{31}P\{^{1}H\}$ NMR spectra for the corresponding platinum(II) complexes, as well as the unsymmetrically substituted S/Se platinum(II) complexes Pt3 and Pt4 show a typically AB spin system. Mass spectra show molecular peaks as well as the loss of the asparagusic acid derivatives. Molecular structures of L2, L3, L5, Pt1 and Pt7 have been characterized. Platinum(II) atoms of Pt1 and Pt7 reside in a slightly distorted square-planar environment and a P1-Pt-P2 angle larger than 90° caused by the steric demand of the PPh_3 groups. For Pt1 the carboxylic function forms intermolecular hydrogen-bonds with another unit leading to a dimeric structure, Figure 5-6.

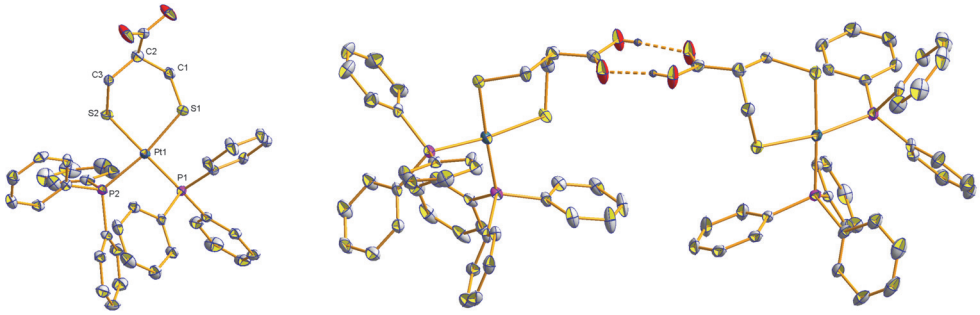

Fig. 5-6: Molecular structure (50% probability) of Pt1.

All platinum(II) complexes have been tested against ovarian cancer cell lines SKOV3 and A2780 as well as their resistant analogues. Results show, that Se/Se-containing compounds exhibit a higher activity in general than their S/S counterparts. Overall, most compounds show a lower or similar activity compared to the reference Cisplatin. To point out, Pt7 is the most active complex with RF lower than 1 and an IC50 value of 4.3 µM compared to 13.5 µM of Cisplatin on SKOV3cis. It was shown that all complexes exhibit lower RF than Cisplatin and are able to circumvent the resistance. Figure 5-7 shows an overview of all platinum(II) complexes compared to Cisplatin. Regarding the mean IC50 value (red line) SARs can be determined as: Se/Se > S/Se > S/S compounds, Se/Se-containing compounds Pt6 and Pt7 show best results of this investigation.

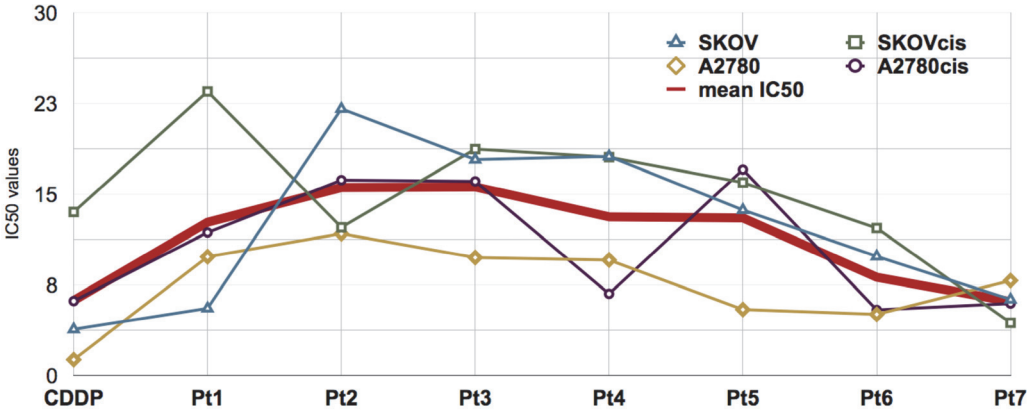

Fig. 5-7: IC50 values for all complexes and Cisplatin on four cell lines, as well as mean IC50 value (red line). All values are in [µM].

To conclude, it was shown that asparagusic acid derivatives can coordinate to platinum(II) and show some interesting results on Cisplatin resistant ovarian cancer cell lines by following a different mode of action.

6. Zusammenfassung

Teil 1: β-Hydroxydithiozimtsäureester Derivate und die dazugehörigen Ruthenium(II), Osmium(II), Platin(II), Palladium(II) und Nickel(II) Komplexe gegen Cisplatin Resistenz in Ovarialkarzinom-Zelllinien

Zimtsäure und dessen Derivate werden bezüglich ihrer antikarzinogenen Wirkung hin untersucht. Es wurde gezeigt, dass β-Hydroxydithiozimtsäureester Derivate Liganden für Metallkomplexe der Metalle Platin(II), Nickel(II) und Palladium(II) sind. Die Untersuchung von synthetischen Zimtsäurederivaten und verschiedener Metallkomplexe ist ein Ziel dieser Arbeit gewesen. Dafür wurden verschiedene Derivate des β-Hydroxydithiozimtsäureesters synthetisiert, ihre chemischen und biologischen Eigenschaften untersucht und mit den verschiedenen Metallkomplexen, auch mit neuartigen Ruthenium(II) und Osmium(II) Verbindungen verglichen. Besonders die letzten beiden Metalle und ihre Verbindungen sind bekannt andere Wirkmechanismen als Cisplatin aufzuweisen. Sie zeigen das Potential als nächste Generation der Metallbasierten Krebsmedikamente.

Die Synthese der β-Hydroxydithiozimtsäureester Derivate geht von den dazugehörigen Acetophenonen aus, diese werden zunächst deprotoniert, Kohlenstoffdisulfid (CS_2) hinzugegeben und abschließend werden die Verbindungen alkyliert mit Methyliodid oder Ethyliodid. Die Rohprodukte wurden säulenchromatographisch aufgereinigt.

Für die dazugehörigen Metallkomplexe werden die β-Hydroxydithiozimtsäureester deprotoniert und in einem zweiten Reaktionsgefäß die Ausgangsverbindungen der Metalle hergestellt. Die Ausgangsverbindungen werden anschließend zu dem Dithioester gegeben. Die Aufreinigung und exakten Reaktionsbedingungen sind je nach Substanzklasse unterschiedlich, für die Ni, Pd und Pt Verbindungen wird die Reaktion bei Raumtemperatur 15 Stunden gerührt, gefolgt von Filtration und Waschschritten. Für alle anderen Komplexe (Ru, Os, Ptdmso) wird die Reaktion unter Stickstoffatmosphäre durchgeführt und eine Vielzahl von Reinigungsschritten, zum Beispiel Säulenchromatographie, sind notwendig. Die

Abbildung 5-1 zeigt ein generelles, vereinfachtes Schema für die Synthese der verschiedenen Substanzklassen dieses Abschnittes.

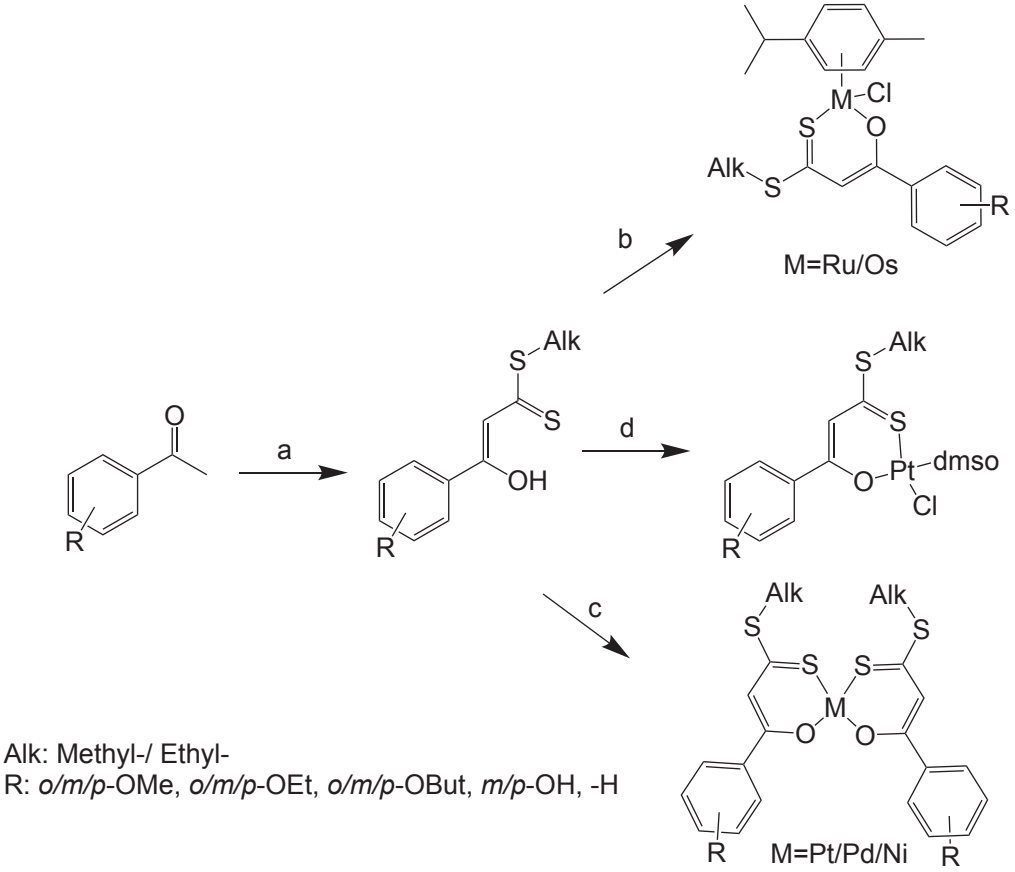

Abb. 5-1: Übersicht der Synthese der Metall(II) Verbindungen mit β-Hydroxydithiozimtsäureester als Liganden. Die Abbildung zeigt eine vereinfachte Darstellung der Synthese, die exakten Reaktionsbedingungen sind in [JH1-JH4] diskutiert. Für a: Deprotonieren mit *t*-BuOK, Hinzugeben von CS_2 und anschließende Alkylierung. Für b: $[(\eta^6\text{-}p\text{-cymene})MCl_2]_2$ wird zum Liganden hinzugegeben. Für c: $NiCl_2$* 6 H_2O / $(PhCN)_2PdCl_2$ oder $(PhCN)_2PtCl_2$ wird hinzugegeben. Für d: $K[PtCl_3(dmso)]$

Alle Verbindungen wurden mittels NMR-Spektroskopie, MS-Spektrometrie und mit Elementaranalysen analysiert. Die Verbindungen zeigten charakteristische Aufspaltungsmuster und Signale in den verschiedenen spektroskopischen und spektrometrischen Experimenten. Vor allem die chemischen Verschiebungen in den NMR Spektren wurde für die verschiedenen Verbindungen diskutiert. Für die β-Hydroxydithiozimtsäureester können verschiedene Aufspaltungsmuster durch unterschiedliche Substitutionen am aromatischen Ring in den ^{1}H NMR Spektren

bei ca. 7 ppm beobachtet werden. Das Methinproton der -C=C-H Doppelbindung erscheint ebenfalls bei ca. 7 ppm, normalerweise hochfeldverschoben zu den Protonen des Aromaten. Diese Signale können in allen Spektren der Metall(II) Verbindungen beobachtet werden, mit einigen spezifischen Charaktertistika in der chemischen Verschiebung einiger Signale nach der Komplexierung an die Metalle. Um ein paar Beispiele zu nennen, zeigt Tabelle 5-1 die Verbindungen mit der Nummer 2 in $^{13}C\{^{1}H\}$ und ^{1}H NMR Spektren. Das Methinproton (Signal Nummer 1) zeigt sich zu Hochfeld verschoben nach der Komplexierung zu Ruthenium(II) und Osmium(II) Verbindungen im Vergleich zum freien Liganden, dagegen wird eine Tieffeldverschiebung für die d^8 Komplexe mit Nickel(II), Palladium(II) und Platinum(II) detektiert. Das dazugehörige ^{13}C Signal (Signal Nummer 3) zeigt keine signifikante Korrelation, verglichen mit dem β-Hydroxydithiozimtsäureester verschiebt es sich bei den Metallkomplexen leicht in verschiedene Richtungen des Spektrums. Das ^{13}C Signal der -C-O-Gruppe zeigt für alle Komplexe eine Tieffeldverschiebung, die Thiocarbonylgruppe hingegen verschiebt sich zu kleineren ppm-Werten (Hochfeldverschiebung). Diese Verschiebungen können mit den Molekülstrukturen bestätigt werden, diese zeigen eine längere Bindung für die Thiocarbonylgruppe in den Komplexstrukturen verglichen zum freien Liganden, und eine Verkürzung der -C-O-Bindungslänge. Diese Charakteristika zeigen die erfolgreiche Komplexierung des Liganden an das jeweilige Metall.

Tab. 5-1: Charakteristische Signale in den NMR Spektren der Verbindungen 2.

Nr.	Signal	L2	Ni2	Pd2	Pt2	Ptdmso2	Ru2	Os2
1	=C-*H*	6.97	7.16	7.16	7.14	7.35	6.64	6.87
2	-*C*=S	217.3	181.4			180.9	185.9	186.7
3	=*C*-H	112.9	115.1	113.0	112.5	112.9	113.4	112.7
4	-*C*-O-	169.1	178.1	178.1		174.2	179.0	174.9

Die verschiedenen Gruppen unterscheiden sich bezüglich ihrer weiteren Liganden voneinander und auf Grund dessen können die verschiedenen Charakteristika der weiteren Liganden interpretiert werden. Die Synthese der Ruthenium(II)

und Osmium(II) Verbindungen gehen von der symmetrischen, bimetallischen Verbindung $[(\eta^6\text{-}p\text{-cymene})MCl_2]_2$ (M= Ru/ Os) aus, welche für den Cymene Liganden zwei Dubletts im ^{1}H NMR Spektrum aufzeigt und ein Dublett für die Isopropylgruppe. Komplexierung des O,S-Chelatliganden führt zu unsymmetrischen Strukturen und zu chemisch nicht-äquivalenten aromatischen Protonen und Kohlenstoffatomen. Diese zeigen im ^{1}H NMR Spektrum vier aromatische Dubletts und zwei Dubletts für die Isopropylgruppe, ebenso wie vier aromatische Kohlenstoffatome (anstelle von zwei) und zwei Signale für die Kohlenstoffatome der Isopropylgruppe (anstelle von einem Signal) im $^{13}C\{^1H\}$ NMR Spektrum. Für die Platin(II) Verbindungen des Typs Ptdmso lassen sich ^{195}Pt Satelliten neben der Protonen der DMSO-Gruppe im ^{1}H-NMR Spektrum erkennen.

Tab. 5-2: Vergleich verschiedener Bindungslängen [Å] für die Verbindungen 1.

Signal	L1	Ru1	Ni1	Pd1	Ptdmso1
C(1)-S(1)	1.681(2)	1.690(2)	1.698(2)	1.703(6)	1.710(3)
C(3)-O(1)	1.334(3)	1.266(2)	1.2583(3)	1.271(7)	1.274(3)
O(1)-M(1)		2.0790(14)	1.8466(17)	2.023(4)	2.015(7)
S(1)-M(1)		2.3544(5)	2.1429(7)	2.2307(16)	2.251(6)

Wie bereits bei den NMR Spektren erwähnt wurde, zeigt sich die Verlängerung der C(1)-S(1)-Bindung und die Verkürzung der C(3)-O(1)-Bindungslänge nach der Komplexierung der Liganden zu den Metallen auch in den Kristallstrukturen. Tabelle 5-2 zeigt einige charakteristische Bindungslängen der Verbindungen 1. Die Länge der Bindungslänge der C(1)-S(1)-Bindung nimmt zu in folgender Reihenfolge: L1 (1.681(2) Å) < Ru1 (1.690(2) Å) < Ni1 (1.698(2) Å) < Pd1 (1.703(6) Å) < Ptdmso1 (1.710(3) Å). Die Bindungslänge der C(3)-O(1)-Bindung wird in folgender Reihenfolge kleiner: L1 (1.334(3) Å) > Ptdmso1 (1.274(3) Å) > Pd1 (1.271(7) Å) > Ru1 (1.266(2) Å) > Ni1 (1.2583(3) Å). Abbildung 5-2 zeigt die Molekülstrukturen der diskutierten Verbindungen. Für die Metall(II) Verbindungen mit Nickel, Palladium und Platin (Ni1, Pd1, Ptdmso1) zeigt sich eine leicht verzerrte quadratisch-planare Koordinationsumgebung, typisch für d^8 Metallkomplexe. Für die

Ruthenium(II) Verbindung (Ru1) liegt eine tetraedische Koordinationsumgebung vor.

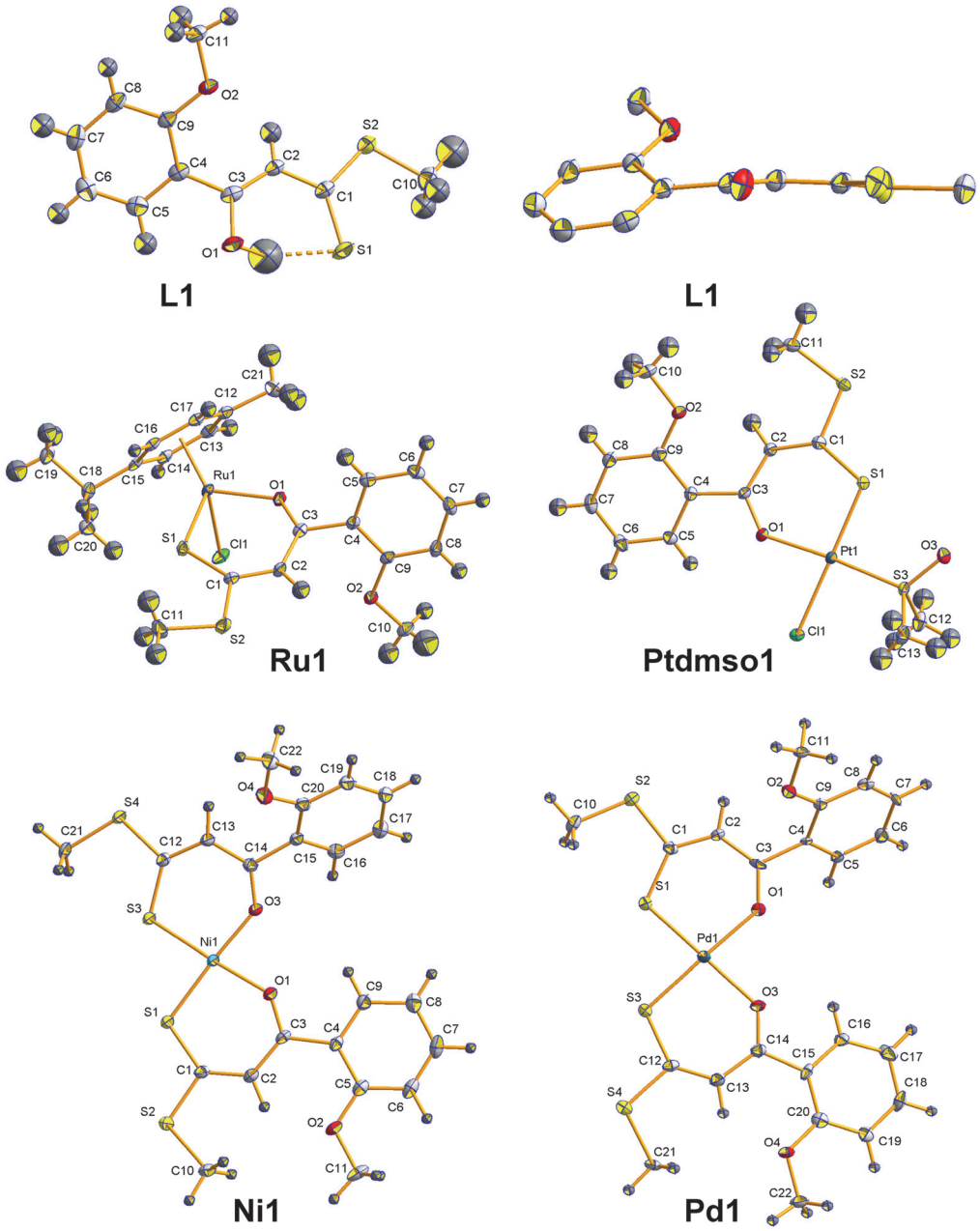

Abb.: 5-2: Molekülstrukturen L1, Ru1, Ptdmso1, Ni1 und Pd1. Die Schwingungsellipsoide sind für eine Aufenthaltswahrscheinlichkeit von 50% dargestellt.

Löslichkeitsexperimente und Stabilitätsuntersuchungen für alle Verbindungen wurden mit unterschiedlichen Techniken durchgeführt, zum Beispiel UV-Vis Spektroskopie und ^{1}H-NMR Spektroskopie, hierbei wurden die Bedingungen variiert. Allgemein lässt sich sagen, dass alle Verbindungen löslich und stabil sind in den organischen Lösungsmitteln Dichlormethan und Chloroform. Die Wasserlöslichkeit der Verbindungen wird durch polare Substituenten am Aromaten erhöht,

für die biologischen Experimente wurden die Verbindungen zunächst in DMSO gelöst. Somit wurden Stabilitätsuntersuchungen unter anderen in dmso-d_6 durchgeführt und mittels ^{1}H-NMR Spektroskopie in Kinetikmessungen nachverfolgt. Dadurch wurde gezeigt, dass die Verbindungen der Substanzklassen: L, Os, Ni, Pd und Ptdmso unter verschiedenen getesteten Reaktionsbedingungen stabil sind. Platin(II) Verbindungen (Pt) zeigten nach 48 Stunden Messung einige unspezifische Veränderungen in den Spektren, was auf die schlechte Löslichkeit der Verbindungen in den Lösungsmitteln zurückgeführt werden kann. Für die Ruthenium(II) Verbindungen ist die Koordination von DMSO Molekülen zu erkennen, einhergehend mit dem Verlust des Arene Liganden. Trotz der Instabilität der Ruthenium(II) Verbindungen zeigen sie vielversprechende biologische Ergebnisse.

Hauptziel dieser Arbeit ist die Erforschung der Metall(II) Verbindungen als potentielle Krebsmedikamente. Hierfür wurden alle Verbindungen und die Referenzsubstanz Cisplatin in *in vitro* Zellkultur MTT Assays gegen die zwei Ovarialkarzinomzelllinien SKOV3 und A2780, wie auch deren Cisplatin resistente Analoga SKOV3cis und A2780cis und die Lungenkarzinomzelllinie A549 untersucht. Wie bereits zuvor erwähnt, wurde DMSO als Lösungsmittel verwendet und der toxische Einfluss bestimmt und bei jedem Versuch als Kontrolle mitgemessen. Der Einfluss des verwendeten 0,5 % DMSO auf die Zellen ist minimal. Zur Bestimmung von Struktur-Aktivitäts-Wirkungsbeziehungen (SARs) konnten bezüglich der verschiedenen Gruppen keine generellen Korrelationen erkannt werden, nur innerhalb der Gruppen lassen sie sich festlegen. Die β-Hydroxydithiozimtsäureester zeigen generell schwache Aktivität gegen alle untersuchten Krebszelllinien und SARs für diese Verbindungsklasse zeigen höhere Aktivität für Verbindungen mit langen Alkylketten am Aromaten. Die besten Ergebnisse zeigte die Verbindung L9 (Tabelle 5-3). Die aktivsten Verbindungen im Allgemeinen sind die Osmium(II) Komplexe, diese zeigen niedrige IC50 Werte für alle untersuchten Zelllinien und die aktivste Verbindung dieser Klasse ist Os10, ein Komplex mit Hydroxylgruppe in *meta*-Position am Aromaten und damit die polarste Verbindung der Klasse (Tabelle 5-3). Somit lässt sich sagen, dass die SARs der Osmium Verbindungen nicht mit den der β-Hydroxydithiozimtsäureester L korrelieren.

Ähnliche Ergebnisse weisen die Verbindungen der Klasse Ptdmso auf, die ebenfalls mit erhöhter Polarität niedrigere IC50 Werte aufzeigen, aktivste Verbindung ist hier Ptdmso16 (Tabelle 5-3). Neben den Os Verbindungen zeigen die Ru und Pd Komplexe die besten Ergebnisse auf. Beide Gruppen korrelieren mit den SARs für die β-Hydroxydithiozimtsäureester und zeigen niedrige IC50 Werte mit erhöhter Lipophilie der Verbindungen, Ru6 und Pd3 sind die aktivsten Verbindungen für diese Klassen. Generell, zeigen die Ni und Pt Verbindungen dieselben SARs wie ihre Pd Analoga, jedoch weisen sie niedrigere Aktivität im Allgemeinen auf (Table 5-3). Tabelle 5-3 zeigt die aktivsten Verbindungen jeder Substanzklasse, ihren IC50 Mittelwert für alle fünf Zelllinien (englisch: MeanIC50) und die Daten der Referenzsubstanz Cisplatin. Besonders Ru6, Pd3 und Os10 sind potentielle Kandidaten für *in vivo* Studien.

Tab. 5-3: Substitutionsmuster und IC50 Mittelwert [µM] für die aktivsten Verbindungen und Cisplatin.

	L9	**Ru6**	**Os10**	**Ni1**	**Pd3**	**Pt4**	**Ptdmso16**	**CDDP**
-R	*p*-OBut	*p*-OEt	*m*-OH	*o*-OMe	*p*-OMe	*o*-OEt	*m*-OH	
-Alk	-Me	-Me	-Me	-Me	-Me	-Me	-Et	
Mean IC50	11.49	3.22	0.97	5.26	3.98	5.49	13.75	6.5

Abbildung 5-3 zeigt die IC50 Mittelwerte aller Substanzen einer Substanzklasse (violett), die IC50 Mittelwerte der Cisplatin sensitiven- (blau) und -resistenten- (rot) Ovarialkarzinomzelllinien. Es kann geschlussfolgert werden, dass generell Palladium(II) und Osmium(II) Komplexe vielversprechende IC50 Werte zeigen im Vergleich zu Cisplatin. Ebenso zeigen sich für alle Verbindungen (außer Pt) niedrigere IC50 Mittelwerte für die Cisplatin resistenten Zelllinien im Vergleich zu den sensitiven Zelllinien, was die Aktivität und Wirkung der Substanzen speziell auf resistente Tumore zeigt. Da dieser Effekt bereits für die β-Hydroxydithiozimtsäureester gezeigt wurde, ist er potentiell Liganden-abhängig. Die Komplexierung mit Metallen führt generell zu niedrigeren IC50 Werten.

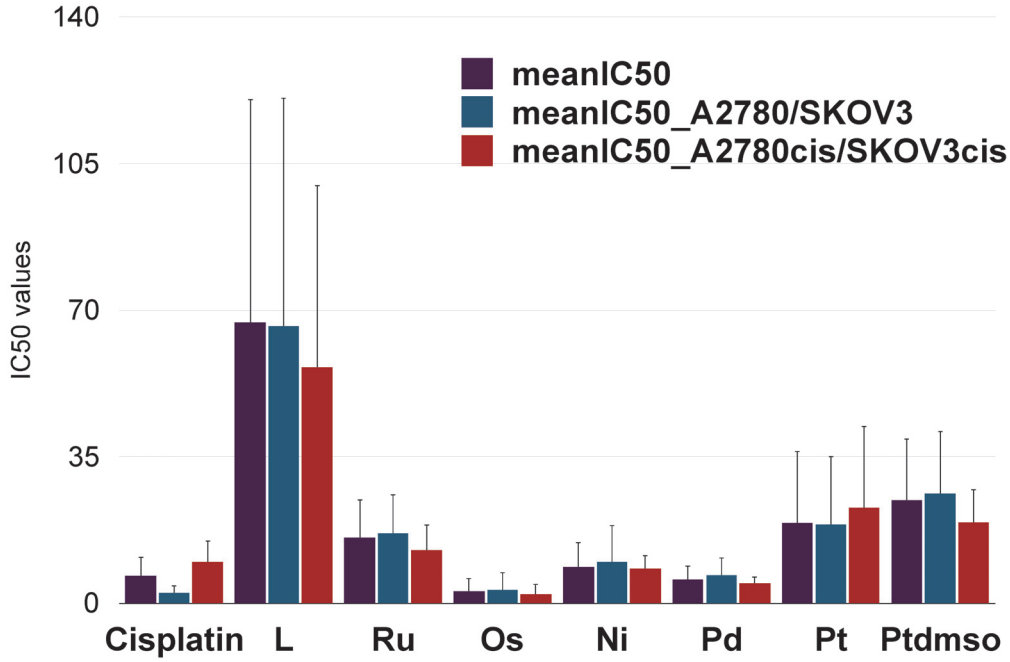

Abb. 5-3: Übersicht der IC50 Mittelwerte [µM] für alle Substanzklassen und Referenz Cisplatin (violett), IC50 Mittelwerte der Cisplatin sensitiven Zelllinien SKOV3 und A2780 (blau) und für die Cisplatin resistenten Analoga (rot).

Um die Aktivität der Verbindungen auf die resistenten Tumore zu bestimmen wurden Resistenzfaktoren (RF) berechnet. Tabelle 5-4 zeigt generell den Anteil von Substanzen mit RF ≤ 1 (zeigt das die Verbindungen aktiver auf die resistenten Zelllinien wirken als auf die sensitiven) für alle Substanzklassen gegen die Ovarialkarzinomzelllinien. Besonders für SKOV3/ SKOV3cis zeigen sich sehr gute Ergebnisse: 67% der Verbindungen L, 65% der Verbindungen Ru, 83% der Pd Verbindungen und 75% aller Ptdmso Komplexe zeigen höhere Aktivität auf die resistente Zelllinie. Hinzugefügt werden muss zudem, dass in den meisten Fällen die RF wesentlich niedriger sind als für Cisplatin, es zeigt sich also, dass diese Verbindungen nicht nur in der Lage sind die Resistenz zu umgehen sondern auch speziell auf resistente Tumore wirken, ein Effekt, der potentiell vom β-Hydroxydithiozimtsäureester Liganden selbst gesteuert wird.

Tab. 5-4: Prozentualer Anteil der RF ≤ 1 auf Ovarialkarzinomazelllinien für alle Substanzklassen.

RF ≤ 1	L	Ru	Os	Ni	Pd	Pt	Ptdmso
SKOV3/ SKOV3cis	67%	65%	25%	50%	83%	50%	75%
A2780/ A2780cis	50%	59%	25%	33%	17%	33%	50%

Die Betrachtung der Wirkung auf die resistenten Zelllinien dieser Arbeit zeigt, dass 22 Verbindungen niedrigere IC50 Mittelwerte zeigen als Cisplatin, Abbildung 5-4. Auch hier zeigt sich erneut, dass die Os, Pd und Ru Verbindungen die besten Ergebnisse erzielen.

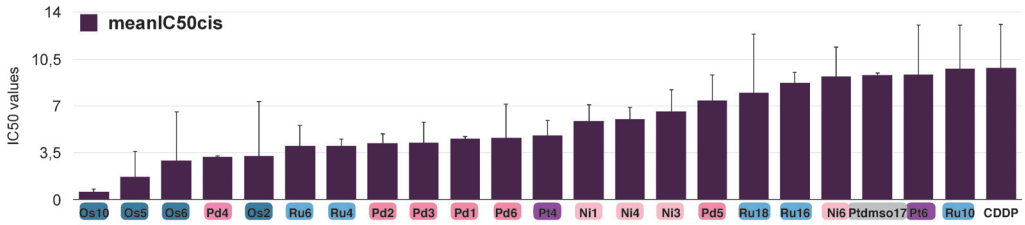

Abb. 5-4: IC50 Mittelwerte [µM] für SKOV3cis und A2780cis für alle Substanzen die niedrigere Werte zeigen als Referenzsubstanz Cisplatin.

Neben den guten Ergebnissen für Os und Pd Verbindungen sind die Ru Komplexe für weitere Untersuchungen ausgewählt worden, vor allem, da in der Literatur (besonders für die RAPTA-Komplexe) gezeigt worden ist, dass sehr gute *in vivo* Ergebnisse erzielt wurden auch wenn die *in vitro* Werte denen von Cisplatin gleichen.

Zusätzlich wurden einige der aktivsten Verbindungen auf drei nicht-karzinogene Zellllinien: Keratinozyten (1), Fibroblasten (2) und der MCF10A (3) unter denselben Bedingungen wie Cisplatin getestet. Wie für Cisplatin bekannt ist, zeigt es toxische Nebenwirkungen und somit konnten die IC50 Werte hier zwischen 3.3 µM und 5.7 µM bestimmt werden. Alle untersuchten Verbindungen zeigen höhere IC50 Werte als Cisplatin für die drei Zelllinien, somit kann geschlussfolgert werden, dass die hier untersuchten Verbindungen eine höhere spezifische

Aktivität auf Krebszelllinien (besonders auf Cisplatin resistente) aber eine geringere Zytotoxizität auf gesunde, proliferierende Zellen besitzen. Dies führt zu einer höheren Selektivität für Tumorzellen und einem großen Vorteil dieser Verbindungen.

Tab. 5-5: IC50 Werte für einige der meist aktivsten Verbindungen auf nicht-karzinogene Zelllinien um die Selektivität und toxische Nebenwirkungen zu bestimmen: Keratinozyten (1), Fibroblasten (2) und MCF10A (3), alle Werte sind in [µM].

Zell-linie	**L6**	**Ru10**	**Os10**	**Ni1**	**Pd3**	**Pt4**	**Ptdmso16**	**CDDP**
1	>100	>100	84.5 (±31.3)	87.0 (±0)	55.0 (±6.7)	>100	72.4 (±17.9)	5.7 (±3.1)
2	>100	>100	>100	84.3 (±8.9)	42.9 (±10.2)	>100	52.4 (15.8)	4.1 (±1.1)
3	>100	16.7 (±4.1)	21.3 (±3.3)	19.6 (±2.6)	28.3 (±16.8)	41.5 (±25.8)	42.6 (±13.5)	3.3 (±0.6)

Die Ptdmso und Ru Verbindungen sind bezüglich ihrer Wirkmechanismen mit verschiedenen Techniken, zum Beispiel Kristallstrukturen und NMR Studien genauer untersucht worden. Es wurde für beide Systeme gezeigt, dass das Binden an die genomische DNA, so wie es für Cisplatin der Fall ist, reduziert ist. Dies wurde untersucht mittels γH2AX-Foci Analysen, 9-Methylguanin NMR Studien und Zellzyklusarrest Experimenten. Die Suche nach anderen Bindungszielen der Substanzen führte zu zwei Kristallstrukturen, A) Ruthenium(II) Verbindung (Ru10) bindet an RNAse A mit dem Verlust des Arene Liganden und B) Platin(II) Verbindung (Pt1) bindet an HEWL mit dem Verlust aller Liganden. Somit kann die höhere Aktivität der Verbindungen verglichen mit Cisplatin auf einen anderen Wirkmechanismus zurückgeführt werden - vermutlich der Interaktion mit Proteinen.

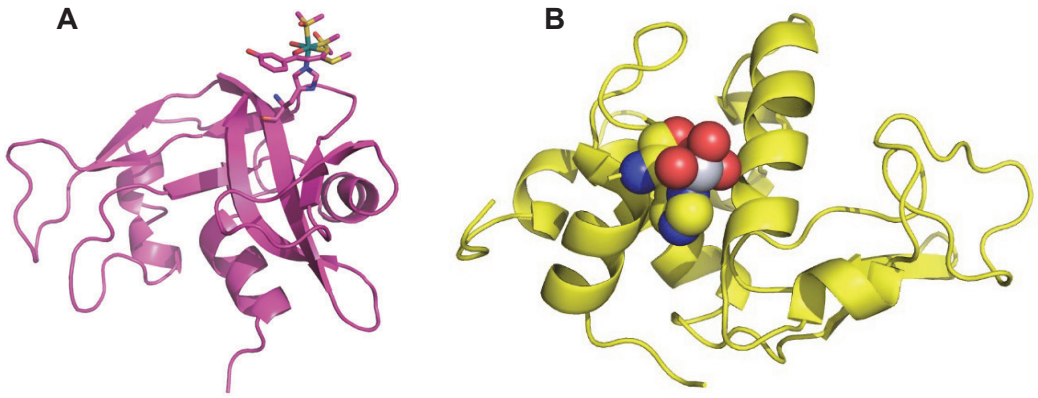

Abb. 5-5: **A**: Interaktionen von Ru10 und RNAse A. **B**: Interaction von Pt1 mit HEWL.

Zusammenfassend wurden in diesem Abschnitt neue Metall(II) Verbindungen mit vielversprechenden cytotoxischen Aktivitäten gegen Cisplatin resistente Zelllinien und mit einem anderen Wirkmechanismus als Cisplatin vorgestellt. Dies kann auch zu der höheren Selektivität der Verbindungen beitragen.

Teil 2: Chemische und biologische Untersuchungen von Platin(II) Komplexen mit Asparagussäure Derivativen als S/S, Se/Se und S/Se-Chelatliganden

Asparagussäure, ein Inhaltsstoff von Spargel, ist ein 1,2-Dithiolan Ringsystem ähnlich der α-Liponsäure welche als Co-Faktor im Pyruvat-Dehydrogenase-Komplex fungiert. Somit wird die Asparagussäure im Hinblick auf ihre pharmakologischen Eigenschaften hin untersucht. Ebenso wurde bereits gezeigt, dass sie und auch das Se/Se Analoga die Aufnahme von Arzneistoffen in die Zelle erhöhen können. Es ist bereits bekannt, dass Asparagussäure selbst an das Platin(II)-Zentrum koordinieren kann. Das Design von Derivativen und die biologische Untersuchung aller Komplexe ist Teil dieser Arbeit. Das Hauptziel der vorliegenden Arbeit lag in der Bestimmung der cytotoxischen Aktivität dieser Verbindungen, besonders gegen Cisplatin resistente Zelllinien, nachdem vielversprechende Ergebnisse bereits in Teil 1 für die Zimtsäure Derivate gezeigt werden konnten.

Die Synthese der Platin(II) Komplexe geht aus von den dazugehörigen Liganden L1-L4 und für Pt2, Pt4 und Pt6 der Synthese der Ausgangsverbindung (dppma)$PtCl_2$. Anschließend wird der dazugehörige Ligand L1-L4 reduziert und die Platin(II) Ausgangsverbindung hinzugegeben $PtCl_2L_2$ (L= dppma oder PPh_3). Für die Darstellung der Verbindungen Pt1 und Pt2 ist eine weitere Syntheseroute über die Deprotonierung der Dihydroasparagussäure möglich.

Die Charakterisierung aller Verbindung erfolgte mit verschiedenen Methoden, inklusive NMR Spektroskopie. Charakteristische ^{195}Pt- und ^{77}Se-Satelliten sind in den $^{31}P\{^{1}H\}$-NMR Spektren aller Platin(II) Komplexe erkennbar, ebenso wie das typische AB-Spin-System für die unsymmetrisch substituierten Verbindungen Pt3 und Pt4. Massenspektren zeigen die Molpeaks der jeweiligen Verbindung und den Verlust des Asparagussäure Liganden. Die Verbindungen L2, L3, L5, Pt1 und Pt7 wurden mittels Molekülstrukturen analysiert. Die Platin(II)-Atome von Pt1 und Pt7 weisen eine leicht verzerrte quadratisch-planare Koordinationsumgebung auf und einen P1-Pt-P2 Winkel größer als 90°, bedingt durch den sterischen Anspruch der PPh_3 Gruppen. Für die Verbindung Pt1 können intermolekulare Wasserstoffbrückenbindungen im Kristall zu einem zweiten Molekül beobachtet werden, dies führt zu einer Dimer-Struktur, Abbildung 5-6.

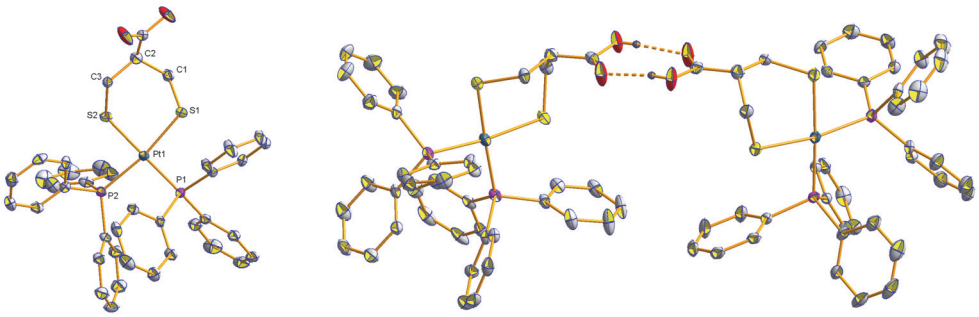

Abb. 5-6: Molekülstrukturen der Verbindung Pt1. Die Schwingungsellipsoide sind für eine Aufenthaltswahrscheinlichkeit von 50% dargestellt.

Alle Platin(II) Verbindungen wurden hinsichtlich ihrer Aktivität auf die Ovarialkarzinomzelllinien SKOV3 und A2780, wie auch deren resistente Analoga, untersucht. Die Ergebnisse zeigen, dass die Se/Se Verbindungen generell eine höhere Aktivität aufweisen als ihre S/S Analoga. Insgesamt zeigen die meisten Verbindungen eine niedrigere oder vergleichbare Aktivität zu Cisplatin, herauszustellen

sind die Ergebnisse der Verbindung Pt7, diese aktivste Verbindung zeigt RF kleiner als 1 und einen IC50 Wert von 4,3 µM im Vergleich zu 13,5 µM von Cisplatin für die Zelllinie SKOV3cis. Alle Komplexe zeigen kleinere RF Werte als Cisplatin und können somit die Resistenz umgehen. Abbildung 5-7 zeigt eine Übersicht aller Platin(II) Verbindungen im Vergleich zu Cisplatin. In Bezug auf die IC50 Mittelwerte, können folgende Struktur-Aktivitäts-Beziehungen erkannt werden: Se/Se > S/Se > S/S Verbindungen, die Se/Se Verbindungen Pt6 und Pt7 zeigen die besten Ergebnisse dieser Untersuchung.

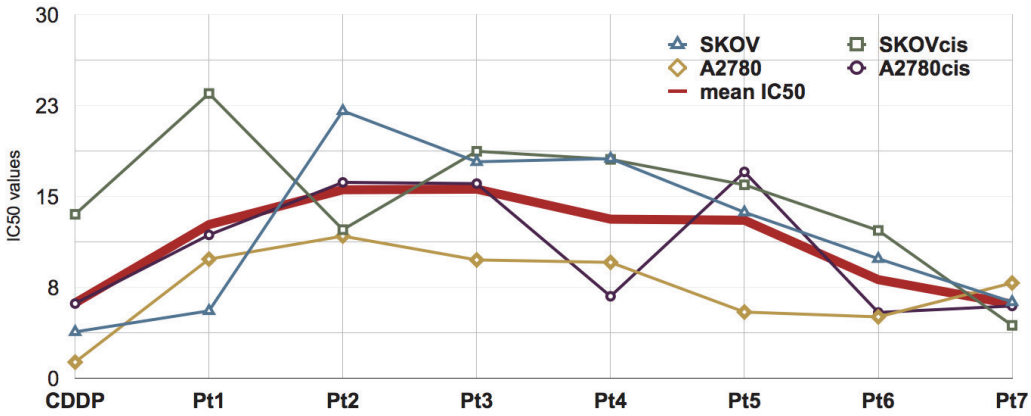

Abb. 5-7: IC50 Werte für alle Platin(II) Komplexe und Cisplatin auf den vier Zelllinien und die IC50 Mittelwerte. Alle Werte sind in [µM].

Zusammenfassend wurde in diesem Teil neue Platin(II) Verbindungen mit Asparagussäure Derivativen als Liganden vorgestellt, die einige interessante Ergebnisse auf Cisplatin resistente Ovarialkarzinomzelllinien und einen anderen Wirkmechanismus als Cisplatin zeigen.

7. References

A

[Abegg, 2017] D. Abegg, G. Gasparini, D. G. Hoch, A. Shuster, E. Bartolami, S. Matile and A. Adibekian, *Journal of the American Chemical Society*, **2017**, 139, 231-238.

[Abramkin, 2010] S. A. Abramkin, U. Jungwirth, S. M. Valiahdi, C. Dworak, L. Habala, K. Meelich, W. Berger, M. A. Jakupec, C. G. Hartinger, A. A. Nazarov, M. Galanski and B. K. Keppler, *J. Med. Chem.*, **2010**, 53, 7356–7364.

[Abu-Surrah, 2002] A. S. Abu-Surrah, T. A. K. Al-Allaf, L. J. Rashan, M. Klinga and M. Leskela, *Eur. J. Med. Chem*., **2002**, 37, 919-922.

[Abu-Surrah, 2008] A. S. Abu-Surrah, H. H. Al-Sa'doni and M. Y. Abdalla, *Cancer Therapy*, **2008**, 6, 1-10.

[Adhireksan, 2014] Z. Adhireksan, G. E. Davey, P. Campomanes, M. Groessl, C. M. Clavel, H. Yu, A. A. Nazarov, C. H. Yeo, W. H. Ang, P. Droge, U. Rothlisberger, P. J. Dyson and C. A. Davey, *Nat. Commun*., **2014**, 5, 3462-3475.

[Adiguzel, 2014] Z. Adiguzel, A. T. Baykal, O. Kacar, V. T. Yilmaz, E. Ulukay and C. Acilan, *J. Proteome Res.*, **2014**, 13, 5240-5249.

[Ahn, 1996] B. Z. Ahn and D. E. Sok, *Curr. Pharm. Design*, **1996**, 2, 247-262.

[Aird, 2002] R. E. Aird, J. Cummings, A. A. Ritchie, M. Muir, R. E. Morris, H. Chen, P. J. Sadler and D. I. Jodrell, *Br. J. Cancer*, **2002**, 86, 1652-1657.

[Al-Allaf, 1998] T. A. K. Al-Allaf and L. J. Rashan, *Eur. J. Med. Chem*., **1998**, 33, 817-820.

[Alam, 2016] M. D. Alam and F. Huq, *Coord. Chem. Rev.,* **2016**, 316, 36-67.

[Alazard, 1982] R.J. Alazard, M. Germanier and N.P. Johnson, *Mutation Res.*, **1982**, 93, 327-337.

[Alessio, 1988] E. Alessio, G. Mestroni, G. Nardin, W. M. Attia, M. Calligaris, G. Sava and S. Zorzet*, Inorg. Chem*., **1988**, 27, 4099-4106.

[Alessio, 1991] E. Alessio, G. Balducci, M. Calligaris, G. Costa, W. M. Attia and G. Mestroni*, Inorg. Chem*., **1991**, 30, 609-618.

[Alessio, 2013] M. Alessio, I. Zanellato, I. Bonarrigo, E. Gabano, M. Ravera and D. Osella, *J. Inorg. Biochem*., **2013**, 129, 52-57.

[Alderden, 2006] R. A. Alderen, M. D. Hall and T. W. Hambley, *JCE*, **2006**, 83(5), 728-734.

[Allardyce, 2001a] C. S. Allardyce and P. J. Dyson, *Platinum Met. Rev*., **2001**, 45, 62-69.

[Allardyce, 2001b] C. S. Allardyce, P. J. Dyson, D. J. Ellis and S. L. Heath, *Chem. Commun*., **2001**, 1396-1397.

[Allardyce, 2001c] C. S. Allardyce and P. J. Dyson, *Dalton Trans*., **2016**, 3201-3209.

[Ang, 2005a] W. H. Ang, C. S. Khalaila, L. Allardyce, L. Juillerat-Jeanneret and P. J. Dyson, *J. Am. Chem. Soc.*, **2005**, 127, 1382-1383.

[Ang, 2005b] W. H. Ang, S. Pilet, R. Scopelliti, F. Bussy, L. Juillerat-Jeanneret and P. J. Dyson, *J. Med. Chem.*, **2005,** 48, 8060-8069.

[Ang, 2011] W. H. Ang, A. Casini, G. Sava and P. J. Dyson, *J. Organomet. Chem.,* **2011**, 696, 898-998.

[Antonarakis, 2010] E. S. Antonarakis and A. Emadi, *Cancer Chemother. Pharmacol.*, **2010**, 1, 1-9.

[Appleton, 1997] T.G. Appleton, *Coord. Chem. Rev*., **1997**, 166, 313-359.

[Arnesano, 2011] F. Arnesano, L. Banci, I. Bertini, I.C. Felli, M. Losacco and G. Natile*, J. Am. Chem. Soc.*, **2011**, 133, 18361-18369.

[Arora, 2010] S. Arora, A. Kothandapani, K. Tillison, V. Kalman-Maltese and S.M. Patrick, *DNA Repair*, **2010**, 9, 745-753.

B

[Baban, 1998] D. F. Baban and L. W. Seymour, *Adv. Drug Delivery Rev*., **1998**, 34, 109-119.

[Baderschneider, 2001] B. Baderschneider and P. Winterhalter, *J. Agric. Food Chem*., **2001**, 49(6), 2788-2798.

[Barnes, 2004a] K. R. Barnes and S. J. Lippard, *Met. Ions Biol. Syst.,* **2004**, 42, 143-177.

[Barnes, 2004b] K. R. Barnes, A. Kutikov and S. J. Lippard, *Chem. Biol*., **2004**, 11, 557-564.

[Beatty, 1996] E. J. Beatty, M. C. Cox, T. A. Frenkiel, B. M. Tam, A. B. Mason, R. T. MacGillivray, P. J. Sadler and R. C. Woodworth, *Biochemistry*, **1996**, 35, 7635-7642.

[Bergamo, 2008] A. Bergamo, A. Masi, P. J. Dyson and G. Sava*, Int. J. Oncol*., **2008**, 33, 1281-1289.

[Bergamo, 2010] A. Bergamo, A. Masi, A. F. A. Peacock, A. Habtemariam, P. J. Sadler and G. Sava, *J. Inorg. Biochem*., **2010**, 104, 79-86.

[Berger, 1989] M. R. Berger, F. T. Garzon, B. K. Keppler and D. Schmahl, *Anticancer Res*., **1989**, 9, 761-765.

[Betanzos-Lara, 2012] S. Betanzos-Lara, O. Novakova, R. J. Deeth, A. M. Pizarro, G. J. Clarkson, B. Liskova, V. Brabec, P. J. Sadler and A. Habtemariam, *J. Biol. Inorg. Chem*., **2012**, 17, 1033-1051.

[Bierle, 2015] L. A. Bierle, K. L. Reich, B. E. Taylor, E. B. Blatt, S. M. Middleton, S. D. Burke, L. K. Stultz, P. K. Hanson, J. F. Patridge and M. E. Miller, *PLOS ONE Staff.*, **2015**, 10, e0138085.

[Bijelic, 2016] A. Bijelic, S. Theiner, B. K. Keppler and A. Rompel, *J. Med. Chem*., **2016**, 59, 5894-5903.

[Bindoli, 2009] A. Bindoli, M. P. Rigobello, G. Scutari, C. Gabbiani, A. Casini and L. Messori, *Coord. Chem. Rev.*, **2009**, 253, 1692-1707.

[Bloemink, 1996] M. J. Bloemink and J. Reedijk, *Met. Ions. Biol. Syst.*, **1996**, 32, 641-685.

[Boccarreli, 2006] A. Boccarelli, F. P. Intini, R. Sasanelli, M. F. Sivo, M. Coluccia and G. Natile, *J. Med. Chem*., **2006**, 49, 829-837.

[Borst, 2000] P. Borst, R. Evers, M. Kool and J. Wijnholds, *J. Natl. Cancer Inst.*, **2000**, 92, 1295-1302.

[Bowler, 1986] B. E. Bowler and S. J. Lippard, *Biochemistry*, **1986**, 25, 3031-3038.

[Brabec, 1993] V. Brabec and M. Leng, *Proc. Natl. Acad. Sci. U. S. A.*, **1993**, 90, 5345-5349.

[Brabec, 2000] V. Brabec, in: L. R. Kelland, N. P. Farrell (Eds.), *Platinum-Based Drugs in Cancer Therapy*, Humana Press Inc., **2000**, 37-61.

[Brabec, 2017] V. Brabec, O. Hrabina and J. Kasparkova, *Coord. Chem. Rev.*, **2017**, 351, 2-31.

[Brodie, 2004] C. R. Brodie, J. G. Collins and J. R. Aldrich-Wright, *Dalton Trans.*, **2004**, 1145-1152.

[Brown, 1993] S. J. Brown, P. J. Kellett and S. J. Lippard, *Science*, **1993**, 261, 603-605.

[Bruijnincx, 2009] P. C. A. Bruijnincx and P. J. Sadler, *Adv. Inorg. Chem*. **2009**, 61, 1-62.

[Bryde, 2009] D. Bryde and A. I. P. M. de Kroon, *Future Med. Chem.*, **2009**, 1, 1467-1480.

[Buettner, 2012] K. M. Buettner and A. M. Valentine, *Chem. Rev.*, **2012**, 112, 1863-1881.

[Burris, 2016] H. A. Burris, S. Bakewell, J. C. Bendell, J. R. Infante, S. F. Jones, D. R. Spigel, G. J. Weiss, R. K. Ramanathan, A. Ogden and D. D. Von Hoff, *ESMO Open,* **2016**, 1, e000154.

[Buss, 2011] I. Buss, D. Garmann, M. Galanski, G. Weber, G. V. Kalayda, B. K. Keppler and U. Jaehde, *J. Inorg. Biochem.*, **2011**, 105, 709-717.

[Butour, 1997] S. Butour, F. Wimmer, F. Wimmer and P. Castan, *Chemico-Biological Interactions***, 1997**, 104, 165-178.

[Büchel, 2013] G. E. Büchel, A. Gavriluta, M. Novak, S. M. Meier, M. A. Jakupec, O. Cuzan, C. Turta, J. B. Tommasino, E. Jeanneau, G. Novitchi, D. Luneau and V. B. Arion, *Inorg. Chem*. **2013**, 52, 6273-6285.

C

[Caires, 1999] A. C. F. Caires, E. T. Almeida, A. E. Mauro, J. P. Hemerly and S. R. Valentini, *Química Nova,* **1999**, 22, 329-334.

[Calandrini, 2014a] V. Calandrini, T.H. Nguyen, F. Arnesano, A. Galliani, E. Ippoliti, P. Carloni and G. Natile, *Chemistry*, **2014**, 20, 11719-11725.

[Calandrini, 2014b] V. Calandrini, F. Arnesano, A. Galliani, T.H. Nguyen, E. Ippoliti, P. Carloni and G. Natile, *Dalton Trans.*, **2014**, 43, 12085-12094.

[Calvert, 1982] A. H. Calvert, S. J. Harland, D. R. Newell, Z. H. Siddik, A. C. Jones, T. J. McElwain, S. Raju, E. Wiltshaw, I.E. Smith, J. M. Baker, M. J. Peckham and K. R. Harrap, *Cancer Chemother. Pharmacol.*, **1982**, 9, 140-147.

[Carmine, 2013] A. Carmine, Y. Domoto, N. Sakai and S. Matile, *Chemistry*, **2013**, 19, 11558-11563.

[Carr, 2002] J. L. Carr, M. D. Tingle and M. J. McKeage, *Cancer Chemother. Pharmacol*., **2002**, 50, 9-15.

[Carr, 2006] J. L. Carr, M. D. Tingle and M. J. McKeage, *Cancer Chemother. Pharmacol*., **2006**, 57, 483-490.

[Carreira,2012a] M. Carreira, R. Calvo-Sanjuań ,M. Sanaú, I. Marzo and M. Contel, *Organometallics*, **2012**, 31, 5772-5781.

[Carreira, 2012b] M. Carreira, R. Calvo-Sanjuań, M. Sanaú, X. Zhao, R. S. Magliozzo, I. Marzo and M. Contel, *J. Inorg. Biochem.*, **2012**, 116, 204-214.

[Cebrian-Losantos, 2007] B. Cebrian-Losantos, A. A. Krokhin, I. N. Stepanenko, R. Eichinger, M. A. Jakupec, V. B. Arion and B. K. Keppler, *Inorg. Chem*., **2007**, 46, 5023-5033.

[Cetinbas, 2010] N. Cetinbas, M. I. Webb, J. A. Dubland and C. J. Walsby, *J. Biol. Inorg. Chem*., **2010**, 15, 131-145.

[Chatlas, 1995] J. Chatlas, R. Vaneldik and B. K. Keppler*, Inorg. Chim. Acta*, **1995**, 233, 59-63.

[Chambers, 1997] A. F. Chambers and L. M. Matrisian, *J. Natl. Cancer Inst*., **1997,** 89, 1260-1270.

[Chatterjee, 2008] S. Chatterjee, S. Kundu, A. Bhattacharyya, C. G. Hartinger and P. J. Dyson, *J. Biol. Inorg. Chem*., **2008**, 13, 1149-1155.

[Chen, 2002] H. M. Chen, J. A. Parkinson, S. Parsons, R. A. Coxall, R. O. Gould and P. J. Sadler, *J. Am. Chem. Soc.*, **2002**, 124, 3064-3082.

[Chen, 2009] D. Chen, V. Milacic, M. Frezza and Q. P. Dou, *Curr. Pharm. Des.*, **2009**, 15, 777-791.

[Cheng, 2006] H. Cheng, F. Huq, P. Beale and K. Fisher, *Eur. J. Med. Chem*., **2006**, 41, 896-903.

[Cheng, 2014] Q. Cheng, H. Shi, H. Wang, Y. Min, J. Wang and Y. Liu, *Chem. Commun*., **2014**, 50, 7427-7430.

[Churusova, 2017] S. G. Churusova, D. V. Aleksanyan, E. Y. Rybalkina, O. Y. Susova, V. V. Brunova, R. R. Aysin, Y. V. Nelyubina, A. S. Peregudov, E. I. Gutusul, Z. S. Klemenkova and V. A. Kozlov, *Inorg. Chem*., **2017**, 56, 9834-9850.

[Clarke, 1974] M. J. Clarke and H. Taube, *J. Am. Chem. Soc*., **1974**, 96, 5413-5419.

[Clarke, 1978] M. J. Clarke, *J. Am. Chem. Soc*., **1978**, 100, 5068-5075.

[Clarke, 1980a] M. J. Clarke, *Inorg. Chem*., **1980**, 19, 1103-1104.

[Clarke, 1980b] M. J. Clarke, S. Bitler, D. Rennert, M. Buchbinder and A. D. Kelman, *J. Inorg. Biochem*., **1980**, 12, 79-87.

[Clarke, 1999] M. J. Clarke, F. Zhu and D. R. Frasca, *Chem. Rev.*, **1999**, 99(9), 2511-2534.

[Clarke, 2002] M. J. Clarke, *Coord. Chem. Rev.*, **2002**, 232, 69-93.

[Clarke, 2003] M. J. Clarke, *Coord. Chem. Rev*., **2003**, 236, 209-233.

[Clavel, 2014] C. M. Clavel, E. Paunescu, P. Nowak-Sliwinska and P. J. Dyson, *Chem. Sci*., **2014**, 5, 1097-1101.

[Cleare, 1973] M. J. Cleare and J. D. Hoeschele, *Bioinorg. Chem.*, **1973**, 2, 187-210.

[Cleare, 1974] M. J. Cleare, in: T. A. Connors, J. J. Roberts (Eds.), *Platinum Coordination Complexes in Cancer Chemotherapy*, Springer, **1974**, 12-37.

[Clifford, 1999] N. M. Clifford, *J. Sci. Food Agric.*, **1999**, 79(3), 362-372.

[Clifford, 2000] N. M. Clifford, *J. Sci. Food Agric.*, **2000**, 80(7), 1033-1043.

[Cohen, 2007] S. M. Cohen, *Curr. Opin. Chem. Biol.*, **2007**, 11, 115-120.

[Coluccia, 1995] M. Coluccia, A. Boccarelli, M. A. Mariggiò, N. Cardellicchio, P. Caputo, F. P. Intini and G. Natile, *Chem. Biol. Interact.*, **1995**, 98, 251-266.

[Coussens, 1996] L. M. Coussens and Z. Werb, *Chem. Biol*., **1996**, 3, 895-904.

D

[Daghriri, 2004] H. Daghriri, F. Huq and P. Beale, *J. Inorg. Biochem*., **2004**, 98, 1722-1733.

[Das, 1978] M. Das and S. E. Livingstone, *Br. J. Cancer,* **1978**, 38, 325-328.

[De, 2011] P. De, M. Baltas and F. Bedos-Belval, *Curr. Med. Chem.*, **2011**, 18, 1672-1703.

[DeConti, 1973] R. C. DeConti, B. R. Toftness, R. C. Lange and W. A. Creasey, *Cancer Res.*, **1973**, 33, 1310-1315.

[Dent, 2001] P. Dent and S. Grant, *Clin. Cancer Res.*, **2001**, 7, 775-783.

[Depenbrock, 1997] H. Depenbrock, S. Schmelcher, R. Peter, B. K. Keppler, G. Weirich, T. Block, J. Rastetter and A. R. Hanauske, *Eur. J. Cancer*, **1997**, 33, 2404-2410.

[Dhar, 2009] S. Dhar and S. J. Lippard, *Proc. Natl. Acad. Sci. U .S .A.*, **2009**, 106, 22199-22204.

[Dilruba, 2016] S. Dilruba and G. V. Kalayda, *Cancer Chemother. Pharmacol.*, **2016**, 77, 1103-1124.

[Dobrova, 2016] A. Dobrova, S. Platzer, F. Bacher, M. M. Milunovic, A. Drobrov, G. Spengler, E. A. Enyedy, G. Novitchi and V. B. Arion, *Dalton Trans.*, **2016**, 45, 13427-13439.

[Dolgova, 2013] N. V. Dolgova, S. Nokhrin, C. H. Yu, G. N. George and O. Y. Dmitriev, *Biochem. J.*, **2013**, 454, 147-156.

[Dorcier, 2005] A. Dorcier, P. J. Dyson, C. Gossens, U. Rothlisberger, R. Scopelliti and I. Tavernelli, *Organometallics*, **2005**, 24, 2114-2123.

[Dorcier, 2006] A. Dorcier, W. H. Ang, S. Bolano, L. Gonsalvi, L. Juillerat-Jeannerat, G. Laurenczy, M. Peruzzini, A. D. Phillips, F. Zanobini and P. J. Dyson, *Organometallics*, **2006**, 25, 4090-4096.

[Dougan, 2006] S. J. Dougan, M. Melchart, A. Habtemariam, S. Parsons and P. J. Sadler, *Inorg. Chem*., **2006**, 45, 10882-10894.

[Durig, 1976] J. R. Durig, J. Danneman, W. D. Behnke and E. E. Mercer, *Chem.-Biol. Interact*., **1976**, 13, 287-294.

[Dyson, 2007] P. J. Dyson, *Chimia*, **2007**, 61, 698-703.

E

[Edreva, 2005] A. Edreva, *Agric. Ecosyst. Environ.*, **2005**, 106, 135-146.

[Ekmekcioglu, 1998] C. Ekmekcioglu, J. Feyertag and W. Marktl, *Cancer Lett.*, **1998**, 128, 137-144.

[Epifano, 2007] F. Epifano, M. Curini, S. Genovese, M. Blaskovich, A. Hamilton and S. M. Sebti, *Bioorg. Med. Chem. Lett.*, **2007**, 17(9), 2639-2642.

F

[Farrell, 1990] N. Farrell, Y. Qu and M. P. Hacker, *J. Med. Chem.*, **1990**, 33, 2179-2184.

[Fedi, 1997] P. Fedi, S. R. Tronick and S. A. Aaronson, In: J. F. Holland, R. C. Bast, D. L. Morton, E. Frei, D. W. Kufe and R. R. Weichselbaum (Eds.), *Cancer Medicine*, Williams and Wilkins, **1997**, 41-64.

[Filak, 2010] L. K. Filak, G. Muhlgassner, M. A. Jakupec, P. Heffeter, W. Berger, V. B. Arion and B. K. Keppler, *J. Biol. Inorg. Chem*., **2010**, 15, 903-918.

[Filak, 2011] L. K. Filak, G. Muhlgassner, F. Bacher, A. Roller, M. Galanski, M. A. Jakupec, B. K. Keppler and V. B. Arion, *Organometallics*, **2011**, 30, 273-283.

[Filak, 2013] L. K. Filak, S. Goschl, P. Heffeter, K. Ghannadzadeh Samper, A. E. Egger, M. A. Jakupec, B. K. Keppler, W. Berger and V. B. Arion, *Organometallics*, **2013**, 32, 903-914.

[Fisher, 2007] D. M. Fisher, P. J. Bednarski, R. Grunert, P. Turner, R. R. Fenton and J. R. Aldrich-Wright, *ChemMedChem*, **2007**, 2, 488-495.

[Flocke, 2016] L. S. Flocke, R. Trondl, M. A. Jakupec and B. K.Keppler, *Invest. New Drugs,* **2016**, 34, 261-268.

[Fotti, 1996] M. Fotti, M. Piattelli, M. Z. Baratta and G. Ruberto, *J. Agric. Food Chem.*, **1996**, 44(2), 497-501.

[Franklin, 2009] R. B., Franklin and L. C. Costello, *J. Cell Biochem.*, **2009**, 106, 750-757.

[Frasca, 1996] D. Frasca, J. Ciampa, J. Emerson, R. S. Umans and M. J. Clarke, *Metal-Based Drugs*, **1996**, 3, 197-209.

[Frezza, 2010] M Frezza, S. Hindo, D. Chen, A. Davenport, S. Schmitt, D. Tomco and Q. P. Dou, *Curr. Pharm. Design*, **2010**, 16, 1813-1825.

[Fricker, 2007] S. P. Fricker, *Dalton Trans.*, **2007**, 4903-4917.

[Frei, 2011] E. Frei, *Diabetol. Metab. Syndr.*, **2011**, 3 (11), doi.10.1186/1758-5996-3-11.

[Friedberg, 2006] E. C. Friedberg, A. Aguilera, M. Gellert, P. C. Hanawalt, J. B. Hays, A. R. Lehmann, T. Lindahl, N. Lowndes, A. Sarasin and R. D. Wood, *DNA Repair (Amst.)*, **2006**, 5, 986-996.

[Fu, 2010] Y. Fu, A. Habtemariam, A. M. Pizarro, S. H. van Rijt, D. J. Healey, P. A. Cooper, S. D. Shnyder, G. J. Clarkson and P. J. Sadler, *J. Med. Chem*., **2010**, 53, 8192-8196.

[Fu, 2011] Y. Fu, A. Habtemariam, A. M. B. H. Basri, D. Braddick, G. J. Clarkson and P. J. Sadler*, Dalton Trans*., **2011**, 40, 10553-10562.

[Fu, 2012] Y. Fu, M. J. Romero, A. Habtemariam, M. E. Snowden, L. J. Song, G. J. Clarkson, B. Qamar, A. M. Pizarro, P. R. Unwin and P. J. Sadler, *Chem. Sci*., **2012**, 3, 2485-2494.

[Fuereder, 2017] T. Fuereder and W. Berger, *ESMO Open*, **2017**, 2, e000239.

G

[Gabano, 2009] E. Gabano, M. Ravera and D. Osella, *Curr. Med. Chem.*, **2009**, 16, 4544-4580.

[Galuzzi, 2011] L. Galluzzi, E. Morselli, O. Kepp, I. Vitale, M. Pinti and G. Kroemer, *Antioxid. Redox. Signal.*, **2011**, 15, 1691-1714.

[Galuzzi, 2012] L. Galluzzi, L. Senovilla, I. Vitale, J. Michels, I. Martins, O. Kepp, M. Castedo and G. Kroemer, *Oncogene*, **2012**, 31, 1869-1883.

[Garbutcheon-Singh, 2013] K. B. Garbutcheon-Singh, P. Leverett, S. Myers and J. R. Aldrich-Wright, *Dalton Trans.*, **2013**, 42, 918-926.

[Giancotti, 1999] F. G. Giancotti and E. Ruoslahti, *Science*, **1999**, 285, 1028-1032.

[Giandomenico, 1995] C. M. Giandomenico, M. J. Abrams, B. A. Murrer, J. F. Vollano, M. I. Rheinheimer, S. B. Wyer, G. E. Bossard and J. D. Higgins, *Inorg. Chem*., **1995**, 34, 1015-1021.

[Gibson, 2009] D. Gibson, *Dalton Trans.*, **2009**, 48, 10681-10689.

[Gibson, 2016] D. Gibson, *Dalton Trans.*, **2016**, 45, 12983-12991.

[Gill, 1984] D. S. Gill, *Platinum Co-Ordination Complexes in Cancer Chemotherapy*, M. Nijhoff Publishers, **1984**.

[Ginzinger, 2012] W. Ginzinger, G. Muhlgassner, V. B. Arion, M. A. Jakupec, A. Roller, M. Galanski, M. Reithofer, W. Berger and B. K. Keppler, *J. Med. Chem*., **2012**, 55, 3398-3413.

[Gopal, 1999] Y. N. V. Gopal, D. Jayaraju and A. K. Kondapi, *Biochemistry*, **1999**, 38, 4382-4388.

[Gordaliza, 2007] M. Gordaliza, *Clin. Trans. Oncol.*, **2007**, 9, 767-776.

[Groessl, 2007] M. Groessl, E. Reisner, C. G. Hartinger, R. Eichinger, O. Semenova, A. R. Timerbaev, M. A. Jakupec, V. B. Arion and B. K. Keppler, *J. Med. Chem*., **2007**, 50, 2185-2193.

[Guichard, 2006] S. M. Guichard, R. Else, E. Reid, B. Zeitlin, R. Aird, M. Muir, M. Dodds, H. Fiebig, P. J. Sadler and D. I. Jodrell*, Biochem. Pharmacol*., **2006**, 71, 408-415.

[Gullo, 1980] J. Gullo, C. L. Litterst, P. J. Maguire, B. I. Sikic, D. F. Hoth and P. V. Woolley, *Cancer Chemother. Pharmacol*., **1980**, 5, 21-26.

H

[Habtemariam, 2006] A. Habtemariam, M. Melchart, R. Fernandez, S. Parsons, I. D. H. Oswald, A. Parkin, F. P. A. Fabbiani, J. E. Davidson, A. Dawson, R. E. Aird, D. I. Jodrell and P. J. Sadler, *J. Med. Chem*., **2006**, 49, 6858-6868.

[Hackl, 2016] C. M. Hackl, M. S. Legina, V. Pichler, M. Schmidlehner, A. Roller, O. Domotor, E. A. Enyedy, M. A. Jakupec, W. Kandioller and B. K. Keppler, *Chem.-Eur. J.*, **2016**, 22, 17269-17281.

[Hall, 2002] M. D. Hall and T. W. Hambley, *Coord. Chem. Rev*., **2002**, 232, 49-67.

[Hambley, 2007] T. W. Hambley, *Dalton Trans.*, **2007**, 4929-4937.

[Hanahan, 2000] D. Hanahan and R. A. Weinberg, *Cells*, **2000**, 100, 57-70.

[Hanahan, 2011] D. Hanahan and R. A. Weinberg, *Cells*, **2011**, 144, 646-674.

[Hanif, 2010] M. Hanif, P. Schaaf, W. Kandioller, M. Hejl, M. A. Jakupec, A. Roller, B. K. Keppler and C. G. Hartinger, *Aust. J. Chem*., **2010**, 63, 1521-1528.

[Harder, 1970] H.C. Harder and B. Rosenberg, *Int. J. Cancer*, **1970**, 6, 207-216.

[Haribabu, 2015] J. Haribabu, K. Jeyalakshmi, Y. Arun, N. S. P. Bhuvanesh, P. T. Perumal and R. Karvembu, *RSC Adv.*, **2015**, 5, 46031-46049.

[Harper, 2007] J. W. Harper and S. J. Elledge, *Mol. Cell.*, **2007**, 28, 739-745.

[Harris, 2005] A. L. Harris, X. Yang, A. Hegmans, L. Povirk, J. J. Ryan, L. Kelland and N. P. Farrell, *Inorg. Chem.*, **2005**, 44, 9598-9600.

[Hartinger, 2008] C. G. Hartinger, M. A. Jakupec, S. Zorbas-Seifried, M. Groessl, A. Egger, W. Berger, H. Zorbas, P. J. Dyson and B. K. Keppler, *Chem. Biodiversity*, **2008**, 5, 2140-2155.

[Haxton, 2009] K. J. Haxton and H. M. Burt, *J. Pharm. Sci.*, **2009**, 98, 2299-2316.

[Hildebrandt, 2016] J. Hildebrandt, *'Quadrupole Action' Platinum(IV) Prodrugs as Anticancer Agents*, Proposal submitted for Minerva Fellowship, **2016**.

[Holford, 1998] J. Holford, F. Raynaud, B. A. Murrer, K. Grimaldi, J. A. Hartley, M. Abrams and L. R. Kelland, *Anticancer Drug. Des.*, **1998**, 13, 1-18.

[Holm, 1996] R. H. Holm, P. Kennepohl and E. I. Solomon, *Chem. Rev*., **1996**, 96, 2239-2314.

[Honecker, 2018] F. Honecker, J. Claßen, J. C. Preiß and W. Dornoff, *Interdisziplinäre Empfehlungen zur Therapie 2018/19*; Taschenbuch Onkologie, W. Zuckerschwerdt Verlag München, 19. Auflage, **2018**.

[Hoskins, 1984] J. A. Hoskins, *J. Appl. Toxicol*., **1984**, 4, 283-292.

[Hotze, 2000] A. C. G. Hotze, A. H. Velders, F. Ugozzoli, M. Biagini-Cingi, A. M. Manotti-Lanfredi, J. G. Haasnoot and J. Reedijk, *Inorg. Chem.,* **2000**, 39, 3838-3844.

[Howle, 1970] J. A. Howle and G. R. Gale, *Biochem. Pharmacol.,* **1970**, 19, 2757-2762.

[Hrazdina, 1992] G. Hrazdina, *Basic Life Sci.*, **1992**, 59 (Plant Polyphenols), 61-72.

[Huang, 1994] J. C. Huang, D. B. Zamble, J. T. Reardon, S. J. Lippard and A. Sancar, *Proc. Natl. Acad. Sci.* USA, **1994**, 91, 10394-10398.

[Huq, 2004] F. Huq, H. Daghriri, J. Q. Yu, H. Tayyem, P. Beale and M. Zhang, *Eur. J. Med. Chem*., **2004**, 39, 947-958.

[Huq, 2007] F. Huq, H. Tayyem, P. Beale and J. Q. Yu, *J. Inorg. Biochem*., **2007**, 101, 30-35.

I

[Iqbal, 2017] B. Y. Iqbal,R. N. Iqbal, M. Ejaz, M. Hussain, F. Yasmeen, H. Saira and M. Imran, *J. Plant. Biochem. Physiol.*, **2017**, 5, 3-6.

[Ito, 2010] Y. Ito and P. Selenko, *Curr. Opin. Struct. Biol.*, **2010**, 20, 640-648.

[Ivanov, 1998] A. I. Ivanov, J. Christodoulou, J. A. Parkinson, K. J. Barnham, A. Tucker, J. Woodrow and P. J. Sadler, J*. Biol. Chem.*, **1998**, 273, 14721-14730.

J

[Jackson, 2009] S. P. Jackson and J. Bartek, *Nature*, **2009**, 461, 1071-1078.

[Jang, 2004] D. S. Jang, M. Cuendet, H. H. Fong, J. M. Pezzuto and A. D. Kinghorn, *J. Agr. Food Chem.*, **2004**, 52, 2218-2222.

[Jansen, 1948] E. F. Jansen, *J. Biol. Chem.*, **1948**, 176, 657-664.

[Jennette, 1974] K. W. Jennette, S. J. Lippard, G. A. Vassiliades and W. R. Bauer, *Proc. Natl. Acad. Sci. U. S. A.*, **1974**, 71, 3839-3843.

[Jiang, 1997] L. Jiang, Y. Chen, G. Tang and W. Tang, *J. Inorg. Biochem*., **1997**, 65, 73-77.

[Johnson, 1978] N. P. Johnson, J. D. Hoeschele, N. B. Kuemmerle, W. E. Masker and R. O. Rahn, *Chem.- Biol. Interact.*, **1978**, 23, 267-271.

[Johnstone, 2013] T. C. Johnstone, J. J. Wilson and S. J. Lippard, *Inorg. Chem.*, **2013**, 52, 12234-12249.

[Johnstone, 2016] T. C. Johnstone, K. Suntharalingam and S. J. Lippard, *Chem. Rev.*, **2016**, 116, 3436-3486.

[Jung, 2007] Y. Jung and S. J. Lippard, *Chem. Rev.*, **2007**, 107(5), 1388-1407.

[Jungwirth, 2011] U. Jungwirth, C. R. Kowol, B. K. Keppler, C. G. Hartinger, W. Berger and P. Heffeter, *Antioxid. Redox. Sign.*, **2011**, 15(4), 1085-1126.

[Jungwirth, 2012] U. Jungwirth, D. N. Xanthos, J. Gojo, A. K. Bytzek, W. Korner, P. Heffeter, S. A. Abramkin, M. A. Jakupec, C. G. Hartinger, U. Windberger, M. Galanski, B. K. Keppler and W. Berger, *Mol. Pharmacol*., **2012**, 81, 719-728.

K

[Kalayda, 2008] G. V. Kalayda, C. H. Wagner, I. Buss, J. Reedijk and U. Jaehde, *BMC Cancer,* **2008**, 8 (175), doi: 10.1186.1471-2407-8-175.

[Kalayda, 2012] G.V. Kalayda, C. H. Wagner and U. Jaehde, *J. Inorg. Biochem.*, **2012**, 116, 1-10.

[Kandioller, 2009a] W. Kandioller, C. G. Hartinger, A. A. Nazarov, M. L. Kuznetsov, R. O. John, C. Bartel, M. A. Jakupec, V. B. Arion and B. K. Keppler, *Organometallics*, **2009**, 28, 4249-4251.

[Kandioller 2009b] W. Kandioller, C. G. Hartinger, A. A. Nazarov, J. H. Kasser, R. O. John, M. Jakupec, V. Arion, P. J. Dyson and B. K. Keppler, *J. Organomet. Chem*., **2009**, 694, 922-929.

[Kandioller, 2009c] W. Kandioller, C. G. Hartinger, A. A. Nazarov, C. Bartel, M. Skocic, M. A. Jakupec, V. B. Arion and B. K. Keppler, *Chem. - Eur. J*., **2009**, 15, 12283-12291.

[Kapitza, 2005] S. Kapitza, M. Pongratz, M. A. Jakupec, P. Heffeter, W. Berger, L. Lackinger, B. K. Keppler and B. Marian*, J. Cancer Res. Clin. Oncol*., **2005**, 131, 101-110.

[Kastan, 2008] M. B. Kastan, *Mol. Cancer Res.*, **2008**, 6, 517-524.

[Kelland, 2007] L. Kelland, *Nat. Rev. Cancer*, **2007**, 7, 573-584.

[Kelman, 1977] A. D. Kelman, M. J. Clarke, S. E. Edmonds and H. J. Peresie, *J. Clin. Hematol. Oncol*., **1977**, 7, 274-288.

[Kemp, 2007] S. Kemp, N. J. Wheate, D. P. Buck, M. Nikac, J. G. Collins and J. R. Aldrich-Wright, *J. Inorg. Biochem.,* **2007**, 101, 1049-1058.

[Keppler, 1986] B. K. Keppler and W. Rupp, *J. Cancer Res. Clin. Oncol*., **1986**, 111, 166-168.

[Keppler, 1987] B. K. Keppler, W. Rupp, U. M. Juhl, H. Endres, R. Niebl and W. Balzer, *Inorg. Chem*., **1987**, 26, 4366-4370.

[Keppler, 1989] B. K. Keppler, M. Henn, U. M. Juhl, M. R. Berger, R. Niebl and F. E. Wagner, *Prog. Clin. Biochem. Med*., **1989**, 10, 41-69.

[Khalaila, 2005] I. Khalaila, C. S. Allardyce, C. S. Verma, and P. J. Dyson, *Chembiochem: Eur. J. Chem. Biol.*, **2005**, 6, 1788-1795.

[Kieler-Ferguson, 2013] H. M. Kieler-Ferguson, J. M. J. Frećhet and F. C. Jr. Szoka, *Wiley Interdiscip. Rev.: Nanomed. Nanobiotechnol.*, **2013**, 5, 130-138.

[Kieller, 1962] J. Kieller, *Biochem. Pharmacol*., **1962**, 11, 453-456.

[Kilpin, 2014] K. J. Kilpin, S. Crot, T. Riedel, J. A. Kitchen and P. J. Dyson, *Dalton Trans*., **2014**, 43, 1443-1448.

[Kirsch, 1998] D. G. Kirsch and M. B. Kastan, *J. Clin. Oncol.*, **1998**, 16, 3158-3168.

[Kostova, 2006] J. Kostova, *Curr. Med. Chem.*, **2006**, 13, 1085-1107.

[Kratz, 1993] F. Kratz, *Metal Complexes in Cancer Chemotherapy*, VCH-Weinheim, **1993**.

[Kratz, 1994] F. Kratz, M. Hartmann, B. K. Keppler and L. Messori, *J. Biol. Chem.*, **1994**, 269, 2581-2588.

[Kratz, 2008] F. Kratz, *J. Controlled Release*, **2008**, 132, 171-183.

[Krause-Heuer, 2009] A. M. Krause-Heuer, R. Grünert, S. Kühne, M. Buczkowska, N. J. Wheate, D. D. Le Pevelen, L. R. Boag, D. M. Fisher, J. Kasparkova, J. Malina, P. J. Bednarski, V. Brabec and J. R. Aldrich-Wright, *J. Med. Chem.*, **2009**, 52, 5474-5484.

[Kroemer, 2007] G. Kroemer, L. Galluzzi and C. Brenner, *Physiol Rev*, **2007**, 87, 99-163.

[Kron, 1999] P. A. Kroon and G. Williamson, *J. Sci. Food. Agri.*, **1999**, 79, 355-361.

[Kurzwernhart, 2012a] A. Kurzwernhart, W. Kandioller, C. Bartel, S. Bachler, R. Trondl, G. Muhlgassner, M. A. Jakupec, V. B. Arion, D. Marko, B. K. Keppler and C. G. Hartinger, *Chem. Commun*., **2012**, 48, 4839-4841.

[Kurzwernhart, 2012b] A. Kurzwernhart, W. Kandioller, S. Bachler, C. Bartel, S. Martic, M. Buczkowska, G. Muhlgassner, M. A. Jakupec, H. B. Kraatz, P. J. Bednarski, V. B. Arion, D. Marko, B. K. Keppler and C. G. Hartinger, *J. Med. Chem*., **2012**, 55, 10512-10522.

L

[Legin, 2016] A. A. Legin, S. Theiner, A. Schintlmeister, S. Reipert, P. Heffeter, M. A. Jakupec, J. Mayr, H. P. Varbanov, C. R. Kowol, M. Galanski, W. Berger, M. Wagner and B. K. Keppler, *Chem. Sci.*, **2016**, 7, 3052-3061.

[Leijen, 2015] S. Leijen, S. A. Burgers, P. Baas, D. Pluim, M. Tibben, E. van Werkhoven, E. Alessio, G. Sava, J. H. Beijnen and J. H. Schellens, *Invest. New Drugs,* **2015**, 33, 201-214.

[Lemaire, 1991] M. A. Lemaire, A. Schwartz, A. R. Rahmouni and M. Leng, *Proc. Natl. Acad. Sci. U. S. A.*, **1991**, 88, 1982-1985.

[Lentz, 2009] F. Lentz, A. Drescher, A. Lindauer, M. Henke, R. A. Hilger, C. G. Hartinger, M. E. Scheulen, C. Dittrich, B. K. Keppler and U. Jaehde, *Anti-Cancer Drugs*, **2009**, 20, 97-103.

[Liu, 1995] L. Liu, W. R. Hudgins, S. Shack, M. Q. Yin and D. Samid, *Int. J. Cancer*, **1995**, 62, 345-350.

[Liu, 2013] D. Liu, C. He, A. Z. Wang, and W. Lin, *Int. J. Nanomed.*, **2013**, 8, 3309-3319.

[Liu, 2014] D. Liu, C. Poon, K. Lu, C. He and W. Lin, *Nat. Commun*., **2014**, 25(5), 4182-4193.

[Livingstone, 1970] S. E . Livingstone and A. E. Mihkelson, *Inorg. Chem*., **1970**, 9, 2545-2551.

[Long, 1990] E. C. Long and J. K. Barton, *Acc. Chem. Res.*, **1990**, 23, 271-273.

[Lukasehv, 1998] M. E. Lukashev and Z. Werb, *Trends Cell. Biol.*, **1998**, 8, 437-441.

M

[Ma, 2005] E. S. Ma, W. D. Bates, A. Edmunds, L. R. Kelland, T. Fojo and N. Farrell, *J. Med. Chem.*, **2005**, 48, 5651-5654.

[Ma, 2015] L. L. Ma, R. Ma, Y. P. Wang, X. Y. Zhu, J. L. Zhang, H. C. Chan, X. F. Chen, W. J. Zhang, S. K. Chiu and G. Y. Zhu, *Chem. Commun*., **2015**, 51, 6301-6304.

[Maurya, 2015] M. R. Maurya, B. Uprety, F. Avecilla, S. Tariq and A. Azam, *Eur. J. Med. Chem.*, **2015**, 98, 54-60.

[Mayr, 2017] J. Mayr, P. Heffeter, D. Groza, L. Galvez, G. Koellensperger, A. Roller, B. Alte, M. Haider, W. Berger, C. R. Kowol and B. K. Keppler, *Chem. Sci.*, **2017**, 8, 2241-2250.

[Mazumder, 2012] M. E. Mazumder, P. Beale, C.Chan, J. Q.Yu and F. Huq, *ChemMedChem*, **2012**, 7, 1840-1846.

[Meggers, 2009] E. Meggers, *Chem. Commun.,* **2009**, 1001-1010.

[Meier, 2013] S. M. Meier, M. Novak, W. Kandioller, M. A. Jakupec, V. B. Arion, N. Metzler-Nolte, B. K. Keppler and C. G. Hartinger, *Chem.-Eur. J.,* **2013**, 19, 9297-9307.

[Meier-Menches, 2018] S. M. Meier-Menches, C. Gerner, W. Berger, C. G. Hartinger and B. K. Keppler, *Chem. Soc. Rev.,* **2018**, 47, 909-928.

[Mello, 1995] J. A. Mello, S. J. Lippard and J. M. Essigmann, *Biochemistry*, **1995**, 34, 14783-14791.

[Mendoza-Ferri, 2009] M. G. Mendoza-Ferri, C. G. Hartinger, A. A. Nazarov, R. E. Eichinger, M. A. Jakupec, K. Severin and B. K. Keppler, *Organometallics*, **2009**, 28, 6260-6265.

[Merlino, 2016] A. Merlino, *Coord. Chem. Rev.,* **2016**, 326, 111-134.

[Mertz, 1993] W. Mertz, *Nutr. Rev.*, **1993**, 51, 287-295.

[Messori, 2000a] L. Messori, P. Orioli, D. Vullo, E. Alessio and E. Iengo, *Eur. J. Biochem*., **2000**, 267, 1206-1213.

[Messori, 2000b] L. Messori,F. G. Vilchez, R. Vilaplana, F. Piccioli, E. Alessio and B. K. Keppler, *Metal-based Drugs*, **2000**, 7, 335-342.

[Messori, 2014] L. Messori and A. Merlino, *Dalton Trans.*, **2014**, 43, 6128-6131.

[Messori, 2016] L. Messori and A. Merlino, *Coord. Chem. Rev.,* **2016**, 315, 67-89.

[Michels, 2013] J. Michels, I. Vitale, L. Senovilla, D. P. Enot, P. Garcia, D. Lissa, K. A. Olaussen, C. Brenner, J. Soria, M. Castedo and G. Kroemer, *Cell Cycle*, **2013**, 12, 877-883.

[Mitchell, 2014] S. C. Mitchell and R. H. Waring, *Phytochemistry*, **2014**, 97, 5-10.

[Monti-Bragadin, 1975] C. Monti-Bragadin, L. Ramani, L. Samer, G. Mestroni and G. Zassinovich, *Antimicrob. Agents Chemother*., **1975**, 7, 825-827.

[Morris, 2001] R. E. Morris, R. E. Aird, P. D. Murdoch, H. M. Chen, J. Cummings, N. D. Hughes, S. Parsons, A. Parkin, G. Boyd, D. I. Jodrell and P. J. Sadler, *J. Med. Chem*., **2001**, 44, 3616-3621.

[Muggia, 2015] F. M. Muggia, A. Bonetti, J. D. Hoeschele, M. Rozencweig and S. B. Howell, *J. Clin. Oncol.*, **2015**, 33(35), 4219-4226.

[Muhammad, 2014] N. Muhammad and Z. Guo, *Curr. Opin. Chem. Biol.*, **2014**, 19, 144-153.

[Murray, 2016] B. S. Murray, M. V. Babak, C. G. Hartinger and P. J. Dyson, *Coord. Chem. Rev.*, **2016**, 306, 86-114.

[Mügge, 2011] C. Mügge, C. Rothenburger, A. Beyer, H. Gorls, C. Gabbiani, A. Casini, E. Michelucci, I. Landini, S. Nobili, E. Mini, L. Messori and W. Weigand, *Dalton Trans.*, **2011**, 40, 2006-2016.

[Mügge, 2014] C. Mügge, R. Liu, H. Goerls, C. Gabbiani, E. Michelucci, N. Ruediger, J. H. Clement, L. Messori and W. Weigand, *Dalton Trans.*, **2014**, 43, 3072-3086.

[Mügge, 2016] C. Mügge, T. Marzo, L. Massai, J. Hildebrandt, G. Ferraro, P. Rivera-Fuentes, N. Metzler-Nolte, A. Merlino, L. Messori and W. Weigand, *Inorg. Chem.*, **2015**, 54, 8560-8570.

N

[Nakabayaski, 2015] Z. Nakabayashi, T. Yang, T. Nishizawa, T. Mori and K. Saito, *Journal of natural products*, **2015**, 78, 1179-1183.

[Natella, 1999] F. Natella, M. Nardini, M. Di Felice and C. Scaccini, *J. Agric. Food Chem.*, **1999**, 47(4), 1453-1459.

[Ndagi, 2017] U. Ndagi, N. Mhlongo and M. W. Soliman, *Drug Des. Dev. Ther.*, **2017**, 11, 599-616.

[Negrini, 2010] S. Negrini, V. G. Gorgoulis and T. D. Halazonetis, *Nat. Rev. Mol. Cell Biol.*, **2010**, 11, 220-228.

[Neumann, 2015] W. Neumann, B. C. Crews, L. J. Marnett and E. Hey-Hawkins, *ChemMedChem*, **2015**, 9, 1150-1153.

[Niksch, 2010] T. Niksch, H. Gorls, M. Friedrich, R. Oilunkaniemi, R. Laitinen and W. Weigand, *Eur. J. Inorg. Chem.*, **2010**, 74-94.

[Nowak-Sliwinska, 2011] P. Nowak-Sliwinska, J. R. van Beijnum, A. Casini, A. A. Nazarov, G. Wagnieres, H. van den Bergh, P. J. Dyson and A. W. Griffioen, *J. Med. Chem*., **2011**, 54, 3895-3902.

O

[Oberoi, 2013] H. S. Oberoi, N. V. Nukolova, A. V. Kabanov and T. K. Bronich, *Adv. Drug Delivery Rev.*, **2013**, 65, 1667-1685.

[Ohi, 2012] H. Ohi, M. Ashizaki and M. Obata, *Chem. Biodivers*., **2012**, 9(9), 1903-1915.

[Ohno, 2011] A. Ohno, K. Inomata, H. Tochio and M. Shirakawa, *Curr.Top.Med.Chem*., **2011**, 11, 68-73.

[Orvig, 1999] C. Orvig and M. J. Abrams, *Chem. Rev*., **1999**, 99, 2201-2204.

[Ott, 2007] I. Ott and R. Gust, *Arch. Pharm*., **2007**, 340, 117-126.

[Ozols, 2003] R. F. Ozols, B. N. Bundy, B. E. Greer, J. M. Fowler, D. Clarke-Pearson, R. A. Burger, R. S. Mannel, K. De Geest, E. M. Hartenbach and R. Baergen, *J. Clin. Oncol.*, **2003**, 21, 3194-3200.

P

[Pascoe, 1974] J. M. Pascoe and J. J. Roberts, *Biochem. Pharmacol*., **1974**, 23, 1345-1357.

[Pathak, 2014] R. K. Pathak, S. Marrache, J. H. Choi, T. B. Berding and S. Dhar, *Angew. Chem., Int. Ed.,* **2014**, 53, 1963-1967.

[Paunescu, 2015] E. Paunescu, P. Nowak-Sliwinsky, C. M. Clavel, R. Scopelliti, A. W. Griffioen and P. J. Dyson, *ChemMedChem*, **2015**, 10, 1539-1547.

[Peacock, 2006] A. F. A. Peacock, A. Habtemariam, R. Fernandez, V. Walland, F. P. A. Fabbiani, S. Parsons, R. E. Aird, D. I. Jodrell and P. J. Sadler, *J. Am. Chem. Soc*., **2006**, 128, 1739-1748.

[Peacock, 2007a] A. F. A. Peacock, A. Habtemariam, S. A. Moggach, A. Prescimone, S. Parsons and P. J. Sadler, *Inorg. Chem*., **2007**, 46, 4049-4059.

[Peacock, 2007b] A. F. Peacock, M. Melchart, R. J. Deeth, A. Habtemariam, S. Parsons and P. J. Sadler, *Chem.–Eur. J.,* **2007**, 13, 2601-2613.

[Peacock, 2007c] A. F. A. Peacock, S. Parsons and P. J. Sadler, *J. Am. Chem. Soc*., **2007**, 129, 3348-3357.

[Persons, 2000] D. L. Persons, E. M. Yazlovitskaya and J. C. Pelling, *J. Biol. Chem.,* **2000**, 275, 35778-35785.

[Petruzzella, 2017] E. Petruzzella, J. P. Braude, J. R. Aldrich-Wright, V. Gandin and D. Gibson, *Angew. Chem., Int. Ed*., **2017**, 56, 11539-11544.

[Petruzzella, 2018] E. Petruzzella, R. Sirota, I. Solazzo, V. Gardin and D. Gibson, *Chem. Sci.*, **2018**, 9, 4299-4307.

[Petrylak, 2007] D. P. Petrylak, O. Sartor, F. Witje, J. Ferrero, W. R. Berry, A. Koletsky, S. Falcon, F. E. Nathan, M. E. Petrone and C. A. Sternberg, *Proc. Am. Soc. Clin. Oncol*., **2007**, 145.

[Phillips, 2004] A. D. Phillips, L. Gonsalvi, A. Romerosa, F. Vizza and M. Peruzzini, *Coord. Chem. Rev.,* **2004**, 248, 955-993.

[Pichler, 2013] V. Pichler, J. Mayr, P. Heffeter, O. Domotor, E. A. Enyedy, G. Hermann, D. Groza, G. Kollensperger, M. Galanksi, W. Berger, B. K. Keppler and C. R. Kowol, *Chem. Commun*., **2013**, 49, 2249-2251.

[Pielak, 2009] G. J. Pielak, C. Li, A. C. Miklos, A. P. Schlesinger, K. M. Slade, G. F. Wang and I. G. Zigoneanu, *Biochemistry*, **2009**, 48, 226-234.

[Pizarro, 2010] A. M. Pizarro, A. Habtemariam and P. J. Sadler, in: G. Jaouen and N. Metzler-Nolte (Eds.), *Medicinal Organometallic Chemistry*, Springer, **2010**, 21-56.

[Planells-Cases, 2015] R. Planells-Cases, D. Lutter, C. Guyader, N. M. Gerhards, F. Ullrich, D. A. Elger, A. Kucukosmanoglu, G. Xu, F. K. Voss, S. M. Reincke, T. Stauber, V. A. Blomen, D. J. Vis, L. F. Wessels, T. R. Brummelkamp, P. Borst, S. Rottenberg and T. J. Jentsch, *EMBO J*., **2005**, 34, 2993-3008.

[Prager, 1966] R. H. Prager and H. M. Thregold, *Aust. J. Chem*., **1966**, 19, 451-454.

[Prasad, 1995] A. S. Prasad, *Nutrition*, **1995,** 11, 93-99.

[Prasad, 2002] A. S. Prasad and O. Kucuk, *Cancer Metastasis Rev.*, **2002**, 21, 291-295.

R

[Rademaker-Lakhai, 2004] J. M. Rademaker-Lakhai, D. van den Bongard, D. Pluim, J. H. Beijnen and J. H. Schellens, *Clin. Cancer Res*., **2004**, 10, 3717-3727.

[Raveendran, 2016] R. Raveendran, J. P. Braude, E. Wexselblatt, V. Novohradsky, O. Stuchlikova, V. Brabec, V. Gandin and D. Gibson, *Chem. Sci*., **2016**, 7(3), 2381-2391.

[Reedijk, 1999] J. Reedijk and J. M. Teuben, in: B. Lippert (Ed.), *Cisplatin. Chemistry and Biochemistry of a Leading Anticancer Drug,* VHCA, Wiley- VCH, **1999**, 339-362.

[Reedijk, 2003] J. Reedijk, *Proc. Natl. Acad. Sci. U. S. A.*, **2003**, 100, 3611-3616.

[Riedl, 2017] C. A. Riedl, L. S. Flocke, M. Hejl, A. Roller, M. H. Klose, M. A. Jakupec, W. Kandioller and B. K. Keppler, *Inorg. Chem*., **2017**, 56, 528-541.

[Romero-Canelon, 2013] I. Romero-Canelon and P. J. Sadler, *Inorg. Chem*., **2013**, 52, 12276-12291.

[Rosenberg, 1965] B. Rosenberg, L. Vancamp and T. Krigas, *Nature*, **1965**, 205, 698-699.

[Rosenberg, 1969] B. Rosenberg, L. Vancamp, J. E. Trosko and V. H. Mansour, *Nature*, **1969**, 222, 385-386.

[Rothenburger, 2006] C. Rothenburger, M. Galanski, V. B. Arion, H. Gorls, W. Weigand and B. K. Keppler, *Eur. J. Inorg .Chem.*, **2006**, 3746-3752.

S

[Safaei, 2006] R. Safaei, *Cancer Lett.*, **2006**, 234, 34-39.

[Saha, 2012] P. Saha, C. Descôteaux, K. Brasseur, S. Fortin, V. Leblanc, S. Parent, E. Asselin and G. Bérubé, *Eur. J. Med. Chem.*, **2012**, 48, 385-390.

[Salemme, 2016] A. Salemme, A. R. Togna, A. Mastrofrancesco, V. Cammisotto, M. Ottaviani, A. Bianco and A. Venditti, *Brain research bulletin*, **2016**, 120, 151-158.

[Samimi, 2004] G. Samimi, R. Safaei, K. Katano, A. K. Holzer, M. Rochdi, M. Tomioka, M. Goodman and S. B. Howell, *Clin. Cancer Res.,* **2004**, 10, 4661-4669.

[Saumweber, 1998] R. Saumweber, C. Robl and W. Weigand, *Inorg. Chim. Acta,* **1998**, 269, 83-90.

[Sava, 1989] G. Sava, S. Pacor, S. Zorzet, E. Alessio and G. Mestroni, *Pharmacol. Res.*, **1989**, 21, 617-628.

[Sava, 1992] G. Sava, S. Pacor, G. Mestroni and E. Alessio, *Anti-Cancer Drugs*, **1992**, 3, 25-31.

[Sava, 1994] G. Sava, S. Pacor, M. Coluccia, M. Mariggio, M. Cocchietto, E. Alessio and G. Mestroni, *Drug Invest.*, **1994**, 8, 150-161.

[Schmid, 2007a] W. F. Schmid, R. O. John, G. Muhlgassner, P. Heffeter, M. A. Jakupec, M. Galanski, W. Berger, V. B. Arion and B. K. Keppler, *J. Med. Chem*., **2007**, 50, 6343-6355.

[Schmid, 2007b] W. F. Schmid, R. O. John, V. B. Arion, M. A. Jakupec and B. K. Keppler, *Organometallics*, **2007**, 26, 6643-6652.

[Schmidlehner, 2016] M. Schmidlehner, L. S. Flocke, A. Roller, M. Hejl, M. A. Jakupec, W. Kandioller and B. K. Keppler, *Dalton Trans*., **2016**, 45, 724-733.

[Schneider, 2013] V. Schneider, M. L. Krieger, G. Bendas, U. Jaehde and G. V. Kalayda, *J. Biol. Inorg. Chem.*, **2013**, 18, 165-174.

[Schubert, 2003] K. Schubert, R. Saumweber, H. Görls and W. Weigand, *Z. Anorg. Allg. Chem.*, **2003**, 629, 2091-2096.

[Schubert, 2005] K. Schubert, H. Görls and W. Weigand, *Heteroatom. Chemistry*, **2005**, 16(5), 369-378.

[Schubert, 2006] K. Schubert, T. Alpermann, T. Niksch, H. Görls and W. Weigand, *Z. Anorg. Allg. Chem.*, **2006**, 632, 1033-1042.

[Schubert, 2007] K. Schubert, H. Görls and W. Weigand, *Z. Naturforsch.*, **2007**, 62b, 475-482.

[Scolaro, 2005] C. Scolaro, A. Bergamo, L. Brescacin, R. Delfino, M. Cocchietto, G. Lau- renczy, T. J. Geldbach, G. Sava and P. J. Dyson, *J. Med. Chem*., **2005**, 48, 4161-4171.

[Serrano, 2011] F. Serrano, A. Matsuo, P. Monteforte, A. Bechara, S. Smaili, D. Santana, T. Rodrigues, F. Pereira, L. Silva, J. Machado, E. Santos, J. Pesquero, R. Martins, L. Travassos, A. Caires and E. Rodrigues, *BMC Cancer*, **2011**, 11, 296-313.

[Shahidi, 2010] F. Shahidi and A. Chandrasekara, *Phytochem. Rev.*, **2010**, 9, 147-170.

[Sharma, 2011] P. Sharma, *J. Chem. Pharm. Res.*, **2011**, 3(2), 403-423.

[Sharma, 2017] S. D. Sharma, *Am. J. PharmTech Res.*, **2017**, 7, 1-19.

[Shiraishi, 1989] T. Shiraishi, M. K. Owada, M. Tatsuka, T. Yamashita, K. Watanabe and T. Kakunaga, *Cancer Res.*, **1989**, 49, 2374-2378.

[Shnyder, 2011] S. D. Shnyder, Y. Fu, A. Habtemariam, S. H. van Rijt, P. A. Cooper, P. M. Loadman and P. J. Sadler, *MedChem-Comm.*, **2011**, 2, 666-668.

[Siemeling, 2010] U. Siemeling, F. Bretthauer and C. Bruhn, *J. Organomet. Chem.*, **2010**, 695, 626-629.

[Simonyan, 1993] A. V. Simonyan, *Khim.-Farm. Zh.*, **1993**, 27(2), 21-22.

[Skobe, 1998] M. Skobe and N. E. Fusenig, *Proc. Natl. Acad. Sci. U. S. A.*, **1998**, 95, 1050-1055.

[Smith, 1996] C. A. Smith, A. J. SutherlandSmith, B. K. Keppler, F. Kratz and E. N. Baker, *J. Biol. Inorg. Chem*., **1996**, 1, 424-431.

[Soldevila-Barreda, 2015] J. J. Soldevila-Barreda and P. J. Sadler, *Curr. Op. Chem. Biol.*, **2015**, 25, 172-183.

[Sova, 2012] M. Sova, *Med. Chem.*, **2012**, 12, 749-767.

[Spreckelmeyer, 2014] S. Spreckelmeyer, C. Orvig and A. Casini, *Molecules*, **2014**, 19, 15584-15610.

[Stathopoulos, 2012] G. P. Stathopoulos and T. Boulikas, *J. Drug Delivery*, **2012**, 2012, 581363-581373.

[Stepanenko, 2013] I. N. Stepanenko, G. E. Büchel, B. K. Keppler, V. B. Arion in: R. H. Kretsinger, V. N. Uversky, E. A. Permyakov (Eds.), *Encyclopedia of Metalloproteins*, Springer Science and Business Media, **2013**, 1596-1614.

[Stewart, 2007] D. J. Stewart, *Crit. Rev. Oncol. Hematol.*, **2007**, 63, 12-31.

[Strebhart, 2008] K. Strebhardt and A. Ullrich, *Nat. Rev. Cancer*, **2008**, 8, 473-480.

[Sudimack, 2000] J. Sudimack and R. J. Lee, *Adv. Drug Delivery Rev.*, **2000**, 41, 147-162.

[Süss-Fink, 2010] G. Süss-Fink, *Dalton Trans.*, **2010**, 39, 1673-1688.

[Szwajgier, 2005] D. Szwajgier, J. Pielecki and Z. Targonski, *Acta Sci. Pol., Technol. Aliment.*, **2005**, 4(2), 129-142.

T

[Takahara, 1995] P. M. Takahara, A. C. Rosenzweig, C. A. Frederick and S. J. Lippard, *Nature*, **1995**, 377, 649-652.

[Tapiero, 2003] H. Tapiero, D. M. Townsend and K. D. Tew, *Biomed. Pharmacother.*, **2003**, 57, 386-398.

[Thimann, 1969] K. V. Thimann, In: M. B. Son (Eds.), *Physiology of plant growth and development*, **1969**, McGrew-Hill, 2-45.

[Thompson, 2003] K. H. Thompson and C. Orvig, *Science*, **2003**, 300, 936-939.

[Thornberry, 1998] N. A. Thornberry and Y. Lazebnik, *Science*, **1998**, 281, 1312-1316.

[Trondl, 2014] R. Trondl, P. Heffeter, C. R. Kowol, M. A. Jakupec, W. Berger and B. K. Keppler, *Chem. Sci.*, **2014**, 5, 2925-2932.

[Trynda-Lemiesz, 1999] L. Trynda-Lemiesz, B. K. Keppler and H. Kozlowski, *J. Inorg. Biochem.*, **1999**, 73, 123-128.

[Tsao, 2004] R. Tsao and Z. Deng, *J. Chromatogr. B*, **2004**, 812, 85-89.

[Tshuva, 2009] E. Y. Tshuva and D. Peri, *Coord. Chem. Rev.*, **2009**, 253, 2098-2115.

U

[Ulukaya, 2011] E. Ulukaya, F. Ari, K. Dimas, E. I. Ikitimur, E. Guney and V. T. Yilmaz, *Eur. J. Med. Chem.*, **2011**, 46, 4957-4963.

V

[Vaisman, 1998] A. Vaisman, M. Varchenko, A. Umar, T. A. Kunkel, J. I. Risinger, J. C. Barrett, T. C. Hamilton and S. G. Chaney, *Cancer Res.*, **1998**, 58, 3579-3585.

[van Rijt, 2009] S. H. van Rijt, A. F. A. Peacock and P. J. Sadler, in: A. Bonetti, R. Leone, F. M. Muggia and S. B. Howell (Eds.), *Platinum and Other Heavy Metal Compounds in Cancer Chemotherapy – Molecular Mechanisms and Clinical Applications*, Humana Press, **2009**, 73-79.

[van Rijt, 2010] S. H. van Rijt, A. Mukherjee, A. M. Pizarro and P. J. Sadler, *J. Med. Chem*., **2010**, 53, 840-849.

[Vander Heiden, 2009] M. G. Vander Heiden, L. C. Cantley and C. B. Thompson, *Science*, **2009**, 324, 102-1033.

[Veikkola, 1999] T. Veikkola and K. Alitalo, *Cancer Biol.*, **1999**, 9, 211-220.

[Velders, 2000] A. H. Velders, H. Kooijman, A. L. Spek, J. G. Haasnoot, D. de Vos and J. Reedijk, *Inorg. Chem.,* **2000**, 39, 2966-2967.

W

[Wang, 2000] X. Wang, J. L. Martindale and N. J. Holbrook, *J. Biol. Chem.*, **2000**, 275, 39435-39443.

[Wang, 2003] F. Wang, H. M. Chen, S. Parsons, L. D. H. Oswald, J. E. Davidson and P. J. Sadler, *Chem.–Eur. J*., **2003**, 9, 5810-5820.

[Wang, 2005] F. Y. Wang, J. Bella, J. A. Parkinson and P. J. Sadler, *J. Biol. Inorg. Chem*., **2005**, 10, 147-155.

[Wang, 2013] X. Wang and Z. Guo, *Chem. Soc. Rev.*, **2013**, 42, 202-224.

[Warburg, 1956a] O. Warburg, *Science*, **1956**, 123, 309-314.

[Warburg 1956b] O. Warburg, *Science*, **1956**, 124, 269-270.

[Weigand, 1993] W. Weigand, R. Saumweber and P. Schulz, *Z. Naturforsch.*, **1993**, 48b, 1080-1088.

[Weiss, 2014] A. Weiss, R. H. Berndsen, M. Dubois, C. Müller, R. Schibli, A. W. Griffioen, P. J. Dyson and P. Nowak-Sliwinska, *Chem. Sci*., **2014**, 5, 4742-4748.

[Weiss, 2015] A. Weiss, D. Bonvin, R. H. Berndsen, E. Scherrer, T. J. Wong, P. J. Dyson, A. W. Griffioen and P. Nowak-Sliwinska, *Sci. Rep*., **2015**, 5 (8990), doi: 10.1038/srep08990.

[Weitman, 1992] S. D. Weitman, R. H. Lark, L. R. Coney, D. W. Fort, V. Frasca, V. R. Jr. Zurawski and B. A. Kamen, *Cancer Res.*, **1992**, 52, 3396-3401.

[Wexselblatt, 2012] E. Wexselblatt and D. Gibson, *J. Inorg. Biochem.,* **2012**, 117, 220-229.

[Wheate, 2010] N. J. Wheate, S. Walker, G. E. Craig and R. Oun, *Dalton Trans*., **2010**, 39, 8113-8127.

[Whetten, 1998] R. W. Whetten, J. J. Mackay and R. R. Sederoff, *Ann. Rev. Plant Physiol. Plant Mol. Biol*., **1998**, 49, 585-609.

[Wimmer, 1989] F. Z. Wimmer, S. Wimmer, P. Castan, S. Cros, N. Johnson and E. Colacio Rodrigez, *Anticancer Res.,* **1989**, 9, 791-794.

[Wu, 2005] Y.-S. Wu, K. R. Koch, V. R. Abratt and H. H. Klump, *Arch. Biochem. Biophys.*, **2005**, 440, 28-37.

Y

[Yamasaki, 2011] M. Yamasaki, T. Makino, T. Masuzawa, Y. Kurokawa, H. Miyata, S. Takiguchi, K. Nakajima, Y. Fujiwara, N. Matsuura, M. Mori and Y. Doki, *Br. J. Cancer*, **2011**, 104, 707-713.

[Yanagawa, 1972] H. Yanagawa, N. Takahash, T. Kato, Y. Kato and Y. Kitahara, *Tetrahedron Lett.*, **1972**, 2549-2552.

[Yang, 2012] J. Yang, X. Sun, W. Mao, M. Sui, J. Tang and Y. Shen, *Mol. Pharmaceutics*, **2012**, 9, 2793-2800.

[Yang, 2015] T. Yang, M. Chen, T. Chen and A. Thakur, *Oncol. Lett.*, **2015**, 10, 2584-2590.

[Yeh, 2002] P.Y. Yeh, S. E. Chuang, K. H. Yeh, Y. C. Song, C. K. Ea and A. L. Cheng, *Biochem. Pharmacol*., **2002**, 63, 1423-1430.

Z

[Zalba, 2013] S. Zalba and M. J. Garrido, *Expert. Opin. Drug Delivery,* **2013**, 10, 829-844.

[Zhang, 2006] S. Zhang, K. S. Lovejoy, J. E. Shima, L. L. Lagpacan, Y. Shu, A. Lapuk, Y. Chen, T. Komori, J. W. Gray, X. Chen, S. J. Lippard and K. M. Giacomini, *Cancer Res.*, **2006**, 66, 8847-8857.

[Zhao, 1999] G. Zhao, H. Lin, P. Yu, H. Sun, S. Zhu, X. Su and Y. Chen, *J. Inorg. Biochem.*, **1999**, 73, 145-149.

[Zhao, 2005] Y. Y. Zhao, R. Mandal and X. F. Li, *Rapid Commun. Mass Spectrom*. *RCM*, **2005**, 19, 1956-1962.

[Zisowsky, 2007] J. Zisowsky, S. Koegel, S. Leyers, K. Devarakonda, M. U. Kassack, M. Osmak and U. Jaehde, *Biochem. Pharmacol*., **2007**, 7, 298-307.

8. Acknowledgements

Bedanken möchte ich mich bei Prof. Dr. W. Weigand für das interessante Thema und die Möglichkeit diese Doktorarbeit anzufertigen. Besonders für sein Engagement bezüglich der Kooperationen zur Frauenklinik in Jena und zur School of Pharmacy in Jerusalem, durch die diese interdisziplinäre Arbeit erst ermöglicht werden konnte. Neben meinem einjährigen Aufenthalt in Israel gewährte er mir die Möglichkeit auf nationalen und internationalen Tagungen meine Ergebnisse zu präsentieren, besonders die Konferenzen auf Mallorca und in Budapest werden mir in Erinnerung bleiben. Ebenso unterstützte er mich bei den von mir gewählten Weiterbildungen, vor allem im Rahmen der GDCh und der Graduierten-Akademie in Jena und meinem BWL-Masterstudium neben der Promotion. Nur durch sein Vertrauen in mich und die fachliche und persönliche Beratung war es möglich diese Arbeit anzufertigen.

Großer Dank gilt Dr. Norman Häfner für die fachliche Betreuung der biologischen Arbeiten seit der Masterarbeit. Seine freundliche und entspannte Art hat das Zusammenarbeiten und Publizieren sehr angenehm gestaltet. Ich konnte mich stets darauf verlassen, dass Norman mir mit einem fachlichen Rat zur Seite steht, Fragen beantwortet oder sehr schnell Manuskripte, Poster, Proposals, Abstracts (und die Doktorarbeit) durchliest. Auch während der Arbeiten im Labor war er immer zur Stelle wenn etwas „ganz schnell“ erledigt werden musste. Besonders aber auch, da seine Überlegungen und Experimente meine Arbeiten sinnvoll ergänzt haben.

Prof. Dr. M. Dürst und Prof. Dr. I. B. Runnebaum gilt mein Dank für die Möglichkeit die biologischen Arbeiten selbstständig in den Laboren der Frauenklinik durchführen zu können. Besonders für das Vertrauen das in mich, als „nicht-Biologin“, gesetzt wurde, bin ich sehr dankbar.

Dem gesamten Team des Labors der Frauenklinik gilt mein Dank für die angenehme Arbeitsatmosphäre und die Unterstützung. Es war mir immer eine Freude in die Klinik gehen zu dürfen um meine Experimente durchzuführen und mich nett zu unterhalten. Besonderer Dank gilt hier Dr. Daniel Kritsch, der meine Arbeiten sinnvoll ergänzt hat.

Acknowledgements

Meinem F-Praktikanten Lars Gabriel möchte ich danken für die Ergebnisse während seines Praktikums bei mir.

אני רוצה להודות Professor Dani Gibson שנתן לי את ההזדמנות לעבוד בקבוצה שלו במשך יותר משנה, לעזרה בעת הכתיבה לקבלת המלגה ולעצותיו.
גם אם השנה לא היתה קלה כל הזמן הייתי שמחה ללמוד ממנו, בכימיה ובנושאים אישיים .

Bedanken möchte ich mich bei meinen Stipendiengebern, der Max-Planck Gesellschaft für das Minerva Stipendium und der COST Action CM 1105 für meine Aufenthalte an der Hebrew University Jerusalem in Israel. Besonders für die freundliche Atmosphäre und der großartigen Unterstützung der Minerva-Stiftung möchte ich mich bedanken, das jährliche Stipendiaten Treffen in Rehovot bleibt mir in Erinnerung.

Der Graduierten Akademie Jena gilt mein Dank für die Aufnahme in das Zertifikatsprogramm „Führung in Wirtschaft und Gesellschaft“ durch das ich die Möglichkeit hatte viele nützliche Kurse zu besuchen.

I like to thank Prof. Dr. A. Merlino and G. Ferraro for their cooperation and the experiments on my ruthenium and platinum complexes.

Dr. H. Görls möchte ich danken für die Vielzahl an Kristallstrukturen, die er für mich gemessen hat und die Unterstützung bei den Anfertigungen dieser für die Publikationen. Es war immer wieder schön einen Anruf zu erhalten und begeistert die fertige Struktur zu bekommen. Der Anruf „*Ich hätte grade etwas Zeit, haben Sie nicht noch zufällig Kristalle?*“ ist ein Highlight der Doktorarbeitszeit. Auch für seine persönliche Unterstützung hin und wieder möchte ich mich bedanken.

Mein Dank gilt Frau B. Rambach und Frau G. Sentis in der NMR-Abteilung für die vielen Messungen, auch über Nacht oder über Wochenenden, die immer unkompliziert und freundlich angefertigt wurden.

Bei Sarah Tippner möchte ich mich bedanken für die vielen bürokratischen Aufgaben, die erledigt werden mussten und die sie mir abgenommen hat. Es war auch immer wieder schön einfach einmal im Sekretariat bei ihr vorbei zu schauen und etwas von der guten Laune mitzunehmen.

Acknowledgements

Susanne Spanngenberg gilt mein Dank für die organisatorischen Aufgaben in der Arbeitsgruppe, die sie durchführt und für ihre Hilfe bei der Chemikalienbestellung, es war wirklich sehr schön immer reichlich Lösungsmittel zum Säulen zur Verfügung zu haben.

Bedanken möchte ich mich bei Dr. R. Fischer für die Unterstützung bei der Durchführung der AC1-Praktika.

Mein Dank gilt weiterhin den technischen Mitarbeitern des Instituts für Anorganische und Analytische Chemie, der MS-Abteilung und der Abteilung für die Durchführung der Elementaranalysen.

Prof. Dr. R. Walter gilt mein Dank dafür, dass ich durch meine BWL-Masterarbeit eine andere Sichtweise auf das Thema meiner Doktorarbeit und die Forschung auf diesem Gebiet erlangen konnte. Durch seine Unterstützung konnte ich das Thema einmal ökonomisch betrachten und habe dadurch eine andere Sicht auf die chemische Forschung an Arzneistoffen erhalten, die mir sonst verwehrt geblieben wäre und auch zur Diskussion dieser Arbeit beigetragen hat.

Mein BWL-Masterstudium neben der Promotion zu absolvieren ging nur durch Unterstützung. Für die vielen Mitschriften der von mir verpassten Vorlesungen oder gleich ganzen Ordnern an Materialien, dem gemeinsamen Lernen vor Prüfungen und vor allem dem Mut machen es nicht aufzuegeben bedanke ich mich bei meinen (BWL-)Freundinnen: Caro, Merve, Johanna und Nancy. Durch eure Hilfe konnte ich gelassen im Labor arbeiten, die Promotion an erste Stelle setzen und war trotzdem gut vorbereitet bei den BWL-Prüfungen. Ich habe mich immer gefreut, wenn ich gestresst aus dem Labor in eine Vorlesung gerannt bin, zu wissen, dass eine von euch für mich einen Platz freihält.

Bedanken möchte ich mich bei Dr. Ralf Trautwein für seine persönliche und fachliche Unterstützung während der Zeit. Durch seine ruhige, gelassene und vernünftige Art hat er mir vieles beigebracht und mein Arbeiten erleichtert.

Bei Alexander Kiefer bedanke ich mich vor allem für die gemeinsame Zeit, aber auch die fachlichen Ratschläge und Diskussionen und das parallele Abschließen der Dissertationszeit.

Prof. Dr. Christian Kowol gilt mein Dank in erster Linie für die tolle Freundschaft, die in den letzten Jahren entstanden ist, aber auch durch immer wieder fachliche

und persönliche Ratschläge und Diskussionen. Besonders dafür, dass er sich Zeit genommen hat, durch seine Anmerkungen meine Arbeit zu unterstützen bin ich ihm sehr dankbar.

Mein Dank gilt Martin Klapper für die Freundschaft seit dem Bachelor Studium, er hat alle Höhen und Tiefen mit mir durchlebt und auf seinen Rat und sein offenes Ohr ist immer Verlass.

היה כיף לחיות שנה שלמה בישראל, אך לפעמים גם קשה.

הזמן הטוב ביותר שלי לתואר הדוקטורוט היה שם , ובזה רוצה להודות ל-"החברים הישראלים שלי:"

- Liora, השותפה היפה שלי שבילינו הרבה זמן ביחד.

- Verena, Marga and Daniel- מפני שתמיד היה לכם זמן לבירה והיתה לי הזדמנות מיוחדת לבקר את הארץ איתכם.

- Hannah, במיוחד לפעם הראשונה בישראל שהראתה לי כל כך הרבה דברים ועל החוויה שלנו בנסיעה לאילת.

- Dahie, על הידידות ,על כך שלימדת אותי עברית וערבית ולקחת אותי ברכב שלך כשהייתי עצלנית ללכת ברגל.

- Balsam, על הזמן הרב שבילינו יחד, על הביקור בגן החיות.

הרגשתי כמו בבית כאשר שבילינו עם החברים שלך , כך שהראית לי חיים אחרים של המדינה.

- Thorsten, and the rest of the Minerva-people - על ערבי הפאב הגדולים בתל-אביב, ברחובות ובירושלים.

9. Curriculum Vitae

Name	Jana Hildebrandt

Work Experience

07/2018 -	Consultant at Accenture Strategy Life Sciences, Hamburg
10/2014 – 06/2018	Scientific Employee at Friedrich-Schiller Universität Jena, Institute for Inorganic and Analytical Chemistry
12/2016 – 12/2017	PhD Student at Hebrew University Jerusalem
01/2011 – 03/2011	Student (Hilfswissenschaftler) at Friedrich-Schiller Universität Jena, Institute for Organic Chemistry

International Work Experience

12/2016 – 12/2017	PhD Student at the Hebrew University Jerusalem (Israel), School of Pharmacy, Minerva-Fellowship, Max-Planck Gesellschaft
03/2016 – 04/2016	Guest researcher at the Hebrew University Jerusalem (Israel), School of Pharmacy, Fellowship: COST-Action CM1105
09/2012-10/2012	Guest researcher at the Università degli Studi di Firenze (Italy), Fellowship: DAAD

Education

10/2014-	PhD Student at the Friedrich-Schiller Universität Jena (Institute for Inorganic and Analytical Chemistry), Uniklinikum Jena (Department of Gynecology) and the Hebrew University Jerusalem (School of Pharmacy)
10/2014 – 03/2018	Master of Science in Business Administration at Friedrich-Schiller Universität Jena Title of Master thesis: Marktanalyse ausgewählter Arzneistoffe in der Pharmaindustrie. Eine wirtschaftshistorische Studie.

10/2012 – 09/2014	Master of Science in Chemical Biology at Friedrich-Schiller Universität Jena Title of Master thesis: Synthese und Untersuchung der biologischen Aktivität von Ruthenium- und Platinkomplexen
10/2009 – 09/2012	Bachelor of Science in Chemistry at Friedrich-Schiller Universität Jena Title of Bachelor thesis: Mechanistische Untersuchungen zur Wirkungsweise von Pt(II)-Komplexen mit O,S-chelatisierenden Liganden
08/1996 – 06/2009	High School degree (Abitur) at Albertus-Magnus Gymnasium Friesoythe

Certifiactes, Prices and Fellowships

11/2017	Certificate: Führung für Nachwuchsführungskräfte (GDCh-Fortbildungskurs)
11/2017	Certificate: Deskriptiv-und Interferenzstatistik mit SPPS (Graduiertenakademie Jena)
10/2017	Certificate: New Business Development (GDCh-Fortbildungskurs)
02/2017	Poster Prize: der GDCh, DPhG, SCS: Frontiers in Medicinal Chemistry (Bern)
02/2017	Certificate: BWL für Chemiker (GDCh-Fortbildungskurs)
12/2016	Fellowship: Minerva-Stiftung der Max-Planck-Gesellschaft
12/2016	Certificate: Führung in Wirtschaft und Gesellschaft (Inhalte u.a.: BWL kompakt, Teambildung, Führung, Projektmanagement, Zeitmanagement) (Graduiertenakademie Jena)
09/2016	Poster prize: Mitteldeutsches Anorganiker Nachwuchssymposium (Halle/Saale)
09/2016	Certificate: Geprüfter Projektmanager Wirtschaftschemie (GDCh-Fortbildungskurs)
09/2013	Certificate: Qualitätssicherung in der Analytischen Chemie (FSU Jena)

Conferences

10.9.2017– 14.09.2017	Poster presentation: GDCh-Wissenschaftsforum Chemie 2017, Berlin

12.2.2017– 15.2.2017	Poster presentation: Frontiers in Medicinal Chemistry, Tagung der GDCh/DPhG/SCS, Bern
15.09.2016	Oral and Poster presentation: Mitteldeutsches Anorganisches Nachwuchssymposium, Halle/Saale
26.8.2016– 01.09.2016	Poster presentation: 13th European Biological Inorganic Chemistry Conference (EuroBIC 13), Budapest
24.07.2016– 29.07.2016	Oral and Poster presentation: 27th International Symposium on Organic Chemistry of Sulfur, Jena
24.07.2016	Oral presentation: Deutsch-polnisches premeeting im Rahmen der 27th ISOCS, Jena
27.4.2016– 30.4.2016	Oral presentation: Early Career Investigator Communication: 3rd International Symposium on Functional Metal Complexes that Bind to Biomolecules - 4th Whole Action Meeting of the COST Action CM1105, Palma de Mallorca
23.4.2016	Poster presentation: 8th Postgraduate Symposium on Cancer Research, Dornburg
13.03.2016– 16.03.2016	Poster presentation: Frontiers in Medicinal Chemistry, Tagung der GDCh/DPhG, Bonn
30.8.2015– 02.09.2015	Poster presentation: GDCh-Wissenschaftsforum Chemie 2015, Dresden
25.04.2015	Poster presentation: 7th Postgraduate Symposium on Cancer Research, Dornburg

Language Skills

English	Fluently
Hebrew	Basic skills (Alef)
French	School (Delf Diploma A1 and A2)

Jana Hildebrandt

10. Declaration of authorship/ Selbstständigkeitserklärung

I declare that this thesis and the work presented herewith are my own and have been generated by me as the result of my own original research.

Ich erkläre, dass ich die vorliegende Arbeit selbstständig und unter Verwendung der angegeben Hilfsmittel, persönlichen Mitteilungen und Quellen angefertigt habe.

Jena, _____

Jana Hildebrandt